

**Heat and mass exchange within the Soil-Plant canopy- Atmosphere system:
A theoretical approach and its validation.**

Promotoren:

dr. ir. L. Wartena
emeritus hoogleraar in de landbouweerkunde en
omgevingsnatuurkunde

dr. ir. J. Goudriaan
persoonlijk hoogleraar bij vakgroep Theoretische Productie-Ecologie

Co-promotor:

dr. ir. A. F. G. Jacobs
universitair hoofddocent meteorologie

11102201, 2024

Rushdi M. M. El-Kilani

**Heat and mass exchange within the Soil-Plant canopy- Atmosphere system:
A theoretical approach and its validation.**

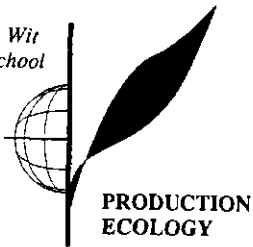
Proefschrift

ter verkrijging van de graad van doctor
op gezag van de rector magnificus
van de Landbouwniversiteit Wageningen,
dr. C. M. Karssen,
in het openbaar te verdedigen
op dinsdag 18 februari 1997
des namiddags te vier uur in de Aula

1511 931572

ISBN 90-5485-644-0

*The C.T. de Wit
Graduate School*



This study was carried out at the Department of Meteorology in coordination with The Department of Theoretical Production Ecology of the Wageningen Agricultural University, The Netherlands with the main financial support by the Wetenschappelijk Onderzoek voor de Tropen (WOTRO), Directoraat Generaal Internationale Samenwerking (DGIS), Dossiernummer WB 76-129, and the Agricultural University of Wageningen.

All rights reserved.

Copyright © 1997 by R. M. M. El-Kilani

No part of this material protected by this copyright notice, apart from bibliographic data and brief quotations embodied in critical reviews, may be reproduced, re-recorded, published or utilized in any form or by any means, electronic or mechanical, including photocopying, recording or by any information storage and retrieval system, without written permission from the copyright owner.

Printed in The Netherlands.

WAGENINGEN
LANDBOUWUNIVERSITEIT
WAGENINGEN

Stellingen

behorende bij het proefschrift

**Heat and mass exchange within the Soil-Plant canopy- Atmosphere system:
A theoretical approach and its validation.**

door Rushdi M. M. El-Kilani,

*in het openbaar te verdedigen op 18 februari 1997 in de
Aula van de Landbouwwuniversiteit in Wageningen.*

1. A numerical result is not a proof, it still can be an artifact.

This thesis

2. The problem of intermittency in canopy climate modelling is caused by the combined effect of:

- 1) the existence of a separation in the length scales responsible for transport and

- 2) the ability of the leaves and the soil as sources and sinks to respond to temperature and vapour pressure variations due to this intermittency or scale separation.

This thesis

3. The reason behind the failure of the K theory approach, namely that the length scale of transport is much larger than the scale of $\frac{\partial c}{\partial z}$, is the same which would lead to a failure of random walk modelling, since this would lead to non-independent movement of the particles at different heights.

This thesis

4. The manner in which a well-buffered soil behaves with respect to the input of a certain pollutant, i.e. the relation between the adsorbed phase to the mobilized phase, shows that there is a limit to soil tolerance to mismanagement.

Inspired by a curve in Stigliani, W. M., 1995. Global perspectives and Risk assessment. In: Biogeodynamics of pollutants in soils and sediments, eds. Salomons, W., and Stigliani, W. M., pp. 331-343. Springer-Verlag, Berlin.

5. In simulating any dynamical system, if any of the scales of intermittency leads to the creation of nonvanishing correlations between behavioural aspects of the system components within a time scale *less than our step of simulation*, we have to:

- 1) include the effect of these correlations on the large-time averaged set of equations describing the system behaviour or

- 2) reduce our time step of simulation and take account of the correlations explicitly.

This thesis.

6. The maintenance of biodiversity is crucial to the existence and the welfare of this planet.

7. The use of too much animal protein in the diet of people in developed countries represents a wasteful conversion of grains to animal protein masses, which could

otherwise be used for securing the food requirements of a large number of people in the underdeveloped countries.

8. Genetically engineered micro-organisms, which are capable of breaking down persistent pollutants, could represent a future option of environmental rehabilitation.
9. Rehabilitation of damaged ecosystems and the development of environmental friendly manufacturing processes will require a lot of capital investment, which will not be met by research and development departments of multinational companies alone, unless a decisive power by the people materializes, expressed in market behavioural trends and their willingness to even sacrifice some of their standard of living.
10. There were times in history of Mankind when a massive loss of heritage and knowledge occurred. To prevent such a loss of heritage in future, the role of the book versus a compact disk or any computer medium as a way of dispersing knowledge will remain crucial.
11. Power training and condition training are complementary to each other.
12. Dilution is not the solution to pollution.
13. Before Mankind can colonize other planets, it has to answer the question of achieving a sustainable ecosystem management on planet earth first.
14. To reduce the delay time of an improved management regime for ecosystems, a stronger public awareness about the extent of the current and projected damage to these systems and the resulting devaluation of our resources has to be created. A translation of this awareness into a political decision force has to materialize.
15. Short sighted commercial interests to meet the rising expectations of human beings and to introduce an unsustainable way of living should not be allowed to be the main motivation behind the destruction of our ecosystems.

This thesis

16. A degraded environment will touch everybody's pocket.

الحمد لله

El-Hamedo le ALLAH

Thanks to ALLAH

*To My Mother
To whom I am
gratefully indebted.*

Foreword

Sitting down and looking back at the six years which it took to finish the work presented in this thesis, I think of the all the times and the branching points through which this work has passed and the pitfalls which became only clear after the work was finished. For partly avoiding me such pitfalls and for all other things in life, I would like to acknowledge and thank **ALLAH** the merciful for his grace and mercy which he extended to me.

I would like also to extend my gratitude and thanks to **all the people** whom God made available to prepare the stage, help, support and guide this work during its different stages.

First of all, I would like to thank my promoter Prof. **L. Wartena** for his guidance, encouragement and the freedom which he granted me to continue this work. He was a source of encouragement and an example of a good teacher which I would like to follow for the rest of my days. I would like to thank him for his patience in keeping up with my lousy datelines. I would like to thank him for his trust in me, his reading and commenting on the manuscript during the different stages.

I would like to thank my promoter Prof. **J. Goudriaan** for his supervision and the freedom which he gave me to pursue this work in the way I liked. I thank him for putting up with my lengthy way of writing. I remember that day in the month of Ramadan (fasting month for Moslems) when I went to him to discuss the possibility of him supervising my Ph.D. study. It was a discussion about my M. Sc. work which ended in accepting me as a Ph.D. student. I thank him for granting this chance to me. I remember the time back in Cairo in 1984 when I looked at a book of Pudoc about crop micrometeorology. It was Prof. Goudriaan's Ph.D. thesis. At that minute, I was wondering if it could be possible for me to do a work like this and have Prof. Goudriaan as my promoter. It was a wish which ALLAH brought true. I would like to thank his wife **Trijnie** for her kindness and understanding.

I would like to thank my co-promoter Dr. **A. F. G. Jacobs** for his supervision and continuous checking up of how things are going. I would like to thank him for his positive attitude toward this work and for keeping the trust that this work will end up in the right result. Our first encounter was during the Climatology course taught within the M.Sc. course in Soil science and Water management. His way of teaching and modesty were what encouraged me to approach him to do my M. Sc. research under his supervision. I thank him for his friendly and encouraging attitude during all the years we have worked together.

I would like also to thank Prof. **J. Wieringa** for volunteering to correct the English manuscript before sending it to the reading committee. I appreciate his encouraging comments on the work.

I would like to thank Dr. **L. Kroon** and his family for their hospitality during the several times they invited me to their house. I appreciate his encouragement during the progress of this work and him pushing me to send articles to international journals.

I would like to thank Prof. **C. Stigter** and his wife for friendly attitude and encouragement.

I would like to thank Dr. **J. H. van Boxel** for his encouragement; either during my study period in the M.Sc. course or during my Ph.D. I would like to thank him especially for allowing me to use the high quality data set collected by him during his Post. Doc. years in the department of Meteorology. This data set was extremely valuable for the parameterization of some processes in that model. His data set gave the proof that I was conceptually right in my approximations. Thank you very much. I certainly hope we can continue working together.

I would like to thank Dr. **W. A. J. van Pul** for allowing me to use his data set, collected during his Ph.D. study, for validating the model results. His data set was very helpful in completing the validation. I had no access to other data set. He saved me the time and the trouble in collecting one. Thank you very much. I also certainly hope we can continue working together.

I would like to thank Dr. **Michael Saraber** for his friendly attitude, encouragement and his interest and appreciation of ancient Egyptian civilization.

I would like to thank **Gerrie van den Brink** for her encouragement and her friendship (Who knows, maybe it works in Sweden). I would like to thank all her colleagues in the secretariaat for their friendship.

I would like to thank the people of the electronic and mechanical workshop, either retired or currently working there, for their friendly and encouraging attitude toward me. I thank **Fritz** and **Ton Antonysen** for all the nice time we had together, discussing different topics of life. I would like to thank **Dick van Welgraven**, **Teun Jansen**, **Willy Hillen** and **Johan Birnie** for their positive and friendly attitudes. I should have put more time in their friendship by learning Dutch. That would have helped communication better. All of them gave me positive encouragement during my stay in the Netherlands.

I would like to thank **Kees van de Dries** for his tolerance and help with computer problems whenever they arise. I remember the day when he had to come to the department at 4.00 AM. on the weekend because I forgot to phone the security service. I am sorry for this and I thank him for allowing me to use his computer for the computationally demanding MATHCAD runs.

I would like to thank my previous and current Ph.D. colleagues for their friendship. **Bert Heusinkveld**, thanks for stressing that there are more things in life (in general) than just modelling. I appreciate your patience in pushing me to do other things. **Cor Jacobs**, thanks for your friendship (how is .ife?). **Joost Nieveen** (thanks for tolerating the mess in our room. Inshaa ALLAH, it goes all right). **Bart van den Hurk**, thank you and your wife for your friendship. **Anna** and **Petra Verhoef**, thank you both for your friendship. I know Anne more than I know Petra but since they are identical twins. I think I know both equally well. **Berenice** and **Arnold Moene**, thanks for all the friendship during our neighbourhood years and working years. **Theo Jetten** (thanks for all the years we were neighbours and for the trust and confidence you had in me after you left to another job). **Job Verkaik** (thanks for your friendship). **Aafka Atzema** (thank you for your friendship).

I would like to thank my colleagues from the Ph.D. discussion group for their support. namely; **Harry Lovenstein**, **Anne Marie van dam**, **Marcos Silveira Bernardes**, **Martina Mayus**, **Koen Kramer**, **Jereon Geroot**, **Bjørn Dirks**, **Johan Warringa** and **Herman Peppleelenbos**. They were a source of help by diversifying my background.

Financial support for a main part of this project has to acknowledged to **WOTRO**, **DGIS** and the **Wageningen Agricultural University**.

I would like to thank **Shell Oil company** for supporting the flight costs to the 22 conference on Agricultural and Forest Meteorology held in Atlanta Jan. 28 - feb 2, 1996.

I would like to thank **Stichting 'Fonds Landbouw Export-Bureau 1916/1918'** for contributing to the costs of printing this book.

I would like to thank the student affairs of the university for their support from the first day till the end. Thanks are due to **Ankie lamberts**, **Marianne Wijkniet** for their friendship . Thanks are also due to Mr. **E. Kamphuis**, mw. **J. Hermans** and mw. **Bea Jansen**.

I would like to thank Dr. **S. Slager** and mr. **C. van Heijst** for their support and encouragement

I would like to thank all my teaches in Egypt and the Netherlands who were the reason behind my advancement and my way of thinking. They were a source of enlightenment for me. From them I would like to mention particularly Prof. Dr. **H. El-Shaaer**, Previous Head Agronomy department, Faculty of Agriculture, Cairo University who deceased last year for his tolerance and patience with me during my M. Sc. in Egypt. Also, I would like to thank Prof. Dr. **E. El-Beisaary** for teaching me during my undergraduate years and for standing up by me in my attempt to come to the Netherlands. I would like to thank Prof. Dr. **I. Habib** for his moral support and teaching me during my undergraduate years. I would like to Thank Prof. Dr. **Dief** for his support and stand up next to me. Thanks are also due to Prof. Dr. **F. Hanna** for his support. I would like also to thank Prof. Dr. **M. F. Kandill** for teaching me during my undergraduate years and for his support as the head of the Soil Science Department. During my final undergraduate year, I did a literature research topic with him about Soil water plant relationships which could be looked upon as a beginning toward my Ph.D. thesis.

I would like to thank Prof. Dr. **N. Bassiouni** for her role as my M.Sc. promoter in Egypt. Maybe, we had our differences but I hope it is all right now.

I would like to thank some Egyptian colleagues who came to the Netherlands during different times of my study for their encouragement, support and hospitality. I mention Dr. **M. Hellal**, Dr. **G. Naser**, Dr. **G. Mansour**, Dr. **A. Metwalli** and **T. Metwalli** for their encouragement and trying to help with some affairs back in Egypt. They were a source of relief and I had by them a good ear for some emotional problems.

I would like to thank **Ahmed Robert Smit** and his wife **Nahla** for their friendship and hospitality. In the same way, I would like to thank **Hussein** and his wife **Elizabeth** and their kids for their friendship.

I would like to thank **family Zandberg** uit Zevenaar for their hospitality during my early years of stay in the Netherlands. May be life took us in different directions, but I surely appreciate you friendship and kindness.

I would like to thank **family Jordens**, the ex-director of the M. Sc. Course in Soil Science and Water management for their hospitality and kindness.

I would like to thank my friend **Laurent Minere** and his wife **Saskia** for their friendship and encouragement

I would like to thank my friend **Ashraaf El-Sawaf** for his friendship and support during all the years we have known each other from high school till now.

I would like to thank **my father** for all the help he could supply during my early years of study and for his good intentions and his prayers for me. There was a misunderstanding but, El-hamedo le ALLAH, it worked out fine. I wish you Inshaa ALLAH extended life and good health.

I would like to thank my deceased cousin, **Kamal Kamel Kilani** for all the support, financially and morally, which he extended to me during my undergraduate and graduate study years in Egypt. He gave me a place to stay for seven years before I moved to The Netherlands. My dear Cousin, Now I can not repay you back your stand up next to me all those years, but I surely hope and pray that ALLAH Al-Mighty will reward you in the Judgement day and will forgive you and me for all our sins.

I would like to extend my thanks for **his wife** and **Amin Kamel Kilani** for their support and encouragement.

I would like to thank my step-father **Mohamed Islam** for his stand up next to my mother, in her support for us during my under graduate years, especially during those last seven years. before I moved to the Netherlands. His standing by us made it possible for my mother to help us in the best way she can.

I would like to apologize to my brother **Tosson** and my sisters **Mariam**, **Shreen** and **Ayat** for missing too much of their childhood and teenage years.

Finally, I would like to express my gratitude and thanks to **my mother**, for all the trouble she took to make things work for us. Above all, she left her homeland (South Africa) and family and came to Egypt to fight an uphill fight to make things better for us. Mother, I think no words are enough to express my thanks.

ABSTRACT

Heat, mass and momentum transfer between the canopy air layer and the layer of air above has a very intermittent nature. This intermittent nature is due to the passage at the canopy top of coherent structures which have a length scale at least as large as the canopy height. The periodic passage of these coherent structures at the canopy top leads to the ejection of the air inside the canopy and the replacement of this air by fresh air from above. It is through this process of ejection and sweep that the coherent structures become responsible for most of the large time average flux.

This study considers the effect of these coherent structures on the modelling and the dynamics of interaction between the plant canopy and the soil with the layer of air above and the effect of these coherent structures on the soil temperature profile. So, three parts are considered: Modelling, mathematical analysis and validation.

In the Modelling part: a discussion of the limitations of the available approaches and a suggestion of an intermittency approach are given.

First, there is a qualitative analysis of the effect of these coherent structures and their role in the momentum, heat and mass transfer on the validity of the Eulerian approaches used to describe canopy flow. We outline the limitations of these approaches and later suggest an intermittency approach to describe heat and mass transfer between the canopy layer and the layer of air above. We describe the used averaging procedure, the resulting correlations, the closure parameterization used and their justification.

Then we give a discussion of the effect of these coherent structures on the Lagrangian model approach qualitatively and then quantitatively and a method to correct for this is suggested.

From this, a mathematical analysis of the effect of coherent structures on the soil temperature profile is done by first analysing the effect of coherent structures on the mean temperature and vapour pressure deficit of the air. It is shown from the equations governing the system's behaviour that there is a non linearity in the canopy system. The effect of this non linearity depends on the ratio between the period between consequent gust intrusions into plant canopy with respect to the air time constants. The effect of this non linearity on the soil temperature profile is shown through its effect on the coefficients of an Eigenfunction expansion of the soil temperature profile. Different scenarios for the effect of different parameters such as the stomatal resistance, the turbulent transport coefficient and the period between gust intrusion are studied and explained.

In the validation part, a comparison of a simulation for 7 days against a data set shows that the model gives very good agreement between the radiative environment and the temperature and vapour pressure of the air. Anyhow there is an interplay between three degrees of freedom. These are represented by the turbulent transport coefficient, the stomatal resistance and the gust intrusion into plant canopy.

Subject headings: micrometeorology / Canopy turbulence / Random walk models / Numerical and Mathematical models; the canopy soil system / Soil heat flux.

TABLE OF CONTENTS

	Page
Foreword	
Abstract	
1. General Introduction	1
1. 1. The importance of theoretical studies for heat and mass exchange in the soil plant atmosphere continuum and the motivation behind such studies.	1
1.1.1. Aim of the proposed study.....	5
1.2. A general description of the interactions of the components of the Canopy-Soil-Atmosphere system and the feedbacks involved.	6
1.2.1 The averaging problem (an elementary discussion).	8
1.3 The organization of this thesis.	12
2. The Quantification of The Energy Sources and Sinks within Plant Canopies.	14
2.1 Introduction.	14
2.2 The interaction between the plants and the radiation field.	17
2.2.1. The short wave radiation	20
2.2.1.1 Direct radiation interception	20
2.2.1.2 The diffuse short wave radiation	21
2.2.2 The long wave radiation.	25
2.3 The energy budget of the leaves*.	26
2.3.1 Definition of the boundary conditions for the solution of leaf energy budget.	28
2. 3. 1. 1 The numerical implementation.	29
2.4 The resistances to heat flux from the leaves to the inter canopy air stream.	33
3. Turbulent Transport within and close above Plant Canopies.	34
3.1 Introduction	34
3.2 A qualitative description of the turbulent transport within plant canopies and its relation to the governing equations.....	34
3.3 Implications of intermittency for Eulerian modelling	38
3.3.1 Counter gradient transport:	51
3.4 The governing equations.	53
3.5 The averaging procedures.	56
3.6. An intermittency approach:	60
3.6.A) The ensemble averaging approach.	60
3.6.1 The closure assumptions:	66

3.6.2 The parameterization of K_M values during the gust and the quiescence period.	67
3.6.B) The time averaging approach.	71
3.6.C) The variances and turbulent flux equations and their time variation	74
3.6.D) The importance of the pressure fluctuation on the dispersion of the correlations	78
3.7. Implications of intermittency for Lagrangian modelling as applied to canopy flow.	80
3.7.1 Introduction.	80
3.7.2 Random walk models as applied to canopy flow.	80
3.7.3 A sequence of events.	83
3.7.3.1 What is the probability of random walk model runs creating such correlations on its own ?	87

**4. The Interactions between the Soil and the Canopy: Modelling* And
Mathematical Analysis**** 90

4.1 The interaction between the plants and the soil and the systems of equations solved to simulate that interaction*:	90
4.2. Intermittency in the canopy soil system**:	93
4.2.a. Definition of the problem.	98
4.2.1 A quantitative treatment: The nonlinearity of the canopy system.	102
4.2.1.1. The effect of intermittency on the canopy air system.	102
4.2.1.2: The effect of the intermittency on the soil temperature profile and the soil heat flux:	111
4. 2.1.2.a. The formulation and the solution of the problem :	111
4. 2.1.2.b. Coupling the soil to the canopy air layer.	116
4.2.1.2.II.1 One layer model.	117
An approximate form for one layer canopy	117
4.2.1.2.III. Several layers model (for the canopy layers)	120
1. The approximate form for n layer canopy	121
2. The more exact form for n layer canopy.	127
The effect on intermittency on the soil heat flux from the more exact form: The MATHCAD® runs.	131
4.2.2 An analysis of source and scalar profile behaviour during a gust cycle:	147
4.2.3 A simulation of different scenarios by the use of the more exact form.	151
4.2.4. Sensitivity analysis on the approximate form: The inverse matrix A^{-1}	172
4.3 The relation between the large eddy length scale, d' and d_{mean} and the correlation between the transport and the source.	173
4.4 Assumptions used in solving the energy budget for soil layers*:	179
4.4.1. The governing equations	181
4.4.2 Defining the energy forcing on the soil surface.	183
4.5 Calculating the liquid water flux through soil layers*:	187

4.5.2 Quantification of the sink term for H ₂ O with different soil layers*	188
4.5.3 The stomatal resistance of water stressed plants*	192
4.6 The coupling between heat and water transport, gas flux and soil resistance to vapour flux under drying conditions.	183
5. The Canopy-Soil-Layer of Air close above Interaction model, CANOPY.	196
5.1 The logical order of the solution.....	196
5.2 The listing of the program.	198
5.2.1 The momentum solution (MOMNTM subroutine).	213
5.2.2 The Tridiagonal Matrix algorithm (THOM Subroutine).	218
5.2.3. The short wave radiation solution (NORMN subroutine).	219
5.2.4. The soil temperature and moisture solution and canopy air state variables solution (CYCLE subroutine).	223
5.2.5. The soil heat conductivity submodel (BERGE subroutine).	224
5.2.6. The soil water submodel solution (HYDRO subroutine).	225
5.2.7. The photosynthesis model (PHOTO subroutine).	230
5.2.8. The coupling coefficients for mass transport (Water and CO ₂). (EQCOEM subroutine).	231
5.2.9. The coupling coefficients for sensible heat transport (EQCOEH subroutine).	234
5.2.10. The sources and sinks within plant canopy (ENERGD subroutine).	237
5.2.11 The plant water potential and plant water uptake submodel (PLANT subroutine).	251
5.2.12 The Stomatal and Boundary layer resistances submodel (RESIS subroutine).	258
5.2.13 The calculation of the fluxes (FLUX subroutine).	261
5.2.14 The root distribution model (ROOTDN subroutine).	264
5.2.15 The initial profiles (INITAI and INIT subroutines).	264
5.2.16 The boundary conditions (RADBOU subroutine).	268
5.3 common files	270
5.4 List of abbreviation for CANOPY	274
6. Measurements & model validation.	284
6.1 Introduction	284
6.2 Validation	286
6.3 The data set used to validate the model	287
6.3.1 Comparison against the measured data.	288
6.3.2 Results	290

6.3.2.1. The first run.	290
6.3.2.2. The second run.	299
Discussion of the second run.	307
Conclusions	310

APPENDIXES:

Appendix 1: (A.1):

Appendix 1.A: Reynolds averaging of Navier Stokes Equations and the assumptions required.	311
---	------------

Appendix 1 b: Random Walk Models and the effect of intermittency in its derivation.	316
---	------------

Appendix 2: (A.2): The dynamic Behaviour of The Canopy Soil System.

2.1 The energy equation of the leaves.	320
2.2 The sensible heat equation of the canopy air layers.	321
2.3 The latent heat equation of canopy air layers.	325
2.4 The vapour pressure deficit of the canopy air layers.	326
2.5 The soil temperature equation solution and the effect of intermittency on the change of the boundary condition for the energy equation at the soil surface.	330
2.6. The n layers canopy model	334
2.6.1 The approximate form	334
2.6.2 The more exact form	337
2.7 The change in the equilibrium temperature of the leaves.	339
2.8 The fluxes from the leaves to the air (the sources).	341
2.9 The mean temperature, vapour pressure and vapour pressure deficit of the air.	342
2.10 The inverse matrix A^{-1}	343
2.11 Discretization of the transport equations.	346

Appendix 3:

List of symbols.	347
-----------------------	-----

Appendix 4:

The input file for the run	358
Summary.	361
Samenvatting.	369
Molakhas (Arabic summary)	377
List of references.	384
Curriculum Vitae.	390

CHAPTER 1

GENERAL INTRODUCTION

In the first part of this chapter, the main aspects for the motivation of undertaking theoretical studies and modelling of the soil plant atmosphere interaction will be discussed and an outline of the aim of this work will be given. In the second part of this chapter, a qualitative description of the exchange processes within the soil plant atmosphere will be given. In the third part, we will give a general description of the hypothesis used for solving heat and mass exchange in this thesis. The last part contains a general description of the organisation of this thesis.

1.1 The importance of theoretical studies for heat and mass exchange in the Soil-Plant-Atmosphere Continuum and the motivation behind such studies

The demands which are laid on the existing ecosystems by human needs, due to population growth and rising expectations, are quite enormous and the effects of satisfying these demands put a large stress on the existing ecosystems. In contrast to older civilizations, the current civilisation has the power to exert its own demands and fulfil them by the expenditure of fossil fuel or other forms of energy. In older civilisations, the input of energy which was exerted by humans on ecosystems was always limited. They managed to survive and live according to what their ecosystems supplied. There was always a co-existence between what the human beings wanted and what the eco-system supplied them with. This co-existence was dictated, sometimes accompanied with harsh facts, by what the eco-systems could supply (Hillel, 1992). But the main difference here is that modern civilisation can exert and fulfil its own short term needs without consideration of what the existing eco-system can sustainably supply. The stress strain relationship of the existing eco-systems is in a much further range than in earlier times. The relationship between humans and their ecosystems will still ultimately be dictated by the ecosystem's ability to meet our demands, but the possibility of transport of goods has reduced the dependence on local eco-systems with the result that a feedback on the management regimes of these eco-systems is delayed even further. The final outcome could even be harsher than in earlier times due to the backlash occurring when a global failure in the existing ecosystems occurs. This difference is very dangerous. We need in this case to answer the inevitable question of how we can maximise the degree of satisfaction of the human expectations without stressing the existing ecosystems to the point of irreversible damage and to answer the question: how far is this point (i.e. defining the stress strain relationships of these eco-systems)? And, if our expectations should be reduced accordingly?!

So far, there is no scientific quantitative solution to this problem in spite of its urgency.

Optimising our management regimes would require an understanding of how our ecosystems respond to these regimes. This understanding cannot be achieved by a trial and error process of trying different management regimes and if it does not work, to try something different. This is because of two reasons:

1) Ecosystems have very large time constants and so their response to shifting them from an

already achieved equilibrium, due to an introduction of a certain management regime, will only show after a considerable period of time (few generations).

2) We can not take the risk of losing the ecosystem in which we live. The state of the new equilibrium which this system achieves after a certain disturbance of its equilibrium must be predicted, since this new equilibrium state should still be life sustaining. This is a question of survival.

As a consequence of this, we see that in both the more developed (developed) and the less developed (or underdeveloped) countries, there is a need to have scientifically based means of managing our own ecosystems in an optimal way. For the time being, we have no means of predicting all the short and long term ecosystems responses to certain management regimes, so we can appreciate the consequences of our deeds or the disturbances which we introduce to these ecosystems. We suffer then from a trial and error approach in managing them. We exert our own demands on the existing ecosystems and expect the tolerance levels of these systems to be quite high. By the time we find out the consequences of our deeds from these trial and error approaches, it could be too late to do anything about it.

From the previous paragraphs, we see that our options are very limited. Since experimenting with an ecosystem can be very dangerous and the time delay in getting a response could be very long, the trial and error approach would then be useless in optimising our management regimes. Trying instead to understand the web of physical, chemical and biological processes which control the response of such a complicated system to a certain set of environmental conditions (in which the management regime is expressed) and implementing this understanding in models is the only option we have to predict and manage our ecosystems. But the problem of validating these models remains: how can we validate a model whose results can be checked only by a comparison with the real system that needs a large period of time and that is unique? The only possible way then is trying to understand the underlying physical processes and the interactions between the different components of this large system and putting this understanding into models or submodels describing the ecosystem components. We have to do our best in refining these sub models and validating them separately and then coupling them together in the right way. In the end, we hope that everything goes right and the built-up model simulates closely enough the real system. Another problem which shows up here, is the time scale of the different submodels and the time scale of the big model and how to extrapolate from the submodel level describing submodel processes to the whole eco-system level. This lumping of submodel processes to a higher level requires the correct inclusion of the effect of the sum of correlations between the lumped submodel processes, within the time or the spatial scale of the large model, on the solution of the higher level model.

The selection of which processes and what level of detail is required to achieve validity of models at higher levels requires an insight into which processes in the lower level are decisive in determining the behaviour of the model upper level. All the above underlined steps require implementing some assumptions by the modeller which reflect his biased view of how he thinks reality works. This means, which processes he thinks are important and which are not, how the submodels should be coupled or what kind of correlations from the lower level to the higher one should be included and how they should be parameterized. Continual validation of these assumptions by comparing against measurements or data sets is

a necessity. The scarcity or complete absence of such data sets with the increase in the time scale of the simulated processes is a problem which we have. The correct way then of integrating from lower level to a higher level is not an easy problem to solve. This will be discussed in chapter 6. But an essential rule is that we should start with submodels which are valid, i. e. all the physical processes which are described in detail in these submodels should be modelled correctly.

Due to differences in the time resolution (time steps) of the different scales of models, these valid submodels can later be used to obtain valid closure parameterization for higher level models. In these submodels, all the parameterizations included in it, either obtained from a lower or a higher level models, should also be valid. This chain of parameterizations, which represents a method of including information from a wide variety of time scales, without the need to run the equivalent submodels coupled, should be correct. In the spatial scales, the integration between different levels should allow for interaction between heterogeneous subdomains within the integrated domain.

The problem lies as shown from previous paragraphs in how to understand the limiting physical processes which govern the response of a very dynamical system (the eco-system) to a certain set of environmental conditions. One point worth mentioning here, is that averting natural cyclic climatic changes is not the issue, but the point is that these changes or catastrophes should not be human induced due to mis-management.

To give an example of this, Egypt had an eco-system for a period of ten thousand years. This eco-system was represented by the Nile flooding its plain once a year. The old Egyptians built dikes to keep the water of the flood in big basins. Water would then infiltrate into the soil and saturate the subsoil and in the process leach the amounts of salt accumulated during the previous year. This amount of water stored within the profile would be used to grow one crop a year. Then a change in the natural hydrological cycle of that system was introduced by building a dam. This led to the possibilities of a more frequent irrigation regime and securing water supply during low flood years. This change here expresses the demands exerted by the Egyptian people on their eco-system and their way to fulfil this demand. The question now comes to the response of this ecosystem to this demand and the way of exerting it. I am not here questioning the need to build such a dam. In fact, this dam helped to save Egypt from drought in the last few years. This is here an example representing the sometimes justified expectation of a certain people and their way of exerting this demand from their eco-system. But one does not want to replace a harsh reality with a delayed much harsher one. The answer to the question if something like this will exceed the limits of tolerance of this ecosystem remains to be seen. I am stating here that we neither were nor are aware of the effect which such changes of the natural hydrological cycle have on our ecosystem. Now we have obtained a high ground water table which leads to salinization and to a loss of the land which we had for millennia and which now we are losing due to mismanagement and failure to cope with the results of changes we have introduced to the hydrological cycle. This ecosystem has not yet achieved its new state of equilibrium. It could be argued that this could have been foreseen. In fact, some effects have been overseen or predicted already in the preliminary studies preceding the project (Said 1993, Hemdan 1961), but no one could then have told, nor can now tell, how the final equilibrium will be. A complete study on the dynamical behaviour of this ecosystem and its tolerance limits is not available. A compromise has always to be

found between the expectation of a certain people and the disturbances they introduce to their ecosystems. This compromise has to lie within the tolerance limits of their ecosystems. It is my concern as an Egyptian (and I think of all the people there) that the new state of equilibrium should be life sustaining.

To give an example from the more developed or developed countries, the management of the river Rhine eco-system in Europe has not been very good either. The earlier policy of dumping high amounts of micropollutants into the river, which were adsorbed to the suspended solids and later sedimented, led to the formation of highly polluted beds. National inventories have shown that in Dutch inland waters, 34% of the beds exceed the test value and 27% exceed the warning value (Cuwo, 1990). Dredged spoils between test and warning value must be stored under Isolate, Store and Monitor (ISM) conditions. If the warning value is exceeded, then research into the necessity for cleaning and storage under strict ISM conditions is urgent because of risks to public health and environment. During some 20 years of environmental incubation, for some higher chlorinated benzines, polychlorinated biphenols, dioxins and furans, significant losses in the sediment core layers were observed. The concentration of other few lower chlorinated dioxins and furans and two biphenyls in core layers that was deposited around 1970 showed no significant differences (Beurskens *et al*, 1994). This indicated no disappearance has occurred within the studied period. Downward transport of some of these pollutants is a very limited possibility because of their hydrophobic nature. Even with the significant improvement in water quality, the polluted sediment problem is a serious one. This proves that, due to the memory of the system, a bad management regime will still leave a scar for a long time to come and that there is a need for an introduction of rehabilitation measures and new manufacturing processes which are environmental friendly. The situation has improved a lot during the eighties. In the seventies, laboratory species suffered acute toxicity after exposure to the Rhine water (Sloof, 1983). Nowadays, water has to have a 25-fold concentration increase to induce mortality in water fleas, but less than 5% of the toxicity can be explained by identified compounds (Hendricks 1994 and Hendricks *et al* , 1994).

From these two given examples, it is shown that both the developed and under-developed world suffer from problems of ecosystem mis-management. This problem stems *most probably* from a lack of understanding and appreciation of how the ecosystem works and how it should be managed. I say *most probably* since one hopes that short sighted commercial interests to meet the rising expectations of human beings and to introduce an unsustainable way of living is not, or will not be, the main motivation behind the destruction of our ecosystems. For an appreciation of the extent of the damage to our ecosystems, see e.g. Seager *et al*. (1995).

Quantifiable sustainable ecosystem management requires all the efforts and co-operation between all the people who can do something about it. It also becomes clear that the difference between what we can call a useful science of immediate benefit to an underdeveloped country and a more theoretical science, which may seem of no immediate use to a third world country or an underdeveloped country, is very vague. From my point of view and from the previous argument, I think that there is no such difference in the aspect of ecosystem management.

I do not deny the fact that there are some problems about which something can and

should be done now, such as the starvation in Africa. We cannot wait till we find all the answers that we need to know to manage our ecosystem. Those people should be fed right away. But looking to short term problems should not make us forget the point, that these countries in the end should be able to develop their own resources and manage their own ecosystems in such a way, that they become self-dependent as much as their ecosystem can sustainably allow. That should not be done by duplication or the adaptation of production systems, which could lead to environmental degradation, but by self sustaining systems which are socially and culturally acceptable. In more developed countries, attention should be given to sustainable management of our ecosystems, rehabilitation of damaged ones and the development of environmental friendly manufacturing processes.

In a striven-for wise ecosystem management, ecosystem managers should be able to predict correctly the response of the ecosystem to a certain set of management regimes. From these, we should be able to choose the ones which are self sustaining in the sense of achieving enough production or maximising self-sufficiency or human expectations of the population and keeping the environment intact. From these technically available options, we could choose, as a society what is socially and culturally acceptable. But first of all, a correct prediction of the ecosystem response to a certain management regime is needed because it is on this prediction, that we will base our management decision.

How should we attack the problem of managing such an ecosystem? I believe that understanding how such an ecosystem really works in its sub-components, and trying to integrate all this understanding into how the whole system responds to different management regimes, is the best way to manage such a system. The point is that our understanding should be clear because we cannot experiment with ecosystems and check the validity of a large model describing their behaviour. So, we try to refine our understanding of the governing processes in the subsystems.

One of these subsystems affecting the dynamical behaviour of the whole ecosystem is the Soil-Vegetation-Layer of air close above system. This subsystem is the region where the interaction between the lithosphere, biosphere, hydrosphere and atmosphere takes place. This interaction and its modelling, on different time scales is what controls the ecosystem behaviour. The study and modelling of the dynamical behaviour of this subsystem, on a time scale of second to days, is what constitutes the main theme of this Ph.D. study. The dynamic behaviour of this subsystem is represented by the radiative and non-radiative (heat and water vapour) energy and mass (CO₂) transfer between the different components of this subsystem and how it is controlled.

I feel fortunate to have the chance to work in this area of research. The proposed study is to contribute theoretically, as well as experimentally, to the understanding of these complicated processes.

1. 1. 1 Aim of the proposed study

The aim of the proposed research is to develop a dynamic multi-layered model for describing radiative and non-radiative energy and mass exchange within and between the soil, its vegetated layer (aggregates of plants with a spatial arrangement) and the layer of air close above it. We would like to have a valid model, describing the physical interaction between the

plants, the soil and its environment. We need to refine our understanding of the effect, which the intermittency of the turbulent transport within and close above plant canopies and the resulting coupling of the vegetation layer with the layer above it, could have on the thermal and moisture regimes of soils. This intermittency is due to the existence of large coherent structures at the layer of air above the canopy and their interaction with the canopy layer. The time scale of these coherent structures lies in the range of 40-1000 s. We would like to know if these small time scale processes have a net residual effect on the integrated behaviour of the system, represented by the integration of the soil heat flux, thus leading to a different soil temperature profile through affecting the energy partition at the soil surface. The question here is equivalent to: What level of detail is needed to model the canopy soil system, and do we lose some information by large-time interval averaging (10-20 minutes averaging) ?

This appreciation or understanding could be achieved by:

1) Formulating an intermittent turbulent transport model which considers the effect of coherent eddy structures on heat and mass transport within plant canopies and the resulting coupling of the plant canopy-soil layer to the layer of atmosphere above it. In order to achieve this, the appropriate set of exchange equations for momentum, heat and mass (H_2O and CO_2) have to be formulated and solved, numerically, under a certain set of boundary conditions. Considerations should be given to the feedbacks involved.

and/or

2) In addition to describing the governing equations and the numerical implementation of these equations in a completely numerical model, a mathematical analysis of the governing equations, describing heat and mass transfer between the canopy layer and layer of air above, is used to analyse the behaviour of the system and the effect of turbulent transport intermittency on that behaviour. This analysis gives a justification to the numerical results of the model, since a numerical result is not a proof. It is difficult to justify without an analytical evidence, since, in spite of being highly improbable, it still could be an artifact.

A qualitative analysis of an equivalent system of equations (the averaged Navier Stokes) will also show some of the limitations of the available approaches used to describe heat and mass transfer within and close above plant canopies in which no or an implicit account of intermittency is considered.

1.2 A general description of the interactions of the components of the canopy-soil-atmosphere system and the feedbacks involved

Within the canopy layer, the plants act as interceptors of the radiant energy in the short and long wave band and convert this energy into other forms of energy: non-radiative (mainly sensible and latent heat, and to a much less degree: chemical) or into radiant energy in a different wave length band.

The partition of this available energy (absorbed energy in the short and long wave bands) is dependent on the resistances to the fluxes from the plant organs to the surrounding environment, and on the boundary conditions (i.e. the temperature and the vapour pressure) in close proximity to the leaves.

The non-radiative energy exchange between the plants and the inter-canopy air stream

determines the amounts of non-radiative energy exchange (sensible and latent) which the turbulent transport mechanisms, between the canopy air layers (small scale transport) and between these layers and the layer of air above the canopy (large scale transport), have to evacuate.

The exchange processes of momentum, heat and mass between the air layers in close proximity to the plants and the air stream above the canopy have a very stochastic and intermittent character. The plants interact with the air flow as obstacles, converting mean kinetic energy into turbulent kinetic energy and as sources or sinks of heat and mass.

Within the soil layer, the plants modify and alter the soil climate through affecting the energy and mass input into the soil beneath it through the effect of shading and interception. It does also alter the thermal characteristics of the soil layers through the roots acting as sinks with varying strength for H₂O in different layers of the soil, altering in the process the thermal and moisture characteristics of the soil. The plants modify the turbulent transport between the canopy air layers and between these air layers and the layers of air above it, thus affecting heat and mass exchange between the soil and the air above it. The plants exudate supply the heterotrophic microbial population with sources of energy (organic carbon) and so alter in the process the physical and the chemical environment of the plant roots.

The soil in turn affects plants through its moisture, temperature and salt regimes. The moisture regime within the soil determines the availability of moisture for plants. This in turn affects the plant partition of the available energy between the different pathways through its effect on the stomatal resistance. This in turn affects the microclimate within the plant canopy. The soil also affects the root distribution through the soil mechanical and chemical properties (e.g. root penetration resistance, aeration and pH). All of these processes affect plant growth and development.

Within the atmosphere layer, the surface properties affect the development and structure of turbulence in the atmosphere above it, due to the interaction of the soil-vegetation layer with the radiation field and the subsequent forcing from the ground on the atmosphere above. This structure of turbulence will affect the canopy soil system through its intermittency. I think that the development and structure of turbulence in the atmosphere above responds to a large scale representation of the surface below, so a detailed model of the canopy climate is not needed to describe the forcing from the ground or the vegetation layer on the atmosphere. A big leaf model, with a fitted resistance to account for the atmosphere effect on the canopy, could suffice. The effect of the atmospheric surface layer on canopy microclimate has to be accounted for, since the large scale eddy structure will determine the intermittency of the gust penetration into the canopy. That fitted resistance will be a function of the canopy state. That is not only the stomatal resistance. It will be shown in chapter 4.1 that the canopy responds in a nonlinear way to the formulation of turbulent transport resistance.

Within the plants, the microclimate in close proximity determines the rate of physiological processes (e.g. CO₂ assimilation) and so the amount of reserves used for shoot and root growth. The plants respond much more to the average meteorological conditions than to the instantaneous ones, due to the response time of physiological processes being larger than the actual time of gust penetration, so a time-averaged profile can be used to model the potential production process. A detailed description then of the micrometeorology stochastically is not needed, but the effects of this stochasticity should be included in the time

mean. The effect of production processes within the plants, as affected by weather, on the soil shows through the partition of these assimilates between shoot and root growth (source-sink relationships), which controls within a larger time scale the feed back from plants on the soil. A functional description is not yet possible, so measured values for that partition are usually used (e.g. Van Heemst, 1988). The source-sink relationships are controlled genetically and environmentally. For example, the actual growth of the roots happens where the soil mechanical resistance is below a certain minimum (a function of the soil structure, porosity and moisture content: Misra *et al* (1988), Dexter (1987), Hillel and Toplaz (1976) , Bar-Yosef and Lambert (1981)) and where the aeration is good enough (also dependent on moisture content and pore size distribution, Blackwell and Wells, 1983). This affects the root distribution within different layers. The active root distribution, and its conductance, control the regions of water uptake by plant roots, and so the soil moisture regime.

As we can see, the exchange processes between the components of the Soil-Plant Canopy-Atmosphere Continuum are very complex and there are a lot of feedbacks which make a suggested numerical procedure to model the physical behaviour of the system quite complex and lengthy. One main point here, is that time scale differences exist between different processes. Within one time scale, this requires the integration or inclusion of processes on a lower level in the correct way and the delivery of a good result (which simulates reality well) to be integrated on its effect to the higher and lower level. That brings us to the averaging problem as discussed here and in chapter 3 and 4.

1.2.1 The averaging problem (an elementary discussion)

In the soil layer, averaging is done by assuming a **REV (Representative Elementary Volume)** approach, in which this volume is larger than the discontinuities of the pore soil system, while it is smaller than the scale over which there are gradients in the system. This justifies the gradient theory, since transport processes work on a smaller scale than these gradients.

In the above soil part, this assumption is not valid, since most of the transport happens in a very short interval of time by large scale coherent structures (gusts), and the scale over which this gust works is larger than the distance over which gradients develop.

For the above ground parts, in existing models, we try to model (simplify) this exchange process by averaging in time and place. So, we eliminate the time variation of this intermittent process by assuming it averaged in time. This averaging procedure leads to the closure problem and also to the fact that we try to represent a very intermittent process in which most of the transport happens in a small fraction of the averaging time by a continuous term in the turbulent transport equations. It has been shown by several workers (e.g. Finnigan and Raupach 1987) that the largest scales of motions (events or coherent structures) are the most effective ones in the turbulent transport between the canopy air layers and the air stream above.

Does the large-time interval averaging, in which we lose the details of the process, represent a loss of information which could affect the large-time response of the simulated system? We suggest, from the nonlinearity of the canopy turbulent transport equations, that a large-time interval averaged value for a term in these governing equations is not the same as a

fluctuating in time one with the same mean. So, we think it is important to make a division between the different time scales (and so implicitly the different length scales of motion and their contribution to the total transport).

A compromise to be made is to maintain the minimum degree of resolution without losing details of the flow which may affect the long term response of the system.

I think that there are three approaches to visualise the plants and their role as energy interceptors, converters and dischargers in the soil atmosphere system.

The first approach is taking the plants as individuals with a given spatial arrangement, which are interacting with the airflow above with all its intermittency. So the problem here is treated in all its time intermittency and spatial heterogeneity (after averaging of course for small scale turbulence). This approach is probably not needed. In the lower limit (no averaging for small scale turbulence), this approach goes to **Direct Numerical Simulation (DNS)** of the Navier-Stokes equations. The spatial and time resolution which is required for this approach would exceed by far the capabilities of the available computers.

The second approach is applying some kind of averaging spatially, i.e. treating the plants as a layer in which the variation in the horizontal directions are smoothed out. This spatial averaging is done to eliminate the horizontal heterogeneity of the canopy elements (a uniform dense crop with no gaps) or to treat the canopy as composed of two or more uniform subdomains (e.g. an orchard; row crop or intercropping). In all of these, averaging in time is within a small time scale. Thus in every time step, a term for the large scale transport will either be turned on or off depending on the probability of a gust penetrating into the canopy at the considered time step. In this case, the transport will be separated into one or more length scales, which will then have two different frequencies.

The third approach, by averaging in place (space scale larger than the small scale of heterogeneity of the plant canopy and the largest scale of transport) or in time (time interval larger than the largest time scale contributing to momentum and scalar transport and a space scale larger than the small scale heterogeneity) and that would lead to a different kind of closure problem, in which we lose account of the different scales of motion contributing to the transport and also of the intermittency of the problem. This is the common way of averaging which is used in the Eulerian approach models. We get terms in the turbulent transport equation which are assumed to be active all the time. These terms and their parameterization are obtained from large-time interval averaging. The values obtained are not possible to use for time steps smaller than the time averaging. So we lose detail of the intermittency of the problem which is, as we shall see, important to the large term response of the system. At the same time, these terms can not be used for modelling small scale transport within time steps smaller than the large scale transport, since they include in them some of the contribution of the large scale transport.

Li *et al.* (1985) tried to describe the transport in two time-averaged components; local and nonlocal transport in a first order closure model. This approach is also not successful since it needs a parameterization for the non-local term in an averaged in time process. These terms are then obtained by optimisation. A curve fitting method is just replaced by another curve fitting method.

In the present thesis, we follow the second approach. We will show that intermittency considerations make a difference in the solution depending on the time constants of the

system, and that the second approach is the minimum required degree of detail. I think that we would agree when we say that small scale turbulence has a small time scale and small effect in transporting heat and mass between the canopy air space and the layer above and it would require a large time to achieve an equilibrium profile. Large scale transport, on the other hand, is efficient in achieving most of the transport between canopy layers and the layers of air above with a larger time scale, and it requires much less time to achieve equilibrium. We will assume that a separation in the scales of transport exists. The averaging procedure of the instantaneous turbulent transport equations remains to yield averaged equations, but the interval of integration will be modified to account for the contribution of different scales of motion to the total transport. So in the equations a term, which represents the effect of the gust or large scale of motion has to be introduced. This term has to be turned on or off depending on the probability of a gust penetrating into the plant canopy during a certain time step. But the question remains how to determine this probability distribution.

To get an answer to which probability distribution one should use to simulate the gust penetration into plant canopies, one can use two approaches:

The first is observations made by other workers e.g. Shaw and McCartney (1985); Shaw, Ward and Aylor (1979); who tried to fit measured time series of wind velocities inside plant canopies to some statistical distributions. But even if they fit, the question of applying these distributions to general situations (universality) arises, since these wind regimes are functions of the interaction of the canopy layer with the airflow above.

The second approach is somewhat functional: trying to describe the interaction between the canopy layer and the air flow above it. There is an attempt by Raupach *et al* (1989) to define the coherent eddy structure within plant canopies in the case of thermally near-neutral canopies. In their paper, they assumed that the dynamic stability or the shear is the most important in generating eddies. This assumption ignores the importance of thermal stability on eddy generation.

In all above mentioned averaging cases, the following steps should be followed:

1) Quantification of the radiant energy interception within the plant canopy and at the soil surface (this process is the source of all energy transformation within the ecological system). Averaging in time is done with a time scale small enough to follow the diurnal radiation changes, if we neglect the effect of leaf fluttering and the wavy movement of the canopy elements. This means that there are no differences between approach 2 and 3. However, there are differences between whether or not we average in space, since in the latter we treat the plants as a turbid homogeneous medium.

2) The partition of this intercepted energy between different pathways (radiative and non-radiative energy exchanges). That partition determines the amount of source or sink terms for the non-radiative energy exchanges which has to be discharged or satisfied through the turbulent exchange processes between the canopy air layers and the air stream above.

Concerning *these two steps*, theory already exists which describes these two steps, and there are several approaches to calculate the source strengths.

3) Developing and solving a valid set of equations to describe the canopy turbulent transport processes. Here, the averaging in time and place will determine the complexity of the solution. We will do averaging in place and time according to the second approach, since we would like to study the intermittency of the process and show its effect on the simulated mean concentration and sources profiles. We would like to take account of the different length scales (here two categories) and so different time scales and their contribution to the total transport.

So during gust penetration, a term of large scale transport will be turned on, while in the interval between gusts (the quiescence periods), the turbulent transport equations will be solved using different closure assumptions for the small scale turbulence. The effect of using different approaches on the form of turbulent transport equations and the final solution will be studied. A parameterization for the local transport during the quiescence period will be used. This is done according to a statistical distribution of the values of the vertical velocity variance within time. A modification for a random walk model to account for intermittency will be shown.

In solving the resultant nonsteady state canopy turbulent transport equations, a nonsteady solution for the leaves will be used.

4) Quantification of the interaction between the soil and the canopy above it. That is done through two processes, the effect of the vegetative part of the canopy on the interception of the short wave coming in, and in incrementing the downward long wave radiation since the plants are warmer than the sky so the plants increase the long wave coming in. The plants shield the soil from the colder sky. The second process is through the roots action. This is done through the use of a root distribution as a function of depth. The sink term in the soil volume is determined using the solution of the equations for water transport to the leaves from the soil.

5) Quantification of the energy balance of the different soil layers and solving the non-steady energy balance equation for the different soil layers till the depth where $dT/dt = 0$, taking account of the sink distribution. Partition between latent and sensible heat fluxes does not occur only at the surface, but there is a regression of the evaporation front. The model considers coupled heat and mass transport through the soil.

The effect of all these processes will be integrated through time and the long term effect on soil heat storage will be checked.

This model should be able to describe the interactions between a vegetated soil layer with the atmosphere in semi-arid regions, where the thermal behaviour of the soil is varying strongly with time due to the variation of moisture content of the soil between subsequent water applications, and where it to assume a soil profile which is always within the early stages of drying is not valid anymore.

So in short, in the study, several points will be discussed:

1) The effect of intermittency on the existing available approaches (Eulerian as well as Lagrangian) used for describing heat and mass transport within the Soil-Plant Canopy-Layer of air close above system (section 3.3, section 3.7 and section 4.3).

2) The introduction of an intermittency approach to describe heat and mass transport within this layer, the parameterization or the used closure assumptions and their justification (Section 3.6).

3) The development of a complete numerical canopy soil model, using in its turbulent part an intermittency approach and including the resulting feedbacks (chapters 2, 4 and 5).

4) Analysis of the nonlinearity of the system and also when intermittency does make a difference in the solution for the canopy air layers (section 4.2.1.1).

5) The effect of this non-linearity on the soil heat flux and the soil temperature profile (section 4.2.1.2).

6) Analysing the effect of the different forms of the turbulent transport equations (continuous versus intermittent due to the use of different averaging schemes) on the soil heat flux, the air temperature and vapour pressure profiles and the sources (MATHCAD[®] runs and section 4.2.2).

7) Validation of such a model (Chapter 6).

1.3 The organization of this thesis

This thesis consists of three parts. Two of them are intimately related: a modelling part indicated by (*) superscript and an analysis part indicated by (**) superscript. The third part is a validation part (chapter 6). The modelling part is just describing how the modelling and the consideration of feedbacks between different systems of equations was done without further analysis of the equations behaviour (e.g. chapter 2 or section 4.1.2). In the mathematical analysis part, we give an analysis (either quantitatively or analytically) of the systems of equation describing transport and describe its behaviour and the consequences of this behaviour on the validity of certain assumptions or on the nonlinearity of the system. (e.g. section 3.3 and section 4.2, respectively).

We would like to draw the attention of the reader to the following: In this thesis, especially, the analysis part, we start with a global view of the problem, discard certain processes which we think insignificant while going through it, concentrate on some other processes, derive some conclusion from the different pieces of the problem and then use these several conclusion from here and there to come to a major conclusion concerning the system and the approaches used to describe it.

In some parts of the text; we use a different font (letter type) as a way of explaining things in a more extensive way, we would suggest to skip it during a first reading. That would not disturb the continuity of the story.

In chapter 2, we discuss the modelling of the energy sources and sinks within plant canopies.

In chapter 3, we discuss in a qualitative way the effect of intermittency on the turbulent

transport of heat, momentum and the validity of available approaches, whether Eulerian or Lagrangian. We also discuss a suggested intermittent approach and the closure assumptions used and their justification. The effect of intermittency is considered through its effect on the turbulent transport correlations.

In chapter 4, we analyse the effect of intermittency on the sources and sinks within plant canopies and the soil temperature profile. We show a nonlinearity in the system and the effect of this nonlinearity on the system behaviour (the canopy and the soil) in a semi-analytical way. We also discuss some modelling aspects concerning soil heat, moisture fluxes. We also discuss the modelling of plant water uptake and stomatal resistance. The effect of intermittency here is discussed through its effect on the sources and sinks or on the correlations between the fluxes and the sources. We will also discuss the sensitivity of an approximate model to certain parameters.

In chapter 5, we include a description of the numerical model with a reduced listing.

In chapter 6, we discuss the model validity.

CHAPTER 2

THE QUANTIFICATION OF ENERGY SOURCES AND SINKS WITHIN PLANT CANOPIES*

In this chapter, we will explain how the energy sources and sinks within the plant canopy have been quantified. In the first part, an introduction, a qualitative description of the interactions between the plants and the radiation field in which they exist will be given. In the second part, we will treat the equations which are used to describe this interaction. In the third part, we will treat the partition of the total absorbed energy between different pathways. In the fourth part, we will mention the quantification of the resistances for heat and mass and CO₂ sinks or sources within plant canopies.

2.1 Introduction

The mere existence of the plants with their three dimensional configuration, i.e. the stem carrying the branches with the leaves appended to it, leads to the plants interacting with the surrounding radiation field. This interaction is represented by the leaves or the plant parts intercepting radiant energy and then reflecting, absorbing or transmitting this intercepted energy. The partition of the intercepted energy between reflection, absorption and transmission depends mostly on the spectral properties of the plant pigments and water.

The amount of absorbed radiant energy in the different regions of the spectrum determines the radiative energy load which the plants have to dissipate or disperse. This dissipation takes place through the radiative and non-radiative energy exchange between the plants and the surrounding medium. The radiative energy exchange is represented by the long wave emission of the leaves. The non-radiative energy exchange is represented by the sensible and latent heat which is delivered by the leaves to the inter canopy air stream. The conditions under which the absorbed radiation load equals the radiative and non-radiative energy exchange between the leaves and the surrounding media determine the plant organ surface temperature. Into this balance also goes the contribution of the change of heat storage within plant tissues.

The temperature and vapour pressure of the air in conjunction with the radiation load on plant surfaces, given certain surface resistances, determine the temperature of the plant surfaces and constitute the environmental conditions, which should lie within the domain of viability of the cytoplasm of the living tissues. We can call the range of these environmental conditions, under which this condition can be achieved, the domain of existence of plants. Within these domains of existence, which are species dependent, there will be subranges within that domain in which conditions for plant productivity are optimised. By plant productivity, we could mean the net assimilation rate for short time intervals or integrated over a longer period, the total plant dry matter production or another certain criteria. In this way, we have expressed a one direction effect of the environmental conditions on the plants.

The environmental conditions are not only the vapour pressure, temperature of the air and the radiation load. There are other factors like the moisture and salt regimes of the soil. In this thesis, we will assume that the effect of the other environmental conditions is shown through

the effect of these other environmental conditions on the resistance of the plant surfaces to different forms of energy exchanges (i.e. through the stomatal resistance). This will affect the surface temperature. We consider that the temperature of the surface, in combination with the short wave radiation load, internal CO₂ concentration, tissue water potential and ionic status of the plant tissue as the window through which the inner plant processes see and respond to the physical and chemical (abiotic) environment. The effect of nutrient status within the soil on the plant inner processes is not considered here. We will treat the quantification of the effect of the other environmental conditions in detail in chapter 4.

Now, to get our qualitative picture of the whole system clear, let us come to the question if the relation between the environmental conditions, expressed as the temperature, vapour pressure of the air and the radiation load on the plant, is a one way direction relationship?. i.e. do they impose a certain load or stress on the plant with no feedback from the plant on them?.

Considering the net result of the feedback between the radiation load and the plant surface temperature, this feedback is small and is only due to the interaction between the plant surface temperature and the long wave radiation field. There is no feedback between the plant surface and the short wave radiation. So the solution of the short wave radiation is independent of our final solution of the vapour pressure and temperature of the air (i.e. there is no feedback).

On the other hand, the temperature and vapour pressure of the air are not passive to the inputs of non-radiative energy from the plant organs into them. The canopy air layers have an ability to exchange heat, water vapour and other constituents due to turbulent motions which mix the air between canopy air layers. These turbulent motions are either externally or internally induced. The internal induction of turbulent motions could be due to the dynamic effects of the canopy elements. These dynamic effects are represented by the leaves working as drag media extracting momentum from the flow field, as converters of mean kinetic energy into turbulent kinetic energy, and mostly as obstacles to the intrusion of air flow from above the canopy. This last effect leads to the appearance of high positive pressure-velocity correlation inside the canopy. These high positive velocity-pressure correlations lead to the coupling of the inner canopy flow to the flow above. We will come to this point in chapter 3. The thermal induction is due to the effect of density stratification on the degree of mixing (stability effects).

If the energy load by the leaves on the air layers (i.e. the amounts of delivered sensible and latent heat from the leaves into them) is not evacuated to the layer of atmosphere above the canopy, a build-up (whether positive or negative) of vapour pressure and temperature of the air would result. This build-up would then lead to an enhancement or inhibition of the exchange of these delivered amounts between the canopy air layers, or between these air layers and the layer of atmosphere above. This exchange would then lead to relaxation of the energy load. Somewhere, an equilibrium is achieved depending on the time constants of the turbulent transport mechanisms and the loading terms. The situation, concerning the air layers within the canopy, is then represented by an equilibrium between two forces;

The first is a forcing term, which is represented by the non-radiative energy exchange from the leaves to the inter-canopy air stream.

The second is the non-radiative energy (turbulent) exchange between the canopy air layers, which tends to relax the first force. The degree of build-up of vapour pressure and air

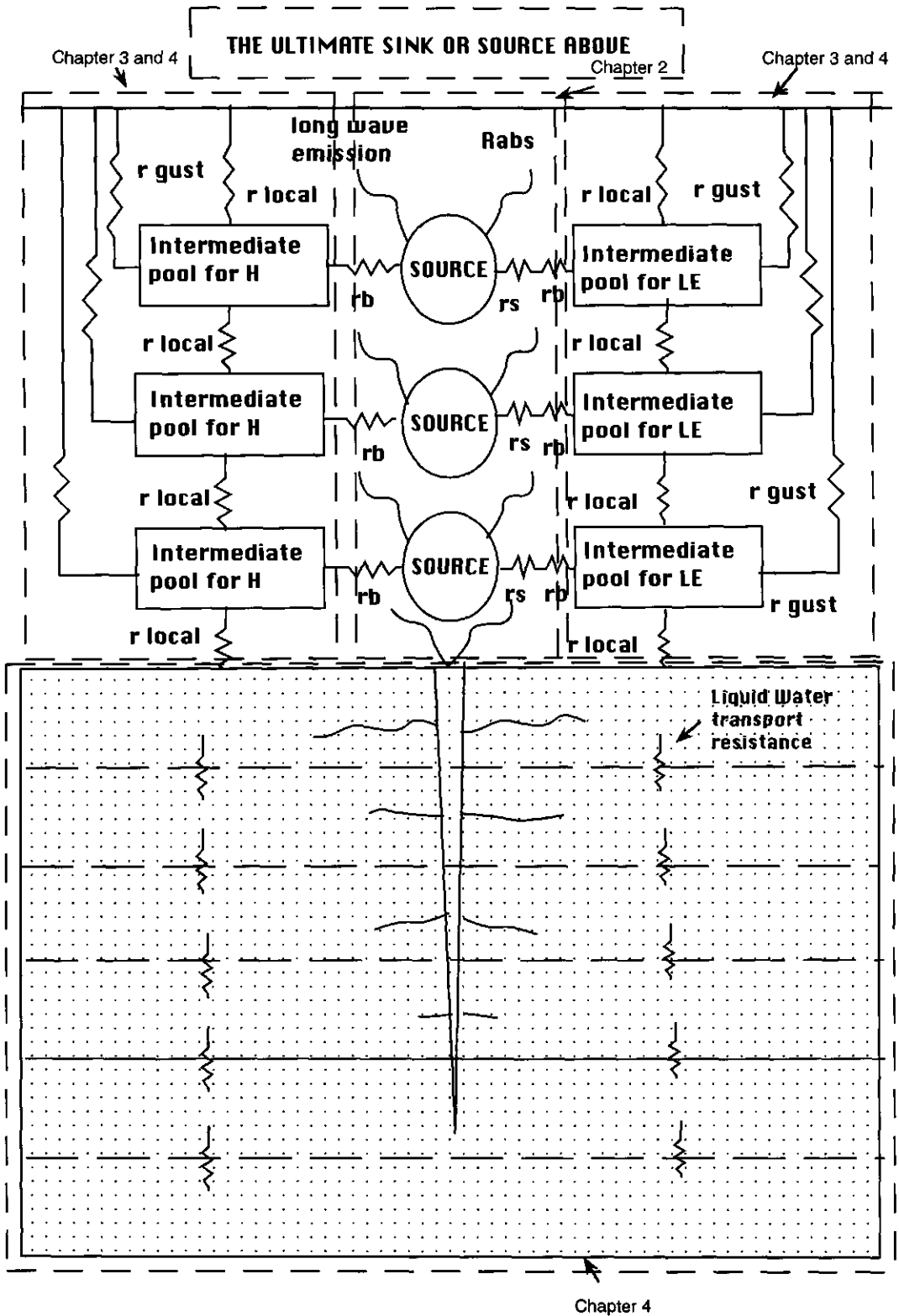


Fig. 2.1 : The areas covered within this thesis in its different chapters

temperature, which is required to maintain equilibrium between these two effects, determines the temperature and vapour pressure of the air. This in turn will control the partition of the absorbed energy between different pathways, i.e. radiative and non-radiative, and so the amounts of non-radiative energy which is delivered from the leaves into the canopy air layers.

From the above description, we see that the components of the canopy air system are interrelated like a system of resistances or *springs*, and the state of that system will depend on the forcing terms imposed on its components and the different relaxation terms relaxing these forcing terms. For canopy air layers, these different relaxation terms are represented by turbulent transport mechanisms between canopy air layers which tend to relax the energy sources with the canopy. For the leaves, the forcing term is the radiation loading, while the relaxing term is the nonradiative energy delivered from the leaves to the air. We can include the role of the soil in this system through its effect on modifying the resistances of the plant surfaces to energy exchanges in one direction. In the other direction, the plants affect the non-radiative energy input to the soil surface, the boundary conditions for the energy budget solution at the soil surface, and the thermal and moisture characteristics of the soil layers.

Figure 2.1 gives us an overview of the interactions between the plants and its environment. The circles in the figure represent the leaves within different canopy layers and their role as interceptors and converters of radiant energy into other forms of energy (i.e. non-radiative energy or radiant energy in another waveband). The partition depends on the vapour pressure and temperature of the air and the resistances to the different forms of fluxes. In this chapter, we will cover these processes in the above-ground part of this figure.

In the next part of this chapter, we will introduce the equations used to quantify the forcing on the canopy air system due to the leaves. We will assume that the temperature and vapour pressure of the air and the surface resistance are already known. This means that we will cover the first part of the system, i.e. the forcing due to radiation loading under a certain state of environmental conditions (vapour pressure, temperature of the air and plant surface and boundary layer resistances). The restoring or relaxation mechanisms which are due to the turbulent exchange between the canopy air layers will be covered in Chapter 3. The effect of surface resistance on the forcing, due to its effect on the partition between radiative and non-radiative energy exchange, will be covered in chapter 4.

2.2 The interaction between the plants and the radiation field

The word radiation field in the previous paragraphs is used to describe the fact that for every point in this field there exists a magnitude and direction. There is a magnitude of the radiation intensity or radiance, depending on the direction of the beam. In every point in the x,y,z space there are infinite number of values for this radiation flux, depending on the direction of radiation and the width of cone from which this value is integrated. For every plane passing through a certain point in the x, y, z space, there will be two values (the irradiances on the upper and lower surfaces) that represent the integrated values from the two corresponding hemispheres above and below it.

In the case of a plant canopy, we will assume that the plant canopy elements (the leaves) are represented by a turbid homogeneous medium, dispersed uniformly in the x, y direction, but varying in the z direction depending on the profile of the leaf area density (m^2 leaf at one

side/m³ air).

The first step in the interaction between a leaf element and a beam of radiation is the leaf physically intercepting the incident beam. The probability of interception depends on the projection of the leaf perpendicular to the direction of the incoming beam, which is the effective area for interception of radiation and is dependent on the cosine of the angle between the leaf normal and the incident radiation. So, for a beam of light incident from a certain direction, the probability of interception of this beam in a certain layer is equal to the area density projected in the direction of the incoming beam divided by the sine of the angle of elevation. In equation

$$I_{i,k} = LAI_k \cdot \frac{|\cos \phi_{i,k}|}{\sin \beta} \quad (2.2.1)$$

where

β is the angle of elevation of the incoming radiation

LAI_k is the incremental leaf area index with a surface perpendicular to direction k .

$I_{i,k}$ is the probability of radiation incident from a direction i being intercepted by LAI_k

$\sin \beta$ determines the effect of the beam angle of inclination on increasing the travel length through the canopy of the incident beam of light. $\phi_{i,k}$ is the angle between the directions of the incident beam and the leaf normal. The cosine of this angle represents the fraction of the leaf area projected in the direction of the incident beam or equivalently

$$I_d = \exp(-LAI_k \cdot \frac{|\cos \phi_{i,k}|}{\sin \beta}) \quad (2.2.2)$$

where

I_d is the probability of a certain beam incident from a direction i not being intercepted by a surface with a normal which has a direction k .

A whole canopy layer has a certain probability distribution for its leaf normals and is subjected to a certain distribution for the incoming radiation from the different zones of the sky or from the layer above it. To get a representative value of the non-interception probability coefficient for this layer, a weighed average of the non-interception probability coefficients for the different leaf angle classes and different zones of the sky should be taken. In this model, to calculate energy sources and sinks within plant canopies, a multi-directional reflection and transmission model is not needed. The minimum level of detail we have to go into, while still maintain a reasonable level of accuracy, is by taking three leaf angle classes and three different zones of the sky as suggested by Goudriaan (1988).

The projection of the leaves for the different leaf inclination classes is calculated as a function of the leaf inclination class and the angle of elevation of the incoming radiation using the following functions:

$$|\cos \phi_{1,\beta}| = \text{MAX}(0.25, 0.93 \sin\beta) \quad (2.2.3.a)$$

$$|\cos \phi_{2,\beta}| = \text{MAX}(0.47, 0.68 \sin\beta) \quad (2.2.3.b)$$

$$|\cos \phi_{3,\beta}| = 1 - 0.26 \left(|\cos \phi_{1,\beta}| - |\cos \phi_{2,\beta}| \right) \quad (2.2.3.c)$$

where :

$|\cos \phi_{i,\beta}|$ is the fraction of leaf area in angle class i projected into the direction of the incoming radiation.

The extinction coefficient, $K_{ex,i,\beta}$, for a leaf inclination class i and radiation angle of elevation β is equal to

$$K_{ex,i,\beta} = |\cos \phi_{i,\beta}| / \sin\beta \quad (2.2.4)$$

Here, we end up with nine $K_{ex,i,\beta}$ (three zones of the sky multiplied by three leaf angle classes) coefficients which determine the relation between the leaf inclination class, the angle of elevation of the incoming radiation, and the effective leaf area intercepting radiation in the light path. An average extinction coefficient, K_{av} , for each of the three zones of the sky is found by the linear addition of the contribution of the three leaf classes. Goudriaan (1988) uses a weighted mean of the average extinction functions, $\exp(K_{av} \text{LADMID}(J) dz(J))$, by multiplying these with the weights of the contributions of the different zones of the sky to the incoming radiation (0.178, 0.514 and 0.308) for the standard overcast sky. $\text{Ladmid}(J)$ is the average leaf area density in the middle of the layer. The product ($\text{Ladmid}(J) dz(J)$) represents the leaf area increments within layer (J). The resulting expression gives the probability of non-interception i.e. that an incident diffuse radiation will not be intercepted by the foliage elements within layer J .

Once a beam of radiation has been intercepted, it will be reflected (R) (either specularly R_s or diffusely R_d), absorbed (R_a) or transmitted (either transparently T_t or diffusely T_d). See figure 2.2. A more detailed discussion is given by Den Dulk (1989). These fractions for the intercepted beam will be dependent on the angle of incidence. Therefore, in a detailed canopy radiation model, these fractions cannot be simply introduced as model parameters. But in this study, we are not interested in simulating the details of the angular distribution of the reflected and transmitted radiation within the plant canopy. So, we neglect the specular reflection fraction (which can be significant in a detailed radiation model) and the transparently transmitted radiation fraction, which is small compared with other fractions unless the leaves are very thin, this would lead to the reflection and the transmission coefficients of the leaves mostly dependent on the spectral properties of the plant pigments and water.

Concerning the spectral properties of the leaves, a leaf reflects and transmits very little radiation at the ultraviolet and visible wavelengths (an average value for the whole band of 0.1 and 0.1, respectively) and, as a result, has high absorption at the wave length band of 0.4 - 0.7 μm except in the green (0.55 μm). In the near infrared NIR (0.7-1.4 μm), the leaves show

higher reflectance and transmittance (average values of 0.4 and 0.4, respectively). This is due to a gap in the absorption spectrum between regions in the ultraviolet and visible wave bands, where electronic energy transitions dominate the spectrum, and the intermediate and far infrared (long) ($>3.0 \mu\text{m}$) wave band, where vibrational and rotational energy transitions dominate. The vibration-rotation absorption bands of liquid water enter the spectrum in the near infrared and, although weak at shorter wavelengths, they begin to dominate the spectrum at wave lengths greater than $1.4 \mu\text{m}$. The result is that reflectance and transmittance of a leaf rapidly diminish at longer wavelengths, and absorptance increases, with nearly complete absorptance at wave lengths greater than $2\mu\text{m}$ (Gates, 1980). So, the leaves are almost black bodies for the long wave radiation, showing reflectance of less than 0.05 and transmittance of zero. The leaves also act as a source for long wave emission since they, as all other bodies, emit radiation according to Stephan-Boltzmann law.

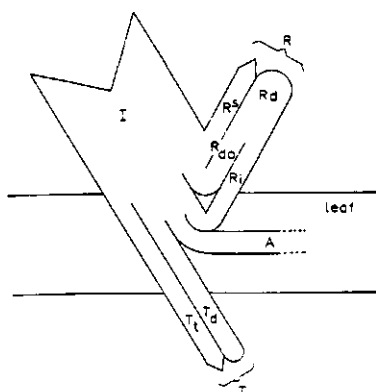


Fig. 2.2 Scheme of the distribution of the radiation I that incidents on a leaf over the five possible output destinations. Rs (specular reflection), Rd(diffuse radiation), A (absorption), Td (diffuse transmission), Tt(transparent transmission), Taken from Den Dulk(1989).

With this in mind, the radiation profiles have been calculated for three wave bands; the visible, the near infrared and the long wave radiation.

2.2.1. The short wave radiation

2.2.1.1 Direct radiation interception

For a direct beam, the probability that a beam of light, incident from a certain direction, will not be intercepted till a given depth in the canopy is given by

$$IBB(J) = \exp(-0.5 \text{ CUMLA}I(J) / \sin\beta) \quad (2.2.5)$$

and

$$Ib(J) = \exp(-0.5 \text{ LADMID}(J) \text{ DZ}(J) / \sin\beta) \quad (2.2.6)$$

where

IBB(J) is the cumulative probability that a direct beam will not be intercepted by the leaf elements above Layer J, Ib(J) is the probability that an incident radiation will not be intercepted by the leaf elements of layer J, and CUMLA I(J) is the cumulative leaf area in the layers above layer J.

The third component (III) represents the multiplication of $IBB(J+1)$ by $[1 - I_b(J+1)]$ which would represent the joint independent probabilities of a direct beam, which managed to get to the upper boundary of the layer (J+1), being intercepted by the elements of that layer and so contributing to the diffuse radiation fluxes at the upper and lower boundaries of this layer. This joint probability multiplied by the transmittance (τ_x) of the leaf represents the probability of a direct beam intercepted in a layer (J+1) contributing to the downward diffuse radiation flux density at the upper boundary of the layer below (J).

The second set of equations for the upward diffuse radiation fluxes (eq. 2.2.8) contains three equivalent terms;

The first of these represent the contribution of the upward radiation flux density at the lower boundary of a canopy layer (J) to the upward radiation flux density at the upper

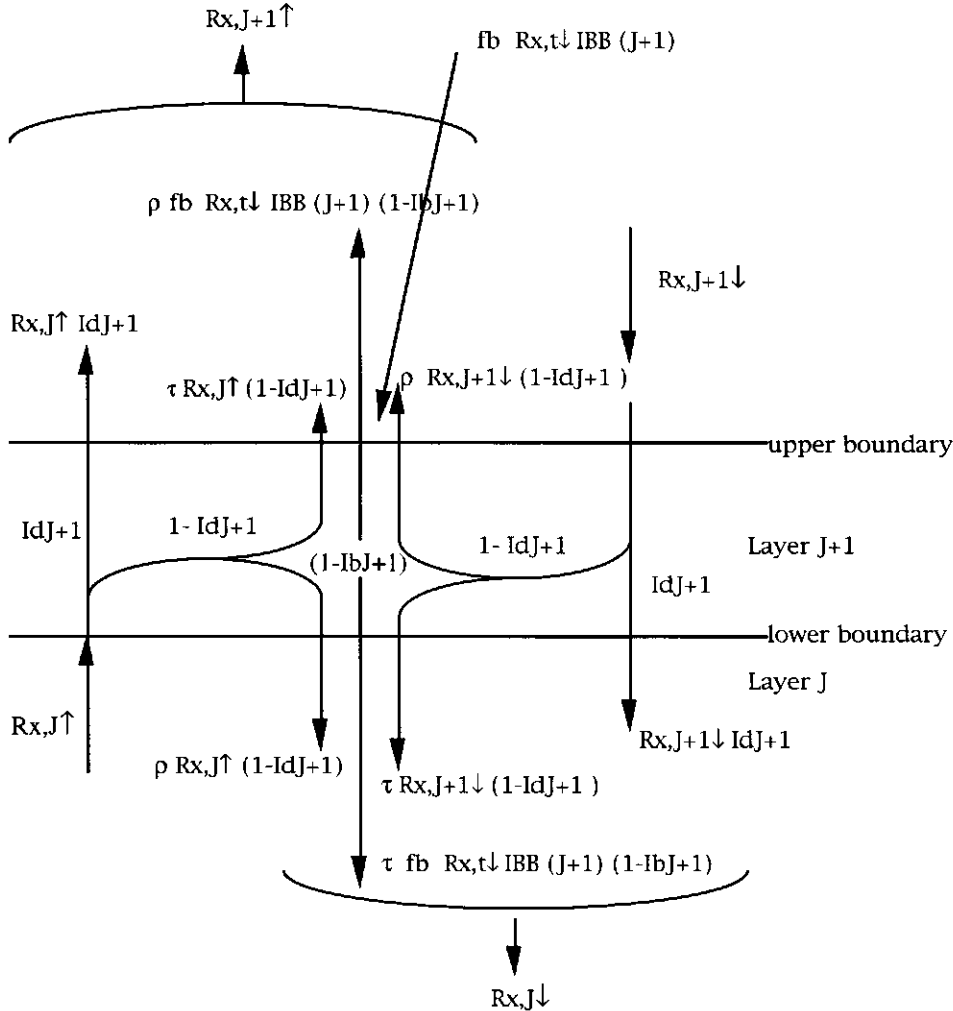


Fig. 2.3: The components of radiation fluxes above and below Layer J+1

boundary of this layer, after being intercepted and then transmitted, or managing to pass the canopy layer (J) non-intercepted.

The second of these terms represent the contribution of the downward radiation flux at the upper boundary of the canopy layer(J) after being intercepted and reflected to the upward radiation flux at upper boundary of this layer.

The third of these terms represents the contribution of the direct beam of radiation, which managed to get unintercepted to the upper boundary of layer (J) and then was intercepted within this layer and subsequently reflected, thus contributing to the upward diffuse radiation flux density at the upper boundary of the layer(J).

These two sets of equations for the downward and upward diffuse radiation fluxes represent then a set of discretized numerical equations needed to describe the downward and upward diffuse radiation fluxes. These two set of equations are applied for two wavelength bands (the visible, NIR). They could also be used for the longwave band after taking into account that the leaves emit radiation in the longwave band, since there is a dispersed source within the canopy for the long wave radiation.

There is one condition for these two sets of equations: The canopy layers should be thin enough to ensure that the probability of leaf overlap is negligible. This permits us to make an estimate of the reflected (or transmitted) radiation from the product of intercepted radiation and the leaf reflectance or transmittance. If layers are not chosen thin enough (leaf area index increments in the range of 0.1), scattering will be overestimated (Norman, 1982).

To increase the thickness of the layer without degrading the radiation profile estimates, use could be made of two approaches. The first is use of the Poisson's probability distribution to describe the probability of leaf overlap within a certain layer and to derive a thick layer reflection and transmission coefficients as suggested by Norman (1982), where the thick layer transmission and reflection coefficients $RL_{x,J}$ and $Trans_{x,J}$, respectively, are expressed as:

$$RL_{x,J} = \sum_{I=1}^{I=3} \rho_x^I Id_J (-\ln Id_J)^{I-1} / I! \quad (2.2.9)$$

$$Trans_{x,J} = \sum_{I=0}^{I=3} \tau_x^I Id_J (-\ln Id_J)^{I-1} / I! \quad (2.2.10)$$

The layer equations take the form:

$$R_{x,J} \downarrow = R_{x,J+1} \downarrow Trans_{x,J+1} + R_{x,J} \uparrow RL_{x,J+1} + f_b R_{x,t} \downarrow IBB_{(J+1)}(1 - I_b J_{+1}) \tau_x \quad (2.2.11)$$

$$R_{x,J} \uparrow = R_{x,J-1} \uparrow Trans_{x,J} + R_{x,J} \downarrow RL_{x,J} + f_b R_{x,t} \downarrow IBB_{(J)}(1 - I_b J) \rho_x \quad (2.2.12)$$

The other approach is to use the analytical solution of Kubelka-Munk equations defining the thick layer reflection coefficients. From equation 2.2.7 and 2.2.8, not including the contribution of the direct beam to the diffuse radiation, and substituting $d_j = (1-d_j)$ where d_j is the probability of being intercepted for a beam of diffuse radiation, the layer equations take the form :

$$R_{X,J}\downarrow = R_{X,J+1}\downarrow [\tau_X d_{J+1} + (1-d_{J+1})] + R_{X,J}\uparrow [\rho_X d_{J+1}] \quad (2.2.13)$$

$$R_{X,J}\uparrow = R_{X,J-1}\uparrow [\tau_X d_J + (1-d_J)] + R_{X,J}\downarrow [\rho_X d_J] \quad (2.2.14)$$

Decomposing and rearranging the equations, we get:

$$R_{X,J}\downarrow - R_{X,J+1}\downarrow = R_{X,J+1}\downarrow d_{J+1} [\tau_X - 1] + R_{X,J}\uparrow d_{J+1} \rho_X \quad (2.2.15)$$

and

$$R_{X,J}\uparrow - R_{X,J-1}\uparrow = R_{X,J-1}\uparrow d_J [\tau_X - 1] + R_{X,J}\downarrow d_J \rho_X \quad (2.2.16)$$

taking the limit when ΔZ approaches zero, considering that d_j is a decreasing function of z (+ upwards) opposite also to the direction of forward scattering and equal to

$$d_j = 1 - \exp(-K_{av} \text{Ladmid}_j dz_j) \quad (2.2.17)$$

or in case of small leaf area increments

$$d_j = K_{av} \text{Ladmid}_j dz_j \quad (2.2.18)$$

$$\begin{aligned} -\Delta R_X\downarrow &= R_X\downarrow d [\tau_X - 1] \\ &+ R_X\uparrow d \rho_X \\ \Delta R_X\uparrow &= R_X\uparrow d [\tau_X - 1] \\ &+ R_X\downarrow d \rho_X \end{aligned} \quad (2.2.19)$$

These are exactly the Kubelka-Munk equations (Gates 1980, Den Dulk 1989).

$$\begin{pmatrix} \frac{d R_X\downarrow}{d\text{lai}} \\ \frac{d R_X\uparrow}{d\text{lai}} \end{pmatrix} = \frac{d}{d\text{lai}} \begin{pmatrix} \tau_X - 1 & \rho_X \\ -\rho_X & -[\tau_X - 1] \end{pmatrix} \begin{pmatrix} R_X\downarrow \\ R_X\uparrow \end{pmatrix} \quad (2.2.20)$$

where $\frac{dd}{d lai}$ is the derivative of the interception coefficient with respect to $d lai$ (lai is leaf area increments)

2.2.2 The long wave radiation

The treatment of the long wave radiation in plant canopies is more complicated since the plants emit in the long wave region $> 3 \mu m$, so there is a dispersed source of this radiation within the canopy.

For calculating the long wave radiation fluxes into different layers, the long wave emission by the leaves in the long wave band, according to the Stephan-Boltzmann's law, should be considered.

With an emissivity of approximately 0.95 in this region, the leaves are almost black bodies to long wave radiation. By using the same layers equations of Norman (1979) and taking into account that transmittance is zero and reflectance is almost zero (a value of 0.05), we will neglect thermal scattering within the canopy (a negligible error). That will simplify the calculations, since we avoid an iterative procedure to calculate the upwelling and downwelling long wave radiation profiles.

By substituting the values of τ_x and ρ_x for the long wave radiation band and inserting the long wave emission term in the long wave radiation profile equation, the layer equations expressing the incoming upward and downward long wave radiation into a layer reduce to :

$$R_{l\downarrow,J} = R_{l\downarrow,J+1} Id_{l\text{ong},J+1} + \epsilon\sigma T_{l\text{eaf},J}^4 (1-Id_{l\text{ong},J}) \tag{2.2.21}$$

$$R_{l\uparrow,J} = R_{l\uparrow,J-1} Id_{l\text{ong},J} + \epsilon\sigma T_{l\text{eaf},J}^4 (1-Id_{l\text{ong},J}) \tag{2.2.22}$$

where

$R_{l\downarrow,J}$ is the downward long wave radiation flux density at layer J upper boundary.

$R_{l\uparrow,J}$ is the upward long wave radiation flux density at layer J upper boundary.

ϵ is leaf emissivity (assumed 1.0).

σ is Stephan-Boltzmann constant, $5.67 \cdot 10^{-8} \text{ Wm}^{-2}\text{K}^{-4}$

$T_{l\text{eaf},J}$ is the leaf temperature at layer J in K.

The incoming long wave radiation from the sky at the upper boundary of the canopy is calculated from the sky temperature, the degree of cloudiness and the sky emissivity (Campbell, 1977) or as measured. Here, the assumption is made for the calculation of long wave distribution that it follows the uniform overcast sky condition (UOC). This assumption was used in calculating the coefficients $Id_{l\text{ong},J}$.

The total amount of absorbed radiative energy was determined by the divergence of the short wave radiation profile (visible and NIR) plus an equation to determine the amount of the long wave absorbed by the leaves in different layers.

$$\begin{aligned}
 R_{\text{abs},J\downarrow} = & R_{\text{down},J}(1 - I_{\text{dlong},J}) + R_{\text{up},J-1}(1 - I_{\text{dlong},J}) \\
 & + \epsilon \sigma T_{\text{leaf},J}^4 - 2 \text{LADMID}_J \text{DZ}_J - 2(1 - I_{\text{dlong},J}) \epsilon \sigma T_{\text{leaf},J}^4
 \end{aligned}
 \tag{2.2.23}$$

where

The different terms are

I = the contribution of the downwelling long wave radiation flux density above the layer(J) upper boundary to the absorbed long wave within layer J

II = the contribution of the upwelling long wave radiation above the layer (J-1) upper boundary to the absorbed long wave radiation within layer J.

III = the long wave production per layer, is equal to the long wave emission per m² leaf surface multiplied by the leaf area (two sided) contained in the layer.

IV = the contributions of the foliage elements in the layer to the upwelling and downwelling long wave radiation fluxes.

The difference between III and IV represents the effect of mutual shading of the leaves and the un-directional (isotropic) long wave emission by an isothermal foliage element in a certain layer on long wave radiation, being intercepted by some other foliage elements in the same layer. The difference between III and IV will go to zero when leaf area density in the layer goes to zero.

In these equations, the temperature of the leaf surfaces within different layers is required, which is not known at the beginning. An iterative procedure was then used in which the divergence of the short wave radiation profile within canopy layers (independent of the solution) plus the extinction of the incoming long wave radiation at the upper and lower boundaries of the canopy were used as a first estimate of the total absorbed (short and long wave) radiation by the leaves surfaces (i.e. no emission by the leaves). This first estimate and an initial temperature and vapour pressure of the air were used to evaluate surface temperature of the leaves at different layers, and a source term for long wave emission within different canopy layers was added. The calculation of the long wave radiation profile was then possible and a new total absorbed radiation was estimated. The procedure was repeated till an equilibrium or steady state solution of the leaf was achieved. This solution was later used as an initial leaf surface temperature for a non steady energy budget solution for the upper and lower surfaces of the leaves.

2.3 The energy budget of the leaves*

The energy budget equation of the leaves is a conservation equation which relates the amount of the total absorbed radiation ($R_{\text{abs,total}}$) or net radiation (R_n) to the amounts of radiative and non-radiative energy exchange from the leaves to the surrounding media. We need to solve this equation under a certain set of environmental conditions (i.e. the vapour pressure and temperature of the air), given a certain set of surface resistances, to calculate the delivery of sensible and latent heat from the leaves into inter-canopy air stream. These delivered amounts represent the sources or sinks for non-radiative energy exchange within the canopy layers. We mentioned earlier that the vapour pressure and temperature of the air are

not the only environmental conditions, but we consider, in this thesis, that all the other abiotic environmental conditions affect the plants through their effect on the surface resistance to non-radiative energy exchange. This equation for a steady state solution reads as follows:

$$R_{abs,total} = \underbrace{\rho C_p (\overline{T_{leaves,J}} - \overline{T_{air,J}})}_I / r_{bh,J} + \underbrace{\frac{\rho C_p}{\gamma (r_{leaf,v,J} + r_{bv,J})}}_{II} [e_s(\overline{T_{leaves,J}}) - e_J] + \underbrace{\epsilon \sigma \overline{T_{leaf,J}^4}}_{III} \quad (2.3.1)$$

or

$$R_n = \underbrace{\rho C_p (\overline{T_{leaves,J}} - \overline{T_{air,J}})}_I / r_{bh,J} + \underbrace{\frac{\rho C_p}{\gamma (r_{leaf,v,J} + r_{bv,J})}}_{II} [e_s(\overline{T_{leaves,J}}) - e_J] \quad (2.3.2)$$

where:

ρC_p is the volumetric heat capacity of the air under constant pressure in $J m^{-3} K^{-1}$. $\overline{T_{leaves,J}}$ is the average temperature of the leaf surface in layer J in $^{\circ}C$ or K. $\overline{T_{air,J}}$ is the average temperature of the air in layer J. $r_{bh,J}$ is the boundary layer resistance for heat in $s m^{-1}$. γ is the psychrometric constant ($67 Pa K^{-1}$). $e_s(\overline{T_{leaves,J}})$ is the saturated vapour pressure at the average leaf temperature in Pa. $r_{leaf,v,J}$ is the leaf stomatal resistance in layer J in $s m^{-1}$. $r_{b,v,J}$ is the boundary layer resistance for water vapour in $s m^{-1}$. e_J is the vapour pressure of the air in layer J in Pa.

The first term stands for the sensible heat flux (H) from the leaves in Wm^{-2} . The second term represents the latent heat flux (λE or LE) from the leaves expressed in Wm^{-2} leaf surface. The use of one-sided or two-sided leaf area depends on how the resistances in the above equations were defined and how the value of R_n is defined. In here, we used the fluxes defined for one side of the leaf surface

There are several methods to solve the above mentioned energy equation. The most widely used is, according to Penman (1948), getting rid of the unknown surface temperature by using a linearization of the saturated vapour pressure at the leaf temperature, using the following approximation.

$$e_s(\overline{T_{Leaves,j}}) = e_s(\overline{T_{air,j}}) + s [(\overline{T_{Leaves,j}} - \overline{T_{air,j}})] \quad (2.3.3)$$

where S is slope of the saturated vapour pressure temperature curve at the temperature of the air. This would lead to the elimination of the unknown surface temperature and the determination of LE and H.

$$\lambda E = \frac{s R_n + \rho C_p D r_H^{-1}}{s + \gamma^*} \quad (2.3.4)$$

where D is the saturation vapour pressure deficit of the air, λ is the latent heat of vaporisation in J kg^{-1} .

$$\gamma^* = \gamma (r_{b,v} + r_s) / r_{b,h} \quad (2.3.5)$$

From this, an estimate of the surface temperature is made by the use of

$$\overline{T}_{\text{leaves},J} = \overline{T}_{\text{air},J} + \frac{H r_{b,h},J}{\rho C_p} \quad (2.3.6)$$

Another approach as suggested by, Paw U (1987) and Paw U & Gao (1988), is by the use of a fourth order polynomial function for the saturated vapour pressure at the temperature of the surface and substitute it into eq. 2.3.1. It is then possible to put the energy equation (for the steady state) in a fourth order polynomial with the temperature of the surface as the unknown.

A third approach would be the use of an iterative solution, e.g. Newton-Raphson method (Press *et al* 1992).

2.3.1 Definition of the boundary conditions for the solution of the leaf energy budget

During day time, the exchange between the canopy air space and the air above is modulated by the existence of coherent structures at the layer of air above the canopy. These structures represent the main mechanism of heat and mass transport between the canopy and the air above (see chapter 3). In the presented model, a gust term in the turbulent transport equation is introduced. i.e. a sudden intrusion into the canopy air layer by air from above the canopy. From an assumed refreshment effect of the coherent structure on the air inside the canopy, the temperature and vapour pressure of the air are known just after the gust intrusion and the sources or sinks can be calculated. A follow-up of the exchange between the canopy air layers and the layers of air above keeps track of the buildup of the temperature, vapour pressure of the air and the consequent source variation within time.

During night time, the situation is much more complicated. The long wave radiation loss at the upper portion of the canopy leads to the appearance of a radiative energy sink at the canopy top. The leaves in the top of the canopy start cooling. When the air is not saturated, a sensible heat flux from the air in close contact with the leaves to the leaves is initiated. Depending on the sensible heat flux from the air above and below, cooling of the air starts. The cooling of the air continues till the leaves reach the dew point temperature of the air. In this stage, a contribution of latent heat flux from the air to the leaves also starts. The contribution of latent heat flux in comparison to sensible heat flux (Bowen ratio) in supplying the radiative sink at the canopy top depends on the moisture content of the air brought in contact with the leaves, and whether that air is left long enough in contact with the leaves, that it cools enough to reach the air dew point temperature. The contribution of the air above and below to the air layer in contact with leaves is dependent on the active turbulent transport mechanism and the feedback from the radiative sink on it.

The sink in the canopy top leads to a heat flux from the air below in contact with the soil, which initiates an upward soil heat flux. The unstable profile in the lower part of the canopy enhances turbulent heat transport from the lower canopy air to the top of the canopy. In the layer above the canopy, the downward sensible and latent heat flux from the air above to the upper canopy elements partly compensates for the radiative cooling of the canopy elements. Such transport is hindered by the stability of the air in this region. In case of light wind speed at the canopy top, there will be little dynamic coupling between the canopy air space and the air above. This puts an extra role on the soil as a source to meet the needs of an unsatisfied sink at the canopy top. The whole equilibrium is achieved anyhow, but at what temperature of the canopy elements? This is dependent on the radiative cooling and the feedback between this radiative cooling and the transport processes (a picture of such a flow regime is shown in page 167). In cases of strong dynamic coupling between the above canopy air and the canopy (i.e. a strong shear), a gust term is turned on and the temperature gradient at the layer above the canopy will be reduced. This increases the relative contribution of the air above the canopy in meeting the demands of the radiative sink at the canopy top.

The flow regimes can change drastically during night hours; from clear skies to cloudy skies, stronger wind to lighter wind, or dry air to moist air. All these processes determine the relative contribution of the sensible and latent heat flux in both of the energy fluxes from below and above (i.e. Bowen ratio and dewrise to dewfall ratio) to the radiative sink.

Shortly after sunrise, the net radiation balance changes sign. The radiative cooling, which represents the forcing for dew formation, is gone. But it takes some time, till the wind regime at the canopy top starts picking up and a coupling of the flow between the canopy air space and the air above is achieved. The realization of this coupling depends on the stability regime within and close above the canopy. That coupling will enhance the drying process of the leaves within the canopy. During the drying process, the difference of the surface resistance between the dry and the wet part of the leaves and the fraction of the wet and dry surface is important in determining the time constants of the canopy air layers and the value of the equilibrium vapour pressure of the air layers as shown in sect.4.2. The difference in the surface resistance between the dry and wet surface of the leaves will depend on the stomatal resistance of the dry part and how it is controlled (sect.4.5.3). We thus considered the development of the fractional wet area on both the upper and lower surface of the leaves. In principle, this model can be coupled to an interception model plus a plant pathogen model.

2. 3. 1. 1 The Numerical Implementation

In principle, the above given equations are enough to calculate the energy partition on the plant surfaces and so the steady state energy sources and sinks within plant canopy. The thermal time constants of the leaves lie within the cycle of the gust intrusion, and the variation of the source with time inside the canopy is affected by the storage in the leaves. So we decided, in the numerical calculation, to use a nonsteady state solution of the leaf surfaces.

A numerical implementation is given here. An analytical treatment of the whole system of equations (the leaves and the air) is given in sec. 4.2. The energy equation for a certain surface reads as follows:

$$\rho C_J = \frac{\partial T_J}{\partial t} = -\text{div } \mathbf{q} + S \quad (2.3.7)$$

where: ρC_J is the volumetric heat capacity of plant material in $\text{J m}^{-3} \text{K}^{-1}$ for plant material. It is assumed that the leaf mass is composed mainly of water, \mathbf{q} is the energy flux (whether radiative or non radiative) to the leaf segment. S are the sources and sinks with the leaf segment or volume in $\text{J m}^{-3} \text{s}^{-1}$. $\frac{\partial T_J}{\partial t}$ is the temperature rate of change in K s^{-1} .

This equation expresses the rate of change of energy storage within the plant tissue in the form of sensible heat due to two effects; the first is negative the divergence of the radiative and non-radiative energy fluxes. The second effect is the sources and sinks within the plant tissue. An evaporation flux from the leaf to the surrounding air could be looked at as a sink term for energy or as a non-radiative energy flux from the leaf surface to the surrounding air, and so it would be considered as a component in the divergence term.

For the upper boundary of the upper surface of the leaf, we have

$$q_u = -R_{n,\text{short}} + \rho C_P (T_J^{t+dt} - T_{\text{air}})/r_{bh} \quad (2.3.8)$$

where

q_u is the energy flux at the upper surface of the leaf (+ upwards). $R_{n,\text{short}}$ is the net short wave radiation. This value was estimated from the divergence of the downward diffuse short wave radiation flux plus the divergence of the direct radiation (mainly down) flux divided by the total leaf area increment in the layer (conventionally expressed as one-side). A negative sign was used since this energy is directed into the upper surface. The second term in the previous equation represents the sensible heat flux from the leaf to the air (+). The superscript, $t+dt$, expresses the time level of the superscripted variable.

For the lower boundary of the upper segment (half the leaf thickness) of the leaf

$$q_{u,l} = -\lambda \nabla T \quad (2.3.9)$$

where $q_{u,l}$ is the amount of heat conduction from the upper segment leaving through the lower boundary of that segment. The source term is expressed by

$$S = R_{\text{long, absorbed}} - \frac{\rho C_P}{\gamma(r_{\text{leaf},v,J} + r_{bv,J})} [e_s(T_J^{t+dt}) - e_{\text{air}}] - \epsilon \sigma T_{\text{leaf}}^{t+dt}{}^4 \quad (2.3.10)$$

The amount of $R_{\text{long, absorbed}}$ was determined by the use of eq 2.2.23.

$$\begin{aligned} R_{\text{long, absorbed}, J \downarrow} &= R_{\text{down}, J} (1 - I_{d\text{long}, J}) + R_{\text{lup}, J-1} (1 - I_{d\text{long}, J}) \\ &+ \epsilon \sigma T_{\text{leaf}, J}^4 - 2 \text{LADMID}_J \text{DZ}_J - 2(1 - I_{d\text{long}, J}) \epsilon \sigma T_{\text{leaf}, J}^4 \end{aligned} \quad (2.3.11)$$

this amount was divided by the leaf area increment. The terms are as explained in eq 2.2.23

In the source term expression (eq 2.3.10), we see we had the temperature of the leaf segment at the end of time step (an implicit approximation). To linearize, we used

$$S = R_{\text{long, absorbed}} - \frac{\rho C_p}{\gamma(r_{\text{leaf,v,J}} + r_{\text{bv,J}})} [e_s(T_1^t) - e_{\text{air}}] - \epsilon \sigma T_{\text{leaf}}^t{}^4 - \frac{\rho C_p}{\gamma(r_{\text{leaf,v,J}} + r_{\text{bv,J}})} \left[\frac{\partial e_s(T_1)}{\partial T} \right] \Delta T - 4\epsilon \sigma T_{\text{leaf}}^t{}^3 \Delta T \quad (2.3.12)$$

where

$$\Delta T = T_1^{t+dt} - T_1^t \quad (2.3.13)$$

The same procedure is done for the lower surface of the leaf. The final discretized equations will form a set of linearized algebraic equations. These can be solved by the use of an implicit scheme with the knowledge of the temperature and vapour pressure of the air at the beginning of the time step and the incoming radiation fluxes. The shortwave radiation flux is independent of the solution (the temperature of the leaf surfaces). The effect of the solution on the long wave emission by the leaves is considered within the linearization, while the effect of the leaf warming on incrementing the upwelling and downwelling longwave radiation profiles and on the divergence of long wave radiation is considered within another iteration within the solution of the longwave radiation profiles. Even, if this last effect is not considered, it is taken care of automatically at the beginning of the new time step. I think the effect of neglecting this within a single time step would not be important.

The simulation of the amount of dew on the upper and lower surfaces of the leaves at different height was done. A consideration of the complete qualitative picture, as given in sect.2.3.1., was done by updating the boundary condition for wind (i.e. the dynamic coupling) and the incoming long wave radiation. We considered the possible combinations of the upper and lower surfaces being wet and dry and followed the drying process for the upper and lower surface of the leaves. A variation of the surface resistances between the upper and lower surface resistances could also be due to a different response of the upper and lower stomata to radiation. The different radiation loads, for the upper and lower surface, would be equalized by the strong coupling between the two surfaces. A leaf in the upper part of the canopy at night sees the colder sky, while the lower side of the leaf sees the warmer vegetation and the soil below.

Considering the possible combinations of the upper and lower surfaces of the leaves being wet or dry, we assumed that for a certain time step there is no correlation between the position of the wet and dry spots on the upper and lower surface of the leaf, i.e. they have independent probability distributions. (This correlation through time steps is considered through the heat conduction from the upper to the lower surface for the different combinations). This leads to a probability distribution of the leaf segments being the product of the probability of the upper and lower surface being dry or wet. We had four segments (w,w), (w,d), (d,w) and (d,d). The first position in an ordered pair stands for the lower surface and the symbols w and d stand for the surface being wet or dry respectively. So, an ordered pair (w,d) means a leaf segment with lower surface wet and the upper surface dry. These

probabilities were determined by multiplying the different combinations of the wet and dry fractions for the upper and lower surfaces. These fractions were calculated from the total amounts of dew which were given initially for the first time step or were calculated from the pervious time step. An assumption was made about a constant average thickness of the water film layer on the upper and the lower surface of the leaf. From this value, the amount of dew (initial or calculated) was converted into equivalent wet areas on the upper and lower surfaces of the leaf. The circular drops were assumed as cylinders with a fixed height. So the cumulative variation of dew was expressed as an expansion or shrinkage of the wetted area. Another assumption was made about the ability of the upper and lower surface of the leaf to hold water. It was assumed arbitrarily that the water film thickness on the leaf upper surface is twice as large as that of the water film on the lower surface. This is rather arbitrary, but it can be changed to express the condition of surface wettability.

When the fraction wet area exceeds one, dripping then starts and not before. So there is no account for stem flow or dew dripping from the leaves due to the leaf fluttering by the wind.

From the above procedure, we have four combination of leaf segments. For each of them , we get a temperature of the upper and lower segments with half leaf thickness. The neighbouring segments could have different temperatures. The coupling between the wet and dry surface on the same side of the leaf is not as strongly coupled as the coupling between the upper and lower surface. This coupling was considered explicitly, not implicitly, i.e. as determined at the beginning of the time step. The importance of the degree of coupling of a wet and a dry spot on the same side of the leaf is shown by the inverse of this ratio:

$$\frac{n \Pi r^2}{n 2 \Pi r d} = \frac{r}{2 d} \quad (2.3.14)$$

where r is the radius of the representative drop diameter for the surface (could be different for the lower and upper surface). n is the number of drops per m^{-2} leaf surface. d is the leaf thickness in m . The coupling or the amount of lateral heat conduction between the wet and dry spots on the same side of the leaf was considered by the use of the following equation.

$$C_H = -\lambda 2 \Pi r d \frac{(T_{wet} - T_{dry})}{\Delta x} n$$

$$d \approx \Delta x \quad (2.3.15)$$

$$C_H = -\lambda 2 \Pi r (T_{wet} - T_{dry}) n$$

λ is the heat conduction coefficient of the plant material in $W m^{-1}K^{-1}$. Δx is the distance over which the temperature gradient between a dry and a wet spot is taken. This distance can not exceed the thickness of the leaf so $d \approx \Delta x$. This leads to the third equation in eq (2.3.15). This expresses lateral heat conduction for m^{-2} leaf surface with all its possible combinations. To express this per m^{-2} of one combination, we take an averaged weight of lateral heat conduction from different kinds of neighbours on the same surface for a certain combination. This equals

$$\text{conduh}_{\text{leaves},i,l,x,y} = \frac{2 \lambda}{r_l} \sum_{K=1}^2 \sum_{J=1}^2 \text{Pr}_{K,J} (T_{\text{leaves},i,l,K,J} - T_{\text{Leaves},i,l,x,y}) \quad (2.3.16)$$

where $\text{conduh}_{\text{leaves},i,l,x,y}$ is the horizontal heat conduction for leaves in leaf layer i , on side l with wetness condition x, y . $\text{Pr}_{K,J}$ is the probability of existence of combination K,J and r_l is the characteristic diameter of the water drops on side l .

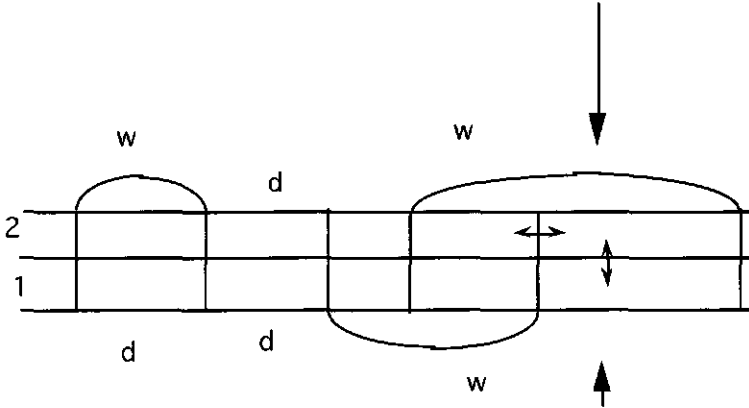


Figure 2.4 showing the different combination of wetness for the upper and lower surface.

This term is added then to the heat balance equation of the leaves, i,l,x,y for $l=1$ and $l=2$ for the lower and upper surfaces respectively. The non-steady equation is solved and new values for the temperature of the lower and upper surface of the leaves are obtained.

2.4 The resistances to heat flux from the leaves to the inter canopy air stream

In the energy budget equations, there appear two resistances: the boundary layer resistance and the stomatal resistance.

The boundary layer resistance is calculated according to the formulas suggested by Gates (1980) and Monteith & Unsworth (1990) and will be referred to within the computer listing in the subroutine **RESIS** or subroutine **MOMNTM**.

The stomatal resistance is calculated according to:

- 1) a radiation effect.
- 2) a soil moisture potential effect which regulates the sensitivity the stomatal resistance to leaf water potential, as suggested by Tardieu and Davies (1993).

The quantification of CO_2 sink within plant canopies was calculated by using a photosynthetic model as explained by Goudriaan (1982).

CHAPTER 3

TURBULENT TRANSPORT WITHIN AND CLOSE ABOVE PLANT CANOPIES **,*

3.1 Introduction

In this chapter, the governing equations for describing momentum, heat and mass transport within plant canopies, and the averaging procedures used, will be discussed. Several approaches, used for modelling heat and mass exchange between the canopy air layer and the layer of air above it and the assumption behind these approaches, will be covered. The implications of intermittency on these approaches (Eulerian and Lagrangian) will be considered.

First, a qualitative presentation of heat, mass and momentum exchange between the canopy and the layers of air above will be given. From this qualitative presentation, a qualitative picture of what is wrong with second and higher order closure models will be given. The governing equations and the averaging procedures used to describe canopy flow and some of their limitations with long time interval averaging will be shown. A suggested averaging scheme in which we try to separate between the different contributions of length scales to the total transport and some of its limitations will be considered. The used closure assumptions, in this intermittent approach, will be discussed and justified. Second, a quantitative picture of the nonuniformity of the terms in the governing equations will be given. All of these points give a theoretical justification for the suggested method. Then, a consideration of the effect of coherent structures existence on the random Lagrangian approaches used for describing heat and mass transfer within plant canopies will be made.

3.2 A qualitative description of the turbulent transport within plant canopies and its relation to the governing equations

Momentum, heat and mass transport within and close above plant canopies has a very intermittent nature. This intermittent nature is due to the passage at the canopy top of

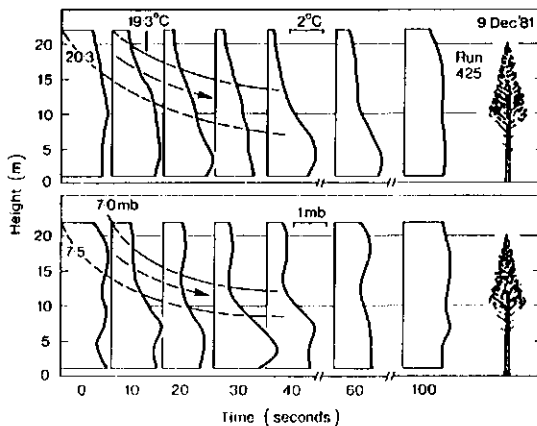


Fig. 3.1 Profiles of temperature (top) and vapour pressure (bottom) in Uriarra forest during and after the passage of a gust. Baseline for temperature, 18.5 °C, and for vapour pressure 6.5 mb. Dashed lines are contours of constant temperature and vapour pressure. Arrows depict the penetration of the gust. Taken from Denmead and Bradley (1985), with the kind permission of Kluwer Academic Publishers.

coherent structures which have a length scale larger than the canopy height and which have a period of a few minutes. During the passage of these coherent structures at the canopy top, most of the exchange of sensible, latent heat and a high fraction of momentum exchange between the canopy air space and the layer of air above take place. In the period of time between the passage of two consecutive coherent structures, called a quiescence period, a build up (look at fig.3.1 taken from Denmead and Bradley (1985)) of the temperature and vapour pressure follows. This build up represents then the amount of non-radiative energy and mass which has been delivered by the leaves and the soil surface, representing the sources or sinks, into the inter canopy air stream and which has not been evacuated by the turbulent transport processes active then to the layer of air above. In this period, a minor fraction of the total averaged flux between the canopy air layer and the layer of air above is observed. Given ample time between the passage of two consecutive coherent structures, an equilibrium profile would be achieved.

Any how, in the quiescence period, the profiles of temperature, vapour pressure and CO₂ reflect the distribution of the non-radiative energy and mass sources within height and they represent a high value of storage, for the energy and mass exchange of the leaves, within the canopy air space. The profiles, in the quiescence period, are characterised then by the existence of a large hump (a positive or a negative one, depending on the sign of our sources). During the passage of the next coherent structure, the ejection and sweep phases of this structure would lead to the refreshment or the replacement of the air within the canopy, partially or fully, with fresh air from above leading in the process to a rapid change in energy storage within the canopy air layers which represents a high fraction of the total averaged flux. So, during a very short interval of time compared to the total averaging time, a major fraction of the total averaged flux is achieved. In an averaging procedure, in which we use time intervals of averaging larger than the largest time scale of turbulent transport, the profiles in the quiescence period, in which there is little transport, would dominate the long-time averaged profiles since those occupy most of the averaging time. The large time interval averaged flux at the canopy top is controlled mainly by the ejection and sweep phases of the passage of the coherent structures, which occupy a very short interval (fraction) of the total

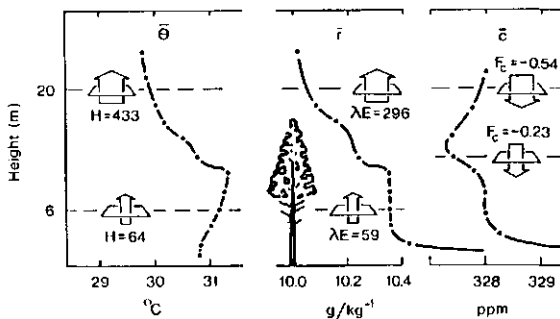


Fig. 3.2 Mean profiles of potential temperature, θ , mixing ratio, \bar{r} and CO₂ concentration, \bar{c} , observed in Uriarra forest over a period of one hour near noon and flux densities of sensible heat, H , (in Wm^{-2}) λE , Latent heat (in Wm^{-2}) and CO₂, F_c (in $mg\ m^{-2}\ s^{-1}$) at different heights. Taken from Denmead and Bradley (1985) with the kind permission of Kluwer Academic Publishers.

averaging time. This would lead to an anomaly in the flux profile relationship. An attempt to fit an in-time-averaged profile to an in-time-averaged flux, which are controlled by two different processes and which do not occur simultaneously, leads automatically to the failure of the K-theory approach to describe heat and mass transport within such a canopy.

A characteristic example of this situation is apparent in fig.3.2, as given by Denmead and Bradley (1985). Notice the value of the averaging time (one hour). Figure 3.1 expresses a characteristic sequence of events (an example of heat evacuation during the coherent structure passage and the buildup during the quiescence period) for a forest. There is no accompanying flux trace of sensible and latent heat flux at canopy top, but the sudden change in the non-radiative energy stored in the canopy must have expressed itself in a sudden increase in the flux between the canopy air space and the layer of air above.

Figure 3.3a shows an identical example of a space-time domain temperature map for a maize canopy. A space-time domain map is a graph representing on its horizontal and vertical axis the time and space (height), respectively. This space-time coordinate axis represents an area which is occupied by different values of temperatures. This is similar to the graphs by Wilczak (1984) and Gao *et al.* (1989). By looking at this figure, we see a contour map of temperature values occupying different regions in the space-time domain. This map was obtained by using a measurement set which was available at the Meteorology Dept., Wageningen Agricultural University. The details of the measurement are given by Jacobs *et al.* (1992) and Van Boxel (1988) and will be given briefly in chapter 6 (on validation). These maps (fig.3.3 a, b) were obtained by placing temperature sensors and hot bulb anemometers at different heights which measured, continuously (few hours within certain days) with 5 Hz and 1 Hz frequencies the temperature and wind speed signals respectively. The measurement heights here were (0.1, 0.2, 0.3, 0.4, 0.7, 1.0, 1.4 m) within a maize canopy which had a height of 1.7 metres and which had a cumulative one sided plant area index (PAI) of 3.6. The PAI is the sum of leaf area index (LAI) and stem area index.

The map (3.3.a) shows regions or islands of high temperature which are interspersed by regions of lower temperatures. We see that the heights of the centroid of these temperature island is centred around the one metre height which corresponds to the maximum plant area height. Next, we look at the net radiation (R_n) time series graph (fig.3.4) as measured above the canopy, which is taken as a measure for the incoming short wave radiation at the canopy top. We see that in most of the cases there is no correspondence between the two signals (air temperature and R_n). So, the variation of the air temperature within time was not due to an intermittency in the sources within the canopy due to time variations of the incoming short wave radiation due to cloudiness. From a look at a space-time domain map of wind speed within the canopy (fig.3.3.b), we see that regions of temperature island disappearance correspond with high wind speed regions inside the canopy. The conclusion we can draw from this is that the disappearance of the temperature islands is due to the passage of coherent structures which have accelerated the air within the lower part of the canopy air space and later replaced all the air within the canopy air space with fresh air from above, thus achieving a high fraction of the flux. During the passage of these coherent structures, there is an absence of observable vertical gradients both in temperature and wind speed. In the period between the passage of two coherent structures, a build up of temperature, shown by temperature islands, occurs which represents the amount of energy delivered by the leaves

into the inter canopy air stream and not evacuated by the turbulent transport mechanisms during that period to the layer of air above the canopy. This process of renewal and buildup represents an intermittency in the turbulent transport of momentum, heat and mass between the canopy air space and the layer of air above.

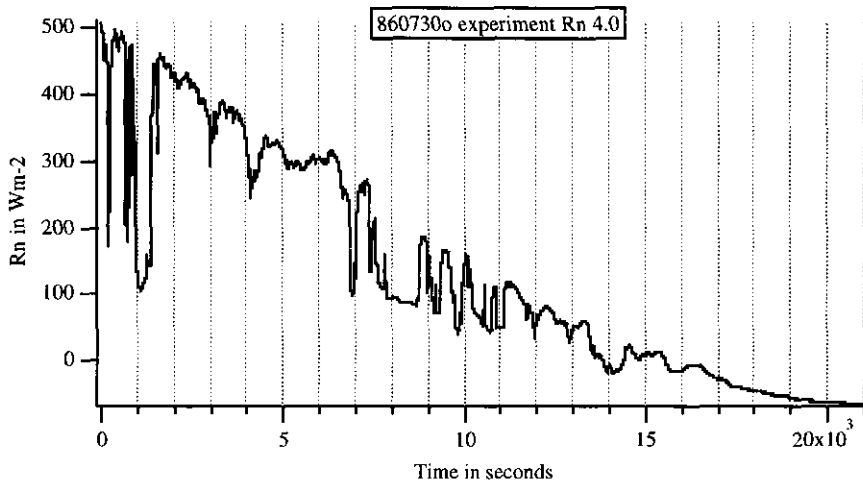


Fig. 3.4 The behaviour of R_n as a function of time for the shown segment of the data set in fig. 3.3, 3.14 and 3.16.

3.3 IMPLICATIONS OF INTERMITTENCY FOR EULERIAN MODELLING

The problem in first order closure models, as we have seen, is that most of the averaged flux and the averaged profiles occupy different regions in the time domain. In our procedure of averaging, we try to fit an averaged profile to an in-time averaged flux. The averaged profile does not control the direction of most of the averaged flux which occurs mainly during the ejection and sweep phases of the coherent structure passage. The averaged scalar profiles are characterised by the existence of a secondary maximum or minimum, depending on the sign of our sources, while the averaged scalar fluxes are directed upwards or downwards respectively. This is called counter-gradient transport. Counter-gradient transport is also observed in momentum transport but has a somewhat different explanation due to the higher role the pressure plays in the momentum transport in comparison to scalar transport (see Shaw *et al*, 1990). We will come to this explanation later. There is more than what we have said to counter gradient transport (Look at Sect. 3.3.1).

The problem of canopy turbulent transport and failure of K-theory approach could also be expressed in the length scales of turbulent transport within plant canopies in relation to the canopy scale and the time or space distribution of these length scales. In the period of passage of the coherent structures at the canopy top, the length scale of the transport is larger than the canopy height and transport is not controlled by a local gradient. In the quiescence period, the length scale of transport is quite small in comparison to the canopy height and the source distribution. This leads to a build up of the storage of non radiative energy within canopy air

space which reflects the source distribution within height. This buildup of storage establishes a local gradient which controls the direction of a short-time averaged flux. If turbulence within plant canopy were small scaled in relation to the source distribution or the canopy height, this would lead always to the validity of down gradient transport. The Lagrangian integral time scale would have been small, and the effects of the superposition of the near field concentration field on the total one would have been minor. We would not have seen then this cycle of build-up and depletion. We would not have seen a jump in the scalar fluxes signal above the canopy (see for example Denmead and Bradley 1985, fig. 8). If the length scale of transport were always large compared to the canopy height or source distribution, we would have seen no or very little build up of the vapour pressure or temperature of the air within the canopy and no jump in the flux signal at the canopy top. In this case, the Lagrangian treatment would have not been valid (a conclusion we make from Sect. 3.7). The change of the storage within the canopy would have played no role in the transformation of the signal at the leaf surface to the signal at the canopy top. The signal at the canopy top would be coupled more to the forcing signal (the solar radiation) affected by the time constants of the leaves, and there would be no delay due to turbulent transport or equivalently due to the storage change within the canopy air.

Meanwhile, we have come to two important questions, which we try to tackle:

1a) Is intermittency in turbulent transport due to the existence of coherent structures, with a length scale larger than the canopy height and which have a certain frequency, a characteristic feature of canopy flow ?

2a) What consequences does this have on the approaches used for modelling heat and mass transport within plant canopies and their validity ?

Concerning the first question 1a about the universality of coherent structures existence in canopy flow and their effect on intermittent transport, the work of several authors in numerous papers shows signs of this universality. Finnigan (1979) in his study on momentum transfer on wheat crop, had found that most of the transfer occurred when gusts originating from near the top of the equilibrium boundary layer penetrated the canopy. The velocity and shear stress profiles at these times were quite different from those during lighter winds. Much of the same mechanism appeared to influence the transport of scalars in an experiment in a Uriarra forest (Denmead & Bradley 1985). Shaw *et al.* (1983) and Shaw (1985) showed, from measurements made in a corn canopy, that relatively large fractions of the total Reynolds stress occurred in a small fraction of the total time. In his example, near the top of the canopy about 50% of the momentum transfer occurred in 6% of the total time.

Gao *et al.* (1989) have shown that time/height cross sections of scalar contours and velocity vectors portray details of flow structures associated with the scalar ramps. A ramp is a gradual increase or decrease in the signal terminated by a sudden decrease or increase respectively, depending on the stability of the air above the canopy. He has concluded from the magnitude of the temperature drop that the cold air originates well above the canopy (what he considered at least twice the canopy height) because the mean temperature profile shows only a slight vertical temperature gradient in the above canopy atmosphere. In the same study, in a data set which were collected under near neutral stability (run B in the study), there were ramp patterns in humidity but not in temperature because the mean temperature gradient was too weak. Although the mean humidity gradient was apparently

sufficient to allow ramp production, the moisture flux did not contribute to destabilizing the flow, as indicated by the relatively large magnitude of the Monin-Obukhov length ($L=-1063$ m). Therefore, without significant buoyancy effects, shear must be the major factor in the dynamics of structures associated with the ramps. From the latter study, we see from the ramp patterns (fig.1.a of the last study) at different heights that the coherent structures associated with such ramps must have a horizontal and a vertical extension which is larger than the canopy height. The word horizontal comes here because the highest two measurements were on a tower 25 metres to the west.

Raupach *et al.* (1989) give an explanation why coherent structure existence would be a characteristic feature of canopy flow. They show from examining data on turbulence statistics in seven uniform, thermally near-neutral canopies that despite their great morphological variations, these canopies have a number of universal characteristics. One of these characteristics was the existence of an inflection point in the mean velocity profile $U(z)$ near $z=h$. These seven canopies include: two forests, two corn canopies and three wind tunnel model canopies. The height of the canopies (h) varied over a factor of 400 and U^* ranged over a factor of 10 or more. Assuming an analogy between turbulent flows in plane mixing layer and turbulent flows in the vicinity of plant canopies, and from a linear stability theory analysis of the early stages of transition of this flow to turbulence, theorems due to Rayleigh second theorem and Fjortoft (Drazin and Reid, 1981) show that a necessary condition for the Rayleigh equation to have an unstable mode is that the mean velocity $U(z)$ must have an inflection point at which du/dz is a maximum. Also Tollmien (1929,1931) proved that this is a sufficient condition. These unstable modes generate transverse vortex motions, called Kelvin-Helmholtz waves, which are associated with inviscid stability. These transverse Kelvin-Helmholtz waves constitute an entire family of motions which can grow in a mixing layer but are not possible in a laminar boundary layer. Following the primary instability process described by this theory, the subsequent development towards a fully turbulent state includes several instability processes (Ho and Hurre, 1984), most of them non-linear and not describable by linear stability theory. The transverse vorticity in the Kelvin waves collects, under a non-linear self-interaction, into a string of concentrated blobs or cat eyes, linked by braids of vorticity. The concentrated transverse vortices undergo a non-linear, stochastic, pairing process which introduces irregularities in the spacing between vortices and provides a mechanism for the vertical spread of mixing layers. The main process leading to a break-up of the transverse vortices is a three-dimensional secondary instability which produces longitudinal vorticity (i.e. double roller structures as in fig.6 of Raupach *et al.* (1989)). These structures are thought to be essentially those responsible for the main ramp patterns observable on time traces.

So even if coherent structures were not there initially, they will result as a consequence of the existence of an inflection point in the velocity profile. This explains the mechanical induction of the coherent structure.

Coherent structures can be also thermally induced. These coherent structures could be small or large. The small ones could result due to inhomogeneities in the surface heating in the field i.e. hot dry spots (i.e. wide distance between trees in a localized irrigated field). The appearance of these structures will depend on the magnitude of the shear and its ability to smear them out. The larger scale thermal coherent structures which are a characteristic of the

convective mixed layer play also a role in the transport of scalars and momentum while intruding into plant canopies. The structures which are seen in the graphs (3.a and 3.b) are not only the ones which result from dynamic induction. The relationships derived from Raupach *et al* (1989) for the frequency of occurrence which relates to U^*/h , gives a higher frequency than the ones seen in fig.3.3.a. *The ones in these graph are having also a larger duration of the gust intrusion.*

It is assumed by Raupach that the mechanically induced structures are the main ones responsible for the ramp patterns observed on time traces. The role of the thermally induced ones in heat and momentum in atmospheric surface layer is shown from the work of others (Schols, 1984 and Wilczak, 1984). These structures would intrude into the plant canopy leading to the achievement of a large percentage of the flux. The effect of thermal stability on the coherent structure frequency of occurrence has been investigated by Leclerc *et al.* (1991).

The ejection of low momentum fluid, which accompanies the intrusion of the large scale structure, would lead to the development of somewhat instantaneous inflection points, which would also lead to the development of smaller scale coherent structures in a mechanism as explained in Raupach *et al.* (1989). So, from a large scale coherent structure, there would develop a smaller one.

Possibly, there are two populations of coherent structures which are working on heat and mass transport within plant canopies as has been suggested in shear layers (Cantwell, 1981). The duration and the frequency of both populations will differ. These two populations are superimposed upon each other.

From the previous two examples, the forest and the maize, we have seen a common picture of coherent structures with the following characteristic:

- 1) They have a certain frequency of occurrence.
- 2) They have a large length scale larger than the canopy height.
- 3) They intrude into canopy air space, replacing the air inside the canopy with fresh air from above;

such that they become the main agents for heat and mass transfer (also for momentum, with a higher role for the pressure correlation). This intrusion leads to the appearance of a coincidence in the intermittent signals of turbulent transport fluxes at different heights within plant canopy and also a coincidence in the scalar concentrations.

Concerning the second question 2a about the effects of turbulent transport intermittency on available approaches used for modelling heat and mass transport within plant canopies. these available approaches lie mainly under two main categories: Eulerian approaches and Lagrangian ones. The Eulerian approaches include local and non-local approaches. The local approaches include first, second (Wilson and Shaw 1977) and higher (currently maximum third) order closure models (Meyers and Paw U, 1987). The non-local closure includes the transient turbulence approach (Stull, 1988) and the non locality term in a first order closure approach by Li *et al.* (1985). The Lagrangian approach include the random walk models (e.g. Legg & Raupach 1982, Wilson *et al.*, 1981, Flesch and Wilson 1992, Wilson and Sawford 1995). An evaluation of some of these models is given in Baldocchi (1992).

The aim of all available approaches in their application to canopy flow is to predict the state variables of the canopy-soil-layer of air above the canopy system (e.g. air and soil temperature and air vapour pressure at different heights) in response to some forcing

variables (solar radiation, air temperature and vapour pressure at screen height). The whole system is divided into several subsystems: a canopy air plant subsystem, a plant subsystem and a soil plant subsystem. The solution of the state variables describing this system requires the simulation of the response of the different subsystems to the forcing imposed on them and the interaction between them. For the canopy air subsystem, this requires the solution of a coupled set of time- and/or space-averaged turbulent transport equations describing canopy turbulent transport processes (Reynolds averaged Navier Stokes equations). A time step of simulation of a few minutes (e.g. 6-7 minutes) would be good enough to follow a diurnal cycle. In the turbulent transport subsystem, we assume that the same interval should be good enough to follow the sub-system dynamics. We use some closure assumptions to parameterize the effect of the correlation between state variables within this averaging time period on the solution. Within that period, there should be no other cycles of intermittency which have a correlation with a behavioural aspect of our system and which do not in the mean sum up to zero. Ignoring or wrong parameterizations of correlations which do not sum up to zero would lead to a deviation between the observed and the simulated behaviour of our system depending on whether the correlations which affect our system summed up to zero or not. To overcome the problem of having cycles with an interval less than our time of averaging and which we suspect to have non vanishing correlations, we have two options:

1) Put these correlations back in the large-time averaged equations and parameterize them correctly.

or

2) Reduce the time step of simulation and take account of the intermittency cycle and its correlations explicitly.

We always try to optimize our calculation by maximizing our time step of simulation without loss of relevant information. So, we try first to follow the second approach, i.e. large-time interval averaging.

That brings us to a question: 1b) What assumptions do we need for valid averages (appendix 1.A) and the effect of deviating from these assumption on the solution?

The Navier Stokes and their Reynolds averages are nonlinear except for the instantaneous scalar equation and the mean scalar equations in which a first order closure is used. In the case of a linear equation, the equality

$$\overline{f(x)} = f(\bar{x})$$

holds. This means that we can use the mean of an independent variable to determine the mean value of a function. The same large-time interval averaged value for a linear function would have been obtained while considering or not the effect of intermittency on the solution. I think that the justification for using large-time averages on a non-linear equation could have been that, despite the nonlinearity of the equation, the terms were assumed to be more or less uniformly distributed within time. Turbulence was assumed more uniformly distributed, like the space distribution of different sizes of sand particles on a sheet of sand paper. The role of pressure on destroying the correlations, even if they exist, is assumed to be quite large. The rate of solution convergence by going higher with the closure level is assumed to be large, i.e. the value of the initial correlations are

low and more uniformly distributed**. The existence of the coherent structures with a spatial separation and their role in creating non-uniform correlation at high order led to the breakdown of that assumption. Reynolds(1894) has shown that one needs a uniformity of the turbulent* signals within the averaged volume or time interval to obtain a valid averaging of the momentum equation. The combination of nonuniformity of the terms and nonlinearity in these equations make the situation difficult. The averaged system of equation will not be strictly valid. The correction for the deviation from uniformity is attempted through the inclusion of the higher order terms equations, till we arrive at a complete dispersion of the correlations. The solution which we obtain will then be dependent on the assumptions used to close the equation, their validity and the effect of the difference between realistic and assumed ones on the divergence between the simulated and measured behaviour of the system. Adopting valid assumptions to average and describe the exchange processes and comparing the results of this assumptions with reality determines if our assumptions are correct. A difference between the measured and the simulated behaviour could be due to two reasons:

1) Ignoring or wrong parameterization of correlation which do not sum up to zero.

or

2) High sensitivity of the system to these variables at certain regions of its domain of solution i.e. small error in the initial value or the closure assumption results in high error or magnifies with the progression of simulation. *That depends on the path of the system equation solution on its n dimensional phase space and whether very adjacent paths diverge widely later.*

By decomposing the signal into a large scale and a small scale which are more uniformly distributed within the considered intervals, the assumption of uniformity is more valid during the quiescence period. In the intrusion, we used a closure assumption for the effect of coherent structures on the refreshment.

To overcome a hump (a secondary maximum or minimum) in the averaged profile and achieve a flux through it, we need to allow for a higher order term to achieve this and retain some of the information we have lost. Use of a higher order closure model shows a hump in

 ** For this remark, LOOK AT APPENDIX 1.A, there is also a segment of the article which was written by Reynolds (1894) saying that :

" defining S1 to be such that the space variations of $\bar{u}, \bar{v}, \bar{w}$ are approximately constant over this space, we have putting $\overline{u'u'}$, & c., for the mean values of the squares and products of the components of relative-mean-motion, for the equations of mean-mean-motion,

$$\begin{aligned} \rho \frac{d\bar{u}}{dt} = & - \left\{ \frac{d}{dx} (\overline{P_{xx}} + \rho \overline{uu} + \rho \overline{u'u'}) \right. \\ & + \frac{d}{dy} (\overline{P_{yx}} + \rho \overline{uv} + \rho \overline{u'v'}) \\ & \left. + \frac{d}{dy} (\overline{P_{zx}} + \rho \overline{uw} + \rho \overline{u'w'}) \right\} \end{aligned}$$

which equations are approximately true at every point in the same sense as that in which the equations of mean motion are true".

the large-time averaged profile and maintains a flux through it. One may suggest then that by the use of higher order closure models, we can then take account of counter-gradient transport (defined on the mean; there is another definition, look at 3.3.1) and that would explain the whole story. The question is: if through the use of second and higher order closure models, we could put back the information we have lost of non vanishing correlations or phase relationships in our system and get correct solutions of the equations? We mean by these phase relationships, that the passage of coherent structures introduces a lot of correlations (i.e. correlations between vertical wind velocity and heat flux (a third order term) or vertical wind velocity and temperature(a flux) etc.). All these correlations happen within a coherent structure cycle which is less than our time step of simulation. In a numerical solution by second or higher order closure models, two assumptions are made:

- 1) uniformity of these high order terms within our time step of simulation.
- 2) that they have no cycles of change which have correlations not vanishing to zero in the mean or within the time step of simulation. The step of simulation is usually small enough to follow the boundary conditions changes at canopy top, but quite coarse for following the correlations which develop within a coherent structure cycle.

Due to the high nonlinearity of the system, a large-time interval averaged value for a higher order term within our time step of simulation would not be equivalent to a fluctuating-in-time value for that higher order term, which has the same mean, in its effect on the solution. (Appendix 1.A). Also, the behaviour of the higher order terms affects the assumptions used in their closures. To follow what happens perfectly, we have to: 1) go higher with our closure level to include the correlations and keep our time step large till we get a complete dispersion of the correlations. or 2) reduce our time step of simulation and apply the closure assumptions where they are appropriate. This is what we call a continuous versus intermittent treatment.

In second or higher order closure models, to reduce the importance of third order or higher order terms respectively, the ideal situation would be that these terms are homogeneously distributed in time, or, in time and space. If these terms were distributed homogeneously in time but non-homogeneously in space (i.e. in the vertical), the value of the divergence in these terms would have a constant value and could have been measured or parameterized and put directly in the equations. Hence, there would have been no difference between an intermittent and continuous treatment of the closures. If these terms were homogeneously distributed in the time and space domain, the value of the divergence in these terms would have been zero and their importance in the second or higher order closure equations nil (negligible). If these terms were randomly distributed, this would lead to zero correlations and a reduction of the importance of these terms. When neither of the above conditions is satisfied, an ideal situation would be going higher with the closure level (n) till we encounter the higher order term (n+1) in this equation which is completely randomly or homogeneously distributed. This consequently would guarantee for us the convergence of the solution and absence of gain from going higher with the closure level.

But what is the situation of second and higher order closures in our canopy flows? The existence of coherent structures in canopy flow with their characteristics correlates in their passage the fluxes of momentum, heat and mass with one another. This will lead to highly localized values in the time domain map of the correlations between the vertical wind

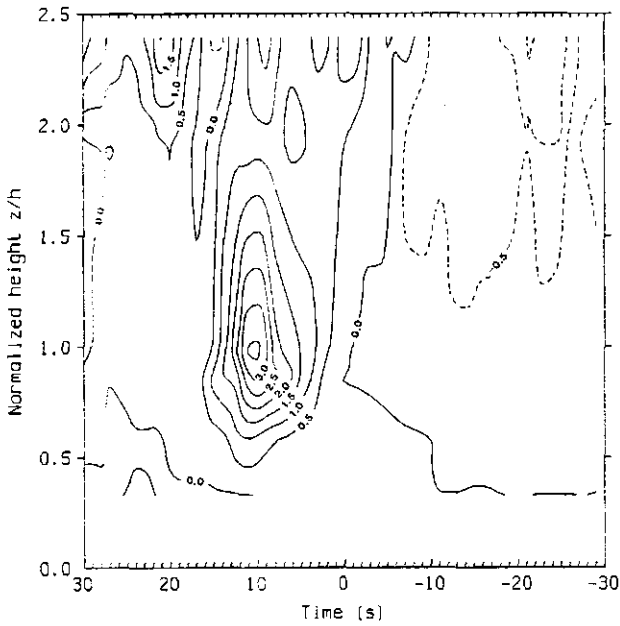


Fig. 3.5.a Vertical cross-section of ensemble averaged $w'u'w'$ fields normalized by u^{*3} with contour interval of 0.5 under unstable condition ($L = -138$ m), during Run A.. Solid lines represent positive $w'u'w'$ and dashed lines represent negative $w'u'w'$. Taken from Gao *et al* 1989, (fig 12.a) with kind permission of Kluwer Academic Publishers.

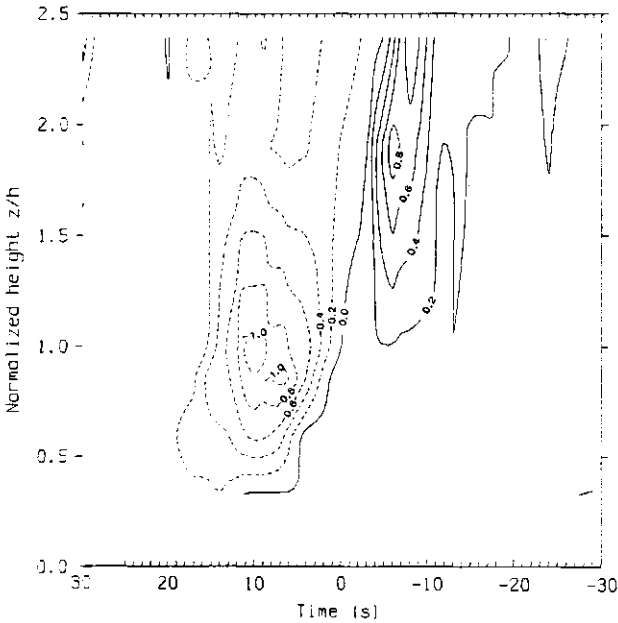


Fig. 3. 5b. The same as fig 3.5a but for $w'w'T'$ normalized by $-T^* u^{*2}$, with contour intervals of 0.2. Taken from Gao *et al* 1989, with kind permission of Kluwer Academic Publishers.

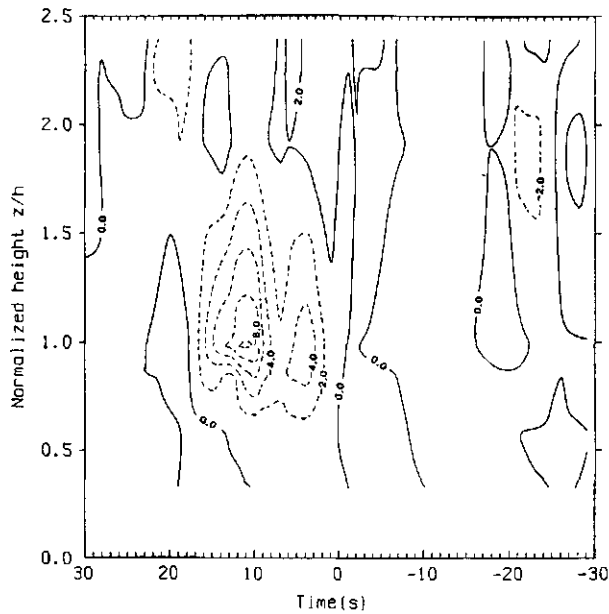
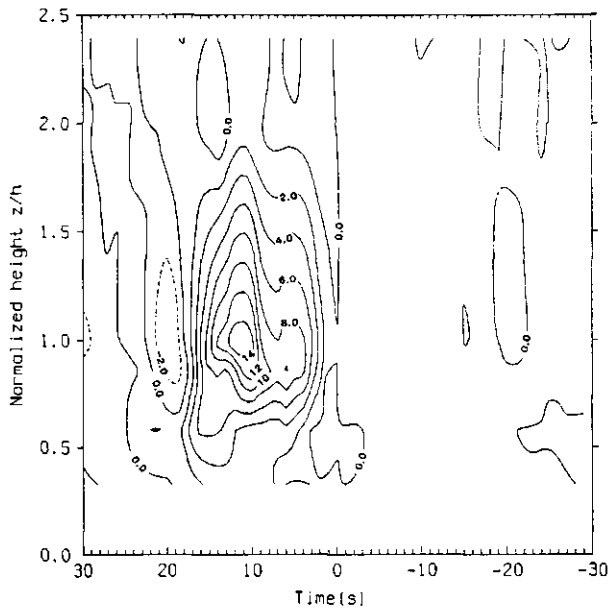


Fig 3.6 a Vertical cross-section of 1-s average momentum flux normalized by the square of the friction velocity calculated at the top of the forest, for the single structure at Run A as shown in figure 3 of Gao *et al* 1989. Contour interval is 2.0. Dashed lines indicate negative $u'w'$ and solid lines indicate positive $u'w'$. Taken from Gao *et al* 1989 with kind permission of Kluwer Academic Publishers.



3.6 b. Vertical cross section of 1-s average heat flux normalized by $-T'u^*$ calculated at the top of the forest for the same single structure as in fig 3 of Gao *et al* 1989. Contour interval is 2.0. Solid lines indicate positive $w'T'$ and dashed lines represent negative $w'T'$. Taken with kind permission of Kluwer Academic Publishers.

velocity and the fluxes of heat (sensible and latent) and mass (CO₂) or between the different fluxes (third and fourth order terms respectively). This leads to an increased importance of the third order terms in the second order equations, and that these third order terms become highly non-homogeneous (Gao *et al.* 1989 fig.12.a and 12.b, included here as fig.3.5 a,b). Still in the third order closure, the fourth order terms would represent a correlation between a momentum, or a variance and a flux which would still be quite large. (see for example Gao *et al.* 1989 fig.8.a and 8.b and their superposition included here as fig.3.6). Both pictures correlate highly since both fluxes occupy almost the same regions in the height-time domain maps. The directional derivative of these fluxes and their correlations is far from homogeneous, which would lead to a difference between a continuous and intermittent treatment. It is important to mention that momentum is transported differently from mass and heat due to the higher role which the pressure correlation terms play in momentum transport. This would lead to a dispersion of the correlation between momentum or velocity variances and scalar fluxes. This would reduce the importance of the fourth order terms, but these fourth order terms would not be completely randomly distributed. Going higher with our closure level till we obtain a complete dispersion of the correlations would require the solution of a large number of equations. It could be that the yield we get in the convergence of the solution by going one level higher is not rewarding, depending on how fast the correlations disperse when going higher, due to the relative importance of the pressure correlation on the momentum and scalar fluxes.

The role of the pressure on dispersing the correlations is a function of the velocity field, since the pressure signal is controlled by the divergence of the flow fields as given by Poisson equation. The elliptic behaviour of the momentum equation makes it difficult to tell what the cause and the effect of this relation. But anyhow, the fluctuating pressure will disperse the correlations between scalar and momentum fluxes around the fringes of the coherent structure where the vertical derivatives are higher. That is where the effect of the pressure on dispersing the correlations is more pronounced. So, the more dispersed, or spatially distributed the events, the better is the dispersion of the correlation by going higher. An example of a static pressure fluctuations is given in fig.3.7b as taken from Shaw *et al.* (1990) and fig.3.7a taken from Conklin and Konner (1994). We see from this figure that the pressure fluctuations are centred around the passage of the coherent structures at the canopy top. This is related to the velocity field which controls the pressure field. The pressure distribution terms will be having a higher effect around the passage of the coherent structures. Since the occurrence of the coherent structure passage is somewhat disperse and the smoothing by the pressure is centred around their fringes, the variation in the higher order term will not smoothed out by the pressure smoothing. The effect will depend on the distance of smoothing due to pressure redistribution effect in relation to the spacing distance between coherent structures. We need an overlap of pressure fields resulting from the passage of subsequent coherent structures. There must be some kind of an optimum or a maximum in the separation between the events which can be smoothed out by the pressure redistribution terms. In canopy flow, the ratio of pressure smoothing distance/distance between coherent structures is much less than one.

To summarize the situation: There are two opposing factors: the role of coherent structures in creating high values for the correlation on higher level and the role of pressure

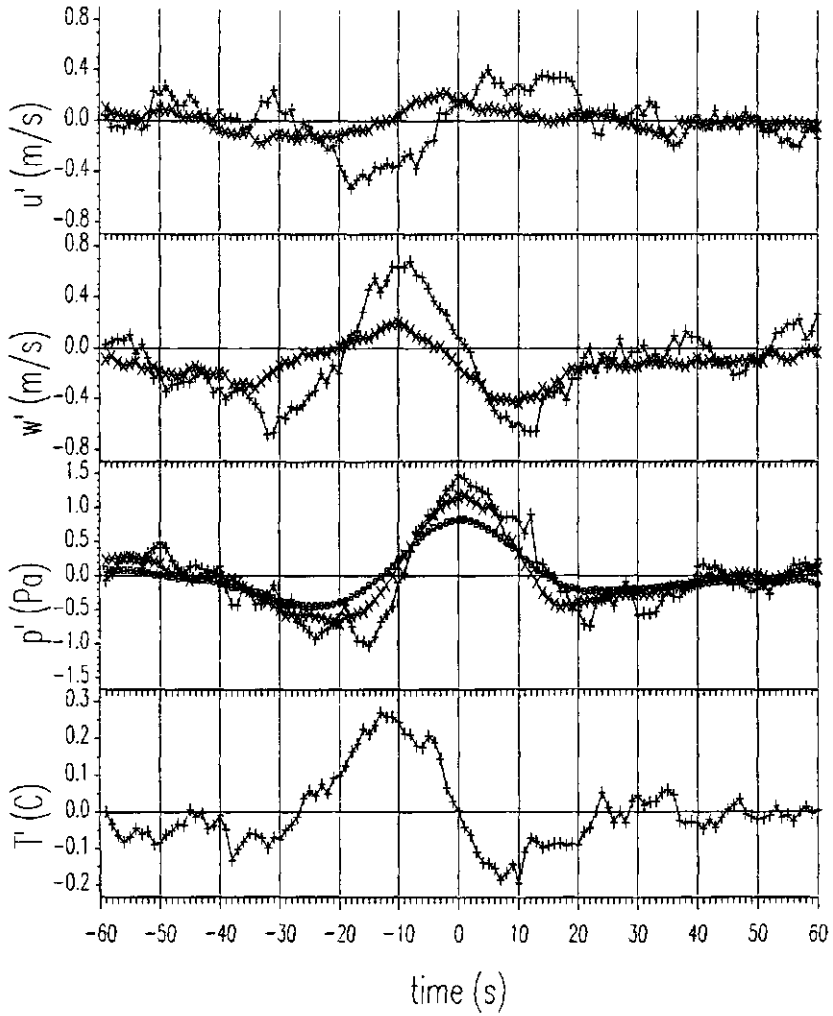


Fig 3.7.a. Ensemble average of 17 pressure pulse events . From top to bottom, Horizontal wind component u' , vertical wind component w' , static pressure p' and temperature T' . +++++ above canopy at 1.3 times canopy height. x-x-x-x within canopy at 0.6 times canopy height. □-□-□ surface. Taken from Conklin and Konner (1994).

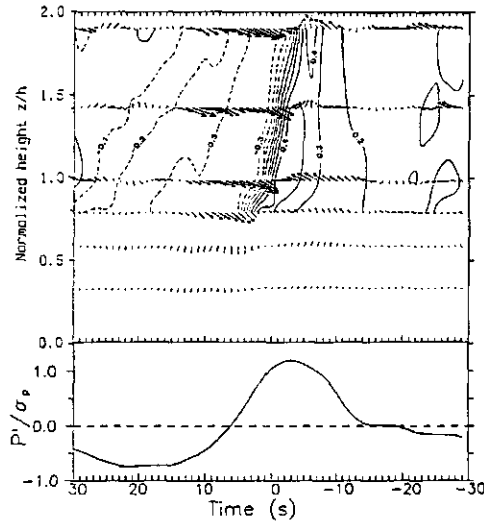


Fig 3.7b. Association between ejection/sweep coherent structure identified by fluctuations in humidity (contour interval $0.1\text{g}/\text{m}^3$) and by fluctuating velocity vectors (maximum arrow length represents 2.0 m/s), and surface static pressure normalized by its unfiltered standard deviation. Each part of the diagram is an ensemble average of events during 30 min period. Taken from Shaw *et al* (1990) with the kind permission of Kluwer Academic Publishers.

correlation in destroying these correlations. It seems to me that due to the large role of coherent structures in achieving high fraction of the fluxes, their length scales and their time distribution, that even our fourth order terms are quite large in their variation. Gao *et al.* (1989) found that the instantaneous (1 second averages) values reach magnitudes which are larger than the 30-min mean fluxes by a factor of 10 for momentum flux and 14 for heat flux. In his ensemble average of 10 events, an attenuation of that factor by a factor of 2 to 3 was observed. Probably, this high attenuation was because no attempt was made to adjust the time scales to match ramps of different duration. This led to smoothing of correlations and masking coherent structure turbulence into small scale turbulence. Had they matched the coherent structures according to their duration, they would have obtained less attenuation. This would have meant a worse situation in the ensemble averages. The adjusting of the time scales to match ramps of different durations would have led to a scaled time map of the correlations. This concurrent occurrence will mean directly very high values for the instantaneous momentum heat flux correlation, which is a fourth order term ($w'u'w't'$). The time map of that fourth order would have regions with very high values. The fourth order map could be approximated by the multiplication of map 8a and 8b of Gao *et al.* (1989), included here as fig.3.6. if we assume that correlations of deviations of instantaneous fluxes from 1 sec mean are minor. The highest order available closure model is a third order closure, in which an assumption of the homogeneous distribution of the fourth order term is made. It is clear from the measurement of Gao *et al.* (1989) that this assumption is far from reality. The distribution of this fourth order correlations is quite non-homogeneous which leads to the invalidity of the following assumption

$$\overline{u_j u_k u_l} = \overline{u_j u_l} \overline{u_k u_l} + \overline{u_k u_l} \overline{u_j u_l} + \overline{u_j u_l} \overline{u_k u_l} \quad (3.3.2)$$

which is valid only for homogeneous (or gaussian) turbulence. This assumption is used also in the closure of the fourth order terms in higher order closure models. Based on this assumption is the closure of the third order term in second order closure model. The same applies to invalidity of

$$\overline{u_i u_j u_k \theta} = \overline{u_i u_j} \overline{u_k \theta} + \overline{u_i u_k} \overline{u_j \theta} + \overline{u_i \theta} \overline{u_j u_k} \quad (3.3.3)$$

The role of the pressure correlation on destroying the above mentioned correlations is quite real, but it seems due to the characteristics of the coherent structures that at least till a fourth order term this role is not effective. In a more homogeneous flow, in which the scales of transport are less effective in correlating fluxes together, the pressure correlation terms would have less trouble in destroying the higher order correlations, since they have lower starting values. The dispersion of these terms when going higher would be quite rapid. The gain of the remaining information would be based on the use of a closure for this homogeneous higher order term.

So, there are two problems: the nonlinearity of the system of equations, so the use of an averaged value for a higher order term is not the same as a fluctuating term with the same mean, and the effect of intermittency on the closure assumptions used.

Now, what is the solution to this problem?

In simulating any system, there are many scales of intermittency. If any of these scales has a correlation which does not sum up to zero with a behavioural aspect (in this case the fluxes and profiles) within our step of simulation, we have to find a way to include this effect in the averaged equations used for describing the system or reduce our time step of averaging. We have seen that the normal way of including the effect with long time interval averaging is increasing the order of the closure, but our convergence rate will be small and at increasing computational costs. If we have no other method with high credibility for parameterizing the effect of the intermittent transport on the closure assumptions, and that is clearly the case, we have to reduce our time step and take account of the intermittency of the transport directly.

The problem, we assume, is in the large interval of averaging used in second or higher order closure without consideration of the circumstances under which the averaging and the closure assumptions for different time periods are valid. We assume that this is due to the variation within time of the length scales of transport; a large scale at and around the passage of the coherent structure and a small scale in the remaining period. This affects the validity of the averaging procedure and the closure assumptions used in higher order closure models. We suggest to put the correlations back at early stages of closure levels. We do this by trying to reduce our time step of simulation and apply the closure assumptions when they are relevant to the scale of transport. This is what we have done, since we assume a separation between a large scale transport, represented by the effect of a coherent structure on heat and mass transport, and a small scale transport, represented by the quiescence period. In the period after the passage of the coherent structure, we could have a problem to parameterize the interaction between large scale and small scale transport.

The assumption of homogeneity of turbulence could be valid in the quiescence period, where the length scale of transport is small compared to the canopy height. It could be that K-

theory works well, with an assumption, in the period between the passage of two coherent structures, if the length scale of turbulence in this period is small enough in comparison to the length scale of the source distribution within the canopy.

For the parameterization of large scale transport, I would like to quote what Raupach *et al.* (1989) wrote: "It is a truism to say that there is presently no theory capable of predicting coherent eddy structure in fully developed turbulence, such as double roller or transverse vortices described above, but there are some theories which provide idealised models of some facets of coherent structures." We here use parameterizations for the coherent structures by including a certain frequency of occurrence, degree of refreshment or intrusion into plant canopies and duration. With the developments in the flow regime simulation, it could be possible later to obtain simulated parameterizations for coherent gust intrusion into plant canopies and put these directly in the model we are suggesting.

In the following pages, we will outline the governing equations for describing momentum, heat and mass transport within plant canopies, and relate the above qualitative picture to the different terms in the averaged equations. We will also show the intermittent nature of the other terms in the flux equation

We will make a comparison between an intermittent and non intermittent approach in describing canopy transport processes in chapter 4 (only for first order).

3.3.1 COUNTER GRADIENT TRANSPORT

In the previous part, we have shown that counter gradient transport emerges when averaging is done over an interval larger than the interval between the passage of two coherent structures. So, while the averaged-in-time profiles are controlled by the profiles at the quiescence period which are accompanied by very little flux, the averaged fluxes are controlled mainly by the ejection and sweep events, which result due to the passage of coherent structures at the canopy top and which occupy a very small fraction of the total time. So due to the averaging procedure, the large-time averaged profiles will have a secondary maximum or minimum depending on the sign of our sources while the averaged flux is positive or negative across this maximum. However, counter-gradient transport occurs not only due to averaging.

Counter gradient transport can also happen instantaneously. This can be shown by considering what happens during the passage of a coherent structure. Due to the velocity field which accompanies the passage of the coherent structure at the canopy top, this leads through the application of the Poisson equation to the appearance of a pressure maximum at the soil surface. This pressure maximum leads to the acceleration of the wind at the lower part of the canopy. There exists then a region of higher wind velocity at the lower part of the canopy through a region of low fluid momentum. This is also some kind of counter-gradient transport for momentum (Shaw and Zhang, 1992). The acceleration of the flow at the lower parts of the canopy leads to the $\frac{\partial u}{\partial x} < 0$. Due to the continuity, this leads to $\frac{\partial w}{\partial z} > 0$, considering that $w_{\text{soil surface}} = 0$, which then represents an ejection phase. After the passage of the inclined shear layer at the canopy top, the horizontal pressure gradient is negative; this leads to the

deceleration of the flow and $\frac{\partial u}{\partial x} > 0$. Because of continuity, this leads to a sweep phase represented by $\frac{\partial w}{\partial z} < 0$. One point worth considering here is that the flow equation is elliptic, so information is transformed upstream and it becomes difficult to tell what is the cause and what is the effect. Some would say that the ejection phase leads to an evacuation of the air mass from the the lower layers within the canopy, so, a sweep must occur which replaces the ejected air. Then, an ejection is a cause and sweep is an effect. In the explanation we have given, the flow field of the coherent structure leads to a pressure maximum which leads to the occurrence of the ejection and the sweep. The explanation could depend on the scale of the coherent structure.

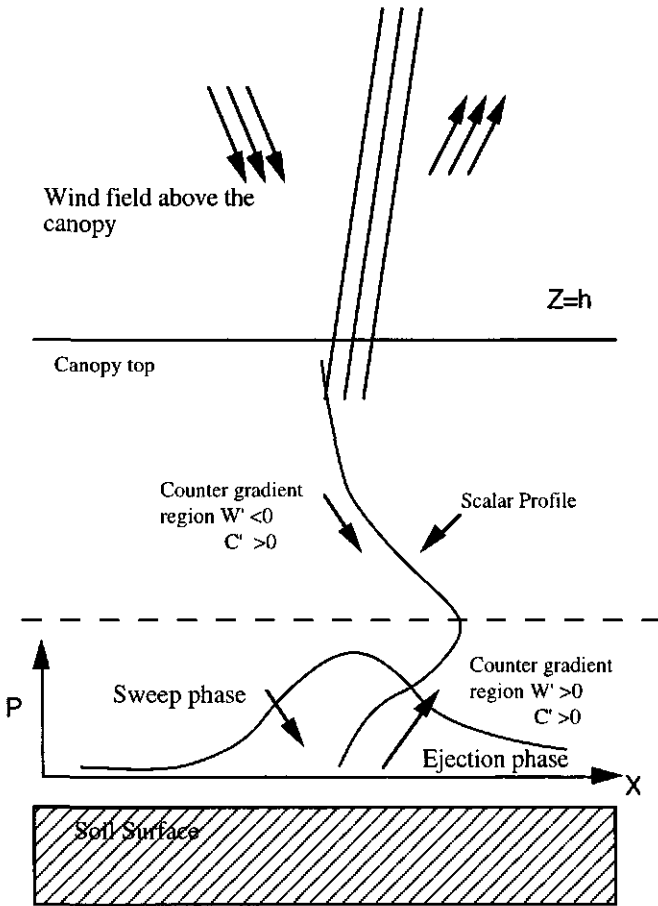


Fig. 3. 8 shows the velocity field and the inclined shear layer at the canopy top as shown by Shaw *et al* (1990) and the resulting pressure field at the soil surface. The occurrence of an ejection phase or a sweep phase in the existence of a concentration profile as shown here leads to an instantaneous counter-gradient scalar transport.

The existence of ejection and sweep phases during the passage of the coherent structures leads with the existence of a scalar profile in the flow field to the appearance of instantaneous scalar counter-gradient transport as shown in fig.3.8. So, the flux in this case has nothing to do with the concentration gradient (the flux could be counter or pro gradient).

3.4 The Governing Equations

There are three fundamental physical principles upon which all of fluid dynamics is based: the conservation of mass, momentum and energy. These are expressed by the fundamental governing equations of fluid dynamics: the continuity, momentum and energy equations. These equations have different forms depending on the way they were derived. The general procedure is defining a finite region of the flow (a control volume) which is bounded by a control surface. The control volume could be moving with the flow such that the same fluid particles are always within it (Lagrangian) or fixed in space with the fluid moving through it (Eulerian). These equations for instantaneous values of a an infinitesimal control volume fixed in space read as :

3.4.1 The continuity equation

$$\frac{\partial \rho}{\partial t} + \nabla \cdot (\rho \mathbf{u}) = 0 \tag{3.4.1}$$

(a list of symbols is given in the appendix 3). Which in the case of canopy or atmospheric boundary layer flow ($Ma^2 \ll 1$, i.e. $V \ll 100 \text{ m s}^{-1}$, low frequency pressure waves $nL \ll a$, $Ma^2 \ll Fr$ and a characteristic length $L \ll 12 \text{ km}$) reduce to the incompressible form:

$$\nabla \cdot \mathbf{u} = 0 \tag{3.4.2}$$

3.4.2 The momentum equation

$$\underbrace{\frac{\partial \rho u_i}{\partial t}}_I + \underbrace{\frac{\partial \rho u_j u_i}{\partial x_j}}_{II} = - \underbrace{\delta_{i3} g}_{III} - 2 \underbrace{\varepsilon_{ijk} \Omega_j u_k}_{IV} - \underbrace{\frac{1}{\rho} \frac{\partial p}{\partial x_i}}_V + \underbrace{\frac{1}{\rho} \frac{\partial \tau_{ij}}{\partial x_j}}_{VI} \tag{3.4.3}$$

where:

- I represents the storage of momentum.
- II represents the advection of momentum.
- III is the action of gravity.
- IV describes the influence of the earth's rotation.
- V describes the pressure gradient forces.
- VI represents the influence of viscous stress

To a close approximation, air in the atmosphere behaves like a Newtonian fluid Thus, the

expression for viscous stress allow us to write term VI as :

$$\text{Term VI} = \left(\frac{1}{\rho} \right) \frac{\partial}{\partial x_j} \left\{ \mu \left[\frac{\partial u_i}{\partial x_j} + \frac{\partial u_j}{\partial x_i} \right] - \delta_{ij} \left(\frac{2}{3} \right) \mu \left[\frac{\partial u_k}{\partial x_k} \right] \right\} \quad (3.4.4)$$

which after differentiation equals:

$$\text{Term VI} = \left(\frac{\mu}{\rho} \right) \left\{ \frac{\partial^2 u_i}{\partial x_j \partial x_j} + \frac{\partial}{\partial x_i} \left[\frac{\partial u_j}{\partial x_j} \right] - \frac{2}{3} \frac{\partial}{\partial x_i} \left[\frac{\partial u_k}{\partial x_k} \right] \right\} \quad (3.4.5)$$

which due incompressibility (eq 3.4.2) reduces to

$$\text{Term VI} = \nu \frac{\partial^2 u_i}{\partial x_j^2} \quad (3.4.6)$$

$$\frac{\partial \rho u_i}{\partial t} + \frac{\partial \rho u_j u_i}{\partial x_j} = - \delta_{i3} g - 2 \epsilon_{ijk} \Omega_j u_k - \frac{1}{\rho} \frac{\partial p}{\partial x_i} + \nu \frac{\partial^2 u_i}{\partial x_j^2} \quad (3.4.7)$$

I
II
III
IV
V
VI

This is the form of equation which is most used as a starting point for turbulence derivation.

3.4.3 The energy equation

The first law of thermodynamics is expressed by the energy equation, which reads for a fixed volume as:

$$\frac{\partial \left[\rho \left(e + \frac{u_i^2}{2} \right) \right]}{\partial t} + \frac{\partial \left[\rho u_j \left(e + \frac{u_i^2}{2} \right) \right]}{\partial x_j} = \rho \dot{q} - \frac{\partial q_i}{\partial x_i} + \frac{\partial u_i \tau_{ij}}{\partial x_j} + \rho u_i g_i \quad (3.4.8)$$

I
II
III
IV
V
VI

where:

I is the time rate of change of a fixed fluid element. That is the sum of its internal energy per unit mass e and its kinetic energy per unit mass $\frac{u_i^2}{2}$.

II is the divergence of energy advection

III is the volumetric heating due to radiation divergence or chemical processes.

IV is the divergence of heat flux.

V is the contribution by the total work (τ_{ij}) to the rate of energy change. This term is the deformation work and increase of kinetic energy

VI is the body forces work.

This equation can be decomposed into two equations: one for kinetic energy and the

other one for internal energy. The internal energy equation reads as:

$$\rho \frac{\partial e}{\partial t} = - \underset{\text{I}}{\nabla \cdot \mathbf{q}} - \underset{\text{II}}{p (\nabla \cdot \mathbf{u})} + \underset{\text{IV}}{\phi} \quad (3.4.9)$$

where:

I represents the internal energy change.

II represents the divergence of the internal energy flux.

III represents the work by volume expansion

IV represents the viscous dissipation.

3.4.3 The Scalar equation

$$\underset{\text{I}}{\frac{\partial c}{\partial t}} + \underset{\text{II}}{u_j \frac{\partial c}{\partial x_j}} = \underset{\text{III}}{v_c \frac{\partial^2 c}{\partial x_j^2}} \quad (3.4.10)$$

The physical interpretation of the terms is as the previous one. This equation is linear.

3.5 The Averaging Procedures

The equations given above are the instantaneous conservation equations for a fluid element (no leaves within it). These equations have to be averaged in some way. There are several approaches for averaging. These could be one or a combination of:

- Ensemble averaging approach.
- or
- Time averaging approach.
- and/or
- Continuous volume averaging approach.
- or
- Control volume averaging approach.

The averaging leads to the appearance of correlations between deviations of the quantities from their averages. These correlations have to be parameterized or solved explicitly by developing their own prognostic equation. In developing those latter equations, still higher order terms appear which have to be solved explicitly and so on. This constitutes the closure problem in turbulence. In this part, we cover the different averaging schemes and the resulting unclosed correlations. We will also discuss the effect of the intermittency on the form of these correlations.

In our canopy soil system, there are several scales of inhomogeneities or intermittencies in the spatial and time domain, respectively. In any time or spatial averaging procedure, the size of the averaged volume or size of the averaged time interval has to satisfy two main criteria, namely equations (3.5.1). These criteria are given in Bear and Bachmat (1990) for spatial averaging in porous media. These criteria would apply automatically to an ensemble average, since in well behaved natural systems, the satisfaction of these two conditions is guaranteed. In time averaging or continuous control volume averaging, there must exist some separation in the scales of inhomogeneities or intermittencies for these two conditions to be satisfied. This is an assumption which we make.

$$\frac{\partial n(x, S)}{\partial S} \Big|_{S=S_0} = 0 \tag{3.5.1.a}$$

$$\frac{\partial \overline{\tilde{n}(x) \tilde{n}(x+h)} \Big|_{x_0, s, h}}{\partial S} \Big|_{S=S_0} = 0 \tag{3.5.1.b}$$

where:

n is the property under averaging,

\tilde{n} is the deviation of this quantity from its mean

S is the volume, time interval or number of ensembles.

S_0 is the chosen volume or number of ensembles or length of time interval

x is the centroid of the averaging domain.

h is the separation distance.

In the spatial domain, we start with a fluid element in the canopy air space. Enlarging that volume to include a representative volume for the air and plant part represents the averaging volume 1. The canopy air space is a multiple interconnected air space, which means that any closed surface within the air space can not be shrunk to a point without crossing a solid space. This volume averaging will lead to the appearance of source terms due to the interaction between the plants and the air. The averaging rules for flow within porous media are given as eq.3.6.1 and eq. 3.6.2. We end up with cubes, in which the effect of plant leaves interaction with the air stream are included in the governing equations. Increasing this volume further to include a representative volume for a certain canopy type with its within row and between row inhomogeneities represents the second larger averaging volume. It is assumed that there are no correlations due to plant geometry which do not sum up to zero when going higher with our averaging volume from the averaging volume 1 to averaging volume 2. Going further with our averaging volume to have a representative volume for a region with two or three types of vegetation represents the third higher averaging volume. In all of these volumes, it is assumed that the given above two criteria hold. This is equivalent to assuming that a separation in the scales of inhomogeneities on the different levels of averaging exists. For all of these levels, the values of the correlations which result due to deviation of the averaged quantities from their means should be defined or parameterized.

In the time domain, there is the annual or diurnal cycle of global radiation. The latter one would represent the cycle of interest in our scale of canopy climate modelling. We need to average with an interval which is small enough to follow the changes in this diurnal cycle (6-7 minutes averages). The small turbulent scales of transport lies within this cycle. Small scale is meant relative to the synoptic scale. Within this time interval lies the different scales responsible for turbulent transport within the canopy. With the time interval of averaging, the values of the correlation which result due to time averaging have to be incorporated in the averaged equations.

There are the several variants in the averaging procedures. Our aim is to have one variant which has an easy parameterization. With different averaging procedures, different terms in the averaged equation will result. Below, we will show the different averaging procedures

Fig.3.9 shows a horizontal extension of a canopy layer with a layer of air above it. This air layer contains coherent structures which are distributed in some manner in the flow field. The structures could be thermally or mechanically induced. The structures which are mechanically induced and the large thermally induced ones will be convected with the flow field. Given enough averaging time, these structures will pass through every point in the field. The small size thermally induced structures will be more localized to the hot spots in the flow field i.e. a hot bare soil surface. They may disperse or move around, with the mean wind, but they will still be localized. The existence of those structures will depend on the heterogeneity of heating at the soil surface and the ability of the wind shear to smear out these small scale thermally induced structures. In a time-spatial average, if they persist in a certain location they will show as a correlation between a vertical wind velocity spatial deviation from its mean and a temperature spatial deviation from the spatial mean (equivalent to term III2 in eq.3.5.2) This is called dispersive flux in the case of canopy flow. The value of this correlation depends on height, since the averaging process by turbulence will need some time to smear them out. The large scale thermally induced structures, will also be convected all

over the flow field. So, given enough averaging time, they would not show up as a spatial deviation from a spatial mean.

We assume that these coherent structures have a double roller structure, as shown in a more detailed manner in fig.3.10, and that these are the main ones responsible for the major part of heat, mass and momentum transport.

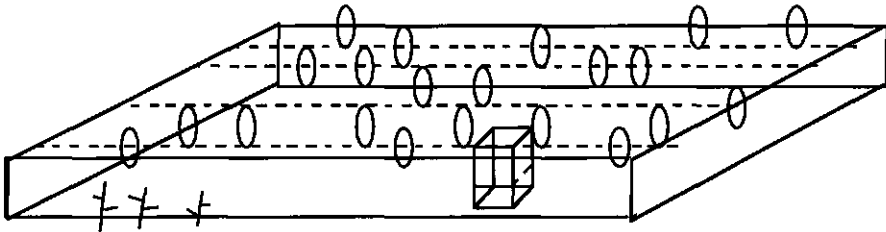


Fig 3.9. A figure shows coherent structures as represented by the ellipsoidal shapes with a certain distribution in a layer of air above a horizontal expansion of a canopy layer. The large parallelepiped volume is the maximum size of averaging volume 2. The inner parallelepiped represents stacked above each other volumes, which have the minimum size of the averaging volume 2. It is assumed that increasing the horizontal extent of these volumes, which are stacked above each other, to a horizontal scale as large as a coherent structure represents no loss of information. A detailed figure representing an inner parallelepiped is shown in fig 3.10. The shaded region in fig. 3.10 represents an intermediate size of averaging volume 2.

In time-averaging procedure, we consider one point in the domain or an averaged volume (which is larger than small scale canopy inhomogeneities) and do the averaging with respect to time interval length larger than the largest time scale of transport. The resulting equation reads as:

$$\begin{aligned}
 \frac{\partial \langle \bar{u}_i \rangle}{\partial t} + \langle \bar{u}_j \rangle \frac{\partial \langle \bar{u}_i \rangle}{\partial x_j} + \frac{\partial \langle \bar{u}_i \bar{u}_j \rangle}{\partial x_j} + \frac{\partial \langle \bar{u}_i'' \bar{u}_j'' \rangle}{\partial x_j} = - \frac{1}{\rho} \frac{\partial \langle \bar{p} \rangle}{\partial x_i} - \frac{1}{\rho} \frac{\partial \langle \bar{p}'' \rangle}{\partial x_i} + \nu \nabla^2 \langle \bar{u}_i \rangle + \nu \nabla^2 \langle \bar{u}_i'' \rangle
 \end{aligned}
 \tag{3.5.2}$$

I II III1 III2 IV V VI VII

where:

- I is the time rate of change of the time mean momentum (component i) of a volume average.
- II is the convection of the time mean momentum of a volume average $\langle \bar{u}_i \rangle$ by the spatial time mean momentum $\langle \bar{u}_j \rangle$
- III1 is the divergence of the turbulent transport due to spatial time averaged correlation between time deviations of the instantaneous momentum from its time mean.
- III2 is the divergence of the turbulent transport due to spatial time averaged correlation between deviations of the time averaged momentum from its spatial time mean (look at eq.3.6.7) . This term is called a dispersive flux, and it represents the effect of correlation

between inhomogeneities in the spatial domain on the total averaged flux

- IV is the gradient of the spatial time averaged pressure.
- V is the spatial time averaged gradient of the spatial deviation of pressure time mean from its spatial time average. This represents the effect of the form drag force by the leaves on the spatial time averaged momentum.
- VI is the effect of molecular diffusion on the divergence of momentum flux.
- VII is the effect of the spatial time averaged divergence of spatial deviation of time averaged momentum from its spatial time averaged values. That term expresses the viscous drag by the leaves on the flow.

We have seen in this procedure of averaging a complete failure of K-theory approach. Averaging spatially within a scale larger than plant parts is required to consider the sources and sinks within plant canopies. So a column or a cube is then considered. Use of second order or higher to obtain a counter-gradient transport has some assumptions, which are not fulfilled, concerning the uniformity of the behaviour of the terms within our time step of simulation and the closure assumptions, as we have shown qualitatively in the first part of this chapter.

Another variant is the spatial averaging procedure with a volume which is larger than the small scale of inhomogeneities and larger than the largest scale of transport. This averaging volume will be comparable to the horizontal volume shown in fig.3.9. It is like taking a snapshot of a representative picture of the flow field.

$$\frac{\partial \langle u_i \rangle}{\partial t} + \langle u_j \rangle \frac{\partial \langle u_i \rangle}{\partial x_j} + \frac{\partial \langle u_i'' u_j'' \rangle}{\partial x_j} = - \frac{1}{\rho} \frac{\partial \langle p \rangle}{\partial x_i} - \frac{1}{\rho} \langle \frac{\partial p''}{\partial x_i} \rangle + \nu \nabla^2 \langle u_i \rangle + \nu \langle \nabla^2 u_i'' \rangle \tag{3.5.3}$$

I
II
III
IV
V
VI
VII

where:

- I is the time rate of change of a spatial average of momentum.
- II is the convection of the spatial averaged momentum $\langle u_i \rangle$ by $\langle u_j \rangle$
- III is the spatial averaged divergence of turbulent momentum flux due to the spatial averaged correlation of momentum from its spatial averages.
- IV is the gradient of the spatial averaged pressure.
- V is the spatial averaged gradient of pressure deviations of the instantaneous values from its spatial mean. This represents the effect of the form drag by the leaves on the air flow.
- VI is the effect of molecular diffusion on the divergence of momentum flux.
- VII is the effect of the spatial averaged divergence of spatial deviation of momentum from its

spatially averaged values. That term expresses the viscous drag by the leaves on the flow.

Problems arise due to the quiescence profiles dominating the spatial averaged profile, since they are represented by a larger number of columns in which there is very little flux, while the averaged flux is mainly controlled by the columns lying under the coherent structures. The number of such columns are quite small in comparison to the total number of columns. This will lead to the same problem as in the time averaging with a time scale larger than the largest scale of transport.

In an attempt to correct for this, we try to go higher with the closure. The objections for this has been raised in Sect. 3.3. In Sect. 3.6.C, a measured time behaviour of the terms in the second order equation is shown.

3.6 AN INTERMITTENCY APPROACH*

We have seen in the first part of this chapter, that the other option for considering the effect of intermittency on the closure assumptions for the higher order terms is to reduce our time step of simulation and to take account of the correlations explicitly. In trying to develop an intermittent turbulent transport model, our averaging volumes and averaging time have to satisfy the two above mentioned criteria (equations 3.5.1). Since the coherent structures have a large cross flow dimension, we need to define an averaging volume such that the horizontal divergence of the fluxes due to the spatial dimension of the coherent structures is equal to zero. We assume that the cross stream dimensions of the coherent structure are larger than the scale of canopy inhomogeneity in that direction, and that there is a divergence zone in the flow which achieves no horizontal divergence of the flux of the momentum and scalar fluxes.

First, we do the volume averaging till averaging volume 1. That will give us parallelepipeds stacked above each other, in which the interaction between the leaves and the air is included. The horizontal layer shown in fig.3.9 constitutes a large number of columns, each representing such a stack of averaged volumes above each other. Increasing the size of the averaging volume from volume 1, where the volume averaging is done for air and leaf, to volume 2 leads, as we have assumed to no appearance of correlations between sources at averaging volume 1 to averaging volume 2. Enlarging the averaging volume from volume 1 to volume 2 then would introduce no loss of information. The averaging volume 2 has a minimum size which includes small scale canopy inhomogeneity. An intermediate size of average volume 2 would have a horizontal extension, which is large enough to include small scale inhomogeneity (i.e. within and between row inhomogeneities) and to be of width as large as the cross-stream dimensions of the coherent structures. The dimensions along the flow are such that small distances can be covered in the buildup process of scalars during the quiescence period. The averaging volume 2 has a vertical thickness which would allow us enough resolution of the vertical profiles within and above the canopy. This volume is represented by the shaded region in fig.3.10. The spatial averaging used is a control volume averaging approach. This process has the same characteristics as the ensemble averaging. In enlarging the averaging volume from 1 to 2, we do not have the problem of the

noncommutivity of spatial averaging and differentiation. We have already done this in obtaining the averaging volume one.

We assume that the canopy flow is a repetition of cycles of refreshment and build up which are caused by repeated passage of coherent structures at the canopy top. We do ensemble averaging on different cycles of coherent structure occurrences by adjusting the occurrence of the ramps associated with the ensembled structures and adjust time scales to match ramps of different durations. This will constitute our ensemble average at different points in the time cycle. This is shown in fig.3.10 by ensemble averaging of three large volumes, each with a counter-rotating double-roller structure in it. The purpose of using these larger volumes is to obtain an ensemble representation of all the stages of the coherent structure. Our averaging volume (the shaded area in the fig.3.10) will be such that along the

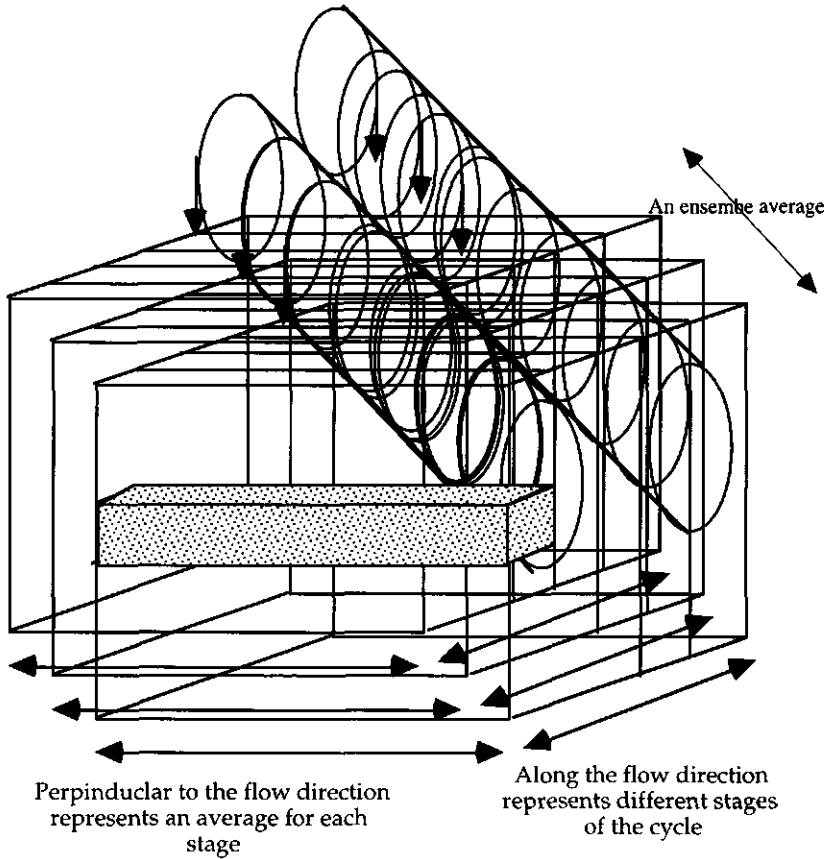


Fig 3.10: An ensemble average of three cycles which were adjusted for the occurrence of the ramp and to match cycles of different durations.

direction of the flow, there is not so much variation, while perpendicular to flow direction, the size should be large enough to have a horizontal divergence of fluxes equal to zero. The profile represented will be an average of several volumes across the flow.

There are two possibilities for the existence of such a volume depending on the distribution of the coherent structure in the flow field. In the case of a complete coverage of the flow field by parallel lines of these coherent structures, which have the same line of vorticity, the existence of high pressures regions under the boundary of the double-roller structures which are counter rotating leads to the satisfaction of condition (eq.3.5.1). In the case of dispersed distribution of the double-roller coherent structures, perpendicular to the flow there will exist a region of no horizontal velocity, due to the canopy drag. The difference in the duration of different gust cycles could be due to a variation in the gust intensity or simply due to that the passage of the coherent structures by the masts, used in the measurement, was along different sections.

We could have done our averaging directly on averaging volume 2. We get then an equation in which the source terms are shown due to the non-commutivity of the spatial differentiation and volume averaging. We then do ensemble averaging on the volume averaged equations.

In fig.3.10, it should be noted that there is a transformation: A particular control volume would occupy different regions in the three big cubes imposed upon each other while keeping each volume height and relative position in relation to its neighbours the same. Because of this, one control volume will see different regions in the gust and no-gust region. In this figure, we tried to superimpose three double-roller coherent structures above each other.

The **spatial averaging rules for a multiply interconnected air space** with moving canopy elements read as:

1. For a time derivative:

$$\frac{\partial}{\partial t} \int_{U_{oa}(t)} e \, dU = \int_{U_{oa}(t)} \frac{\partial e}{\partial t} \, dU + \int_{s\alpha\beta(t)} e \mathbf{u} \cdot \mathbf{n} \, ds \quad (3.6.1)$$

2. For spatial derivative:

$$\frac{\partial}{\partial x_i} \int_{U_{oa}} G_{jkl\dots} \, dU = U_0 \theta \frac{\partial G_{jkl\dots}^\alpha}{\partial x_i} - \int_{s\alpha\beta} G_{jkl\dots} \cos(\mathbf{n}, l\mathbf{x}_i) \, ds \quad (3.6.2)$$

The derivation of these averaging rules are given in Bear and Bachmat (1990). The application of these averaging rules on the instantaneous equation lead to the instantaneous volume averaged equations which read as.

$$\frac{\partial \langle u_i \rangle}{\partial t} + \frac{\partial \langle u_j u_i \rangle}{\partial x_j} = \frac{\partial}{\partial x_j} \left\langle k_u \frac{\partial u_i}{\partial x_j} \right\rangle - \frac{1}{V} \sum_1^m \iint_{s_i} k_u \frac{\partial u_i}{\partial n} \, ds \quad (3.6.3)$$

I
II
III
IV

$$\frac{\partial \langle c \rangle}{\partial t} + \frac{\partial \langle u_j c \rangle}{\partial x_j} = \frac{\partial}{\partial x_j} \left\langle k_c \frac{\partial c}{\partial x_j} \right\rangle - \frac{1}{V} \sum_1^m \iint_{s_i} k_c \frac{\partial c}{\partial n} ds \quad (3.6.4)$$

I
II
III
IV

A similar equation with a continuous volume approach is given in Finnigan (1985). The last term in these equations express the effect of the sources within our averaging volume.

By decomposing the turbulent signal into a small-scale component, which is dominant in the quiescence period, and a large scale component which is dominant during the gust intrusion period, we get

$$\begin{aligned} u_i &= \langle \bar{u}_i \rangle + u_i'' + u_i^s + u_i^l \\ u_j &= \langle \bar{u}_j \rangle + u_j'' + u_j^s + u_j^l \\ c &= \langle \bar{c} \rangle + c'' + c^s + c^l \end{aligned} \quad (3.6.5)$$

where:

u_i, u_j, c are the instantaneous values

$\langle \bar{u}_i \rangle, \langle \bar{u}_j \rangle, \langle \bar{c} \rangle$ are the volume averages of an ensemble mean or the ensemble mean of a volume mean (that does not matter).

u_i'', u_j'', c'' are the deviations of an ensemble mean from its control volume average

u_i^s, u_j^s, c^s are the ensemble deviations due to small scale(s) for u_i, u_j, c respectively

u_i^l, u_j^l, c^l are ensemble deviations due to large scale(l) for u_i, u_j, c respectively

where:

$$\overline{u_i^s + u_i^l} = 0 \quad (3.6.6)$$

$$\overline{u_j^s + u_j^l} = 0$$

$$\overline{c^s + c^l} = 0$$

$$\bar{u}_i = \langle \bar{u}_i \rangle + u_i'' \quad (3.6.7)$$

$$\bar{u}_j = \langle \bar{u}_j \rangle + u_j''$$

$$\bar{c} = \langle \bar{c} \rangle + c''$$

We assume that small-scale turbulence has a gaussian distribution with a time mean of zero. The total probability distribution of canopy turbulence, which describes the sum of the

large scale and small scale turbulence, is positively skewed for the u component and negatively skewed for the w component due to the effect of coherent structures on turbulence statistics. Because of the assumption of the gaussian distribution of small-scale turbulence, the time mean of the probability distribution of large scale turbulence is equal to zero. The region between the total probability distribution of u' and w' turbulence and the small scale turbulence, the latter was assumed to be the same for both u' and w', gives a probability distribution for u_i^l, u_j^l, c^l which will also have a mean of zero. In this averaging scheme, we could have assumed in the division between small-scale and large-scale turbulence that the ensemble mean of both of them is zero, by definition, but that could mean that our $\overline{u_i}, \overline{u_j}, \overline{c}$ would have two different values. We get in the equation for momentum or scalar the following terms:

$$\begin{array}{c}
 \left[\begin{array}{cccc}
 \langle \overline{u_i} \overline{u_j} \rangle & \langle \overline{u_i} \rangle u_j'' & \langle \overline{u_i} \rangle u_j^s & \langle \overline{u_i} \rangle u_j^l \\
 u_i'' \langle \overline{u_j} \rangle & u_i'' u_j'' & u_i'' u_j^s & u_i'' u_j^l \\
 u_i^s \langle \overline{u_j} \rangle & u_i^s u_j'' & u_i^s u_j^s & u_i^s u_j^l \\
 u_i^l \langle \overline{u_j} \rangle & u_i^l u_j'' & u_i^l u_j^s & u_i^l u_j^l
 \end{array} \right]
 \end{array}
 \qquad
 \begin{array}{c}
 \left[\begin{array}{cccc}
 \langle \overline{c} \overline{u_j} \rangle & \langle \overline{c} \rangle u_j'' & \langle \overline{c} \rangle u_j^s & \langle \overline{c} \rangle u_j^l \\
 c'' \langle \overline{u_j} \rangle & c'' u_j'' & c'' u_j^s & c'' u_j^l \\
 c^s \langle \overline{u_j} \rangle & c^s u_j'' & c^s u_j^s & c^s u_j^l \\
 c^l \langle \overline{u_j} \rangle & c^l u_j'' & c^l u_j^s & c^l u_j^l
 \end{array} \right]
 \end{array}$$

1
2

Ensemble averaging for equations 1 will lead to the disappearance of the last two values on the first row and the first column. The u_i'' is assumed negligible due to the fact that coherent structures we are considering are convected, they are moving around and they would not show in u_i'' . We assume no heterogeneity within our averaging volume. In case of coherent structures which are due to inhomogeneity in the field, i.e. between row and within row, u_i'' could be also decomposed to small scale and large scale. Volume averaging will lead to the disappearance of the second element of the first row and the second element on the first column. The $u_i'' u_j^s$, $u_i'' u_j^l$, $u_i^s u_j''$, and $u_i^l u_j''$ are terms representing interaction between scale of transport ; small or large and inhomogeneities of the surface or the volume. In case of complete homogeneities of the volume or inhomogeneities which could be smeared out, the third and fourth elements of the second row and the second column in the case of homogeneous canopy are zero.

The first element of the first row represents the advection by the mean flow which is quite minor. The element $u_i'' u_j''$ represents some kind of dispersive flux. In case of homogeneous canopy, it is zero. The instantaneous Reynolds stress tensor for momentum flux is composed of the last four elements. These are the most important ones. They do not vanish in the ensemble averaging. They represent turbulent fluxes at small and large scale and interaction fluxes. In the period of coherent structure intrusion into plant canopy, $u_i^l u_j^l$ is the most important. In the quiescence period, where the scale of transport is quite small

compared to canopy height, $u_i^s u_j^s$ is the active flux. $u_i^l u_j^s$ and $u_i^s u_j^l$ are important terms in the period around (i.e. before and after) the gust passage. These are interaction terms between two different components of the wind vector. In the case of $i=j$, these terms are zero since, by definition, u_i^l and u_i^s are mutually exclusive. In the case of $i \neq j$, we assume also that we can include these two terms in the gust parameterization and through an exponential decay for transport coefficient after the coherent structure passage. So now, for the averaged equation, we end up with four unclosed terms. This was the case for the momentum equation.

Concerning the scalar equation, the same procedure is applied. Ensemble averaging will lead to the disappearance of the last two values on the first row and the first column. The u_j'' is assumed negligible due to the fact that coherent structures we are considering are convected, they are moving around and they would not show in u_j'' . Volume averaging will lead to the disappearance of second element of the first row and the first element on the second row. In the enlarging process of the averaging volume from 1 to 2, c'' is assumed negligible. There

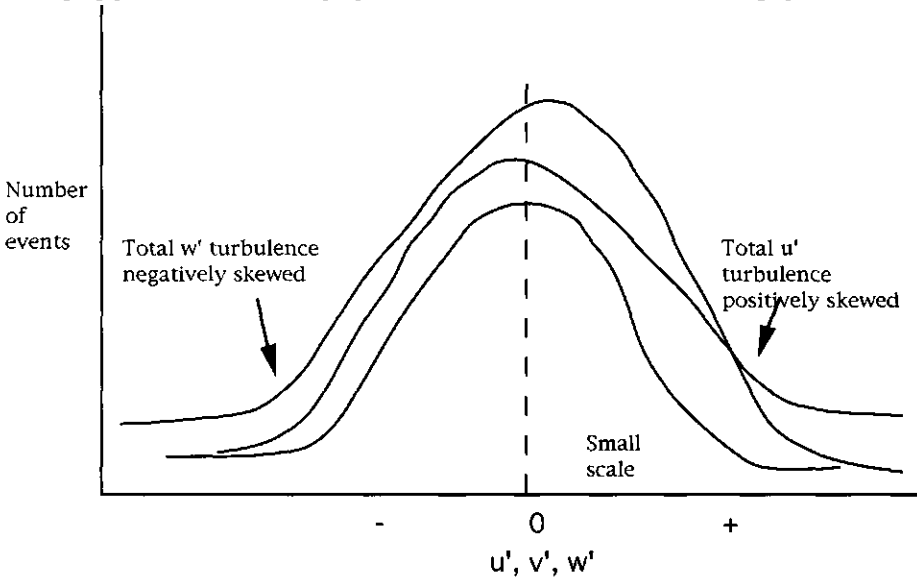


Fig. 3.11: an assumed behaviour of small scale and large scale turbulence.

are no small scale inhomogeneities in c . That will lead to $c^s u_j'' c^l u_j'' c'' u_j^s c'' u_j^l$, which are interaction terms, to be zero in the case of homogeneous canopy or if the inhomogeneities could be smeared out due to the flow being so turbulent or due to being far away from the forcing surface. These terms express the feedback between the inhomogeneities in the surface and the flow. We come back to these terms later (Sect. 3.6.B). The first element of the first row represents advection by mean stream which is quite minor. The element $c'' u_j''$ when averaged represents some kind of dispersive flux. The last four terms $c^s u_j^s$, $c^s u_j^l$, $c^l u_j^s$ and $c^l u_j^l$ we assume are the most important ones. They represent the turbulent flux of the scalar.

The last term is the most important during the gust intrusion. The first is the active flux during the quiescence period. The other two are interaction fluxes. We will discuss next the closure assumptions for these four terms for the mean momentum and scalar equations

3.6.1 THE CLOSURE ASSUMPTIONS

There are two ways to parameterize the effect of the gust intrusion on the mean scalar and the momentum equations:

In the mean scalar equation, the two terms $c'u_j^s$, $c'su_j^s$ in the case of one dimensional flow, are included in the gust intrusion and parameterized, in the first method, by an integrated value for that flux divergence for every layer at the end of the coherent structure passage period, so the state variable of the air at the end of the gust period would become $S_{t+\Delta t} = S_t - \nabla \cdot \text{flux} * \Delta t$. The value $-\nabla \cdot \text{flux} * \Delta t$ is parameterized by defining a refreshment function which represents the change of storage in the non-radiative energy exchange before the intrusion of the gust till the end of the passage period. If the duration of the intrusion is larger than a certain time step, the plants respond to the boundary conditions at the canopy top and there is no storage within the canopy air space.

The second method is by increasing the value of the exchange coefficient (K_m) value to a very high value. That will lead to the same effect.

In figure 3.10, we have identical double-roller structures. But in reality, there will be variations in the size of these structures. So there will be some arbitrariness in the definition of the boundaries of what is small and what is large, but all the structures have been synchronised on the occurrence of the ramp at the downstream end. The dispersion due to sizes or passage of structures at different cross sections shows in the upstream end and the sides.

We obtain this refreshment $Rf(z,t)$ from an assumption of the frequency of occurrence by Raupach, corrected by Paw U *et al.* (1992), or from a measured one and a depth of intrusion and duration. The frequency of intrusion according to Paw U *et al.* (1992) seems much less than the parameterization used in Kaviany (1990) or Bergström and Högström (1989). We see from a data set collected by Van Boxel (1988) that a complete refreshment is not far from reality (fig.3.3). It seems that the air is refreshed completely in the upper layers of the canopy. This is where most of the leaf area is concentrated. The assumption of complete refreshment would make a difference in the boundary conditions for energy partition at the soil surface. This effect depends on the surface resistance of the soil. That will affect the D'/\bar{D} ratio (i.e. vapour pressure deficit fluctuation / mean vapour pressure deficit), as we shall see in Sect.4.3. The $c'u_j^s$ is parameterized by using a local gradient approach. The value of K_m used during the quiescence period could be parameterized either by:

- 1) the use of wind speed time domain map (see for example fig.3.3.b). The square of this map after subtracting a mean value could be assumed to represent a time domain map for turbulent kinetic energy. The obtained value could be used to have an idea about the exchange which is proportional to turbulent kinetic energy. We still need a value for a time scale. This could be the value of the Lagrangian integral time scale during the corresponding period.
- 2) The second method is explained in the following section.

In the momentum equation, we use the second method by defining an increased value of the turbulent exchange coefficient during the first time step after the gust intrusion. That will lead to an enhanced momentum exchange between the above canopy air and the intercanopy air stream. The effect of this on the total solution is quite small due to the effect of the wind speed on the boundary layer resistance, which is a square root function. The first method does not work on the momentum equation.

3.6.2 THE PARAMETERIZATION OF K_m VALUES DURING THE GUST AND THE QUIESCENCE PERIODS

Two detailed data sets, which were collected by Van Boxel (Jacobs *et al* 1992 and Van Boxel 1988) and Van Pul (1992), are used to obtain a picture of the behaviour of K_m during a coherent structure cycle. For the first data set, details of the measurements are given in Jacobs and Van Boxel (1988) and in chapter 3 and chapter 6. For the second data set, we used one dimensional sonic measurements for a certain day (18-8-88) to see the pattern of w' variance behaviour. The selected data for analysis represent few hours of measurement (7 hours for both data sets). For the first data set, a day was selected in which the intermittency in the forcing signal (i.e. the intermittency in the incoming radiation at the canopy top) was low. The selected day was 30 July 1986. The general meteorological characters are given in Jacobs *et al.* (1992). The measurements started at 13.00 GMT. It was a sunny day with moderate wind (about 2 m s^{-1} at 4 m height). A picture of the exchange processes during a period of time when the intermittency in R_n was low, is shown in figures 3.3 and 3. 14.

We used the one dimensional sonic anemometer measurements at a height of 0.45 h to parameterize the transport coefficient during the quiescence period and correlated these values to the time domain maps.

We assumed that the mean vertical wind velocity is zero. So, by squaring all the values of vertical wind velocity, we obtained then the contribution of the different measured values to the averaged value of the w'^2 . We obtained then a mean value of the squared w'^2 . We divided the different readings by the mean value of w'^2 . The result gave us a time series of the ratio of instantaneous w'^2 (1 second averages) to the mean w'^2 . We then did a frequency distribution analysis on the number of events below a certain threshold and how much they contribute to the total mean. This gave us the following figures (fig 3.12, 3.13)

We see from figure 3.12 that for the two time series, during 74% and 67% of the time, the measured instantaneous w'^2 was less than the mean and contributed less than 0.19 and 0.2 respectively to the total w variance. Gusts less than 0.1 (0.077 and 0.08) of the events, thus occupying less than 0.1 of the time, contributed more than 0.51 and 0.37 respectively to the total variance.

Fig 3.13. shows the relative strength of the events, i.e. the cumulative contribution by a certain class of events, which is less than a certain limit, to the total variance, divided by the contributing number of events in the same class. Fig.3.13 is obtained by dividing the solid line over the dashed line in fig.3.12. Fig 3.13 shows that events, which have as relative maximum the value of the mean, have a relative strength of 0.25 and 0.3 respectively, while the events which have a relative maximum of twice the value of the mean had a relative

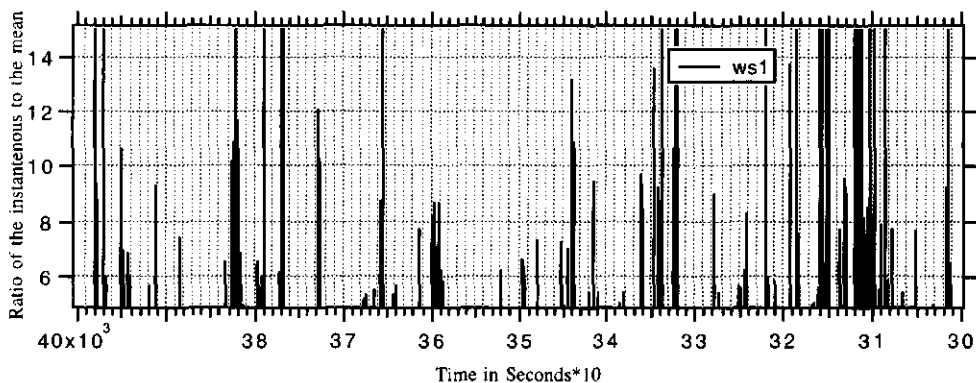


Fig 3.14.a The time occurrence of extreme events of w^2/w^2

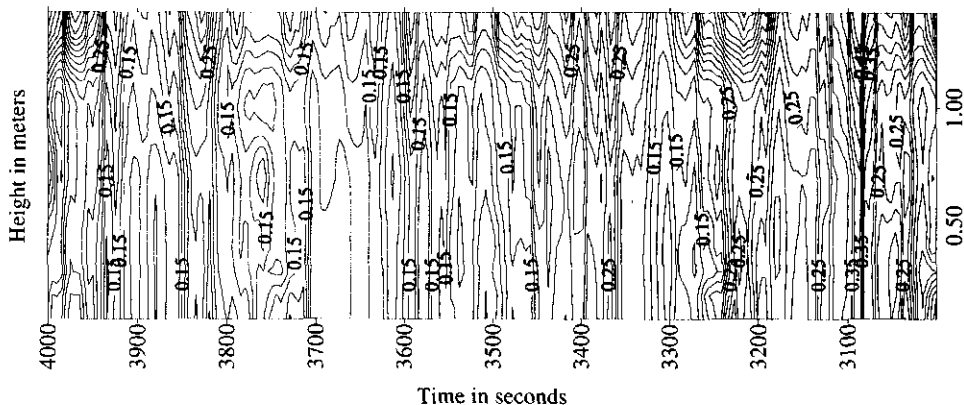


Fig 3.14.b The corresponding wind speed time domain map with time in seconds. Contour interval is 0.02m/s.

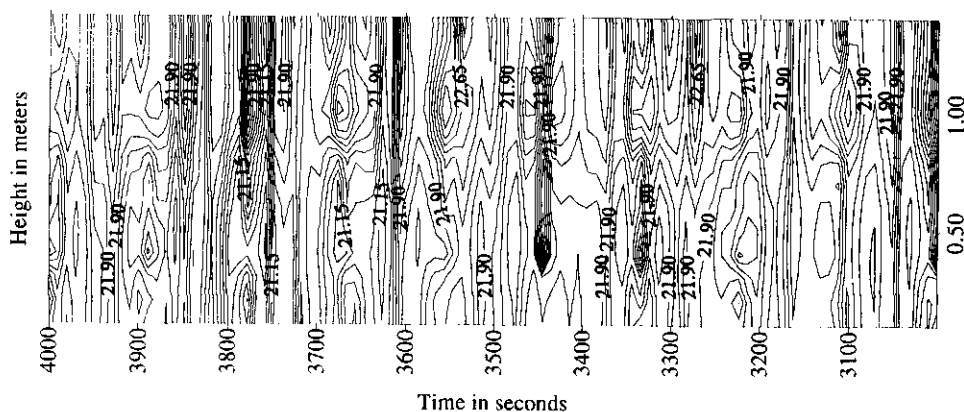


Fig 3.14. c The corresponding temperature time domain map with time in seconds. Contour interval is 0.15 °C.

3.6.B THE TIME AVERAGING APPROACH

In the previous procedure we used volume averaging to obtain an average for a certain segment along and perpendicular to the flow. We then did an ensemble average to obtain a representative average for different gust occurrences. This leads to different gust occurrences imposed above each other, while the same elementary averaging volume would be occupying different regions in the different cubes.

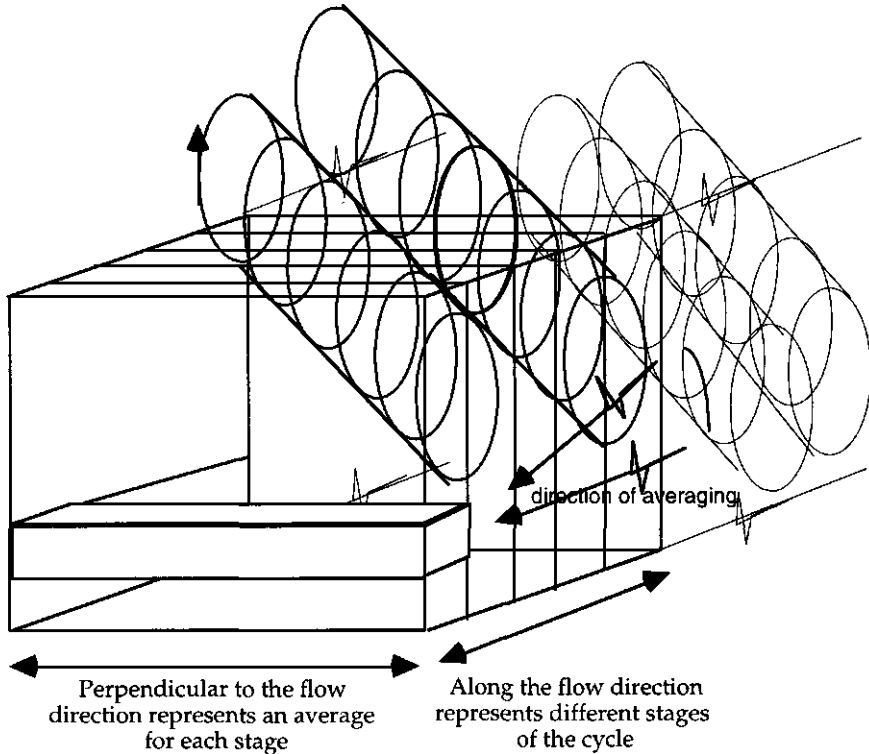


fig 3.15: The averaging is done with respect to time. The several occurrences of the gust passage are imposed upon each other by the use of a detection function, e.g. like VITA method or a visual detection.

In the following procedure, we keep our averaging volume the same and get a representative picture through time averaging.

We decompose the turbulent signal into a small-scale turbulence component which is dominant in the quiescence period and a large-scale component which is dominant during the gust intrusion period. The difference in the division between small-scale and large-scale deviation depends on some detection function.

$$u_i = \langle \overline{u_i} \rangle + u_i'' + u_i^s + u_i^l$$

$$u_j = \langle \overline{u_j} \rangle + u_j'' + u_j^s + u_j^l$$

$$c = \langle \overline{c} \rangle + c'' + c^s + c^l$$

where:

u_i, u_j, c are the instantaneous values

$\langle \overline{u_i} \rangle, \langle \overline{u_j} \rangle, \langle \overline{c} \rangle$ are the volume averages of a time mean

u_i'', u_j'', c'' are the deviations of a time mean from its volume average

u_i^s, u_j^s, c^s are the time deviations due to small scale (s)

u_i^l, u_j^l, c^l are time deviations due to large scale (l) for u_i, u_j, c respectively

We get in the equation for momentum or scalar the following terms.

$$\begin{bmatrix} \langle \overline{u_i} \overline{u_j} \rangle & \langle \overline{u_i} \overline{u_j} \rangle'' & \langle \overline{u_i} \overline{u_j} \rangle^s & \langle \overline{u_i} \overline{u_j} \rangle^l \\ u_i'' \langle \overline{u_j} \rangle & u_i'' u_j'' & u_i'' u_j^s & u_i'' u_j^l \\ u_i^s \langle \overline{u_j} \rangle & u_i^s u_j'' & u_i^s u_j^s & u_i^s u_j^l \\ u_i^l \langle \overline{u_j} \rangle & u_i^l u_j'' & u_i^l u_j^s & u_i^l u_j^l \end{bmatrix} \quad \begin{bmatrix} \langle \overline{c} \overline{u_j} \rangle & \langle \overline{c} \overline{u_j} \rangle'' & \langle \overline{c} \overline{u_j} \rangle^s & \langle \overline{c} \overline{u_j} \rangle^l \\ c'' \langle \overline{u_j} \rangle & c'' u_j'' & c'' u_j^s & c'' u_j^l \\ c^s \langle \overline{u_j} \rangle & c^s u_j'' & c^s u_j^s & c^s u_j^l \\ c^l \langle \overline{u_j} \rangle & c^l u_j'' & c^l u_j^s & c^l u_j^l \end{bmatrix}$$

1 2

We use a control volume average plus a time average. Time averaging leads to the disappearance of the last two elements of the first row and the first column. Volume averaging will lead to the disappearance of the second element in the first row and the second element in the first column. Concerning the third and fourth elements of the second column and the second row, they represent interaction terms between the spatial inhomogeneities and the small scale and large scale turbulence. These terms are related, with a negative feedback to the turbulent fluxes, due to the size of the averaging volume. In the case of large scale coherent structures which are moving around, these structures are not induced by small scale inhomogeneities of the surface. There are two kinds of these coherent structures: large scale thermally induced ones and dynamically induced ones. The dynamically induced ones could be large (Schols 1984 or Run B in Gao *et al* 1989) or small. The generation of the small dynamically induced ones are explained by Raupach *et al* (1989). The large scale thermally induced ones represent a response of the boundary layer above to the forcing from the underlying surface due to energy partition, so they respond to large scale inhomogeneities. In the case of small dynamically induced coherent structures, they also represent a response of the layer of air close to the vegetation to the drag force of the underlying vegetation. These latter will be responding to somewhat smaller scale forcing. The nonuniformity of this latter

forcing will be represented by the ratio of the distance travelled during the life time of that dynamically induced coherent structure to the distance between individual canopy elements and its relation to the averaging volume. This ratio in a way represent an expression of the forcing uniformity. The higher this ratio, or the closer it is to one, the less they will show as a spatial deviation. They will show in the time mean and not in the spatial mean. The decay of that coherent structures with travelling distance and the generation of a new one to take its place homogenize this correlation. The value of $u''C''$ becomes a residual non vanishing correlation. In the first case of a large scale coherent structure, the interaction terms between the large scale and spatial inhomogeneities will be zero by definition. If we were working with an averaging volume which represent two different kinds of vegetation, these two terms would not vanish and they have to be parameterized and the problem would be equivalent to the interaction between small scale spatial inhomogeneities and coherent structures. In the case of dynamically induced structures, with non-uniform drag media below, there would be some interaction between small-scale spatial inhomogeneities and large-scale turbulence. This problem would be present with averaging volume two. In the case of spatial inhomogeneities (i.e. hot spots with a field) which lead to generation of small scale thermally induced coherent structures which will disperse around. The shear will make these coherent structures decay. The ratio also between the hot spots spacing and the travelling distance over which the coherent structure is still alive will control the value of this non vanishing correlation (i.e. the importance of this correlations in our averaging). In this case, a parameterization for this effect has to be included.

In case of complete inhomogeneities, or homogeneities which could be smeared out, the third and fourth element in the second row and second column are zero.

As in the ensemble averaging, the first element in the first row represents the mean convection, the second element in the second row represents the dispersive flux. The third and fourth elements in the third and fourth row represent Reynolds stress term or turbulent scalar flux. They are treated in the same manner as in the ensemble averaging.

3.6.C THE VARIANCES AND TURBULENT FLUX EQUATIONS AND THEIR TIME VARIATION

In Sect.3.1, we have shown qualitatively the limitations of the second and higher order closure models by showing the effect of the coherent structure existence on the uniformity and so on the assumptions used for parameterizing the higher order terms (n+1) in the higher order (n) closure. In this part, we will show the time behaviour of the terms in the second order equations. From this, we will come back to the same conclusions we have derived earlier. In the following equations, we assume no plant parts intersecting the flow. We want to show the intermittency of the terms in the equations.

Our starting point is the turbulent vector or scalar equation which reads as:

$$\begin{aligned} \frac{\partial u_i'}{\partial t} + \bar{u}_j \frac{\partial u_i'}{\partial x_j} + u_j' \frac{\partial \bar{u}_i}{\partial x_j} + u_j' \frac{\partial u_i'}{\partial x_j} &= \delta_{i3} \left(\frac{\theta_v'}{\theta_v} \right) g + f_c \epsilon_{ij3} \overline{u_i' u_j'} - \left(\frac{1}{\rho} \right) \frac{\partial p'}{\partial x_i} + \nu \frac{\partial^2 u_i'}{\partial x_j^2} + \frac{\partial (\overline{u_i' u_j'})}{\partial x_j} \\ \frac{\partial u_k'}{\partial t} + \bar{u}_j \frac{\partial u_k'}{\partial x_j} + u_j' \frac{\partial \bar{u}_k}{\partial x_j} + u_j' \frac{\partial u_k'}{\partial x_j} &= \delta_{k3} \left(\frac{\theta_v'}{\theta_v} \right) g + f_c \epsilon_{kj3} \overline{u_k' u_j'} - \left(\frac{1}{\rho} \right) \frac{\partial p'}{\partial x_k} + \nu \frac{\partial^2 u_k'}{\partial x_j^2} + \frac{\partial (\overline{u_k' u_j'})}{\partial x_j} \end{aligned}$$

I
II
III
IV*
V
VI
VII*
VIII
IX*

(3.6.8)

$$\frac{\partial q'}{\partial t} + \bar{u}_j \frac{\partial q'}{\partial x_j} + u_j' \frac{\partial \bar{q}}{\partial x_j} + u_j' \frac{\partial q'}{\partial x_j} = \nu_q \frac{\partial^2 q'}{\partial x_j^2} + \frac{\partial (\overline{u_j' q'})}{\partial x_j}$$

I
II
III
IV?
VIII
IX*

(3.6.9)

The first two equations are the turbulent fluctuations equations for u_i and u_k , respectively. The third equation is the turbulent fluctuation for a scalar quantity where:

I is the time rate of change of the concerned quantity.

II is the convection term by the mean wind.

III is the production term due to the interaction between the turbulent fluctuations and the mean wind gradient.

IV is also a production term due to the interaction between a turbulent fluctuation in the wind velocity component and the gradient in the turbulent fluctuations of the scalar or the wind component. So it transports the turbulent fluctuations down into the canopy. After deriving the variances equation or the momentum or flux equations, this becomes the turbulent transport term. This term is nonlinear in the first and second equation. In the third equation, it is also nonlinear through the effect of scalar field on the buoyancy flux (term V in the first equation)

VII is the pressure fluctuation term. This term is nonlinear since it is related by the Poisson equation to the velocity field.

The asterisked terms are nonlinear terms in the above equations.

We will use time domain maps of the temperature as an example of a scalar, and the wind speed map as an indication for the wind velocity component. The time domain maps used are included as figures 3.3a,b and 3.14c,b and 3.16a,b. The behaviour of R_n within the corresponding periods for these time maps is shown in fig. 3.4.

We will define the mean as the average value for 16 minutes for different heights within and above the plant canopy. The 16 minutes period represents the time duration of one time map. The regions in the map in which the contour lines are quite separate would have more weight in representing the mean at a certain height. Strong deviations from that mean would be represented by regions in which the contour lines are quite crowded. If we assume Taylor's frozen hypothesis, the time domain maps which give the temperature or wind field passing through a vertical line or a plane would represent a picture of the flow field along a horizontal distance at a certain time. The second term in the equations would be representing the convection by the mean horizontal wind of the turbulent fluctuation, i.e. the role of the mean wind in carrying the wind variation (in strong cases the gust) around. For the vertical component, that term would have no effect since $\bar{w} = 0$. The third term is controlled by u_j' since the mean profiles for the period under consideration (16 minutes) and so their derivatives are constants, the third term will be then a function of u_j' . We can obtain the turbulent fluctuations map of both wind and temperature by subtracting a mean value for different heights. u_j' will be similar to u_j , since it is obtained after subtracting a height dependent constant (i.e. $\overline{u_j(z)}$). u_j' is also highly intermittent as can be seen from the same map (from the following map 3.16.b). q' can be obtained in a similar way by subtracting a height dependent value (i.e. the mean temperature as a function of height $\overline{q(z)}$) from the q map. q' is highly intermittent. The fourth term $u_j' \frac{\partial q'}{\partial x_j}$ represents the interaction between u_j' and the vertical gradient of the turbulent scalar time fluctuations $\frac{\partial q'}{\partial x_j}$ or the transport of q' by turbulent velocity fluctuations. This also represents the instantaneous scalar flux. The

difference between this term and $\frac{\partial(u_j' q')}{\partial x_j}$ gives the effect of the deviation of minus the divergence of the instantaneous heat flux from its mean on the value of the scalar deviations. We can see from the multiplication of the directional derivatives of one map with the other map that this term is highly intermittent. We know also from the measurement of other researchers that this term is highly intermittent. It could reach values as high as 20 times the mean flux (Gao *et al.* 1989). It is clear that the terms in the equations have cycles of intermittency or periodicity which relate to the passage of coherent structures. The same goes for similar terms in the momentum equation. For the extra terms in the momentum equations, especially the pressure correlation terms, there is also strong time variation in the pressure signal due to the passage of coherent structures. An example from a set of measurements of a pressure pulse at different heights is given by Conklin and Konner (1994) and Shaw *et al.* (1990).

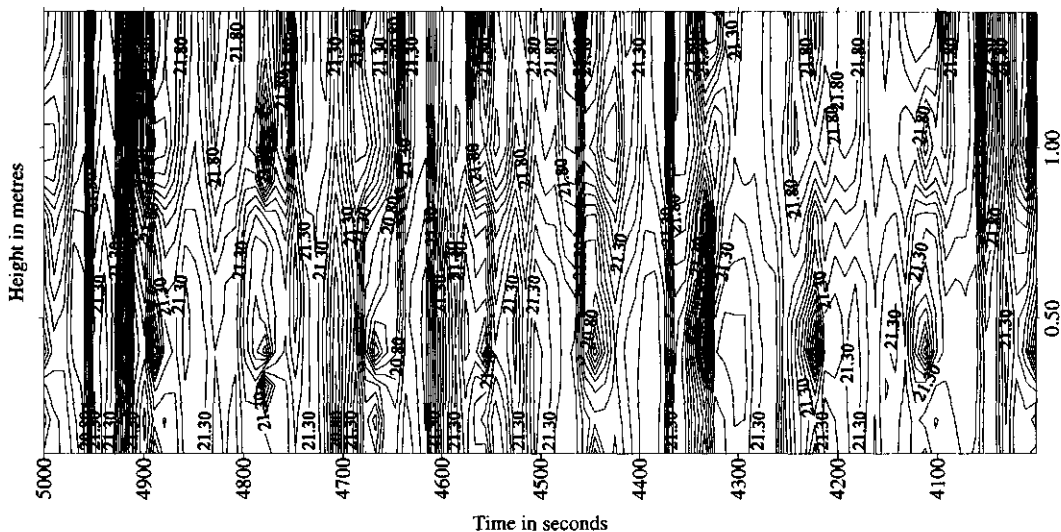


Fig. 3.16 .a A 1 sec averaged temperature time-height domain map representing 1000 sec. The starting time coordinate for the data series is from about 13.45 GMT on July 30 1986 within a maize canopy. Contour interval is 0.1 $^{\circ}$ C.

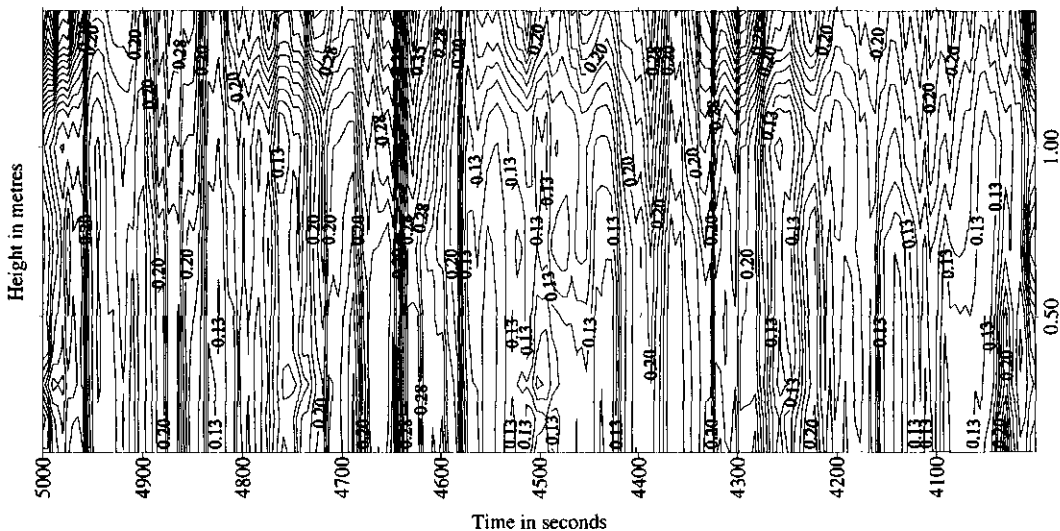


Fig. 3.16.b. A 1 sec averaged wind speed time-height domain map representing 1000 sec. The starting time coordinate for the data series is from about 13.45 GMT on July 30 1986 within a maize canopy. Contour interval is 0.015m/s.

The existence of intermittency in terms in the equations leads to correlations between terms, e.g. fluctuations and fluxes which may not sum up to zero. Trying to take account of this correlation will lead us to develop their prognostic equations. This leads to an attempt of going higher with our closures.

By looking at the higher order level equations before averaging, all the terms have time varying values which is related to the passage of the coherent structures.

$$\begin{aligned}
 & q' \frac{\partial u'_i}{\partial t} + q' \bar{u}_j \frac{\partial u'_i}{\partial x_j} + q' u'_j \frac{\partial \bar{u}_i}{\partial x_j} + q' u'_j \frac{\partial u'_i}{\partial x_j} \\
 & \text{I} \qquad \text{II} \qquad \text{III} \qquad \text{IV} \\
 & = \delta_{i3} \left(\frac{\theta'_v q'}{\theta_v} \right) g + f_c \varepsilon_{ij3} q' u'_j - q' \left(\frac{1}{\rho} \right) \frac{\partial p'}{\partial x_i} + q' v \frac{\partial^2 u'_i}{\partial x_j^2} + q' \frac{\partial (\overline{u'_j q'})}{\partial x_j} \\
 & \text{V} \qquad \text{VI} \qquad \text{VII} \qquad \text{VIII} \qquad \text{IX}
 \end{aligned} \tag{3.6.10}$$

$$\begin{aligned}
 & u'_i \frac{\partial q'}{\partial t} + u'_i \bar{u}_j \frac{\partial q'}{\partial x_j} + u'_i u'_j \frac{\partial \bar{q}}{\partial x_j} + u'_i u'_j \frac{\partial q'}{\partial x_j} = u'_i v q \frac{\partial^2 q'}{\partial x_j^2} + u'_i \frac{\partial (\overline{u'_j q'})}{\partial x_j} \\
 & \text{I} \qquad \text{II} \qquad \text{III} \qquad \text{IV} \qquad \text{VIII} \qquad \text{IX}
 \end{aligned} \tag{3.6.11}$$

The first term in both equations represents the correlation between a turbulent fluctuation of a scalar and a velocity component time derivative or a vector fluctuation and scalar time derivative for eq 3.6.10 , 3.6.11 respectively. The first equation is a nonlinear one. The second is a linear one except for the effect of the scalar on the density. The sum of these two terms constitutes the scalar flux which will be nonlinear. The second term in both equations represents the correlation between q' or u'_i and the convection of u'_i or q' by the mean wind respectively. This is equivalent to the correlation between the q' time domain map multiplied by a height dependent constant multiplied by the horizontal derivative of the other map. In case of vertical wind velocity, this constant is zero.

The third term represents the correlation between momentum flux or scalar flux and the derivative of the mean wind. The momentum or heat flux are highly intermittent signals. We know this from measurement by other researchers (e.g. Finnigan 1979 and Denmead and Bradley, 1985). The fourth term represents the instantaneous correlation between turbulent scalar fluctuations and a divergence of a momentum flux or an instantaneous correlation between turbulent vector fluctuations and the divergence of heat flux. This represents the correlation between one of the maps of fluctuations and the flux divergence of the other map and vice versa. The sum of these two terms (terms IV in eq.3.6.10 and eq.3.6.11) makes the turbulent transport term. During the period of simulation, this term is not uniformly distributed as shown by measurements by Gao *et al.* (1989). Flux divergence is related to the change of storage and the source terms by the general transport equation. During the gust

intrusion period, there is not enough time for the leaves to respond to rapid changes in the temperature or vapour pressure of the air. So the change in the storage around the gust passage is mostly related to the flux divergence. This term is non linear. The concurrent occurrence of a rapid change in q' and u' leads automatically to high values of the triple correlation terms. Trying to take account of intermittency will lead to the development of a third order closure equation which will contain a fourth order term. We showed earlier from the measurements by Gao *et al.* (1989) that this fourth order term is highly nonuniform. The assumption of the uniformity of terms during the time step of simulation is not justified. That brings us to the question: Would a large-time interval averaged value for a term in these equations within our time step of simulation, be as good as a varying in time, value for that term? Due to the high non linearity of these equations, the expected answer to this question is **NO**. Now, what can be gained by getting higher in the closure? The dispersion of the correlation which results from the pressure correlation as explained below will lead to more uniformity of the higher order terms ($n+1$) in the (n) closure equation and that could have allowed, some people, in a way to assume they counteracted the effect of the nonuniformity of the terms at lower level of closures and so they could have regained then the effect of nonuniformity of the terms at the lower levels which was lost due to the averaging. That would have been the case, if not for the nonlinearity of the equations. So, I am not sure that such an assumptions is correct.

The problem of intermittency will also show in the different terms which result from spatial averaging with the existence of plant parts intersecting the flow (Finnigan, 1985). The nonlinearity is even higher there.

3.6.D The importance of pressure fluctuation on the dispersion of the correlations

The dispersion of the correlation comes from the pressure field which leads to acceleration of the flow in the lower parts of the canopy. This means that the turbulent

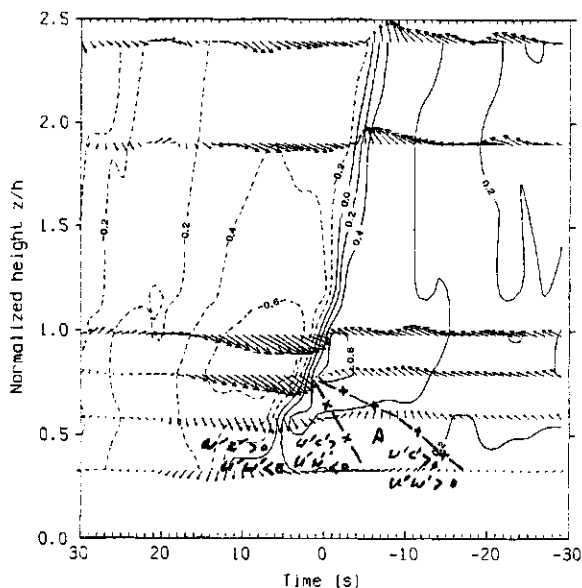


Fig 3.18. Vertical cross section of ensemble averaged and fluctuating velocity fields, under unstable conditions ($L = -138 \text{ m}$), during Run A. Dashed lines are isotherms below the mean, and solid lines are isotherms above the mean. Contour interval is $0.2 \text{ } ^\circ\text{C}$ and the maximum arrow length represents a wind magnitude of 1.9 m/s . Taken from Gao *et al* (1989) with kind permission Kluwer Academic Publishers. In area lined and marked with A notice the regions of different signs of $w'c'$ and $w'u'$.

velocity fluctuations in the lower parts of the canopy will have some kind of phase shift ahead of the temperature or scalar fluctuations. The pressure field (Shaw *et al* 1990) shows a maximum in the soil surface coincident with the passage of the coherent structure at the canopy top. An area of a phase shift in which there a dispersion between momentum and heat fluxes is shown here in figure 6.a, as taken from Gao *et al.* (1989) and included here as figure 3.17 in the area marked by A. Going higher with the closure assumes that there will a rapid dispersion of the higher order correlation such that the information we have missed could be obtained back quickly by going not very high with our closure. It seems as have been shown earlier that this is not happening till the third order closure and that coherent structures and their role in correlating higher order terms is quite important.

There are some reservoirs in the soil canopy system. In this case the canopy air and its storage of scalars and vector quantities which, due to the length scale of the coherent structures, have small time constants for different scalar and vector quantities. That leads to the high correlation in the values of some terms. If, for example, we were dealing with a non-ventilated open top chamber which is closed from the sides, the intrusion into this chamber due to the passage of a coherent structure would have been limited because of the weakness of the return to isotropy terms, and that would have led to lower percent of refreshment and only in the upper layer of the chamber and to an increase in the time constants of the system inside this chamber. The correlation of the fluxes during the gust passage would have been less important in comparison to the quiescence period. The problem of intermittency as we know in canopy flow would have not been there.

Now: what is the sensitivity of the solution to the difference between an assumed and real behaviour of the terms in the turbulent fluxes and variances equations and what is the use of higher order closure models if it takes so many levels of closure to disperse the correlations ? It seems that the rate of correlation dispersion is very low, as shown from the argument presented on Sect. 3.3. It seems, to me, that the use of large-time averaged second closure models leads to the introduction of flux divergence terms in the first order equations. These divergences, being not homogeneous with height, lead to something like the appearance of extra sources or sinks within height and that leads to their simulation of counter gradient transport. (!?). That is all, but this really leaves a lot of questions about the validity of such a solution. The validity of this assumption depends on the answer to the underlined part of above given question. A complete answer to this question needs a complete description of the behaviour of the Reynolds-averaged Navier-Stokes system of equations describing the canopy flow. We will try to give an approximate answer to the underlined part in the appendix 1.A. An attempt to describe the dynamical behaviour of an equivalent system of equations is given in chapter 4. This attempt proves that an intermittency in the turbulent transport does not lead to the same solution as a non-intermittent treatment. A similar mathematical analysis for the second or higher models would be quite complicated. So, we take the proven nonlinearity in the first order as an indication for the existence of a similar dependence on intermittency in the solution of the higher order equations.

3.7 IMPLICATIONS OF INTERMITTENCY FOR LAGRANGIAN MODELLING AS APPLIED TO CANOPY FLOW**

3.7.1. INTRODUCTION

The intrusion of coherent structures into plant canopies leads, during their ejection and sweep phases, to the displacement of the air inside the canopy upwards outside the canopy domain. A replacement of the displaced air by air from above the canopy accompanies this process. The ejected parcels of air from the canopy carry within them the amounts of sensible and latent heat, which have been delivered by the leaves and the soil to these air parcels while they were in contact with the leaves. The result of this process is a net transport of the scalar quantities between the canopy air space and the layer of air above. It has been shown by different researchers that this process is the one responsible for most of the large-time averaged *flux*. In the period of time between the passage of two consecutive coherent structures, the amount of sensible and latent heat which is delivered by the leaves to the intercanopy air stream will be dispersed around due to the scales of motion which are existent then in the flow. These scales of motion are quite small compared to the canopy height. This leads to a small scale mixing and a buildup of the storage of heat and moisture during the quiescence period. This buildup controls the large-time averaged *profiles*.

From this qualitative picture, it is clear that most of the large-time averaged flux occurs due to scales of motion which have a length scale larger than the canopy height and which leads, during their intrusion into plant canopies, to correlation in the motion of air parcels all over the canopy height.

Random walk models are used to describe the averaged concentration field at a certain point within plant canopies. This concentration field at a certain point results from the superposition of different plumes originating from different sources lying at different distances from that point. This superposition of the concentration fields assumes that the particles are moving independently of each other all the time. This assumes that the scales of motion responsible for dispersion, are relatively small in relation to the source distribution within height and that these scales are moving independently. These assumptions are obviously not valid during the gust intrusion period during which most of the large-time averaged flux occurs

In here, we discuss the effect of the deviation from these assumptions on the random walk models as applied to canopy flow. We suggest a method to correct for the effect of the correlation between directions of motion of particles, which are not close neighbours, on the mean concentration profile.

3.7.2. RANDOM WALK MODELS AS APPLIED TO CANOPY FLOW

In random walk models, the following equation is used (Raupach, 1989) and Lamb(1980):

$$c(z,t) = \int_0^t \int_{-\infty}^{+\infty} S(h) \overline{c_e}(z,t;h,t-s) dh ds \quad (3.7.1a)$$

or

$$c(z,t) = \int_{-(t-t_0)}^t \int_{-\infty}^{+\infty} S(h) \bar{c}_e(z,t;h,t_0) dh dt_0 \quad (3.7.1.b)$$

where

$c(z,t)$ is the mean concentration as function of height z and time (t) .

$\bar{c}_e(z,t;h,t_0)$ is the conditional probability density function that a particle being found at height z at time t , given it was released at height h at an earlier time t_0 . The subscript e means that this function is determined for an elementary source. An elementary source is an instantaneous (not continuous) point release of unit source released at t_0 and z_0 .

$S(h)$ is the source strength as a function of height.

The above integration is carried out for all heights and all times since release. For an elementary source, the resulting cloud depth keeps growing as a function of time. The centre of the cloud moves downstream with a velocity equal to the convective velocity of the air, as shown in fig.3.18. Fig.3.18 represents the development of clouds which are resulting from elementary sources, which have been released, all together at a certain moment at the same height, but at different points along the line BF between p_0 and p_1 . In figure 3.18, four of these clouds have been drawn, but with a vertical shift as a drawing trick to show, what happens to each one and the resulting effect on the concentration field at a certain point F, where the concentration field is measured. The clouds on the inclined line AY represent clouds which have the same lifetime (t_1-t_0) . They all have been released at the same moment and at the same height. In this case, at point F, a sensor does not see any more clouds with a lifetime less than $(t-t_0)$, since these clouds are being carried down from further away distances, and once they reach point F and continue being carried away, they will not be replaced by clouds with the same lifetime. The largest cloud which point F will see is the cloud which has a lifetime $(t-t_0)$ equal to the perpendicular distance between the lines p_0 and p_1 divided by the average wind velocity. The point F will keep seeing a concentration as if it was at the centre of a passing train of progressively older clouds (Eulerian), or equivalently the concentration at the centre of a convected progressively older cloud (Lagrangian). In the case of completely homogeneous canopy in the horizontal direction with continuous source releases at a certain height, the effect of a certain cloud being convected on the change of the concentration field at a certain point is compensated for by another cloud which would have the same time-since-release as the cloud which would have just left point F. The net result is that no changes in vertical depth or concentration are felt due to cloud migration. So, the effect of convection need not to be considered when we add all times since release in the above given integral. The shape of the cloud at a certain line PP becomes as shown in fig.3.19 (a continuous plume). This physical picture is clear and expresses the effect of the different previous times-since-release which are felt at the point under consideration. This time integral could be looked at as expressing the effect of different sources further away from the point

under consideration on the total concentration field.

For a continuous release at a certain height or instantaneous releases at different heights for several sources, the assumption of independent movement of the particles in the above integral is made. This problem will automatically occur when representing the time mean of

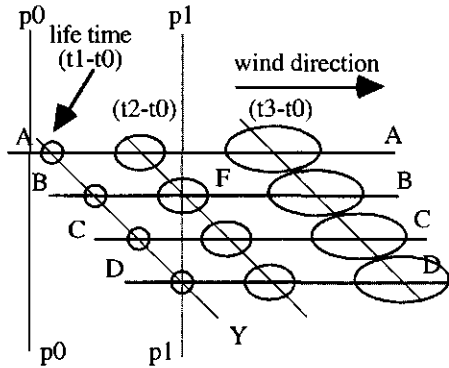


Fig 3.18. shows the concentration field as seen by point F resulting from instantaneous releases of unit sources at one line BF.

continuous releases at different heights. All the particles should be independently moving all the time (for separation times which are much larger than the integral time scale T_L) for all the heights. In the time mean, which we try to represent by an ensemble mean of particles moving independently, the question is : are the particles, which are being emanated by the sources into the canopy air stream, moving independently of each other all the time at all heights? Or is the time mean, which is reality, well represented by an ensemble mean of independently moving particles? The

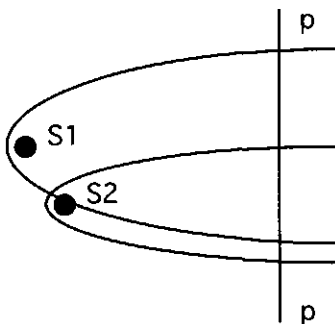


Fig 3.19 The concentration field due to continuous releases.

answer to this question is NO, since measurements show that most of the flux occurs due to organized motion which has a scale larger than the canopy height, leading to correlations between the particles motion at different heights. In that integral, it is assumed that the particles are moving independently of each other, i.e. that the probability of a particle 1 released at height h_1 arriving at height z_1 at a later time since release t_1 (Event A) has

nothing to do with another particle 2 being released at height h_2 arriving at height z_2 at a later time since release t_2 (Event B). z_2 could be equal to z_1 and also t_1 could be equal to t_2 . In case of z_1 equals z_2 , t_1 can not be equal to t_2 , since the particles released a short time after each other at the same height must have a definite correlation in their motion, expressing the persistence in the motion due to turbulence. This time is related to Lagrangian integral time scale and is considered already in the Langevin equation for describing the random motion of a particle. The correlations we are considering are between particles motions at different heights or motions at the same heights but separated at time with time intervals much larger than T_L . These correlations are due to large scale motions. In the case of two particles, the total probability of event particle 1 or particle 2 arriving at a certain height h ($h_1=h_2$) after some time from release t ($t_1=t_2$) equals

$$P(A \cup B) = P(A) + P(B) - P(A \cap B) \tag{3.7.2}$$

The dependence in the motion of the particles affects their destination after a certain time since release. This correlation, or dependence in the occurrence of the two events, should be subtracted from the total probability. The intersection of the events is controlled mainly by the scales of motion which are controlling the dispersion of particle 1 and particle 2. If it occurs that, for some time, the length scale of the structures responsible for dispersion is larger than the vertical distance between h_1 and h_2 , the two particles 1 and 2 will be correlated in their motion, i.e. they will be migrating together. This correlation in the motion should be subtracted from the total superposition. The time distribution (frequency) or the space distribution of the coherent structures and their length scale will determine the effect of these correlations on the total concentration field.

The evaluation of the effect of the correlation on the superposition in a direct way is very difficult. I have no solution this way.

An alternative method which is suggested here is based on what happens during a whole gust cycle, since this will describe the time mean, which is what we are trying to obtain, in a proper way.

3.7.3. A SEQUENCE OF EVENTS

After a gust intrusion into a plant canopy, the whole concentration field is replaced by a concentration field which is equal to the concentration at the canopy top. After the passage of a coherent structure, a certain point inside the canopy will start seeing progressively plumes up to a lifetime(time-since-release) equal to the time interval since the passage of the coherent structure. The concentration field at this point will be a superposition of the concentration fields from plumes with life time less than or equal to the time interval since the coherent structure passage.

During this period, the scales of motion which are responsible for dispersion are quite small in comparison to the source distribution, so there is independent motion of the particles which are being emanated to the air during the period between the passage of two coherent structures. So, the superposition of the concentration fields is possible and eq.3.7.1 would describe the concentration field at a certain point after a large period of time since the gust

passage and not the mean concentration at that point. The actual concentration after a time t is

$$C(z,t) = \int_0^t \int_{-\infty}^{+\infty} S(h) \bar{C}_e(z,t;h,t-s) dh ds \quad (3.7.3)$$

where t is the length of the period since the gust passage.

Mean c should be

$$\bar{c} = \frac{\int_0^{t_{\text{period}}} \left[\int_0^{t_{\text{period}}} \int_{-\infty}^{+\infty} S(h) \bar{c}_e(z,t;h,t-s) dh ds \right] dt}{t_{\text{period}}} \quad (3.7.4)$$

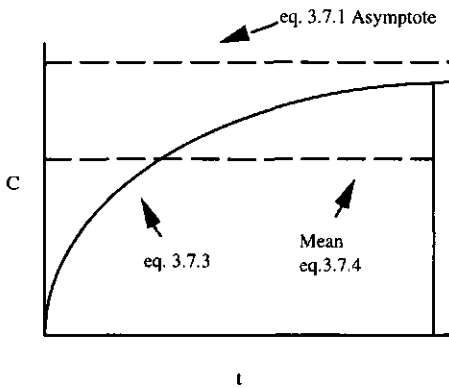


Fig. 3.20 A comparison between the behaviour of eq.3.7.1, 3.7.3 and the mean concentration as suggested here.

The mean concentration field is a function of height and the length of the period between the passage of two coherent structures (t_{period}). It is a weighted mean of eq.3.7.3. The difference between the mean concentration field according to eq.3.7.1 and the time mean of eq.3.7.3 is a larger effect for the earlier stages of the plume development on the mean concentration field. In eq.3.7.1, there is an equal weight for all the stages of the plume development, while in the mean of eq.3.7.4 the earlier stages are weighed more heavily. The author does not know exactly the shape of the development of eq.3.7.3. The curve representing this relation is an approximation.

Since the time mean is the mean we are interested in, the ensemble mean, obtained from equation 3.7. 1, should have been equal to the time mean in case of no correlation between the particles motions. The difference between the time mean as determined by eq.3.7.4 and the ensemble mean as determined by eq.3.7.1 represents the total effect of the correlation

between particle motions due to coherent structures on the mean concentration field.

To make the physical picture more clear, we discuss the difference between a time mean and a spatial mean. In the case of inhomogeneous turbulence, the scales of motion are nonuniformly distributed. The dispersion of particles at a single instant of time at different regions of the flow is controlled by the distribution of these length scales. An example of such a flow is given in fig.3.9. To get a mean spatial picture of the concentration field, we could have a representative number of pictures of the dispersion in different regions as a snapshot and average them. In regions where the length scale of motion is quite large in relation to the source distribution, the movement of all particles emanated now plus all other particles which have been around is controlled by the motion of the air within this parcel. Most of the flux between the canopy air layer and the layer above happens there. In all the other regions, in which the scale of motion is quite small and uniform, particles are being released and transported within each canopy layer.

Now for the time mean, if we have assumed that all the scales of motion keep moving around all over the flow field, one could obtain a time mean concentration field by putting a sensor in a representative spot and then do time averaging. During the passage of a coherent structure, a sensor will be seeing a concentration field equal to a background concentration. The sensor will start seeing plumes from sources lying close up stream. By the passage of time, the sensor will start seeing plumes from sources lying further and further upstream. The concentration field as a function of time will progressively be an addition of all these superimposed plumes. A time mean concentration field is a weighted average of all the time intervals. In case that, the scales of motion responsible for dispersion are not localized, the time and spatial average are exactly equal.

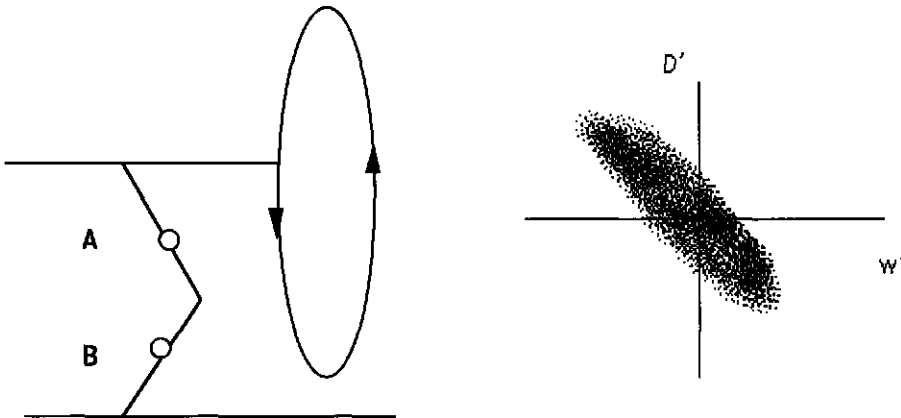


Fig. 3. 21a shows the correlation of the motion of the particles emanating at two different heights due to the passage of the coherent structures. The right hand curve shows the resulting joint probability distribution between w' (vertical velocity deviation) and D' (vapour pressure deficit deviation)

Another point worth consideration is that there is a large inhomogeneity in the value of Lagrangian integral time scale. For coherent structures, which have coherence in motion and persistence, the value of T_L is quite high compared to T_L for small scale turbulence. The

time behaviour of a dispersing plume at a certain height is simulated by considering the Eulerian-determined integral time scale is equal to the Lagrangian integral time scale. The Eulerian integral will see the effect of a coherent structure turbulence passing through the sensor and small scale background turbulence. The particle which has been subjected to a large scale coherent motion will experience much larger persistence in its motion. So there will be some kind of a Lagrangian integral time scale for the coherent motion, which will be much larger than that for back ground turbulence. The Eulerian-determined Lagrangian integral scale emerges from some kind of averaging for Lagrangian integral time scales for both motions. The persistence in the motion during the passage of the coherent structures will be large enough to remove all the wandering particles exposed to it from our domain of interest (the canopy air layers) to a height far above the canopy. The life cycle of a coherent structure is longer than the time required for the particles to be displaced to far above the canopy. The particles displaced upwards will be diluted. A consecutive structure will bring a volume of air from higher up to the canopy which has a lesser concentration. The probability of a particle displaced upwards to return to the canopy air space will be dependent on random motions. The result is that it is highly improbable that all the displaced particles are returned back (Entropy Law). So the effect of a coherent structure on the concentration is not forgotten (irreversible).

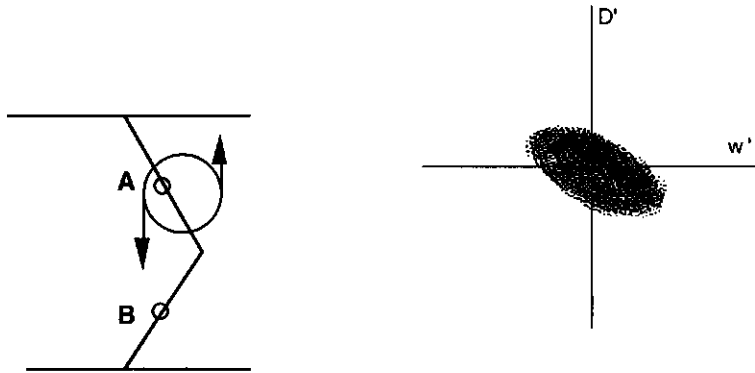


Fig. 3. 21b shows the independence in the motion of the particles motion at point A and B.. The resulting joint probability distribution.

The persistence in the motion term in the Langevin equation is representing the effect of the memory of the particle on its motion. The effect of the gust process is included in an approximate form on the motion of one particle through the generation of its initial velocity, according to some probability representing the occurrence of extreme events. The effect of coherent structures on correlating the motions of different particles, released at different heights and different times which are separated by time intervals much larger than T_L , is not included.

Now, we will discuss the behaviour of the flux as a function of time according to the above given picture. The flux at a certain boundary between two layers will be due to the sum

of component fluxes. Each is determined due to the dispersion, in the vertical, of the particles constituting a certain plume or cloud. The instantaneous flux then at a certain boundary between layers could be expressed as a time integral for of an ensemble average. The time integral is done for different sources with different times-since-release while, the ensemble average is done for a large number of source releases which have the same time-since-release. The instantaneous flux will be a superposition of different fluxes having different times since release i.e. a superposition of eq.4.2.9.a. Each component flux (q_i) has its own diffusivity, which is developing as a function of time as given by the term inside the square bracket in the integral on the left of eq.4.2.9.a. The concentration gradient in eq.4.2.9.a is a concentration gradient resulting from the concentration field due to sources which have the same time since release. The integration of eq. 4.2.9.a leads to eq. 4.2.9.b , which expresses the development of the instantaneous flux as a function of time due to the effect of plumes from sources far away being convected to the point under consideration. The mean flux is given by averaging eq.4.2.9.b.

$$q_1 = \overline{w'c_1'}^{ens} = \left[\overline{w'^2} \tau_L \left\{ 1 - e^{-\frac{t_0-t_1}{\tau_L}} \right\} \right] \frac{\partial \overline{c_1}^{ens}}{\partial z} \quad (4.2.9.a)$$

$$q_{\sum_{i=1}^n} = \int_0^t \overline{w'c_1'}^{ens} dt = \int_0^t \left(\left[\overline{w'^2} \tau_L \left\{ 1 - e^{-\frac{t_0-t_1}{\tau_L}} \right\} \right]_{top} \frac{\partial \overline{c_1}^{ens}}{\partial z} \right) dt_1 \quad (4.2.9.b)$$

$$\overline{q_{i+1}} = \frac{\int_0^t \int_0^t \overline{w'c_1'}^{ens} dt_1 dt}{t} = \frac{\int_0^t \int_0^t \left(\left[\overline{w'^2} \tau_L \left\{ 1 - e^{-\frac{t_0-t_1}{\tau_L}} \right\} \right]_{top} \frac{\partial \overline{c_1}^{ens}}{\partial z} \right) dt_1 dt}{t} \quad (4.2.9.c)$$

In the flux equation, there will be also a near field flux plus the far field component.

3.7.3.1 WHAT IS THE PROBABILITY OF RANDOM WALK MODEL RUNS CREATING SUCH CORRELATIONS ON ITS OWN ?

In random walk models, we run random experiments on different particles emanating at different heights at different times and then we sum the results of all these experiments as an ensemble average. We assume that this is equivalent to the time mean of running these experiments on particles released at different heights at the same time. The two main assumption behind this, are: that the scales of motion responsible for the dispersion of the scalars are small compared to the vertical distribution of the sources, and that these scales are not correlated in their motion. These two assumptions lead to the validity of the independent probabilities of distribution of the dispersing particles from different heights for elementary

sources. In every time step of all the experiments, we expose the particle to a random motion generated by a random number with a gaussian distribution and a certain variance. In a certain time step (let us say n) for one realization, the particle could be exposed to an extreme random number which, when multiplied by the variance and summed with a mean, leads to an expression of an extreme event. In another realization on a neighbouring particle, which starts at time zero and progresses till $t \gg T_L$. In the same time step (n) as for the first realization, if the random number generator has generated the same random number as for the first realization, that would mean that there is at this moment a correlation between the movement of particle 1 and particle 2. This would have expressed the fact, that the length scale of extreme events (i.e. coherent structures of our interest) is much larger than the canopy height or much larger than the source distribution with the canopy. In this case, we would obtain a correlation between the movement of the particles at different heights. The coincidental occurrence in a random walk model of two extreme events at two heights is equal to the probability of occurrence 1 * probability of occurrence 2, since both runs of the random number generator are independent. This will even be less probable for a case of several heights. If the random occurrence of extreme events at two different heights has a time lag of t steps, where $t: 0 - x$, where x is very large number, there will be a decay of the correlation of the particle motion and we will have from the summation independent realization of the flow. The chance of coincidental occurrence of extreme events at the same time step at several height at independent runs of a random number general is extremely low. It is equal to the multiplication of all the probabilities of occurrence at different heights. The increase in the time lag between the occurrence of the extreme events in the independent realization of the random experiment will lead to the disappearance of the correlation in the displacement of the particles at different heights. This will lead to a difference between the total sum of all the independent realizations.

In the case of an extreme events passing through, we use a T_L value which is quite small. It leads to the decay of the effect quite rapidly.

The physical picture of what happens in a plant canopy due to a coherent structure intrusion, and how a flux is generated, is completely different from results of a random walk model. In the latter, we get a counter-gradient transport on the mean due to the superposition of near field dispersion on the far field dispersion. This also happens in real life, but that is not the whole story. The flux resulting from the passage of a coherent structure is due to the positive $W'C'$ during both its ejection and sweep phases, which is resulting from collective motion of particles. The probability of this process, or something similar, within a random walk model is quite low. The diffusion of the particles in random walk is assumed to be due to the sum of persistence component and a random motion component for a large number of independently moving particles. It is a completely different mechanism.

In random walk models, the sequence of events is not considered. This is due to the fact that we assume ensemble averages are equal to time averages. We forget about the correlations of the motions at different heights, which play a role in the time averages but which become randomly occurring with very little probability in the ensemble averages.

It seems to me that the reason behind the failure of K theory approach, i.e. the length scale of transport is much larger than the scale of $\frac{\partial c}{\partial z}$, is the same which would lead to a

failure of random walk modelling, since this large length scale transport is quite large compared to the source distribution within height. That would lead to non independent movement of the particles at different heights.

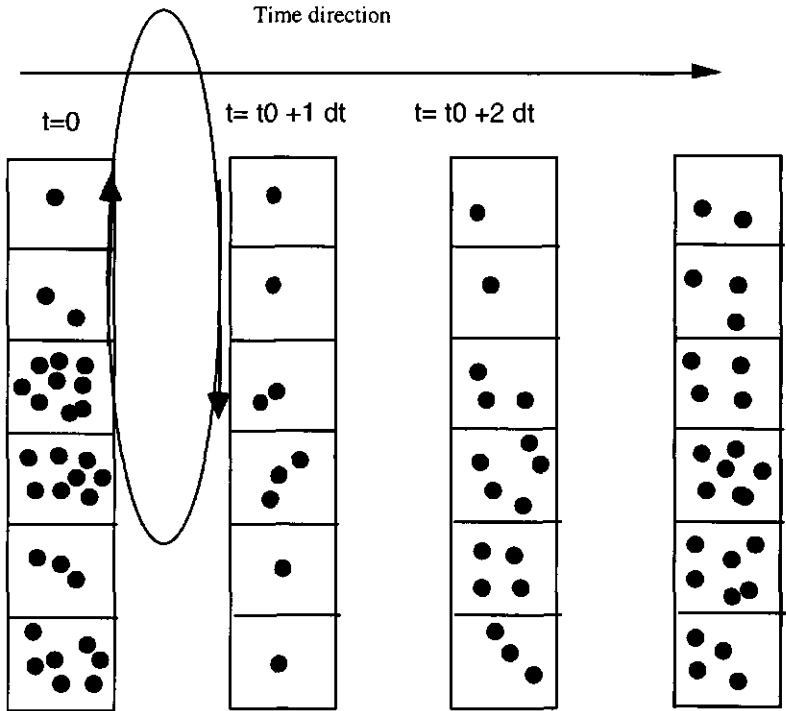


Fig. 3.22 shows what happens in reality in a certain time step due to the existence of coherent structures and the following build up.

The assumptions in random walk models could be valid only in the quiescence period.

To reduce the amount of particle dispersion during the quiescence period, we have to reduce the value of σ_w used in the simulation of the build-up of the temperature and vapour pressure. That will exclude the occurrence of extreme events during the quiescence period. That will lead to smaller absolute values of the initial velocities. Use of smaller T_L will lead to more effect of the random component on the dispersion.

Here, I would like to quote what G. I. Taylor wrote in his original article (1921), page 176: "The migration is still a discontinuous one, however. It suffers also from the disadvantage of depending on a special assumption, namely, that there is a definite correlation between the direction of motion in one infinitesimal element of path, and that in its immediate neighbours, but there is no partial correlation between the directions of motions in paths which are not neighbours." I think this is in complete agreement with what has been said here. The objections to the theoretical proof by Lamb (1980) which states otherwise, i.e. that his derivation is free from any restrictions has been outlined in Appendix 1.b.

CHAPTER 4

THE INTERACTIONS BETWEEN THE SOIL AND THE CANOPY: MODELLING* AND MATHEMATICAL ANALYSIS**

In this chapter, the assumptions used for modelling heat (sensible and latent) and mass exchange between the canopy air space and the soil will be covered. A mathematical analysis will be made about the effect of intermittency on the dynamical behaviour of the canopy soil system. We will cover several points:

- 1) An introduction about the interaction between the plants and the soil and the systems of equations solved to simulate that interaction.
- 2) The time scales of intermittency within the canopy soil system and the effect of this intermittency on the mean temperature and vapour pressure profiles of the air, on their evaluation and on the evaluation of mean sources and sinks within plant canopies. An analytical analysis of the system of equation, used to describe the canopy-soil system will be given. An analysis of the dynamical behaviour of the canopy-soil system under different situations will be carried out. An analytical analysis of the intermittency effect on the soil heat flux (G) and its integration will be given.
- 3) A quantification of the correlation between intermittency of transport and the non radiative energy sources within the plant canopy represented by the plant leaves and the soil.
- 4) The assumptions used in solving the energy budget equations for different soil layers.
- 5) A model for the water uptake by plant roots. This model was used, among other things, to quantify the effect of plants as sinks of water within different soil layers and to calculate the leaf water potential. These sinks were included in an equation to describe water flux between soil layers. We consider the effect of soil water potential on stomatal resistance as suggested by Tardieu *et al* (1993) and Tardieu and Davies (1993).
- 6) The coupling between heat and water transport, gas flux and the soil resistance to vapour flux under drying conditions.

4.1 THE INTERACTION BETWEEN THE PLANTS AND THE SOIL AND THE SYSTEMS OF EQUATIONS SOLVED TO SIMULATE THAT INTERACTION*

4.1.1 The interaction

The interaction between the plants and the underlying soil occurs mainly through four different means (arranged in the length of the process time scale)

- 1) The plants reduce the input of short wave radiation to the soil surface through shading. They also increase the long wave radiation down. Both of these effects lead to a modification of the radiative energy input to the soil (chapter 2).
- 2) The above-ground plant parts affect the turbulent transport regime within plant canopy. They induce the formation of coherent structures, which have a length scale as large as the canopy height and which are intermittent in nature. They also act as sources of non-radiative energy. The former effect leads to a modification of the turbulent exchange coefficient between the canopy air space, the soil surface and the layer of atmosphere above. A

modification of the mean temperature and vapour pressure profiles results. These two effects lead to a modified relaxation, i.e. a different ratio of the partition of the radiative energy absorbed by the soil surface into sensible, latent heat and soil heat flux. Superimposed on this scale of intermittency is the scale of coherent structures, which is induced by the forcing of the vegetated surface as a whole on the PBL (Planetary Boundary Layer). The resulting formation of much larger turbulent coherent structures exerts a large effect on canopy flow. These large coherent structures, with a scale as large as the PBL height, have a lower frequency and larger duration than the ones induced dynamically by the shear at the canopy top. These two kinds of coherent structures affect the temperature, vapour pressure of the air and the sources within plant canopies. They also modulate the flux between the canopy and the layer of air above.

3) The plants act through their roots as sinks for H₂O with different strength within different soil layers, thus affecting the thermal and moisture characteristics of the soil and the heat, water and vapour flux between soil layers. They modify then the thermal and moisture regimes of the soil, which affects the plant surface resistance for latent heat exchange through its effect on the stomatal resistance (sect. 4.5). The soil moisture and thermal regimes also control its salt regime, which controls the ionic environment of the plant roots. This would affect the plant productivity or chances of survival through shifting the environmental conditions into less favourable regions of their domain of existence.

4) The plants supply the heterotrophic microbial population with sources of energy (organic carbon) in the form of root exudates and root and plant residues, which in combination with the contribution of other micro-autotrophs form the source of chemical energy for soil heterotrophic micro-organisms. This interaction alters the soil physical and chemical properties.

The second effect has been covered partly in chapter 2 through the quantification of the canopy sources and sinks for sensible and latent heat. In chapter 3, we considered the behaviour of the coupling between the canopy and the layer of air above. The limitations imposed by intermittency of turbulent transport on the available approaches used for simulating heat and mass transport within and close above plant canopies were considered. An intermittent approach was thus formulated to consider the effect of intermittency on heat and mass transfer within this system. A numerical implementation of this approach was used to model the behaviour of the soil canopy system (chapter 5). In this chapter, we will consider the effect of coherent structures on the mean source and mean scalar profiles from a theoretical (analytical or semi-analytical) point of view, and the difference between an intermittent and non intermittent approaches in simulating these profiles. We will also consider the effect of this difference on the soil heat flux and the *soil temperature profile*. We will also cover the modelling of the plants effect on the soil surface resistance through its effect on the moisture regime of the soil and the feedback from the soil on the plant stomatal resistance (the second effect mentioned in point 3 above).

4.1.2 The systems of equations solved to simulate that interaction*

Quantification of heat and mass transport through any media, whether soil or air, requires the formulation of the appropriately averaged transport equations, the proper

parameterization of their coefficients, and solving these equations under a certain set of initial and boundary conditions. For a dynamic simulation, these boundary conditions have to be updated. For soil layers, we need to know the boundary conditions at the top and the lowest soil layers plus the initial conditions below the soil surface. The above soil surface boundary conditions are the radiative energy input at the soil surface which constitutes the forcing term and the temperature and vapour pressure of the first air layer in contact with soil as a function of time. These last two state variables, in combination with the value of the convective heat transfer coefficient between the soil surface and first air layer, form the necessary above-surface parameters needed to calculate the partition of the available energy at the soil surface. These variables tend to relax the forcing term and determine the soil heat flux (G). A known flux boundary condition, or a flux specified via a heat transfer coefficient and the temperature and vapour pressure of the air, could have been used. These boundary conditions are usually not known, while they have a strong feed back from the simulated system on them within a time scale as the one we are interested in. So, a high degree of resolution and a small time step is required.

For the canopy subsystem, the same boundary conditions at the soil canopy interface are needed to know the amount of sensible and latent heat flux which the soil contributes to the canopy air space. In this way, the soil and the canopy air space represent two coupled subsystems. Lack of knowledge of these boundaries makes the partition of the available energy at the soil surface unknown, and so the amount of available energy which goes to the soil as heat flux (G)

A better way is to treat the canopy and the soil as one system and then solve for the decoupling at the interface (sect. 4.4). The boundary conditions are then defined at e.g. twice the canopy height and deep enough into the soil, where the temperature of the soil is known as a function of time with a good degree of accuracy. Our soil-canopy system would then have no feedback on the boundary conditions, at least not within the time scale in which we are interested.

The problem in solving the coupling then is to define the spatial translation of the boundary conditions from screen height to the soil surface, taking into account the shift and the damping or the deformation which these boundary conditions suffer in their spatial translation downwards toward the soil surface. The spatial translation of the radiative energy input from measured values at screen height to the soil surface is done by considering the extinction of the short wave radiation profiles and the increase of the down welling long wave radiation due to the leaf temperatures through the canopy (chapter 2). For the determination of the temperature and vapour pressure of the air, solving the canopy turbulent transport equations taking into account all the possible sources and sinks and their time variations (chapter 3) is done.

Once the amount of soil heat flux (G) is known, it is used as a heat flux boundary condition for the soil layers or as an extra source in the equation of the first soil layer to calculate the soil temperature profile. Evaporation or condensation from different soil layers due to water vapour flux divergence represent sinks or sources in this equation. The conductivity coefficients for conductive heat flux are determined from the soil texture and an initial soil moisture content according to De Vries (1963, 1975). These coefficients are

updated for different time steps as the soil gets drier. The conductivity for water vapour flux are determined from a tortuosity model as given by Millington and Quirk (1961).

The amount of evaporation from the soil surface is used as a flux boundary condition in the soil moisture flow equation. Evaporation or condensation and water uptake by plant roots from different soil layers go as sinks or sources into this equation. The conductivity coefficients for water are calculated from Van Genuchten's model (1980), if valid, or from fitted functions for $K(\theta)$ or $K(h_m)$ functions where K is the soil hydraulic conductivity as a function of moisture content (Θ) or matric head (h_m).

The amount of water uptake by plant roots is calculated from a system of equations describing the water flow through the plant. For initializing this system of equations, we start at dawn and assume, that plants could have recovered during the previous night from water stress developed during the previous day. We could then assume that water potential is the same as that of the soil at dawn. We use the calculated latent heat flux from the leaves, imposed on the leaf surfaces at different layers in a mass flux form, as a known water flux boundary condition. The soil moisture potential at different soil layers is used as a lower boundary condition (a known water potential boundary condition). The calculated potential difference between the soil and the root at different depths is used, in conjunction with the soil, root and contact resistances, to calculate water uptake from different soil layers. These latter terms go as sink terms in the water transport equations. It is assumed that the soil moisture has a larger time constant than that of the plant water simulation. The amount of water taken up by roots at different soil layers, during one time step of simulation, will not affect the soil water potential. We can then use the soil water potential as a boundary condition for the solution of the plant water transport equations during our time step of simulation.

The whole system of equations is coupled and solved implicitly, using the values of the conductances as updated from the values calculated at the end of the previous time step. The validity of this assumption depends on the sensitivity of conductance changes to state variables changes within the time step of simulation.

4.2 Intermittency in the Canopy Soil System**

In the Canopy Soil System, there are several scales of intermittency superimposed upon each other. The existence of these scales of intermittency and the ability of some system components (here the leaves and the soil surface) to respond to them determine the dynamical behaviour of the system. Intermittency is defined as a change in the value of one of the forcing or driving, relaxing and state variables which control the system behaviour. This change could be gradual or sharp depending on the way time is scaled. Some scales of intermittency are self-induced and have a quick feedback on the canopy system, e.g. dynamically induced coherent structures. Others are also self-induced but have a slower feedback on the canopy soil system, since it requires a mechanism of interaction from a neighbouring system with a larger time constant, e.g. large coherent eddy structures in the PBL above the canopy. Others are externally imposed and could have been self-induced, e.g. cloudiness. The daily cycle of extraterrestrial radiation is completely externally induced. For

the canopy soil system (fig. 4.1), the forcing variable is the shortwave net radiation, $R_{n,short}$, and the long wave radiation, $L(z,t)$, energy load on the plant surfaces and the soil. The short wave radiation loading as a function of height (z) and time (t) has different scales of intermittency superimposed upon each other. These constitute the total functional behaviour of this driving variable. The diurnal cycle of radiation superimposed on it changes by different degrees of cloudiness or leaf flutter are some examples. Cloudiness intermittency, in the time scale we are interested in, is difficult to handle because its time scales are not known and, moreover, it does not have a semi-deterministic form similar to that of the large scale turbulent transport. A good representation of the radiative energy input is done by updating the incoming short and long wave radiation on regular intervals for clear or overcast skies. In other cases, updating a measured incoming short wave radiation signal, once an intermittency is detected, could be used. The independence of the interaction of the plants with the short wave radiative field, from the final solution (temperature and vapour pressure of the air), gives good enough time dependent representation of the short wave energy load $L_S(z,t)$ on the leaves and the soil. This represents $\alpha_r R_S \downarrow A_r$ in eq.4.2.1, which is the energy budget equation for the leaf surface. The net long wave radiation load is the second term in this equation. Leaf longwave emission, sensible and latent heat flux from the leaves to the canopy air layers, and their time variations, would depend on the time scale of variations of the temperature and vapour pressure of the air and also on the variation of the convective latent and sensible heat transfer coefficients between the leaves and the surrounding air (r_b and r_s). The state variables of the air have, in addition to the diurnal time scale, an extra time scale of intermittency due to turbulent transport playing a role in the transport of sensible and latent heat and no role in the transport of radiative energy. So, for energy partition at the leaves and the soil surface, $H(z,t)$ and $LE(z,t)$ will have a different time behaviour from $L(z,t)$. The scale of intermittency in the temperature and vapour pressure of the air within the canopy, due to turbulent transport, is controlled mainly by;

1) the space distribution of the turbulent structures, and how they are convected around in the flow field. This controls, in a certain point in the flow field, the time distribution or the occurrence of these coherent structures and the active length scales of the turbulent transport mechanism and so the time variation of the fluxes

and partly by:

2) the source variation or the source response to this intermittency.

The former tends to mix and move air around leading in the process to scalar quantities transport. This transport has a quasi-deterministic form or periodicity that achieves most of the transport of these quantities between the canopy and the layer of atmosphere above. The induction mechanism of these scales has been briefly discussed in chapter 3. The spatial scale of the mixing processes is quite large compared to the canopy height due to the large length scale of these coherent structures. This introduces mixing across regions where there exists a large difference of these state variables. This leads to a rapid change in the temperature and vapour pressure of the air. The rapid replacement of air parcels within canopy air space represents a rapid change in the turbulent transport coefficient. The resulting rapid variation in the time rate of storage change of these scalar quantities within canopy air layers represents a rapid time change of the flux of these scalar quantities between the canopy air layer and the layer of air above. This change of storage affects the partition of the absorbed radiant energy

at the plant and soil surfaces. The change of storage is shown in fig 4.1 by the curves in the rectangles representing air layers. This storage change depends on the time scale of temperature and vapour pressure changes, their duration and the ability of the leaves to

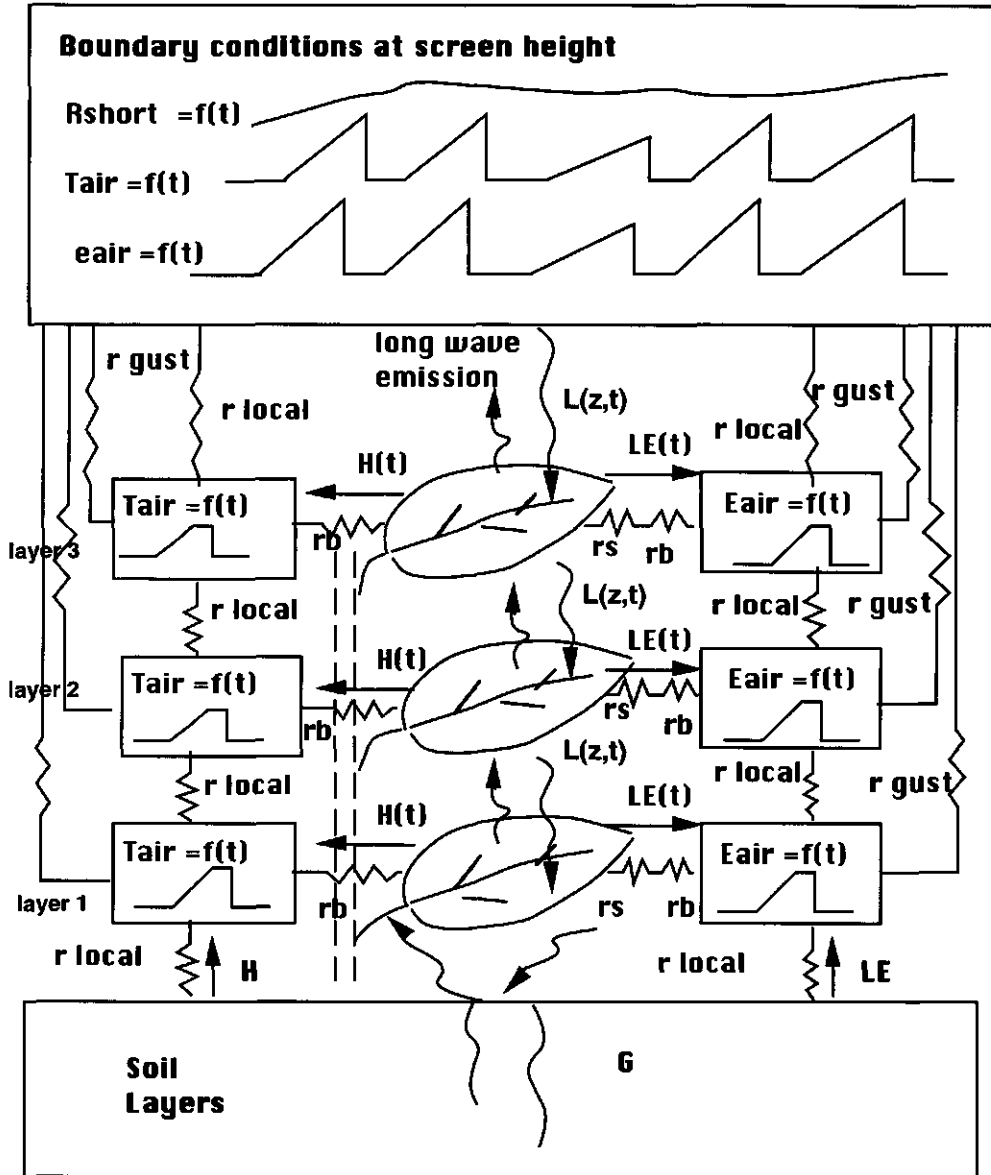


Fig 4.1 A schematic outline which shows the different subsystems and their forcing, relaxing and state variables and their scales of intermittency. The amount of energy which is delivered by the leaves and the soil to the air layers are evacuated by small scale resistance (r_{local}) and a large scale one (r_{gust}) representing the effect of coherent structures. The rest of the symbols are given in appendix 3.

respond to such changes. This ability of the canopy sources to respond to such changes and the coincident reduction in the turbulent transport between the canopy air space and the layer of air above during the quiescence period, see sect.3.6.2, lead to a significant increase in the storage of the scalar quantities during the quiescence periods. These last two factors will relate to the ratio of D/D_{mean} as we shall see later (sect 4.2 or eq.4.2.104). This storage change i.e. build up will modulate the sources again. This interaction between the sources and the storage change represents a correlation between the sources and the temperature or vapour pressure, which we smear out when we average with a time interval larger than the coherent structures cycle of intermittency.

In fig 4.1, an intermittent signal at screen height is also detected at lower levels. That is due to the large scale coherent structure bringing air from much higher heights than screen heights with different temperature and moisture content. Even if the coherent structures were bringing air from screen height only and not from further up, the difference in the temperature and vapour pressure profiles within depth, due to the variation in source distribution, would lead to the appearance of an intermittent temperature and vapour pressure signal at lower depths.

From the previous discussion, the following questions arise, which have to be answered:

1.a) Will the resulting variation in the short-time averaged energy partition at the soil surface and the leaves lead to an appreciable integrated effect in time, on the mean temperature and vapour pressure of the air, in comparison to a large-time averaged model (the gust process is either absent, i.e. first order closure model, or implicitly accounted for, i.e. second or higher order closure models) ?

or equivalently:

1. b) Does intermittency have an effect on the evaluation of the mean sources and sinks within plant canopies? Or equivalently: Does the mean concentration profile differ due to the gust effect?

1c) Is the use of a large-time averaged K_m value equivalent to a fluctuating K_m value with the same mean? or in other words; is the system linear?

1.d) Under what condition is the difference between an intermittent and non intermittent approach significant (more than 10%)?

Equivalently, in the case of a large-time averaged model:

2.a) Does the source build-up correlation affect the evaluation of the large-time averaged mean source or profiles within plant canopies?

2. b) Do normal (large-time averaged models) approaches consider this effect?

3) What difference does this make on the soil heat flux? The latter, when integrated, controls the soil temperature profile, and the question is extended to:

4) What effect does the introduction of an intermittent model have on *the mean temperature of the soil and the air layers?*

In general, there are two methods to answer the above given questions quantitatively either: a) Numerically or b) Analytically or semi-analytically:

a) Numerically by formulating a complete numerical soil-canopy turbulent transport model in which the interaction between the different components of the system is considered. Depending on the level of detail of simulation, a detailed description of intermittency could be included in the model and then numerically integrated or an implicit account of intermittency is followed.

For the detailed consideration, an intermittent model has been introduced. The effect of intermittency in the gust model could be considered by allowing the turbulent transport coefficients to vary as a function of time and/or introducing intermittency as a step function in the state variables of the air. One would then observe the long time behaviour of the simulated model, represented by the soil temperature profile and soil heat flux, under different assumptions. These assumptions would concern the time behaviour of the turbulent transport coefficients.

The implicit or less detailed approach or continuous approach, on the other hand, is done by assuming certain forms of the correlations between the different components of the system which result due to intermittency and include these within our less detailed model.

The distinction between these two simulation methods can be stated briefly as follows: In simulating any dynamical system, there are many scales of intermittency. If any of these scales has a correlation with a behavioural aspect of one of our system components within a time scale less than our step of simulation and which in the considered mean does not sum up to zero, we have to:

1) find a way to include or evaluate the effect of this intermittency behavioural aspect correlation on the large-time averaged set of equations used to describe the total system behaviour

or

2) reduce our time step of simulation and take account of the correlation explicitly.

Now, as we talk about the time mean, is it the five minutes mean or the fifteen seconds mean? The mean value is just a matter of definition, keeping in mind satisfying equations 3.5.1 a,b. In a large-time interval averaging (5-15 minutes mean), the temperature change due to the gust effect will be represented by a deviation from an assumed or a measured mean. In a measured data set, the time mean for a certain interval is well defined. In a simulation trial, the agreement between the simulated and measured mean values of the state variables of the system depends on the correctness of the assumptions used in the modelling process and the sensitivity of the model output to these implemented assumptions. In a large-time averaged model, we need to simulate the corresponding time mean right by putting in and correctly parameterizing the effect of any missing correlations within our averaged time interval in the mean equation. The effect of such an assumption in simulating the mean could be quite severe.

In chapter 3, we have addressed this problem and introduced two other reasons than the source build-up correlations, mentioned above, for the introduction of an intermittent approach. The first is that, due to the nonlinearity of the equations and the nonuniformity of the terms behaviour within large-time interval averaging, a requirement for correct Reynolds averaging of the non-linear Navier Stokes equation is not met (Appendix 1.A). The second is that intermittency leads to a problem with the correlation between the terms during our time step of simulation. The assumptions used to feed the resulting correlations back into the large-time averaged solution, and to close the higher order terms in the Reynolds averaged Navier-Stokes equation, are not met. Intermittency leads to inhomogeneities of these higher order terms which are not homogenized by going higher with the closure. Under such conditions, we do not have a theoretically valid large-time averaged system of turbulent transport equations to describe heat and mass transfer within plant canopies. An intermittent approach for describing heat and mass transport within plant canopies was thus introduced to take account of the intermittency and its correlation explicitly.

The numerical method, especially the more detailed one, would allow for a precise implementation of different scenarios and studying their effect on the behaviour of the simulated system but this, most of the time, comes on the expense of reducing the visibility of the system behaviour.

b) Analytically or semi-analytically by assuming certain simplifications which would allow solving a conservation equation describing a certain aspect of the canopy system behaviour. The analytical approach allows for better visibility of the system behaviour. The simplifications implemented should not reduce the system into idealistic cases, which would make the obtained solution of very limited use. On the other hand, not enough simplifications may produce a form of the equation which could be only solved by numerical methods.

In this chapter, In sh'aa ALLAH, we will answer the above given questions (1, 3 and 4), in a close to analytical form. This would give a more theoretical justification and insight to some of the results reported in sect.4.2 (The MATHCAD® runs). We will cover the assumptions used in the analysis. Question 2 will be answered by scaling of the different terms in the flux equations (sect.4.3)

4. 2. a. DEFINITION OF THE PROBLEM

Since the Penman-Monteith equation (eq.4.1.1) is linear in the vapour pressure deficit, D, assuming no feedback on the resistances (r_b and r_s) within a gust cycle, a different form of the variation from the \bar{D} while keeping the same value of the \bar{D} should give the same value of the mean source, i.e. eq.4.1.2 is valid.

$$\lambda E = \frac{sR_n + \rho C_p D r_H^{-1}}{s + \gamma^*} \tag{4.1.1}$$

$$E(\bar{D}) = \overline{E(D)} \tag{4.1.2}$$

where D is vapour pressure deficit, \bar{D} is its mean and E is energy in the form of evaporation (λE) or sensible heat (H). If a numerically detailed intermittent approach gives a solution

different from a continuous one, it must mean then that this is due to a different value of the simulated mean temperature and vapour pressure of the air, resulting in a different mean D .

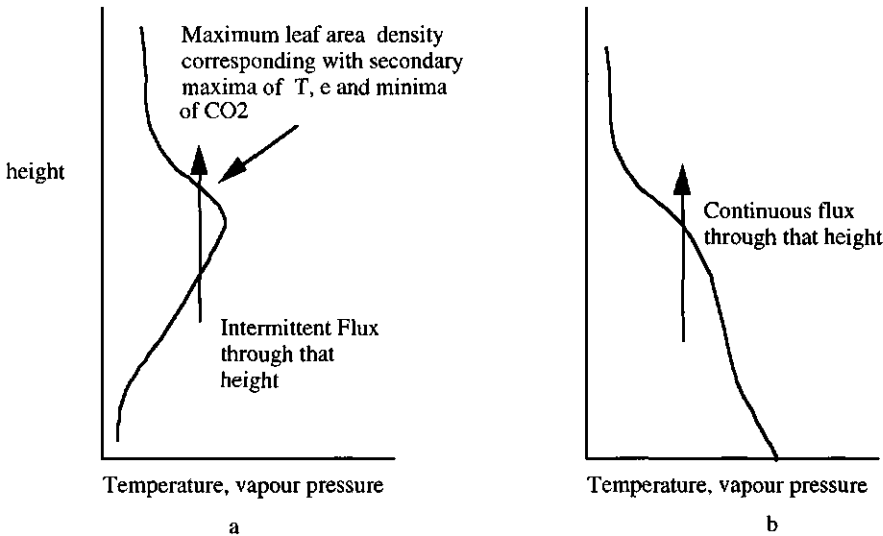


Fig 4.2: Comparison between an intermittent and continuous model approach.

The consideration of the variation in the simulated \bar{D} and \bar{T} values at different heights due to the modelling approach, their feedback on the sources and the agreement with measurement is crucial here. The value of \bar{D} and \bar{T} close to the soil surface, in conjunction with soil thermal conductivity between soil surface and the layer below it, controls the energy partition at the soil surface and so the soil surface heat flux (G).

A clear effect of intermittency on the mean sources or mean scalar profiles is that it allows transport of these scalars through a large-time averaged maximum or minimum by allowing intermittent discharges of the storage of these scalars below the height of that maximum or minimum.

In the case of a gust model in comparison to first order closure model, a gust model maintains a flux through the secondary maximum or minimum by the use of the same mechanism.

The height of this maximum coincides with the height of maximum light interception. In a first order closure model, a negative temperature or vapour pressure gradient is required to maintain an equivalent flux through that height. If we assume that the mean temperature and vapour pressure do not differ at that height for both models, this would mean a higher mean temperature and vapour pressure of the air in the lower part of the canopy in a first order closure model in comparison to a gust model. On the other hand, if we assume that the mean temperature and vapour pressure of the air close to the soil surface do not differ in both approaches, the same condition required to maintain an equivalent large-time averaged flux across the maximum leaf area density height, would mean a lower value of the temperature and vapour pressure of the air at the maximum leaf area density height in a nogust model

compared to the gust model. Both conditions (equality of mean concentrations at the soil surface and the maximum leaf area density) cannot be met at the same flux, fig. 4.2

Coherent structures achieve a large fraction of the total averaged flux without a required local gradient. The buildup process which starts after the gust intrusion is due to the enhancement of the sources and the reduced turbulent transport coefficient. After a gust intrusion, the rate of scalar buildup is higher for maximum source height than for lower canopy parts. This can be shown from the values of the time constants for the different canopy layers and the equilibrium values of vapour pressure deficit with heights. These values, as given by eq.4.2.18, eq.4.2.19 and eq. 4.2.21, show us that the rate of vapour pressure deficit buildup or decrease (toward equilibrium values) will be higher in the highest leaf area density height. That leads to entrapment of the nonradiative energy below this height and a build up process begins. There will be favourable partition toward LE on the expense of H depending on D' being positive or negative, where D' is the vapour pressure deficit variation. D' depends on the value of the layer stomatal resistance being lower or higher than a certain value, as shown on the analysis in the following page or in sect.4.2.1.2. The partition variation (eq.4.2.83.a) below that height will control the development of D within time. An average value of D is given by the integration of eq.4.2.20.

If we, as a result, accept fig.4.2.a as a mean concentration profile due to the gust cycle, a similar profile under a first order closure model means that the heat flux is toward the soil surface and all latent heat flux delivered from the soil surface to inter canopy air stream has to remain trapped below the maximum leaf area density height, which reduces the value of D close to the soil surface, as calculated from a nonintermittent first order closure. For a flux release through that height, a profile like that to the right in fig.4.2 has to develop. So, equality of fluxes and profiles can not be maintained between the two approaches. The resulting difference between the two approaches in the mean temperature and vapour pressure of the air will make a difference in the value of D and the energy partition at the soil surface and so the amount of (G) soil heat flux.

An increase or decrease in the vapour pressure deficit of the air within depth depends on $\left(\frac{\partial e_s}{\partial T} T' - e'\right)$, being greater or less than zero respectively. e' here is $e_2 - e_1$, where e_2 is the vapour pressure at e.g. screen height and e_1 is the vapour pressure at e.g. soil surface or maximum leaf area density height. So is the case for T'. In the case of a first order closure model, e_1 and T_1 can be calculated, assuming a steady state solution.

$$T_2 - T_1 = -\frac{(R_n - G)/(1 + \beta^{-1})}{\rho C_p} \int_{z=1}^{z=2} \frac{1}{K_h} dz \quad (4.1.3)$$

$$e_2 - e_1 = -\frac{\gamma(R_n - G)/(1 + \beta)}{\rho C_p} \int_{z=1}^{z=2} \frac{1}{K_e} dz \quad (4.1.4)$$

where K_h and K_e represent mean time diffusivities. The decrease of mean vapour pressure deficit within height depends on $\beta < \frac{\gamma}{s}$. β here represents an average partition of R_n on plant

surfaces for the whole canopy, which will show as a ratio between the averaged sensible and latent heat fluxes above the canopy top.

$$\beta = \left(\frac{H}{\lambda E} \right) = \frac{\gamma^* R_n - \rho C_p \bar{D} r_h^{-1}}{s R_n + \rho C_p \bar{D} r_h^{-1}} < \frac{\gamma}{s} \quad (4.1.5)$$

where \bar{D} is the effective mean vapour pressure deficit which the sources respond to. The rest of the symbols are explained in the list of symbols. In the case of first order closure, \bar{D} is determined from the solution of eq.4.2.21 which represents the steady state solution, while for a gust model, its average is determined from the integration of eq.4.2.20. From eq.4.1.5, we obtain

$$(\gamma^* R_n - \rho C_p \bar{D} r_h^{-1}) < \frac{\gamma}{s} (s R_n + \rho C_p \bar{D} r_h^{-1}) \quad (4.1.6)$$

dividing both sides by $\gamma^* + s$ and working it out as has been done by Chen (1984) and shown in the appendix (A.2.4)

$$\frac{\gamma^* R_n - \gamma R_n}{\gamma^* + s} < \frac{\rho C_p \bar{D} r_h^{-1} + \gamma / s \rho C_p \bar{D} r_h^{-1}}{\gamma^* + s} \quad (4.1.7)$$

$$\frac{r_s \alpha R_n}{r_b + \alpha r_s} < \frac{\rho C_p \bar{D}}{s r_b + \alpha r_s} \quad (4.1.8)$$

From this expression, we see that for a decrease of mean vapour pressure deficit with height to occur, this requires

$$r_s R_n < \frac{\rho C_p}{\alpha s} \bar{D} \quad (4.1.9.a)$$

or

$$r_s < \frac{\rho C_p}{\alpha s R_n} \bar{D} \quad (4.1.9.b)$$

or a critical stomatal resistance is defined, above which there is an increase and not a decrease of vapour pressure deficit within height. So, if a coherent structure brings a parcel of air which has the same temperature and vapour pressure deficit as the air at a height twice the canopy height, and with a stomatal resistance responding to a large-time averaged mean values of solar radiation, vapour pressure deficit and soil water potential, this air has to attain equilibrium by reducing or increasing its vapour pressure deficit depending on the above inequality. Notice that R_n is also a function of height within the canopy.

In case of comparing a second order closure model to a gust model, the turbulent transport (2 order) equations (sect.3.6.c) contains a divergence turbulent transport terms (third order terms) which lead in their steady state solution to a gradient in the second order terms (fluxes or variances) within height. This is somewhat similar to assuming an extra source (+ or -) within different layers. The assumptions in the averaging and the assumed regaining of the lost information in the higher order terms have been discussed in chapter 3.

If this can be ignored, an estimation of the effect of intermittency on the simulated mean of a large-time averaged second or higher order closure model can be shown by extending these models with a source intermittency correlation or source build-up correlation term and checking its effect on the magnitude of the assumed mean in a simulation model, or by scaling the different terms in the higher order equations. This is done in sect.4.3.

4.2.1 A QUANTITATIVE TREATMENT**: THE NONLINEARITY OF THE CANOPY SYSTEM.

4.2.1.1 THE EFFECT OF INTERMITTENCY ON THE CANOPY AIR SYSTEM**

For the leaf subsystem, the system of equations used to describe the system is the energy balance equation (for derivation and list of symbols, see appendix 2 and 3, respectively).

$$\begin{aligned} \frac{\partial T_1}{\partial t} = & \frac{1}{\rho_s C_s V} [\alpha_r R_s \downarrow A_r + 4\epsilon\sigma T_{air,rad,a}^3 (T_{air,rad} - T_1) - \frac{\rho C_p}{r_{bh}} (T_1 - T_{air}) A_h \\ & - \frac{\rho C_p}{\gamma(r_{bv} + r_s)} (e_s(T_{air}) - e_a) A_l - \frac{\rho C_p}{\gamma(r_{bv} + r_s)} s (T_1 - T_{air}) A_l] \end{aligned} \quad (4.2.1)$$

This equation can be put in the form of (appendix 2)

$$\frac{\partial T_1}{\partial t} = -K_{1,T} (T_1 - T_{1,eq}) \quad (4.2.2)$$

where

$$\frac{1}{\tau_{1,T}} = K_{1,T} = \frac{\rho C_p}{\rho_s C_s \text{ thickness}} \left[\frac{1}{r_R} + \frac{1}{r_{bh}} + \frac{1}{\gamma(r_{bv} + r_s)} s \right] \quad (4.2.3)$$

where $\tau_{1,T}$ represents the thermal time constant of the leaves.

$$\begin{aligned} T_{1,eq} = & \frac{1}{\left[\frac{1}{r_R} + \frac{1}{r_{bh}} + \frac{1}{\gamma(r_{bv} + r_s)} s \right]} \left[\frac{\alpha_r R_s \downarrow}{\rho C_p} + \frac{T_{air,rad}}{r_R} + \frac{1}{r_{bh}} T_{air} \right. \\ & \left. - \frac{1}{\gamma(r_{bv} + r_s)} (e_s(T_{air}) - e_{air}) + \frac{1}{\gamma(r_{bv} + r_s)} s T_{air} \right] \end{aligned} \quad (4.2.4)$$

or

$$T_{l,eq} = \frac{1}{\left[\frac{1}{r_R} + \frac{1}{r_{bh}} + \frac{1}{\gamma(r_{bv}+r_s)} s \right]} \left[\frac{\alpha_r R_s \downarrow}{\rho C_p} + \frac{T_{air,rad}}{r_R} + \frac{1}{r_{bh}} (\bar{T}_a + T'_a + T''_a) \right. \\ \left. - \frac{1}{\gamma(r_{bv}+r_s)} (\bar{D} + D' + D'') + \frac{1}{\gamma(r_{bv}+r_s)} s (\bar{T}_a + T'_a + T''_a) \right] \quad (4.2.5)$$

$T_{l,eq}$ represents the equilibrium temperature of the leaf i.e. the value of the leaf temperature under which a steady state solution of the energy budget equation is achieved. The different terms in the square brackets in eq.4.2.1, numerator of both eq.4.2.4 and eq.4.2.5, represent the effect of different terms within the energy budget on the equilibrium temperature of the leaf. These different terms represent the effects of the short wave radiation load, the long wave radiation load, the sensible heat flux from the leaf to the air and the latent heat flux from the leaf to the air on the leaf equilibrium temperature respectively. The last effect is represented by the last two terms. The equilibrium temperature of the leaf is a weighted mean of the radiative temperature of the environment and air temperature, depending on their relative conductances, plus the decremental effect of air vapour pressure deficit and an incremental effect of the short wave radiative loading (the first term has no resistance). All of these terms contain intermittency as we have discussed before, but the scales of intermittency are different. The intermittencies in the third, fourth and fifth terms are the ones we are interested in (i.e. due to coherent structures existence).

$T_{l,eq}$ and to a much lesser degree $K_{l,t}$ are time dependent functions. Reducing our time step of integration and assuming a time separation between a small scale D' or T' and a large scale D'' or T'' , the last two occur concurrently, the time dependency during one time step is weakened. An integration of eq.4.2.2 over a small time step, assuming close to constant values of these two parameters, could be done. The solution of eq.4.2.2 then follows:

$$T_l = T_{l,eq} \left(1 - e^{-\frac{t}{\tau_{l,T}}} \right) + T_{l,initial} e^{-\frac{t}{\tau_{l,T}}} \quad (4.2.6)$$

$T_{l,eq}$ will be changing between different time steps due to changes in the third, fourth and fifth terms (i.e. the buildup of the temperature and vapour pressure of the air). The importance of $T_{l,eq}$ is that it dictates the direction of leaf temperature change (see sect.4.2.2)

For the canopy air subsystem, the temperature and vapour pressure of the air have a similar kind of equation (A.2.2). For the air temperature equation

$$\rho C_p \frac{\partial T_a}{\partial t} = - \frac{\partial q_h}{\partial z} + s_h \quad (4.2.7)$$

discretized with respect to space, it reads

$$\Delta z \rho C_P \frac{\partial T_a}{\partial t} = -(q_{i+1} - q_i) + S_h \Delta z \quad (4.2.8)$$

The instantaneous flux at a certain boundary between layers, according to sect. 3.7, is expressed as a time integral for of an ensemble average. This is given by eq.4.2.9

$$\bar{q}_{i+1} = \frac{\int_0^t \int_0^t \frac{\partial c_1^{ens}}{w c} dt_1 dt}{t} = \frac{\int_0^t \int_0^t \left(\left[\frac{1}{w^2 \tau_L} \left\{ 1 - e^{-\frac{t_0-t_1}{\tau_L}} \right\}_{top} \right] \frac{\partial c_1^{ens}}{\partial z} \right) dt_1 dt}{t} \quad (4.2.9)$$

The contribution of the near field concentration to the whole concentration field will be always in the solution and it will lead to non-linearity in the superposition of the flux as a function of the transport coefficients or the concentration, since the behaviour of the transport coefficient is dependent on the time since source release, which is a classical result of G. I. Taylor in his original paper (Taylor, 1921).

Inserting that expression (4.2.9.b) in equation 4.2.8, assuming a large-time limit behaviour leads to (Appendix. 2.2).

$$\frac{\partial T_{air}}{\partial t} = -K_{a,T} T_i + K_{a,T} T_{air,eq} \quad (4.2.10)$$

where

$$\frac{1}{\tau_{a,T}} = K_{a,T} = \frac{1}{\Delta z} \left(\frac{K_{top}}{\delta X_{top}} + \frac{K_{bottom}}{\delta X_{bottom}} + \frac{LAD \Delta z}{r_{bh}} \right) \quad (4.2.11)$$

$$T_{air,eq}(t) = \left(\begin{array}{l} \frac{K_{top}}{\delta X_{top}} T_{i+1} + \frac{K_{bottom}}{\delta X_{bottom}} T_{i-1} \\ \left(\frac{K_{top}}{\delta X_{top}} + \frac{K_{bottom}}{\delta X_{bottom}} + \frac{LAD \Delta z}{r_{bh}} \right) T_i \\ + \frac{LAD \Delta z}{r_{bh}} T_i \\ \left(\frac{K_{top}}{\delta X_{top}} + \frac{K_{bottom}}{\delta X_{bottom}} + \frac{LAD \Delta z}{r_{bh}} \right) \end{array} \right) \quad (4.2.12)$$

$T_{air,eq}$ represents the equilibrium temperature of the air layer. This temperature is a weighted mean of the temperature of the air layer below and above and the temperature of the leaves in that layer. The weighting factors depend on the relative strength of the turbulent coupling between the air layers and the relative strength of the coupling to the source, expressed by leaf area increments and leaf temperature. The first two weighting factors will be called the turbulent transport coupling coefficients (symbolized as f_{topt} , f_{lowert} respectively). It is important to notice that $T_{air,eq}$ is a linear function of the transfer coefficients between canopy air layers.

The air layer has two time constants, one active during the gust intrusion and the other active during the quiescence period.

The solution of the air temperature follows

$$T_{air} = T_{air,eq} \left(1 - e^{-\frac{t}{\tau_{a,T}}}\right) + T_{air,initial} e^{-\frac{t}{\tau_{a,T}}} \quad (4.2.13)$$

It should be mentioned that T_{i-1} , T_{i+1} and T_i are functions of time and not constants. $T_{air,eq}$ is also a function of time. We assume an integration of eq.4.2.10 over small time intervals is possible. So, the solution is exponential in K_m within small time intervals. For large time intervals, the whole solution could be proven to behave exponentially as a function of K_m , but in this case, the behaviour of the solution within this large time interval is missing. For example, if the air is initially cooled and then warmed up due to vapour pressure deficit decrease, this behaviour will be missing in our solution. The importance of this is shown in sect.4.2.1.2.b.III.2

For the vapour pressure equation,

$$\frac{\partial e_{air}}{\partial t} = -K_{a,e} e_i + K_{a,e} e_{air,eq} \quad (4.2.14)$$

where

$$\frac{1}{\tau_{a,e}} = K_{a,e} = \frac{1}{\Delta z} \left(\frac{K_{top}}{\delta X_{top}} + \frac{K_{bottom}}{\delta X_{bottom}} + \frac{LAD \Delta z}{(\Gamma_{bv} + \Gamma_s)} \right) \quad (4.2.15)$$

The solution of this equation is:

$$e_{air} = e_{air,eq} \left(1 - e^{-\frac{t}{\tau_{a,e}}}\right) + e_{initial} e^{-\frac{t}{\tau_{a,e}}} \quad (4.2.16)$$

where

$$e_{air,eq}(t) = \left(\frac{\frac{K_{top}}{\delta X_{top}}}{\left(\frac{K_{top}}{\delta X_{top}} + \frac{K_{bottom}}{\delta X_{bottom}} + \frac{LAD \Delta z}{(r_{bv} + r_s)} \right)} e_{i+1} + \frac{\frac{K_{bottom}}{\delta X_{bottom}}}{\left(\frac{K_{top}}{\delta X_{top}} + \frac{K_{bottom}}{\delta X_{bottom}} + \frac{LAD \Delta z}{(r_{bv} + r_s)} \right)} e_{i-1} \right. \\ \left. + \frac{\frac{LAD \Delta z}{(r_{bv} + r_s)}}{\left(\frac{K_{top}}{\delta X_{top}} + \frac{K_{bottom}}{\delta X_{bottom}} + \frac{LAD \Delta z}{(r_{bv} + r_s)} \right)} es(T_l) \right) \quad (4.2.17)$$

The equilibrium vapour pressure ($e_{air,eq}$) of the air will also be a weighted mean of the vapour pressure of the air layers below and above, plus a contribution from the saturated vapour pressure at the temperature of the leaves. The first two terms represent the strength of the turbulent coupling of the vapour pressure in the air layer below and the air layer above to the vapour pressure of the layer under consideration. The first two weighting factors will be called the turbulent transport coupling coefficients for water vapour (symbolized as f_{tope} , f_{lowere}). The factor of the third term $\frac{LAD \Delta z}{(r_{bv} + r_s)}$ represents the strength of the source and its effectiveness in coupling the vapour pressure of the air to that of the leaf. All the three vapour pressure terms in eq.4.2.17 are function of time, so $e_{air,eq}$ is also a function of time. The contribution of the $es(T_l)$ to $e_{air,eq}$ depends on the relative weight of the corresponding conductance. $es(T_l)$ is usually much higher than $e_{i\pm 1}$. The temperature of the leaves has a much larger time constant than that of the air layer. Notice that $e_{air,eq}$ value is a linear function of the transfer coefficients between the canopy air layers.

For the vapour pressure deficit of the air, a non-steady vapour pressure deficit equation can be obtained, as has been done by Chen (1984) for the steady state situation. There is an assumption here concerning the possibility of using the source term for sensible and latent heat in equation A.2.2.1, A.2.3.1, as given by the Penman-Monteith equation. This expression is a steady state solution of the leaf energy budget equation. The effect of this assumption will be discussed in sect.4.2.1.2.b.III. The derivation is done by multiplying the temperature equation by (s) and the vapour pressure equation by $(-\gamma)$ and adding both equations. A further manipulation of the equation, as shown in appendix A.2.4, gives:

$$\frac{\partial D_i}{\partial t} = -K_D D_i + K_D D_{air,eq} \quad (4.2.18)$$

where

$$\frac{1}{\tau_{a,D}} = K_D = \frac{1}{\Delta z} \left(\frac{K_{top}}{\delta X_{top}} + \frac{K_{bottom}}{\delta X_{bottom}} + \frac{LAD \Delta z}{r_b + \alpha r_s} \right) \quad (4.2.19)$$

The solution of this equation is:

$$D_{\text{air}} = D_{\text{air,eq}} \left(1 - e^{-\frac{t}{\tau_{a,D}}}\right) + D_{\text{air,initial}} e^{-\frac{t}{\tau_{a,D}}} \quad (4.2.20)$$

where:

$$D_{\text{air,eq}}(t) = \left(\begin{aligned} & \frac{K_{\text{top}}}{\delta X_{\text{top}}} D_{i+1} + \frac{K_{\text{bottom}}}{\delta X_{\text{bottom}}} D_{i-1} \\ & \frac{\left(\frac{K_{\text{top}}}{\delta X_{\text{top}}} + \frac{K_{\text{bottom}}}{\delta X_{\text{bottom}}} + \frac{\text{LAD } \Delta z}{r_b + \alpha r_s} \right)}{\left(\frac{K_{\text{top}}}{\delta X_{\text{top}}} + \frac{K_{\text{bottom}}}{\delta X_{\text{bottom}}} + \frac{\text{LAD } \Delta z}{r_b + \alpha r_s} \right)} D_{i+1} + \frac{\left(\frac{K_{\text{top}}}{\delta X_{\text{top}}} + \frac{K_{\text{bottom}}}{\delta X_{\text{bottom}}} + \frac{\text{LAD } \Delta z}{r_b + \alpha r_s} \right)}{\left(\frac{K_{\text{top}}}{\delta X_{\text{top}}} + \frac{K_{\text{bottom}}}{\delta X_{\text{bottom}}} + \frac{\text{LAD } \Delta z}{r_b + \alpha r_s} \right)} D_{i-1} \\ & + \frac{\frac{\text{LAD } \Delta z}{r_b + \alpha r_s}}{\left(\frac{K_{\text{top}}}{\delta X_{\text{top}}} + \frac{K_{\text{bottom}}}{\delta X_{\text{bottom}}} + \frac{\text{LAD } \Delta z}{r_b + \alpha r_s} \right)} \left(\frac{s \alpha r_s R_n}{\rho C_p} \right) \end{aligned} \right) \quad (4.2.21)$$

where $\alpha = \left(\frac{\gamma}{\gamma + s}\right)$. The equilibrium vapour pressure deficit of the air ($D_{\text{air,eq}}$), as in the previous two equations, will be a weighted mean of the vapour pressure deficit of the layer above and the layer below plus a fractional contribution, dependent on the value of $\frac{\text{LAD } \Delta z}{r_b + \alpha r_s}$ from $\left(\frac{s \alpha r_s R_n}{\rho C_p}\right)$ in the same layer. This last term equals

$$\left(\frac{s \alpha r_s R_n}{\rho C_p} \right) = \frac{\gamma r_s \frac{s}{\gamma + s} R_n}{\rho C_p} = \frac{\gamma r_s E_{\text{equ}}}{\rho C_p} \quad (4.2.22)$$

It is important to notice that equations 4.2.12, 4.2.17 and 4.2.21 represent the discretized steady state equation for the temperature, vapour pressure and vapour pressure deficit for a canopy air layer (i). Solving a system of n equations for n canopy layers where n takes the value of one or less for the first two equations, while it is greater than one for the third equation, represents the steady state profile for these three equations.

CONCLUSIONS (4.2.1.1):

From the analysis so far,

1) We get four coupled partial differential equations, namely eq.4.2.2, 4.2.10, 4.2.14 and 4.2.18, describing the behaviour of the canopy system, one for the leaves temperature and the other three for the air subsystem. There are several variants for solving the canopy leaf-air subsystem, which lie under two main combinations. These two combinations, each consisting

of three of these equations, can be used to describe the system behaviour completely with different degrees of accuracy.

The first three partial differential equations (temperature of the leaf, temperature and vapour pressure of the air) constitute a complete set of equations which can be used to describe the dynamical behaviour of the system. In this combination, the equations for different layers are coupled through the solution of the last two equations (i.e. the profile solution) i.e. updating the values of T_{i+1} , T_{i-1} , e_{i+1} and e_{i-1} in the $e_{air,eq}$ and $T_{air,eq}$ equations. This description is more accurate, but more complicated than an alternative approach in which the linear dependence of the Penman-Monteith equation on the vapour pressure deficit is used.

The other combination is the R_n equation, temperature of the air and vapour pressure deficit equation of the air. This last equation was derived by assuming a steady state solution of the energy budget equation, so it is less accurate than the first combination.

Concerning the canopy layers, the first combination applies for all canopy layers, possibly with a modified interpretation of the coefficients, while the second combination applies for all canopy layers except the first air layer in contact with the soil layer. The first air layer has its own form of equation (Sect.4.4.2)

2) One learns that the canopy air temperature, vapour pressure of the air and vapour pressure deficit approach asymptotically a steady state solution ($T_{air,eq}$, $e_{air,eq}$ and $D_{air,eq}$ for temperature, vapour pressure and vapour pressure deficit of the air, respectively). After a large time interval (usually $\frac{t}{\tau_{air}} > 3 \rightarrow 4$) since the introduction of a disturbance to the system equilibrium through the gust effect (a step function), the equilibrium solution ($T_{air,eq}$, $e_{air,eq}$ and $D_{air,eq}$) is a linear function of the transfer coefficient between the canopy air layers, assuming no resulting feedback on the leaf temperature. In early stages of the solution development, the solution is behaving as an exponential function of the transfer coefficients and is not linear. The importance of this nonlinearity becomes less once a disturbance due to a gust is introduced and the system is left to attain equilibrium for a long period of time before a new disturbance is introduced. The importance of the exponential period contribution to the total mean is reduced. But, if the ratio of the inverse of the frequency of gust occurrence to the time constants of the canopy air layers is in the range of 0.5 to 3.0, the system will be always in the non-linear part of the solution. The effect of using a mean value of the K_m (transfer coefficients) values is not the same as using a varying in-time value of K_m , which has the same mean, during the whole period or during the lull (the quiescence) period if the ratio of length scales of transport to the source inhomogeneity is quite large. So, depending on the ratio of (frequency)⁻¹/time constants of the layer ($\frac{t}{\tau}$), we have a significant nonlinearity in the solution. In this model we assume two K_m values (one during the gust intrusion phase and the other during the quiescence period), see sect.3.6.2. If the interval between the gust occurrences (inverse of the frequencies) is very small in relation to the time constants, the system will always be close to the initial condition and a linear assumption could be made due to $e^{-x} = (1-x)$ where $x = \frac{t}{\tau}$.

What we are arguing here is that the solution of the mean in the case of the closeness of the $\frac{f^{-1}}{\tau}$ ratio to one will not be a linear function of the transfer coefficients (K_m). So, a mean value of K_m does not yield the same mean temperature and vapour pressure profile as a varying, in time, value of K_m which has same mean. Equivalently, the system is then nonlinear. This case occurs in the case of a non-stressed canopy (i.e. after irrigation) with moderate wind velocity at canopy height. If we assume the value of f^{-1} is dynamically controlled, i.e. no thermal stability effects, its value will be dependent mainly on the friction velocity at the top of the canopy, or, on $U(h)$ divided by the canopy height, while the time constants of the canopy layer will be dependent on the contribution of: 1) the turbulent coupling between canopy layers through a local or short time mean K_m and 2) the stomatal resistance (soil moisture stress dependent) to the value of the time constant. An irrigation or a rain cycle contains the entire range of $\frac{f^{-1}}{\tau}$ ratios. So, the denominator in the above ratio is a variable term. The time distribution of irrigation or rain events will result in a canopy soil system, being in the different regions of the ratio $\frac{f^{-1}}{\tau}$ with different time proportions. The nonlinearity of the solution will always occur. This is an answer to 1c mentioned above.

3) The derivation of these equations, (detailed for sensible heat flux equation) shows that this nonlinearity is not only due to the near field effect, as suggested by Raupach *et al* (1989) or Finnigan (1985), based on Taylor's original paper (1921), in their criticism of the use of K theory approach to describe canopy turbulent transport processes. The nonlinearity, which we are considering here, is at least one order of magnitude larger than the near field effect.

4) From eq.4.2.20 and eq.4.2.21, one learns that $D_{air,eq}$ being higher or lower than $D_{air,initial}$ depends on the value of the third term in 4.2.21 ($\frac{s \alpha r_s R_n}{\rho C_p}$) contributing negatively or positively to $D_{air,eq}$.i.e. being lower or higher than D_{i+1} or $D_{air,initial}$. These last two are equal just after the gust passage. $D_{air,eq}$ being higher or lower than $D_{air,initial}$ depends then on the following equality being satisfied

$$r_s(z) R_n(z) < \frac{D_{initial} \rho C_p}{s \alpha} \quad (4.2.23)$$

So, if a parcel of air is brought into the canopy air space, which has a vapour pressure deficit and temperature not in equilibrium with the $D_{air,eq}$, then it has to be brought to equilibrium. This is in complete agreement with the result derived in eq.4.1.9.

5) In spite of the apparent constancy or the non dependency of the $\frac{s \alpha r_s R_n}{\rho C_p}$ on the gust process, r_s being a function among other things of the mean vapour pressure deficit (Jacobs, 1994), the value of the $D_{air,eq}$ will be a function of intermittency since the weak coupling turbulent coefficients during the quiescence period will lead to an increase of the

fractional contribution of the third term in eq.4.2.21 to $D_{air,eq}$. So, the vapour pressure deficit will be heading toward a different ceiling than that of a no-gust approach. This point is also shown in sect. 4.2.1.2.b.III

One question which arises here is whether it is possible that there would be no net effect of intermittency on the mean in spite of the nonlinear behaviour of the canopy state variables equations due to the change of the ceiling of these state variables, i.e. that the sudden drop and then the exponential increase to a value higher than the one resulting from a no-gust model would neutralize each other.

That would require the value of the mean as determined by eq.4.2.24 or eq.4.2.58 to be equal to the value of the mean as determined by eq.4.2.21, with non-intermittent values for the turbulent transport coupling coefficient. Even if this occurs for a certain layer, the requirement of down-gradient or a co-gradient flux in a nonintermittent model, or the nonequality of the coupling coefficient lead to a deviation between the two approaches for the lower layers.

Concerning the statement of the apparent constancy or the non-dependency of $s \propto r_s \frac{R_n}{\rho C_p}$ on the gust process, r_s is a function of the mean temperature, vapour pressure deficit, as determined by equations given in sect. 4.5.3. R_n is also a weak function of the leaf temperature, so the increase of the leaf temperature will vent some of total absorbed radiation as a long wave emission and reduce the net radiation by $4\sigma T_{abs}^3$ for one K ($5.7 \text{ W m}^{-2} \text{ K}^{-1}$, at 293 K). The incoming longwave radiation is not a function of the solution. A decrease in the outgoing longwave radiation represents an increase in R_n . This represents a cooling of the canopy elements, as seen by an infrared thermometer. So, for a R_n increase of 5.7 W m^{-2} , a decrease of one degree K is required, which represents a lot of storage change. So, even if R_n is almost constant, the nonsteady state term in the energy budget equation is important as also shown in section 4.2.1.2.II.2. (page 127)

The effect of the discussed above nonlinearity and the change of the equilibrium solution, due to coherent structures intermittency on the long term behaviour of the system shows through its effect on:

- 1) the soil temperature profile by affecting the soil heat flux and its integration (sect.4.2.1.2)
- 2) the mean temperature and vapour pressure profile of the air which could affect the physiological process within the plant by changing the values of **GDD** (Growing Degree Days). An integration of the latter could show in a pool of interest to us (i.e. a yield quantity or quality).

We have proven that the vapour pressure deficit behaves nonlinearly as a function of the transport coefficients. The value of the mean vapour pressure deficit is given by eq.4.2.24 or by eq. 4.2.58.

$$\bar{D} = D_{top} \frac{\Delta t_{gust \text{ duration}}}{\text{period}} + D_{equilibrium} \left(1 - \frac{\Delta t_{gust \text{ duration}}}{\text{period}} - \frac{4\tau_{a,D}}{\text{period}}\right) + D_{average} \frac{4\tau_{a,D}}{\text{period}} \quad (4.2.24)$$

The value of the time constant will be controlled mainly, for the quiescence period, by the value of $\frac{LAD \Delta z}{r_b + \alpha r_s}$ in relation to the turbulent coupling in the quiescence period. If the

latter is assumed zero and in case of a canopy with LAI of 5 and r_b of 50 sm^{-1} and a stomatal resistance of 200 sm^{-1} and α of 0.5 gives a time constant of 30 s. With a period of intrusion of 1.5 minutes, the canopy is in the nonlinear phase of the solution and a use of a large-time averaged K_m is not the same as a variable in time K_m value with the same mean. This gives a definite answer to question 1c and 1b.

An advantage of the use of eq.4.2.18 in comparison to the three equations 4.2.2, 4.2.10 and 4.2.14 is that the equilibrium solution is expressed as a function of R_n which is much less dependent on time. The other three equations have a larger time dependency due to the variability of the leaf temperature, air temperature and vapour pressure. So, an integration of the equation with a larger time interval is possible, but there is a loss of information due to assuming a steady state solution of the energy budget equation (sect. 4.2.1.2.b III.2).

The use of the saturation deficit flux as defined by Perrier (1976) and Chen (1984) shows that

$$J = H - (\gamma/s) \lambda E \tag{4.2.25}$$

$$J'_i = - \frac{\frac{\rho C_p}{s} D_i}{r_{b,i} + \alpha r_{s,i}} + \frac{R_{n,i}}{1 + \frac{r_{b,i}}{r_{s,i}} \alpha} \tag{4.2.26}$$

An increase in the air vapour pressure deficit, due to the gust intrusion, will lead to a decrease in the contribution of each layer J'_i to the total flux of J. Using the other expression of cumulative saturation heat flux J (eq.4.2.25), shows that this is only possible by the increase of latent heat flux from the leaves to the air at the expense of sensible heat flux. So, there is a favourable partition of LE at the expense of H depending on the variation of the mean vapour pressure deficit with height. This variation is dependent on a critical Bowen ratio. The favourable partition of the LE/H is also shown in page 163 (eq.4.2.99).

We will later see the importance of the variability of the time constants of the layer, $T_{air,eq}$ and $e_{air,eq}$ on the solution (sect. 4.2.1.2: The MATHCAD® runs).

4.2.1.2: THE EFFECT OF THE INTERMITTENCY ON THE SOIL TEMPERATURE PROFILE AND THE SOIL HEAT FLUX**

4. 2.1.2.a. THE FORMULATION AND THE SOLUTION OF THE PROBLEM

The soil energy budget equation:

The equation of the soil surface energy budget is very similar in form to the leaf surface energy budget equation (4.2.1) except for an extra term expressing the soil heat flux into the lower soil layer.

This equation reads as follows

$$\frac{\partial T_s(L,t)}{\partial t} = \frac{A}{\rho_s C_s V} [\alpha_r R_s \downarrow + (\epsilon \sigma T_{air,rad,a}^4 - \epsilon \sigma T_s^4) - \frac{\rho C_p}{\Gamma_{bh}} (T_s - T_a) - \frac{\rho C_p}{\gamma(\Gamma_{bv} + \Gamma_{s,s})} (e_s(T_s) - e_a) - \frac{\beta}{\delta z} (T_s - T_{s,i-1})] \quad (4.2.27)$$

β is the thermal heat conductivity (in $W m^{-1} K^{-1}$) and δz is the vertical distance between the centres of the uppermost layer and the layer below it. To obtain an analytical solution, this equation has to be cast into a boundary condition to our problem.

$$\beta_L \frac{\partial T_s(L,t)}{\partial x} = \alpha_r R_s \downarrow + 4\epsilon \sigma T_{air,rad,a}^3 T_{air,rad} + \left(\frac{\rho C_p}{\Gamma_{bh}} + \frac{\rho C_p s}{\gamma(\Gamma_{bv} + \Gamma_{s,s})} \right) T_{air} - \frac{\rho C_p}{\gamma(\Gamma_{bv} + \Gamma_{s,s})} D_{air} - \left(4\epsilon \sigma T_{air,rad,a}^3 + \frac{\rho C_p}{\Gamma_{bh}} + \frac{\rho C_p s}{\gamma(\Gamma_{bv} + \Gamma_{s,s})} \right) T_s \quad (4.2.28)$$

The soil temperature, T_s , as function of space (x) and time (t) is formulated as follows:

$$\frac{\partial T_s}{\partial t} = \kappa \frac{\partial^2 T_s}{\partial x^2} + Q(x,t) \quad (4.2.29)$$

subject to the following boundary conditions:

$$\beta_L \frac{\partial T_s(L,t)}{\partial x} + \alpha_L T_s(L) = f(L,t) \quad (4.2.29a)$$

$$\frac{\partial T_s(0,t)}{\partial x} = 0 \quad (4.2.29b)$$

and the initial condition

$$T(x,0) = g(x) \quad (4.2.29c)$$

where

$$f(L,t) = \alpha_r R_s \downarrow + 4\epsilon \sigma T_{air,rad,a}^3 T_{air,rad} + \left(\frac{\rho C_p}{\Gamma_{bh}} + \frac{\rho C_p s}{\gamma(\Gamma_{bv} + \Gamma_{s,s})} \right) T_{air} - \frac{\rho C_p}{\gamma(\Gamma_{bv} + \Gamma_{s,s})} D_{air} \quad (4.2.30)$$

$$\alpha_L = \left(4\epsilon \sigma T_{air,rad,a}^3 + \frac{\rho C_p}{\Gamma_{bh}} + \frac{\rho C_p s}{\gamma(\Gamma_{bv} + \Gamma_{s,s})} \right) \quad (4.2.31)$$

$$Q(x,t) = 0 \quad x \leq L \text{ and } t \geq 0 \quad (4.2.32)$$

The first two terms in $f(L, T)$ express the effect of the short and long wave radiation loading on the increase of the temperature gradient at the soil surface. The last two terms express the effect of the temperature and vapour pressure deficit of the air across the boundary layer of the soil clods on the temperature gradient at the soil surface. The effect of the soil temperature on the soil long wave emission, the latent and sensible heat flux from the soil to the air is expressed in the second term of (4.2.29a). For the other soil layers, the most significant energy flux, neglecting water vapour flux etc., is the conductive soil heat flux.

These boundary conditions (4.2.29a and 4.2.29b) are of the third and second kinds, respectively.

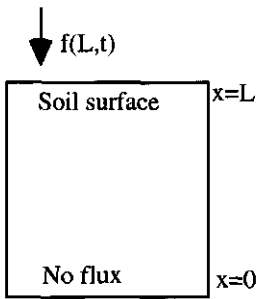


Fig 4.3 The definition of the problem.

The related homogeneous problem, which is given below, satisfies a Sturm-Liouville Eigenvalue problem and as such are complete, i.e. any piecewise smooth function can be expanded in a series of Eigenfunctions. The related homogeneous problem is expressed as:

$$\frac{d^2\phi_n}{dx^2} + \lambda\phi_n = 0 \quad (4.2.33)$$

$$\beta_L \frac{d\phi_n}{dx}(L) + \alpha_L \phi_n(L) = 0 \quad (4.2.33a)$$

$$\frac{d\phi_n}{dx}(0) = 0 \quad (4.2.33b)$$

The Eigenfunction of the related homogeneous problem is

$$\phi_n = C_1 \cos \sqrt{\lambda_n} x \quad (4.2.34)$$

where

$$\sqrt{\lambda_n} = \cot(\sqrt{\lambda_n} L) \frac{\alpha_L}{\beta_L} \quad (4.2.35)$$

C_1 is an arbitrary constant.

The temperature of the soil can then be expressed in the form

$$T(x,t) = \sum_{n=0}^{n=\infty} b_n(t)\phi_n(x) \quad (4.2.36)$$

The problem now is determining the coefficient $b_n(t)$ as a function of time and the effect of intermittency on its value. This problem could be solved by the use of Green's formula to obtain the Eigenfunction expansion of the nonhomogeneous problem. The full details of the solution are given in Appendix 2.5.

The coefficient $b_n(t)$ has a first-order ordinary differential equation which reads:

$$\frac{db_n(t)}{dt} + \lambda_n \kappa b_n(t) = \frac{\kappa \cos(\sqrt{\lambda_n} L) f(L, t)}{\beta_L \int_0^L \phi_n^2(x) dx} \quad (4.2.37)$$

where

$$\frac{\kappa}{\beta_L} = \frac{1}{\rho_s C_s} \quad (4.2.38)$$

Equation (4.2.37) is equivalent to

$$\frac{d(b_n(t) e^{\lambda_n \kappa t})}{dt} = e^{\lambda_n \kappa t} \frac{\cos(\sqrt{\lambda_n} L) f(L, t)}{\rho_s C_s \int_0^L \phi_n^2(x) dx} \quad (4.2.39)$$

The integration of this equation requires an initial condition for $b_n(0)$ which is obtained from the initial temperature profile according to

$$b_n(0) = \frac{\int_0^L g(x) \phi_n(x) dx}{\int_0^L \phi_n^2(x) dx} \quad (4.2.40)$$

The solution of eq. 4.2.39 is given by

$$b_n(t) = b_n(0)e^{-\lambda_n \kappa t} + e^{-\lambda_n \kappa t} \int_0^t \frac{e^{\lambda_n \kappa \tau} \cos(\sqrt{\lambda_n} L) f(L, \tau)}{\rho_s C_s \int_0^L \phi_n^2(x) dx} d\tau \quad (4.2.41)$$

This completes the solution of the soil temperature profile as affected by $f(x,t)$. The $f(x,t)$ can be decomposed into two terms

$$f_1(L,t) = \alpha_r R_s \downarrow + 4\epsilon \sigma T_{\text{air,rad,a}}^3 T_{\text{air,rad}} \quad (4.2.41a)$$

$$f_2(L,t) = \left(\frac{\rho C_p}{r_{bh}} + \frac{\rho C_p s}{\gamma(r_{bv} + r_{s,s})} \right) T_{\text{air}} - \frac{\rho C_p}{\gamma(r_{bv} + r_{s,s})} D_{\text{air}} \quad (4.2.41b)$$

$$b_n(t) = b_n(0)e^{-\lambda_n \kappa t} + \frac{e^{-\lambda_n \kappa t} \cos(\sqrt{\lambda_n} L)}{\rho_s C_s \frac{L}{2} + \frac{\rho_s C_s}{2\sqrt{\lambda_n}} \sin(\sqrt{\lambda_n} L) \cos(\sqrt{\lambda_n} L)} \left(\int_0^t e^{\lambda_n \kappa \tau} f_1(L, \tau) d\tau + \int_0^t e^{\lambda_n \kappa \tau} f_2(L, \tau) d\tau \right) \quad (4.2.42)$$

The physical interpretation of the solution:

To study the physical behaviour of the solution, several remarks can be made:

- 1) The soil temperature profile is expressed by eq.4.2.36. ϕ_n is determined from the solution of the boundary value problem under the given boundary conditions and is determined by the initial condition and is not a function of time. So, its space derivative is fixed in time. The effect of the change of the coefficients $b_n(t)$ controls the change within time of the soil temperature profile and of the soil heat flux. The time development of the solution is a function of $b_n(t)$ only.
- 2) The equality, eq.4.2.36, can not be valid at $x=L$, since ϕ_n satisfies the homogeneous boundary condition while $T(x,t)$ does not. But the derivative at a lower depths is allowed. Nonetheless, we use the notation = , where we understand that the \sim is more proper.
- 3) The first term on the right hand side of eq.4.2.42 expresses the effect of the initial value of the coefficients of an Eigenfunction expansion of the soil temperature profile. The first term, between the parenthesis in the same equation, expresses the effect of the short and longwave radiation loading on the soil temperature profile, $f_1(L,t)$. The second term expresses the effect of the temperature and vapour pressure deficit of the air across the boundary layer of the soil clods, $f_2(L,t)$, on the coefficients of this Fourier series expansion of the soil temperature

profile. These two terms have different scales of intermittency. The second one is the one affected by the existence of coherent structures in the layer of air above the canopy.

4) It is important to notice that the effect of intermittency on the coefficients of this expansion expresses itself in the same way on all wave numbers. So the effect of intermittency needs to be studied on one component only. This is what will be done.

5) The effect of previous intermittencies in $f(L,T)$ dies out at a much faster rates for the higher wave numbers.

6) To evaluate the effect of intermittency on the soil heat flux and the soil temperature profile, one needs to evaluate the effect of intermittency on the value of $f_2(L,t)$ and how this affects $f(L,t)$. That effect shows directly in $b_n(t)$, as given by eq.4.2.42. Then, we need to do a scaling analysis of the different terms in $f_1(L,t)$ and $f_2(L,T)$ to see the effect of intermittency on the values of the boundary condition for the soil heat flux and how much that will affect $b_n(t)$. A direct numerical integration of eq.4.2.42 is also possible.

4. 2.1.2.b. COUPLING THE SOIL TO THE CANOPY AIR LAYER

I. Assumptions:

There are three assumptions in the following analysis,

1) The first soil layer has a much larger time constant compared to that of the total canopy air layer or the first air layer. The time rate of the soil surface temperature change is much lower than that of the canopy air layer. An assumption of a boundary condition for the solution, eq.4.2.29a, being decoupled from the soil surface temperature for small time interval, is thus valid. The effect of the turbulent transport intermittency of the canopy air, during small time intervals, could be checked.

2) The temperature and vapour pressure of the air for the whole period between two gust intrusions follows an equation similar to eq.4.2.13 and eq.4.2.16, respectively. This can be shown from MATHCAD® (a mathematical software for programming and solving equations) runs (fig.4.17.c, fig.4.18.c and fig. 4.19c). In the derivation for these equations, an integration for a small time step was used. During this short time step, relative to the time constants of the canopy air layer, the values of $e_{air,eq}$ and $T_{air,eq}$ and $T_{air,ini}$ and $e_{air,ini}$ in these equations are assumed constant. During the whole gust cycle, they keep changing as a function of time. This will affect the time rate of the air temperature and vapour pressure change for the total period. It will, in reality, be lower for the vapour pressure in earlier stages of the solution and keep increasing later. This will not change the exponential behaviour of the solution. This is the case for vapour pressure, as long as the temperature of the leaves is higher than the dew point temperature of the air. For the temperature, the air temperature could decrease and then increase depending on the vapour pressure of the air being higher or lower than a critical vapour pressure deficit as defined from Penman-Monteith equation. It is also assumed that deviations from steady state solutions are not of serious consequences for the scaling.

3) The third assumption, which is not required for the calculation, but was implemented to obtain scaled values with a hand calculator in the following calculation, is that in eq.4.2.42 a multiplication of $f(L,t)$ by $e^{-\lambda_n \kappa(t-\tau)}$ is required and then integrated. We assumed in the

following scaling, that it could be possible to use the mean of eq.4.2.13 and eq.4.2.16 during a gust interval, with a time period less than the time constant of the soil surface layer to obtain an accurate enough value for the scaled terms in $f(L,t)$.

All these assumptions could be disregarded in the case of the numerical model, since an updating of the state variables is possible.

II. The scaling procedure for a one-layer canopy model:

The analysis procedure is:

1) An equilibrium temperature and equilibrium vapour pressure of the canopy layer is calculated. These are calculated according to eq.4.2.12 and eq.4.2.17 respectively. There is no vapour pressure deficit equation for the first air layer, since in the derivation of a vapour pressure deficit equation, f_{lower} for the air vapour pressure and air temperature equations are not similar, so a common factor can not be obtained in step (A2.4.6). The analysis has to do then with the temperature and vapour pressure equations and obtaining vapour pressure deficit from their combined solution.

$$T_{air,eq} = f_{top} T_{i+1} + f_{lower} T_{i-1} + f_{layer} T_{l,eq} \quad (4.2.43)$$

$$e_{air,eq} = f_{top} e_{i+1} + f_{lower} e_{i-1} + f_{layer} e_s(T_{l,eq}) \quad (4.2.44)$$

In these equations, two approaches were used to calculate the coupling coefficients (f_{lower}, f_{top} or f_{layer}), either a parameterization according to a constant large-time averaged K_M value or a K_M value characteristic of the quiescence period as justified by the analysis given in sect.3.6.2.

The T_{i+1} is the temperature at the upper boundary for the whole canopy and so is the case for the vapour pressure. T_{i-1} is the soil surface temperature and the lower vapour pressure is the saturated vapour pressure at the soil surface temperature. The required temperature of the leaves in the canopy were calculated from eq.4.2.4, in which the temperature of the air and vapour pressure of the air in the canopy layer were eliminated from the equation. This is done by substituting $T_{air,eq}$, $e_{air,eq}$ equations in eq.4.2.4.

The equilibrium temperature of the leaves of the canopy are expressed as

$$T_{l,eq} = \frac{1}{1 - f_{layer,T} - \frac{f_{layer,e} s}{\gamma(r_{bv} + r_s)}} \frac{1}{\left[\frac{1}{r_R} + \frac{1}{r_{bh}} + \frac{s}{\gamma(r_{bv} + r_s)} \right]} \left[\frac{\alpha_r R_s \downarrow}{\rho C_p} + \frac{T_{air,rad}}{r_R} \right. \\ \left. + \frac{f_{top,T}}{r_{bh}} T_{air,top} + \frac{f_{bottom,T}}{r_{bh}} T_{soil} - \frac{e_s(T_{air,top})}{\gamma(r_{bv} + r_s)} + \frac{s}{\gamma(r_{bv} + r_s)} T_{air,top} + \frac{f_{top,e}}{\gamma(r_{bv} + r_s)} e_{air,Top} \right. \\ \left. + \frac{f_{bottom,e}}{\gamma(r_{bv} + r_s)} e_s(T_{soil}) + \frac{f_{layer,e}}{\gamma(r_{bv} + r_s)} e_s(T_{air,top}) - \frac{f_{layer,e}}{\gamma(r_{bv} + r_s)} s (T_{air,top}) \right] \quad (4.2.45)$$

During the gust intrusion phase, the air temperature and vapour pressure becomes equal to the temperature and vapour pressure above the canopy and this becomes the initial value in eq.4.2.46 and eq.4.2.47, respectively. The obtained values for the equilibrium temperature and vapour pressure of the air were replaced in the same equations to obtain the temperature and the vapour pressure of the air.

$$T_{air} = T_{air,eq} \left(1 - e^{-\frac{t}{\tau_{a,T}}}\right) + T_{air,initial} e^{-\frac{t}{\tau_{a,T}}} \quad (4.2.46)$$

$$e_{air} = e_{air,eq} \left(1 - e^{-\frac{t}{\tau_{a,e}}}\right) + e_{initial} e^{-\frac{t}{\tau_{a,e}}} \quad (4.2.47)$$

Two characteristic ratios (2 and 3 respectively) of the period between two consecutive gusts to the time constant of the canopy air were used in eq.4.2.46 and eq.4.2.47. An integral of these last two equations were used in the comparison between the effect of different parameterization of f_{top} , f_{lower} and f_{layer} in $f(L,t)$.

In this analysis the canopy layer was assumed well mixed. This simplifies the calculation for the canopy layer.

In the case studied, we used the following values for the different terms were used:

α_r	$R_s \downarrow$	for the soil is zero, for the canopy it is 200 Wm^{-2} .
$T_{air,rad}$		$10 \text{ }^\circ\text{C}$ for the canopy and for the soil $20 \text{ }^\circ\text{C}$.
$T_{air,top}$		$20 \text{ }^\circ\text{C}$.
T_{soil}		$21 \text{ }^\circ\text{C}$.
e_{top}		1500 Pa
r_R		210 s m^{-1}
$r_{b,h}$		100 sm^{-1}
r_s		200 sm^{-1}
r_{ss}		200 sm^{-1}
K_m		$0.12 \text{ m}^2\text{s}^{-1}$ for a no gust model
K_m		$0.25 \cdot (0.12) \text{ m}^2\text{s}^{-1}$ for a gust model during the quiescence period.
Lad		$3 \text{ m}^2\text{m}^{-3}$
Δz		1 m

The results of the different state variables, under a gust (intermittent) and no-gust (non-intermittent) approach, are given in the following table:

variable	gust	no gust
$T_{l,eq}$	32.95	26.53
$T_{air,eq}$	25.69	21.28
$f_{top,T}$	0.429	0.75
$f_{lower,T}$	0.143	0.062
$f_{layer,T}$	0.429	0.188
$f_{top,e}$	0.692	0.9
$f_{lower,e}$	0.077	0.025
$f_{layer,e}$	0.231	0.075
$e_{air,eq}$	2389	1673

\bar{T}_a	23.23-23.9	21.28
e_{air}	2005-2111	1673
$f_1(L,t)$	114	114
$f_2(L,t)$	442	388
$f(L,t)$	556	502
gust/no-gust forcing ratio		1.108

The two figures, for the mean temperature and vapour pressure, in the gust model are the resulting mean values in the case of the quiescence period being twice or three times as large as the time constant of the canopy layer respectively. The comparison is done for the latter case.

In this one-layer canopy gust model, the calculations show that due to the stronger coupling between the leaves and the canopy air in a gust model compared to a no-gust model, the smaller turbulent transport coefficient during the quiescence period, the resulting higher equilibrium temperature of the leaves and the large ratio between the quiescence period to the time constant of the canopy air layers, the mean temperature and vapour pressure of the air are higher in a gust model compared to a no-gust model.

In this case, that led to an increase in the forcing on the soil temperature profile estimated to be by about 11%. This was due to a canopy layer which was assumed well mixed. The effect of the temperature and vapour increase was felt at the soil surface and so led to a consequent increase in the forcing; $f_2(L,t)$.

Concerning the answer of question 4 about the effect of intermittency on the mean temperature of the air and the soil layers. For the air layers, the time constant is small relative to the time rate of change of the boundary conditions, so an integration of the effect could be shown easily by integrating over small time steps resulting in solutions such as eq.4.2.58. Concerning the soil temperature, the situation differs due to the time constant of the soil reservoir much larger than the time rate of change of the forcing function $f(L,t)$ with its radiative and non radiative components. So, in fact there is no equilibrium temperature but a modified rate of the temperature change of the soil as affected by intermittency. The effect of intermittency on the mean temperature is obtained from evaluating eq.4.2.42 over large time intervals, but it is also shown how the forcing is reduced by following the effect of intermittency on the $f_2(L,t)/f_1(L,t)$. The effect of intermittency on the mean can be evaluated by the value of eq.4.2.36 and averaging. But this will require an integration for a large period of time. We have some results from an early version of the numerical model which shows the effect of intermittency on the mean soil temperature profile (see sect. 4.2.1.2).

In case of two canopy layers, an upper one which has most of the leaf area density and a lower one which has a very low leaf area density, the situation would be reversed. This, we expect, is due to limited turbulent mixing, which would limit the turbulent transport from the top of the canopy down. Also, the low leaf area density in lower part of the canopy will lead to a low equilibrium temperature and vapour pressure of the air and restoration of equilibrium will require a longer period of time as can be seen from eq.4.2.20. This will lead to the effect of the air, which has been brought by the gust intrusion from well above the canopy, to be felt at

soil surface, and a resulting reduction of the forcing with respect to no-gust model will occur. To prove this would require a more numerical model as done in the following section.

CONCLUSIONS (4.2.1.2.B.II):

Before proceeding to study the effect of a two or n layers model, we notice some important results from the analysis of the one layer canopy model,

1) We have seen from section 3.6.2, that most of the contribution to the large-time averaged σ_w^2 comes from events which occupy a very short period of the total time. During most of the time, a small fraction of the total σ_w^2 variance is contributing to the small scale dispersion of the scalars within plant canopies. This leads to a higher coupling, during the quiescence period, between the leaves as sources or sinks to the temperature, vapour pressure of the canopy air layer. The equilibrium temperature and vapour pressure of the air at the end of the quiescence period would have a higher value for a gust model compared to a non-intermittent model. We have seen from section 4.2.1.1, that a mean K_m value does not lead to the same temperature and vapour pressure as a fluctuating K_m value which has the same mean because of the exponential behaviour of the equations. In here, we see that the stronger coupling between the leaves and the air layers lead to a higher equilibrium vapour pressure and temperature of the air.

2) The values of the variation of the forcing, due to the existence of the coherent structures, are significant. In this scaling analyse, we are interested in approximate values to show the importance of the gust process on the behaviour of the system. Detailed numerical modelling is done in chapter 5.

III. A scaling of a two to n layers model:

1. The Approximate form :

In here, we are interested in obtaining the effect of intermittency on the mean temperature and vapour pressure deficit of the air, and use this to scale the effect of intermittency on $f_1(L,t)/f_2(L,t)$ functions. In the case of a multi-layered canopy (two to n vegetation layers) and the layer of air above the canopy, it is not possible to obtain a complete elimination of the temperature and vapour pressure of the canopy air layers, as has been done in eq.4.2.45 for the one layer canopy model. This means that we have to find a way to solve the canopy equation and scale the effect of intermittency easily.

In Section 4.2.1.1, four equations were derived which could be used to describe the canopy behaviour completely. Two combinations, each consisting of three equations, could be used to describe the canopy behaviour with different degrees of accuracy. We will use these two combinations to scale the effect of intermittency on the average temperature and vapour pressure deficit of the air. This is done through the effect of intermittency on the

values of the coefficients of the inverse matrix A^{-1} of the coupling coefficients matrix A between different canopy layers.

We will start first with the less accurate combination, the vapour pressure deficit combination and show how this can be used to describe the canopy behaviour and the effect of intermittency on the soil heat flux. We will call this form **the approximate form**. In the appendix 2.6.1, it is shown that

$$\begin{bmatrix} 1 & 0 & 0 & 0 & 0 & 0 \\ E_2 & -F_2 & G_2 & 0 & 0 & 0 \\ 0 & E_3 & -F_3 & G_3 & 0 & 0 \\ 0 & 0 & E_4 & -F_4 & G_4 & 0 \\ 0 & 0 & 0 & E_5 & -F_5 & G_5 \\ 0 & 0 & 0 & 0 & 0 & 1 \end{bmatrix} \cdot \begin{bmatrix} D_1 \\ D_2 \\ D_3 \\ D_4 \\ D_5 \\ D_6 \end{bmatrix} = \begin{bmatrix} D_{\text{first air layer}} \\ -C_2 \\ -C_3 \\ -C_4 \\ -C_5 \\ D_{\text{upper boundary}} \end{bmatrix} \quad (4.2.48)$$

E_i, G_i are the turbulent transport coupling coefficient between the layer i and the layer below and above respectively and given by

$$E_i = \frac{K_{\text{bottom},i}}{\delta X_{\text{bottom},i}} \quad (4.2.49a)$$

$$G_i = \frac{K_{\text{top},i}}{\delta X_{\text{top},i}} \quad (4.2.49b)$$

while F_i expresses the layer coefficient and equals

$$F_i = \left(\frac{\Delta z_i}{\Delta t} + \frac{K_{\text{top},i}}{\delta X_{\text{top},i}} + \frac{K_{\text{bottom},i}}{\delta X_{\text{bottom},i}} + \frac{\text{LAD} \Delta z_i}{r_{b,i} + \alpha r_{s,i}} \right) \quad (4.2.49c)$$

and C_i expresses the source effect

$$C_i = \frac{\text{LAD} \Delta z}{(r_s \alpha + r_b)} \frac{s r_s \alpha R_n}{\rho C_p} + \frac{\Delta z_i}{\Delta t} D_i^f \quad (4.2.49d)$$

The importance of intermittency shows through decreasing the fractional contribution of the E_i and G_i to the F_i term. In case of solving for a steady state solution, this is done by assuming $\Delta t \rightarrow \infty$, so the first term in F_i and the last one in C_i go to zero. If we assume that intermittency has no effect on some of the terms of C_i and F_i especially r_s, R_n and less importantly s , then intermittency effect shows mainly on the values of the inverse matrix of A (the coupling coefficient matrix). The indirect effect could show through the effect of intermittency on the resulting mean temperature and vapour pressure deficit of the air which

affects the stomatal resistance of the leaves and the value of R_n (the latter through making the leaves warmer or colder). The solution of the above system is

$$\mathbf{A}^{-1} \cdot \mathbf{A} \cdot \mathbf{D} = \mathbf{A}^{-1} \cdot \mathbf{C} \quad (4.2.50)$$

$$\mathbf{D} = \mathbf{A}^{-1} \cdot \mathbf{C} \quad (4.2.51)$$

What the inverse matrix expresses is the contribution of the different values of C_j to a certain value of D_i , as given by

$$D_i = \sum_{j=1}^n A_{ij} C_j \quad (4.2.52)$$

In the example given below, there were no sources with the canopy (i.e. LAD was turned to zero). What we notice is the higher values in the intermittent system of the coefficients A_{ij}^1 where i and $j \neq 1$ or $\neq n$, i.e. the inner elements of the matrix, while the elements in the first column or the last one have still the same value as the non-intermittent system. This means a relative reduction in the role of the upper and lower boundaries of the simulated domain to the equilibrium solution and a higher contribution of the inner layers to the solution at a certain height. The lower mixing during the quiescence period leads then to the establishment of a higher influence of the inner C_i elements to the vapour pressure deficit within a certain layer in comparison to a non gust model, in which a higher value of the turbulent transport coefficient is active all the time. Whether this leads to a higher or lower vapour pressure deficit than that of the boundaries depends on the stomatal resistance and R_n profile, as has been shown on conclusion 4 of sect.4.2.1.1. In the gust approach, the total mean K_M value is the same as in the no-gust model, but during the gust occurrence, most of the turbulence occurs while in the quiescence period, the value of K_M is much lower than the

$$\mathbf{A} = \begin{bmatrix} 1 & 0 & 0 & 0 & 0 & 0 \\ -0.06 & 0.12 & -0.06 & 0 & 0 & 0 \\ 0 & -0.06 & 0.12 & -0.06 & 0 & 0 \\ 0 & 0 & -0.06 & 0.12 & -0.06 & 0 \\ 0 & 0 & 0 & -0.06 & 0.12 & -0.06 \\ 0 & 0 & 0 & 0 & 0 & 1 \end{bmatrix} \quad (4.2.53a)$$

$$\mathbf{A}^{-1} = \begin{bmatrix} 1 & 0 & 0 & 0 & 0 & 0 \\ 0.8 & 13.333 & 10 & 6.667 & 3.333 & 0.2 \\ 0.6 & 10 & 20 & 13.333 & 6.667 & 0.4 \\ 0.4 & 6.667 & 13.333 & 20 & 10 & 0.6 \\ 0.2 & 3.333 & 6.667 & 10 & 13.333 & 0.8 \\ 0 & 0 & 0 & 0 & 0 & 1 \end{bmatrix} \quad (4.2.53b)$$

An example of a matrix with intermittency and its inverse (no sources).

$$A = \begin{bmatrix} 1 & 0 & 0 & 0 & 0 & 0 \\ -0.12 & 0.24 & -0.12 & 0 & 0 & 0 \\ 0 & -0.12 & 0.24 & -0.12 & 0 & 0 \\ 0 & 0 & -0.12 & 0.24 & -0.12 & 0 \\ 0 & 0 & 0 & -0.12 & 0.24 & -0.12 \\ 0 & 0 & 0 & 0 & 0 & 1 \end{bmatrix} \quad (4.2.54a)$$

$$A^{-1} = \begin{bmatrix} 1 & 0 & 0 & 0 & 0 & 0 \\ 0.8 & 6.667 & 5 & 3.333 & 1.667 & 0.2 \\ 0.6 & 5 & 10 & 6.667 & 3.333 & 0.4 \\ 0.4 & 3.333 & 6.667 & 10 & 5 & 0.6 \\ 0.2 & 1.667 & 3.333 & 5 & 6.667 & 0.8 \\ 0 & 0 & 0 & 0 & 0 & 1 \end{bmatrix} \quad (4.2.54b)$$

An example of a matrix with non-intermittency and its inverse (no sources)

mean (0.25-0.3 of the total averaged mean). In this case, LAD was assumed zero for all layers, so all C_i from $i=2$ to $i=n-1$ are zero and the solution leads to a linear interpolation between $D_{\text{first air layer}}$ and $D_{\text{upper boundary}}$ for different canopy layers. In this case also, there is no effect for LAD in F_i coefficients, so there is a decrease of the importance of the source terms in layer coefficient F_i . But the point shown here, is that the contribution of the inner nodes increases in the final solution in the case of a gust model as compared to that of no gust.

The resulting change in the values of these coefficients will be used to check the effect of the closure on the solution (the inverse matrix A^{-1}).

For the air temperature at equilibrium, the following system of equation has to be solved

$$\begin{bmatrix} 1 & 0 & 0 & 0 & 0 & 0 \\ E_2 & -F_2 & G_2 & 0 & 0 & 0 \\ 0 & E_3 & -F_3 & G_3 & 0 & 0 \\ 0 & 0 & E_4 & -F_4 & G_4 & 0 \\ 0 & 0 & 0 & E_5 & -F_5 & G_5 \\ 0 & 0 & 0 & 0 & 0 & 1 \end{bmatrix} \cdot \begin{bmatrix} T_1 \\ T_2 \\ T_3 \\ T_4 \\ T_5 \\ T_6 \end{bmatrix} = \begin{bmatrix} T_{\text{first air layer}} \\ -C_2 \\ -C_3 \\ -C_4 \\ -C_5 \\ T_{\text{upper boundary}} \end{bmatrix} \quad (4.2.55)$$

E_i, G_i are the turbulent transport coupling coefficient between the layer i and the layer below and the layer above respectively and are the same as eq.4.2.49.a and eq.4.2.49.b, while F_i expresses the layer coefficient and equals

$$F_i = \left(\frac{\Delta z_i}{\Delta t} + \frac{K_{\text{top},i}}{\delta X_{\text{top},i}} + \frac{K_{\text{bottom},i}}{\delta X_{\text{bottom},i}} \right) \quad (4.2.56a)$$

$$C_i = \left(\frac{\gamma^* R_n - \rho C_p D r_b^{-1}}{s + \gamma^*} \right) LAD \Delta z + \frac{\Delta z}{\Delta t} T_i^t \quad (4.2.56b)$$

$$T = A^{-1} \cdot C \quad (4.2.57)$$

For steady state solution, $\Delta t \rightarrow \infty$. The first term in F_i and the last one in C_i go to zero.

The solution is obtained by assuming initially isothermal conditions within the plant canopy (i.e. the leaf temperatures equal air temperature), so the longwave radiation profiles and R_n can be calculated. These values of R_n are used to calculate the values of D according to eq.4.2.51, These latter can be used to calculate the temperature and vapour pressure of the air according to eq.4.2.55 and 4.2.57. The amount of sensible heat flux from the leaf to the air can be calculated by the use of Penman-Monteith equation and the calculated D and the assumed R_n . This value of C_i can be used to calculate the leaf temperature at different layers. This will be used to calculate the longwave radiation profile and a new value of R_n . The process is repeated till the solution converges.

This method of solution could be considered a variant of Chen's method (1984), in which the requirement of specifying the saturation heat flux J has been eliminated. D could be calculated directly.

It is to be noticed that the coefficients of C matrix, for air temperature, have an effect of intermittency expressed in their values through the effect of the A^{-1} of equation system (4.2.48) in the calculation of D_i . The calculated T will have an intermittency effect due to changes in the values of C matrix of system (4.2.55) and the values A^{-1} of that system, so it is rather a compound effect.

To obtain an approximate value for mean D , it is assumed that we can integrate eq.4.2.20,

$$D_{air} = D_{air,eql} \left(1 - e^{-\frac{t}{\tau_{a,D}}} \right) + D_{air,initial} e^{-\frac{t}{\tau_{a,D}}} \quad (4.2.20)$$

resulting in

$$\bar{D} = \frac{1}{\text{period}} \int_0^{\text{period}} D_{air} dt \approx \frac{1}{\text{period}} \int_0^{\text{period}} \left(D_{air,eql} \left(1 - e^{-\frac{t}{\tau_{a,D}}} \right) + D_{air,initial} e^{-\frac{t}{\tau_{a,D}}} \right) dt \quad (4.2.58)$$

Since $D_{air,eql}$ and $D_{air,initial}$ are functions of time, it is difficult to integrate eq.4.2.20. It is possible, anyhow, to describe the canopy vapour pressure deficit by an equation similar to 4.2.20

$$\bar{D} \approx D_{air,eql} + \frac{(D_{air,initial} - D_{air,eql})}{\text{Period}} \int_0^{\text{period}} -\tau_{a,D} \left(-\frac{1}{\tau_{a,D}} \right) e^{-\frac{t}{\tau_{a,D}}} dt \quad (4.2.59a)$$

$$\bar{D} = D_{\text{air,eq}} + \frac{(D_{\text{air,initial}} - D_{\text{air,eq}}) \tau_{a,D}}{\text{Period}} \left(1 - e^{-\frac{\text{period}}{\tau_{a,D}}}\right) \quad (4.2.59b)$$

In case of characteristic period for coherent structure intrusion which equals three times the time constant,

$$\bar{D} \approx 0.69 D_{\text{air,eq}} + 0.31 D_{\text{air,initial}} \quad (4.2.60)$$

$D_{\text{air,eq}}$ will be determined from the solution of eq.4.2.48 by the use of a reduced turbulent transport coefficient, assuming that the value of the C matrix are the same for the gust and no-gust approach. This is not exactly true, since there is an effect of intermittency on the mean vapour pressure deficit and temperature of the air, which affects the values of C_i terms through affecting mainly the stomatal resistance and less importantly the value of R_n and s .

In case of the period between two gust intrusions being very large, a profile as shown in fig.4.2.b develops and the resulting D becomes very small due to the required gradient needed to achieve a vapour pressure deficit flux. The end result could be less vapour pressure deficit in a gust model in comparison to a no-gust model. Usually, the time period between two consecutive gust intrusions is usually not large enough for such a profile to develop, so the diffusion from above of low vapour pressure deficit to the soil surface and the decrease of vapour pressure deficit is not allowed to continue, and a mean profile will be an inverse of that shown in fig 4.2.a.

$$D_{\text{air,eq}} = A^{-1} \cdot C \quad (4.2.61)$$

$$\bar{D}_{\text{gust model}} \approx 0.69 A_{\text{gust}}^{-1} C + 0.31 D_{\text{ini}} \quad (4.2.62)$$

The Matrix C is assumed the same in the gust and no-gust model. The deviation between a gust and no-gust model depends on

$$\bar{D}_{\text{gust model},i} = \sum_{j=1}^n (0.69 A_{\text{gust},ij}^{-1} C_j) + 0.31 D_{\text{ini},i} \quad (4.2.63)$$

being higher or lower than

$$\bar{D}_{\text{nogust model},i} = \sum_{j=1}^n A_{\text{nogust},ij}^{-1} C_j \quad (4.2.64)$$

This will depend on the inverse matrix of the coupling coefficient matrix A and how much relative weight it gives to the layers above and below the canopy in determining the vapour pressure deficit of the air layers close to the ground. Even if it matches for a certain layer, the requirement of down-gradient transport will lead to no matching for the other

layers. That shows the importance of defining the inverse matrix symbolically or by the use of Thomas algorithm as given in Patanker (1980).

The inverse matrix A^{-1} is given symbolically in sect. 4.2.4.

The same procedure is done for the calculation of the mean T by solving the eq.4.2.55
The mean temperature of the air is determined by integrating an equation similar to eq.4.2.13, yielding

$$\bar{T} \approx T_{air,eq1} + \frac{(T_{air,initial} - T_{air,eq1})}{\text{Period}} \int_0^{\text{period}} -\tau_{a,T} \left(-\frac{1}{\tau_{a,T}}\right) e^{-\frac{t}{\tau_{a,T}}} dt \quad (4.2.65)$$

$$\bar{T} \approx T_{air,eq1} + \frac{(T_{air,initial} - T_{air,eq1})\tau_{a,T}}{\text{Period}} (1 - e^{-\frac{\text{period}}{\tau_{a,T}}}) \quad (4.2.66 a)$$

$$\bar{T} \approx 0.69 T_{air,eq1} + 0.31 T_{air,initial} \quad (4.2.66b)$$

with an assumption that the effect of the difference between the values of the time constants of T and D make no much difference on the solution. The coefficients Matrix C will not be the same for a gust and no-gust model, because the value of D entering in the coefficients is being affected by the turbulent closure.

$$\bar{T}_{\text{gust model}} \approx 0.69 * A_{\text{gust}}^{-1} C + 0.31 T_{ini} \quad (4.2.67)$$

$$\bar{T}_{\text{nogust}} = A_{\text{nogust}}^{-1} C \quad (4.2.68)$$

$$\bar{T}_{\text{nogust model},i} = \sum_{j=1}^n A_{\text{nogust},ij}^{-1} C_j \quad (4.2.69)$$

$$\bar{T}_{\text{gust model},i} = \sum_{j=1}^n (0.69 A_{\text{gust},ij}^{-1} C_j) + 0.31 T_{ini,i} \quad (4.2.70)$$

The difference of the solution between a gust and no-gust approach for the temperature and vapour pressure is fed into the solution of the first air layer.

There is one problem with this system: This problem is defining the values of vapour pressure deficit for the lowest air layer. For this layer, the lower coupling coefficient is different for the temperature and vapour pressure air equations, so obtaining a common factor in step A.2.4.6 is not possible. So, the above system of equations apply only to the canopy air layers from layer number 2 to layer number n. For the first air layer in contact with soil, obtaining a value of the vapour pressure deficit for the first air layer is done through the use

of the temperature and vapour pressure equations for the first air layer equations. These equations are the same as equations A.2.2.7 and A.2.3.5 for temperature and vapour pressure for the first air layer. The lower coupling coefficient in both these equations have to be replaced by

$$\frac{K_{\text{bottom}}}{\delta X_{\text{bottom}}} = \frac{\rho C_p}{r_{\text{bh,soil}}} \tag{4.2.71a}$$

$$\frac{K_{\text{bottom}}}{\delta X_{\text{bottom}}} = \frac{\rho C_p}{(r_{\text{bv,soil}} + r_{\text{s,soil}})} \tag{4.2.71b}$$

$r_{\text{s,soil}}$ expresses the soil resistance to evaporation. This resistance is somewhat similar to the stomatal resistance of the plants, and it has been parameterized as shown in section 4.6. So we solve the temperature and vapour pressure equations for the first air layer assuming a rather constant temperature of the soil and a feedback from air layer number 2. The solution would converge. One point is that we assume, that the temperature or vapour pressure of the soil are initially the same for the gust and no-gust approach. This method can still be used for checking the forcing variability with the modelling approach. This forcing will control the time rate of soil surface temperature change.

It is important to notice that the whole canopy layers and the first soil layer are coupled, but there is a large difference in the time constants of both systems. That allows assuming that the soil surface temperature is almost constant during a short time interval which is much larger than the time duration of a gust cycle, so the temperature of the soil surface can be treated as a constant in eq.A.2.2.7 & A.2.3.5. The effect of intermittency on the mean value of D and T of the first air layer can be calculated. The resulting mean value of the first air layer D and T will affect the solution of the soil later through eq.4.2.42. So, the whole technique of analysis here depends on the separation of time scales of different system components.

We will stop here with the analysis for the approximate form and continue with the analysis for the more exact form because, we think, it is more relevant.

2. The more exact form (the nonsteady state solution)

There is an enhancing aspect of intermittency on the sources and sinks within plant canopies. The time variation in the turbulent transport coefficient leads, during the gust intrusion phase, to the time constants of the canopy air layer being very small, and an equilibrium solution for the canopy air layers is established very rapidly. This equilibrium during the gust intrusion phase is represented by the canopy air having the same temperature and vapour pressure deficit as the layer of air above. The leaves on the other hand have a much larger time constant in comparison to the canopy air time constant during the gust intrusion phase. So, an equilibrium solution for the air is established within the gust process, while for the leaves it is not. Once the gust process shuts off, there is a strong reduction in the turbulent transport coefficient which reduces the coupling between the air layers and the layer of air above. If the leaves thermal equilibrium had been established before the gust intrusion, the process of gust intrusion represents then a large shift for the system which has to be

restored. The energy storage change within the leaves plays an important part in this. The system is far from a steady state solution and the effect of temperature changes within the system is important.

To estimate the effect of the non-steady term in the energy budget equation of a canopy with a leaf area index of 2 and leaf thickness of 0.001 m and 75 % moisture content in the leaves, a decrease or an increase of 1 K for the leaves would represent about 6270 joules storage change. If this change happened within 60 seconds, this represents 104 Wm^{-2} . This would represent a large ratio with respect to the energy partition on the leaf surfaces.

It has been shown by Paw U(1992) that the radiative surface temperature trace reveals a ramp-like response to the coherent structures. That implies that the value of R_n follows a ramp-like pattern. So, there is a measured change of energy storage within plant tissues.

If hypothetically, the gust duration period were large enough that the leaves have achieved thermal equilibrium, the sudden reduction in the turbulent transport coefficient would lead to the a re-establishment of a new equilibrium. This new equilibrium state would be due to the different weighting coefficients in eq.4.2.12. So the difference in temperature between the leaf and the air will contribute in a different ratio to the equilibrium temperature of the air. We start then with a system which was in equilibrium already and it shifts from that equilibrium due to the change in the weighing coefficients in the air temperature and vapour pressure equilibrium equation. This will later have a feedback on the temperature of the leaves through eq.4.2.5. Things here will go more smoothly than in the previous case, but the initial hypothesis of long gust duration is unrealistic. So in our analysis we will be dealing with nonsteady state solutions, and we will show an example of such a solution.

The more exact equation (nonsteady state solution for air temperature and vapour pressure)

The temperature of the air system follows (A.2.6.2.a)

$$\begin{bmatrix} 1 & 0 & 0 & 0 & 0 & 0 \\ E_2 & -F_2 & G_2 & 0 & 0 & 0 \\ 0 & E_3 & -F_3 & G_3 & 0 & 0 \\ 0 & 0 & E_4 & -F_4 & G_4 & 0 \\ 0 & 0 & 0 & E_5 & -F_5 & G_5 \\ 0 & 0 & 0 & 0 & 0 & 1 \end{bmatrix} \cdot \begin{bmatrix} T_1 \\ T_2 \\ T_3 \\ T_4 \\ T_5 \\ T_6 \end{bmatrix} = \begin{bmatrix} T_{\text{first soil layer}} \\ -C_2 \\ -C_3 \\ -C_4 \\ -C_5 \\ T_{\text{upper boundary}} \end{bmatrix} \tag{4.2.72}$$

$$\mathbf{T} = \mathbf{A}^{-1} \mathbf{C} \tag{4.2.73}$$

where

$$E_i = \frac{K_{\text{bottom},i}}{\delta X_{\text{bottom},i}} \tag{4.2.74a}$$

$$G_i = \frac{K_{top,i}}{\delta X_{top,i}} \quad (4.2.74b)$$

$$F_i = \left(\frac{\Delta z_i}{\Delta t} + \frac{K_{top,i}}{\delta X_{top,i}} + \frac{K_{bottom,i}}{\delta X_{bottom,i}} + \frac{LAD \Delta z}{r_{bh}} \right) \quad (4.2.74c)$$

or

$$F_i = \left(\frac{\Delta z_i}{\Delta t} + \frac{K_{top,i}}{\delta X_{top,i}} + \frac{K_{bottom,i}}{\delta X_{bottom,i}} \right)$$

$$C_i = \frac{T_1}{r_{bh}} LAD \Delta z + \frac{\Delta z}{\Delta t} T_i^t \quad (4.2.74d)$$

or

$$C_i = \left(\frac{(T_1 - T_i)}{r_{bh}} \right) LAD \Delta z + \frac{\Delta z}{\Delta t} T_i^t$$

The effect of intermittency shows also, as before, through the effect of the inverse matrix A^{-1} of the coupling coefficient A on the solution and the memory of the system through T_i^t . In here the initial temperature of the air is kept in the C matrix, since we are solving for the nonsteady state source.

The vapour pressure equation has a similar equation (A.2.6.2.b)

$$\begin{bmatrix} 1 & 0 & 0 & 0 & 0 & 0 \\ E_2 & -F_2 & G_2 & 0 & 0 & 0 \\ 0 & E_3 & -F_3 & G_3 & 0 & 0 \\ 0 & 0 & E_4 & -F_4 & G_4 & 0 \\ 0 & 0 & 0 & E_5 & -F_5 & G_5 \\ 0 & 0 & 0 & 0 & 0 & 1 \end{bmatrix} \cdot \begin{bmatrix} e_1 \\ e_2 \\ e_3 \\ e_4 \\ e_5 \\ e_6 \end{bmatrix} = \begin{bmatrix} e_{\text{first soil layer}} \\ -C_2 \\ -C_3 \\ -C_4 \\ -C_5 \\ e_{\text{cupper boundary}} \end{bmatrix} \quad (4.2.75)$$

$A \quad \cdot \quad e = C$

$$A^{-1} \cdot A \cdot e = A^{-1} \cdot C \quad (4.2.76)$$

$$e = A^{-1} \cdot C \quad (4.2.77)$$

where

$$E_i = \frac{K_{bottom,i}}{\delta X_{bottom,i}} \quad (4.2.78a)$$

$$G_i = \frac{K_{top,i}}{\delta X_{top,i}} \quad (4.2.78b)$$

$$F_i = \left(\frac{\Delta z_i}{\Delta t} + \frac{K_{top,i}}{\delta X_{top,i}} + \frac{K_{bottom,i}}{\delta X_{bottom,i}} + \frac{LAD \Delta z}{(r_{bh} + r_s)} \right) \quad (4.2.78c)$$

or

$$F_i = \left(\frac{\Delta z_i}{\Delta t} + \frac{K_{top,i}}{\delta X_{top,i}} + \frac{K_{bottom,i}}{\delta X_{bottom,i}} \right)$$

$$C_i = \frac{e_s(T_i)}{(r_{bh} + r_s)} LAD \Delta z + \frac{\Delta z}{\Delta t} e_i^t \quad (4.2.78d)$$

or

$$C_i = \left(\frac{(e_s(T_i) - e_i^t)}{(r_{bh} + r_s)} \right) LAD \Delta z + \frac{\Delta z}{\Delta t} e_i^t$$

The temperature of the leaves are determined implicitly (with the knowledge of the T_i^t and e_i^t) by the use of eq.4.2.5 & 4.2.6 or by the use of the numerical implementation as explained in sect. 2.3.1.1.

This represents the more exact system form to solve the canopy equations. One advantage is that it applies for all canopy layers, including the first air layer. Soil layers could be included, if we change the coupling coefficient by the heat conductivity coefficients between different layers. There are no sources and sinks within the soil except for phase transformations. In the numerical model (chapter 5), a nonsteady state solution for a system of discretized equations equivalent to this nonsteady one were used to solve the whole problem.

From here, it seems that the inverse matrix A^{-1} of the coupling coefficient A will control the coupling between the canopy layers and the boundaries above and below.

Now, we want to continue with our scaling analysis and obtain an average vapour pressure deficit and temperature of the first air layer, so we can determine the effect of intermittency on the $f_1(L,t)/f_2(L,t)$ in the forcing functions. We will come back to the discussions of the decoupling procedure for system 4.2.72 and 4.2.75, especially at the soil canopy interface at section 4.4.

A numerical solution by the use of MATHCAD® for few time steps including three gust cycles will be used to show the effect of the intermittency on the values of the mean D and mean T . This model will be run under identical conditions, except for a gust occurring at every tenth time step from the beginning of the simulation in the gust model, which also has a reduced turbulent transport coefficient by a factor of 0.25 compared to the no-gust model.

This model solves the following systems of equations: eq.4.2.5, system of equations 4.2.72 and system of eq.4.2.75. All the variables in these equations will play a role in the solution. These variables include : R_n , $T_{air,rad}$, T_{air} , e_{air} , LAD , K_{top} , K_{bottom} , r_{bh} , r_s and r_{ss} .

To facilitate a comparison, the values of R_{short} , T , will be chosen to represent a rather constant high radiative loading, while the values of the temperature and vapour pressure of the air will be varied to allow for the variability of certain climatic regimes, as is explained on page 143. The leaf area density will be kept constant for all the runs. The values of K_{top} , K_{bottom} , r_s and r_{ss} will be varied to see the sensitivity of the solution (i.e. the f_1/f_2 function and the integrated fluxes at the canopy top).

The effect of intermittency on the soil heat flux from the more exact form:

The MATHCAD runs:

The description of the simulated system:

A six layer canopy with equal layers thickness of 0.2m is defined. The values of all other variables are given in fig.4.4.a. In the case shown: a leaf area density profile of $0.0 \text{ m}^2 \text{ m}^{-3}$ for the lowest two layers and a leaf area density of $4 \text{ m}^2 \text{ m}^{-3}$ for the uppermost four layers was used. A cumulative leaf area index of 3.2 results. A short wave radiation absorption coefficient (α_r) of about 0.8 was used. This leads, in the case of R_{short} being equal to 140 Wm^{-2} leaf surface (one side), to a total short wave radiation loading of about $3.2 * 2 * 140 * 0.8 = 716 \text{ Wm}^{-2}$ for the whole vegetation layer. No absorption of radiation by the soil surface was assumed. Only the effect of intermittency on the state variables of the air and its effect on the forcing on the soil was considered. $T_{\text{air,rad}}$ was set to 15°C , a rather high value, to average for the different longwave radiation loading on the upper and lower surface of the leaves. The time

coeff:= 0.25	$dz_i := 0.2$	$dx_{top_i} = 0.2$	
$R_{\text{short}} := 140.$	$dt := 5.$	$dx_{lower_i} = 0.2$	
$T_{\text{air,rad}} := 15.$		Thick:= 0.0005	
$Lad_i :=$	$k_{lower_i} :=$	$ktop_i :=$	$T_{ini_i} :=$
0.0	0.008	0.016	23.807973
0.0	0.016	0.028	23.986098
4.0	0.028	0.04	24.236366
4.0	0.04	0.08	24.11513
4.0	0.08	0.08	23.8934
4.0	0.08	0.08	23.490263
$cumlai := \sum_i Lad_i \cdot dz_i$			$T_{\text{airtop}} = 20.0$
cumlai= 3.2			$T_{\text{air}_{m,j}} := 20.0$
$Total_Load := cumlai R_{\text{short}} 2 \cdot \alpha_r$			$e_{\text{air}_{m,j}} = 1500$
Total_Load= 716.8			$T_{\text{air}_{0,0}} := 20$
$rbh_m := 100.$			$e_{\text{air}_{m,0}} = 1500.$
$rbhs = 100.$			
$rs_m = 600$			$e_{\text{airtop}} = 1500$
$rss = 200.$			
$T_{\text{leaves}_{i,j}} := 23.0$			$T_{\text{soil}} = 21.$

Fig. 4.4.a: The parameters used in the run.

step of simulation will be changed in the last run to check the sensitivity of the solution to the period between gust intrusions into plant canopies, since in this simplified model an intrusion of air into plant canopy occurs every tenth time step. The difference between the gust and no-gust approach on the forcing f_2 functions and the fluxes will be checked. In the no-gust run, the value of (coeff= 1) was used. Everything else was the same.

The solution procedure of the governing equations is exactly the same as the model presented in chapter 5, except for the solution of the absorbed radiation. There is no calculation of the short and longwave radiation profiles. The amount of absorbed radiation is assumed the same for unit leaf surface for all heights. To avoid the effect of storage change within the leaves on the solution, the gust model was run first using an arbitrary initial leaf temperature profile and the final temperature of the leaves were used as initial values of the leaf temperature in a new run. This process was repeated till the difference in storage change in the leaves didn't contribute more than 1 Wm^{-2} for the whole canopy layer. The same initial leaf temperatures profile was also used in the no-gust model. This latter step does not really matter, since in the comparison between a gust and no-gust model, the equilibrium solution of the no-gust model (i.e. the final time step) is compared against the mean values of the gust model.

The results of the run specified in fig.4.4.a is used to show the limitations of the use of the value of f_2 functions alone as a criteria for the effect of intermittency on the canopy soil system. The results for the gust model give a value of 398.1 Wm^{-2} for the f_2 function, while for the no-gust model a value of 396.1 Wm^{-2} was obtained, not a significant difference. The

The higher turbulent coupling coefficients in the no-gust model (f_{topt} , f_{lowert} , f_{topte} , f_{lowere}), as given by eq.4.2.12 and 4.2.17 respectively, couple the canopy layers more to the boundary conditions above, while for the gust model the higher f_{layert} and f_{layere} couple these layers during the quiescence period more to the temperature and vapour pressure of the leaves. These latter are affected by the vapour pressure and temperature of the air as given by eq.4.2.5. The higher temperature and vapour pressure of the air resulting from the coupling of these latter to the temperature and vapour pressure of the leaves will affect the temperature of the leaves further, and a buildup starts.

We notice the higher bulge in the gust model, compared to the no-gust model, in the mean temperature, vapour pressure and vapour pressure deficit profiles. The first bulge corresponded to a counter-gradient transport, while the existence of a smaller bulge in the no-gust model corresponded to a negative flux (downwards) due to the temperature of the soil during the simulation being set to 21 °C. There was also a maximum difference in the mean temperature of the air of about one degree °C and a difference in the mean temperature of the leaves in the middle of the canopy of about 0.5 °C. Looking at the equilibrium air temperature and vapour pressure profiles (fig.4.4.c), we see that in spite of being initially lower than those of the nogust model, they pick up rapidly that the mean values of those in the gust model become higher than the equilibrium ones in the no-gust model.

A new run with a reduced value of the stomatal resistance (300 sm^{-1}) was done. The other parameters are as in fig.4.5.a. For the gust model, the resulting f_2 function was 397.6 Wm^{-2} . The resulting sensible and latent heat flux from the soil to the air were 0.29 and 41.9 Wm^{-2} . The averaged sensible and latent heat fluxes at the canopy were: 126.9 and 352.1 Wm^{-2} . This corresponded to total sources within the canopy of 126.6 and 310.2 Wm^{-2} (a value of $436. \text{ Wm}^{-2} R_n$ with a Bowen ratio on plant surfaces of 0.41). The values of the mean profiles is given in fig.4.5.d.e.

In the case of no-gust model, the resulting f_2 function was 395.2 Wm^{-2} . This is also an insignificant difference. The resulting sensible and latent heat flux from the soil to air were: 2.0 and 46.9 Wm^{-2} . The fluxes at the canopy top of sensible and latent heat were: 138.8 and 362.1 Wm^{-2} . This corresponded to total sources within the canopy of 136.7 and 315.2 Wm^{-2} (a value of $451 \text{ Wm}^{-2} R_n$ with a Bowen ratio on plant surfaces of 0.435). The resulting mean profiles are shown in fig.4.5.d for the no-gust model. So, there is a somewhat large difference between the gust model and no-gust in the value of R_n and the partition on plant surfaces.

In this run, within the gust model, there was a favourable partition toward sensible heat on the account of latent heat, as can be seen from fig. 4.5.b,

coeff = 0.25		dxtop _i = 0.2
Rshort = 140.	dz _i = 0.2	dxlower _i = 0.2
Tairrad = 15.	dt = 5.	Thick = 0.0005
Lad _i =	klower _i =	ktop _i =
0.0	0.008	0.016
0.0	0.016	0.028
4.0	0.028	0.04
4.0	0.04	0.08
4.0	0.08	0.08
4.0	0.08	0.08
$\text{cumlai} = \sum_i \text{Lad}_i dz_i$		
$\text{cumlai} = 3.2$		
$\text{Total_Load} = \text{cumlai} R_{\text{short}} 2 \cdot \text{ar}$		
$\text{Total_Load} = 716.8$		
rbh _m = 100.		Tairtop = 20.0
rbhs = 100.		Tair _{m,j} = 20.0
rs _m = 300		ear _{m,j} = 1500
		Tair _{0,0} = 20
		ear _{m,0} = 1500.
rss = 200.		earitop = 1500
Tleaver _{i,j} = 23.0		Tsoil = 21.

Fig.4.5.a : A run with a reduced stomtal resistance.

in spite of the observed behavior of decreased vapour pressure deficit with time during the quiescence period. This case corresponds to Bowen ratio less than γ/s and condition 4.2.85 not being satisfied. There was a maximum difference of 0.5 °C for the temperature of the air and the leaves. It is clear from fig.4.5.b that the gust intrusion leads to an increase in the value of R_n , since it leads to more coupling between the plant and the upper boundary, but it seems that the adverse effect of the lower coupling coefficient during the quiescence period dominates.

Looking at the coupling coefficients for this run and the previous one, we see that the first air layer of the canopy has a higher coupling to the soil vapour pressure in the gust model, so the vapour pressure of the soil contributes more to the equilibrium vapour pressure of the first air layer and the transport to the layer above contributes less. This leads to the buildup of vapour pressure which reduces the soil latent heat flux. The

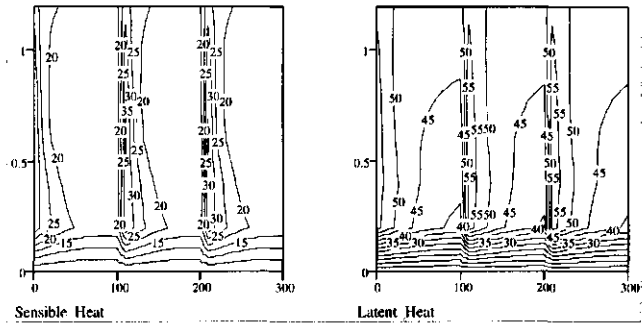


Fig.4.5.b: Sources behaviour within time in Wm-2 leaf surface (one side)

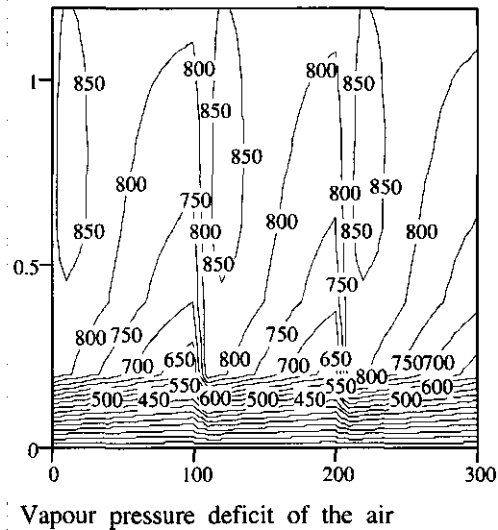


Fig 4.5.c: vapour pressure deficit behaviour within time in seconds*1/2

Mean_Tleaves_eq <i>i</i>	Mean_Taireq <i>i</i>	Mean_eaireq <i>i</i>	Tairmean	Eairmean	Dmean	Mean_Tleav <i>e</i> _{<i>i</i>}
22.73	21.037	1.825·10 ³	20.84	1.745·10 ³	721.286	22.723
22.789	21.187	1.746·10 ³	21.071	1.719·10 ³	782.95	22.786
22.983	21.476	1.767·10 ³	21.385	1.746·10 ³	804.3	22.982
22.882	21.328	1.728·10 ³	21.277	1.717·10 ³	816.154	22.88
22.703	21.086	1.683·10 ³	20.637	1.605·10 ³	829.8	22.702
22.382	20.663	1.61·10 ³	20.637	1.605·10 ³	829.8	22.379

Fig 4.5.d : The mean profiles in the gust model for run 4.5.a

bottleneck of transport then is the turbulent transport between the canopy first air layer and the air layer which is in direct contact with the soil surface. This latter has a thickness as large as the displacement boundary layer (about 1 cm thickness). This transport works on moving latent heat from this air layer to the one above. We notice that the third and higher canopy layers have higher turbulent transport coupling coefficients. This leads to the lower

$T_{leaveseq}^l_{i,30}$	$T_{aireq}^l_{i,30}$	$caireq^l_{i,30}$	$T_{air}^l_{i,30}$	$cair^l_{i,30}$	$D_{air}^l_{i,30}$	$T_{leaves}^c_{i,30}$
22.654	20.832	$1.704 \cdot 10^3$	20.832	$1.704 \cdot 10^3$	759.835	22.641
22.584	20.81	$1.672 \cdot 10^3$	20.811	$1.672 \cdot 10^3$	789.32	22.577
22.544	20.798	$1.653 \cdot 10^3$	20.798	$1.653 \cdot 10^3$	806.144	22.543
22.412	20.65	$1.618 \cdot 10^3$	20.65	$1.618 \cdot 10^3$	818.525	22.412
22.293	20.506	$1.59 \cdot 10^3$	20.506	$1.59 \cdot 10^3$	825.208	22.293
22.119	20.289	$1.551 \cdot 10^3$	20.289	$1.551 \cdot 10^3$	832.544	22.119

Fig 4.5.e : The equilibrium profiles for the nogust model for run 4.5.a

The nogust model coupling coefficients			The gust model coupling coefficient		
$f_{lopt} =$	$f_{lower} =$	$f_{layert} =$	$f_{lopt} =$	$f_{lower} =$	$f_{layert} =$
0	0	0	0	0	0
0.889	0.111	0	0.667	0.333	0
0.636	0.364	0	0.636	0.364	0
0.562	0.393	0.045	0.495	0.347	0.158
0.649	0.325	0.026	0.602	0.301	0.096
0.49	0.49	0.02	0.463	0.463	0.074
0.49	0.49	0.02	0.463	0.463	0.074
$f_{lopt} =$	$f_{lower} =$	$f_{layert} =$	$f_{lopt} =$	$f_{lower} =$	$f_{layert} =$
0	0	0	0	0	0
0.96	0.04	0	0.857	0.143	0
0.636	0.364	0	0.636	0.364	0
0.584	0.409	0.007	0.562	0.393	0.045
0.664	0.332	0.004	0.649	0.325	0.026
0.499	0.499	0.003	0.49	0.49	0.02
0.499	0.499	0.003	0.49	0.49	0.02

equilibrium vapour pressure in the no-gust model compared to a gust model. The favourable effect of the gust process on the average flux is through refreshing the air inside the canopy, which represents a large percentage of the flux. If the time interval between two coherent structures is quite large, the enhancement of the average flux due to the storage depletion with the gust passage will be adversely compensated by the lower turbulent transport coefficient during the quiescence period. The resulting buildup will increase the average forcing on the soil. This relates to the time period between consequent gust intrusions into plant canopies in relation the time required for the build-up to occur and the resulting adverse effect on the soil latent heat flux to express itself. To get an enhanced effect due to the gust process on the soil heat flux, a parcel of air has to be brought in contact with the soil and maintain, during its contact time, a lower vapour pressure than the one obtained with a no-gust model such that the resulting mean vapour pressure has to be lower than the one obtained with a no-gust model. A new gust intrusion will replace this parcel of air with a fresh dry air before the adverse effect of buildup shows on the forcing. This requires a low leaf area density in the lower part of the canopy and lower turbulent mixing, which will lead to low diffusion of low vapour pressure deficit downward. Increasing the thickness of the first air layer in contact with the soil will lead to the same effect, since the first air layer will require a large period of time to maintain equilibrium. All of these variables relate to increasing the value of the time constant of the first or higher air layers in contact with the soil.

To show this, we did another run in which the turbulent transport coefficients were reduced

as shown in the fig.4.6.a.

The value of the obtained f_2 function in the gust model is 395.2 Wm^{-2} . The sensible and latent heat flux from the soil to the air were 4.27 and 40.6 Wm^{-2} . The storage change within the canopy was less than 0.09 Wm^{-2} for the whole canopy layer. The resulting averaged sensible and latent heat fluxes at the canopy top were 127.8 and 351.1 Wm^{-2} . This corresponded to total sources within the canopy (excluding the soil) of 123.5 and 310.5 Wm^{-2} for sensible and latent heat respectively. This corresponds to a Bowen ratio on plant surfaces of about 0.4.

In the case of no-gust model, the value of f_2 function was equal to 412.4 Wm^{-2} . The resulting sensible and latent heat flux at the canopy top were 136.7 and 345.8 Wm^{-2} . This corresponded to total sources within the canopy (excluding the soil) 135.8 and 315.9 Wm^{-2} . The resulting Bowen ratio was about 0.44. So in this case, there was a difference in the forcing function f_2 on the soil surface. The corresponding value of the boundary condition, given by eq.4.2.28 in the case of a gust model was -81.4 versus -64.42 Wm^{-2} for the no-gust model.

The first two terms in eq.4.2.28 represent the radiative energy load. The shortwave radiation load on the soil was set to zero. In the case of a positive one, the difference of about 17 W m^{-2} could represent an important difference in the boundary condition for the soil surface. Looking at the boundary condition, we notice that a calculation of the equilibrium temperature of the soil surface, assuming no storage within the soil, would mean in the case of αL (as

```

coeff:= 0.25      dz1:= 0.2      dxtop1:= 0.2
                                dxlower1:= 0.2
                                dt:= 5.
Rshort:= 140.      Thick:= 0.0005
Tairrad:= 15.
Lad1:=            klower1:=      ktop1:=      Tlinj1:=
0.0               0.0008         0.0016     22.757457
0.0               0.0016         0.0028     22.429896
4.0               0.0028         0.04        23.263929
4.0               0.04           0.08        23.075605
4.0               0.08           0.08        22.84354
4.0               0.08           0.08        22.456774

cumlai:= sum(Lad1*dz1, i)      Tairtop:= 20.0
cumlai= 3.200                 Tairmj:= 20.0
Total_Load:= cumlaiRshort2-ar  cairmj:= 1500
Total_Load= 716.800          Tair0,0:= 20
rbhm:= 100.                  cairm,0:= 1500.
rbhs:= 100.                  cairtop:= 1500
rsm:= 300
rss:= 200.
Tleaves1,j:= 23.0           Tsoil:= 21.

```

Fig.4.6.a: A run with reduced turbulent transport coefficient.

Mean_Tleaves_eq <i>i</i>	Mean_Taireq <i>i</i>	Mean_eaireq <i>i</i>	Tairmean <i>i</i>	Eairmean <i>i</i>	Dmean <i>i</i>	Mean_Tleaves <i>i</i>
22.632	20.893	$2.138 \cdot 10^3$	20.556	$1.763 \cdot 10^3$	660.142	22.62
22.326	21.221	$1.765 \cdot 10^3$	20.518	$1.605 \cdot 10^3$	812.229	22.323
23.118	21.743	$1.798 \cdot 10^3$	21.602	$1.766 \cdot 10^3$	819.329	23.117
22.954	21.443	$1.739 \cdot 10^3$	21.389	$1.729 \cdot 10^3$	822.458	22.953
22.749	21.157	$1.69 \cdot 10^3$	20.671	$1.609 \cdot 10^3$	831.16	22.747
22.404	20.697	$1.614 \cdot 10^3$	20.671	$1.609 \cdot 10^3$	831.16	22.402

Fig.4.6. b The mean profiles for a gust model in run 4.6.a

given by eq.4.2.31) being equal to 26.7, an increase to about $0.7 \text{ }^\circ\text{C}$. The resulting temperature difference is calculated from the summation of equation of 4.2.36.

$T_{leaves,eq}^i_{i,30}$	$T_{air,eq}^i_{i,30}$	$e_{air,eq}^i_{i,30}$	$T_{air}^i_{i,30}$	$e_{air}^i_{i,30}$	$D_{air}^i_{i,30}$	$T_{leaves}^i_{i,30}$
23.185	20.925	$1.975 \cdot 10^3$	20.924	$1.972 \cdot 10^3$	506.042	23.123
22.756	20.831	$1.762 \cdot 10^3$	20.831	$1.761 \cdot 10^3$	703.258	22.719
22.514	20.779	$1.641 \cdot 10^3$	20.779	$1.641 \cdot 10^3$	814.696	22.504
22.393	20.637	$1.611 \cdot 10^3$	20.637	$1.611 \cdot 10^3$	823.453	22.386
22.280	20.496	$1.585 \cdot 10^3$	20.496	$1.611 \cdot 10^3$	828.435	22.274
22.113	20.285	$1.548 \cdot 10^3$	20.285	$1.585 \cdot 10^3$	834.144	22.108
		$1.548 \cdot 10^3$		$1.548 \cdot 10^3$		

Fig 4.6.c The equilibrium solution in the no-gust model for run 4.6.a

The resulting mean profiles in the gust model give in fig.4.6.b while for the no-gust model they are given in fig.4.6.c. There is a difference in the temperature of the leaves about 0.5°C .

The value of the time constants for air temperature of the first, second, third and fourth canopy air layers (excluding the first cm thickness of air in contact with the soil) in this last run, as given by eq.4.2.11, were 16.6 and 36.36, 2.87 and 1.20 s respectively. Those for the vapour pressure of the air have values of 21.42, 36.36, 3.47 and 1.29 s respectively. The duration between gust intrusions into plant canopies was 50 sec. These time constants would be lower for all layers than the ones calculated graphically for the whole gust cycle since $T_{air,eq}$ and $e_{air,eq}$ keep changing between different time steps. So, the ratio of the period between gust intrusions into the plant canopy and the time constants was close to one. That led to a residual effect of the gust intrusion on the forcing function f_2 on the soil. The value of the used turbulent transport coefficient, in the previous run, could have been too small, so another run in which the thickness of the first two layers were increased to 0.6 m and 0.4m respectively. The value of the turbulent transport coefficient was increased to the values shown in fig.4.7.a.

The value of f_2 function in the case of the gust model is 387.1 Wm^{-2} . This corresponded to a value of -89.5 Wm^{-2} for the flux boundary condition given by eq. 4.2.28. The averaged sensible and latent heat flux at the canopy top were 131.1 and 359.6 Wm^{-2} . This corresponded to sensible and latent heat sources within the canopy (excluding the soil) of 125.1 and 311.6 Wm^{-2} respectively. The mean profiles are shown in fig.4.7.b. The values of the air temperature time constants for the first, second, third and fourth layers are 26.6, 24.0, 3.7 and 1.4 s respectively. The values of these time constants for the vapour pressure for the

coeff = 0.25	$dz_1 = 0.2$	$dx_{top_1} = 0.2$	
Rshort = 140.	dt = 5.	$dx_{lower_1} = 0.2$	
Thick = 0.0005		$dz_1 = 0.4$	$dz_2 = 0.4$
Tairrad = 15.		$dx_{top_1} = 0.4$	$dx_{lower_1} = 0.4$
		$dx_{top_2} = 0.3$	$dx_{lower_2} = 0.4$
			$dx_{lower_3} = 0.3$
Lad ₁ =	klower ₁ =	ktop ₁ =	Tinj =
0.0	0.004	0.008	22.461759
0.0	0.008	0.014	22.493279
4.0	0.014	0.02	23.164818
4.0	0.02	0.08	22.96947
4.0	0.08	0.08	22.776066
4.0	0.08	0.08	22.423835
$cumlai = \sum_i Lad_i dz_i$			Tairtop = 20.0
cumlai = 3.200			Tair _{m,j} = 20.0
Total_Load = cumlaiRshort2:ar			eair _{m,j} = 1500
Total_Load = 716.800			Tair _{0,0} = 20
rbh _m = 100.			eair _{m,0} = 1500.
rbhs = 100.			
rs _m = 300			eairtop = 1500
rss = 200.			
Tleaves _{1,j} = 23.0			Tsoil = 21.

Fig. 4.7.a : A run with increased thickness for the first two layers.

Mean_Tleaves_cq _i	Mean_Taireq _i	Mean_eaireq _i	Tairmean _i	Eairmean _i	Dmear _i	Mean_Tleaves _i
22.372	20.853	1.950·10 ³	20.420	1.655·10 ³	747.749	22.364
22.385	21.162	1.718·10 ³	20.622	1.611·10 ³	822.037	22.382
23.025	21.659	1.789·10 ³	21.479	1.745·10 ³	820.478	23.023
22.861	21.329	1.720·10 ³	21.270	1.708·10 ³	824.669	22.860
22.690	21.081	1.677·10 ³	20.635	1.603·10 ³	832.125	22.689
22.376	20.660	1.607·10 ³	20.635	1.603·10 ³	832.125	22.373

Tleaveseq _{i,30}	Taireq _{i,30}	eaireq _{i,30}	Tair _{i,30}	eair _{i,30}	Dair _{i,30}	Tleaves _{i,30}
22.930	20.945	1.832·10 ³	20.941	1.828·10 ³	652.590	22.874
22.725	20.919	1.723·10 ³	20.917	1.722·10 ³	755.363	22.689
22.640	20.910	1.677·10 ³	20.909	1.677·10 ³	798.742	22.620
22.395	20.633	1.614·10 ³	20.633	1.614·10 ³	820.432	22.384
22.281	20.494	1.587·10 ³	20.494	1.587·10 ³	826.450	22.273
22.114	20.283	1.549·10 ³	20.283	1.549·10 ³	833.161	22.108

Fig. 4.7.b The mean profiles and the equilibrium ones for the gust and no-gust respectively.

same layers are 24.5, 24.0, 4.9 and 1.55 s respectively.

For the no-gust model, the resulting f2 function was 403.8 Wm⁻². This corresponded to a value of -72.81 Wm⁻² for the boundary condition given by eq.4.2.28. This is about 17 Wm⁻² difference between the gust and no-gust approach with the lower value for the gust model. This difference represents in the case of αL, as given by eq.4.2.31, being equal to 27 Wm⁻² K⁻¹, an increase in the no-gust model of about 0.6 °C. The sensible and latent heat flux at the canopy top were 136.0 and 351.5 Wm⁻². This corresponded to total sensible and latent heat sources within the canopy (excluding the soil) of 135.7 and 314.4 Wm⁻² (total Rn on plant surfaces of 449.8 Wm⁻² with a Bowen ratio of 0.430.

Reducing the soil resistance to 100 sm⁻¹ (recently irrigated) and doing the same run as before, we see that for the gust model, the value of the forcing function f2 becomes equal to 463.23 Wm⁻² with a value of -109.41 Wm⁻² for the flux boundary condition given by eq.4.2.28. The storage change was 0.31 Wm⁻² for the whole canopy layer. The sensible and latent heat flux at the canopy top were 131.2 and 377.5 Wm⁻². This corresponded to total sources within the canopy of about 125.1 and 311.3 Wm⁻² with a Bowen ratio on plant

coeff = 0.25	dz ₁ = 0.2	dxtop ₁ = 0.2	
Rshort = 140.	dt = 5.	dxlower ₁ = 0.2	
Thick = 0.0005	dz ₁ = 0.4	dz ₂ = 0.4	
Tairrad = 15.	dxtop ₁ = 0.4	dxlower ₁ = 0.2	
	dxtop ₂ = 0.3	dxlower ₂ = 0.4	
		dxlower ₃ = 0.3	
Lad _i =	klower _i =	ktop _i =	Tlin _i =
0.0	0.004	0.008	22.461759
0.0	0.008	0.014	22.493279
4.0	0.014	0.02	23.164818
4.0	0.02	0.08	22.96947
4.0	0.08	0.08	22.776066
4.0	0.08	0.08	22.423835
cumlai = ∑ _i Lad _i dz _i			Tairtop = 20.0
cumlai = 3.200			Tair _{m,j} = 20.0
Total_Load = cumlaiRshort 2-ar			eair _{m,j} = 1500
Total_Load = 716.800			Tair _(0,0) = 20
rbh _m = 100.			eair _{m,0} = 1500.
rbhs = 100.			
rs _m = 300			eairtop = 1500
rss = 100.			
Tleaves _{i,j} = 23.0			Tsoil = 21.

Fig. 4.8.a: A run with reduced soil resistance to evaporation.

of 400.5 Wm^{-2} . This corresponded to a value of -76.1 Wm^{-2} for the flux boundary condition as given by eq.4.2.28. The resulting averaged sensible and latent heat flux at the canopy top were 52.4 and 274.4 Wm^{-2} . This corresponded to sources within the canopy (excluding the

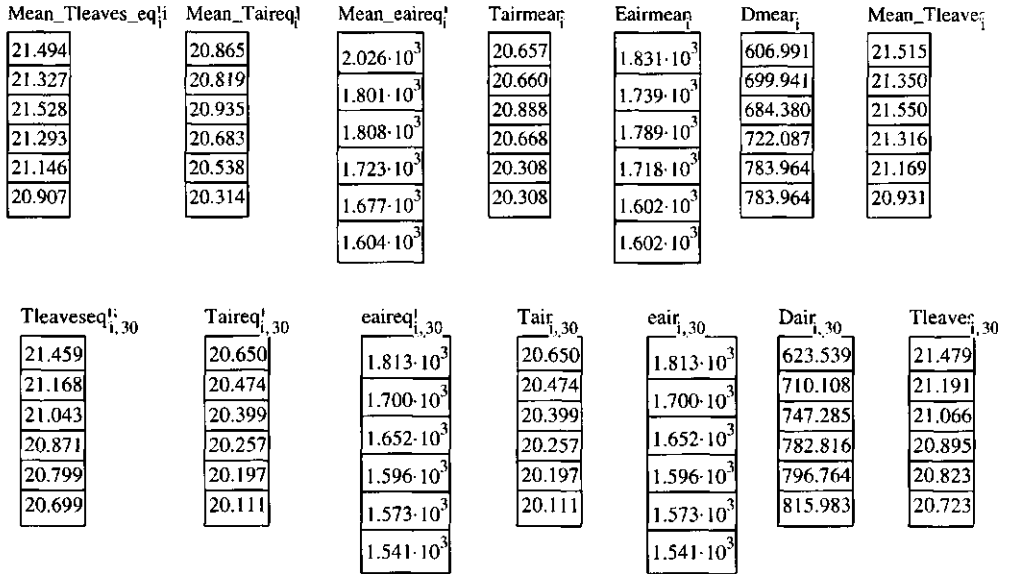


Fig 4.10.b The mean profiles in the gust model and the equilibrium in the no-gust mode for 4.10.a respectively

soil) of 49.4 and 238.4 Wm^{-2} . The resulting profiles are given above.

In the case of no gust model, f2 function had a value of 399.4 Wm^{-2} . This corresponded to a value of -77.2 Wm^{-2} for the flux boundary condition, as given by eq.4.2.28. This is again a non significant difference. The value of the sensible and latent heat at the canopy top were 53.1 and 292.8 Wm^{-2} . This corresponded to sources within the canopy (excluding the soil) of 48.9 and 252.4 Wm^{-2} corresponding to a Bowen ratio of 0.193 . There is a difference in the value of Rn on the plant surfaces. The values of the mean profiles in the gust model and equilibrium ones in the no-gust model are given below.

So, the effect of the ratio of the time period between two consecutive gust intrusion into plant canopies with respect to the time constants of the first and higher canopy layers, close to the soil, determine the effect of the gust intrusion on the soil.

To have a global evaluation of the sensitivity of the forcing function f2 and the flux boundary condition to intermittency, we will show the values of this function under different temperature and vapour pressure deficit regimes. We mean by these regimes that, depending on the climatic regime, a tropical, cold humid or dry arid climate, there will be a certain range of values for the temperature and vapour pressure deficit which can occur simultaneously. These values will control the value of the f2 function and the value of the flux boundary condition given by eq.4.2.28. The buildup or decrease of the vapour pressure deficit, depending on the stomatal resistance being higher or lower than the critical one as defined by

eq.4.1.9, will lead to a certain equilibrium value. To obtain a value for the vapour pressure and air temperature close to the soil surface, we ran the MATHCAD model using the boundary conditions representing the mean values of temperature and vapour pressure for a certain month (August) for different climatic regime. The selected regimes were a hot humid climate regime (Djakarta, Indonesia, Sukanto, 1969), hot arid (Cairo, Egypt, Griffiths and Soliman, 1972) and cold humid (De Bilt, The Netherlands, Arlery, 1970 respectively. The details of the runs are given in sec.4.2.3. The temperature and vapour pressure deficit values at the initial and the end of the quiescence were considered as the range of variation in the values going into the f2 function expression. The following matrices were obtained. These matrices help to give an idea on the variation of the value of f2 function which will be integrated by the soil to constitute the soil temperature.

$$f2_value_{m,nd} := \left[\frac{pcp}{rbhr} + pcp \frac{s(Tair_m)}{\gamma(rbv + rsoil)} \right] \cdot Tair_m - \frac{pcp}{\gamma(rbv + rsoil)} \cdot Dair_{nd}$$

644.463	641.478	638.493	635.508	632.523	629.538	626.553
665.658	662.673	659.687	656.702	653.717	650.732	647.747
687.374	684.389	681.404	678.419	675.434	672.449	669.464
709.627	706.642	703.657	700.672	697.687	694.702	691.716
732.430	729.445	726.460	723.475	720.490	717.505	714.520

Tair_m :=	Dair_nd :=
27	300
27.5	350
28	400
28.5	450
29	500
	550
	600

$$f2_value_{m,nd} := \left[\frac{pcp}{rbhr} + pcp \frac{s(Tair_m)}{\gamma(rbv + rsoil)} \right] \cdot Tair_m - \frac{pcp}{\gamma(rbv + rsoil)} \cdot Dair_{nd}$$

485.721	473.781	461.841	449.900	437.960	426.020	414.079
561.795	549.855	537.915	525.974	514.034	502.094	490.154
645.583	633.643	621.703	609.762	597.822	585.882	573.941
737.956	726.016	714.075	702.135	690.195	678.254	666.314
839.858	827.917	815.977	804.037	792.097	780.156	768.216

Tair_m :=	Dair_nd :=
24	1000
26	1200
28	1400
30	1600
32	1800
	2000
	2200

$$f2_value_{m,nd} := \left[\frac{pcp}{rbhr} + pcp \frac{s(Tair_m)}{\gamma(rbv + rsoil)} \right] \cdot Tair_m - \frac{pcp}{\gamma(rbv + rsoil)} \cdot Dair_{nd}$$

383.419	377.448	371.478	365.508	359.538	353.568	347.598
414.186	408.216	402.245	396.275	390.305	384.335	378.365
446.409	440.439	434.468	428.498	422.528	416.558	410.588
480.174	474.204	468.234	462.264	456.294	450.323	444.353
515.572	509.602	503.632	497.662	491.691	485.721	479.751

Tair_m :=	Dair_nd :=
20	500
21	600
22	700
23	800
24	900
	1000
	1100

The change in the value of the soil boundary condition due to gust intrusion will be represented by the difference the between two entries in these matrices. The first one of these matrices represents the values obtained for a hot humid region. The second is a dry arid region and the third is for a cold humid region. The value of the vapour pressure deficit and the air temperature, specified with the vectors to the right of each matrix, are the ones obtained within the canopy after the gust intrusion for an air with the specified values given in the runs at sect.4.2.3. The rows represent the values for a certain value of the temperature vector shown to the right of the matrix, while the column represent the value for a certain vapour pressure deficit. Depending on the initial and final temperature and vapour pressure deficit of the air, the forcing function can experience a large variation as can seen for the elements in the three matrices.

To show the integrated effect of a gust versus no-gust case on the temperature of the soil and the mean temperature of the air, we ran a simplified version of the model included in Chapter 5 for a period of 11 days for a gust and nogust model. This version of the model did not take account of the effect of water uptake by plant roots or the effect of evaporation on

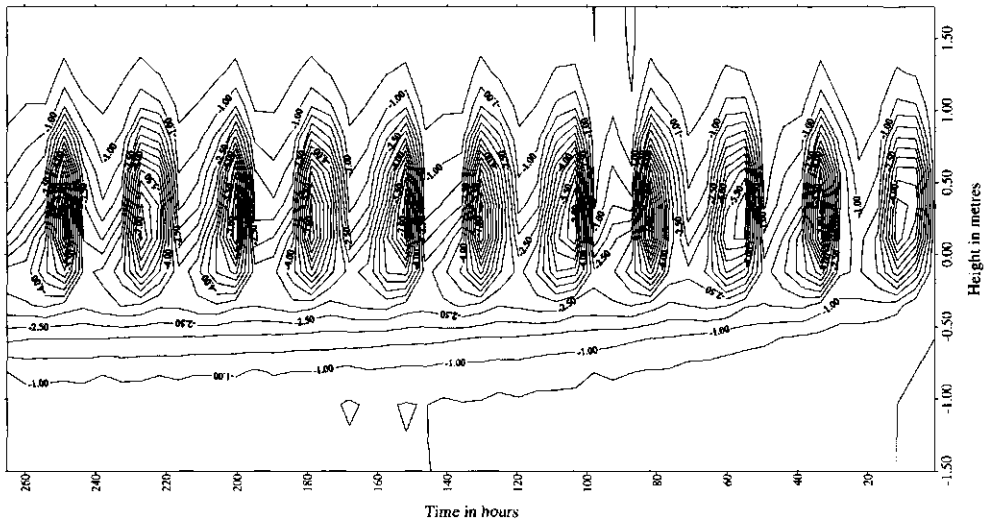


Fig 4.12.a : The mean temperature difference (a gust - no gust) models for the boundary conditions specified in fig 4.13.

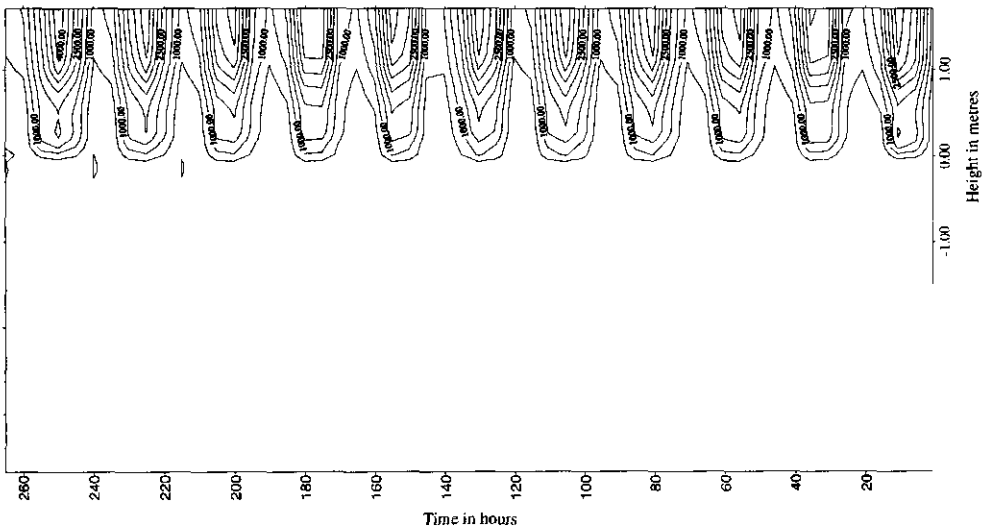


Fig. 4.12b The difference in the mean vapour pressure deficit (a gust- no gust) models for the boundary conditions specified in fig. 4.13.

reducing the moisture content of the soil. The soil resistance to evaporation was minimal ($r_{ss} = 0.0$). The boundary conditions used in the run were somewhat typical of a rather hot sunny summer day in Egypt. These boundary conditions (i.e. the incoming short wave radiation, friction velocity, temperature and vapour pressure are shown in fig.4.13). The gust intrusion during day time was assumed constant with a period of 1.5 minutes. In here, we show the difference within time between the gust and no gust model in the mean temperature and vapour pressure deficit for the two models. The results shown (fig 4.12 a,b) give the day

difference of the simulated mean temperature of the air and the soil and the vapour pressure deficit between a gust model and no-gust model. We notice in here the very high temperature and vapour pressure deficit differences (- 9 °C and more than a 1000 Pa) between the two models. This difference could be explained on the basis of the used parameterization for the turbulent transport coefficients, the low leaf area density and the higher stomatal resistance in the lower part of the canopy. All of these led to an increase in the time constants of the mean vapour pressure deficit of the canopy air layers close to the surface. This increase in the value of the layers time constants and the short period (90 seconds) between consecutive gust intrusions led to the high vapour pressure deficit accompanying the gust intrusion, to be felt at the soil surface. The values of these high time constants could be seen from fig.4.14 showing the decrease of the vapour pressure deficit of the layers close to the soil. The resulting mean vapour pressure deficit in the case of a the gust model was much higher than the no-gust model. The use of a soil

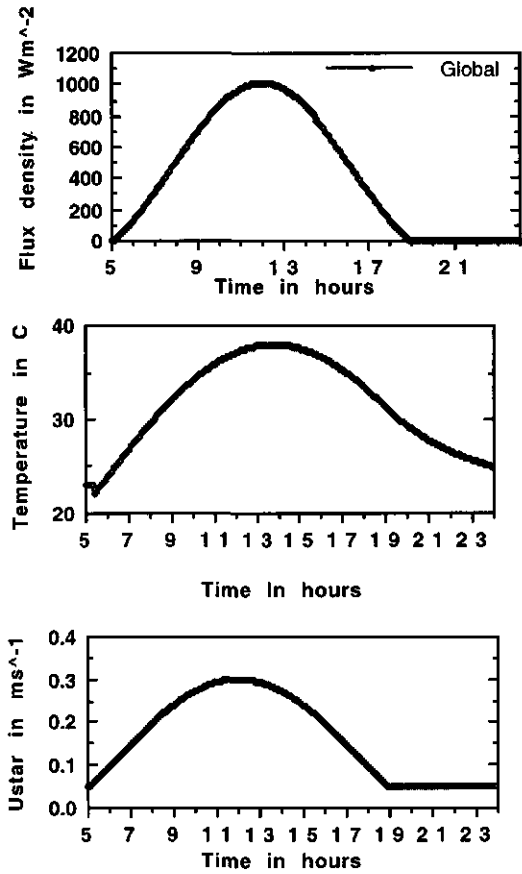


fig.4.13 The boundary conditions for the run

resistance to evaporation with a value of zero led to an enhanced effect of intermittency on the value of f2 function. A zero soil resistance would increase the latent heat flux from the soil to the air, trying in the process to lower the value of the vapour pressure deficit of the first air layer, so having a negative feedback on the effect of the vapour pressure deficit on the soil temperature, but due to the whole dynamics (i.e. the period between two gust intrusions and its ratio to the time constants of the first air layer) that effect of the higher vapour pressure deficit, in the case of a gust model, was felt at the soil surface.

The lower turbulent transport coefficient was due to the use of the following parameterization

$$\begin{aligned}
 n &= 2.0 \\
 \text{DISPL} &= 0.63 * Z(\text{IT}) \\
 \text{Imix}(\text{it}) &= \text{M1} * \text{Karmen} * (z(\text{it}) - \text{displ}) \\
 \text{km}(\text{IT}) &= \text{LMIX}(\text{IT}) * \text{ustar} \\
 \text{KM}(\text{I}) &= \text{KM}(\text{IT}) * \text{EXP}(-n * (1 - z(\text{I}) / z(\text{IT})))
 \end{aligned}$$

The mean values of the simulated vapour pressure deficit in the gust model are much higher than the value of the mean simulated vapour pressure deficit of the no-gust model. (283, 348 and 455 Pa for the layer number 1, 2 and 3 respectively) as can be seen from the fig.14.a . That was a difference of about 1200 Pa. The behaviour of the temperature of the first air layers is shown in the following figures. The temperature of the soil surface was about 35 C and 42 C for the gust and no gust model respectively. This would lead to a difference in the flux boundary condition of at least about 150 Wm^{-2} . The lower loading is for the gust model. This is a rather high value, but this is due to the high vapour pressure deficit difference between the two approaches. The difference between the simulated heat flux for the gust .vs. no gust model is about 100 Wm^{-2} at 0.01 m depth. The cumulative leaf area index was 2.19. The amount of soil short wave radiation absorbed was 322 Wm^{-2} .

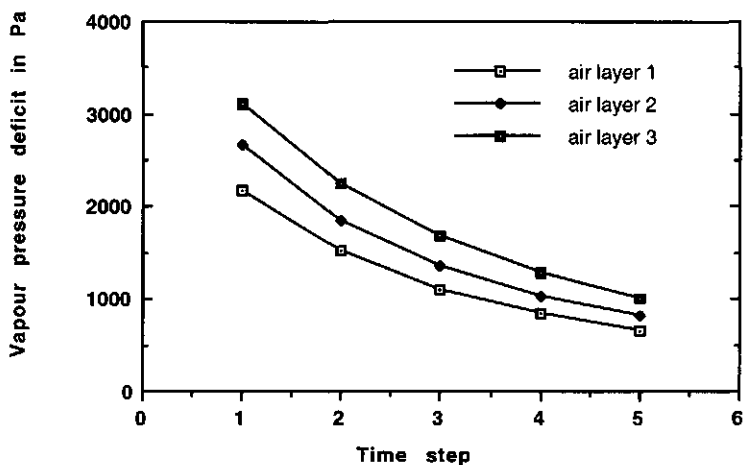


Fig 4.14. a The vapour pressure deficit within the quiescence period

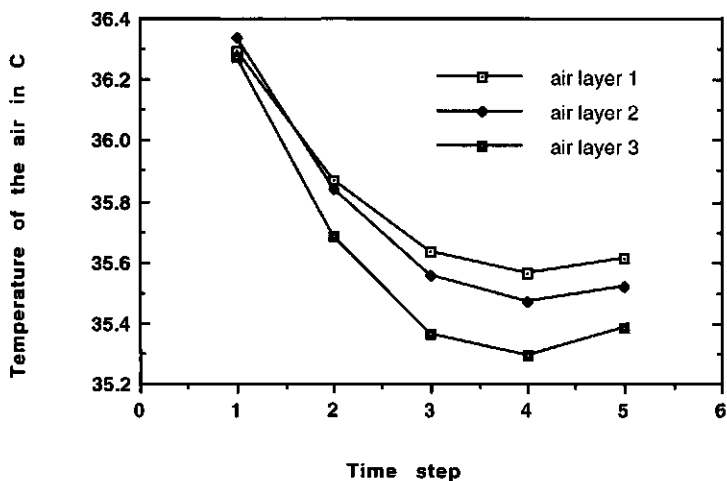


Fig 4.14. b : The behaviour of temperature f during the quiescence period.

4.2.2 AN ANALYSIS OF SOURCE AND SCALAR PROFILE BEHAVIOUR DURING A GUST CYCLE

1. The scalar profiles

The importance of turbulent transport intermittency is that it brings into the canopy air space a parcel of air, which has a temperature and a moisture content that is not in equilibrium with the value deduced by limited turbulent transport coefficients during the quiescence period and the leaves stomatal resistance, and leaves this air parcel within the canopy air space. The maintenance or restoration of a "height-dependent equilibrium" of the temperature and moisture content requires a partition of non-radiative energy, from the leaves to the air, which is different from the equilibrium situation. This constitutes the change in the source. But what is meant by 'height-dependent equilibrium'?

There are two options on answering that question, :

- 1) either using the temperature and vapour pressure equations of the air eq.4.2.12 and 4.2.17 or
- 2) using the vapour pressure deficit equation of the air. eq.4.2.21.

The 'height-dependent' equilibrium temperature and vapour pressure of the air are given by eqs. 4.2.12 and 4.2.17. These two equations are the discretized nonintermittent transport equations and they represent the steady state solution of the air after a large $\nu\tau$. The time constants for air temperature and vapour pressure are the inverse of eq.4.2.11 and eq.4.2.15 respectively, and they have different values due to the stomatal resistance. The development of an equilibrium situation depends on the time interval between the gust intrusion into plant canopies in relation to the air layer time constants.

As long as the air has a dew point temperature which is lower than the leaf temperature, the humidifying (increase of vapour pressure) of the air occurs as given by eq.4.2.16 and 4.2.17. The relative contribution of the different conductance factors in eq.4.2.17 determines the equilibrium vapour pressure. The warming or cooling of the air depends on the air which came in, being warmer or colder than the leaves, and the degree of humidifying of the air within time. The behaviour of D as a function of time, whether it increases or decreases, depends on the behaviour of $T_a(t)$ and $e_a(t)$ for different layers and is given by

$$D' = s T' - e' \tag{4.2.80}$$

$$\frac{\partial D}{\partial t} = s \frac{\partial T}{\partial t} - \frac{\partial e}{\partial t} \tag{4.2.81}$$

For negative $\frac{\partial D}{\partial t}$, this requires

$$\frac{\partial e}{\partial t} / s > \frac{\partial T}{\partial t} \tag{4.2.82}$$

For condition 4.2.82 to be satisfied, $\frac{\partial T_{air}}{\partial t}$, $\frac{\partial e_{air}}{\partial t}$ equations, as given by eq.4.2.10 and 4.2.14 with updating $e_{air,eq}$ and $T_{air,eq}$ and given that $K_{a,e} \leq K_{a,T}$, show that the third factor in $e_{air,eq}$ eq. 4.2.17 should be high enough to compensate for $K_{a,e}$ being lower than $K_{a,t}$

The comparison between the expressions of eqs. 4.2.12 and 4.2.17 show that the first and second coupling coefficients are lower for the temperature equation than those for the vapour pressure equation. The third coupling coefficient is lower for the vapour pressure than the equivalent term in the temperature. Even so, the multiplication of the third term by the saturated vapour pressure under certain combination of D, radiation load and the stomatal resistance value would be able to compensate for the relative stronger turbulent coupling coefficients in the vapour pressure equation.

Anyhow, given enough time between consecutive gust intrusions, $D_{\text{equilibrium}}$ is reached and it is determined from $D_{\text{equilibrium}} = e_s(T_{l,\text{eq}}) - e_{\text{air,eq}}$. In the extreme case of assuming zero turbulent transport during the quiescence period, one sees that $D_{\text{equilibrium}} = 0$. That would mean according to $T_{\text{air,eq}}$ that leaf temperature is equal to air temperature and that air is saturated. This means a complete shutoff of sensible and latent heat flux from the leaves to the air, so that thermal radiation is the only way to get rid of the short wave radiation load. This situation is extreme, since before this equilibrium is established and, if there were no coherent structures existent to prevent its realization, the resulting thermal instability of the air will lead to turbulent transport initiation and that equilibrium will never be established. The actual progress toward that hypothetical equilibrium (i.e. $D_{\text{equilibrium}} = 0$ and $R_n = 0$) will depend on the degree of turbulent coupling between the canopy air layers and the air layers above on one side and the leaves stomatal resistance and leaf area increment on the other side (i.e. the three coefficients in eq. 4.2.17). The turbulent coupling will vent some of the total absorbed radiation as sensible and latent heat flux from the leaves to the air (R_n). So, the resulting observed value of R_n is due to the existence of some transport mechanisms which allow some venting of the total absorbed radiation into sensible and latent heat. There will be an equilibrium between what is delivered by the leaves into the intercanopy air stream and what is evacuated to the layers above and below. The final partition will depend on the temperature and vapour pressure buildup which is allowed to occur, i.e. how much is the temperature and vapour pressure of the leaves is allowed to be coupled to the air through the effect of the stomatal resistance.

If the integration of eq. 4.2.80 is not zero within the quiescence period, there will be a time mean decrease or increase of D within depth. The mean vapour pressure deficit D and air temperature, as given by eqs. 4.2.102 and 4.2.100, respectively, are a weighed time mean of the air vapour pressure deficit and temperature of the different periods (gust intrusion, buildup and equilibrium phase 1, 2 in fig.4.23). This controls the time mean source. The mean source will be different from the source due to the gust intrusion depending on the second term in eq. 4.2.24 being different from D_{top} . This difference is due to the ability of the canopy to see and respond to D_{top} . If the $D_{\text{equilibrium}}$ did not differ from the D_{top} , D_{mean} will then be equal to D_{top} , and the variation of D and T_{air} , due to the gust will not affect the evaluation of the mean source. This could be due to:

- 1) coherent structures moving air, which has the same D due to small ratio of the length scale of transport to the source inhomogeneity
- or
- 2) the canopy is too sluggish (very high values of air time constants with respect to the gust interval) due to a very high stomatal resistance, low leaf area increments and/ or very strong

turbulent coupling all the time. Another analysis of showing the same effect is shown by the analysis starting by eq. 4.2.103.

There is another option through the use of the vapour pressure deficit equation. The equilibrium vapour pressure deficit is given by equation 4.2.21. We see that the third term in vapour pressure deficit equilibrium ($\frac{s \alpha r_s R_n}{\rho C_p}$), in the case of complete shutoff of the sensible and latent heat flux, becomes equal to the equilibrium vapour pressure. But if there is no exchange, R_n is not a constant anymore. Warming of the leaves reduces R_n by $4\epsilon\sigma T_{abs}^3$ $Wm^{-2}K^{-1}$ and equilibrium becomes achieved by reducing R_n till D becomes zero. The rest of the story is the same as in the previous paragraph.

2. The sources:

The leaves as sources respond to intermittency by modifying the energy partition on its surfaces to retain equilibrium. Equation 4.2.83 represents a Bowen ratio for plant surfaces, a ratio between H/LE fluxes from the leaves to the inter canopy air layers.

$$\frac{H}{LE} = \frac{\gamma(r_{bv}+r_s)(T_s-T_a)}{r_b \left[(e_s(T_{air})-e_{air}) + \frac{\partial e_s}{\partial T} (T_s-T_a) \right]} \quad (4.2.83.a)$$

$$\gamma^* = \gamma(r_{bv}+r_s)/r_b \quad (4.2.84)$$

$$\frac{H}{LE} = \frac{\gamma^*}{\left[\frac{D}{(T_s-T_a)} + \frac{\partial e_s}{\partial T} \right]} \quad (4.2.83.b)$$

This equation requires no condition of a steady state situation in its application. The fluxes here could be also due to heat storage change in the leaves. The time variation of the energy partition will be dependent, within the time scale we are interested in, on the $\frac{D}{(T_s-T_a)}$ variation of the air

The variation of D just after or during the gust passage is related to the height from which the parcel of air has been brought and the amount of build-up which was allowed to occur before the gust intrusion. The variation of D within time around the passage of coherent structures is related to a large distance difference in D. That difference within height, whether positive or negative is related to a large-time averaged β for the whole canopy being less or greater than γ/s . This relates to the stomatal resistance and R_n profile, as has been shown in sect.4.2.1 and conclusion 4 in sect.4.2.1.1.

In the first case, there will be a sudden increase of D around the passage of the coherent structure and a decrease in the quiescence period toward an equilibrium value as given by eq.4.2.21.

The time variation of (T_s-T_a) around the passage of coherent structures is related mainly to the time variation of air temperature, since the leaf temperature will be almost constant. T'' is related then to a large distance difference in T_a .

A negative deviation of $\left(\frac{H}{LE}\right)''$, or, $\frac{\partial\left(\frac{H}{LE}\right)}{\partial t} < 0$ corresponds to a decrease in Bowen ratio on plant surfaces (i.e. an increase in latent heat flux in comparison to sensible heat flux). The behaviour of $\left(\frac{H}{LE}\right)''$ during the quiescence period is related to the buildup process of D and $(T_s - T_a)$, the latter being now controlled not only by T_a , but also by T_s and how it will manage to keep track of the equilibrium temperature and the resulting difference $(T_s - T_a)$.

The sensitivity of the $\left(\frac{H}{LE}\right)''$ in response to temperature and vapour pressure variation is dependent on the magnitude of γ^*

$$\frac{\partial\left(\frac{H}{LE}\right)}{\partial t} = -\gamma^* \frac{\left[\frac{\partial D}{\partial t} \frac{D}{(T_s - T_a)} \frac{\partial(T_s - T_a)}{\partial t} + \frac{\partial\left(\frac{\partial e_s}{\partial T}\right)}{\partial t} \right]}{\left[\frac{D}{(T_s - T_a)} + \frac{\partial e_s}{\partial T} \right]^2} \quad (4.2.85)$$

For $\frac{\partial\left(\frac{H}{LE}\right)}{\partial t} < 0$ this requires, neglecting the third term between brackets in the numerator of eq. 4.2.85, the following inequality to hold.

$$(T_s - T_a) \frac{\partial D}{\partial t} - D \frac{\partial(T_s - T_a)}{\partial t} \geq 0 \quad (4.2.86)$$

Inequality 4.2.86 shows, as can be seen from (4.2.83.b), that the effect of vapour pressure deficit increase on increasing latent heat flux has to be higher than the effect of the air temperature change on increasing the $(T_s - T_a)$ difference.

We have several cases depending on the value of β for the whole canopy which represent then a relation between the sensible and latent heat flux above the canopy top, the sign of $(T_s - T_a)$ and $\frac{\partial(T_s - T_a)}{\partial t}$.

$$\begin{aligned} (T_s - T_a) > 0 &\Rightarrow \frac{\partial D}{\partial t} \geq \frac{\partial(T_s - T_a)}{\partial t} \\ \beta < \frac{\gamma}{s} &\Rightarrow \\ (T_s - T_a) < 0 &\Rightarrow \frac{\partial D}{\partial t} \leq \frac{\partial(T_s - T_a)}{\partial t} \end{aligned} \quad (4.2.87)$$

The other case $\beta > \gamma/s$ would apply for a canopy which is either:

1) having a high value of sensible heat partition in relation to latent heat flux due to high values of γ^* or

2) a canopy acting as a sink for both sensible and latent heat, due to radiative cooling at the canopy top at cold nights, which is compensated less by dewfall than by sensible heat flux from above.

4.2.2.1) DAYTIME SITUATION (non stressed canopy), $\beta < \gamma/s$

During daytime, latent heat flux is positive (i.e. upwards) which corresponds mostly to a negative $W'D'$ correlation (vapour pressure deficit flux) depending on $\beta < \gamma/s$. There are two possibilities for the corresponding joint probability $T'D'$ distribution. The first possibility:

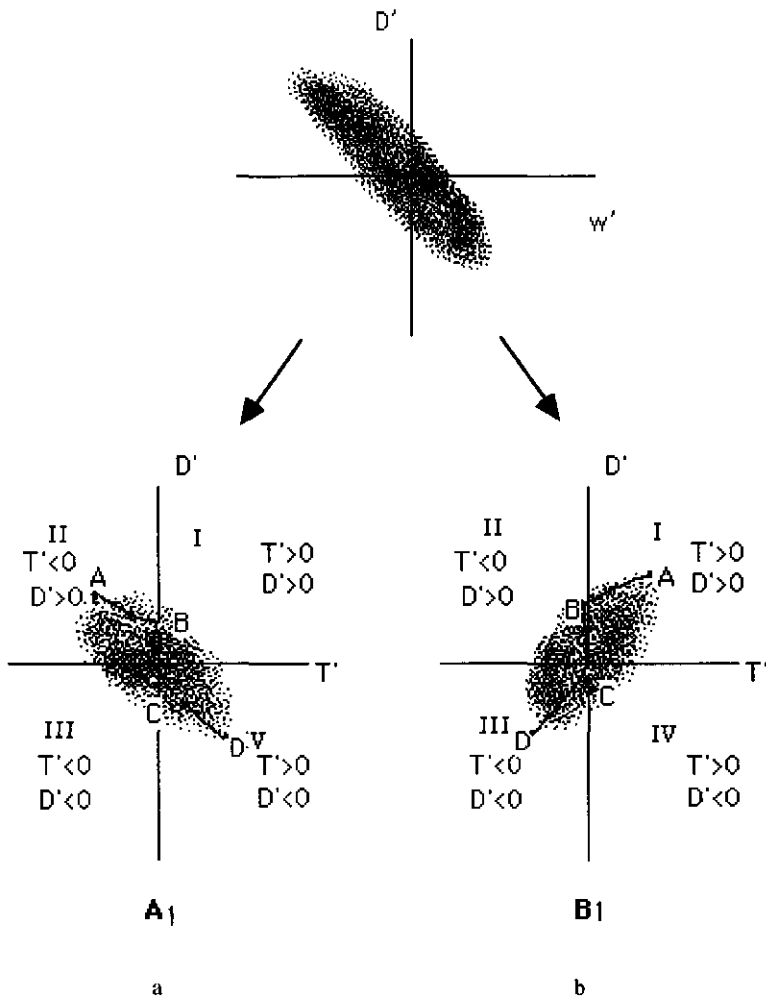


Fig 4.15: Joint probability between T' and D' for two kinds of situations in which vapour pressure deficit flux is negative.

$\overline{T'D}$ is positive (i.e. downward moving air is usually drier and warmer). This situation implies a negative sensible heat flux (**B1**). This situation represents a non stressed canopy in an advective case, or possibly in a non-advective case, in a warm arid region. The second possibility: $\overline{T'D}$ is negative (i.e. downward moving air is usually drier and colder) (**A1**). This applies for situations in more humid, colder regions. These two situations represent two different scenarios (**B1** and **A1**) in fig. 4.3. There is a third scenario **C1** which is similar to **A1**, but with much less absolute value of the slope of the correlation line between $\overline{T'D}$ representing the situation in the humid tropics. Since $\beta < \gamma/s$ is the required condition for the time mean decrease of D with height, the time variation of D around the passage of the coherent structure is positive and then negative in the quiescence period. Depending on the $T''D''$ correlation case, T'' is determined. In scenario **B1**, during the gust intrusion, T'' is positive while in scenario **A1**, T'' is negative. During the quiescence period, $(T_s - T_a)$ could be positive or negative depending on the behaviour of vapour pressure buildup which affects the behaviour of T_s and on the behaviour of T_a . In the quiescence period, $(T_s - T_a)$ variation is always positive due to vapour pressure buildup.

$T''D''$, e'' or T', e', D' are related to the time rate of change in T, e, D . During the gust intrusion period, $T''D''$, e'' are related more to a large-distance difference in D, T, e as shown by eqs. 4.2.14, 4.2.10, since then $e_{air,eq}$ and $T_{air,eq}$ in these equations are equal to e_{top}, T_{top} . The sign of $(T_s - T_a)$ depends on the value of vapour pressure buildup before the gust intrusion, and whether it exceeds a critical value of D . There are then three possibilities depending on the value of $(T_s - T_a)$ and β , which is still less than $\beta < \gamma/s$

1) Above the canopy, the averaged $\beta < 0$ due to $H < 0$. This represents scenario **B1**. The time mean of $(T_s - T_a) < 0$, but due to vapour pressure buildup, $(T_s - T_a)$ is an increasing function of time during the quiescence period, and could be positive just before the gust intrusion. Condition (1) in eq.4.2.87 always holds, since $\frac{\partial(T_s - T_a)}{\partial t} = -T''$, with T'' being positive.

2) The same as 1, except that $(T_s - T_a)$ is negative due to vapour pressure buildup being not high enough, due either to somewhat high stomatal resistance (not very high, otherwise, we get $\beta > \gamma/s$ situation) or to that the period between the gusts is small. So, D before the gust will be high.

$$\frac{\partial D}{\partial t} \leq \frac{\partial(T_s - T_a)}{\partial t} \quad (4.2.88)$$

The satisfaction of eq.4.2.87 depends on the build-up which may not be large enough. So D is relatively high and $(T_s - T_a)$ is small.

3) $\gamma/s > \beta > 0 \Rightarrow H > 0 \Leftrightarrow (T_s - T_a) > 0$, A required condition for $\frac{\partial(\frac{H}{LE})}{\partial t} < 0$, is $\frac{\partial D}{\partial t} \geq \frac{\partial(T_s - T_a)}{\partial t}$, which means that the intruding air is colder than the ejected air (Scenario **A1**). There are two

different scenarios here. This also means that the intruding air has to be colder than the leaves. If that was not the case and the intruding air is warmer than the leaves, we would have a logical contradiction. Assuming this air is warmer than the leaves, it will start cooling and humidifying due to vapour pressure buildup $\beta < \gamma/s$, the vapour pressure deficit will reach a critical D, the leaves will start being warmer than the air, and a heat source develops and due to the large contact time between the leaves and the air (i.e. a large interval between gusts) the air becomes warmer than the air which initially came in (a sensible heat flux positive). The incoming air has to be automatically colder than the leaves. $\frac{\partial(T_s - T_a)}{\partial t}$ is positive with (Ts-Ta) positive

given: $T_{air,in} < T_{air,out}$ sensible heat flux positive

assuming

$$T_{air,in} > T_{leaves} \Rightarrow T_{leaves} > T_{air,out} \Rightarrow T_{air,in} > T_{air,out} \tag{4.2.89}$$

which contradicts our initial assumption.

So, the satisfaction of that condition (4.2.86) depends on the situation.

There is a case of scenario B1, in which the incoming air is warmer than the air within the canopy. There would be a negative heat flux with the gust intrusion, but due to an accidentally large period between two consecutive gust intrusions, the air cooled first and then warmed, such that the air became warmer than the air which initially came in. The sensible heat flux at the canopy top due to a local gradient would be positive, and if that lasts long enough, it would more than compensate the negative heat flux accompanying the gust flux. The next coherent structure would not be able to bring a warmer air than the outgoing one and that would be similar to case A1. The effect is a positive sensible heat flux due to a gust intrusion and a reduction of the air temperature around the plants. This case corresponds to the area in quadrant II in fig. B1.

4.2.3. A SIMULATION OF THE DIFFERENT SCENARIOS BY THE USE OF MORE EXACT FORM

The intrusion of coherent structures, with a large length scale in relation to the source distribution within height, introduces a parcel of air with a different temperature and moisture content into the canopy air space and leaves it there. The whole canopy air is replaced then by fresh air from above in a very short time. This is represented by very small time constants for the exchange processes during the gust intrusion. That expresses the very rapid change in the uppermost curve in (fig 4.16). The value of $T_{l,eq}$, as given by eq.4.2.5 will experience a sudden change. $T_{l,eq}$ change will depend on the net effect of the fourth term in comparison to the third and the fifth terms in eq.4.2.5. There are four combinations of D' and T'. These combinations are shown in fig 4.15 a, b. The upper most regions in Quadrant I and III in the joint probability distribution represent extreme events. Fig.4.3.a,b represent assumed shapes

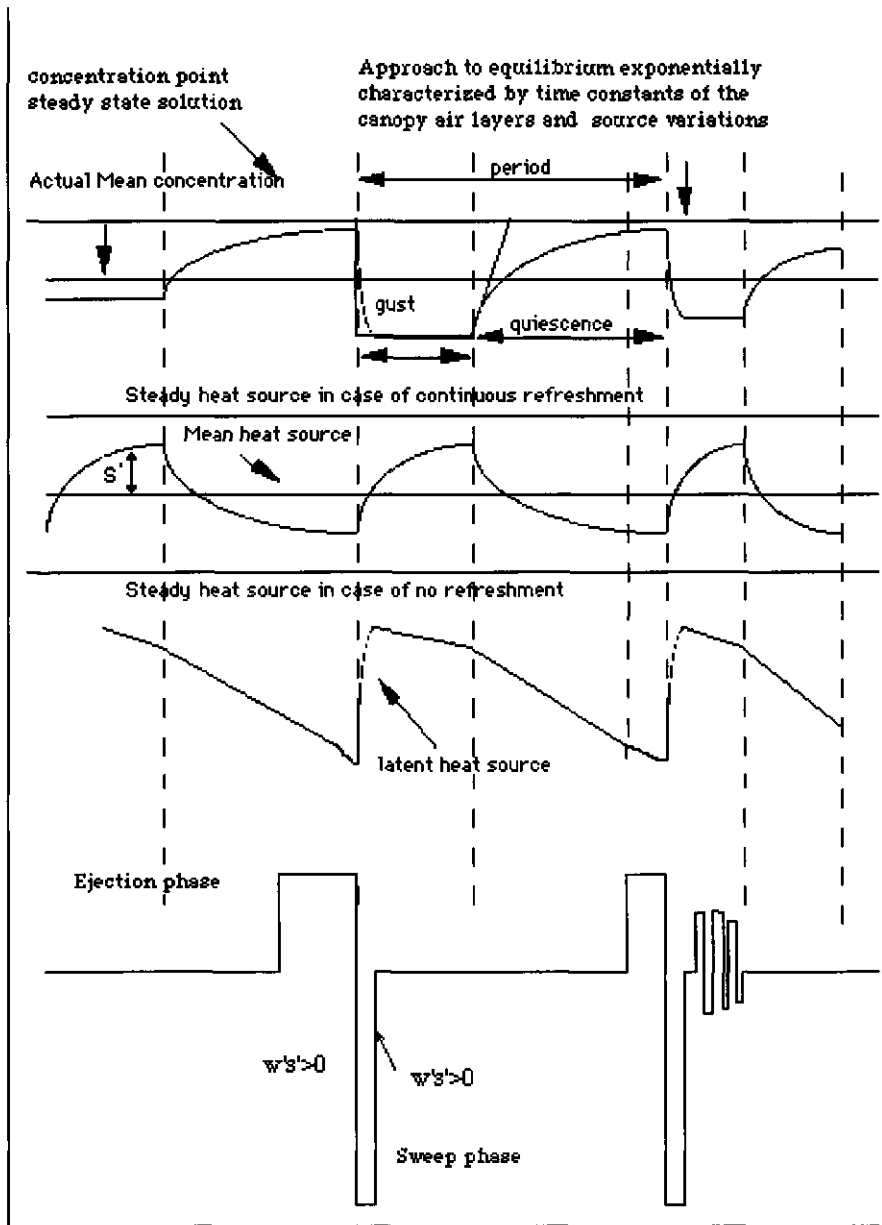


Fig 4.16: A hypothetical case of a gust cycle, showing in the upper graph the behaviour of the state variables of the air (i.e. temperature and vapour pressure). In the second and the third curves, the probable behaviour of the sensible and latent heat sources is shown. The lower one represents the behaviour of the vertical wind speed, being positive during ejection with a low value and highly negative during the sweep phases. There will be a net result on the $w's'$

of the joint probability distribution between T' and D' , and real measured ones represent the solution of the conservation equations.

Scenario B₁:

This scenario represents a warm arid region. We will first discuss the time behaviour of the leaf temperature, the temperature and vapour pressure of the air for a general case, where the intruding air has a $T' > 0$ and a $D' > 0$ and then proceed with an explanation of a particular case for this scenario by the use of MATHCAD.

A: gust intrusion phase:

We start with point A on the W'D' joint probability distribution (fig.4.15 b). We have $D' > 0$ and $T' > 0$, the sign of the fourth term shows that $\Delta T_{l,eq} < 0$ (The leaves are then cooling or heating at a lower rate depending on T_{leaves} being higher or lower than T_{leq}) if $(s + \gamma(r_{bv} + r_s)/r_{bh}) \leq D'/T'_{air}$ (appendix 2.7). During the active exchange period between the canopy air and the layer of air above, there will be no or very little build-up of the temperature and vapour pressure of the air. The value of $T_{l,eq}$ after an initial sudden change will be quite constant, and the sensible and latent heat flux from the leaves will be governed by the equation A.2.8.1 and A.2.8.6 respectively. During this phase of gust intrusion (Quadrant I), we will assume then that $\Delta T_{l,eq}$ is negative. The rapid change in D leads to a change in H/LE in favor of LE and a reduction of H will result. The leaf temperatures then will be moving toward a lower new equilibrium temperature. The sensible heat flux from the air to the leaves could reverse sign, depending on D change. The temperature and vapour pressure of the air will respond to the changing leaf temperature according to equation 4.2.10, 4.2.11 and 4.2.12 for air temperature and eq.4.2.14, 4.12.15 and 4.2.17 for air vapour pressure. The coupling between the canopy air and the air above is very strong. The time constants of the canopy air layer are then so small and controlled mainly by the first two terms in eq.4.2.11 and 4.2.15. The air equilibrium temperatures and vapour pressure, during this phase will be equal to $e_{air,top}$ and $T_{air,top}$. This is represented by the upper curve in fig.4.16. It is highly improbable that the leaves manage to attain equilibrium during the intrusion period. The leaves have a time constant of 100 sec or so, which is quite large in relation to the gust duration.

B: Quiescence Period (a probable build-up phase):

Once the gust mechanism of exchange is shut off, the quiescence period starts. The turbulent transport coefficient reduces and the time constant of the canopy air layers increases. The effect of the leaf temperature terms in eq.4.2.12 and 4.2.17 shows that the sources become more important in controlling the temperature and vapour pressure of the air. There will be a start of a build-up of the vapour pressure of the air since $es(T_l)$ of the leaves is higher than e_i , (positive latent heat flux due to leaf temperature being higher than dew point temperature) in $e_{air,eq}$ as given by eq.4.2.17. The temperature of the air will cool or warm according to eq.4.2.12 and 4.2.13 depending on the $T_{air,eq}$, being higher or lower than $T_{air,initial}$. This relates to the third term in eq. 4.2.12 (initial leaf temperature) being higher or lower than

$T_{i,initial}$ in the $T_{air,eq}$. The slope of $\Delta D/\Delta T$ on the joint probability (fig 4.15.b) is controlled by eq.4.2.90. With air vapour pressure buildup and the assumed air cooling, the slope of D^C/T^C is positive. The canopy air will move to a new coordinate on the T'D' joint probability

$$\frac{D^c}{T^c} = \frac{\partial e_s}{\partial T} \frac{\frac{\partial e_{air}}{\partial t} \Delta t}{\frac{\partial T_{air}}{\partial t} \Delta t} \tag{4.2.90}$$

distribution figure (in this case toward the center of the figure 4.15.b). The resulting change in D' and T' will have a feedback on the solution of the leaf eq.4.2.6 through changing $T_{l,eq}$ (eq.4.2.5) into a new value. New $\Delta T_{l,eq}$ could be positive or negative. If it is negative, this means that the equilibrium temperature of the leaf is even deviating further from the one just after the gust passage. It would mean then that the build-up of the vapour pressure is not allowed to occur (i.e. the canopy is still coupled to the air above, which contradicts our initial assumption of weak coupling during the quiescence period or there is a very high value for stomatal resistance which leads to a decrease of vapour pressure deficit within time, e.g. fig.4.4.d). But in the latter case, our initial assumption of positive D' within the gust intrusion would not be correct. So, $\Delta T_{l,eq}$ must be positive, i.e. the equilibrium temperature of the leaves is moving back to its initial value before the gust intrusion. Another way of looking at it is by considering the definition of the equilibrium

temperature of the leaf, as given on page 103 and how it relates to the coupling, since a gust will couple the leaf more to the upper boundary and less to the radiation loading. It brings that upper boundary just across the boundary layer resistance of the leaf. A decrease in the turbulent coupling will couple the leaf more to the radiation field and less to the temperature and vapour pressure of the air above. So, if the equilibrium temperature of the leaves were higher before the gust intrusion, a shutoff of the gust mechanism, with no change in the radiation loading, must mean a return of the equilibrium temperature of the leaf to its original high value. The temperature of the leaf will move toward this new equilibrium level with lower absolute value of the rate as compared to the rate just after the gust intrusion, as can be seen from eq.4.2.2. The temperature of the leaf will keep feeding back into the temperature and vapour pressure of the air. The vapour pressure will keep increasing, while the air temperature will decrease or increase depending on the third term in eq.4.2.12. being higher or lower than the air temperature at the beginning of each time step.

```

coeff:= 0.25      dz1:= 0.2      dxtop1:= 0.2
Rshort:= 100.    dt:= 10.        dxlower1:= 0.2
Thick:= 0.0005  dz1:= 0.4      dz2:= 0.4
Tairrad:= 22.   dxtop1:= 0.4    dxlower1:= 0.2
                dxtop2:= 0.3    dxlower2:= 0.4
                dxlower3:= 0.3

Lad1:=          klower1:=     ktop1:=      Thin1:=
0.1             0.004          0.008      29.55739
0.1             0.008          0.014      28.305683
4.0             0.014          0.02       28.069028
4.0             0.02           0.08      27.908253
4.0             0.08           0.08      27.85413
4.0             0.08           0.06      27.806613

cumlai:= sum(Lad1,dz1)
cumlai= 3.280
Total_Load:= cumlai/Rshort*2*ar
Total_Load= 524.800
rbhm:= 100.
rbhs:= 100.
rs_m:= 300
rss:= 200.
Tleaver:= 27.0

Tairtop:= 30.0
Tair_mj:= 30.0
eair_mj:= es(18.4)
Tair0_0:= 30.
eairtop:= es(18.4)
Tsoit:= 32.
eairtop= 2.118*10^1

```

Fig 4.17.a A run for a warm arid region

Anyhow, with time the feedback between eq.4.2.2, eq.4.2.10 and eq.4.2.14 will go on and the whole system moves back to equilibrium as dedicated by the limited turbulent transport coefficients and stomatal resistance. The details will differ depending on the particular case. We will discuss one case later. Anyhow, since our initial assumption is of $\beta < \gamma/s$, this means that the build-up of vapour pressure of the air will continue, leading to a negative D' till a critical value of D has been reached. At this point, leaf temperature and air temperature will become equal and sensible heat flux reverses sign. H will be an increasing function of time and LE is a decreasing one. After the sensible heat flux change, the air starts warming and D develops according to eq.4.2.90. The solution of the temperature and vapour pressure and leaf temperature will progress toward an equilibrium solution, given by the solution of system 4.2.2, 4.2.10 and 4.2.14 simultaneously.

In below , we give results of detailed simulations for a canopy of six layers, as was done with the sensitivity analysis of the f_2 function. We now want to see the interaction under specific boundary conditions between the profiles and the sources. We have three runs representing a warm arid region (Griffiths and Soliman, 1969), a humid cold region (Arlery, 1970) and a tropical (hot humid) region (Sukanto, 1969). The boundary conditions are shown in figures 4.17.a, 4.18.a and 4.19.a. The procedure explained in page 131 is the same one used here to control the run such that no contribution of the leaf heat storage to the fluxes occurs. In fig. 4.17.b, the upper left figure shows the temperature of the air (T_{air}), equilibrium temperature of the leaves ($T_{leaveseq}$), as given by eq. 4.2.5 and temperature of the leaves (T_{leaves}) respectively. The upper right figure shows the changes of the equilibrium temperature of the leaves between different time steps due to the vapour pressure deficit changes between time steps ($\Delta T_{leqDair}$), air temperature changes ($\Delta T_{leqTair}$) and the sum of both (ΔT_{leqS}). The lowest two figures are the same as the upper ones, except being for layer number 2.

In fig 4.17 c, most left figures are the same as the upper left figure in fig.4.17.b, for air layers 1, 2, 3 and 5. Layer one is the lowest layer in the canopy. The figures in the middle show the behaviour of the sensible heat sources ($Leaves_{sh}$) and latent heat sources ($Leaves_{lh}$) for the same layers. The rightmost figures show the behaviour of the vapour pressure and vapour pressure deficit of the air for the same layers.

One of the early impressions made from these runs that the state variables of the air (i.e. temperature, vapour pressure and vapour pressure deficit) and the sources follow within the whole gust cycle an exponential behaviour. Another impression which can be drawn is the much larger variation of the value of the equilibrium temperature of the leaves in the lower layers of the canopy as compared to that in the upper layers. This is due to the lower layers being less coupled during most of the time to the boundary above, so the gust represents a large shift from the mean variables of the air, which leads then to a large shift from equilibrium. For the upper layers, the shift due to the gust is relatively not so strong since they are more strongly coupled. So, it seems that the gust effect has to do with the ratio of the deviation to the mean. We will come to this conclusion also in eq.4.2.99.

Fig.4.17.b and fig. 4.17.c show that, for the second air layer, the intruding air was warmer (T' was positive and vapour pressure D' is positive). The change in the equilibrium temperature of the leaves was negative ($\Delta T_{leqDair}$) while that due to air temperature ($\Delta T_{leqTair}$) was positive. The total sum of both components was negative (condition A.2.7.4 being satisfied), so the equilibrium temperature of the leaves in that layer experienced

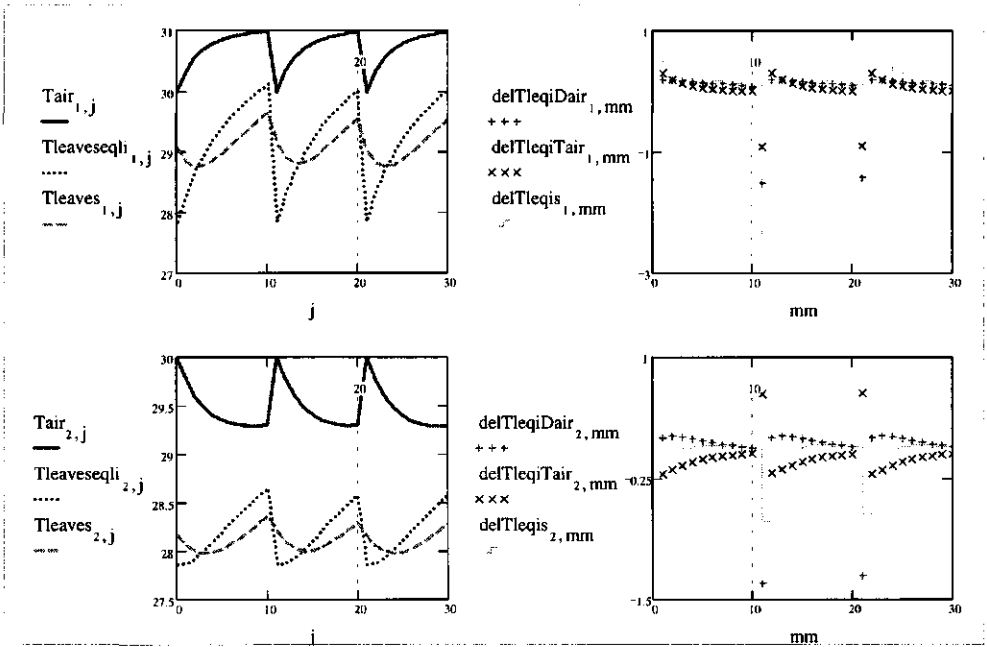


Fig 4.17.b: The behaviour of the equilibrium temperature of the leaves

a sudden negative change. That change caused the equilibrium temperature of the leaf curve to cross the temperature of the leaf curve (the second figure in the first column of fig 4.17.c) Due to this, the leaf temperature curve in the same figure (Tleaves) suddenly reverted direction. With leaves cooling, the air started to cool down, since the leaves are acting as a sink in eq.4.2.12. This was due to the high vapour pressure deficit of the air which led to (delTleqiDair) being highly negative. The air was being humidified at the expense of leaf heat storage and negative sensible heat flux from the air to the leaf. With the gust mechanism shut off, a large fraction of the water vapour delivered by the leaves to the air accumulated within the layer and the air cooled. This led to a decrease in the vapour pressure deficit within time (eq.4.2.90). The feedback on the equilibrium temperature was negative. The leaves within the next time step were still cooling but with a higher rate (less negative) due to the positive change in $T_{l,eq}$. The air cooled and kept humidifying (D^C/T^C between consecutive time steps being positive) with a resulting increase in $T_{l,eq}$. Inevitably, the temperature of the leaves and the equilibrium temperature of the leaf met with a resulting no further decline in leaf temperature. In this case, the air temperature was still higher than this meeting point, since the intruding air was warm enough to maintain a positive temperature difference with the leaf. The negative sensible heat flux from the leaf to the air will continue, but from now on the leaf will start warming, and the heat storage within the leaf will increase. The negative change in storage with the leaf and the air so far represented the contribution of the storage to the sources (in this case latent heat sources). This change represented the variation in the source which could sum in the average to a value higher or lower than a no-gust model, depending on the time period between two gust intrusions. Due to the decrease of vapour pressure deficit, the leaves kept warming till a critical D' was reached in which the temperature of the air

becomes equal to the temperature of the leaf. In this case, or scenario, the period between gust intrusions was not large enough to allow this. This would represent then case 2, discussed within sect.4.2.2.1 (eq.4.2.88).

The time mean will be controlled mainly, by the build-up during the quiescence period. If the value of D during the quiescence period is low, compared to the gust intrusion phase, the numerator in $D/(T_s - T_a)$ will have a large time variation which represents a large variation in H/LE ratio. The importance of the gust process here is that it leads, due to a large difference in D profile, to a different solution of the energy budget equation of the leaves and the soil surface which affect the resulting mean.

The variation of the sources as a function of time is controlled by the feedback between the profiles and the leaf temperature. The effect of that disturbance depends on the frequency of occurrence and the degree of the build-up of temperature and vapour pressure which is allowed to occur.

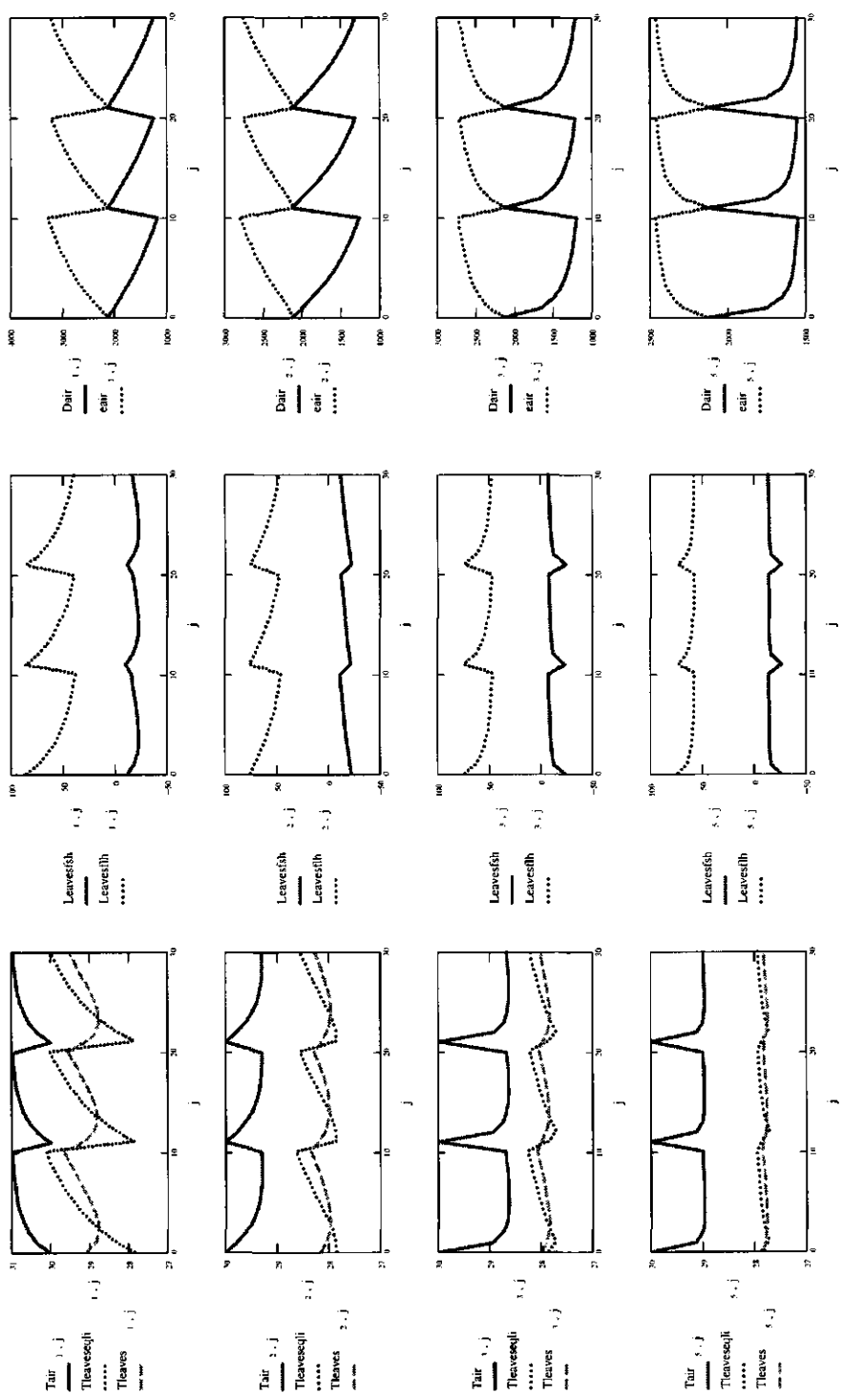


Fig. 4.17.c: Simulation of a warm arid region.

In the following scenario A_1 and C_1 , the same analysis applies in the sense of the feedback between the system of eq.4.2.2 , 4.2. 10 and 4.2.14 with the differences of the initial W'd' coordinate and the effect of this T1,eq and whether this led to a decrease or an increase in the leaf temperature and the resulting change in the behavior of the sources and the feedback on the profiles.

Scenario A_1 :

In scenario A, the incoming air will be drier and colder than the air ejected from plant canopy. The values for this run are obtained from Arlery (1970). They represent the averaged temperature and vapour pressure for the month of August for De Bilt, The Netherlands.

The discussion of this run follows the same line as above except that the intruding air is colder than the ejected air (T' negative and D') positive. In here, the temperature of the leaves was always higher than air. So, there was always a positive source within the canopy. This was due to the lower vapour pressure deficit compared to scenario B1. The intrusion led to an increase in both the sensible and latent heat flux from the leaves to the air. This was achieved at the expense of heat storage within the leaves, which were trying to adopt to the change in the boundary conditions for the solution of the energy budget equation of the leaf surfaces. In the process, and due to the lower turbulent coupling between the air in the middle of the canopy and the air above, the air changed its temperature and vapour pressure with a resulting feedback on the leaf temperature. So, everything was

```

coeff := 0.25   dz1 := 0.2   dxtop1 := 0.2
Rshort := 100.  dt := 10.     dxlower1 := 0.2
Thick := 0.0005 dz1 := 0.4   dz2 := 0.4
Tairrad := 15.  dxtop1 := 0.4  dxlower1 := 0.2
                                dxtop2 := 0.3  dxlower2 := 0.4
                                dxlower3 := 0.3

Lad1 :=      klower1 :=      ktop1 :=      Tlin1 :=
| 0.1 |      | 0.004 |      | 0.008 |      | 22.121194 |
| 0.1 |      | 0.008 |      | 0.014 |      | 21.754356 |
| 4.0 |      | 0.014 |      | 0.02  |      | 21.932505 |
| 4.0 |      | 0.02  |      | 0.08  |      | 21.682033 |
| 4.0 |      | 0.08  |      | 0.08  |      | 21.524594 |
| 4.0 |      | 0.08  |      | 0.06  |      | 21.266762 |

cumlai := ∑i Ladi dzi      Tairtop := 20.0
cumlai = 3.280              Tairm,j := 20.0
Total_Load = cumlai Rshort 2: ar  eairm,j := 1600
Total_Load = 524.800          Tair0,0 := 20.
rbhm := 100.              eairtop := 1600
rbhs := 100.                Tsoil := 22.
rsm := 300
rss := 200.
Tleaveri,j := 22.0          eairtop = 1.600·103

```

Fig.4.18.a Run for a cold humid region

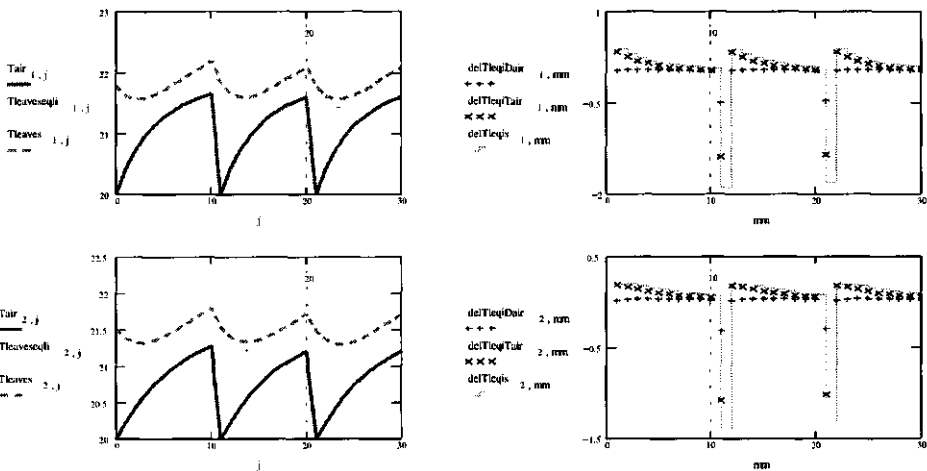


Fig 4.18.b: The behaviour of the equilibrium temperature of the leaves.

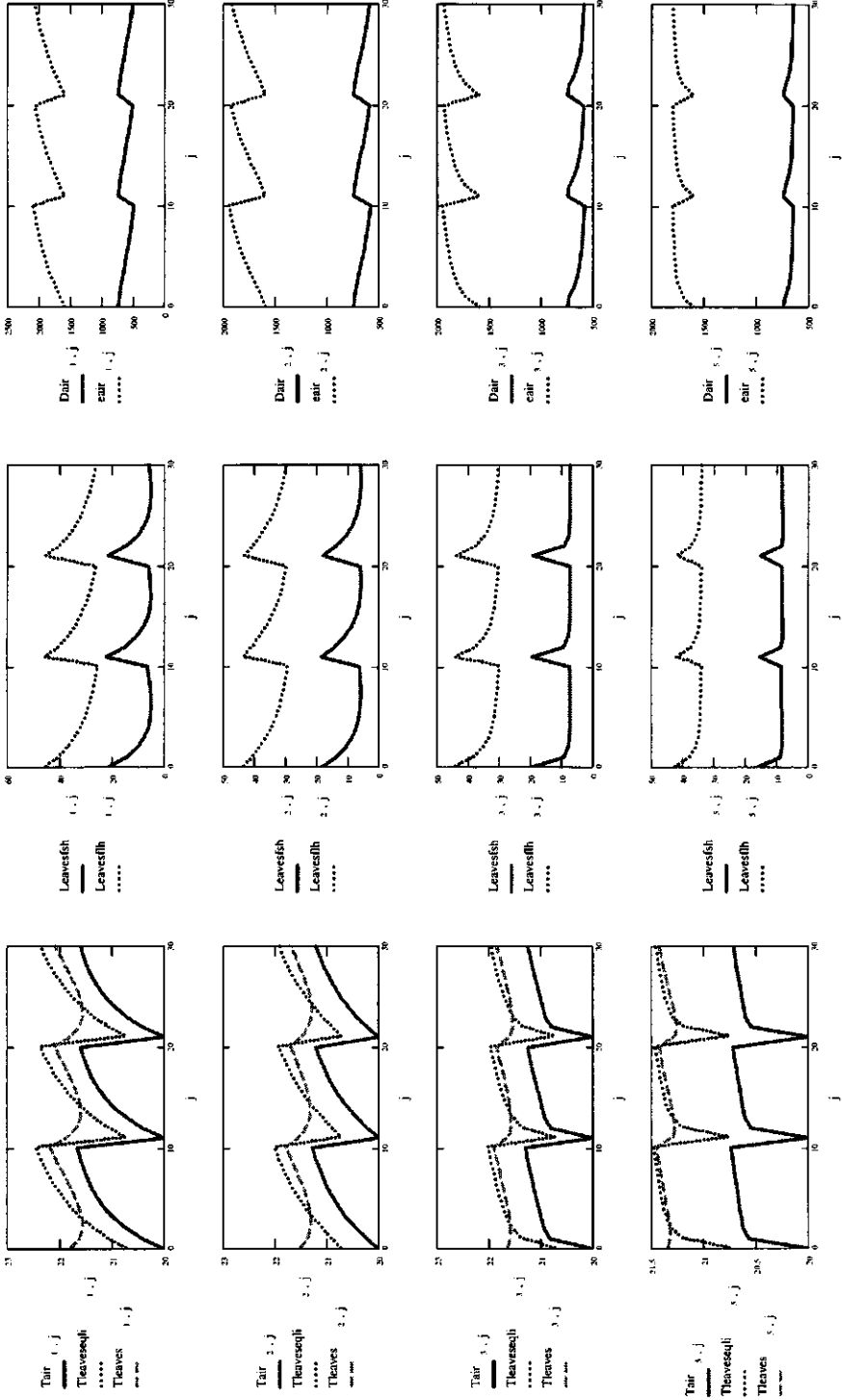


Fig 4.18.c: A simulation of a cold humid region.

moving back to equilibrium.

Scenrio C1

The values of the boundary conditions for this run were obtained from (Sukanto, 1969) The values for this run are shown in fig.4.19.a.

What is noticed here, especially in fig. 4.19.b, is that in comparison to fig.4.17.b, the changes in the equilibrium temperature of the leaves due to vapour pressure deficit changes were much lower (in absolute value) than the more negative changes in the equilibrium temperature of the leaves due to temperature changes. So the gust process introduces a reduction of the leaf temperature, due more to the lower air temperature than due to the higher vapour pressure deficit introduced by the gust intrusion. So, in this case, there will an increase in the sensible heat flux due to the gust process.

```

coeff = 0.25  dz1 = 0.2  dxtop1 = 0.2
Rshort = 100.  dt = 10.  dxlower1 = 0.2
Thick = 0.00095  dz1 = 0.4  dz2 = 0.4
Tairrad = 22.  dxtop1 = 0.4  dxlower1 = 0.2
              dxtop2 = 0.3  dxlower2 = 0.4
              dxlower3 = 0.3

Lad1 =
0.1  0.004  0.008  29.324384
0.1  0.008  0.014  28.957338
4.0  0.014  0.02  28.98552
4.0  0.02  0.08  28.697913
4.0  0.08  0.08  28.539547
4.0  0.08  0.06  28.289065

klower1 =
0.004
0.008
0.014
0.02
0.08
0.08

ktop1 =
0.008
0.014
0.02
0.08
0.08
0.06

Tini1 =
29.324384
28.957338
28.98552
28.697913
28.539547
28.289065

cumlai = sum(Lad1, dz1)
cumlai = 3.280
Total_Load = cumlaiRshort2-ar
Total_Load = 524.800

rbtm = 100.
rbhs = 100.
Rm = 300.
rse = 200.
Tleaves1,j = 27.0
Tairtop = 27.0
Tairm,j = 27.0
eairm,j = 0.85*es(Tairm,j)
Tair0,0 = 27.
eairtop = 0.85*es(Tairtop)
Tsoil = 29.
eairtop = 3.036*10^3
    
```

Figure 4.19.a run for a humid tropic region

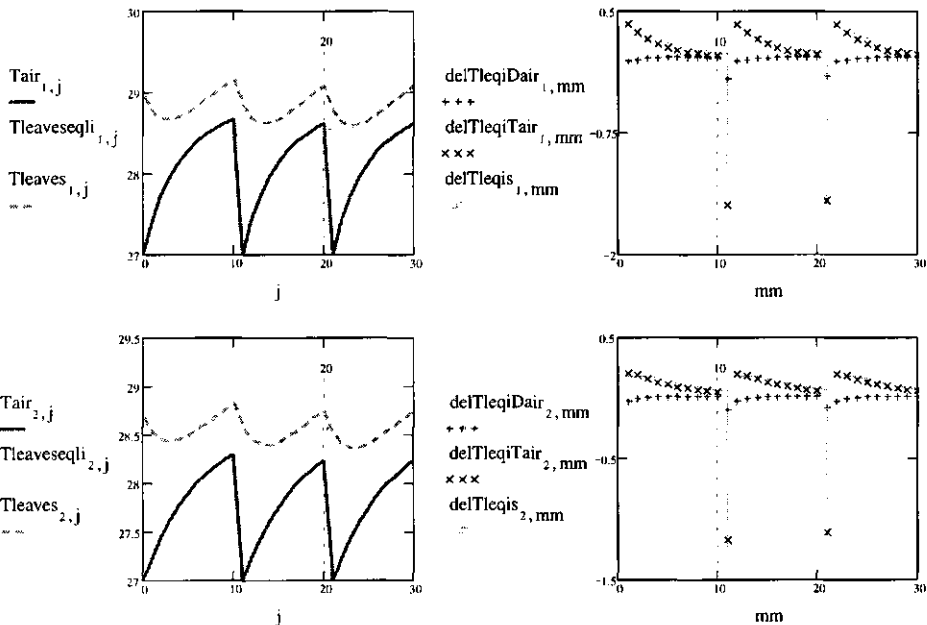


Fig.4.19.b: the behaviour of the leaves temperature.

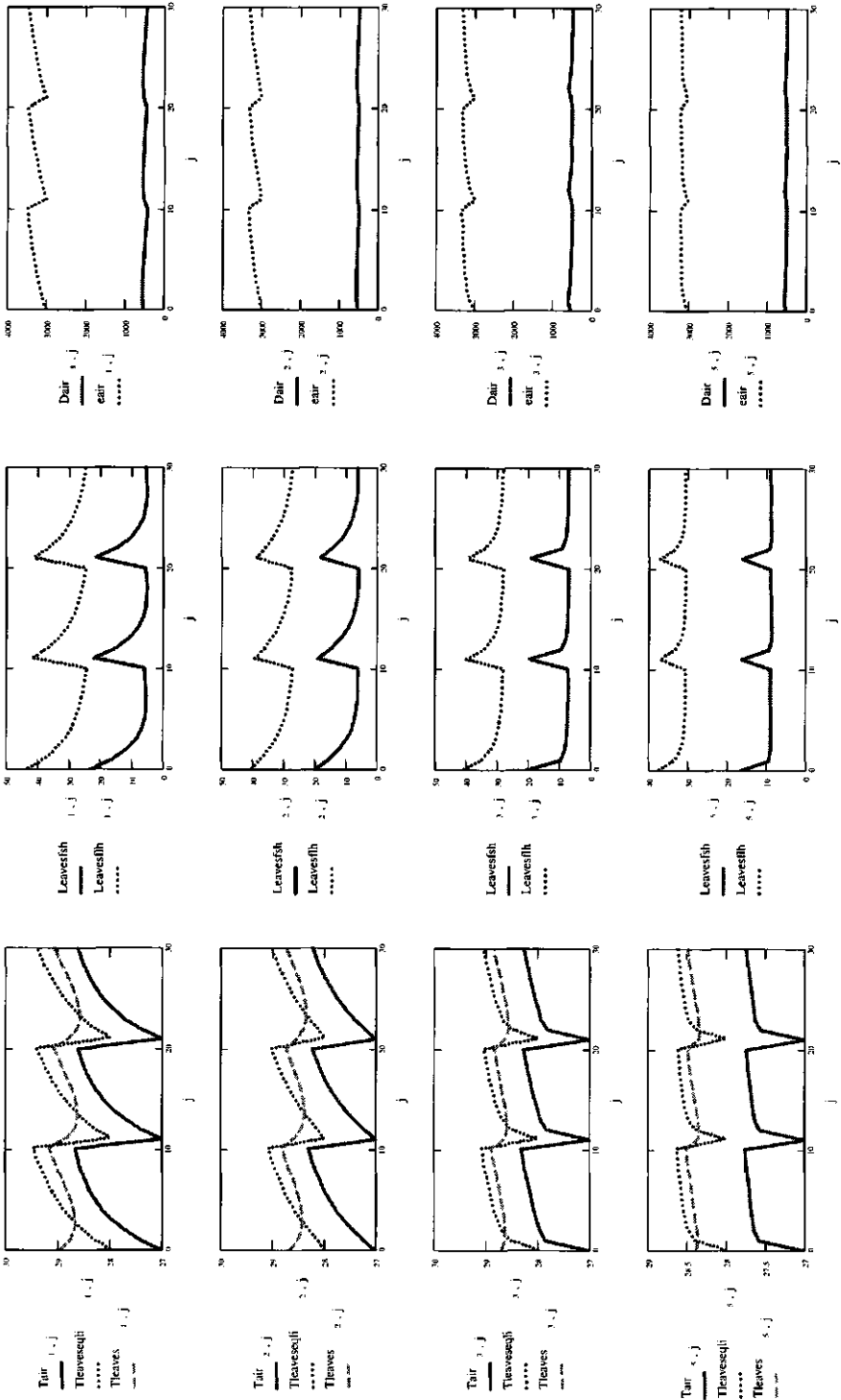


Fig.4.19.c: A simulation of a hot tropic region.

2) NIGHT-TIME SITUATIONS:

Radiative cooling for the canopy elements at night-time and the concentration of these canopy elements at the upper portion of the canopy, leads to the appearance of a heat sink at the canopy top. This sink will be filled up by heat flux from the soil, in the form of thermals transporting warm air from the soil surface to the sink at canopy top. Dew rise, and dew fall from above, compensate the remaining sink deficit at canopy top. The fractional contribution of each of these sources to the sink at the maximum leaf area density height is dependent on the coupling between different heights. The degree of coupling is function of the thermal stability. The coupling from above the canopy air to the canopy top depends on the occurrence of intrusions of air from above. This depends on the existence of a critical shear at the canopy top, which overcomes the thermal stability effects due to the unfilled sink at the canopy top. So at night there are two situations, depending on the shear at canopy top, 1) a coupled canopy or 2) decoupled canopy.

In case of light wind speed at the canopy top, there will be little dynamic coupling between the canopy air space and the air above. This leads to the soil acting as a source to satisfy an unfilled sink at the canopy top.

1) Coupled canopy:

The picture here is similar to colder, more humid air coming down

2) Decoupled canopy:

There is no intermittency due to gust intrusion from above, while there will be circulations of air transporting sensible and latent heat from the warm wet soil surface to the colder canopy top. Look at fig 4.20 and 4.21. This figure is taken after midnight and shows for a segment of 1000 sec duration the temperature and the wind field observed within plant canopies. In this picture, we average the 5 Hz into 1 Hz frequency. The picture clearly shows the radiative cooling at the upper parts of the canopy plus the high temperature regions at the lower parts of the canopy. By looking at the simultaneously measured wind speed, one sees higher values of this absolute wind as measured by hot bulb anemometers. There could be two explanation for this: the intrusion of coherent structures at the canopy top even at night, which could be seen at some of the occasions, or the buoyancy term acting as a source for turbulent kinetic energy, leading to the turbulent transport of heat from lower regions of the canopy to the upper regions of the canopy. Look at the tongues of the temperature islands which extend upwards to the canopy air space. This problem is considered to be similar to the Bernard-Raleigh convection problem (Jacobs *et al.* 1994). The centroid of the radiative cooling by the plants represents the cooler upper surface, and the hotter soil represents the lower hotter surface.

Most of the generation of turbulence within canopy is due to the positive buoyancy flux at the soil surface, due to the soil heat flux from the soil to the canopy layers, which is driven by the residual radiative cooling at the canopy top.

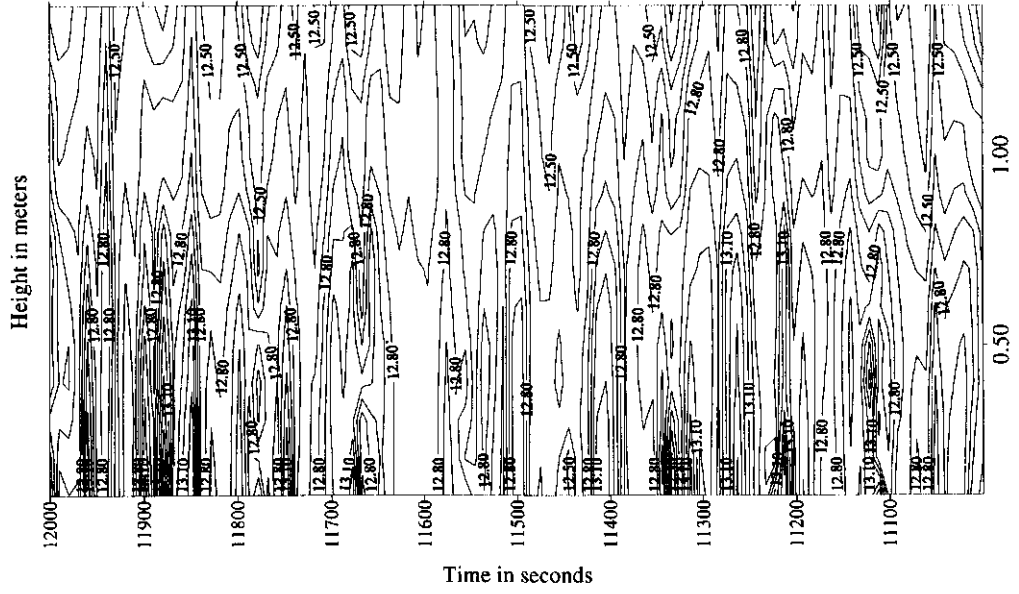
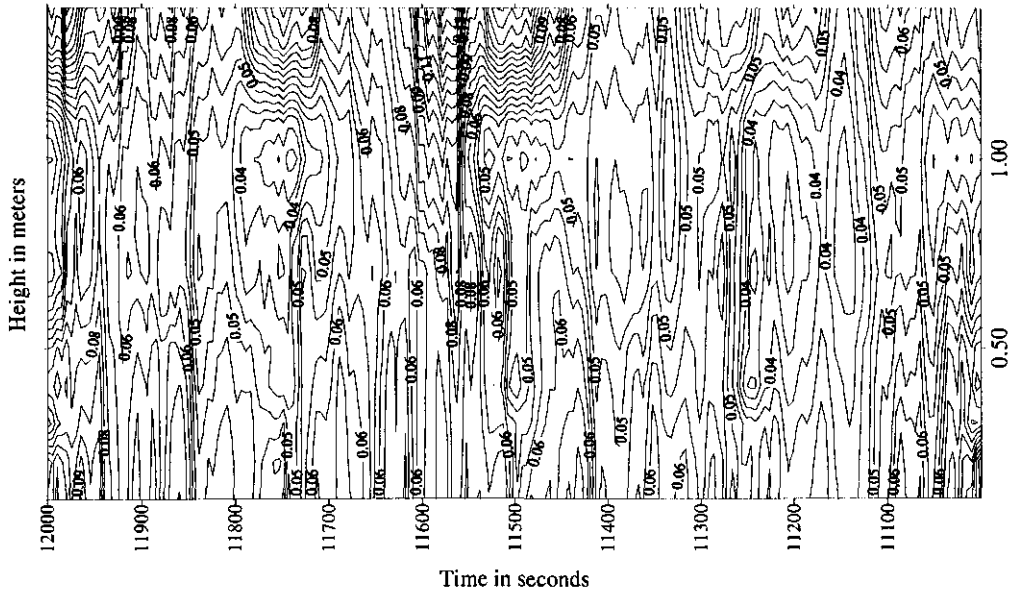


Fig 4. 20 Space time domain maps for a coupled canopy at night. The upper figure shows windspeed and the lower one shows temperature. contour intervals are 0.01m/s and 0.1 °C.

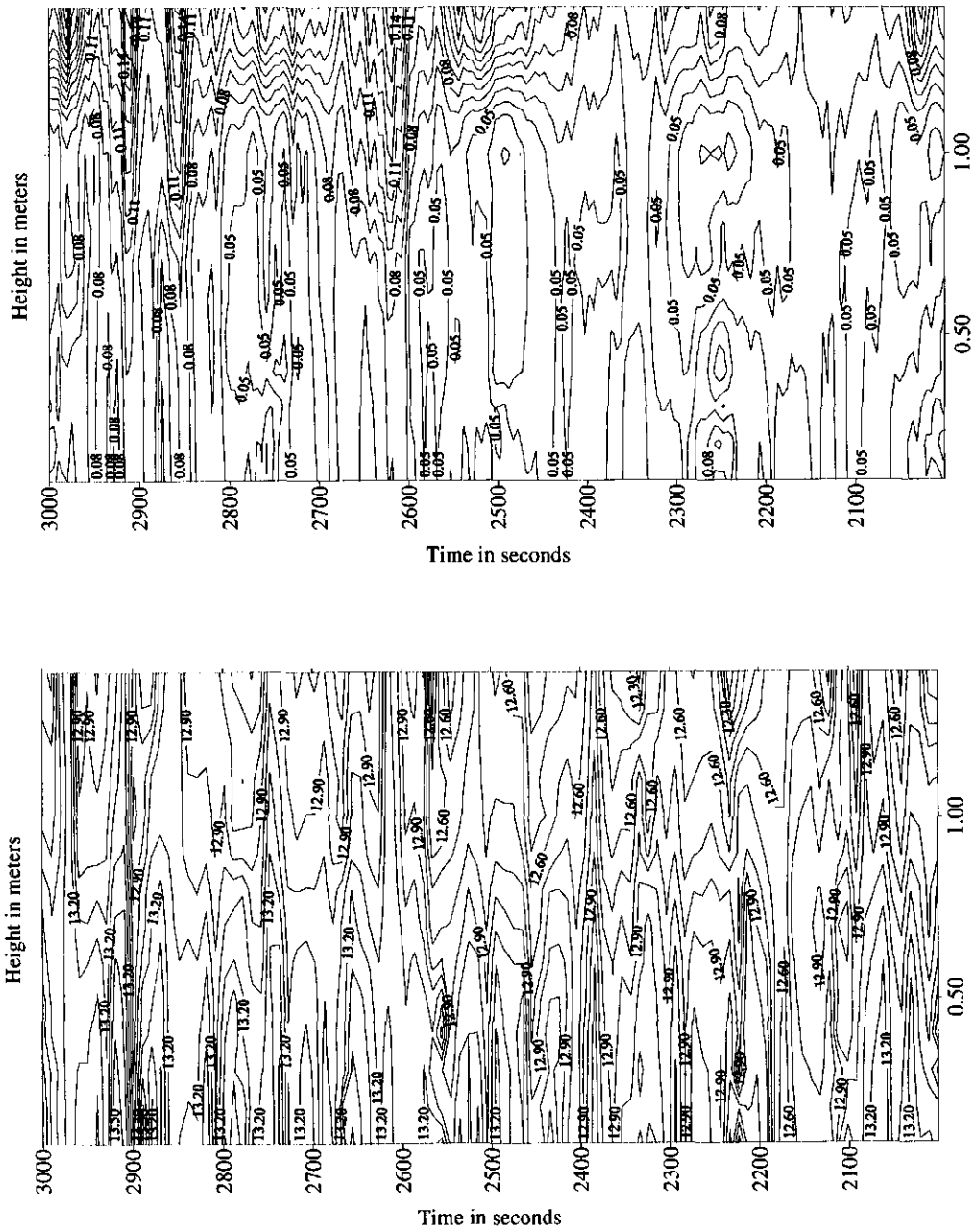


Fig 4. 21 Space time domain maps for a de-coupled canopy at night. The upper figure shows windspeed and the lower one shows temperature. contour intervals are 0.005m/s and 0.1 °C.

The average we obtain in a measured data set is an average of the above explained processes. If the system is nonlinear, an approximation of these processes in a large-time averaged model in a functional (cause-effect) manner is not possible. Obtaining an approximation in a multi-layered model could be done from a detailed model by inverse computing of a matrix, which relates the final solution to the initial with a certain set of averaged sources.

A large-time averaged measured flux could, however, be obtained from a large-time averaged measured surface temperature by the use of a fitted large-time averaged conductances. But this conductance can not be used for a smaller time scale than the one it was obtained from. To obtain conductances means for small time scale, we need to satisfy equation 3.5.1 a,b by the use of ensemble averaging for identical periods of the gust cycle.

The effect of intermittency on shift from equilibrium could be shown by the use of Penman-Monteith equation for latent heat and sensible heat, if storage can be neglected or if an equivalent resistance can be defined. This method here could be also used as an approximation to check the sensitivity of the energy partition as defined by Bowen ratio to the variation in the simulated mean D. Let us decompose D into a mean and a deviation from that mean due to large scale and small scale turbulence. Penman-Monteith equation for sensible heat flux reads as

$$H = \frac{\gamma^* R_n - \rho C_p D r_H^{-1}}{s + \gamma^*} \quad (4.2.91)$$

and for latent heat as

$$\lambda E = \frac{s R_n + \rho C_p D r_H^{-1}}{s + \gamma^*} \quad (4.2.92)$$

By putting the triple decomposition

$$D = \bar{D} + D' + D'' \quad (4.2.93)$$

where D is the instantaneous vapour pressure deficit. D', D'' represent time deviations from the mean due to small scale turbulence and large scale turbulence, respectively,

$$\overline{D' + D''} = 0.0 \quad (4.2.94)$$

$$\bar{D} + \bar{D}' = D_1 \quad (4.2.95)$$

$$H = \frac{\gamma^* R_n - \rho C_p \bar{D} r_H^{-1} - \rho C_p D' r_H^{-1} - \rho C_p D'' r_H^{-1}}{s + \gamma^*} \quad (4.2.96)$$

$$\lambda E = \frac{s R_n + \rho C_p \bar{D} r_H^{-1} + \rho C_p D' r_H^{-1} + \rho C_p D'' r_H^{-1}}{s + \gamma^*} \quad (4.2.97)$$

Dividing

$$\frac{H}{\lambda E} = \frac{\gamma^* R_n - \rho C_p D_1 r_H^{-1} - \rho C_p D'' r_H^{-1}}{s R_n + \rho C_p D_1 r_H^{-1} + \rho C_p D'' r_H^{-1}} \quad (4.2.98)$$

Dividing by $\rho C_p D_1 r_H^{-1}$ both numerator and denominator,

$$\frac{H}{\lambda E} = \frac{\frac{\gamma^* R_n}{\rho C_p D_1 r_H^{-1}} - 1 - \frac{D''}{D_1}}{\frac{s R_n}{\rho C_p D_1 r_H^{-1}} + 1 + \frac{D''}{D_1}} \quad (4.2.99)$$

The relation between D'' and D_1 depends on the frequency of refreshment and its value and the time constants of the canopy layers. D_1 , or \bar{D} , is not independent. It will depend on D'' and the period between the passage of two gusts in relation to the time constants of the canopy air layers. The equations of the mean are given. This relation 4.2.98 could be also used to see the effect of the estimation of the mean D by assuming that D'' is the deviation between two means determined by two modelling approaches (e.g. a gust and no-gust approach). In the following three equations, we use the criterion of being four times the value of the air layers time constant as an indication for equilibrium establishment.

$$\bar{T} = T_{top} \frac{\Delta t_{gust\ duration}}{period} + T_{air,eq} \left(1 - \frac{\Delta t_{gust\ duration}}{period} - \frac{4 \tau_{a,T}}{period} \right) + T_{average} \frac{4 \tau_{a,T}}{period} \quad (4.2.100)$$

$$\bar{e} = e_{top} \frac{\Delta t_{gust\ duration}}{period} + e_{air,eq} \left(1 - \frac{\Delta t_{gust\ duration}}{period} - \frac{4 \tau_{a,e}}{period} \right) + e_{average} \frac{4 \tau_{a,e}}{period} \quad (4.2.101)$$

$$\bar{D} = D_{top} \frac{\Delta t_{gust\ duration}}{period} + D_{equilibrium} \left(1 - \frac{\Delta t_{gust\ duration}}{period} - \frac{4 \tau_{a,D}}{period} \right) + D_{average} \frac{4 \tau_{a,D}}{period} \quad (4.2.102)$$

The ratio of $\frac{D'}{D_{mean}}$ if we assume a complete refreshment which is satisfied becomes

$$\frac{D'}{D_{mean}} = \frac{D_{top} \cdot D_{mean}}{D_{mean}} \quad (4.2.103)$$

$$\frac{D'}{D_{mean}} = \frac{D_{top}}{1} \quad (4.2.104)$$

By looking at the value of D_{mean} ,

$$D_{\text{mean}} = \frac{D_{\text{top}}}{D_{\text{top}} \frac{\Delta t_{\text{gust duration}}}{\text{period}} + D_{\text{equilibrium}} \left(1 - \frac{\Delta t_{\text{gust duration}}}{\text{period}} - \frac{4 \tau}{\text{period}}\right) + D_{\text{average}} \frac{4 \tau}{\text{period}}} \quad (4.2.105)$$

$$D_{\text{equilibrium}} = e_s(T_{\text{air,eq}}) - e_{\text{air,eq}} \quad (4.2.106)$$

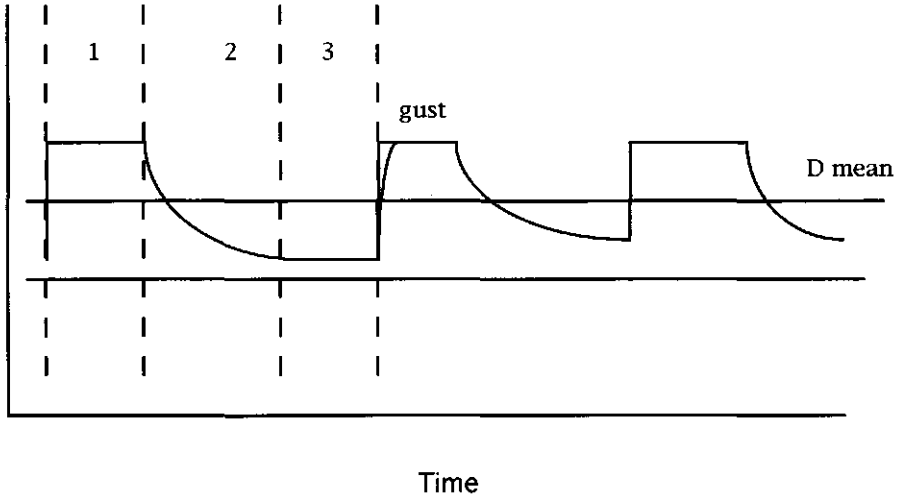


Fig 4.22 The assumed behaviour of the vapour pressure deficit within time.

The maximization of this value requires a low value of relative gust duration and a minimum $D_{\text{equilibrium}}$. A low value of $D_{\text{equilibrium}}$ means from

$$e_{\text{air,eq}} = \left(\frac{\frac{K_{\text{top}}}{\delta X_{\text{top}}}}{\left(\frac{K_{\text{top}}}{\delta X_{\text{top}}} + \frac{K_{\text{bottom}}}{\delta X_{\text{bottom}}} + \frac{\text{LAD} \cdot \Delta z}{(r_{\text{bv}} + r_s)} \right)} e_{i+1} + \frac{\frac{K_{\text{bottom}}}{\delta X_{\text{bottom}}}}{\left(\frac{K_{\text{top}}}{\delta X_{\text{top}}} + \frac{K_{\text{bottom}}}{\delta X_{\text{bottom}}} + \frac{\text{LAD} \cdot \Delta z}{(r_{\text{bv}} + r_s)} \right)} e_{i-1} \right) + \frac{\frac{\text{LAD} \cdot \Delta z}{(r_{\text{bv}} + r_s)}}{\left(\frac{K_{\text{top}}}{\delta X_{\text{top}}} + \frac{K_{\text{bottom}}}{\delta X_{\text{bottom}}} + \frac{\text{LAD} \cdot \Delta z}{(r_{\text{bv}} + r_s)} \right)} e_s(T)$$

a canopy with a low stomatal resistance and weak coupling between canopy air layers and the layers of air above the canopy during the quiescence period. The importance of small scale mixing leads to increased importance of the coupling between different canopy layers, but for every one of these the stomatal resistance has to be low to have a high value of $e_{\text{air,eq}}$.

The problem of stomatal resistance and soil surface parameterization is discussed in the end of this chapter. The problem of small scale mixing during the quiescence period was discussed in chapter 3.

In case of a canopy which is strongly coupled all the time, the effect of intermittency would not be there, since D_{top} will be close to D_{mean} . The value of energy partition will depend on the value of stomatal resistance.

Statement 1: The problem of intermittency in canopy climate modelling is the combined effect of: 1) the existence of a separation in the length scales responsible for transport and 2) the ability of the leaves and the soil as sources and sinks to respond to temperature and vapour pressure variations due to this intermittency or scale separation.

Statement 2: The problem of higher order correlations and their non-uniform distributions within time or space, which we discussed in chapter 3, would not have been there if the canopy elements were not able to respond to temperature and vapour pressure variations introduced by gust intrusions.

Explanation of statement 2: During the quiescence period, the amount of sensible and latent heat energy, which is delivered by the leaves into the intercanopy air stream and which is not evacuated to the layer of air above, represent a change of storage of nonradiative energy within the canopy air space. During the gust intrusion phase, the discharge of these stored amounts represent a flux at the canopy top. During the gust intrusion phase, there is a downward momentum flux. Correlated with momentum flux, there will be a high latent and sensible heat flux represented by evacuation of nonradiative stored energy within the canopy air layers. If the canopy elements were very sluggish (i.e. in an extreme case metallic leaves: no transpiration and completely reflective non-absorbing leaves), there would be no change of latent heat storage in the first case, and also no storage of sensible heat in the second case within the canopy air space during the quiescence period. That would mean no flux of latent heat and sensible heat during the gust intrusion phase and so no correlation between momentum flux and heat fluxes (i.e. fourth order terms). The situation is not so extreme (i.e. metallic leaves), but the more sluggish the canopy elements, the less is the inhomogeneity of the time or space distribution of the higher order terms.

4.2.4 SENSITIVITY ANALYSIS ON THE APPROXIMATE FORM: THE INVERSE MATRIX A^{-1}

What we want to show here is the effect of intermittency due to the parameterizations of turbulent transport coefficient during the quiescence period on the inverse matrix A^{-1} . It will be shown that for the steady state solution, all the inner values of the matrix are multiplied by a coefficient which equals the ratio between the parameterization due to the no-gust model to that of the gust model. So, if the ratio of K_m value between a gust and no gust approach is 0.25, all the inner elements of the inverse matrix are multiplied by a ratio of 1/0.25. This is not a trivial difference.

To show this, the inverse matrix was obtained symbolically for equation system 4.2.72 by the use of Gauss-Jordan elimination. What we want to obtain is a ratio between the values of the corresponding elements of two inverse matrices for the matrix A , as given by eq.4.2.72. The matrix A had two parameterizations, one due to the gust model, and the other one is due to a continuous parameterization, in which the K_m value had a higher value (twice the gust parameterization, but constant in time with large-time interval averaging). To do this, some intermediate steps are shown in Appendix A.2.10 to obtain these ratios.

The coefficients E_i , G_i and F_i are defined according to equations 4.2.74. In the case of a gust model these coefficients have a value (let us assume $1/\alpha$ times as large as the gust model). In the case of a steady state solution $\Delta t \rightarrow \infty$, So F_i equals the sum of E_i and G_i .

In reducing the second column to a value one for the second row, we get the ratios $-G_2/f_2$, E_2/F_2 , $1/F_2$, E_3E_2/F_2 , $F_3-(E_3G_2/F_2)$, E_3/F_2 . The third, the fourth and the fifth terms are affected by the gust process. $1/F_2$ is twice as large as the case of a gust model and $F_3-(E_3G_2/F_2)$ is half the value in the case of no-gust model. Later in the derivation, we call this quantity F_3' . E_3' which equals E_3E_2/F_2 for a gust model is also half the value of that in a no-gust model.

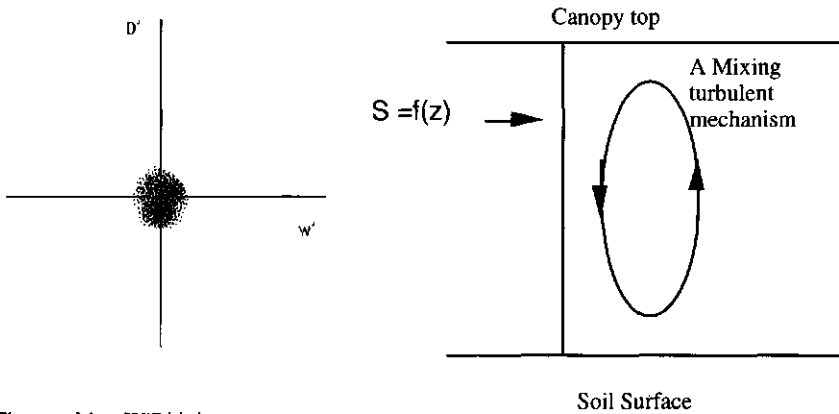
In reducing the third column to a value of one for the third row, we get ratios such as : E_iE_3'/F_3' . This quantity, which we call later E_i' , is also half the value in a gust model compared to that of the no-gust model. The same applies to $F_i-E_iG_3/F_3'$ which will later be called F_i' . The ratio between the gust and no-gust coefficient applies to those coefficients with higher i 's.

Now, looking at the inverse matrix of our system A^{-1} , we see that every element of that matrix consists of an addition of terms. Each of these terms is a multiplication or a division of F_i, E_i, G_i terms. We see that for the inner elements of the inverse matrix, the number of elements constituting the numerator is always one less than the number of elements constituting the denominator, so a factor of $1/\alpha$, where α has been defined earlier as the ratio between K_m values for a gust and no-gust, goes out.

For the elements constituting the first and last columns, we see that the number of elements going into the numerator and the denominator are the same. So, no reduction comes out, and these elements of the matrices for the no-gust and gust model are the same.

4.3 THE RELATION BETWEEN THE LARGE EDDY LENGTH SCALE, D' AND D_{MEAN} AND THE CORRELATION BETWEEN THE TRANSPORT AND THE SOURCE

Assume that the canopy has a large vertical extension compared to the scale of the mixing structure and has a constant source distribution as function of height. A large-scale structure would mix air layers which would have the same temperature and moisture content, and this would have made no effect on the source terms of the canopy. The joint probability distribution of w' and D' would have then a correlation of zero. All the points of that probability would lie with the origin. We allow some dispersion due to randomness



The resulting $W'D'$ joint probability distribution.

Fig 4.23.a shows a hypothetical case of a transport mechanism with a length scale less than the canopy height with uniform source distribution

This would be close to what is happening with small scale turbulence: mixing the air inside the canopy which have moisture contents (D' vapour pressure deficit variations) reflecting the vertical distribution of the sources.

Due to the large scale of the coherent structure in relation to canopy height, vertically downward moving parcels of air tend to be drier (i.e. lower vapour pressure) and they replace more humid air from within the canopy, which is pushed upwards. The downward vertically displaced parcels tend to remain within the canopy air space, so their humidity deficit is felt for a large period of time by the canopy, while the more humid parcels which were displaced upwards have left the canopy space so their effect is not felt. In this case, the joint probability distribution between w' and D' has a correlation which is not equal to zero. The outside regions of this probability represent the effect of extreme events. If the canopy was large enough, this effect would not have been there, since the vertically moving parcels will have a moisture content which reflects the rather constant source distribution.

In the joint probability distribution $W'D'$, there exists three domains. These are represented by domain 1, 2 and 3 respectively in the detailed $W' D'$ diagram (fig 4.24). The

leaves have a very low capacitance for water vapour. They respond immediately to water vapour deficit of the air. The response magnitude will be dedicated by the magnitude of stomatal resistance. Domain 1 and 2 include small scale deviation of D . Part or none of

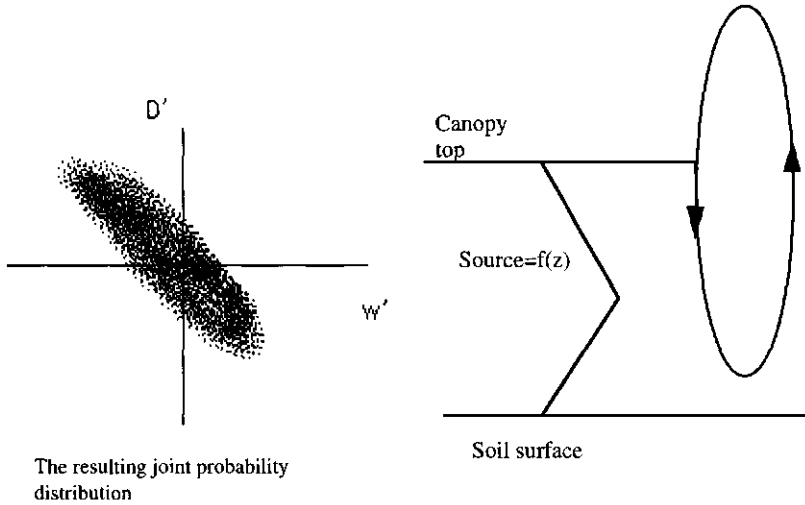


Fig.4.23 b shows a hypothetical case of the joint probability distribution resulting from a large length scale.

these deviations will not be seen by the leaves. These are represented by the symmetric area 1. (that area is very small indeed). *In case of very sluggish leaves with very high time constants, they may not even see the deviations due to large scale turbulence D'' .* This depends on the limit of the RC multiplication, where R is the resistance of the leaf and C is the capacitance of the leaf for water vapour and if RC goes to a limit. The first term is very large (R) while the second term is very small (C). The part which the leaves see and responds to is the area between the outer limits of area 3 and area 1. \bar{D}_1 , as has been defined by eq.4.2.95 could be a spatial mean within small number of layers. That would have been the mean if the gust process did not occur.

From eq.4.2.97, it could be shown that the latent heat source

$$\lambda E_1 = \lambda E_1 \left[1 + \frac{\rho C_p D'' r_H^{-1}}{s R_n + \rho C_p D_1 r_H^{-1}} \right] \quad (4.3.1)$$

$$\lambda E_1 = \frac{s R_n + \rho C_p \bar{D} r_H^{-1} + \rho C_p D' r_H^{-1}}{s + \gamma^*}$$

where

λE_1 is the instantaneous rate if there was no low frequency component or if turbulence was fine-structured, i.e. no large-scale structures.

If there was no large scale turbulence, D'' would have been zero. Superimposed on the figure is the line ABCD which represents the points on the joint probability distribution

which are contributed by an extreme event. Point A represents the start of a sweep phase in which a high negative vertical wind velocity is coincident with a large vapour pressure deficit

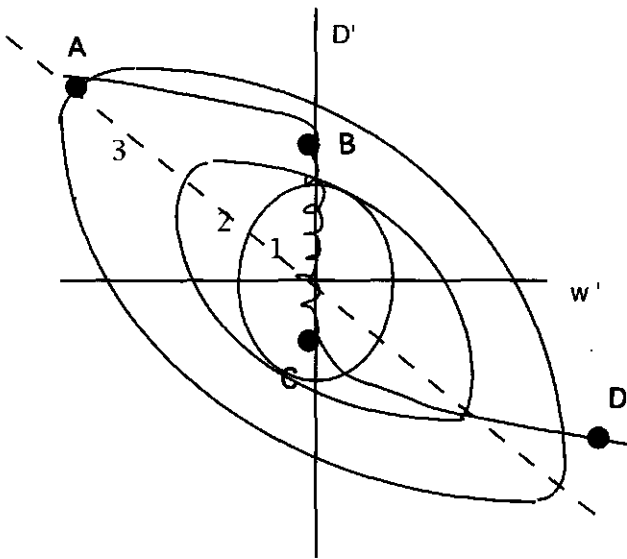


Fig 4.24. Areas in the joint probability distribution of $w'd'$

value. This lasts till point B. We notice there could be very small change in D' value during that period. This is due to the air being actively coupled to the layer of air above in the case of a longer duration sweep, since the leaves can not change the moisture content so rapidly during that stage. After the gust passage, the dry air which has replaced the more humid air has small absolute values of vertical wind velocity, and at the early stages of build up it has high positive values of vapour pressure deficit (high D'' with low absolute W'). With time the air starts humidifying, leading to the movement in time along the twisted line from point B to point C. The twisting in the line is due to small scale mixing within a variable source profile. With the arrival of the following gust, or the passage of the next coherent structure, the air will have humidified (a lower D) and will have a positive W'' (an ejection) and the line moves back to point close to point A.

It is clear that there will be deviation of the source strength due to D'' (a Penman-Monteith result). S' (source deviation) is a linear relation in D' or D'' (the part inside the brackets in eq. 4.3.1). If there is a correlation between w' and D'' depending on the shape of fig 4.24, this correlation will show as correlation in $w's'$. The variation of W'' with D'' is not linear since there are some periods, as we have explained in which D'' is positive and W'' is non existent (after the passage of the coherent structure). But we usually know that the contribution of $W''d''$ to the total saturation heat flux (the integration of $w'd'$) is about 40-50%.

If we assume some form of the joint probability function relating D'' to W'' , S as given by 4.3.1 becomes

$$S = S_1 + S_1 \frac{\rho C_p [-aw'' + \text{random } \sigma_w] r_H^{-1}}{sR_n + \rho C_p D_1 r_H^{-1}} \quad (4.3.2)$$

that leads to

$$S' = S_1 \frac{\rho C_p [-aw'' + \text{random } \sigma_w] r_H^{-1}}{sR_n + \rho C_p D_1 r_H^{-1}} \quad (4.3.3)$$

$$w'S'' = S_1 \frac{\rho C_p [-aw'' + \text{random } \sigma_w] r_H^{-1}}{sR_n + \rho C_p D_1 r_H^{-1}} \quad (4.3.4)$$

The average of this component is not vanishing to zero. In the case of using time steps larger than the scale of the source variations due to D'' or W'', we need to consider the effect of w'D' correlation on the source term which would lead in the end to a correlation between s'w'. This term will affect the mean source profile. It will go into the turbulent flux equation.

$$u_i' \frac{\partial q_i'}{\partial t} + u_i' \bar{U}_j \frac{\partial q_i'}{\partial x_j} + u_i' u_j' \frac{\partial \bar{q}}{\partial x_j} + u_i' u_j' \frac{\partial q_i'}{\partial x_j} = u_i' v_q \frac{\partial^2 q_i'}{\partial x_j^2} + u_i' \frac{\partial (\overline{u_j' q_i'})}{\partial x_j} + u_i' \left\langle \int \int_{S_i} k_c \frac{\partial c}{\partial n} ds \right\rangle \quad (4.3.5)$$

This equation which represents the multiplication of turbulent velocity component with the turbulent scalar equation. This equation is the same as 3.6.11 except for the last term, which represents the correlation between the source variation and u_i variation. This equation is added to equation 4.3.6 to get the turbulent flux equation (eq.4.3.7). This latter will have this term (term XI) which will not vanish to zero. If we assume that the large-time averaged turbulent flux equation is valid, this last term represents the correlation between the sources and the profiles, which we have lost account of due to the intermittency introduced by the existence of coherent structures.

$$\begin{aligned} & q_i' \frac{\partial u_i'}{\partial t} + q_i' \bar{U}_j \frac{\partial u_i'}{\partial x_j} + q_i' u_j' \frac{\partial \bar{U}_i}{\partial x_j} + q_i' u_j' \frac{\partial u_i'}{\partial x_j} \\ & \quad \text{I} \quad \text{II} \quad \text{III} \quad \text{IV}^* \\ & = \delta_{i3} \left(\frac{\theta_v' q_i'}{\theta_v} \right) g + f_c \varepsilon_{ij3} q_i' u_j' - q_i' \left(\frac{1}{\rho} \right) \frac{\partial p'}{\partial x_i} + q_i' v \frac{\partial^2 u_i'}{\partial x_j^2} + q_i' \frac{\partial (\overline{u_j' u_i'})}{\partial x_j} \\ & \quad \text{V}^* \quad \text{VI} \quad \text{VII}^* \quad \text{VIII} \quad \text{IX}^* \end{aligned} \quad (4.3.6)$$

$$\begin{aligned}
& \frac{\partial q' u_j'}{\partial t} + \overline{U_j} \frac{\partial q' u_i'}{\partial x_j} + u_j' u_i' \frac{\partial \overline{q}}{\partial x_j} + q' u_j' \frac{\partial \overline{U_i}}{\partial x_j} + u_j' \frac{\partial q' u_i'}{\partial x_j} \\
& \quad \text{I} \quad \text{II}^* \quad \text{III1}^* \quad \text{III2}^* \quad \text{IV}^* \\
& = \delta_{i3} \left(\frac{\theta_v q'}{\theta_v} \right) g + f_c \varepsilon_{ij3} q' u_j' - q' \left(\frac{1}{\rho} \right) \frac{\partial p'}{\partial x_i} + u_i' v_q \frac{\partial^2 q'}{\partial x_j^2} + q' v \frac{\partial^2 u_i'}{\partial x_j^2} + u_i' \frac{\partial (u_j' q')}{\partial x_j} + q' \frac{\partial (u_i' u_j')}{\partial x_j} \\
& \quad \text{V} \quad \text{VI} \quad \text{VII}^* \quad \text{IX1} \quad \text{IX2} \quad \text{X1} \quad \text{X2} \\
& + u_i' \left\langle \iint_{s_i} k_c \frac{\partial c}{\partial n} ds \right\rangle \quad (4.3.7) \\
& \quad \text{XI}
\end{aligned}$$

This equation is non linear. Averaging this equation, if it is assumed valid (look at appendix 1.a), and assuming stationary, horizontal homogeneity, vertical wind velocity zero, neglecting Coriolis force term and molecular divergence terms, will lead to the disappearance of the first, second, sixth, ninth and tenth terms. The remaining terms will represent a balance between production (III), turbulent transport (IV), buoyancy (V), pressure(VII) and source vertical velocity correlation term. We neglect the effect of buoyancy, assuming that the coupling by the gust process of the canopy air layer to the layer above leaves no time or very little time for thermal stability effects to work. On the other hand, the effect of stability is somewhat included in the gust process since gust frequency is somewhat controlled by stability effects. The term (III1), in the case of assuming horizontal homogeneity, represents a correlation between a vertical wind velocity variance and a vertical gradient in the concentration. The second (III2) is a correlation between a moisture or scalar flux and the mean wind velocity gradient. The gust process also affects the other terms (IV, VII) in the equation, as has been shown on Sect. 3.6.C. The gradient in the turbulent transport term expresses the effect of turbulent transport on moving the flux. The flux in a steady state situation is equal to the mean source and estimating the value of the term in eq.4.3.4 could be used to scale the sources vertical velocity correlation. The coefficient a in eq.4.3.4 represents the time averaged slope of the joint probability distribution of $W'D'$. It has to be a weighed slope of all the points on fig.4.24. This slope is determined by the general climate since it will determine the initial value of D after the gust intrusion (i.e. the extreme values at upper left part of the graph) and the build-up or decrease of the vapour pressure deficit which is allowed to occur (i.e. the lower right part of the graph). The latter will determine the end value and the period of time over which the value of D stays at a certain limit. This slope is not the apparent slope on the joint probability $W'D'$ distribution figure.

In the two examples given below, the values of that slope were determined from a MATHCAD® runs to calculate the end value of vapour pressure deficit for point D. Looking at the values of $D_{air_{nd}}$ at page 143, we get an impression of the values of the change of D' due to gust intrusions. It is about the difference between the first element and the last element in $D_{air_{nd}}$. This gives very close values of the D' and D_{mean} as the ones assumed in eq.4.3.10 and 4.3.9, for the warm arid and cold humid regions. We assumed that the value of points A and D in fig 4.24 were accompanied by -0.3 ms^{-1} at the gust intrusion phase and by $+0.3 \text{ ms}^{-1}$

in the ejection phase. These D_{ind} were obtained from MATHCAD® runs, as has been explained on page 143. This values give a value of the coefficient a in eq.4.3.2 in the order of $-6000 \text{ Pa}\cdot\text{m}^{-1}$. Concerning the random part, which leads to the dispersion of points $W'D'$ around the line, we assumed that it is related mainly to small scale mixing. The coefficient a in eq.4.3.2 is the time mean of the relation between D' and W' , and not the apparent slope on figure 4.25. This time mean is really difficult to obtain since it relates to the build-up. A parcel of air could remain still for a large period of time in which its vapour pressure deficit does not deviate a lot from the one introduced by the gust intrusion. This increases the actual slope determined above, compared to the apparent one.

We do not have direct values for this equation, but there are some measurements which are given in fig.3 of Finnigan 1985, which give some idea of the order of the terms, if we assume about the same ratio between the terms for the latent heat flux equation. In the following scaling, we will compare the value of one of the production terms III1 to the source vertical velocity correlation term. Let assume that the mean latent heat source is 400 Wm^{-2} . This leads to a vapour pressure gradient of about $(400 \cdot 67 / 1200 = 22 \text{ Pa}\cdot\text{m}^{-1})$. Assume a vertical velocity standard deviation of about 0.3 ms^{-1} . This gives a values of about $2 \text{ Pa}\cdot\text{ms}^{-2}$ for the term III1 in eq. 4.3.8. Now, estimating the $W''s''$ term as given equation 4.3.4, assuming the same numbers as given below (eq. 4.3.8) and a leaf area density of $1 \text{ m}^2\text{m}^{-3}$, we get

$$W''s'' = 400 \cdot 1200 (6000 \cdot 0.3 \cdot 0.3 / 50) / (312 \cdot 600 + 1200 \cdot 1600 / 50) = 22.9 \text{ J m}^{-2} \text{ s}^{-2} \quad (4.3.8)$$

This value would equal about $(22.9 \cdot 67 / 1200 = 1.28 \text{ Pa m s}^{-2})$. So, the resulting variation in term XI would be of the same order as term III1.

Solving the averaged equation will yield $\overline{q'u'_i}$ for different layers, the divergence of which will go into the solution of the mean concentration profile (first order). This term will go into a large-time averaged model, if the averaging is assumed valid.

The problem of obtaining a representative average has shown up also in obtaining representative values for the transport coefficients between canopy air layers, and these coefficients obtained within a time resolution larger than the time scale of variations lead to different solution of the temperature and vapour pressure of the air outside the boundary layer of the leaves than the ones obtained with a time resolution smaller than the time scale of variations. If this is case, what is the proper procedure for parameterizing the averaged in time turbulent transport coefficients? We need a separation in scale and ensemble averaging of characteristic periods. This problem has been dealt with in chapter 3.

There is also the effect of the increase of the absolute wind speed observed during the intrusion on the boundary layer resistance. We will neglect that effect, assuming that the sweep duration is not large. That is not always the case. (look at the diagrams where the duration of the gust can last 10-15 seconds).

Let us come to a measured example which shows the effect. The figures are taken from: FAO IRRIGATION AND DRAINAGE PAPER 24: "Crop Water Requirements", page 17.

$$\begin{array}{l} T_{\max} 35 \text{ }^\circ\text{C}, T_{\min} 22 \text{ }^\circ\text{C}, R.H_{\max} 80 \%, R.H_{\min} 30 \%, \\ T_{\text{mean}} \qquad \qquad \qquad \qquad \qquad \qquad \qquad \qquad \qquad 28.5 \text{ }^\circ\text{C} \end{array}$$

es at 35 °C	56.2 mbar
ea at noon time	16.9 mbar
es -ea at noon time	39.3 mbar

e _a at 28.5 °C	38.9 mbar
R _n at noon time	600 W m ⁻²

Let us assume that D mean is half of this value and D'' will be half of the above given value

$$\frac{\rho C_p D'' r_H^{-1}}{s R_n + \rho C_p D_1 r_H^{-1}} = \frac{1200 * 1600 / 50}{312 * 600 + 1200 * 1600 / 50} = 0.17 \quad (4.3.9)$$

In the case of Dutch conditions (Goudriaan 1977, p.175), the net radiation ranged from -84 to 690 W m⁻². The temperature ranged from 13.5 to 20.6 °C, humidity ranged from 11.2 to 15 mbar. We took the values at noontime.

$$\frac{\rho C_p D'' r_H^{-1}}{s R_n + \rho C_p D_1 r_H^{-1}} = \frac{1200 * 500 / 50}{145 * 690 + 1200 * 500 / 50} = 0.107 \quad (4.3.10)$$

The relation between D'' and D₁ depends on the frequency of refreshment and its value and the time constants of the canopy layers. D₁ or D_{mean} is not independent . It will depend on D'' and the period between the passage of two gusts in relation to the time constants of the canopy air layers.

4.4 ASSUMPTIONS USED IN SOLVING THE ENERGY BUDGET FOR THE SOIL LAYERS*

In this section, we will deal with the solution of system of eq.4.2.72 and eq.4.2.75 for the soil part, as has been done in the numerical model. Since the air in the soil pores is almost saturated, depending on the soil water moisture potential, the solution of the soil temperature equation and the soil moisture potential gives directly the soil air vapour pressure. The divergence of water vapour flux accompanied by phase transformations (or the divergence of liquid water movement within a soil which has a thermal gradient) can lead to extra heat transport. Water vapour pressure gradient and water vapour diffusivity, as affected by air-filled porosity and tortuosity, go into determining the water vapour flux between soil layers. Temperature gradient can lead to moisture flux. So, heat and mass transfer are coupled. Solving for the temperature and moisture content of the soil requires taking account of the coupling.

In here, we will deal with this coupling, the parameterization of the heat and mass fluxes, their conjugate forces, the sinks within soil layers, the forcing at the soil surface due to energy partition, and the conductivity terms or the diffusivity terms for the different fluxes. But first, we will talk about differences between heat and mass transfer within the soil and the canopy air and the resulting consequences of these differences.

In the soil layers, the scale over which the transport mechanisms works is quite small compared with the length scale of the gradients of the state variables. The gradient transport approach is then applicable. Most of the heat transport is done either by conduction through the contact points between the soil particles and the water films forming a meniscus around them, or by convection of water, either in its liquid state or by diffusion of water in its vapour state. The spatial scale of convection is quite small and the time scale for appreciable transport distances is normally quite large compared with the time scale which is needed for equilibrium between the moving liquid and the immersed media, so local thermodynamic equilibrium assumption for the soil layers is valid. A multiphase medium (the soil with its solid particles, liquid and gaseous phases) can be treated as a single continuum. This can be seen from applying eq.4.2.11 and eq.4.2.15 to the soil layers. These equations were derived for the canopy layers, but assuming that $LAD \cdot dz$ for the soil layers is the specific soil surface, multiplied by the soil particles, density multiplied by the soil layer thickness, multiplied by a reduction factor to account for the active area of exchange between the soil particles and the surrounding air, make these equations applicable for the soil part. The boundary layer resistance for heat transfer from the surface of soil particles to the soil air is quite small. Both of these make the time constant very small. The K_{top} and K_{bottom} here are considered as the conductive heat transport coefficients, as determined from the De Vries model (1963, 1975). In applying this heat equation (4.2.12) for the soil layers, there is no coupling between heat and mass. The coupling comes from the solution of water vapour transport equation and the soil water transport equation. Water vapour transport depends on the vapour pressure gradient. The conductivity terms in this equation are the water vapour diffusivity coefficients. With water convective flux between different layers, the effect of turbulent fluctuation of heat and scalar within the water (what is called dispersive flux) is quite small and we can assume that the flux happens only due to convection by water in its liquid state. Convective heat flux by liquid water stream, in non isothermal soil, is very minor with respect to water vapour flux divergence (Berge 1990).

In the canopy air space, the spatial scale over which the turbulent transport works is quite large compared with the canopy scale, the local thermodynamic equilibrium approach is not strictly applicable. During the period of large active scale motion, this assumption is gone and the leaves will have no time to respond to the rapidly varying temperature and vapour pressure of the air, but to the final arrangement of these layers after the large scale motion has reshuffled the vertical arrangement of the air inside the canopy. The existence of temperature difference between the immersed surface (i.e. the leaves) and the air, which is large compared to the total temperature difference between the system boundaries, makes a multiphase media treatment a necessity to take account of the interfacial heat and mass transfer between the leaf and the surrounding air. So, an equation for the leaf energy budget is required. In the case of the soil, no such equation is required for the solid phase of the soil. But a specification of the heat flux at the surface of the soil and the sources within the soil layers is needed. The sources could be considered as the water phase transformation due to water vapour flux divergence. What is required here is water vapour diffusivity as determined by air-filled porosity and tortuosity, which is a function of the soil moisture content.

4.4.1 THE GOVERNING EQUATIONS

For the heat and mass transfer within soil, there are two available approaches. One is based on the thermodynamics of irreversible processes (Taylor and Cary, 1964; Cary, 1965; Weeks *et al.*, 1968; Bolt and Groenvelt, 1972) and the other approach is a mechanistic one (Krischer and Rohnalter, 1940; Philip and De Vries, 1957) which is based on the hydrodynamics and heat conduction.

We follow the first one. From the study of entropy production due to irreversible processes occurring within a system, it is possible to specify the flows and their conjugate forces such that Onsager reciprocal relationships (1931) of the phenomenological equations coefficients are satisfied, i.e.

$$L_{kj} = L_{jk} \quad (4.4.1)$$

The flux of a certain entity is

$$J_i = \sum_{k=1}^n L_{ik} X_k \quad (4.4.2)$$

where X_k is the conjugate force which produces the i th flow and L_{ij} is the direct coefficient which relates the flux to the driving force X_i . The other L_{jk} 's relate the different forces (X_k) to a flux j .

For coupled heat and water transport, the system of equations is

$$J_w = L_{ww} X_w + L_{wT} X_T \quad (4.4.3)$$

$$J_T = L_{Tt} X_T + L_{Tw} X_w \quad (4.4.4)$$

$$L_{wT} = L_{Tw} \quad (4.4.5)$$

The first term on the right hand side of eq.4.4.3 is the Darcy Buckingham equation and the following term accounts for the additional contribution to water flow due to the temperature gradient.

The entropy production term multiplied by temperature, which was called the dissipation function by Rayleigh, equals (Katchalsky and Curran, 1965).

$$T \sigma = J_s \cdot \text{grad} (-T) + \sum_{i=1}^n J_i \cdot \text{grad} (-\mu_i) \quad (4.4.6)$$

where J_s is the entropy flux, J_i is the mass flux of species i . In here, we will follow the approach given by Berge (1990) in scaling the different terms within the flux equation as determined from the entropy divergence term eq. 4.4.7

$$J_q = T J_s + \sum_i \mu_{w_i} J_{w_i} \quad (4.4.7)$$

where J_q is heat flux and J_{w_i} are the different mass fluxes of water in its different states i and μ_{w_i} is the chemical potential of the state.

Berge (1990) started with eq.4.4.7 and ended up with eq.4.4.8

$$C \frac{\partial T}{\partial t} = - \frac{\partial}{\partial z} (- \lambda \frac{\partial T}{\partial z} - J_v \Delta H_v) \quad (4.4.8)$$

$$\rho C_p \frac{\partial T}{\partial t} = - \frac{\partial q_h}{\partial z} + s_h \quad (4.4.9)$$

$$\frac{\rho C_p}{\gamma} \frac{\partial e}{\partial t} = - \frac{\partial q_{le}}{\partial z} + s_{le} \quad (4.4.10)$$

where C is the volumetric heat capacity of the soil in $J m^{-3} K^{-1}$ at time t . The first term within brackets on the right hand side of eq.4.4.8 expresses the conductive soil heat flux and the second one is the divergence of the water vapour flux multiplied by latent heat of vapourization which then expresses the contribution of latent heat flux divergence to the heat equation and which could be considered as an extra heat source in the heat flux equation within soil layers (4.4.9). Equation 4.4.10 is solved implicitly from the solution of eq.4.4.9 and the solution of the soil water potential model as explained in 4.5. The calculated water vapour pressure and the use of a tortuosity model as given by Millington and Quirk (1961) allows the calculation of water vapour flux divergence which goes as an extra sink, in addition to water uptake by plant roots, in the water transport equation

The coefficients λ for heat conductivity between different soil layers were determined by the use of the textural composition and the moisture content of the soil at the beginning of each time step by the use of De Vries model. (1963, 1975). The value of ρC_{soil} was determined by the knowledge of the soil composition and the initial moisture content (at the beginning of the time step), according to eq. 4.4.11.

$$C_s = f_q C_q + f_c C_c + f_o C_o + \theta C_w + f_a C_a \quad (4.4.11)$$

The sensible heat flux equation is discretized equation according to Patanker (1980), as shown in the appendix (A.2.11) with the source linearization as a function of the soil water potential and temperature

$$r.h = \exp\left(\frac{\psi M}{RT}\right) \quad (4.4.12)$$

where r.h. is the relative humidity of the soil air.

The whole set of equations for the canopy and soil was solved as a single matrix, i.e. system eq.4.2.72 and eq.4.2.76, with taking account for the different conductivity and capacitance terms for the soil and the air.

The decoupling of the energy budget equation at soil surface is required to consider the feedback, as has been explained in sect.4.1 between the canopy layer and the soil.

4.4.2 DEFINING THE ENERGY FORCING ON THE SOIL SURFACE

To define the forcing at the soil surface, a decoupling procedure for the sensible and latent heat flux at the soil surface was used. For the soil surface (layer number 0), an extra source goes into the heat equation (eq.4.4.9) due to radiation fluxes

$$S_h = R_s \downarrow - R_s \uparrow + R_L \downarrow - R_L \uparrow - \frac{\rho C_p}{\gamma} (e_{soil,1}^{t+\Delta t} - e_{soil,1}^t) \frac{\Delta z}{\Delta t} \theta_{air \text{ filled}} + \frac{\rho C_p}{\gamma} \frac{D_{vapour}}{\Delta z} (e_{soil,2} - e_{soil,1}) - \frac{\rho C_p}{\gamma} \frac{(e_{soil,1}^t - e_1^t)}{r_{b,v} + r_{ss,soil}} \quad (4.4.13)$$

where R_s and R_L are the short and long wave radiation flux densities respectively. The arrows indicate upward and downward directions. The subscript indicate short and long wave. The short wave fluxes are independent from the solution. The long wave radiation fluxes have very weak dependency. The sensitivity of the long wave emission to ΔT is quite small about $6 \text{ Wm}^{-2}\text{K}^{-1}$ at $20 \text{ }^\circ\text{C}$ ($4\epsilon\sigma T_{soil,abs}^3$). So, an initial soil surface temperature could be used to calculate the total R_n value for the soil (the sum of the first four terms). The radiation fluxes have been evaluated from the theory in chapter 2. The fifth term is the change in the soil temperature due to the change in vapour pressure within the soil air. The sixth term represents the water vapour flux from the soil layer below to the first soil layer, while the last term in eq. 4.4.13 stands for the latent heat flux from the soil to the canopy air space. This last term goes as an extra source term into the equations of the latent heat flux of the first air layer. It was added to the discretized equation of layer 1 (the first air layer). The value of latent heat flux from the soil surface was also used as an upper flux boundary condition for the system of equations describing liquid water flow through the soil.

To estimate this value, an iterative procedure was followed, in which an initial estimate was made depending on the vapour pressure of the soil, the vapour pressure of the first air layer, the soil resistance to evaporation and the soil boundary layer resistance.

In the model, the effect of soil dryness on the soil surface resistance was included as explained in section 4.6. The value of the lower boundary transport coefficient for layer 1 equals

$$\rho C_p \frac{K_{bottom}}{dz_{bottom}} = \frac{\rho C_p}{r_{b,h}} \quad (4.4.14)$$

where $r_{b,h}$ is determined from the average wind velocity in the first air layer and using a characteristic dimension of the soil clods as a characteristic dimension of the soil surface. The same approach of using the definition of Nusselt number in defining the resistance terms for heat transfer from the leaves was used here. The values of $r_{b,h}$ is explicitly defined.

The soil and air temperature equations are solved first, using the initial estimate of the decoupling for sensible and latent heat flux at the soil surface according to expression 4.4.25. If the solution of the vapour pressure of the first air layer proves to need a correction, as will be explained below, a new estimate of the decoupling is done which is used to calculate a new value of soil heat flux which goes as an extra sink into the first soil layer equation eq.4.4.13.

A problem which shows here is the different time constants or heat and vapour capacities of the different media constituting the domain of our simulated system. Let us assume that a parcel of dry air comes in contact with a wet soil. If the soil has a low surface resistance, the soil will respond to this contact by delivering a high amount of latent heat flux. If the total amount of delivery is calculated from the initial estimate, the total latent heat flux to the first air layer could exceed the capacity of the first air layer. This capacity is represented by this layer not having a vapour pressure higher than the saturated vapour pressure of the air at the temperature of this layer. In real life, integration is done instantaneously, and there will be a feedback from the build-up of the vapour pressure in the first air layer on the latent heat flux from the soil surface to this layer. To follow this process, we need either to reduce our time step of simulation, or to find a way to have a numerical feedback in our solution and to obtain an integrated value for the latent heat flux from the first soil layer to the first air layer. The source of the problem for the soil layer is that the soil has very high thermal inertia, which is represented by the $\rho C_{soil} \Delta z$ of the first soil layer. This inertia term represents a large amount of energy, which exceeds by large the net radiation at the soil surface. A decrease of a fraction of a degree K in the temperature of first soil layer ΔT can lead to an energy supply, which exceeds the total net radiation at the soil surface. The sensitivity of the sensible heat flux to this temperature difference between the first soil and air layers is quite small. On the contrary, a small change in the temperature of the first soil layer Δt is equivalent to high amount of latent heat release from the first soil layer to the first air layer. The time constant of the first soil layer is very large and we have a problem of two neighbouring elements with very disparate time constants.

The first air layer **

To take account of the feedback, we use the latent heat flux equations for the first air layer.

$$\frac{\rho C_p \partial e_1}{\gamma \partial t} = - \frac{\partial q_e}{\partial z} + S_{e,v} \quad (4.4.15)$$

where q_e represents the latent heat flux and $S_{e,v}$ represents the latent heat sources in $W m^{-3}$

$$\Delta Z_1 \frac{\rho C_p}{\gamma} \frac{\partial e_1}{\partial t} = - (q_1 - q_0) + S_{e,v} \Delta Z_1 \quad (4.4.16)$$

where ΔZ_1 is the thickness of the first air layer in m. The latent heat flux at the upper boundary of layer 1; q_1 is

$$q_1 = - \frac{\rho C_p}{\gamma} \frac{K_{top}}{dz_{top}} (e_1 - e_2) \quad (4.4.17)$$

and the latent heat flux from the soil to the first air layer; q_0 is :

$$q_0 = \frac{\rho C_p}{\gamma (r_{b,v} + r_{s,soil})} (e_{soil} - e_1) \quad (4.4.18)$$

Rearranging leads to :

$$\Delta Z_1 \frac{\rho C_p}{\gamma} \frac{\partial e_1}{\partial t} = - \left(\frac{\rho C_p}{\gamma} \frac{K_{top}}{dz_{top}} + \frac{\rho C_p}{\gamma (r_{b,v} + r_{s,soil})} \right) e_1 + \frac{\rho C_p}{\gamma} \frac{K_{top}}{dz_{top}} e_2 + \frac{\rho C_p}{\gamma (r_{b,v} + r_{s,soil})} e_{soil} + S_{e,v} \Delta Z_1 \quad (4.4.19)$$

let

$$k = \left(\frac{\rho C_p}{\gamma} \frac{K_{top}}{dz_{top}} + \frac{\rho C_p}{\gamma (r_{b,v} + r_{s,soil})} \right) \quad (4.4.20)$$

and

$$e_{air,eqli,1} = \left(\frac{1}{k} \frac{\rho C_p}{\gamma} \frac{K_{top}}{dz_{top}} e_2 + \frac{1}{k} \frac{\rho C_p}{\gamma (r_{b,v} + r_{s,soil})} e_0 + \frac{S_{e,v} \Delta Z_1}{k} \right) \quad (4.4.21)$$

Then, the equations take the form:

$$\frac{\partial e_1}{\partial t} = \frac{k\gamma}{\rho C_p \Delta Z_1} (e_{air,eqli,1} - e_1) \quad (4.4.22)$$

which has the well-known solution

$$e_1 = e_{air,eqli,1} (1 - \exp \frac{t}{\tau}) + e_{initial,1} \exp \frac{t}{\tau} \quad (4.4.23)$$

where

$$\frac{1}{\tau} = \frac{k\gamma}{\rho C_p \Delta Z_1} \quad (4.4.24)$$

and, τ is the time constant of the layer. Notice the little dependence of $e_{\text{air},l,\text{eq},1}$ on the solution. The first and last term have a feedback from the solution.

From this, an account of the effect of the water vapour accumulation on the latent heat flux from the soil is done through the calculation of the time constant of the first air layer and the ratio of the time step of simulation to this time constant. The magnitude of this ratio, $\Delta t/\tau_{\text{first air layer}}$, will determine whether an asymptotic solution ($e_{\text{air},l,\text{eq},1}$) will be achieved. If $\Delta t/\tau_{\text{first air layer}} \geq 3$, the initial state of the water vapour would have a negligible effect on the water vapour concentration at $t+\Delta t$. The capacity of the layer could be used to determine the integrated value of latent heat flux from the first soil layer to the first air layer. An asymptotic flux will be approached, in which the flux from the first soil layer is equal to the turbulent flux between the first air layer and the second air layer, after deducting for the contribution of the leaves within the first air layer to this flux and to the water vapour content within the first air layer. In case of ($\Delta t/\tau_{\text{first air layer}} < 0.1$) we assume there would be no problem of a feedback which is numerically ignored, and using an initial estimation of the latent heat flux from the soil surface to the first air layer would offer no problems. In cases of ($3 > \Delta t/\tau_{\text{first air layer}} > 0.1$), a numerical integration within a time step of $0.1 \Delta t$ of the latent heat flux from the soil to the first air layer is carried out, assuming very little dependence of the integrated contribution on the water vapour concentration of the second air layer. The correctness of this assumption can be checked by the time constant of the second air layer, which is usually much larger than the time constant of the first air layer. An iterative method has been used to find the correct contribution, since the value of $e_{\text{air},l,\text{eq},1}$ has little dependency on the solution. This approach is used for the uncoupling of the sensible and latent heat flux at the soil surface. The evaluated latent heat flux goes as an extra source for the canopy first air layer and as a sink in the heat equation of the first soil layer. It is equated after being divided by the length of the time step to:

$$\frac{\rho C_p (e_{\text{soil},1} - e_1^s)}{\gamma (r_{b,v} + r_{ss,\text{soil}})} \quad (4.4.25)$$

in equation (4.4.13).

A question which arises here is the correct choice of thickness for the first air layer and the frequency of refreshment. Both of these parameters will determine the total integrated latent heat flux from the first soil layer to the first air layer.

The thickness of the first air layer will be equal to the displacement boundary layer thickness. This boundary layer has been estimated according to Monteith and Unsworth (1990). It equals

$$\delta/l = 5 (\text{Re})^{-0.5}$$

This boundary layer thickness has a value of about 1 cm, assuming a wind velocity close to the soil of about 0.25 ms^{-1} and characteristic dimension of the soil clods of 0.05 m.

The sensitivity of the integrated latent heat flux from the soil to the air needed to saturate the first air layer is not high. It can be checked by calculating the amount of latent heat required to saturate that air layer. Assuming a vapour pressure deficit of 2000 Pa for the air which comes in contact with the soil, and no temperature difference between the soil and the air, the latent heat flux from the soil to the air required to saturate that air layer is $1200/67 \cdot 2000 \cdot 0.01$. That represents an amount of latent heat extra, averaged over 90 s, of about 4 Wm^{-2} . So, if we overestimate twice the frequency from once every 90 s to twice every 90 s, this is the error we get. So, a rather careful assumption of the gust intrusion rate is enough. It does not have to be very accurate. The most dangerous effect on the calculation comes though an error in the refreshment of the air within the lower part of the canopy, the turbulent transport coefficients there and the resistance of the system to latent heat flux and the effect of all of these on the mean vapour pressure deficit of the first air layer (excluding this displacement boundary layer) as has been explained by the run of MATHCAD®.

4.5 CALCULATING THE LIQUID WATER FLUX THROUGH SOIL LAYERS*

The value of the latent heat flux from the first soil layer to the first air layer, as calculated from 4.4, is used as an upper flux boundary condition in a system of equations describing liquid water transport through the soil. Our starting point is always replacing the continuity equation of the species under consideration to the general transport equation. We then discretize and define our conductivity and source or sink terms. The sink term for water uptake by plant roots from different soil layers will be determined in the next section. The extra source term which results from a negative value for vapour flux divergence is calculated explicitly from the soil temperature and soil water potential profiles and from a tortuosity model according to Millington and Quirk (1961). The conductivity terms for liquid water flux between different soil layers are calculated explicitly and modelled by the use of Van Genuchten model (1980) as given by eq.4.5.1, or by the use of fitted function for the measured values $K(h_m)$ and $h_m(\theta)$.

$$K(\theta) = K_s S^{1/2} (1 - (1 - S^{1/m})^m)^2 \quad (4.5.1)$$

$$h_m = -\frac{1}{\alpha} (S^{1/m} - 1)^{1/n} \quad (4.5.2)$$

where

$$S = \frac{\theta - \theta_r}{\theta_s - \theta_r} \quad (4.5.3)$$

The water general transport equation which was solved is the following.

$$\frac{\partial \theta}{\partial t} = \frac{\partial}{\partial z} \left(K(\psi) \frac{\partial \psi}{\partial z} \right) + S_w \quad (4.5.4)$$

where ψ is the soil water moisture potential and $K(\psi)$ is the soil hydraulic conductivity as a function of ψ . The determination of the divergence of the water flux and water uptake was used to calculate the new moisture content from the initial one, to avoid numerical incompatibilities between the results obtained from different approaches used in the calculation due to the numerical precision.

4.5.2 QUANTIFICATION OF THE SINK TERM FOR H₂O WITH DIFFERENT SOIL LAYERS*

The plants as autotrophic organisms need to intercept solar energy, and trap this radiative energy into chemical energy by transforming H₂O and CO₂ to energy-rich compounds. The plant leaves with large specific surface area, m² kg⁻¹ and coloured pigments allow the plants to intercept the required radiant energy. The anatomical features of the leaves allow the plants to exchange CO₂ and O₂ with the surrounding environment. These anatomical features (the existence of stomata) let the plants lose water vapour through the stomata, allowing the plants in the process to get rid of a fractional part of their radiation load. The lost amount of water from the plant leaves has to be replaced, otherwise the leaf water potential would drop to lower values causing an undesirable water stress on the plant metabolic processes. The amount of energy or water which is used in the photosynthesis process is quite negligible compared to the total amount of energy absorbed, or to the amount of water transpired to the surrounding environment.

When the evaporative demand by the atmosphere or the evacuation of the latent heat, delivered by the plants into the inter-canopy air stream, to the atmosphere above is quite high and the soil and water movement through the soil-plant continuum is not a limiting factor, in the sense that the plants manage to meet this demand under reasonable leaf water potentials and reasonable leaf temperatures, there would be no problem. But once these leaf water potentials and leaf water status become limiting, due to too high water potential drop between the soil and the leaves, the plants would have to respond by increasing their stomatal resistance as a valve to maintain reasonable turgor pressure, and at the same time they must have a reasonable partition between sensible and latent heat (meaning reasonable leaf temperatures) and maintain a reasonable flux of CO₂ into the leaves. High drop in water potential between the soil and the leaves could be due to high flux density or high resistances, either in the plant or mostly due to the development of high resistances in the soil within the advanced stages of drying. The ability of the plant to interact with the radiation field in which it exists, and the resulting radiation load and the partition of this radiation in a way which is life sustainable, depends on the environmental conditions lying within the domain of existence of these plants.

The ability of the plants to modify the environment in which they exist is limited and is affected by the environmental conditions themselves. The survival of the plants or their well-being depends on the final resulting solution for this feed and feed-back mechanism and if this solution lies within the domain of existence of plants.

In this thesis, concerning the modelling of water movement within plants, we assumed the validity of the cohesion theory for explaining water ascent in plants, in spite of some arguments introduced to the invalidity to this theory by Zimmerman *et al.* (1993). His

measurement of water pressures in the xylem do not agree with the cohesion theory. Following this theory, water pressures which is much less than atmospheric will develop in the xylem vessels. This will lead to cavitation and embolism. Several explanation were given for the maintenance of water columns under negative water pressures which are below atmospheric pressure (Pickard, 1980). Zimmerman *et al* (1993) argues for several other mechanisms, which could be responsible for water ascent in plants without the need for very low negative pressure values as predicted by cohesion theory. These mechanisms include osmotic forces, capillary forces and the development of gradients in interfacial forces along gas-liquid interfaces of a necklace of tiny air bubbles adhering to the inner wall of a capillary and water. These gradients result due to the existence of solute or temperature gradients. This is called *marangoni* convection. The required occurrence of air bubbles in the xylem vessels seems in contradiction, but he argues that the occurrence of moderate cavitation in the xylem elements lead to the introduction of these air bubbles and that it could a strategy by the plant for survival under moderate cavitation. I wonder if the measurement by a xylem pressure probe as shown in fig. 5 of his paper does not lead to the leakage of air along the region of contact between the measuring microcapillary and the plant tissues to the xylem vessel. This would prevent the development of very low negative tensions, even if it was developing otherwise, due to the intrusive nature of the measurement. There is a recent study (Pockman *et al* . 1995) showing that xylem conduits remained water-filled and conductive to species-specific values ranging from -1.2 to below -3.5 MPa. Kramer and Boyer (1995) state that the main difficulty is that the pressure probe must penetrate the xylem water column while it is under tension, which may disrupt the tension. Thus, there probably are as many errors in measurements with pressure probe as with the pressure chamber (Scholander *et al* 1964).

Our starting point is the conservation equation for water within plant water transporting tissues (the xylem elements). Conservation of water , assumed incompressible, requires that the rate of change of a cell volume must equal the difference between the inflow rate and the outflow rate.

$$\frac{\partial V}{\partial t} = A (-\nabla \cdot q_w) + S_w \tag{4.5.5}$$

where V is the volume change of water the due to water flux divergence. q_w is the water flux density in ms^{-1} . S_w are the water sources or sinks in the plant tissue, expressed in $m^3 s^{-1}$.

$$q_w = -K \frac{\partial \Psi}{\partial z} \tag{4.5.6}$$

K_w is the hydraulic conductance with the plant tissue in $m^2 s^{-1} MPa^{-1}$. Ψ is the total water potential which is the sum of the gravitational, metric and osmotic component potential in MPa.

To relate this equation to the total water potential, this equation can be expressed (Molz and Ferrier, 1980) as

$$\frac{\partial V}{\partial \psi} \frac{\partial \psi}{\partial t} = A K \frac{\partial^2 \psi}{\partial x^2} + S_w \quad (4.5.7)$$

$$\frac{\partial V}{\partial \psi} \approx \frac{V_0}{\xi + \Pi} \quad (4.5.8)$$

The modulus of elasticity ξ will determine the reduction in the cross-section of the conducting xylem element due to water tension. With progression of negative water potential, embolism will occur, that will introduce relief of the tension but will reduce the conductance of the tissue. Π is the osmotic pressure of the water in the xylem in MPa. S_w are water sources or sinks within the tissue. Since we are solving a one dimensional flow equation, so, we consider lateral water flow to the storage tissue or the lateral branches as a sink or a source.

The previous equations are describing water flow through an area with no change in the cross section (the number of xylem elements multiplied by the an average area for each xylem element). In the case of following the water movement through an appreciable length of the plant, the number of the xylem elements reduces with height due to xylem elements branching into the plant lateral branches. The area will be given by.

$$A = \Pi r^2 n \quad (4.5.9)$$

We will assume a rate of decline with height for the area available to water transport proportional with the decline of the leaf area with height. There is another source for decline of the xylem available for water movement. This occurs mainly due to the shrinkage in the cross sectional area for the xylem elements due to high water negative potential which exceeds the negative pressure required to withdraw air through the intervessel pit membranes or through the wall pores (Zimmermann, 1983). This leads to the introduction of air bubbles to the system and embolism or cavitation. That effect will be included in the definition of K (the hydraulic conductance in $m^2 s^{-1} MPA^{-1}$). So, K will be a function of ψ depending on the water potential within the xylem.

The resulting equation would read for a certain segment of a plant stem as :

$$\frac{1}{\xi + \pi} A_i \frac{\Delta z}{\Delta t} (\psi_i^{t+dt} - \psi_i^t) = \frac{K_{top}}{\delta z_{top}} (\psi_{i+1}^{t+dt} - \psi_i^{t+dt}) - \frac{K_{bottom}}{\delta z_{bottom}} (\psi_i^{t+dt} - \psi_{i-1}^{t+dt}) + \left[\frac{\psi_L^t - \psi_i^{t+dt}}{R_L} \right] \left[\frac{\psi_i^{t+dt} - \psi_s^t}{R_S} \right] \quad (4.5.10)$$

where the last two terms express the exchange of water between the a lateral branch and the storage tissue within the plant respectively. The R_L express the resistance to water flow between the lateral and the xylem elements of the main stem through the petiole (petiole resistance). The R_S express the resistance for water flow between the xylem elements and the

surrounding storage elements in the same segment. We have used the values of the water potential of the storage tissue at time step t (explicit) since we assumed that during Δt , which is 15 seconds, it would not change to affect the solution. The values of the water potential of the lateral were assumed also at the beginning of the time step.

For the lateral branches, the same equation was assumed. For the first node of the lateral branch, the water exchange with the main branch was included, while for the other nodes, a sink term was included through the calculation of transpiration from the leaf surface attached to that node. The amount of transpiration is calculated from the partition of energy on the leaf surface (chapter 2).

The calculation of the water potential in the points of the lateral branching is done iteratively by calculating the value of the ψ at the points of branching assuming a certain potential of the first node in the lateral. Once a value of ψ in the main stem is determined, this is used with the latent heat flux at lateral to determine the water potential at the different nodes. The potential at the first node is thus determined, which is used again to calculate a new ψ for the point of branching on the main stem. This whole process is repeated till the whole solution converges.

For the underground part, we assumed no storage tissue for water, the fourth term in the right hand side of eq. 4.5.10 is then assumed zero. For the exchange of water between the root tissue and the soil, we replace the value of R_L (lateral resistance) in the right-hand side by a total resistance for water transport between the soil outside the draw down region (in the middle region between two roots) and the root. This total resistance is the series sum of three resistances: a root resistance, a soil resistance and a contact resistance. The root resistance was calculated from a root area distribution, which is assumed exponential in depth according to eq. 4.5.11, by multiplying it with a total root density. From the root area in every soil layer and a specific conductance for the root tissue for the species under consideration (Glinski and Lipiec, 1990 and Gerwitz and Page. 1974), we calculated a root resistance. In the model here, we assumed that the total area of the root surface area is an effective area for water uptake.

$$P(i) = e^{-f|z|} \cdot e^{-f|z(i-1)|} \tag{4.5.11}$$

The soil resistance is dependent of the distribution of the root in the soil volume and is calculated according to Gardner (1960) by assuming a uniform distribution of the root area in every soil layer.

$$R_{soil} = \frac{1}{4 \pi K(\theta) L_a} \ln(d^2/r^2) \tag{4.5.12}$$

The contact resistance is a resistance due to the development of air pockets between the root and the soil. With the advanced stages of drying, these air pockets reduce the contact area between the root surface and the soil. This resistance plays a role in decoupling or reducing the hydraulic coupling between the root and the very dry soil layers. In this case so far, it was assumed zero, but it could be implemented by reducing the contact region between the soil particles and the root by a fraction which equals the air filled porosity, and so also increasing the draw-down curve around the effective regions of water uptake. This is equivalent to

increasing the root resistance and soil resistance by multiplying both by (1- air filled porosity).

Water uptake from different soil layers is calculated by the use of the calculated difference of water potential at root surface and the soil and the total soil resistance according to

$$S = - (\Psi_{\text{soil}} - \Psi_{\text{root}}) / (r_{\text{root}} + r_{\text{contact}} + r_{\text{root}}) \quad (4.5.13)$$

This goes as a sink term into eq.4.5.4. The water potential at the root surface is used also to calculate the production rate of abscisic acid (ABA), which is used as a signal for soil dryness detected by the guard cells which control the stomatal aperture.

4.5.3 THE STOMATAL RESISTANCE OF WATER STRESSED PLANTS

In this part, we will use the approach suggested by Tardieu and Davies (1993) to parameterize the effect of the water stress on plant stomatal resistance.

We can summarize this approach as follows: the effect of the soil dryness on the stomatal resistance of maize is mediated through the production of abscisic acid in the root which is transported through the transpiration stream in the xylem vessels to the leaves. The sensitivity of the leaf response to the abscisic signal is dependent on the leaf water potential. The concentration of abscisic acid in the xylem vessels is dependent on the production rate of abscisic acid, which is soil moisture potential dependent, to the water flux density from the root to the shoot as given by eq.4.5.14. The importance of the abscisic acid (ABA) concentration in comparison to its flux (concentration · water flux density to the leaf) is difficult to answer, due to the complex pattern of ABA distribution in apoplast and to the factors that control membrane permeability (i.e. pH). There is a lot of evidence for the role of ABA in stomatal control in maize (Tardieu *et al.*, 1993). The success of Tardieu and Davies in using the concentration signal is not to say that the role of other factors (e.g. cytokinin, pH and mineral status) is not important, but that role of ABA is central. The importance of the concentration signal versus the quantity is discussed by Gowing *et al.* (1993). Anyhow, the response functions as suggested by Tardieu (1993) for maize are as follows.

$$[ABA] = J_{ABA} / (J_w + b) = (a \Psi_r) / (J_w + b) \quad (4.5.14)$$

$$g_s = g_{s,\text{min}} + \alpha \exp \left\{ [ABA] \beta \exp(\delta \Psi_l) \right\} \quad (4.5.15)$$

The values used for these parameters in eqs. 4.5.14 and 4.5.15 are given within the subroutine **PLANT** and **RESIS**, respectively. In the model, we used a multiplicative effect of absorbed light and dryness of the soil.

4.6 THE COUPLING BETWEEN HEAT AND WATER TRANSPORT, GAS FLUX AND SOIL RESISTANCE TO VAPOUR FLUX UNDER DRYING CONDITIONS

We now come to the question of defining the soil surface resistance to evaporation as defined or needed in eq.4.4.13. Here, we used a tortuosity model as suggested by Millington and Quirk (1961).

Concerning the effect of the air filled porosity on the diffusivity for water vapour, the water vapour flux equation was expressed in an energy flux form

$$J_v = - \frac{\rho C_p}{\gamma} \beta D_g \varepsilon_g \frac{\partial e(\psi, T)}{\partial z} \quad (4.5.16)$$

where J_v is the vapour flux in $J m^{-2} s^{-1}$, and β is an enhancement factor. In here, we will assume it equal to 1. For more details, see Berge (1990). D_g is the water vapour molecular diffusivity in free air. $e(\psi, T)$ is the water vapour pressure as a function of the soil water potential and soil temperature. ε_g is the tortuosity. Tortuosity tries to take account for the effects which lead to a reduction of the diffusivity from its free air value to the its actual value in the soil. This reduction comes due to two reasons: the actual area available for diffusion of water vapour from one location to the other isn't the same as the apparent area (the total cross sectional area), and the actual length of path which the water vapour molecules have to follow in its travel from one point to the other is longer than the apparent distance between two points. These two effects lead to a reduction of the vapour diffusivity from its free value. Tortuosity depends on soil structure, total porosity and air filled porosity. All of these affect the three-dimensional structure or configuration of the void space and its continuity. In her, we will use a model for tortuosity, Millington and Quirk (1961), to obtain a value for the soil surface resistance to evaporation.

$$J_v = - \frac{\rho C_p}{\gamma} \beta D_g A_a \frac{A_e \Delta z}{A_a \Delta l} \frac{\partial e(\psi, T)}{\partial z} \quad (4.5.17)$$

where

A_a is the apparent area available for diffusion (the whole cross-sectional area). since we are working with fluxes for unit area, A_a equals unity. All the other areas are fraction of this unit area. A_e is the actual or effective area available for diffusion. This latter could be made equal to

$$A_e = A_{porosity} \frac{A_{air\ filled}}{A_{porosity}} \quad (4.5.18)$$

where

$A_{porosity}$ is the total porosity in a cross-section perpendicular to the direction of the flux. We assume this equal to the total porosity (a uniform projection of total porosity from three dimension to two dimension). $A_{air\ filled}$ is the air-filled porosity in a cross-sectional area. This could be also be assumed equal to air-filled porosity.

According to Millington and Quirk (1961), tortuosity as a function of porosity and air filled porosity equals

$$\xi_g = a^{10/3} / \varphi^2 \quad (4.5.19)$$

where a is the air filled porosity and φ is the total porosity. Equating eqs.4.5.16 and 4.5.17, leads to

$$\xi_g = a^{10/3} / \varphi^2 = A_{\text{porosity}} \frac{A_{\text{air filled}} \Delta z}{A_{\text{porosity}} \Delta L} \quad (4.5.20)$$

and using the approximation of $A_{\text{air filled}}$ and A_{porosity} being equal to a and φ respectively. This gives us

$$\frac{\Delta z}{\Delta L} = a^{7/3} / \varphi^2 \quad (4.5.21)$$

This function gives the ratio between the apparent length of the path between two nodes in the soil column and the actual length which the water vapour travels between the two nodes. In case of complete dryness of the soil, the air filled porosity equals the total porosity. So, the above given ratio on the right hand side of eq.4.5.21 should equal one. Thus, we reduced exponent from 7/3 to 6/3.

For soil layers lower than the first soil layer this equation tells that, when the air filled porosity becomes equal to zero, the $\frac{\Delta z}{\Delta L}$ goes to zero. That, we would expect for the water vapour diffusion path within the soil volume. But for the top soil layer, the water films surrounding soil particles would be filling all the soil pores and the water film would not be withdrawn into the soil pores. Water vapour would be travelling a distance of zero with respect to the thickness of the first soil layer. We expect then that $\frac{\Delta z}{\Delta L}$ goes to infinity. Since the measured distance between the centre of the first soil layer and the soil top would be overestimating the distance of diffusion which is from the soil surface to the soil surface (0.0), so, the above given ratio goes to infinity. So for the soil surface resistance we took the inverse of eq.4.5.21 as an estimate for the ratio between the actual length travelled and the measured length. In the case of completely dry soil, that ratio goes to one.

To cast this length into a resistance, we used the following equation.

$$r_{s,\text{soil}} = dz(0) a^{6/3} / (\varphi^2 D_g) \quad (4.5.22)$$

This $r_{s,\text{soil}}$ goes in determining the convective latent heat transfer coefficient between the soil and the first air layer which is given as $Ht_e = \frac{\rho C_p}{\gamma (r_{b,v} + r_{s,\text{soil}})}$ which is used in eq.4.4.13.

Concerning the decoupling of energy at lower depths within the soil, the decoupling of energy at the soil surface as has been explained at Sect. 4.4.2 is the first step. Within every soil layer, if the moisture content is high enough at the lower surface of this soil layer and low enough at the upper surface of that layer, and if there is temperature gradient such that there is a positive water vapour flux divergence, this means that water vapour which is leaving the upper boundary of this layer is more than what is entering from below. This lower incoming flux from below is due to the low air-filled porosity at the lower boundary. That flux divergence will represent a negative water sink at the water conservation equation and a negative heat sink in the soil temperature equation. This water vapour flux divergence will come at the expense on the soil heat flux coming from the upper boundary of that layer and leaving from its lower boundary. So, this model, due to its simulation of water vapour flux divergence and low thickness of different soil layers, allows for the decoupling of the available energy (G) into sensible and latent heat flux at different depths automatically.

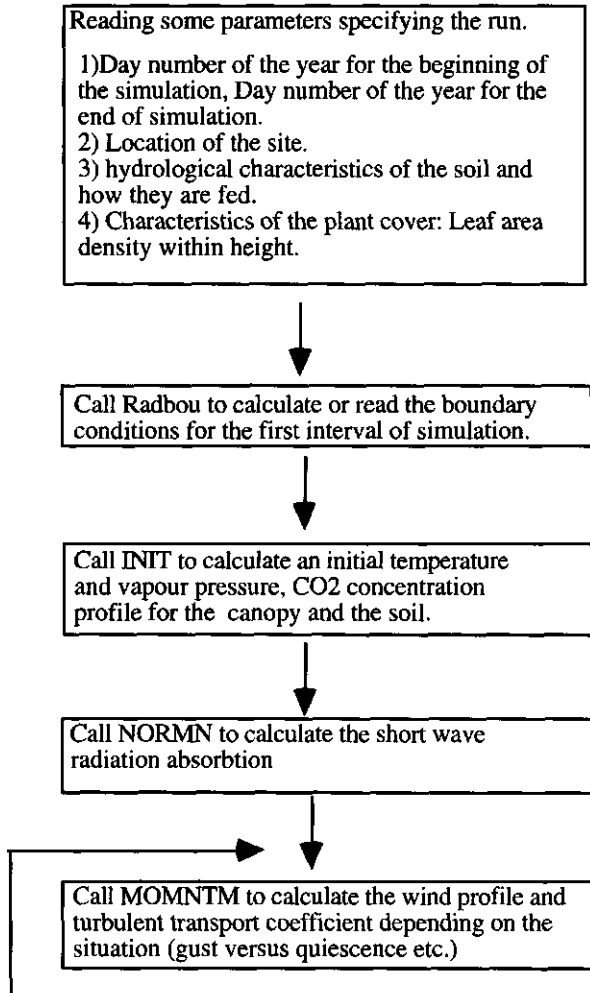
CHAPTER 5

THE CANOPY-SOIL-LAYER OF AIR CLOSE ABOVE INTERACTION MODEL (CANOPY)

5.1 THE LOGICAL ORDER OF THE SOLUTION:

The broad outlines for the logical order of the solution is given here. A detailed order is shown with the listing.

with the solution, for every time step, since we assume no effect of stability on the momentum solution, the momentum equation is solved first.



Call RESIS to calculate the boundary layer and stomatal resistances for different canopy layers and the soil surface resistance.

Call ENERGD to calculate energy sources and sinks within plant canopy depending on the solution of the energy budget equation.

Call PLANT to calculate from the latent heat flux imposed on the leaves the plant water potential and the soil water uptake by plant roots.

Branching point A
(depending on eq. 4.2.24 and the ratio of timestep to the time constant for the first air layer).

Call CYCLE1 to calculate temperature, vapour pressure, Co₂ concentration for the canopy layers and the soil.

Call Flux to calculate heat and mass transfer between different layers due to small scale mixing

Integrate within time the fluxes at the canopy top and within space the storage within the canopy.

Update the soil moisture and air temperature, vapour pressure and CO₂ concentration

PROGRAM CANOPY

CANOPY-SOIL-LAYER OF AIR CLOSE ABOVE INTERACTION
AUTHOR: RUSHDI M. M. EL-KILANI.

Date : June 1989
Updated : Tue Sep 6, 1994 15:27:33
We hope for the best
: : : : : :

Monaco 6 (expanded 1.75)

This program calculates the radiative and non radiative heat and mass exchange for a plant canopy layer and the exchange between this layer and the soil, and the layer of air close above the canopy (about twice the canopy height)

In this model, an intermittent approach is used to simulate the effect of coherent structures intrusion into the plant canopy on the partition of the available energy at the leaves and the soil and the integration of that effect on the system.

A complete description of the governing equations, the assumptions used in their parameterizations and in the modelling are given in the accompanying thesis. An explanation of the logic involved in the calculation is shown within this program.

This work was carried out by the author while studying and working as a Ph.D. student at the

Meteorology Department
Wageningen Agricultural University
Duivendaal 2
Wageningen
The Netherlands

This work was carried out under the supervision of

Prof. Dr. L. Wartena
Previous Head Meteorology Department,
Wageningen Agricultural University.
and
Prof. Dr. J. Goudriaan
Department Of Theoretical Production Ecology,
Wageningen Agricultural University.
and
Dr. Ir. Adrie. F. G. Jacobs
Department Of Meteorology,
Wageningen Agricultural University.

The author is very grateful for their supervision and guidance during the execution of this work.

The current address of the author is:

Rushdi M. M. El-Kilani
Soil Science Department,
Faculty of Agriculture,
Cairo University.
Giza, Egypt.

IMPLICIT NONE

FOR COMPATIBILITY WITH MACTRAN 3.0
\$INCLUDE:ALIMIT.FOR/L
\$INCLUDE:ABLANK.FOR/L
\$INCLUDE:AENERG.FOR/L
\$INCLUDE:AFLUX.FOR/L
\$INCLUDE:ANRMM.FOR/L
\$INCLUDE:ARDBOU.FOR/L
\$INCLUDE:AROOTD.FOR/L
\$INCLUDE:ACOEFF.FOR/L
\$INCLUDE:AEQCOE.FOR/L
\$INCLUDE:ACONST.FOR/L
\$INCLUDE:APLANT.FOR/L
\$INCLUDE:ABERGE.FOR/L
\$INCLUDE:AMHYDRO.FOR/L

INTEGER I,J,ITRA,ITRM,CHOICE,K,L
INTEGER OUTPL,INDEX,INDEXC,INDEXS
INTEGER DAY,RU,ITRF,WAYIN,RAININ
INTEGER FREQ1,FREQ2,PASS
INTEGER DAYEND,GUST,COUNT,INI,INIH
INTEGER FLAG,LOOP,MSZ,SOILIN
INTEGER INDEXI(IS:IH)

CHARACTER*21 FILENAME

REAL FACTOR,CHECK4,RAINM,WFTH(1:2)

REAL GL,RLINN,RLOUT
REAL RATIO,TOTEVP

REAL BTNOON,RTIME,TIMER,RA

REAL AVGDLT,BUDLT,NUMDLT
REAL WINDTP,DTEMP,WTEMP,SHRTN,WIND25,SHEAR
REAL PSISOL(IS:0),VGAS(IS:0),FE(IS:IH),CPHASE(IS:0)
REAL START,TIMEW,TIMEG
REAL HEE(IT,1:2,1:2,1:2)

```

REAL TEMPLF(IT,1:2,1:2,1:2),TEMLFN(IT,1:2,1:2,1:2)
1 ,AVGTLF(1:IT)
1 ,RABLT(IH,1:2)
1 ,ID(1:IT),FRAC(1:IT,1:2,1:2),CUMDEW(1:IT,1:2)
1 ,RDIR(1:IT,1:2)

REAL TOTUP

REAL ERRCBH,ERRCAV,ERR

REAL U(0:ITB),UNEW(0:ITB),DRA(0:ITB),ANAMOM(1:IH)

REAL GRASH(0:IT),NU(0:IT),NUFREE(0:IT)
1 ,NUFORC(0:IT),REYNOL(0:IT)

REAL RICHA1,RICHA2,PHI1,PHI1
REAL RICHA31,RICHA32

REAL TIMEC(1:IH)

1 REAL*8 TEMA1N(IS:ITB),EAI1RNW(IS:ITB),NCO2(IS:ITB),
STORAH(IS:IH),TEMPOR(IS:IH)
1 REAL*8 EXTRAS(IS:IH),EXTRAL(IS:IH)

REAL NSO(IS:0),XH(IS:0),YH(IS:0)
REAL STORAV(IS:IH),STORAC(IS:IH)
REAL TOTLQ,TOTLE,TOTASE,TOTASQ
REAL SATVAP(IS:ITB),VPDAIR(IS:ITB)
REAL KLE(IS:IH),KCO2(IS:IH)

REAL KRATIO(1:IH) ! KH/KM RATIO FOR THE LOCAL TERM.
REAL*8 EM(0:ITB),GM(0:ITB),FM(0:ITB)
REAL DM(0:ITB)

REAL CUMCRN,CUMTRN,CUMBRN

REAL CUMTLE,CUMTQ,CUMTC
REAL STPREH,STPREV,STPREC
REAL SDPRHC,SDPRVC,SDPRCC
REAL LOCALH,LOCALV,LOCALC

REAL AVGH,AVGLE,AVGRN,AVGTRN,AVGBRN
REAL AVGSTH,AVGSTE,AVGSTC
REAL AVG1TH,AVG1TE,AVG1TC

REAL CUMSE,CUMSH
REAL AVGSLE,AVGSH

REAL CUMSRN,CUMSS,CUMSG
REAL AVGSRN,AVGSS,AVGSG

REAL AVGTLE,AVGTQ

REAL CUDCRN,CUDTRN,CUDBRN

REAL CUDTLE,CUDTQ,CUDTC
REAL SDPREH,SDPREV,SDPREC
REAL SDPRHC,SDPRVC,SDPRCC
REAL LDCALH,LDCALV,LDCALC

REAL AVDH,AVDLE,AVDRN,AVDTRN,AVDBRN,AVDCO2
REAL AVDSTH,AVDSTE,AVDSTC
REAL AVD1TH,AVD1TE,AVD1TC

REAL CUDSE,CUDSH
REAL AVDSLE,AVDSH

REAL CUDSRN,CUDSS,CUDSG
REAL AVDSRN,AVDSS,AVDSG

REAL AVDTLE,AVDTQ

REAL DT1

REAL GAMMAT(1:IT),FG(1:IT,1:2)
REAL RLEAF(IT,1:2),HEND(1:IT,1:2),RCUTI(IT,2)
REAL LAYER(1:IT)

REAL KSOIL
REAL SOILTM(IS:0)
REAL TOTALE,TRNST,EVAPOT,EAIR1

REAL TOTSTH,TOTSTE,TOTSTC

REAL ESAIR2,CHECK2,RATIOS
REAL CAPAC,CAPAC3,TIMEC2,DTINT,DELTAC,CUMSLE
REAL ESAIR,EAIRS,CAPAC1,CAPAC2,TIMECO,TIMEC3,TIMECE,RATIO1
REAL RATIO2,W,M,WME,W

REAL IEAIR

CHARACTER T
REAL SATUV2,SATUD2,X
LOGICAL CH,CN,ON

```



```

*****
$INCLUDE:VALUES.DAT/L

OPEN (36,FILE='INPUT2.DAT',STATUS='OLD')

T= CHAR(9)

READ(36,*) DAYNUM
READ(36,*) DAYEND
READ(36,*) LATI
READ(36,*) P,C
READ(36,*) A,B
READ(36,*) AVGDLT
READ(36,*) BUDLT
READ(36,*) WAYIN
READ(36,*) SOILIN
READ(36,*) HYDRIN
READ(36,*) RAININ
READ(36,*) TMIN(1),TMIN(2)
READ(36,*) TMAX
READ(36,*) RHMAX(1), RHMAX(2)
READ(36,*) RHMIN(0),RHMIN(1)
READ(36,*) RAINM

IF (WAYIN.NE.1) THEN
  OPEN(29,FILE='RBOUDI.DAT',STATUS='UNKNOWN')
ENDIF

READ(36,*) ITA,IHA,ISA
READ(36,*) FACTOR
READ(36,*) GUST
READ(36,*) OUTPL
READ(36,*) CLOUDN
READ(36,*) WFTH(1),WFTH(2)
READ(36,*) LP,NP,ALPHA
READ(36,*) ZROOT
READ(36,*) TROOTD
READ(36,*) SROOTC
READ(36,*) PLANTN
READ(36,*) THICKN
READ(36,*) BASEDI

RADE = PI/180.

C ! Calculating the declination of the sun, day length, elevation of the sun at noon
C ! time, time of sun set and air temperature at sun set (if not given in the input
C ! file r'boudi.dat)
DECLIN = -(23.45*RADE)*COS(RADE*(360*(DAYNUM+10)/365))
SINDE = SIN(DECLIN)
DAYLNG =12.+24./PI*ASIN(TAN(LATI*RADE)*TAN(DECLIN))
NGHTLN =24.0-DAYLNG
BTNOON =PI/2+DECLIN-LATI*RADE
SINOON =SIN(BTNOON)
SUNSET =12+0.5*DAYLNG
BB =12-0.5*DAYLNG+C
YSN =(TMAX-TMIN(2))*SIN((PI*(DAYLNG-C))
1 /((DAYLNG+2*P))+TMIN(2))

C ! reading the depth of different soil layers, their structural composition
C ! (volume fraction of clay, quartz and organic matter),volumetric moisture content,
C ! matric head, residual moisture content, saturated hydraulic conductivity and root
C ! radius.
DO 10 I=ISA,0,1
  READ (36,*) Z(I),FC(I),FQ(I),FO(I),THETA(I),HM(I),
  : THETAR(I),KSTATU(I),RADIUS(I)

  POR(I) = 1.-(FC(I)+FQ(I)+FO(I))
  THETAS(I)=POR(I)
10 CONTINUE

C ! Reading leaf area density profile and the number of branches per layer
DO 20 I=0,IHA,1
  READ (36,*) Z(I),LAD(I),BRANCN(I)
  LAD(I)=LAD(I)*FACTOR
20 CONTINUE

C ! Reading the initial amount of dew in joules m-2 for lower and upper surfaces of
C ! the leaves, the wet and dry fraction for the lower and upper surfaces of the
C ! leaves and the characteristic water drops radius for lower and upper surfaces
C ! respectively.
DO 30 I=1,ITA,1
  READ(36,*) CUMDEW(I,1),CUMDEW(I,2),FRAC(I,1,1),
1 FRAC(I,2,1),RDIR(I,1),RDIR(I,2)
  FRAC(I,1,2)=1.-FRAC(I,1,1)
  FRAC(I,2,2)=1.-FRAC(I,2,1)
30 CONTINUE

C ! Reading the length of time step for the whole model and for the subroutine PLANT
C ! (in case of numerical instabilities due to small leaf thickness) .
READ(36,*) DT,DT1

C ! Reading the depths of soil layers at which a transition of the soil moisture
C ! characteristics occurs and the coefficients of the polynomials used to describe
C ! the Hm(theta) and Kstatu(theta) functions for these different layers.

```

```

DO 31 I=0,NLA,1
  READ(36,*) DEPTH(I)
  READ(36,*) HMC(I,0),HMC(I,1),HMC(I,2)
1    ,HMC(I,3),HMC(I,4),HMC(I,5)
  READ(36,*) KUSA(I,0),KUSA(I,1),KUSA(I,2)
1    ,KUSA(I,3),KUSA(I,4),KUSA(I,5)
31  CONTINUE

  DZ(IHA+1) =0.0
  DZ(ISA) =0.0

C    ! Calculating the depth of the centre of different soil and canopy layers and
C    ! their thicknesses
DO 50 I=ISA+1,IHA,1
  ZCENTER(I)=(Z(I)+Z(I-1))/2
50  DZ(I)=Z(I)-Z(I-1)
CONTINUE

C    ! Assigning different soil layers to their corresponding moisture characteristics.
INDESO(ISA)=NLA

DO 23 I=ISA+1,-1,1
  K=NLA
1023 CONTINUE
  IF (Z(I).LT.DEPTH(K)) THEN
    INDESO(I) = K
  ELSE
    K=K-1
    GOTO 1023
  ENDIF
23  CONTINUE
  INDESO(0)=0

C    ! Calculating the leaf area density in the middle of each canopy layer, leaf area
C    ! increments and the cumulative leaf area for different layers.
CUMLAI(IHA)=0
DO 70 I= IHA,1,-1
  LADMID(I)=(LAD(I-1)+LAD(I))/2
  LEAINC(I)=LADMID(I)*DZ(I)
70  CUMLAI(I-1)= CUMLAI(I)+LEAINC(I)
CONTINUE

C    ! calculating the matric heat from volumetric moisture content, given fitted soil
C    ! moisture characteristics.
IF (HYDRIN.NE.1) THEN
DO 333 I= ISA,0,1
  NSO(I)=THETAS(I)/THETA(I)

  XH(I) = ALOG10(NSO(I))
  YH(I) = HMC(INDESO(I),0)
:      +HMC(INDESO(I),1)*XH(I)
:      +HMC(INDESO(I),2)*XH(I)**2
:      +HMC(INDESO(I),3)*XH(I)**3
:      +HMC(INDESO(I),4)*XH(I)**4
:      +HMC(INDESO(I),5)*XH(I)**5

  HM(I) = -(10.)*YH(I)
  HM(I) =HM(I)/100.

  IF(INDESO(I).EQ.0) THEN
    HM(I)=HM(I)*20.0
  ENDIF
333  CONTINUE
ENDIF

PASS= 0
START=REAL(NINT(BB))-0.5

C    ! Starting time of the calculation.
TIME = START
RTIME=TIME
COUNT=0
CORR= MOD(COUNT,OUTPL)

C    ! Call RADBOU to calculate or read the boundary conditions at the canopy top.
1  CALL RADBOU(DTEMP,IEAIR,WINDTP,WIND25,CLOUDN,
  RLOUT,RLINN,WAYIN,CORR,MINUTE,T,TIMER)

U(IHA+1) =WINDTP
TEMAIR(IHA+1) = DTEMP
EAIR(IHA+1) = IEAIR
SHEAR = WIND25/2.2

C    ! Call Rootdn to calculate root area distribution and root Conductance at different
C    ! depths
CALL ROOTDN

```

```

C      ! Call INIT to calculate the initial soil temperature profile and different plant
C      ! hydraulic resistances
      CALL INIT(SOILTM,
:      ELASTI,OSMOTI,
:      KXYLUM,RLS,RS,
:      PSIXYL,PSIS,
:      PSISOL,HM,DX,
:      VOLUME,TOTDX,
:      RADIUS,RDENST,
:      TIME,KSOIL,
:      SOILIN)

      ITRM= 0
      ITRA= 0

      INDEX=0
      SOILLE=0.0
      INI=0
      INIH=0

C      ! The calculating Loop for the number of simulated days.
      DO 5000 DAY=DAYNUM,DAYEND,1

C      ! initializing some daily reservoirs.
      TOT EVP=0.0; STOR TH=0.0; STOR TV=0.0; STOR TC=0.0

      STOR HT=0.0; STOR VT=0.0; STOR CT=0.0

      TOT STE=0.0; TOT STH=0.0; TOT STC=0.0

      CNLFGT=0.0; CNLFGV=0.0; CNLFGC=0.0

      CNLFST=0.0; CNLFSV=0.0; CNLFSC=0.0

      RA=START
      RAINC = 0

C      ! Calculating for every time interval of averaging = AVGDLT = 30 minutes.
      DO 4500 WHILE (RA.LT.24.0)
        NUMDLT=REAL(INT(AVGDLT/BUDLT))

C      !initializing some reservoirs for AVGDLT period.
        SDPREH=0.0; SDPREV=0.0; SDPREC=0.0

        SDPRHC=0.0; SDPRVC=0.0; SDPRCC=0.0

        CUDCRN=0.0; CUDTRN=0.0; CUDBRN=0.0

        CUDTLE=0.0; CUDTQ=0.0; CUDTTC=0.0

        LDCALH=0.0; LDCALV=0.0; LDCALC=0.0

        CUDSRN=0.0; CUDSE=0.0; CUDSH=0.0

        CUDSG=0.0; CUDSS=0.0

C      ! Calculating for every interval of time with a length equal to Budlt (period of
C      ! updating the boundary conditions) = 15 minutes
      DO 4000 RU= 1,NUMDLT,1
        TIME=RA+(REAL(RU-1))*BUDLT
        RTIME=TIME

        RATIO=AMAX1((SINBTA/SIN00N),0.0)

C      ! a counter for output control and an example.
        CORR=MOD(COUNT,OUTPL)
        IF (CORR.EQ. 0) THEN
          WRITE(FILENAME,'(I3,45,F6.3,A3)' )DAYNUM,
1          'AIRB',TIME,'DAT'
          OPEN(UNIT=4,FILE=FILENAME,STATUS='UNKNOWN')
          ENDIF

        CH = ((SINBTA.LT.0.0). AND. (INDEX.LT.1))
        CN = ((SINBTA.GE.0.0) .OR. CH)

        IF (CN) THEN
          IF(SINBTA.LT.0.0) THEN
C      !
          INDEX=1

C      ! not active part
          CALL FREQM(INTERVAL,DURATION,
C      1 INTENSITY,REFRE)
          ELSE
            INDEX=0

C      ! not active part
          CALL FREQM(INTERVAL,DURATION,
C      1 INTENSITY,REFRE)

```

```

        ENDIF
C      ! Call NORMN to calculate the short wave radiation
C      ! profile and the absorbed short wave per layer.
        CALL NORMN(IINI,DIRECT,SINBTA,TIME)
    ENDIF

C      ! Calculate the period between two consecutive gust intrusions into plant canopy C
C      ! as a function of the measured shear at the canopy top (rather arbitrary).
        IF (SHEAR.LE.0.2) THEN
C          ! No intrusion
            FREQ1=6
            FREQ2=10
        ELSEIF (SHEAR.LT.0.4) THEN
C          ! once every three minutes.
            FREQ1=5
            FREQ2=12
        ELSEIF (SHEAR.LT.0.8) THEN
C          ! once every 2.5 minutes.
            FREQ1=6
            FREQ2=10
        ELSEIF (SHEAR.LT.1.0) THEN
C          ! once every 1.5 minutes.
            FREQ1= 10
            FREQ2=6
        ELSEIF (SHEAR.GE.1) THEN
C          ! once every 75 seconds.
            FREQ1= 12
            FREQ2= 5
        ENDIF

    ON=.FALSE.

C      !The calculation MASTER LOOP for every gust cycle (Refreshment and then buildup)
C      ! FREQ1 times within a BULDT period (i.e. 15 minutes).
    DO 3000 MINUTE=1,FREQ1,1
        INDEXS=1
C      ! the first period after the gust passage. (an increases turbulent transport
C      ! coefficient.

        IF (MINUTE.EQ.1) THEN
C          ! Calculate an initial wind profile for the momentum calculation.
            CALL INITAI(U,RATIO,TIME,USTAR,WAYIN)
        ENDIF

C      ! Call MOMNTM to calculate the momentum solution.
        CALL MOMNTM(ITRM,INDEXS,FLAG
        :      ,DU
        :      ,U,UNEW,LMIX,DRA,KM
        :      ,ANAMOM,GRASH,NU,USTAR
        :      ,TIME,SHEAR,SINBTA
        :      ,RICHAR1,RICHAR2,PHIM1
        :      ,PHIM1,RICHAR31,RICHAR32)

C      ! To calculate the fluxes resulting from mixing due to Richardson number being
C      ! less than a critical value. This did not work, It led to much overestimated
C      ! mixing.
        IF ((FLAG.EQ.31).OR.(FLAG.EQ.32)) THEN
            CALL FLUX(FLAG,
            :      TEMAIN,EAIRNW,NCO2,
            :      STORAH,SH,SL,SINK,
            :      STORAV,STORAC,
            :      PCSOIL,VGAS,
            :      TOTALQ,TOTLE,TOTASE,TOTASQ,SOILLE,
            :      DT,TIMEW,SOILRN)

C      ! Integrating Non Local Flux Due to Stability
            CNLFST= CNLFST+ NLFLST
            CNLFSV= CNLFSV+ NLFLSV
            CNLFSC= CNLFSC+ NLFLSC

        DO 444 I=1,IHA,1
            TEMAIR(I)= TEMAIR(IHA+1)
            EAIR(I) = EAIR(IHA+1)
            CO2CON(I)= CO2CON(IHA+1)
        444 CONTINUE

            IF (FLAG.EQ.31) THEN
                FLAG =1
            ELSEIF(FLAG.EQ.32) THEN
                FLAG=2
            ENDIF
        ENDIF
    ENDIF

C      ! Call RESIS to calculate the boundary layer resistance for the leaves
C      ! and the soil surface resistance under different Regimes
C      ! (Forced convection, free or mixed) for sensible and latent heat.
        CALL RESIS(ITRM,ITRA,FLAG,

```

```

1      LEFL,RCUT1,
1      GRASH,NU,REYNOL,NUFORC,NUFREE,
1      LIGHT,UNEW,GAMMAT,FG,AVGTLF,
1      RB,RST,RLEAF,CUMDEW,
1      HT,HE,HEND,PGR,VGAS,
1      PSIS,TIME,ABACON)

C      ! Call ENERGD to calculate the longwave radiation profile and the total absorbed C
C      ! energy and its partition (i.e. sources sinks with plant canopies at different
C      ! heights)
C      CALL ENERGD(ITRA,RTIME,MS2,
:         SH,SL,HT,HE,HEND,HEE,
:         TEMPLF,TEMLFN,AVGTLF,
:         RABL,RABLT,
:         RAB,KAV,LIGHT,ENESAB,
:         ID,FRAC,CUMDEW,
:         RDIR,WPTH,SINBTA,RLOUT,RLINN,
:         DT,TOTENE,SOILSN,ON)

C      ! Once the amount of latent heat flux is calculated for the Leaves, Call PLANT
C      ! to calculate the water potential within different plant parts and Water uptake
C      ! by Plant roots and Abscisic Acid Concentration to be used later for the stomatal
C      ! resistance calculation.
C      CALL PLANT(INI,
:         DT,DT1,
:         RADIUS,RADIU2,LV,KWATER,
:         SL,ROOTRS,
:         PSISOL,
:         TOTUP,F,RTIME,START,DAYNUM)

C      ! initializing certain counters for one gust cycle.
C      STPREH=0.0; STPREV=0.0; STPREC=0.0
C      STPRHC=0.0; STPRVC=0.0; STPRCC=0.0
C      CUMCRN=0.0; CUMTRN=0.0; CUMBRN=0.0
C      CUMTLE=0.0; CUMTQ=0.0; CUMTC=0.0
C      LOCALH=0.0; LOCALV=0.0; LOCALC=0.0
C      CUMSRN=0.0; CUMSE=0.0; CUMSH=0.0
C      CUMSG=0.0; CUMSS=0.0

C      ! A time counter.
C      TIMEG =TIME+REAL(MINUTE-1)*REAL(FREQ2)*15./3600.
C      RTIME =TIMEG

C      ! An estimation of the ratio of the time step to the time constant of the
C      ! first air layer (section 4.4.1).
C      GL =PCP/GAMMA*KM(1)/(0.5*(DZ(1)+DZ(2)))
C      TIMEC3 =1./((GL+HE(0,1,2))
C      RATIO1 =GL*TIMEC3
C      RATIO2 =HE(0,1,2)*TIMEC3
C      WM =GL*TIMEC3*EAIR(2)
C      1      +HE(0,1,2)*TIMEC3*EAIR(0)+SL(1)*TIMEC3
C      ! eq.
C      SOILLE =HE(0,1,2)*(EAIR(0)-EAIR(1))
C      SOILH =HT(0)*(TEMAIR(0)-TEMAIR(1))
C      ESAIR =SATUV2(SNGL(TEMAIR(1)))
C      EAIRS =SATUV2(SNGL(TEMAIR(0)))

C      ! Calculating the capacitance of the first air layer for water vapour.
C      CAPAC1=PCP/GAMMA*(ESAIR-EAIR(1))*DZ(1)
C      CAPAC2=PCP/GAMMA*(EAIR(0)-EAIR(1))*DZ(1)
C      CAPAC3=PCP/GAMMA*(WM-EAIR(1))*DZ(1)
C      IF ((CAPAC3 .LE. 0.0) THEN
C          CAPAC=0.0
C          TIMECO=0.001
C          RATIOS=10.
C      ELSE IF ((CAPAC2 .LT. 0.0) THEN
C          CAPAC =MIN(CAPAC1,CAPAC3)
C      1      CHECK4=HE(0,1,2)*(EAIR(0)-EAIR(1))
C          +SL(1)-GL*(EAIR(1)-EAIR(2))
C          IF (CHECK4.NE.0.0) THEN
C              TIMECO= CAPAC/CHECK4
C          ELSE
C      C      ! to avoid deviding by zero.
C          TIMECO =10E-10
C          ENDIF
C          IF (TIMECO.LT.0.0)THEN
C              RATIOS =10.

```

```

ELSE
  RATIOS= DT/TIMECO
ENDIF

ELSE
  CAPAC =MIN(CAPAC1,CAPAC2,CAPAC3)
  CHECK4=HE(0,1,2)*(EAIR(0)-EAIR(1))
1  +SL(1)-GL*(EAIR(1)-EAIR(2))
    IF (CHECK4.NE.0.0) THEN
      TIMECO= CAPAC/CHECK4
    ELSE
      TIMECO =10E-10
    ENDIF
    IF (TIMECO.LT.0.0)THEN
      RATIOS =10.
    ELSE
      RATIOS= DT/TIMECO
    ENDIF
ENDIF

C  ! First Branching Point (Branching Point A depending on section 4.4.1)
  IF (RATIOS.GT.3.0) THEN
    INDEXC=1
1  WRITE(*,*) 'WM HAS BEEN REACHED '
    , 'DURING THE FIRST 15 SECONDS'
    DO 145 ITRA=1,20,1
    IF (ITRA.EQ.1) THEN
1  SOILLE=PCP/GAMMA*(WM-EAIR(1))*DZ(1)/DT
    -SL(1)+1.0*GL*(WM-EAIR(2))
    ELSE
1  SOILLE=PCP/GAMMA*(WM-EAIR(1))*DZ(1)/DT
    -SL(1)+1.0*GL*(WM-EAIRNW(2))
    ENDIF

C  ! Call CYCLE1 to calculate the temperature, vapour pressure and Co2 concentration
C  ! profile within the system and the volumetric soil moisture content and the soil
C  ! water potential profile
    CALL CYCLE1(INIH,ITRA,PASS,
    :   TEMAIN,EAIRNW,NC02,VGAS,EXTRAS,EXTRAL,
    :   PSISOL,AVGTLF,
    :   RLEAF,
    :   GAMMAT,FG,RAINM,
    :   PHIM,KRATIO,FE,WM,INDEXI,TEMPOR)

C  ! Check the convergence of the solution.
    WME =WM
    WM =GL*TIMEC3*EAIRNW(2)
1  +HE(0,1,2)*TIMEC3*EAIRNW(0)
1  +SL(1)*TIMEC3
    ERR =ABS(WM-WME)
    IF ((ERR.LE.1).AND.(ITRA.GT.1))THEN
      GOTO 146
    ENDIF
145 CONTINUE
146 CONTINUE

C  ! Second option of (Branching Point A). Initial estimate of SOILLE is good enough.
    ELSE IF (RATIOS.LT.0.1) THEN
      SOILLE=SOILLE
      INDEXC=3
      CALL CYCLE1(INIH,ITRA,PASS,
      :   TEMAIN,EAIRNW,NC02,VGAS,EXTRAS,EXTRAL,
      :   PSISOL,AVGTLF,
      :   RLEAF,
      :   GAMMAT,FG,RAINM,
      :   PHIM,KRATIO,FE,WM,INDEXI,TEMPOR)
    ELSE

C  ! Third option of (Branching Point A). (integrate numerically).
    INDEXC=2
    LOOP =NINT(DT*10./TIMECO)
    LOOP =LOOP+1
    DTINT =DT/REAL(LOOP)
    EAIR1 =EAIR(1)
    ESAIR2 =SATUV2(SNGL(TEMAIR(2)))
1  TIMEC2 =PCP/GAMMA*(ESAIR2-EAIR(2))*DZ(2)/
    (GL*(EAIR1-EAIR(2))

```

```

1          -PCP/GAMMA*KM(2)/(0.5*(DZ(2)+DZ(3)))
1          *(EAIR(2)-EAIR(3))
1          +SL(2))

CHECK2  =TIMEC0/TIMEC2

CUMSLE=0.0

DO 1503 I=1,LOOP,1

CUMSLE=DTINT*HE(0,1,2)*(EAIR(0)-EAIR1)+CUMSLE
DELTAC=DTINT*(HE(0,1,2)*(EAIR(0)-EAIR1)
1          +SL(1)-PCP/GAMMA*KM(1)/
1          (0.5*(DZ(1)+DZ(2)))*(EAIR1-EAIR(2)))
EAIR1=EAIR1+DELTAC*GAMMA/(PCP*DZ(1))

IF (EAIR1 .GE. WM) THEN
EAIR1=MIN(EAIR5,WM)
CUMSLE=PCP/GAMMA*DZ(1)*(EAIR1-EAIR(1))
GOTO 1504
ENDIF

1503 CONTINUE

INDEXC=3

1504 CONTINUE

SOILLE=CUMSLE/DT

IF (INDEXC.EQ.3) THEN
ITRF=9
ELSE ITRF=20
ENDIF

DO 147 ITRA=1,ITRF,1

C      ! Remark 1 (calculate the solution (state variables and fluxes)
CALL CYCLE1(INIH,ITRA,PASS,
:          TEMAIN,EAIRNW,NC02,VGAS,EXTRAS,EXTRAL,
:          PSISOL,AVGTLF,
:          RLEAF,
:          GAMMAT,FG,RAINM,
:          PHIM,KRATIO,FE,WM,INDEXI,TEMPOR)

WME =WM
WM  =GL*TIMEC3*EAIRNW(2)
1  +HE(0,1,2)*TIMEC3*EAIRNW(0)
1  +SL(1)*TIMEC3

ERR =ABS(WM-WME)

IF ((ERR.LE.1).AND. (ITRA.GT.1)) THEN
GOTO 148
ENDIF
147 CONTINUE
148 CONTINUE
ENDIF

C      ! integrate within canopy height the sensible and latent heat sources.
TOTLE =0.0
TOTALQ =0.0

DO 222 I=1,ITA
TOTLE=TOTLE+SL(I)
TOTALQ=TOTALQ+SH(I)
222 CONTINUE

C      ! Calculate the resulting fluxes of sensible latent heat and Co2 for the canopy-
C      ! soil system
CALL FLUX(FLAG,
:          TEMAIN,EAIRNW,NC02,
:          STORAH,SH,SL,SINK,
:          STORAV,STORAC,
:          PCSOIL,VGAS,
:          TOTALQ,TOTLE,TOTASE,TOTASQ,SOILLE,
:          DT,TIMEW,SOILRN)

C      ! Integrate for all the canopy height and 15 seconds time step interval
TRNST =(TOTLE*DT)/LAMDA
EVAPOT =TRNST+(SOILLE*DT)/LAMDA
TOTEVP =TOTEVP+EVAPOT

TOTSTE =TOTSTE+TOTLE*DT
1  -FLUXVT(IHA)*DT+SOILLE*DT

TOTSTH =TOTSTH+TOTALQ*DT
1  -FLUXHT(IHA)*DT+FLUXHB(1)*DT

```

```

ERRCAH      =TOTALQ-FLUXHT(IHA)+FLUXHB(1)-STORM
ERRCAV      =TOTLE-FLUXVT(IHA)+SOILLE-STORV
C           ! Integrate within time of the local above the canopy fluxes and the storage within
C           ! the canopy.
LOCALH      =LOCALH+CFLXHT(IHA)
LOCALV      =LOCALV+CFLXVT(IHA)
LOCALC      =LOCALC+CFLXCT(IHA)

STPREH      =STPREH+STOREH
STPREV      =STPREV+STOREV
STPREC      =STPREC+STOREC

STPRHC      =STPRHC+STORHC
STPRVC      =STPRVC+STORVC
STPRCC      =STPRCC+STORCC

CUMCRN      =CUMCRN+RNETOT*DT
CUMTRN      =CUMTRN+(RNSTOP+RLNTP)*DT
CUMBRN      =CUMBRN+(RNSBTM+RLNBTM)*DT

CUMTLE      =CUMTLE+TOTLE*DT
CUMTQ      =CUMTQ +TOTALQ*DT
CUMTC      =CUMTC+

CUMSRN      =CUMSRN+SOILRN*DT
CUMSH      =CUMSH +FLUXHB(1)*DT
CUMSE      =CUMSE +SOILLE*DT
CUMSG      =CUMSG +FLUXHB(0)*DT
CUMSS      =CUMSS +STORAH(0)*DT

C           ! An example for output control, i.e. will not be repeated. It is left to the
C           ! user of the model to add such a segment where ever he wants.

IF ((CORR.EQ.0).AND. (MINUTE.EQ.1)) THEN
  WRITE(4, '(A1)') '*'
  WRITE(4, *) '(3) I', T, 'Z(I)', T, 'TEMAIR', T,
:   'TEMAIN', T, 'EAIR', T, 'EAIRNW', T, 'CO2CON',
:   T, 'NCO2', T, 'SATVAP', T, 'VPDAIR', T

  WRITE(4, *) FREQ2
  DO 3210 I=ISA, IHA, 1

  WRITE (4, *) I, T, Z(I), T, TEMAIR(I), T, TEMAIN(I), T,
:   EAIR(I), T, EAIRNW(I), T, CO2CON(I), T, NCO2(I), T,
:   SATVAP(I), T, VPDAIR(I), T

3210  CONTINUE
  ENDIF

C           ! Calculations for the second time step after the passage of the gust for FREQ2
C           ! times i.e. till the end of the quiescence period with time intervals of 15
C           ! seconds.
DO 2000 ITRM=2, FREQ2, 1

INDEXS=2

C           ! Update the Soil total water potential (!!not including osmotic)
HM(ISA)=HMNEW(ISA)
PSISOL(ISA)=HMNEW(ISA)+Z(ISA)

DO 225 I=ISA+1, 0
  IF (HYDRIN.NE.1) THEN
    THETA(I)=THETAN(I)
  ENDIF

  HM(I)=HMNEW(I)
  PSISOL(I)=HMNEW(I)+ZCENTER(I)
225  CONTINUE

C           ! Update the temperature, the vapour pressure and the Co2 concentration
C           ! for the next time step.
DO 149 I=ISA, IHA, 1
  TEMAIR(I)=TEMAIN(I)
  EAIR(I) =EAIRNW(I)
  CO2CON(I)=NCO2(I)
  EXTRAS(I)=0.0
  EXTRAL(I)=0.0
  INDEXI(I)=0
149  CONTINUE

C           ! Calculate the momentum equation solution for each interval within the quiescence
C           ! period.
CALL MOMNTM(ITRM, INDEXS, FLAG
:   , DU
:   , U, UNEW, LMIX, DRA, KM
:   , ANAMOM, GRASH, NU, USTAR

```



```

:         ,TIME,SHEAR,SINBTA
:         ,RICHAR1,RICHAR2,PHIMI
:         ,PHIH1,RICHAR31,RICHAR32)

C       ! If a large scale mixing occurs due to Richardson number being less than a
C       ! critical value =0.25, this did not work. It lead to too much mixing.
IF ((FLAG.EQ.31).OR.(FLAG.EQ.32)) THEN
  CALL FLUX(FLAG,
:         TEMAIN,EAIRNW,NC02,
:         STORAH,SH,SL,SINK,
:         STORAV,STORAC,
:         PCSOIL,VGAS,
:         TOTALQ,TOTLE,TOTASE,TOTASQ,SOILLE,
:         DT,TIMEW,SOILRN)
  CNLFST= CNLFST+ NLFLST
  CNLFSV= CNLFSV+ NLFLSV
  CNLFSC= CNLFSC+ NLFLSC
  DO 445 I=1,IHA,1
    TEAIR(I)= TEAIR(IHA+1)
    EAIR(I)  = EAIR(IHA+1)
    COZCON(I)= COZCON(IHA+1)
445    CONTINUE
  IF (FLAG.EQ.31) THEN
    FLAG =1
  ELSEIF(FLAG.EQ.32) THEN
    FLAG=2
  ENDIF
ENDIF

  CALL RESIS(ITRM,ITRA,FLAG,
1     LEFL,RCUTI,
1     GRASH,NU,REYNOL,NUFORC,NUFREE,
1     LIGHT,UNEW,GAMMAT,FG,AVGTLF,
1     RB,RST,RLEAF,CUMDEW,
1     HT,HE,HEND,POR,VGAS,
1     PSIS,TIME,ABACON)

C       ! Update the temperature of the leaves for the different segments.
DO 1490 I=1,ITA,1
  DO 1491 J=1,2,1
    DO 1492 K=1,2,1
      IF(CIPRC(I,K,J).NE.0)THEN
        TEMPLF(I,1,K,J)= TEMLFN(I,1,K,J)
        TEMPLF(I,2,J,K)= TEMLFN(I,2,J,K)
      ENDIF
1492    CONTINUE
1491    CONTINUE
1490  CONTINUE

C       ! Calculate energy sources and sinks within plant canopy.
CALL ENERGD(ITRA,RTIME,MS2,
:         SH,SL,HT,HE,HEND,HEE,
:         TEMPLF,TEMLFN,AVGTLF,
:         RABL,RABLT,
:         RAB,KAV,LIGHT,ENESAB,
:         ID,FRAC,CUMDEW,
:         RDIR,WPTH,SINBTA,RLOUT,RLINN,
:         DT,TOTENE,SOILSN,ON)

CALL PLANT(INI,
:         DT,DTI,
:         RADIUS,RADIUZ,LV,KWATER,
:         SL,ROOTRS,
:         PSISOL,
:         TOTUP,F,RTIME,START,DAYNUM)
  TIMEW=TIME+REAL(MINUTE-1)*REAL(FREQ2)*15./3600.
1     +REAL(ITRM-1)*15/3600.
  RTIME=TIMEW

C       ! First option of (Branching Point B).
IF(EAIR(1).EQ. WM) THEN
  INDEXC=1
  DO 1001 ITRA=1,20,1
    IF (ITRA .EQ.1) THEN

C       ! Calculating the Soil latent heat flux
1     SOILLE=PCP/GAMMA*(WM-EAIR(1))*DZ(1)/DT
1     +PCP/GAMMA*KM(1)/(0.5*(DZ(1)+DZ(2)))
      *(WM-EAIR(2))-SL(1)
  ELSE

C       ! Updating the Soil latent heat flux
1     SOILLE=PCP/GAMMA*(WM-EAIR(1))*DZ(1)/DT
1     +PCP/GAMMA*KM(1)/(0.5*(DZ(1)+DZ(2)))
      *(WM-EAIRNW(2))-SL(1)
  ENDIF

```

```

CALL CYCLE1(INIH,ITRA,PASS,
: TEMAIN,EAIRNW,NCO2,VGAS,EXTRAS,EXTRAL,
: PSISOL,AVGTLF,
: RLEAF,
: GAMMAT,FG,RAINM,
: PHIM,KRATIO,FE,WM,INDEXI,TEMPOR)

WME =WM
WM =GL*TIMEC3*EAIRNW(2)
1 +HE(0,1,2)*TIMEC3*EAIRNW(0)
1 +SL(1)*TIMEC3

ERR =ABS(WM-WME)

IF ((ERR.LE.1) .AND. (ITRA.GT.1))THEN
GOTO 1116

ENDIF

1001 CONTINUE
1116 CONTINUE

C ! Second option of (Branching point B).
ELSE
INDEXC=3
WM =GL*TIMEC3*EAIR(2)
1 +HE(0,1,2)*TIMEC3*EAIR(0)+SL(1)*TIMEC3
SOILLE =HE(0,1,2)*(EAIR(0)-EAIR(1))

CALL CYCLE1(INIH,ITRA,PASS,
: TEMAIN,EAIRNW,NCO2,VGAS,EXTRAS,EXTRAL,
: PSISOL,AVGTLF,
: RLEAF,
: GAMMAT,FG,RAINM,
: PHIM,KRATIO,FE,WM,INDEXI,TEMPOR)

3105 CONTINUE

IF (EAIRNW(1) .GT.WM) THEN
EAIRNW(1)= WM
INDEXC=1
DO 1002 ITRA=1,20,1
IF (ITRA .EQ.1) THEN
SOILLE =PCP/GAMMA*(WM-EAIR(1))*DZ(1)/DT
1 +PCP/GAMMA*KM(1)/(0.5*(DZ(1)+DZ(2)))
1 *(WM-EAIR(2))-SL(1)
ELSE
SOILLE =PCP/GAMMA*(WM-EAIR(1))*DZ(1)/DT
1 +PCP/GAMMA*KM(1)/(0.5*(DZ(1)+DZ(2)))
1 *(WM-EAIRNW(2))-SL(1)
ENDIF

CALL CYCLE1(INIH,ITRA,PASS,
: TEMAIN,EAIRNW,NCO2,VGAS,EXTRAS,EXTRAL,
: PSISOL,AVGTLF,
: RLEAF,
: GAMMAT,FG,RAINM,
: PHIM,KRATIO,FE,WM,INDEXI,TEMPOR)

WME =WM
WM =GL*TIMEC3*EAIRNW(2)
1 +HE(0,1,2)*TIMEC3*EAIRNW(0)
1 +SL(1)*TIMEC3

ERR =ABS(WM-WME)

IF ((ERR.LE.1) .AND. (ITRA.GT.1)) THEN
GOTO 1117
ENDIF

1002 CONTINUE
1117 CONTINUE

ENDIF
ENDIF

```

```

1100  CONTINUE
C      ! Calculate the fluxes between different layers.
      CALL FLUX(FLAG,
:       TEMAIN, EAIRNW, NCO2,
:       STORAH, SH, SL, SINK,
:       STORAV, STORAC,
:       PCSOIL, VGAS,
:       TOTALQ, TOTLE, TOTASE, TOTASQ, SOILLE,
:       DT, TIMEW, SOILRN)

      DO 3111 I=ISA, IHA, 1
          SATVAP(I)=SATUV2(SNGL(TEMAIR(I)))
          VPDAIR(I)=SATVAP(I)-SNGL(EAIR(I))
3111  CONTINUE

      TOTLE =0.0
      TOTALQ =0.0

      DO 111 I=1, ITA
          TOTLE =TOTLE+SL(I)
          TOTALQ =TOTALQ+SH(I)

111  CONTINUE
C      ! integrate within canopy height the sensible and latent heat sources.
      TRNST =(TOTLE*DT)/LAMDA
      EVAPOT =TRNST+(SOILLE*DT)/LAMDA
      TOTEVP =TOTEVP+EVAPOT

      TOTSTE =TOTSTE+TOTLE*DT
1      -FLUXVT(IHA)*DT+SOILLE*DT
      TOTSTH =TOTSTH+TOTALQ*DT
1      -FLUXHT(IHA)*DT+FLUXHB(1)*DT

      ERRCAH =TOTALQ-FLUXHT(IHA)+FLUXHB(1)-STORH
      ERRCV =TOTLE-FLUXVT(IHA)+SOILLE-STORV

      LOCALH =LOCALH+CFLXHT(IHA)
      LOCALV =LOCALV+CFLXVT(IHA)
      LOCALC =LOCALC+CFLXCT(IHA)

      STPREH =STPREH+STOREH
      STPREV =STPREV+STOREV
      STPREC =STPREC+STOREC

      STPRHC =STPRHC+STORHC
      STPRVC =STPRVC+STORVC
      STPRCC =STPRCC+STORCC

      CUMCRN =CUMCRN+RNETOT*DT
      CUMTRN =CUMTRN+(RNSTOP+RLNTP)*DT
      CUMBRN =CUMBRN+(RNSBTM+RLNBTM)*DT

      CUMTLE =CUMTLE+TOTLE*DT
C      CUMTQ =CUMTQ +TOTALQ*DT
      CUMTC =CUMTC+

      CUMSRN =CUMSRN+SOILRN*DT
      CUMSH =CUMSH +FLUXHB(1)*DT
      CUMSE =CUMSE +SOILLE*DT
      CUMSG =CUMSG +FLUXHB(0)*DT
      CUMSS =CUMSS +STORAH(0)*DT

2000  CONTINUE

      IF ((GUST.EQ.1).AND.(SHEAR.GT.0.2)) THEN

          FLAG=4
          CALL FLUX(FLAG,
:           TEMAIN, EAIRNW, NCO2,
:           STORAH, SH, SL, SINK,
:           STORAV, STORAC,
:           PCSOIL, VGAS,
:           TOTALQ, TOTLE, TOTASE, TOTASQ, SOILLE,
:           DT, TIMEW, SOILRN)

          CNLFGT= CNLFGT+ NLFLGT
          CNLFGV= CNLFGV+ NLFLGV
          CNLFGC= CNLFGC+ NLFLGC

          FLAG=0

          DO 2500 I=IHA+1, 1, -1
              TEMAIR(I) =DTEMP
              EAIR(I) =IEAIR
              CO2CON(I) =300.
2500  CONTINUE

```

```

DO 2501 I=ISA,0,1
  TEMAIR(I) = TEMAIN(I)
  EAIR(I) = EAIRNW(I)
  CO2CON(I) = NCO2(I)
2501 CONTINUE

ELSE

DO 2502 I=IHA+1,ISA,-1
  TEMAIR(I)=TEMAIN(I)
  EAIR(I)=EAIRNW(I)
  CO2CON(I)=NCO2(I)
2502 CONTINUE

ENDIF
DO 2601 I=ISA,IHA,1
  EXTRAS(I)=0.0
  EXTRAL(I)=0.0
  INDEXI(I)=0
2601 CONTINUE

HM(ISA)=HMNEW(ISA)
PSISOL(ISA)=HMNEW(ISA)+Z(ISA)

DO 223 I=ISA+1,0
C ! Updating the soil moisture content
  IF(CHYDRIN.NE.1) THEN
    THETA(I)=THETAN(I)
  ENDIF
C ! or Updating the soil water moisture potential.
  HM(I)=HMNEW(I)
  PSISOL(I)=HMNEW(I)+ZCENTER(I)
223 CONTINUE

C ! Obtaining averages over the whole gust cycle for storage of sensible, latent heat
C ! and CO2 with the canopy.
AVG1TH =STPREH/(DT*REAL(FREQ2))
AVG1TE =STPREV/(DT*REAL(FREQ2))
AVG1TC =STPREC/(DT*REAL(FREQ2))

AVG2TH =STPRHC/(DT*REAL(FREQ2))
AVG2TE =STPRVC/(DT*REAL(FREQ2))
AVG2TC =STPRCC/(DT*REAL(FREQ2))

C ! Obtaining averages over the whole gust cycle of (????)
AVGTLT =CUMTLE/(DT*REAL(FREQ2))
AVGTQ =CUMTQ/(DT*REAL(FREQ2))
AVGH =LOCALH/(DT*REAL(FREQ2))
AVGLE =LOCALV/(DT*REAL(FREQ2))
AVGRN =CUMCRN/(DT*REAL(FREQ2))
AVGTRN =CUMTRN/(DT*REAL(FREQ2))
AVGBRN =CUMBRN/(DT*REAL(FREQ2))

AVGSRN =CUMSRN/(DT*REAL(FREQ2))
AVGSH =CUMSH/(DT*REAL(FREQ2))
AVGSE =CUMSE/(DT*REAL(FREQ2))
AVGSS =CUMSS/(DT*REAL(FREQ2))
AVGSG =CUMSG/(DT*REAL(FREQ2))

LDCALH =LDCALH+LOCALH
LDCALV =LDCALV+LOCALV
LDCALC =LDCALC+LOCALC

SDPREH =SDPREH+STPREH
SDPREV =SDPREV+STPREV
SDPREC =SDPREC+STPREC

SDPRHC =SDPRHC+STPRHC
SDPRVC =SDPRVC+STPRVC
SDPRCC =SDPRCC+STPRCC

CUDCRN =CUDCRN+CUMCRN
CUDTRN =CUDTRN+CUMTRN
CUDBRN =CUDBRN+CUMBRN

CUDTLE =CUDTLE+CUMTLE
CUDTQ =CUDTQ +CUMTQ
CUDTC =CUDTC+

CUDSRN =CUDSRN+CUMSRN
CUDSH =CUDSH +CUMSH
CUDSE =CUDSE +CUMSE
CUDSG =CUDSG +CUMSG
CUDSS =CUDSS +CUMSS

ITRM =1

C ! Updating the leaf temperatures (old = new)
DO 1495 I=1,ITA,1

```

```

DO 1496 J=1,2,1
DO 1497 K=1,2,1
IF(IPR(I,K,J).NE.0)THEN
  TEMPLF(I,1,K,J)= TEMLFN(I,1,K,J)
  TEMPLF(I,2,J,K)= TEMLFN(I,2,J,K)
ENDIF
1497 CONTINUE
1496 CONTINUE
1495 CONTINUE

3000 CONTINUE
COUNT =COUNT+1
CORR=MOD(COUNT,OUTPL)

C      !
      CALL RADBOU(DTEMP,IEAIR,WINDTP,WINDZ5,CLOUDN,
1      RLOUT,RLINN,WAYIN,CORR,MINUTE,T,TIMER)

      U(IHA+1) =WINDTP
      TEMAIR(IHA+1)= DTEMP
      EAIR(IHA+1) = IEAIR
      SHEAR      = WINDZ5/2.2

      IF ((GUST.EQ.1).AND.(SHEAR.GT.0.2)) THEN

        FLAG=4
        CALL FLUX(FLAG,
        :      TEMAIN,EAIRNW,NC02,
        :      STORAH,SH,SL,SINK,
        :      STORAV,STORAC,
        :      PCSOIL,VGAS,
        :      TOTALQ,TOTLE,TOTASE,TOTASQ,SOILLE,
        :      DT,TIMEW,SOILRN)

        CNLFGT= CNLFGT+ NLFLGT
        CNLFGV= CNLFGV+ NLFLGV
        CNLFGC= CNLFGC+ NLFLGC

        FLAG=0

        DO 4100 I=IHA+1,1,-1
          TEMAIR(I) =DTEMP
          EAIR(I)   =IEAIR
          CO2CON(I) =300.
4100 CONTINUE

        ELSE

          CO2CON(IHA+1) =300.

        ENDIF

        IF (CORR.EQ.0) THEN
          CLOSE(4)
        ENDIF

4000 CONTINUE

        AVD1TH =SDPREH/(AVGDLT*3600)
        AVD1TE =SDPREV/(AVGDLT*3600)
        AVD1TC =SDPREC/(AVGDLT*3600)

        AVD5TH =SDPRHC/(AVGDLT*3600)
        AVD5TE =SDPRVC/(AVGDLT*3600)
        AVD5TC =SDPRCC/(AVGDLT*3600)

        AVDTLE =CUDTLE/(AVGDLT*3600)
        AVDTQ  =CUDTQ /(AVGDLT*3600)
        AVDHL  =LDCALH/(AVGDLT*3600)
        AVDLE  =LDCALV/(AVGDLT*3600)
        AVDRN  =CUDCRN/(AVGDLT*3600)
        AVDTRN =CUDTRN/(AVGDLT*3600)
        AVDBRN =CUDBRN/(AVGDLT*3600)

        AVDSRN =CUDSRN/(AVGDLT*3600)
        AVDSH  =CUDSH/(AVGDLT*3600)
        AVDSLE =CUDSE/(AVGDLT*3600)
        AVDSS  =CUDSS/(AVGDLT*3600)
        AVDSG  =CUDSG/(AVGDLT*3600)

        RA=RA+AVGDLT

4500 CONTINUE

        DAYNUM = DAYNUM+1

        TMIN(1) = TMIN(2)
        RHMAX(1)= RHMAX(2)
        RHMIN(0)= RHMIN(1)

        READ(36,*) TMIN(2)

```

```

READ(36,*) TMAX
READ(36,*) RHMAX(2)
READ(36,*) RHMIN(1)
READ(36,*) RAINM

DECLIN  = -(23.45*RADE)*COS(RADE*(360*(DAYNUM+10)/365))
SINDE  = SIN(DECLIN)
DAYLNG  = 12.24 / PI * ASIN(TAN(LATI*RADE)*TAN(DECLIN))
NGHTLN  = 24.0 - DAYLNG
BTNOON  = PI/2 + DECLIN - LATI*RADE
SINNOON = SIN(BTNOON)
SUNSET  = 12 + 0.5*DAYLNG
BB      = 12 - 0.5*DAYLNG + C
TSN     = (TMAX - TMIN(2)) * SIN((PI*(DAYLNG - C))
1        / (DAYLNG + 2*P)) + TMIN(2)

TIME=0.0
START=TIME

1 CALL RADBOU(DTEMP, IEAIR, WINDTP, WINDZ5, CLOUDN,
  RLOUT, RLINN, WAYIN, CORR, MINUTE, T, TIMER)

U(IHA+1) = WINDTP
TEMAIR(IHA+1) = DTEMP
EAIR(IHA+1) = IEAIR
SHEAR      = WINDZ5/2.2

CLOSE(2)

IF ((GUST.EQ.1).AND. (SHEAR.GT.0.2)) THEN

DO 410 I=IHA+1,1,-1

  TEMAIR(I) = DTEMP
  FAIR(I)   = IEAIR
  CO2CON(I) = 300.

410 CONTINUE

ELSE

  CO2CON(IH+1) = 300.

ENDIF

COUNT = 0

5000 CONTINUE
6000 CONTINUE
7000 CONTINUE
1111 CONTINUE

END

CCCCCCCCCCCCCCCCCCCCCCCCCCCCCCCCCCCCCCCCCCCCCCCCCCCCCCCCCCCCCCCC
C
SUBROUTINE MOMNTH(ITRM,INDEXS,FLAG
:      ,DU
:      ,U,UNEW,LMIX,DRA,KM
:      ,ANAMOM,GRASH,NU,USTAR
:      ,TIME,SHEAR,SINBTA
:      ,RICHAR1,RICHAR2,PHIM1
:      ,PHIH1,RICHAR31,RICHAR32)
CCCCCCCCCCCCCCCCCCCCCCCCCCCCCCCCCCCCCCCCCCCCCCCCCCCCCCCCCCCCCCCC

IMPLICIT NONE
INTEGER ITRM

$INCLUDE:ALIMIT.FOR/L
$INCLUDE:ABLANK.FOR/L

C      ! These variable have a one to one correspondence with the Global Variables
C      ! within the Call statement of this subroutine.
INTEGER INDEXS,FLAG
REAL*8 DU(0:IH)

REAL U(0:ITB),UNEW(0:ITB),LMIX(1:2,0:IH),
1  DRA(0:ITB),KM(0:ITB),ANAMOM(1:IH)
REAL GRASH(0:IT), NU(0:IT)

REAL USTAR,TIME,SHEAR,SINBTA
REAL RICHAR1,RICHAR2,PHIM1,PHIH1
REAL RICHAR31,RICHAR32

CHARACTER T

```

CCCCC

```
C      ! Local variables needed for the subroutine calculation.
      INTEGER I,J,K,ILP,ITER,IHELP
      REAL UNON(1:5,0:IH)      ! wind speed nondimensionalized (ms-1)
      REAL UNEWK(1:5,0:IH)     ! Wind speed (ms-1)
      REAL SIGMAW(1:IH)        ! vertical velocity variance (ms-1)
      REAL TL(1:ITB)           ! Lagrangian integral time scale (s)
C
      REAL KMD(1:5,0:IH)       ! Km value calculated for every layer by 5 different
      REAL KMDD(1:5,0:IH)      ! assumptions
C
      ! Thomas Algorthin Coefficients for the momentum equation.
      REAL F(0:ITB)
      REAL G(0:ITB)
      REAL E(0:ITB)
      REAL D(0:ITB)
C
      REAL KARMEN,CD,FACTOR     ! Von Karmen constant, Drag Coefficient, Factor
      REAL N,DISPL,Z0           ! for quiescence respectively
      REAL C0,C1,C2             ! Displacement height(m) and Roughness length(m).
C
      REAL WSTAR,FLUXS,ALPHA,GR,ETA ! Empirical Coefficients for calculating vertical
      REAL HSTAR,DCLDSD,DIFF,DIFFER ! velocity variance,
      REAL SIGMAT,DLEAF         ! And Lagrangian integral time scale (Raupach ).
      REAL WEIGHT               ! w*, equivalent flux for the case of free convection
      REAL ESP                  ! within the plant canopy.
      REAL ERRMAX
C
      REAL HSTAR,DCLDSD,DIFF,DIFFER ! h* (height of the radiative sink at the canopy top at
      REAL SIGMAT,DLEAF         ! night)
      REAL WEIGHT               ! characteristic dimension of clods, molecular
      REAL ESP                  ! diffusivity for water.
      REAL ERRMAX
C
      REAL SIGMAT,DLEAF         ! temperature variance, Characteristic dimension of
      REAL WEIGHT               ! the leaf.
      REAL ESP                  ! A WEIGHTING FACTOR.
      REAL ERRMAX
C
      *****
C
      *****
      KARMEN = 0.41
      CD = 0.16
      ESP = 0.0000001
      N = 2.5
      DISPL = 0.63 *Z(ITA)
      Z0 = 0.25*(Z(ITA)-DISPL)
      DCLDSD = 0.05
      GR = 9.81
      ETA = 14.2E-6
      DIFF = 20.2E-6
      C0 = 0.25
      C1 = 1.25
      C2 = 0.3
      DLEAF = 0.05
      T=CHAR(9)
C
      ! The period after the gust intrusion, an increased turbulent transport
      ! coefficient is used.
      IF((INDEXS.EQ.1).AND.(SHEAR.GT.0.2)) THEN
      FLAG=3.0
C
      ! For other periods, a reduced turbulent transport coefficient is used according
      ! to Sect.3.6.2.
      ELSEIF (SHEAR.GT.0.2) THEN
      FACTOR =0.25
      FLAG=0
      ELSEIF (SINBTA.GE.0.) THEN
C
      RICAR31 = GR/(Z73+TEMAIR(22))
      1 *((TEMAIR(22)-TEMAIR(15))
C
      1 +0.38*((TEMAIR(22)+273.15)*EAIR(22)
C
      1 -(TEMAIR(15)+273.15)*EAIR(15))/10E5)
C
      1 /(2./4.*SHEAR**2)
C
      IF ((RICAR31.LT.0.25).AND.(ITRM.NE.0)) THEN
      THERE IS AN EJECTION
C
      FLAG =31
      DIFFER = TEMAIR(0)-TEMAIR(35)
C
      ELSE
```

```

FLAG= 1
DIFFER = TEMAIR(0)-TEMAIR(15)
C   ENDIF

ELSEIF (SINBTA. LT.0.) THEN
C   RICHA32 = GR/(273+TEMAIR(35))
C   1 *((TEMAIR(35)-TEMAIR(15))
C   1 +0.38*((TEMAIR(35)+273.15)*EAIR(35)
C   1 -(TEMAIR(15)+273.15)*EAIR(15))/10E5)
C   1 /(.74.*SHEAR**2)

C   IF ((RICHA32.LT.0.25).AND.(ITRM.NE.0)) THEN
C   THERE IS AN EJECTION
C   FLAG =32
C   DIFFER =TEMAIR(0) -TEMAIR(35)
C   ELSE
C   FLAG =2
C   DIFFER= TEMAIR(0)-TEMAIR(15)
C   ENDIF
C   ELSE
C   WRITE(26,*) 'THERE IS A MISTAKE LOOP '
C   ENDF
C   IF (FLAG.EQ.0) THEN
C   LMIX(1,0)=0
C   LMIX(2,0)=0
C   ! Mixing length determinations with the canopy (LI et al. (1985) and Goudriaan
C   ! (1977))
C   DO 300 I=1,ITA, 1
C   LMIX(1,I)= KARMEN * Z(I)/ (1.5 + 2.5 * LAD(I))
C   LMIX(2,I)= (4*DLEAF/(3.14*(LAD(I)+0.01)))**0.5
300 CONTINUE

C   DO 400 I = ITA+1 ,IHA
C   LMIX(1,I)= LMIX(1,ITA) + KARMEN
C   * (Z(I)-Z(ITA))/(1+0.015*(Z(I)-Z(ITA)))
C   LMIX(2,I) = KARMEN*(Z(I)-DISPL-Z0)
400 CONTINUE
901 CONTINUE
C   KMD(3,ITA) =LMIX(2,ITA)*USTAR
C   .....
C   WEIGHT =0.5
C   DO 1380, K=1,5,1
C   DO 1350 ITER=1,30,1
C   IF (ITER.GT.15) THEN
C   WEIGHT=1.0
C   ENDF
C   DU(0)= ABS(U(1)-U(0))/(0.5*DZ(1))
C   KMD(K,0)=0.0
C   DO 1400 I= 1,ITA,1
C   DU(I) = ABS(U(I+1)-U(I))
C   /(.5*(DZ(I+1)+DZ(I)))
C   KMD(1,I) = LMIX(1,I)**2*DU(I)*FACTOR
C   KMD(2,I) = LMIX(2,I)**2*DU(I)*FACTOR
C   KMD(3,I) =KMD(3,ITA)*EXP(-N *(1-Z(I)/Z(ITA)))
C   *FACTOR
C   KMD(4,I) = 0.3**2*FACTOR
C   SIGMAW(I) = USTAR*(C0+(C1-C0)*Z(I)/Z(ITA))
C   TL(I) = Z(ITA)/USTAR
C   1 *AMAX1(CZ,KARMEN*(Z(I)-DISPL-Z0)
C   1 / (C1**2*Z(ITA)))
C   KMD(5,I)=SIGMAW(I)**2*TL(I)*FACTOR
C   DRA(I)= CD * LADMID(I)* ABS(U(I))*DZ(I)
1400 CONTINUE

```



```

DO 1450 I=ITA+1,IHA,1
  DU(I) = ABS(U(I+1)-U(I))
  /(.5*(DZ(I+1)+DZ(I)))

  KMD(1,I) = LMIX(1,I)**2*DU(I)*FACTOR
  KMD(2,I) = LMIX(2,I)**2*DU(I)*FACTOR
  KMD(3,I) = LMIX(2,I)**2*DU(I)*FACTOR
  KMD(4,I) = 0.3**2*FACTOR

  SIGMAW(I) = C1*USTAR
  TL(I) = Z(ITA)/USTAR
  *AMAX1(C2,KARMEN*(Z(I)-DISPL-20)
  /((C1**2*Z(ITA)))
  KMD(5,I)=SIGMAW(I)**2*TL(I)*FACTOR

1450 CONTINUE
  DRA(I)= CD * LADMID(I)* ABS(U(I))*DZ(I)

  E(0)=0.0
  G(0)=0.0
  F(0)=1.0
  D(0)=0.0 ! THE BOUNDARY CONDITION FOR WIND.

DO 1401 I=1,IHA,1
  E(I)=KMD(K,I-1)/(.5*(DZ(I-1)+DZ(I)))
  G(I)=KMD(K,I)/(.5*(DZ(I)+DZ(I+1)))
  D(I)=0.0 *U(IHA+1)*Z(I)
  F(I)=E(I)+G(I)+DRA(I)

1401 CONTINUE

  E(IHA+1)=0.0
  G(IHA+1)=0.0
  F(IHA+1)=1.0
  D(IHA+1)=U(IHA+1)

CALL THOMM(IHA,E,G,D,F,UNEW)

DO 1700 I= 1, IHA,1
  UNEW(I) = (1- WEIGHT)* U(I) + WEIGHT* UNEW (I)
  UNEWK(K,I) = UNEW(I)

1700 CONTINUE

  ERRMAX=0.0

DO 1750 I=1,IHA,1
  ANAMOM(I)=-F(I)*UNEW(I)+G(I)*UNEW(I+1)
  + E(I)*UNEW(I-1)+D(I)

  ERRMAX = MAX(ERRMAX,ABS(ANAMOM(I)))

1750 CONTINUE

  IF(ERRMAX.GE. ESP) THEN
    DO 1800 IHELP=0,IHA+1,1
      U(IHELP) = UNEW(IHELP)
    CONTINUE

    GOTO 1350
  ENDIF

GOTO 1375
1350 CONTINUE

1375 CONTINUE

DO 1376 I=1,IHA,1
  UNON(K,I)= UNEWK(K,I)/USTAR ! OR CHECK
  KMDD(K,I) = KMD(K,I)

1376 CONTINUE

1380 CONTINUE
DO 1390 I=0,IHA,1

  KM(I) =KMD(5,I)

1390 CONTINUE

C !Calculating stability functions in case of no gust intrusion.
C !(shear at the canopy top .Le. 0.2)
ELSE
  RICHAR1= GR/(273+TEMAIR(30))
  *(TEMAIR(IHA+1)-TEMAIR(30))
  /(.2*(CU(IHA+1)-SHEAR*2.2)/2.5)**2)

  IF (RICHAR1. LE.-0.1) THEN
    PHIM1 = (1-16*RICHAR1)**(-0.25)
    PHIH1 = (1-16*RICHAR1)**(-0.5)
  ELSE
    RICHAR1 = AMIN1(0.199, RICHAR1)
    PHIM1 = (1-5*RICHAR1) ** (-1)
    PHIH1 = (1-5*RICHAR1) ** (-1)
  ENDIF

```

```

C      ! Grashof number determined for the top soil layer taking the temperature
C      ! difference over a large distance to avoid feedbacks within short timesteps to C
C      ! avoid possible
C      ! instabilities in the solution.
GRASH(0)= GR*DIFFER*DCLDLS**3/(273*ETA**2)
C      ! All the following formulas are taken from the appendix Of Monteith & Unsworth
C      ! (1990)
      IF (DIFFER.LT.0.0) THEN
C      ! Monteith & Unsworth (1990), Table A.5 formula (ii)
          NU(0) = 0.23* ABS(GRASH(0))**0.25
      ELSEIF (DIFFER.EQ.0.0) THEN
          DIFFER =0.2
          GRASH(0)= GR*DIFFER*DCLDLS**3/(273*ETA**2)
C      ! Monteith & Unsworth (1990), Table A.5 formula (i)
          NU(0) = 0.5 * GRASH(0)**0.25

      ELSEIF (GRASH(0) .LE. 10E5) THEN
C      ! Monteith & Unsworth (1990), Table A.5 formula (ii)
          NU(0) = 0.5 * GRASH(0)**0.25
      ELSE
C      ! Monteith & Unsworth (1990), Table A.5 formula (i)
          NU(0) =0.13*GRASH(0)**0.33
      ENDIF
C      ! Flux of heat calculated according to that difference
      FLUXS = NU(0)*ABS(DIFFER)*1200*DIFF/DCLDLS

C      ! W* calculated to Jacobs et al 1996
      WSTAR= (FLUXS*0.7*Z(ITA)*GR/(273.+TEMAIR(15)))**0.33
C      ! resulting vertical velocity variance
      SIGMAT= FLUXS/WSTAR

DO 2500 I=1,ITA,1
C      ! LAYER .EQ. 0.7 *Z(ITA)
C      ! An assumption
      UNEW(I) = WSTAR
C      ! Equating the flux in Jacobs et al (1996) to a gradient transport equation
C      ! in the calculation of Grashof number for the
C      ! soil layer, a use of temperature difference over ?? was used. This leads
C      ! also to slower feed back of the temperature of the air on the soil heat flux to
C      ! the air at night (stabilizing numerical effect).

      KM(I) = SIGMAT**1.5
      * (KARMEN*0.7*Z(ITA)*GR/(273.+TEMAIR(15)))**0.5
2500 1 * 0.15* 0.7*Z(ITA)/ABS(DIFFER)
      CONTINUE

C      ! Km above the canopy.
      DO 2600 I=ITA+1,IHA,1
          UNEW(I) = USTAR/KARMEN*(ALOG((Z(I)-DISPL)/ZO))
          KM(I) = KARMEN*USTAR*(Z(I)-DISPL)/PHIM1
2600 CONTINUE

      ENDIF

      IF ((CORR.EQ.0) .AND. (MINUTE.EQ.1)) THEN
          WRITE(2,*) '(1), ITER, I, Z(I), UNEW(I), UNON(I),
: LAD(I), ANAMOM(I), KM(I) '
          WRITE(2,*) ' U(0)=' ,U(0)
          WRITE(2,*) ' FLAG =', FLAG
          DO 1900 I=1,IHA,1

              IF (FLAG.EQ.0) THEN

                  WRITE(2,*) ITER,T,I,T,Z(I),T,
: UNON(1,I),T, UNON(2,I),T,UNON(3,I),T,
: UNON(4,I),T, UNON(5,I),T,
: LAD(I),T,ANAMOM(I),T,
: KMDD(1,I),T,KMDD(2,I),T,KMDD(3,I),T,KMDD(4,I),T,
: KMDD(5,I),T

                  ELSE

                  WRITE(2,*) I,T,Z(I),T,
: LAD(I),T,KM(I),T,UNEW(I),T

                  ENDIF

1900 CONTINUE

      ENDIF

      RETURN
      END

```

```

CCCCCCCCCCCCCCCCCCCCCCCCCCCCCCCCCCCCCCCCCCCCCCCCCCCCCCCCCCCC
C
  SUBROUTINE THDM(IHS,ISS,CT,BT,DT,AT,UNEWT)
C
  ! Thomas Algorithm Solution (according to Patankar 1980)
C
CCCCCCCCCCCCCCCCCCCCCCCCCCCCCCCCCCCCCCCCCCCCCCCCCCCCCCCCCCCC
  IMPLICIT NONE
  INTEGER IHS,ISS
  INTEGER I
$INCLUDE:ALIMIT.FOR/L
  REAL*8 AT(IS:ITB),BT(IS:ITB)
  REAL*8 CT(IS:ITB),DT(IS:ITB)
  REAL*8 P(IS:ITB),Q(IS:ITB)
  REAL*8 UNEWT(IS:ITB)
  REAL DENOM
C*****
C
C      Solution By Thomas Algorithm
C*****
      P(ISS)= BT(ISS)/AT(ISS)
      Q(ISS)= DT(ISS)/AT(ISS)
      DO 100 I=ISS+1,IHS+1
          DENOM =AT(I)-CT(I)*P(I-1)
          P(I) =BT(I)/DENOM
          Q(I) =-(DT(I)+CT(I)*Q(I-1))/DENOM
100      CONTINUE
          UNEWT(IHS+1) =Q(IHS+1)
          DO 200 I=IHS,ISS,-1
              UNEWT(I)= P(I)*UNEWT(I+1)+Q(I)
200      CONTINUE
          RETURN
      END
CCCCCCCCCCCCCCCCCCCCCCCCCCCCCCCCCCCCCCCCCCCCCCCCCCCCCCCCCCCC
C
  SUBROUTINE THOMS(ISS,CT,BT,DT,AT,UNEWT)
C
CCCCCCCCCCCCCCCCCCCCCCCCCCCCCCCCCCCCCCCCCCCCCCCCCCCCCCCCCCCC
  IMPLICIT NONE
  INTEGER IHS,ISS
  INTEGER I
$INCLUDE:ALIMIT.FOR/L
  REAL*8 AT(IS:0),BT(IS:0)
  REAL*8 CT(IS:0),DT(IS:0)
  REAL*8 P(IS:0),Q(IS:0)
  REAL*8 UNEWT(IS:0)
  REAL DENOM
C*****
C
      P(ISS) =-BT(ISS)/AT(ISS)
      Q(ISS) =-DT(ISS)/AT(ISS)
      DO 100 I=ISS+1,0
          DENOM =AT(I)-CT(I)*P(I-1)
          P(I) =BT(I)/DENOM
          Q(I) =-(DT(I)+CT(I)*Q(I-1))/DENOM
100      CONTINUE
          UNEWT(0)= Q(0)
          DO 200 I=-1,ISS,-1
              UNEWT(I)=P(I)*UNEWT(I+1)+Q(I)
200      CONTINUE
          RETURN
      END

```

```

CCCCCCCCCCCCCCCCCCCCCCCCCCCCCCCCCCCCCCCCCCCCCCCCCCCCCCCCCCCCCCCCCCCCCCCCCCCCCCCCCCCCCCCC
C
      SUBROUTINE THOMM(IHS,CT,BT,DT,AT,UNENT)
C
CCCCCCCCCCCCCCCCCCCCCCCCCCCCCCCCCCCCCCCCCCCCCCCCCCCCCCCCCCCCCCCCCCCCCCCCCCCCCCCCCCCCCCCC

      IMPLICIT NONE
      INTEGER I,IHS

$INCLUDE:ALIMIT.FOR/L

      REAL AT(0:ITB),BT(0:ITB)
      REAL CT(0:ITB),DT(0:ITB)

      REAL*8 P(0:ITB)
      REAL*8 Q(0:ITB)

      REAL UNENT(0:ITB)
      REAL DENOM

C-----

      P(0)= BT(0)/AT(0)
      Q(0)= DT(0)/AT(0)

      DO 100 I=1,IHS+1
          DENOM    =AT(I)-CT(I)*P(I-1)
          P(I)     =BT(I)/DENOM
          Q(I)     =(DT(I)+CT(I)*Q(I-1))/DENOM
100      CONTINUE

      UNENT(IHS+1)= Q(IHS+1)

      DO 200 I=IHS,0,-1
          UNENT(I)=P(I)*UNENT(I+1)+Q(I)
200      CONTINUE

      RETURN
      END

```

```

CCCCCCCCCCCCCCCCCCCCCCCCCCCCCCCCCCCCCCCCCCCCCCCCCCCCCCCCCCCCCCCCCCCCCCCCCCCCCCCCCCCCCCCC
C
      SUBROUTINE NORMN(IINI,DIRECT,SINBTA,TIME)
C
CCCCCCCCCCCCCCCCCCCCCCCCCCCCCCCCCCCCCCCCCCCCCCCCCCCCCCCCCCCCCCCCCCCCCCCCCCCCCCCCCCCCCCCC

      IMPLICIT NONE

$INCLUDE:ALIMIT.FOR/L
$INCLUDE:ABLANK.FOR/L
$INCLUDE:ANRNM.FOR/L

      SAVE / ANORMN /

      REAL IINI(2),DIRECT(1:2),SINBTA,TIME

      CHARACTER T

CCCCCC
C
      THIS SUBROUTINE CALCULATES THE SHORT WAVE
C
      RADIATION PROFILE WITHIN THE CANOPY
C
      ACCORDING NORMAN'S APPROACH (1979,1982)
C
      IMPLEMENTING GOUDRIAAN APPROACH TO CALCULATE
C
      THE NON-INTERCEPTION FACTORS, THE BARE
C
      BONES OF LEAF ANGLE DISTRIBUTION IN
C
      RADIATION MODELS. AGRICULTURAL AND FOREST
C
      METEOROLOGY 43 (1988) 155- 169.
C
      AUTHOR :RUSHDI EL-KILANI.
C
      DATE   : 17-10-1988.
C-----
C
      ... DATA ELEMENTS ...

      INTEGER I,J,K,L,RXITR,IHELP
      REAL OPR,X
      REAL KE(1:3,1:3)          ! ARRAY OF CALCULATED KEXT.
      REAL BSKY (1:3)          ! SKY ZONES ANGLES.
C
      REAL OPRO (1:3,1:3)      ! LEAF AREA PROJECTION FOR DIFFERENT ZONES OF
C
      REAL FQ(1:3)             ! THE SKY AND DIFFERENT LEAF ANGLE CLASSES.
C
      REAL IDL(1:IH)           ! FREQUENCY DISTRIBUTION OF LEAF AREA ON ANGLE CLASSES.
C
      REAL RxDWN(1:2,0:IH)    ! ID COEFFICIENTS IN NORMAN EQUATIONS EQ.2.2.7
C
      REAL RxDWN(1:2,0:IH)    ! RADIATION FLUX DOWNWELLING IN WAIT M-2
C
      REAL RxDWN(1:2,0:IH)    ! PER CANOPY LAYER SURFACE.
C
      REAL RxDWN(1:2,0:IH)    ! UPWELLING RADIATION FLUX .
C
      REAL RXUC(1:2,0:IH)     ! UPWELLING RADIATION FLUX (PREVIOUS ITER).
C
      REAL RxDN(1:2,0:IH)     ! DOWNWELLING RADIATION FLUX (PREVIOUS ITER).

```



```

DO 501 I=1,IHA,1
      ! ACCORDING TO NORMAN(1982)
TRANSM(I,1)= IDL(I)+ TRANLF(J)*IDL(I)*(-ALOG(IDL(I)))
:         + 0.5*TRANLF(J)**2*IDL(I)*(-ALOG(IDL(I)))**2
:         +(TRANLF(J)**3 *IDL(I)*(-ALOG(IDL(I)))**3)/6
:                                     !EQ. 2.2.10
RLAYER(I,1)= RXREF(J)*IDL(I)*(-ALOG(IDL(I)))
:         +0.5 * RXREF(J)**2*IDL(I)*(-ALOG(IDL(I)))**2
:         +(RXREF(J)**3 *IDL(I)*(-ALOG(IDL(I)))**3)/6
:                                     ! EQ. 2.2.9
ABSORB(I,1)=(1-SCATER(J))*(-ALOG(IDL(I)))
:         +0.5*SCATER(J)*(1-SCATER(J))*(-ALOG(IDL(I)))**2
:         +(RXREF(J)**2+TRANLF(J)**2
:         *(-ALOG(IDL(I)))**3/6
:         *(1-SCATER(J)))
TOTA(I,1)=TRANSM(I,1)+RLAYER(I,1)+ABSORB(I,1)
TURNER(I,1)=1./TOTA(I,1)
TRANSM(I,1)=TRANSM(I,1)*TURNER(I,1)
RLAYER(I,1)=RLAYER(I,1)*TURNER(I,1)
ABSORB(I,1)=ABSORB(I,1)*TURNER(I,1)

EKDL=IDL(I)**KH
      ! ACCORDING TO JAN GOUDRIAAN
      ! 26-9-1989
DEEL=(1.-RCROP*RCROP*EKDL**EKDL)
TRANSM(I,2)=EKDL*(1.-RCROP*RCROP)/DEEL
RLAYER(I,2)=RCROP*(1.-EKDL*EKDL)/DEEL
ABSORB(I,2)=(1.-TRANSM(I,2)-RLAYER(I,2))
TOTA(I,2)=TRANSM(I,2)+RLAYER(I,2)
TURNER(I,2)=1.0

RXUP(J,I)=0.0
RXU(J,I)=0.0
RXDN(J,I)=0.0

501 CONTINUE

RXUP(J,0) =0.0
RXU(J,0) =0.0
RXDN(J,0) =0.0
RXDWN(J,IH)=(1-DIRECT(J))*IINI(J)

DO 591 K=1,2,1
TOTALE=0.0
RXITR=0

DO 550 RXITR =1,100,1
DO 510 I=IHA,1,-1
RXDWN(J,I-1)=RXDWN(J,I)*TRANSM(I,K)
:         +RXUP(J,I-1)*RLAYER(I,K)
:         +RXDIR(J,I)*TRANLF(J)*(1-IBL(I))
:                                     ! EQ 3.9
510 CONTINUE

RXUP(J,0)=RXDWN(J,0)*SOILRF(J)
:         +RXDIR(J,0)*SOILRF(J)

DO 520 I=1,IHA,1
RXUP(J,I)=RXUP(J,I-1) * TRANSM(I,K)
:         +RXDWN(J,I)*RLAYER(I,K)
:         +RXDIR(J,I)*RXREF(J)*(1-IBL(I))
:                                     ! EQ 3.10
520 CONTINUE

DO 530 IHLP=0,IHA,1
IF ((ABS(RXUP(J,IHLP))-RXU(J,IHLP)).GE.EPP).OR.
: (ABS(RXDWN(J,IHLP))-RXDN(J,IHLP)).GE.EPP) THEN
DO 540 I=0,IHA,1
RXU(J,I)=RXUP(J,I)
RXDN(J,I)=RXDWN(J,I)
540 CONTINUE
GOTO 550
ENDIF

530 CONTINUE
GOTO 580

550 CONTINUE

```

```

580  CONTINUE
      IF (J.EQ.1) THEN
          TOTALE=0.0
      ENDIF

      DO 560 I=IHA,1,-1
          ! CALCULATE THE DIVERGENCE OF SHORT WAVE RADIATIVE FLUXES.
          RXDAB(J,I,2) = RXDIR(J,I)-RXDIR(J,I-1)
          RXDAB(J,I,1) = 0.0 ! FOR THE TIME BEING
                              ! MOSTLY CORRECT FOR
                              ! ONE DIMENSIONAL CASE
          RXABS(J,I,2) = RXDWN(J,I)-RXDWN(J,I-1)
          RXABS(J,I,1) = RXUP(J,I-1)-RXUP(J,I)

          RXABST(J,I,1)=RXDAB(J,I,1)+RXABS(J,I,1)
          RXABST(J,I,2)=RXDAB(J,I,2)+RXABS(J,I,2)

          ! SUMMING THE ABSORBED DIRECT AND DIFFUSE RADIATIONS
          ! FOR THE VISIBLE AND NIR BANDS.
          TOTALE=TOTALE+RXABST(J,I,1)+RXABST(J,I,2)
      DO 560  CONTINUE
591  CONTINUE
590  CONTINUE

      SOILSN= (RXDIR(1,0)+RXDWN(1,0))*(1.-SOILRF(1))
              +(RXDIR(2,0)+RXDWN(2,0))*(1.-SOILRF(2))

      DO 600 I=1,IHA,1
          LIGHT(I,2) =0.5*(RXDWN(2,1)+RXDWN(2,I-1))
                   +0.6*0.5*(RXDIR(2,1)+RXDIR(2,I-1))
          LIGHT(I,1) =0.5*(RXUP(2,I-1)+RXUP(2,I))
                   +0.6*0.5*(RXDIR(2,I)+RXDIR(2,I-1))

          ! AN AVERAGE VALUE IS TAKEN.
          ! A STRATIFICATION BY LEAF ANGLE CLASSES SHOULD BE MADE.
          VISIAB(I,1)= RXABST(2,I,1)
          VISIAB(I,2)= RXABST(2,I,2)
          ! ABSORBED VISIBLE RADIATION PER CANOPY LAYERS.
          ENESAB(I,1)= VISIAB(I,1)+ RXABST(1,I,1)
          ENESAB(I,2)= VISIAB(I,2)+ RXABST(1,I,2)
          ! ABSORBED SHORT WAVE RADIATION.
          RAB(I,1)= ENESAB(I,1)/DZ(I)
          RAB(I,2)= ENESAB(I,2)/DZ(I)
          ! ABSORBED SHORT WAVE ABSORBED PER M^3 CANOPY AIR.

          IF (LADMID(I).GT.0.0)THEN
              RABL(I,1)=RAB(I,1)/LADMID(I)
              RABL(I,2)=RAB(I,2)/LADMID(I)
          ! ABSORBED SHORT WAVE ABSORBED PER M^2 LEAF SURFACE.
          ELSE
              RABL(I,1)=0.0
              RABL(I,2)=0.0
          ENDIF
600  CONTINUE

      RNSHRT= RXDIR(1,IHA)-RXDIR(1,0)+RXDIR(2,IHA)-RXDIR(2,0)
              +RXDWN(1,IHA)-RXDWN(1,0)+RXUP(1,0)-RXUP(1,IHA)
              +RXDWN(2,IHA)-RXDWN(2,0)+RXUP(2,0)-RXUP(2,IHA)

      RNSTOP = RXDIR(1,IHA)+RXDIR(2,IHA)
              +RXDWN(1,IHA)-RXUP(1,IHA)
              -RXDWN(2,IHA)-RXUP(2,IHA)

      RNSBTM = -RXDIR(1,0)-RXDIR(2,0)
              +RXUP(1,0)+RXUP(2,0)
              -RXDWN(1,0)-RXDWN(2,0)

      TOTENE=0.0

      DO 700 I=IHA,1,-1
          TOTENE=TOTENE+ENESAB(I,1)+ENESAB(I,2)
700  CONTINUE

      RADERR=TOTENE-RNSHRT

      RETURN
      END

```

CC

```
SUBROUTINE CYCLE1(INIH,ITRA,PASS,
: TEMAIN,EAIRNW,NCO2,VGAS,EXTRAS,EXTRAL,
: PSISOL,AVGTLF,
: RLEAF,
: GAMMAT,FG,RAINM,
: PHIM,KRATIO,FE,WM,INDEXI,TEMPOR)
```

CC

IMPLICIT NONE

```
$INCLUDE:ACONST.FOR/L
$INCLUDE:ALIMIT.FOR/L
$INCLUDE:ABLANK.FOR/L
$INCLUDE:AENERG.FOR/L
$INCLUDE:AFLUX.FOR/L
$INCLUDE:ANRMN.FOR/L
$INCLUDE:ARDBOU.FOR/L
$INCLUDE:AROOTD.FOR/L
$INCLUDE:ACOEFF.FOR/L
$INCLUDE:AEQCOE.FOR/L
$INCLUDE:APLANT.FOR/L
$INCLUDE:ABERGE.FOR/L
$INCLUDE:AHYDRO.FOR/L
```

```
INTEGER ICHECK,I,ITR
INTEGER INDEXI(IS:IH)
```

```
REAL*8 TEMAIN(IS:ITB),EAIRNW(IS:ITB),NCO2(IS:ITB)
REAL*8 EXTRAS(IS:IH),EXTRAL(IS:IH),TEMPOR(IS:IH)
REAL SATVAP(IS:ITB),VPDAIR(IS:ITB)
```

```
REAL VGAS(IS:0)
```

```
REAL PSISOL(IS:0),AVGTLF(1:IT),RLEAF(IT,1:2)
REAL GAMMAT(1:IT),FG(1:IT,1:2)
REAL KRATIO(1:IH) ! KH/KM RATIO FOR THE LOCAL TERM.
REAL PHIM(1:IH) ! STABILITY CORRECTION FOR MOMENTUM
REAL FE(IS:IH)
REAL WM
REAL SATUV2,SATUD2,X
REAL RAINM
```

```
$INCLUDE:VALUES.DAT/L
```

```
DO 151 ITR=1,2,1
```

```
C ! Call HYDRO to calculate the solution of the soil water flow equation taking into
c ! account the sink terms in this equation due to water uptake by plant roots and
C ! the divergence of water vapour flux.
CALL HYDRO(INIH,TEMAIN,
: DT,VGAS,
: POR,SOILLE,SL,
: PSISOL,ROOTUP,RAINM,TIME)
```

```
C ! Call BERGE to calculate the soil Thermal Conductivity (Wm-1K-1) and soil thermal
C ! capacities (J M-3 K-1).
CALL BERGE(ISA,VGAS,THETA)
```

```
C ! Call PHOTO to calculate net Photosynthesis as a sink term in the Co2 Conservation
C ! equation
CALL PHOTO(ITRA,
: AVGTLF,
: RST,RB,RLEAF,
: VISIAB,GAMMAT,FG,SINK)
```

```
C ! Call EQCOEM to calculate the temperature of the different soil and canopy layers
C ! taking into account sources with the canopy and the soil ( water phase changes).
CALL EQCOEM(TEMAIN,SENFL,HMNEW,TORTU,RHSOIL,HM
: ,CHSOIL,PCSOIL,VGAS,VAPFLT,VAPFLB,VAPFDV
: ,EXTRAS,SOILRN,PASS,INDEXI)
```

```
C ! Call EQCOEM to calculate the vapour pressure and CO2 concentration for different
C ! canopy and soil layers.
CALL EQCOEM(TEMAIN,EAIRNW,NCO2
: ,HMNEW,HM,TORTU,RHSOIL
: ,VGAS,PHIM,KRATIO,FE
: ,EXTRAL,WM,SOILRN,PASS,INDEXI)
```

```
C !
CALL THOM(INA,ISA,ELE,GLE,DLE,FILE,EAIRNW)
CALL THOM(INA,ISA,ECO2,GC02,DC02,FC02,NCO2)
```

```
ICHECK =0
```

```
C ! A loop to check if any of the layers has an oversaturation and
C ! to correct back for this
DO 3102 I=ISA,IHA,1
```

```
SATVAP(I)=SATUV2(SNGL(TEMAIN(I)))
VPDAIR(I)=SATVAP(I)-SNGL(EAIRNW(I))
```

```
IF (VPDAIR(I).LT.0.0) THEN
```



```

        INDEXT(I)-1
    ENDIF
    IF (INDEXT(I).EQ.1) THEN
        DSDT(I) = SATUD2(SNGL(TEMAIN(I)))
        EXTRAS(I)=-PCP*VPDAIR(I)*DZ(I)
        / (DT*GAMMA)
        INDEXT(I)= 1
        ICHECK=1
    ELSE
        EXTRAS(I) =EXTRAS(I)
        EXTRAL(I) =EXTRAL(I)
    ENDIF
3102 CONTINUE
    IF (ICHECK.EQ.0) THEN
        GOTO 152
    ENDIF
151 CONTINUE
152 CONTINUE

    RETURN
    END

```

CC

```

SUBROUTINE BERGE(ISS,FA,W)
C      THIS SUBROUTINE IS TRANSLATED FROM AN CSMP PROGRAM WRITTEN BY
C      TEN BERGE IN HIS PH.D THESIS ( HEAT AND WATER TRANSPORT AT
C      THE BARE SOIL SURFACE) 1986 PAGE A17
CCCCCCCCCCCCCCCCCCCCCCCCCCCCCCCCCCCCCCCCCCCCCCCCCCCCCCCCCCCCCCCCCCCCCCCCCCCCCCCCCCCCCCCCCCCCCCCCCCCCCCCCCCCC

```

```

IMPLICIT NONE
INTEGER N,I,ISS

```

```

$INCLUDE:ALIMIT.FOR/L
$INCLUDE:ACONST.FOR/L
$INCLUDE:ABERGE.FOR/L

```

```

REAL FA(IS:0),W(IS:0)
REAL KFCSA(IS:0)
REAL KFSAC(IS:0)
REAL KFCSW(IS:0)
REAL KFSWC(IS:0)
REAL CHSL02(IS:0),CHSL05(IS:0)
REAL CHA,CHW,CHQ,CHC,CHO
REAL GA,GW,GQ,GC,GO
REAL KAW,KQW,KOW,KCW,KWA,KQA,KOA,KCA

```

```
CHARACTER T
```

```
$INCLUDE:VALUES.DAT/L
```

```

GA=0.05; GO=0.5; GW=0.14
GC=0.0; GQ=0.14
CHA=2.5E-2;CHC=2.92; CHQ=8.8
CHW=0.57; CHO=0.25

```

```
T=CHAR(9)
```

```

KAW =0.66/(1.+((CHA/CHW)-1.)*GA)+0.34/
: (1.+((CHA/CHW)-1.)*(1.-2*GA))
KQW =0.66/(1.+((CHQ/CHW)-1.)*GQ)+0.34/
: (1.+((CHQ/CHW)-1.)*(1.-2*GQ))
KOW =0.66/(1.+((CHO/CHW)-1.)*GO)+0.34/
: (1.+((CHO/CHW)-1.)*(1.-2*GO))
KCW =0.66/(1.+((CHC/CHW)-1.)*GC)+0.34/
: (1.+((CHC/CHW)-1.)*(1.-2*GC))
KWA =0.66/(1.+((CHW/CHA)-1.)*GW)+0.34/
: (1.+((CHW/CHA)-1.)*(1.-2*GW))

```

```

      KQA  =0.66/(1.+((CHQ/CHA)-1.)*GQ)+0.34/
:      (1.+((CHQ/CHA)-1.)*(1.-2*GQ))
      KOA  =0.66/(1.+((CHO/CHA)-1.)*GO)+0.34/
:      (1.+((CHO/CHA)-1.)*(1.-2*GO))
      KCA  =0.66/(1.+((CHC/CHA)-1.)*GC)+0.34/
:      (1.+((CHC/CHA)-1.)*(1.-2*GC))

DO 100 I=0,ISS,-1
  FA(I)  =1.-(FC(I)+FQ(I)+FO(I)+W(I))
  CHSL02(I)=1.25*(KWA*0.02*CHW+KOA*FO(I)*CHO+
:           KQA*FQ(I)*CHQ+KCA*FC(I)*CHC
:           +(POR(I)-0.02)*CHA)
:           /(KWA*0.02+KOA*FO(I)+KQA*FQ(I)
:           +KCA*FC(I)+(POR(I)-0.02))

  CHSL05(I)=(1.*0.05*CHW+KOW*FO(I)*CHO
:           +KQW*FQ(I)*CHQ+KCW*FC(I)*CHC
:           +KAW*(POR(I)-0.05)*CHA)
:           /(0.05+KOW*FO(I)+KQW*FQ(I)
:           +KAW*FC(I)+KAW*(POR(I)-0.05))

  KFCSA(I)=KOA*FO(I)*CHO+KQA*FQ(I)*CHQ
:           +KCA*FC(I)*CHC

  KFSA(I) =KOA*FO(I)+KQA*FQ(I)+KCA*FC(I)

  KFCSW(I)=KOW*FO(I)*CHO+KQW*FQ(I)*CHQ
:           +KAW*FC(I)*CHC

  KFSW(I)=KOW*FO(I)+KQW*FQ(I)+KAW*FC(I)
100 CONTINUE

DO 150 I=0,ISS,-1
  PCSOIL(I)= FC(I)*CCLAY+FQ(I)*CQUARZ
:           +FO(I)*CORGNC+W(I)*CWATER

  IF(W(I).LE.0.02) THEN
:     CHSOIL(I)=1.25*(CHW*W(I)*KWA+FA(I)*CHA+KFCSA(I))
:           /(KFSA(I)+KWA*W(I)+FA(I))

    CHSOIL(-3)=0.004

  ELSE IF (W(I).LE.0.05) THEN
:     CHSOIL(I)=CHSL02(I)
:           +(W(I)-0.02)*(CHSL05(I)-CHSL02(I))/0.03

  ELSE
:     CHSOIL(I)=W(I)*CHW+FA(I)*KAW*CHA+KFCSW(I)/
:           (W(I)+KAW*FA(I)+KFSW(I))

  ENDIF
150 CONTINUE

RETURN
END

```

```

CCCCCCCCCCCCCCCCCCCCCCCCCCCCCCCCCCCCCCCCCCCCCCCCCCCCCCCCCCCCCCCCCCCCCCCCCCCC
C

```

```

SUBROUTINE HYDRO(INIH,TEMAIN,
: DT,VGAS,
: POR,SOILLE,SL,
: PSISOL,ROOTUP,RAINM,TIME)

```

```

CCCCCCCCCCCCCCCCCCCCCCCCCCCCCCCCCCCCCCCCCCCCCCCCCCCCCCCCCCCCCCCCCCCCCCCCCCCC

```

```

IMPLICIT NONE
INTEGER INIH

```

```

$INCLUDE:ALIMIT.FOR/L
$INCLUDE:ABLANK.FOR/L
$INCLUDE:ACONST.FOR/L
$INCLUDE:AHYDRO.FOR/L

```

```

SAVE /ACONST/

```

```

REAL*8 TEMAIN(IS:ITB),SL(IB:IH)
REAL X(IS:0),Y(IS:0),NSON(IS:0),NSONN(IS:0),K(IS:0)

```

```

1 REAL VGAS(IS:0),
1 POR(IS:0),
1 PSISOL(IS:0),ROOTUP(IS:0)

```

```

REAL DT,SOILLE
REAL SATUV2,SATUD2
REAL RAINM,MOISTU,DIFFER,DIFFE1

```

```

CCCCC

```

```

INTEGER I,INDIC,J

```

```

REAL*8 PSISL(IS:0)
REAL S(IS:0) ! relative saturation.
REAL SPHASE(IS:0),WPHASE(IS:0)
REAL STT,CTT
REAL CPHASE(IS:0) !
REAL FE(IS:0) ! hydraulic conductivity at the intephase

REAL THETAD(IS:0) !moisture content difference between saturation and residual
REAL THETDP(IS:0) ! the same but at the interphase.
REAL THETRP(IS:0) ! residual at the interphase
REAL KWATE(IS:0) ! hydraulic conductivity
REAL ICSOIL(IS:0)
REAL CSOIL(IS:0) ! d(theta)/d(hm)
REAL THETR(IS:0) ! inverse of the above
REAL HMPR(IS:0)

```

```

c The coefficients of the discretized equation for water flow as given Appendix 2.11

```

```

REAL*8 CBLOCK(IS:ITB)
REAL*8 BBLOCK(IS:ITB)
REAL*8 DBLOCK(IS:ITB)
REAL*8 ABLOCK(IS:ITB)

```

```

CHARACTER T

```

```

CCCCCCC

```

```

$INCLUDE:VALUES.DAT/L

```

```

T=CHAR(9)
MP=1-1/NP

```

```

c ! If given Theta calculate according to the non commented part of the loop.

```

```

DO 20 I=ISA,0,1
  THETAD(I)= THETAS(I)-THETAR(I)
  S(I) = (1+(ABS(ALPHA*HM(I)))**NP)**(-MP)
  ! IF GIVEN HM(I) AND THETA(HM) FUNCTION
  S(I) = (THETA(I)-THETAR(I))/THETAD(I)

```

```

  IF(HYDRIN.EQ.1) THEN

```

```

    S(I) = (1+(ABS(ALPHA*HM(I)))**NP)**(-MP)
    ! IF GIVEN HM(I) AND THETA(HM) FUNCTION

```

```

  c IF(INIH.EQ.0) THEN

```

```

    HM(I)= -1/ALPHA*(S(I)**(-1/MP)-1)**(1/NP)

```

```

  c ENDIF

```

```

    CSOIL(I)=-1*THETAD(I)*
    (-MP)*(1+(ABS(ALPHA*HM(I)))**NP)**(-MP-1)
    *NP*(ABS(ALPHA*HM(I)))**(NP-1)*ALPHA
  endif

```

```

  THETA(I)=S(I)*THETAD(I)+THETAR(I) !NOT IF THETA IS GIVEN

```

```

  VGAS(I) =POR(I)-THETA(I)

```

```

20 CONTINUE

```

```

  SPHASE(ISA)=S(ISA)
  WPHASE(ISA)=THETA(ISA)

```

```

DO 30 I=ISA+1,-1,1
  WPHASE(I)=THETA(I)-DZ(I)
  *(THETA(I)-THETA(I+1))/(DZ(I)+DZ(I+1))

```

```

  THETDP(I)= THETAD(I)-DZ(I)
  *(THETAD(I)-THETAD(I+1))/(DZ(I)+DZ(I+1))

```

```

  THETRP(I)= THETAR(I)-DZ(I)
  *(THETAR(I)-THETAR(I+1))/(DZ(I)+DZ(I+1))

```

```

  SPHASE(I)=(WPHASE(I)-THETRP(I))/THETDP(I)

```

```

  IF (HYDRIN.EQ.1) THEN
    KWATER(I)=KSATU(I)*SPHASE(I)**LP
    *(1-(1-SPHASE(I))**(1/MP))**MP)**2
  endif

```

```

30 CONTINUE

```

```

  IF (HYDRIN.EQ.1) THEN

```

```

      KWATER(0)=KSATU(0)*S(0)**LP
:      * (1-(1-S(0))*(1/MP))**MP)**2
      ENDIF
IF (HYDRIN.NE.1) THEN
  DO 33 I= ISA,0,1
    NSON(I)=THETAS(I)/THETA(I)
    X(I) = ALOG10(NSON(I))
    K(I) = KUSA(INDES0(I),0)
:      +KUSA(INDES0(I),1)*THETA(I)
:      +KUSA(INDES0(I),2)*THETA(I)**2
:      +KUSA(INDES0(I),3)*THETA(I)**3
:      +KUSA(INDES0(I),4)*THETA(I)**4
:      +KUSA(INDES0(I),5)*THETA(I)**5
    KWATE(I)=((10.)**K(I))
    KWATE(I)=KWATE(I)*1.16E-7
    ICSOIL(I)=-HM(I)*(ALOG(10.))*
:      (HMC(INDES0(I),1)
:      +2*HMC(INDES0(I),2)*X(I)
:      +3*HMC(INDES0(I),3)*X(I)**2
:      +4*HMC(INDES0(I),4)*X(I)**3
:      +5*HMC(INDES0(I),5)*X(I)**4)/THETA(I)
    CSOIL(I)=1./ICSOIL(I)
33  CONTINUE
    KWATER(0) =KWATE(0)
    DO 36 I=ISA,-1,1
      FE(I) =DZ(I+1)/(DZ(I)+DZ(I+1))
      KWATER(I)=((1-FE(I))/KWATE(I)+FE(I)
1      /KWATE(I+1))**(-1)
36  CONTINUE
      ENDIF
      PSISOL(ISA)=HM(ISA)+Z(ISA)
      DO 34 I=ISA+1,0
        PSISOL(I)=HM(I)+ZCENTER(I)
34  CONTINUE
c      The coupling coefficients for the water flux equation.
      EW(ISA) =0.0 !lower
      GW(ISA) =0.0 !upper
      FW(ISA) =-1.0 ! for the layer (look at Patanker 1980)
      DW(ISA) =-PSISOL(ISA)
      DO 100 I=ISA+1,-1,1
        EW(I)=KWATER(I-1)/(0.5*(DZ(I-1)+DZ(I)))
        GW(I)=KWATER(I)/(0.5*(DZ(I)+DZ(I+1)))
        IF (INIH .EQ. 0) THEN
1          FW(I)=EW(I)+GW(I)
          +CSOIL(I)*DZ(I)/DT
          ! FIRST ASSUMPTION NO WATER PHASE CHANGES IN THE SOIL LAYERS
1          DW(I)=CSOIL(I)*DZ(I)/DT* PSISOL(I)
          -ROOTUP(I)
        ELSE
1          FW(I)=EW(I)+GW(I)
          +CSOIL(I)*DZ(I)/DT
1          DW(I)=CSOIL(I)*DZ(I)/DT* PSISOL(I)
          -ROOTUP(I)
1          -(SL(I)+VAPFDV(I))
1          /(LAMBDA*1000) ! FOR LATER USE
        ENDIF
c      !PER UNIT WEIGHT
100  CONTINUE
      EW(0)=KWATER(-1)/(0.5*(DZ(-1)+DZ(0)))
      GW(0)=0.0
      IF (INIH .EQ. 0) THEN
        FW(0)=EW(0)+GW(0)

```

```

1          +CSOIL(0)*DZ(0)/DT
          DW(0)=CSOIL(0)*DZ(0)/DT*PSISL(0)
1          -SOILLE/(LAMDA*1000)-ROOTUP(0)
          ELSE
          FW(0)=EW(0)+GW(0)
1          +CSOIL(0)*DZ(0)/DT
          DW(0)=CSOIL(0)*DZ(0)/DT*PSISL(0)
1          -SOILLE/(LAMDA*1000)
1          -ROOTUP(0)
1          -(SL(0)-VAPFLB(0))
1          /(LAMDA*1000) ! FOR LATER USE
          ENDIF
1000      CONTINUE

          CALL THOMS(ISA,EW,GW,DW,FW,PSISL)
          HMNEW(ISA)=REAL(PSISL(ISA))-Z(ISA)
          DO 40 I=ISA+1,0,1

          HMNEW(I) =REAL(PSISL(I))-ZCENTER(I)
          QWATER(I-1)=-EW(I)*(REAL(PSISL(I))
1          -REAL(PSISL(I-1)))
          C      QWATER(I-1)=-EW(I)*(PSISOL(I)
          C      -PSISOL(I-1))
          HMPR(I)=HM(I)
          THETR(I)=THETA(I)
40      CONTINUE
          HMPR(0) =HM(0)
          THETR(0) =THETA(0)
          QWATER(0) =0.0
          C      QWATER(ISA-1)
          C      IS NOT SPECIFIED, CAN BE COUPLED TO A REGIONAL HYDROLOGICAL MODEL.
          IF (HYDRIN.NE.1) THEN

          DO 59 I=ISA+1,0,1
          C      NEWTON _RAPHSON METHOD OF SOLUTION
          DO 10 J=1,10,1
          THETAN(I)=THETR(I)+(HMNEW(I)-HMPR(I))*CSOIL(I)
          NSONN(I)=THETAS(I)/THETAN(I)
          X(I) = ALOG10(NSONN(I))
          Y(I) = HMC(INDESO(I),0)
          :      +HMC(INDESO(I),1)*X(I)
          :      +HMC(INDESO(I),2)*X(I)**2
          :      +HMC(INDESO(I),3)*X(I)**3
          :      +HMC(INDESO(I),4)*X(I)**4
          :      +HMC(INDESO(I),5)*X(I)**5
          HMPR(I) =-(10.)*Y(I)/100.
          IF(INDESO(I).EQ.0) THEN
          HMPR(I)=HMPR(I)*20.
          ENDIF
          IF ((ABS(HMPR(I)-HMNEW(I))).GT.0.001) THEN
          ICSOIL(I)=-HMPR(I)*(ALOG(10.))*
          :      (HMC(INDESO(I),1)
          :      +2*HMC(INDESO(I),2)*X(I)
          :      +3*HMC(INDESO(I),3)*X(I)**2
          :      +4*HMC(INDESO(I),4)*X(I)**3
          :      +5*HMC(INDESO(I),5)*X(I)**4)/THETAN(I)
          CSOIL(I) =1./ICSOIL(I)
          THETR(I)=THETAN(I)
          ELSE
          GOTO 101
          ENDIF
10      CONTINUE
101     CONTINUE

```

```

59   CONTINUE
      ENDIF
      DO 60 I=ISA+1,-1,1
          IF (INIH. EQ. 0) THEN
              THETN(I)=THETA(I)
              +((QWATER(I-1)-QWATER(I))
              -ROOTUP(I))/DZ(I)*DT
1              ! FOR LATER USE
1              ELSE
              THETN(I)=THETA(I)
              +((QWATER(I-1)-QWATER(I))
              -ROOTUP(I))*DT/DZ(I)
              -(SL(I)+VAPFDV(I))*DT/DZ(I)
1              /(LAMDA*1000)
1              ! FOR LATER USE
          ENDIF
60   CONTINUE
      IF (INIH. EQ. 0) THEN
          THETN(0)=THETA(0)+((QWATER(-1)-QWATER(0))
1          -ROOTUP(0))*DT/DZ(I)
1          -SOILLE*DT
1          /(DZ(0)*LAMDA*1000.)
      ELSE
          THETN(0)=THETA(0)+((QWATER(-1)-QWATER(0))
1          -ROOTUP(0))*DT/DZ(I)
1          -SOILLE*DT
1          /(DZ(0)*LAMDA*1000.)
1          -(SL(0)+VAPFLB(0))*DT/DZ(0)
1          /(LAMDA*1000) ! FOR LATER USE
      ENDIF
      DO 53 I =ISA,0,1
          IF (THETAN(I).LT.THETAR(I)) THEN
              EW(I) = 0.0
              GW(I) = 0.0
              ROOTUP(I)=0.0
              FW(I)=1.0
              DW(I)=PSISOL(I)
              INDIC = 1
          ENDIF
53   CONTINUE
      IF (INDIC. EQ. 1) GOTO 1000
      INIH=1
      DO 70 I=ISA,0,1
          C      VGAS(I)      =POR(I)-THETN(I)
          C      VGAS(I)      =POR(I)-THETAN(I)
              TORTU(I)      = VGAS(I)**(10./3.)/POR(I)**2
1              RH5OIL(I)    =EXP(SNGL(PSISL(I))*GR*MOLE
              /(RR*(SNGL(TEMAIR(I))+273.15)))
70   CONTINUE
      IF ((TIME.GT.12.00).AND.(RAINM.GT.2.0).
1      AND.(RAINC.EQ.0))THEN
          MOISTU=0.0
          DO 80 I=0,ISA,-1
          C      If it rained , humidify the soil.
              MOISTU=MOISTU+AMAX1((0.2-THETAN(I)),0.0)*DZ(I)
              DIFFER=(RAINM*0.9)/1000.-MOISTU
          IF (DIFFER.GT.0.0) THEN
              THETAN(I)= AMAX1(0.2,THETAN(I))
              DIFFE1 = DIFFER
          ELSE
              THETAN(I)= THETAN(I)+
1              ((RAINM*0.9)/1000.-DIFFE1)/DZ(I)
              GOTO 1011

```



```

C*****
T=CHAR(9)
DO 100 I=1,ITA,1
    GM(I)=0.0
    GAMMAT(I)=GAMM25(1)*EXP(0.07*(AVGTLF(I)-25))
        ! IN PPM
C
IF ((AVGTLF(I).LE.2.5) .OR.(AVGTLF(I).GE.40)) THEN
    GM(I)=0.0
ELSE
    IF (AVGTLF(I).LE.30) THEN
        GM(I)= (AVGTLF(I)-2.5)/27.5* 0.005 ! IN M/S
        RM(I)= 1/GM(I)
    ELSE
        GM(I) = (40- AVGTLF(I))/10*0.005 ! IN M/S
        RM(I) = 1/GM(I)
    ENDIF
ENDIF
IF (GM(I).EQ. 0 ) THEN
    FNC(I,1)=0.0
    FN(I,1) =0.0
    FNC(I,2)=0.0
    FN(I,2) =0.0
ELSE
    FNC(I,1)=(CO2CON(I)-GAMMAT(I))*1.833/
        (RM(I)+1.3*RB(I)+1.6*RST(I,1))
    FNC(I,2)=(CO2CON(I)-GAMMAT(I))*1.833/
        (RM(I)+1.3*RB(I)+1.6*RST(I,2))
        ! IN MG PER SQUARE METER PER SECOND.
C
    FNMAX(I,1)= FMM(1) *(1-EXP (-FNC(I,1)/FMM(1)))
    FNMAX(I,2)= FMM(1) *(1-EXP (-FNC(I,2)/FMM(1)))
    RD(I)= RD20(1) *EXP(0.07*(AVGTLF(I)-20))
    FGMAX(I,1)= FNMAX(I,1)+0.5*RD(I)
    FGMAX(I,2)= FNMAX(I,2)+0.5*RD(I)
    EFF(I)= EFF0(1)*(CO2CON(I)-GAMMAT(I))/
        (CO2CON(I)+2*GAMMAT(I))
    H(I,1)= VISIAB(I,1)/(DZ(I)*LADMID(1))
    H(I,2)= VISIAB(I,2)/(DZ(I)*LADMID(I))
    FG(I,1)= FGMAX(I,1)
        *(1-EXP(-EFF(I)*H(I,1)/FGMAX(I,1)))
    FN(I,1)= FG(I,1) -0.5*RD(I)
    FG(I,2)= FGMAX(I,2)
        *(1-EXP(-EFF(I)*H(I,2)/FGMAX(I,2)))
    FN(I,2)= FG(I,2) -0.5*RD(I)
ENDIF
100 SINK(I)=(FN(I,1)+FN(I,2))*LADMID(I)*DZ(I)
CONTINUE
RETURN
END

```

```

C*****
C

```

```

SUBROUTINE EQCOEM(TEMAIN,EAIRNW,NC02
: ,HMNEW,HM,TORTU,RHSOIL
: ,VGAS,PHIM,KRATIO,FE
: ,EXTRAL,WM,SOILRN,PASS,INDEXI)

```

```

C*****
C

```

```

IMPLICIT NONE

```

```

$INCLUDE:ALIMIT.FOR/L
$INCLUDE:ABLANK.FOR/L
$INCLUDE:ACOEFF.FOR/L
$INCLUDE:AEQCOE.FOR/L
$INCLUDE:ACONST.FOR/L

```

```

SAVE/ ACOEFF/,/ACONST/,/AEQCOE/

```



```

C      1 +EXP(HMNEW(I)*GR*MOLE/(RR*(TEMAIN(I)+273.15)))
C      1 *SATUV2(SNGL(TEMAIR(I)))
C      1 *MOLE/(RR*(TEMAIN(I)+273.15))
C      1 *(HMNEW(I)-HM(I)))
C
C      SL(I)=PCP/GAMMA* DZ(I)/DT*VGAS(I)
C      1 *(RH5OIL(I)*DSDT(I)
C      1 *(TEMAIN(I)-TEMAIR(I)))
C      1 +EXP(HMNEW(I)*GR*MOLE/(RR*(TEMAIN(I)+273.15)))
C      1 *SATUV2(SNGL(TEMAIR(I)))
C      1 *MOLE/(RR*(TEMAIN(I)+273.15))
C      1 *(HMNEW(I)-HM(I)))
C
C      1 SH(I)=-PCP/GAMMA*DSDT(I)*DZ(I)/DT*VGAS(I)
C      1 *(TEMAIN(I)-TEMAIR(I))
C
C      ECO2(I)=0.0
C      GCO2(I)=0.0
C      FCO2(I)=1.0
C      DCO2(I)=CO2CON(I)
C      SINK(I)=0.0
C
C      ECO2(I)=DBLE(CO2DIF*TORTU(I))
C      GCO2(I)=DBLE(CO2DIF*TORTU(I))
C      FCO2(I)=DBLE(ECO2(I)+GCO2(I)+DZ(I)/DT*VGAS(I))
C      DCO2(I)=DBLE(VGAS(I)*DZ(I)/DT*CO2CON(I))
C      SINK(I)=0.0
C      SINK(I)=0.0 !LATER AFUNCTION DEPENDENT ON
C      SOIL TEMPERATURE
C
300    CONTINUE
C
C      IF (INDEXI(1). EQ.1) THEN
C
C      ELE(1) =0.0
C      GLE(1) =0.0
C      FLE(1) =1.0
C      DLE(1) =DBLE(SATUV2(SNGL(TEMAIN(1))))
C
C      ELSE
C
C      ELE(1) =0.0
C      GLE(1) =PCP/GAMMA*KH(1)/(0.5*(DZ(1)+DZ(2)))
C      FLE(1) =ELE(1)+GLE(1)+PCP/GAMMA*DZ(1)/DT
C      DLE(1) =DBLE(SL(1)+SOILLE
C      1 +PCP/GAMMA*DZ(1)/DT*EAIR(1))
C
C      DLE(1) =0.0
C      1 +PCP/GAMMA*DZ(1)/DT*EAIR(1)
C
C      ENDIF
C
C      ECO2(1)=DBLE(CO2DIF*TORTU(0)) ! AN AVERAGING HAS TO BE DONE
C      GCO2(1)=DBLE(KH(1)/(0.5*(DZ(1)+DZ(2))))
C      FCO2(1)=DBLE(ECO2(1)+GCO2(1)+DZ(1)/DT)
C      DCO2(1)=DBLE(-SINK(1)/1.833+DZ(1)/DT*CO2CON(1))
C      DCO2(1)=0.0/1.833+DZ/DT*CO2CON(1)
C
C
C      DO 500 I=2, IHA, 1
C
C      IF (INDEXI(I). EQ.1) THEN
C
C      ELE(I) =0.0
C      GLE(I) =0.0
C      FLE(I) =1.0
C      DLE(I) =DBLE(SATUV2(SNGL(TEMAIN(I))))
C
C      ELSE
C
C      ELE(I)=PCP/GAMMA*KH(I-1)/(0.5*(DZ(I-1)+DZ(I)))
C      GLE(I)=PCP/GAMMA*KH(I)/(0.5*(DZ(I)+DZ(I+1)))
C      FLE(I)=ELE(I)+GLE(I)+PCP/GAMMA*DZ(I)/DT
C      DLE(I)=DBLE(SL(I)+PCP/GAMMA*DZ(I)/DT*EAIR(I))
C
C      DLE(I)=0.0 +PCP/GAMMA*DZ(I)/DT*EAIR(I)
C
C      ENDIF
C
C      ECO2(I)=DBLE(KH(I-1)/(0.5*(DZ(I-1)+DZ(I))))
C      GCO2(I)=DBLE(KH(I)/(0.5*(DZ(I)+DZ(I+1))))
C      FCO2(I)=DBLE(ECO2(I)+GCO2(I)+DZ(I)/DT)
C      DCO2(I)=DBLE(-SINK(I)/1.833+DZ(I)/DT*CO2CON(I))
C      DCO2(I)=-0.0/1.833+DZ(I)/DT*CO2CON(I)
C
500    CONTINUE

```

```

      ELE(IHA+1)   =0.0
      GLE(IHA+1)   =0.0
      FLE(IHA+1)   =1.0
      DLE(IHA+1)   =EAIR(IHA+1)

      ECO2(IHA+1)  =0.0
      GCO2(IHA+1)  =0.0
      FCO2(IHA+1)  =1.0
      DCO2(IHA+1)  =CO2CON(IHA+1)

```

```

PASS =1
RETURN
END

```

```

CCCCCCCCCCCCCCCCCCCCCCCCCCCCCCCCCCCCCCCCCCCCCCCCCCCCCCCCCCCCCCCCCCCCCCCC
SUBROUTINE EQCOEH(TEMAIN,SENFL,HMNEW,TORTU,RHSOIL,HM
:      ,CHSOIL,PCSOIL,VGAS,VAPFLT,VAPFLB,VAPFDV
:      ,EXTRAS,SOILRN,PASS,INDEXI)
CCCCCCCCCCCCCCCCCCCCCCCCCCCCCCCCCCCCCCCCCCCCCCCCCCCCCCCCCCCCCCCCCCCCCCCC

```

```

      IMPLICIT NONE

$INCLUDE:ALIMIT.FOR/L
$INCLUDE:ABLANK.FOR/L
$INCLUDE:ACOEFF.FOR/L
$INCLUDE:AEQCOE.FOR/L
$INCLUDE:ACONST.FOR/L

      SAVE/ACOEFF/,/ACONST/,/AEQCOE/

      REAL*8 TEMAIN(IS:ITB),SENFL(IB:IH,1:2,1:2,1:2)
      REAL*8 EXTRAS(IS:IH)

      REAL CHSOIL(IS:0),PCSOIL(IS:0)
1     ,VGAS(IS:0)
      REAL HMNEW(IS:0),HM(IS:0)
      REAL RHSOIL(IS:0)
      REAL TORTU(IS:0)
      REAL VAPFLT(IS:0)
      REAL VAPFLB(IS:0)
      REAL VAPFDV(IS:0)

      REAL SATUV2,SATUD2,X
      INTEGER INDEXI(IS:IH)

      INTEGER PASS
      REAL SOILRN
      CHARACTER T

CCCCCC

      INTEGER I

      REAL CPHASE(IS:0)
      REAL FE(IS:IH)
      REAL ENHANC

```

```

CCCCCCCCCCCCCCCCCCCCCCCCCCCCCCCCCCCCCCCCCCCCCCCCCCCCCCCCCCCCCCCCCCCCCCCC
$INCLUDE:VALUES.DAT/L

      ENHANC =1.0
      T=CHAR(9)
      IF (PASS .EQ. 0) THEN
      DO 10 I=ISA,0,1
      VAPFDV(I)=0.0
10     CONTINUE
      DO 20 I=ISA,IHA,1
      EXTRAS(I)=0.0
      INDEXI(I)=0
20     CONTINUE
      ENDIF

      DO 50 I=ISA,-1,1
      FE(I)      =DZ(I+1)/(DZ(I)+DZ(I+1))
      CPHASE(I)  =(C1-FE(I))/CHSOIL(I)+FE(I)

```

```

C      1      CPHASE(I)      /CHSOIL(I+1)**(-1)
      =FE(I)*CHSOIL(I)+(1-FE(I))*CHSOIL(I+1)

50      CONTINUE

      ! THE TREATMENT OF THE BOUNDARY CONDITIONS

EH(ISA) =0.0
GH(ISA) =0.0
FH(ISA) =1.0
DH(ISA) =TEMAIR(ISA)

C      HERE DEFINE CPHASE

DO 100 I=ISA+1,-1,1

      EH(I)=CPHASE(I-1)/(0.5*(DZ(I-1)+DZ(I)))
      GH(I)=CPHASE(I)/(0.5*(DZ(I)+DZ(I+1)))
      DSDT(I)=SATUD2(SNGL(TEMAIR(I)))

      FH(I)=EH(I)+GH(I)
1      +PCSOIL(I)*DZ(I)/DT
1      +PCP/GAMMA*DZ(I)/DT*VGAS(I)
1      *(RHSOIL(I)*DSDT(I)
1      +EXP(HMNEW(I)*GR*MOLE/(RR*(TEMAIR(I)+273.15)))
1      *DSDT(I)
1      *MOLE/(RR*(TEMAIR(I)+273.15))
1      *GR*(HMNEW(I)-HM(I)))

      DH(I)=DBLE(PCSOIL(I)*DZ(I)/DT*TEMAIR(I)
1      -VAPFDV(I)
1      +PCP/GAMMA*DZ(I)/DT*VGAS(I)
1      *(TEMAIR(I)*RHSOIL(I)*DSDT(I)
1      -EXP(HMNEW(I)*GR*MOLE/(RR*(TEMAIR(I)+273.15)))
1      *(SATUV2(SNGL(TEMAIR(I)))-DSDT(I)*TEMAIR(I))
1      *MOLE/(RR*(TEMAIR(I)+273.15))
1      *GR*(HMNEW(I)-HM(I))))

100     CONTINUE

DO 150 I=1,IHA,1

C      KH(I)= (LMIX(I)/PHIM(I)*KRATIO(I))**2*DU(I)
      KH(I)= KM(I)

150     CONTINUE

C      EH(0)      =CPHASE(-1)/(0.5*(DZ(-1)+DZ(0)))
      GH(0)      =0.0      ! THE SOIL IS COMPLETELY DECOUPLED.
      GH(0)      =HT(0)    ! DEPENDING ON ONE ASSUMPTION.

      DSDT(0)    =SATUD2(SNGL(TEMAIR(0)))

      FH(0)=EH(0)+GH(0)
1      +PCSOIL(0)*DZ(0)/DT
1      +PCP/GAMMA*DZ(0)/DT*VGAS(0)
1      *(RHSOIL(0)*DSDT(0)
1      +EXP(HMNEW(0)*GR*MOLE/(RR*(TEMAIR(0)+273.15)))
1      *DSDT(0)
1      *MOLE/(RR*(TEMAIR(0)+273.15))
1      *GR*(HMNEW(0)-HM(0)))

C      DH(0)= DBLE(PCSOIL(0)*DZ(0)/DT*TEMAIR(0)
C      +0.0*DSDT(0)*TEMAIR(0))
C

1      DH(0)= DBLE(PCP/GAMMA*DZ(0)/DT*VGAS(0)
1      *(TEMAIR(0)*RHSOIL(0)*DSDT(0)
1      -EXP(HMNEW(0)*GR*MOLE/(RR*(TEMAIR(0)+273.15)))
1      *(SATUV2(SNGL(TEMAIR(0)))-DSDT(0)*TEMAIR(0))
1      *MOLE/(RR*(TEMAIR(0)+273.15))
1      *GR*(HMNEW(0)-HM(0)))
1      +SOILRN
1      -SOILLE
1      -VAPFLB(0)
1      +PCSOIL(0)*DZ(0)/DT*TEMAIR(0))

C      EH(1)=HT(0)
      EH(1)=0.0
      GH(1)=PCP*KH(1)/(0.5*(DZ(1)+DZ(2)))
      FH(1)=EH(1)+GH(1)+PCP*DZ(1)/DT
      DH(1)=DBLE(SH(1)+PCP*DZ(1)/DT*TEMAIR(1)
1      + EXTRAS(1))
C      DH(1)=0.0 +PCP*DZ(1)/DT*TEMAIR(1)

DO 400 I=ITA+1,IHA,1

      SH(I)      =0.0
      SL(I)      =0.0

```

```

400 CONTINUE
DO 200 I=2, IHA, 1
    EH(I)=PCP*KH(I-1)/(0.5*(DZ(I-1)+DZ(I)))
    GH(I)=PCP*KH(I)/(0.5*(DZ(I)+DZ(I+1)))
    FH(I)=EH(I)+GH(I)+PCP*DZ(I)/DT
    DH(I)=DBLE(SH(I)+PCP*DZ(I)/DT*TEMAIR(I)
1      +EXTRAS(I))
C      DH(I)=0.0+PCP*DZ(I)/DT*TEMAIR(I)
200 CONTINUE
    EH(IHA+1) =0.0
    GH(IHA+1) =0.0
    FH(IHA+1) =1.0
    DH(IHA+1) =TEMAIR(IHA+1)
CALL THOM(IHA, ISA, EH, GH, DH, FH, TEMAIN)
DO 300 I=ISA+1, 0, 1
    SH(I)=-PCP/GAMMA*DZ(I)/DT*VGAS(I)
1    *(RHSOIL(I)*DSDT(I)
1    *(TEMAIN(I)-TEMAIR(I))
1    +EXP(HMNEW(I)*GR*MOLE/(RR*(TEMAIN(I)+273.15)))
1    *SATUV2(SNGL(TEMAIN(I)))
1    *MOLE/(RR*(TEMAIN(I)+273.15))
1    *GR*(HMNEW(I)-HM(I)))
    SL(I)= PCP/GAMMA*DZ(I)/DT*VGAS(I)
1    *(RHSOIL(I)*DSDT(I)
1    *(TEMAIN(I)-TEMAIR(I))
1    +EXP(HMNEW(I)*GR*MOLE/(RR*(TEMAIN(I)+273.15)))
1    *SATUV2(SNGL(TEMAIN(I)))
1    *MOLE/(RR*(TEMAIN(I)+273.15))
1    *GR*(HMNEW(I)-HM(I)))
    IF (I.NE. 0) THEN
VAPFLT(I)= ENHANC*PCP/GAMMA*VAPDIF*TORTU(I)*
1    (SATUV2(SNGL(TEMAIN(I))))
1    *EXP(HMNEW(I)*GR*MOLE/(RR*(TEMAIN(I)+273.15)))
1    -SATUV2(SNGL(TEMAIN(I+1)))
1    *EXP(HMNEW(I+1)*GR*MOLE/(RR*(TEMAIN(I+1)+273.15)))
1    /(DZ(I)+DZ(I+1))
VAPFLB(I)= ENHANC*PCP/GAMMA*VAPDIF*TORTU(I-1)*
1    (SATUV2(SNGL(TEMAIN(I-1))))
1    *EXP(HMNEW(I-1)*GR*MOLE/(RR*(TEMAIN(I-1)+273.15)))
1    -SATUV2(SNGL(TEMAIN(I)))
1    *EXP(HMNEW(I)*GR*MOLE/(RR*(TEMAIN(I)+273.15)))
1    /(DZ(I-1)+DZ(I))
VAPFDV(I)=VAPFLT(I)-VAPFLB(I)
    ELSE
VAPFLT(I) = SOILLE
VAPFLB(I)= ENHANC*PCP/GAMMA*VAPDIF*TORTU(I-1)*
1    (SATUV2(SNGL(TEMAIN(I-1))))
1    *EXP(HMNEW(I-1)*GR*MOLE/(RR*(TEMAIN(I-1)+273.15)))
1    -SATUV2(SNGL(TEMAIN(I)))
1    *EXP(HMNEW(I)*GR*MOLE/(RR*(TEMAIN(I)+273.15)))
1    /(DZ(I-1)+DZ(I))
VAPFDV(I)= VAPFLT(I)-VAPFLB(I)      !IN JOULE M-2 S-1
    ENDF
300 CONTINUE
RETURN
END

```



```

C      REAL LWLEFI(1:IT,1:2,1:2)      ! LEAF SURFACE (ONE SIDE) LINEAR SOLUTION.
C      REAL NORMAN(1:IT,1:2)          ! LONG WAVE EMISSION (ONE SIDE) IN WATT M-2
C      REAL ESTLFF(1:IT,1:2,1:2,1:2) ! LEAF SURFACE. LINEAR SOLUTION.
C      REAL ESTLFF(1:IT,1:2,1:2,1:2) ! LONG WAVE FLUX DENSITY (UPWELLING AND
C      REAL ESTLFF(1:IT,1:2,1:2,1:2) ! DOWNWELLING) INCREMENTS IN WATT M-2
C      REAL ESTLFF(1:IT,1:2,1:2,1:2) ! CANOPY LAYER SURFACE.
C      REAL ESTLFF(1:IT,1:2,1:2,1:2) ! SATURATED VAPOUR PRESSURE AT LEAF
C      REAL ESTLFF(1:IT,1:2,1:2,1:2) ! TEMPERATURE IN PASCAL.

REAL CONDUV(1:IT,1:2,1:2)      ! vertical heat conduction
REAL CONDUH(1:IT,1:2,1:2,1:2) ! horizontal heat conduction
REAL SUM(1:IT,1:2)
REAL ERR(1:IT,1:2,1:2,1:2)    ! ERROR (LINEAR AND NEWTON ITERATION)
C      REAL ERR3(1:IT,1:2,1:2,1:2)    ! ERROR (LINEAR AND NEWTON ITERATION)

REAL ERROL(1:IT)
REAL WAMOUN(1:IT,2)           ! water amount
REAL DRIP(1:IT,2)            ! dripping
REAL VOLUMN(1:IT,2)          ! water volume
C      REAL REMAIN(1:IT,1:2,1:2,1:2)    ! REMAINING COMPONENT.

REAL TEMSKY                   ! TEMPERATURE OF THE SKY
REAL SKYEMS                   ! SKY EMISSIVITY
REAL CLEARS                   !
REAL TEMDIF                   ! TEMPERATURE DIFFERENCE.
REAL FACTOR                   !
REAL SKYLIN                   ! INCOMING LONGWAVE RADIATION FROM THE SKY
REAL TOTLE,TOTALQ

REAL TOTPRO(1:IT)            ! total probability
REAL ITOTPR(1:IT)           ! probability (yes 1 or no 0)

REAL CONVER
REAL ESPP                     ! THE FULFILLED CRITERIA.
REAL KCON
REAL MAXSH
DATA TEMDIF/2.0/
DATA FACTOR/0.1/             ! A FACTOR DEPENDENT ON THE TYPE OF CLOUDS.

```

.....

\$INCLUDE:VALUES.DAT/L

```

KCON   =273.15                ! CONVERTING TO ABSOLUTE TEMPERATURE

ESPP   =0.0001
MAXERR =0.0
MAXER1 =0.0

T      =CHAR(9)

LA     =0
LL     =2
LB     =LL+1

IF (ITRA.LT.1) THEN
  CHECK=0
  CHOICE=0
  IF (CHOICE.EQ.0) THEN
    MS1=0
    MS2=0
  ELSE IF(CHOICE .EQ.1) THEN
    MS1=1
    MS2=0
  ELSE IF(CHOICE.EQ.2) THEN
    MS1=0
    MS2=1
  ELSE
    MS1=1
    MS2=2
  ENDIF
DO 111 I=1,IFA,1
DO 112 J=1,2,1
DO 113 K=1,2,1

```

```

        TEMPLF(I,1,K,J) =SNGL(TEMAIR(I))
        TEMPLF(I,2,J,K) =SNGL(TEMAIR(I))
        TEMLFN(I,1,K,J) =SNGL(TEMAIR(I))
        TEMLFN(I,2,J,K) =SNGL(TEMAIR(I))

        ESTLFF(I,1,K,J) =SNGL(EAIR(I))
        ESTLFF(I,2,J,K) =SNGL(EAIR(I))

        ESTLFI(I,1,K,J) =SNGL(EAIR(I))
        ESTLFI(I,2,J,K) =SNGL(EAIR(I))

        LWLFN(I,1,K,J) =0.0
        LWLFN(I,2,J,K) =0.0
        NONST(I,1,K,J) =0.0
        NONST(I,2,J,K) =0.0
113      CONTINUE
112      CONTINUE
111      CONTINUE

DO 211 I=1,ITA,1
DO 212 J=1,2,1
        CUMDWA(I,J)= CUMDEW(I,J)/(LEAINC(I)*LAMDA)
        VOLUMD(I,J)= PI*RDIR(I,J)**2*WFTH(J)
        NUMDRP(I,J)= CUMDWA(I,J)/(VOLUMD(I,J)*1000.)
        FRAC(I,J,2)= CUMDWA(I,J)/(1000.*WFTH(J))

        IF (FRAC(I,J,2) .LT. 0.0001) THEN

                INDEXD(I,J,2) =0
                INDEXD(I,J,1) =1
                FRA(I,J,2) =0.000
                FRA(I,J,1) =1.000

        ELSE IF(FRAC(I,J,2).GE.1) THEN

                INDEXD(I,J,2) =1
                INDEXD(I,J,1) =0
                FRA(I,J,1) =0.000
                FRA(I,J,2) =1.000

        ELSE

                INDEXD(I,J,1) =1
                INDEXD(I,J,2) =1
                FRA(I,J,1) =FRA(I,J,1)
                FRA(I,J,2) =FRA(I,J,2)

        ENDIF
212      CONTINUE

        PR(I,1,1)= FRA(I,1,1)*FRA(I,2,1)
        PR(I,1,2)= FRA(I,1,1)*FRA(I,2,2)
        PR(I,2,1)= FRA(I,1,2)*FRA(I,2,1)
        PR(I,2,2)= FRA(I,1,2)*FRA(I,2,2)
        IPR(I,1,1)= INDEXD(I,1,1)*INDEXD(I,2,1)
        IPR(I,1,2)= INDEXD(I,1,1)*INDEXD(I,2,2)
        IPR(I,2,1)= INDEXD(I,1,2)*INDEXD(I,2,1)
        IPR(I,2,2)= INDEXD(I,1,2)*INDEXD(I,2,2)

211      CONTINUE

DO 200 I=1,ITA,1
        ID(I)= 0.25*EXP(-KAV(1)*LEAINC(I))
1         +0.5*EXP(-KAV(2)*LEAINC(I))
1         +0.25*EXP(-KAV(3)*LEAINC(I))

        LWAIR(I)= EMISSIV*SBOLTZ
1         *(TEMAIR(I)+273.15)**4

        ESTAIR(I)=SATUV2(SNGL(TEMAIR(I)))
C        EAIR(I)=ESTAIR(I)          !DDDDDDDDDDDDDD
        SSAIR(I)=SATUD2(SNGL(TEMAIR(I)))

DO 201 J=1,LL,1
        LEAFLT(I,J)= THICKN/REAL(LL)

201      CONTINUE
200      CONTINUE

DO 155 I=1,ITA,1

```



```

DO 153 J=1,2,1
DO 154 K=1,2,1

      IF(IPR(I,K,J). NE.0) THEN

          TEMPLF(I,1,K,J)=-273.10
          ESTLFF(I,1,K,J)=0.0
          SSLEAF(I,1,K,J)=0.0

          TEMPLF(I,2,J,K)=-273.10
          ESTLFF(I,2,J,K)=0.0
          SSLEAF(I,2,J,K)=0.0

          DO 169 INTERS=1,10,1

              ELH(0)=0.0
              GLH(0)=0.0
              FLH(0)=1.00
              DLH(0)=TEMAIR(I)

              ELH(1)= HT(I)
C          ELH(1)=0.0          !NO COUPLING DDD0DDD

              GLH(1)= 4*EMSSIV*SBOLTZ
1              *(0.5*(TEMPLF(I,1,K,J)+TEMPLF(I,2,J,K)))
1              +273.15)**3
1              +KW/(0.5*(LEAFLT(I,1)+LEAFLT(I,2)))

              DLH(1)= RABL(I,1)
1              -HE(I,1,K)*(ESTLFF(I,1,K,J)-EAIR(I))
1              -EMSSIV*SBOLTZ*(TEMPLF(I,1,K,J)+273.15)**4
1              +(4*EMSSIV*SBOLTZ*(TEMPLF(I,1,K,J)+273.15)**3
1              +HE(I,1,K)*SSLEAF(I,1,K,J))*TEMPLF(I,1,K,J)

              FLH(1)=ELH(1)+GLH(1)
1              +HE(I,1,K)*SSLEAF(I,1,K,J)
1              +4*EMSSIV*SBOLTZ*(TEMPLF(I,1,K,J)+273.15)**3

              ELH(LL) = 4*EMSSIV*SBOLTZ*
1              (0.5*(TEMPLF(I,LL,J,K)+TEMPLF(I,LL-1,K,J))
1              +273.15)**3
1              +KW/(0.5*(LEAFLT(I,LL-1)+LEAFLT(I,LL)))

              GLH(LL) = HT(I)

              DLH(LL)= RABL(I,2)
1              -HE(I,2,J)*(ESTLFF(I,2,J,K)-EAIR(I))
1              -EMSSIV*SBOLTZ*(TEMPLF(I,2,J,K)+273.15)**4
1              +(4*EMSSIV*SBOLTZ*(TEMPLF(I,2,J,K)+273.15)**3
1              +HE(I,2,J)*SSLEAF(I,2,J,K))*TEMPLF(I,2,J,K)

              FLH(LL) = ELH(LL)+GLH(LL)+HE(I,2,J)*SSLEAF(I,2,J,K)
1              +4*EMSSIV*SBOLTZ*(TEMPLF(I,2,J,K)+273.15)**3

              ELH(LL+1) = 0.0
              GLH(LL+1) = 0.0
              FLH(LL+1) = 1.00
              DLH(LL+1) = TEMAIR(I)

              DO 158 N=0, LB, 1

                  CBLOCK(N) = ELH(N)
                  BBLOCK(N) = GLH(N)
                  ABLOCK(N) = FLH(N)
                  DBLOCK(N) = DLH(N)

158          CONTINUE

          CALL THOM(LL, LA, CBLOCK, BBLOCK, DBLOCK, ABLOCK, TMLF)

          TEMLFN(I,1,K,J)=TMLF(1)

C          DO 160 N=2, LL-1, 1
C              TEMLFN(I,N,J)=TMLF(N)
C160          CONTINUE

          TEMLFN(I,LL,J,K)=TMLF(LL)

          DO 555 N =1,2,1

              ANALG(N)=- FLH(N)*TMLF(N)+GLH(N)*TMLF(N+1)
              +ELH(N)*TMLF(N-1)+DLH(N)

```

```

555      CONTINUE

      FLUXUP(I,1,K,J)=GLH(1)*(TEMLFN(I,1,K,J)-TEMLFN(I,2,J,K))
      FLUXBT(I,1,K,J)=-ELH(1)*(TEMLFN(I,1,K,J)-SNGL(TEMAIR(I)))
      SOURC(I,1,K,J)=RABL(I,1)
1      -HE(I,1,K)*(ESTLFF(I,1,K,J)-EAIR(I))
1      -EMSSIV*SBOLTZ*(TEMLP(I,1,K,J)+273.15)**4
      LINEAR(I,1,K,J)=(HE(I,1,K)*SSLEAF(I,1,K,J)
1      +4*EMSSIV*SBOLTZ*(TEMLP(I,1,K,J)+273.15)**3)
1      *(TEMLFN(I,1,K,J)-TEMLP(I,1,K,J))

      TOTALL(I,1,K,J)=-LINEAR(I,1,K,J)-FLUXUP(I,1,K,J)
1      +FLUXBT(I,1,K,J)+SOURC(I,1,K,J)

      FLUXUP(I,2,J,K)=GLH(2)*(TEMLFN(I,2,J,K)-SNGL(TEMAIR(I)))
      FLUXBT(I,2,J,K)=-ELH(2)*(TEMLFN(I,2,J,K)-TEMLFN(I,1,K,J))
      SOURC(I,2,J,K)=RABL(I,2)
1      -HE(I,2,J)*(ESTLFF(I,2,J,K)-EAIR(I))
1      -EMSSIV*SBOLTZ*(TEMLP(I,2,J,K)+273.15)**4
      LINEAR(I,2,J,K)=(HE(I,2,J)*SSLEAF(I,2,J,K)
1      +4*EMSSIV*SBOLTZ*(TEMLP(I,2,J,K)+273.15)**3)
1      *(TEMLFN(I,2,J,K)-TEMLP(I,2,J,K))

      TOTALL(I,2,J,K)=-LINEAR(I,2,J,K)-FLUXUP(I,2,J,K)
1      +FLUXBT(I,2,J,K)+SOURC(I,2,J,K)

      TOTAE(I,K,J)=TOTALL(I,1,K,J)+TOTALL(I,2,J,K)
1      MAXERR=MAX(MAXERR,ABS(TOTALL(I,1,K,J))
      ,ABS(TOTALL(I,2,J,K)),ABS(TOTAE(I,K,J)))

      ESTLFF(I,1,K,J)=
1      SATUVZ(TEMLFN(I,1,K,J))

      SSLEAF(I,1,K,J)=
1      SATUDZ(TEMLFN(I,1,K,J))

      ESTLFF(I,2,J,K)=
1      SATUVZ(TEMLFN(I,2,J,K))

      SSLEAF(I,2,J,K)=
1      SATUDZ(TEMLFN(I,2,J,K))

1      IF ((ABS(TEMLP(I,1,K,J)-TEMLFN(I,1,K,J)).GT.ESPP).OR.
      (ABS(TEMLP(I,2,J,K)-TEMLFN(I,2,J,K)).GT.ESPP)) THEN
          TEMLP(I,1,K,J)=TEMLFN(I,1,K,J)
          TEMLP(I,2,J,K)=TEMLFN(I,2,J,K)
      ENDIF

169      CONTINUE
      ELSE

      FLUXUP(I,1,K,J) =0.0
      FLUXBT(I,1,K,J) =0.0
      SOURC(I,1,K,J) =0.0
      LINEAR(I,1,K,J) =0.0
      TOTALL(I,1,K,J) =0.0

      FLUXUP(I,2,J,K) =0.0
      FLUXBT(I,2,J,K) =0.0
      SOURC(I,2,J,K) =0.0
      LINEAR(I,2,J,K) =0.0
      TOTALL(I,2,J,K) =0.0
1      TOTAE(I,K,J)=TOTALL(I,1,K,J)
      +TOTALL(I,2,J,K)
      MAXERR=MAX(MAXERR,ABS(TOTAE(I,K,J)))

      ENDIF

      HEE(I,1,K,J) = HE(I,1,K)
      HEE(I,2,J,K) = HE(I,2,J)

154      CONTINUE
153      CONTINUE

155      CONTINUE

      INDIC=1
      ENDIF
      IF (MS2.EQ.0) THEN
          ITERI=4
      ELSE
          ITERI=1

```

```

ENDIF
C .....
C SOLUTION BY ITERATION TO SOLVE FOR THE ABSORBED ENERGY
C (THE SUM OF THE LONG WAVE (?) AND SHORT WAVE)
C .....
C
C   TEMAIR(0)=TEMAIR(IHA)
C   LWPROD(0)=SOILEM*SBOLTZ*(TEMAIR(0)+273.15)**4
C   LWLAYR(0)=LWPROD(0)
C .....
C CALCULATION OF THE LONG WAVE UPPER BOUNDARY CONDITION
C ACCORDING TO MONTEITH (1973)
C CALCULATING THE TEMPERATURE OF THE SKY AND THE SKY
C EMSSIVITY GIVEN THE CLOUDINESS OF THE SKY (CAMPBELL 1977)
C .....
C
C   TEMSKY = 1.2*TEMAIR(IHA+1)-21.
C   CLEARS = 0.65+0.007*TEMAIR(IHA+1) ! FOR A COMPLETELY CLEAR SKY.
C   SKYEMS = CLEARS*(1+ 0.1 * CLOUDN**2)
C   SKYEMS = 1.0 !DDDDDDDD
C
C   IF(WAYIN.EQ.1) THEN
C     SKYLIN = SKYEMS*SBOLTZ
C     1      *(TEMAIR(IHA+1)+273.15)**4
C   SKYLIN = SBOLTZ*(TEMSKY+273.15)**4
C
C   ELSE
C     SKYLIN=RLINN
C   ENDIF
C   ITRQ=1
C   DO 2000 ITRQ=1,50,1
C     DO 250 I=1,ITA
C       DO 251 J=1,2,1
C         DO 252 K=1,2,1
C           IF(IPR(I,K,J).NE.0) THEN
C             1 LWLFN(I,1,K,J)= EMSSIV*SBOLTZ
C               *(TEMLFN(I,1,K,J)+273.15)**4
C             1 SENSH(I,1,K,J)= HT(I)
C               *(TEMLFN(I,1,K,J)-TEMAIR(I))
C             IF (MS2.EQ.0) THEN
C               1 ESTLF(I,1,K,J)=
C                 SATUVZ(TEMLFN(I,1,K,J))
C               1 SSLEAF(I,1,K,J)=
C                 SATUDZ(TEMLFN(I,1,K,J))
C             ELSE
C               1 ESTLF(I,1,K,J)=
C                 SATUVZ(TEMLPF(I,1,K,J))
C               1 SSLEAF(I,1,K,J)=
C                 SATUDZ(TEMLPF(I,1,K,J))
C             ENDIF
C             1 LWLFN(I,2,J,K)= EMSSIV*SBOLTZ
C               *(TEMLFN(I,2,J,K)+273.15)**4
C             1 SENSH(I,2,J,K)= HT(I)
C               *(TEMLFN(I,2,J,K)-TEMAIR(I))
C             IF (MS2.EQ.0) THEN
C               1 ESTLF(I,2,J,K)=
C                 SATUVZ(TEMLFN(I,2,J,K))
C               1 SSLEAF(I,2,J,K)=
C                 SATUDZ(TEMLFN(I,2,J,K))
C             ELSE
C               1 ESTLF(I,2,J,K)=
C                 SATUVZ(TEMLPF(I,2,J,K))

```

```

1          SSLEAF(I, 2, J, K)=
          SATUD2(TEMLFN(I, 2, J, K))

          ENDIF

CONDUH(I, 1, K, J) = 1./RDIR(I, 1)*
1          (REAL(IPR(I, 2, 2))*PR(I, 2, 2)*
1          (TEMLFN(I, 1, 2, 2)-TEMLFN(I, 1, K, J))
1          +REAL(IPR(I, 2, 1))*PR(I, 2, 1)*
1          (TEMLFN(I, 1, 2, 1)-TEMLFN(I, 1, K, J))
1          +REAL(IPR(I, 1, 2))*PR(I, 1, 2)*
1          (TEMLFN(I, 1, 1, 2)-TEMLFN(I, 1, K, J))
1          +REAL(IPR(I, 1, 1))*PR(I, 1, 1)*
1          (TEMLFN(I, 1, 1, 1)-TEMLFN(I, 1, K, J)))

CONDUH(I, 2, J, K) = 1./RDIR(I, 2)*
1          (REAL(IPR(I, 2, 2))*PR(I, 2, 2)*
1          (TEMLFN(I, 2, 2, 2)-TEMLFN(I, 2, J, K))
1          +REAL(IPR(I, 2, 1))*PR(I, 2, 1)*
1          (TEMLFN(I, 2, 2, 1)-TEMLFN(I, 2, J, K))
1          +REAL(IPR(I, 2, 1))*PR(I, 2, 1)*
1          (TEMLFN(I, 2, 1, 2)-TEMLFN(I, 2, J, K))
1          +REAL(IPR(I, 2, 1))*PR(I, 2, 1)*
1          (TEMLFN(I, 2, 1, 1)-TEMLFN(I, 2, J, K)))

C          CONDUH(I, 2, 2)= REAL(INDEXD(I, 2, 1))
C          *REAL(INDEXD(I, 2, 2))
C          *2.*PI*RDIR(I, 2)*NUMDRP(I, 2)
C          *(TEMLFN(I, 2, 1)-TEMLFN(I, 2, 2))

C          CONDUH(I, 2, 1)=-CONDUH(I, 2, 2)

C          CONDUH(I, 1, 2)= REAL(INDEXD(I, 1, 1))
C          *REAL(INDEXD(I, 1, 2))
C          *2.*PI*RDIR(I, 1)*NUMDRP(I, 1)
C          *(TEMLFN(I, 1, 1)-TEMLFN(I, 1, 2))

C          CONDUH(I, 1, 1)=-CONDUH(I, 1, 2)

1          LEFLUX(I, 1, K, J) = HEE(I, 1, K, J)
          *(SATUV2(TEMLFN(I, 1, K, J))-EAIR(I))

1          LEFLUX(I, 2, J, K) = HEE(I, 2, J, K)
          *(SATUV2(TEMLFN(I, 2, J, K))-EAIR(I))

1          ENERG(I, 1, K, J) = LWLFN(I, 1, K, J)
          +SENSH(I, 1, K, J)
          +LEFLUX(I, 1, K, J)
          +FLUXUP(I, 1, K, J)
          +NONST(I, 1, K, J)

1          ENERG(I, 2, J, K) = LWLFN(I, 2, J, K)
          +SENSH(I, 2, J, K)
          +LEFLUX(I, 2, J, K)
          -FLUXBT(I, 2, J, K)
          +NONST(I, 2, J, K)

1          ERR(I, 1, K, J) = RABL(I, 1)+CONDUH(I, 1, K, J)
          -ENERG(I, 1, K, J)          ! FOR A LEAF SURFACE

1          ERR(I, 2, J, K) = RABL(I, 2)+CONDUH(I, 2, J, K)
          -ENERG(I, 2, J, K)          ! FOR A LEAF SURFACE

1          MAXER1= MAX(MAXER1, ERR(I, 1, K, J), ERR(I, 2, J, K))

ELSE

CONDUH(I, 1, K, J) = 0.0
CONDUH(I, 2, J, K) = 0.0
LWLFN(I, 1, K, J) = 0.0
LWLFN(I, 2, J, K) = 0.0
LEFLUX(I, 1, K, J) = 0.0
LEFLUX(I, 2, J, K) = 0.0

ENDIF

252          CONTINUE
251          CONTINUE
250          CONTINUE

1100         CONTINUE

DO 1555 IDE=1, ITA, 1
TOTACO(IDE)=0.0
DO 1556 J=1, 2, 1
DO 1557 K=1, 2, 1
TOTACO(IDE)=TOTACO(IDE)
1 +REAL(IPR(IDE, K, J))*PR(IDE, K, J)*CONDUH(IDE, 1, K, J)
1 +REAL(IPR(IDE, K, J))*PR(IDE, K, J)*CONDUH(IDE, 2, J, K)

```

```

IF (LEFLUX(IDE,J,1,K).LT.0.0) THEN
  HEE(IDE,J,1,K) = HT(IDE)/(GAMMA*0.93)
ELSE
  HEE(IDE,J,1,K)=HEND(IDE,J)
ENDIF
HEE(IDE,J,2,K)=HT(IDE)/(GAMMA*0.93)

1557 CONTINUE
1556 CONTINUE
1555 CONTINUE

DO 1200 I=1,ITA,1
  LWPROD(I)=0.0
  DO 1201 J=1,2,1
    NORMAN(I,J)=0.0
    DO 1202 K=1,2,1

      LWPROD(I)= LWPROD(I)
1      +LWLFN(I,1,J,K)*REAL(IPR(I,J,K))
1      *PR(I,J,K)*LADMID(I)
1      +LWLFN(I,2,K,J)*REAL(IPR(I,J,K))
1      *PR(I,J,K)*LADMID(I)

      IF(J.EQ.1) THEN

        NORMAN(I,J)= NORMAN(I,J)
1      +(LWLFN(I,J,K,1)
1      *REAL(IPR(I,K,1))*PR(I,K,1)
1      +LWLFN(I,J,K,2)
1      *REAL(IPR(I,K,2))*PR(I,K,2))
1      *(1-ID(I))

      ELSE IF(J.EQ.2) THEN

        NORMAN(I,J)= NORMAN(I,J)
1      +(LWLFN(I,J,K,1)
1      *REAL(IPR(I,1,K))*PR(I,1,K)
1      +LWLFN(I,J,K,2)
1      *REAL(IPR(I,2,K))*PR(I,2,K))
1      *(1-ID(I))

      ENDIF

1202 CONTINUE
1201 CONTINUE
  LWLAYR(I)=LWPROD(I)*DZ(I)
1200 CONTINUE
  RLDOWN(IT)= SKYLIN
  DO 1400 I=ITA-1,0,-1

    RLDOWN(I)= RLDOWN(I+1)*ID(I+1)
1      +NORMAN(I+1,1)
C      ! EQ 2.2.21
1400 CONTINUE

    RLUP(0)= LWPROD(0)
      +(1-SOILEM)*RLDOWN(0)
C

    DO 1500 I=1,ITA,1

      RLUP(I)= RLUP(I-1)*ID(I)+NORMAN(I,2)
C      ! EQ. 2.2.22

1500 CONTINUE
  CONVER=0.0
  DO 1600 I=1,ITA,1

    RABLW(I,2) = RLDOWN(I)*(1-ID(I))
1      +0.5*LWLAYR(I)-NORMAN(I,2) ! EQ 2.2.23.A
    RABLW(I,1) = RLUP(I-1)*(1-ID(I))
1      +0.5*LWLAYR(I)-NORMAN(I,1) ! EQ 2.2.23.B
    RABTOT(I,1) = ENESAB(I,1)+RABLW(I,1)
C      ! UPDATING THE ABSORBED RADIATION.

```

```

C      RABTOT(I,2) = ENESAB(I,2)+RABLW(I,2)
          ! UPDATING THE ABSORBED RADIATION.
RABLT(I,1) = RABTOT(I,1)/LEAINC(I)
RABLT(I,2) = RABTOT(I,2)/LEAINC(I)
SUM(I,1)=0.0
SUM(I,2)=0.0
DO 1601 J=1,2,1
DO 1602 K=1,2,1
    IF (IPR(I,J,K).NE.0) THEN
        SUM(I,1)= SUM(I,1)
1          -ENERG(I,1,J,K)
1          *REAL(IPR(I,J,K))*PR(I,J,K)
        SUM(I,2)= SUM(I,2)
1          -ENERG(I,2,K,J)
1          *REAL(IPR(I,J,K))*PR(I,J,K)
    ENDIF
1602    CONTINUE
1601    CONTINUE
ERR2(I,1)= RABLT(I,1)+SUM(I,1)
ERR2(I,2)= RABLT(I,2)+SUM(I,2)
ER(I,1) = RABL(I,1)+SUM(I,1)
ER(I,2) = RABL(I,2)+SUM(I,2)
CONVER = MAX(CONVER,ERR2(I,1),ERR2(I,2))
1600    CONTINUE
DO 1700 I=1,ITA,1
DO 1701 J=1,2,1
C      IF ((ABS(ERR2(I,J))-ER(I,J)).GE.ESPP)
C          .AND.(ABS(ERR2(I,J)).GT.ESPP)) THEN
          ! TO SEE IF THE SOLUTION IMPROVES.
1      IF ((ABS(RABLT(I,J))-RABL(I,J)).GE.ESPP) .OR.
          (ITRQ.EQ.1)) THEN
          DO 1710 IHHELP=1,ITA,1
          DO 1711 JHELP=1,2,1
1          RABL(IHHELP,JHELP)
          =RABLT(IHHELP,JHELP)
          IF(MS2.EQ.0) THEN
              DO 1712 KHELP=1,2,1
              DO 1713 LHELP=1,2,1
1          TEMPLF(IHHELP,JHELP,KHELP,LHELP)
          =TEMLFN(IHHELP,JHELP,KHELP,LHELP)
1713          CONTINUE
1712          CONTINUE
          ENDIF
1711          CONTINUE
1710          CONTINUE
          INDIC=2
          GOTO 2500
          ENDIF
1701    CONTINUE
1700    CONTINUE
          GOTO 2100
2500    CONTINUE
DO 165    I=1,ITA,1
DO 163    J=1,2,1
DO 164    K=1,2,1
    IF(IPR(I,K,J).NE.0) THEN
        DO 179 INTERS=1,ITERI,1
            ELH(0) = 0.0
            GLH(0) = 0.0

```

```

      FLH(0) = 1.00
      DLH(0) = TEMAIR(I)

      ELH(1) = HT(I)

      GLH(1) = 4*EMSSIV*SBOLTZ
1      *(0.5*(TEMLF(I,1,K,J)+TEMLF(I,2,J,K))
1      +273.15)**3
1      +KW/(0.5*(LEAFLT(I,1)+LEAFLT(I,2)))

      DLH(1) = RABL(I,1)+CONDUH(I,1,K,J)
1      -HEE(I,1,K,J)*(ESTLFI(I,1,K,J)-EAIR(I))
1      -EMSSIV*SBOLTZ*(TEMLF(I,1,K,J)+273.15)**4
1      +(4*EMSSIV*SBOLTZ
1      *(TEMLF(I,1,K,J)+273.15)**3
1      +HEE(I,1,K,J)*SSLEAF(I,1,K,J))
1      *TEMLF(I,1,K,J)
1      +REAL(MS2)*LEAFLT(I,1)/DT*CWATER
1      *TEMLF(I,1,K,J)

      FLH(1)= ELH(1)+GLH(1)+HEE(I,1,K,J)*SSLEAF(I,1,K,J)
1      +4*EMSSIV*SBOLTZ*(TEMLF(I,1,K,J)+273.15)**3
1      +REAL(MS2)*LEAFLT(I,1)/DT*CWATER

      ELH(LL) = 4*EMSSIV*SBOLTZ
1      *(0.5*(TEMLF(I,LL,J,K)+TEMLF(I,1,K,J))
1      +273.15)**3
1      +KW/(0.5*(LEAFLT(I,LL-1)+LEAFLT(I,LL)))

      GLH(LL) = HT(I)

      DLH(LL) = RABL(I,2)+CONDUH(I,2,J,K)
1      -HEE(I,2,J,K)*(ESTLFI(I,2,J,K)-EATR(I))
1      -EMSSIV*SBOLTZ*(TEMLF(I,LL,J,K)+273.15)**4
1      +(4*EMSSIV*SBOLTZ
1      *(TEMLF(I,LL,J,K)+273.15)**3
1      +HEE(I,2,J,K)*SSLEAF(I,2,J,K))
1      *TEMLF(I,LL,J,K)
1      +REAL(MS2)*LEAFLT(I,LL)/DT*CWATER
1      *TEMLF(I,LL,J,K)

      FLH(LL) = ELH(LL)+GLH(LL)+HEE(I,2,J,K)*SSLEAF(I,2,J,K)
1      +4*EMSSIV*SBOLTZ*(TEMLF(I,LL,J,K)+273.15)**3
1      +REAL(MS2)*LEAFLT(I,LL)/DT*CWATER

      ELH(LL+1) = 0.0
      GLH(LL+1) = 0.0
      FLH(LL+1) = 1.00
      DLH(LL+1) = TEMAIR(I)

      DO 161 N=0,LL+1,1

          CBLOCK(N) = ELH(N)
          BBLOCK(N) = GLH(N)
          ABLOCK(N) = FLH(N)
          DBLOCK(N) = DLH(N)

161      CONTINUE

1116     CONTINUE

      CALL THON(LL,LA,CBLOCK,BBLOCK,DBLOCK,ABLOCK,TMLF)

      TEMPLN(I,1,K,J)=TMLF(1)

C      DO 162 N=2,LL-1,1
C          TEMPLN(I,N,J)=TMLF(N)
C162     CONTINUE

      TEMPLN(I,LL,J,K)=TMLF(LL)

      DO 55 N =1,2,1

          ANALG(N)=-FLH(N)*TMLF(N)+GLH(N)*TMLF(N+1)
          +ELH(N)*TMLF(N-1)+DLH(N)

55      CONTINUE

      FLUXUP(I,1,K,J)=GLH(1)*(TEMPLN(I,1,K,J)-TEMPLN(I,2,J,K))
      FLUXBT(I,1,K,J)=-ELH(1)*(TEMPLN(I,1,K,J)-SNGL(TEMAIR(I)))

      SOURC(I,1,K,J)=RABL(I,1)+CONDUH(I,1,K,J)
1      -HEE(I,1,K,J)*(ESTLFI(I,1,K,J)-EAIR(I))
1      -EMSSIV*SBOLTZ*(TEMLF(I,1,K,J)+273.15)**4

      LINEAR(I,1,K,J) = (HEE(I,1,K,J)*SSLEAF(I,1,K,J)
1      +4*EMSSIV*SBOLTZ*(TEMLF(I,1,K,J)+273.15)**3)

```

```

1      *(TEMLFN(I,1,K,J)-TEMLPF(I,1,K,J))
NONST(I,1,K,J)=REAL(MS2)*LEAFLT(I,1)/DT*CWATER
1      *(TEMLFN(I,1,K,J)-TEMLPF(I,1,K,J))
TOTALL(I,1,K,J)=-LINEAR(I,1,K,J)-NONST(I,1,K,J)
1      -FLUXUP(I,1,K,J)+FLUXBT(I,1,K,J)
1      +SOURC(I,1,K,J)

FLUXUP(I,2,J,K)=GLH(2)*(TEMLFN(I,2,J,K)-SNGL(TEMAIR(I)))
FLUXBT(I,2,J,K)=-ELH(2)*(TEMLFN(I,2,J,K)-TEMLFN(I,1,K,J))
SOURC(I,2,J,K)=RABL(I,2)+CONDUH(I,2,J,K)
1      -HEE(I,2,J,K)*(ESTLFI(I,2,J,K)-EAIR(I))
1      -EMSSIV*SBOLTZ*(TEMLPF(I,LL,J,K)+273.15)**4

LINEAR(I,2,J,K)= (4*EMSSIV*SBOLTZ
1      *(TEMLPF(I,LL,J,K)+273.15)**3
1      +HEE(I,2,J,K)*SSLEAF(I,2,J,K))
1      *(TEMLFN(I,2,J,K)-TEMLPF(I,2,J,K))

NONST(I,2,J,K)=REAL(MS2)*LEAFLT(I,LL)/DT*CWATER
1      *(TEMLFN(I,2,J,K)-TEMLPF(I,2,J,K))
TOTALL(I,2,J,K)=-LINEAR(I,2,J,K)-NONST(I,2,J,K)
1      -FLUXUP(I,2,J,K)+FLUXBT(I,2,J,K)
1      +SOURC(I,2,J,K)

TOTAE(I,K,J)=TOTALL(I,1,K,J)+TOTALL(I,2,J,K)
MAXERR=MAX(MAXERR,ABS(TOTALL(I,1,K,J))
1      ,ABS(TOTALL(I,2,J,K)),ABS(TOTAE(I,K,J)))

IF (MS2.EQ.0) THEN
    TEMPLF(I,1,K,J) =TEMLFN(I,1,K,J)
    TEMPLF(I,2,J,K) =TEMLFN(I,2,J,K)
    ESTLFI(I,1,K,J) =SATUV2(TEMLFN(I,1,K,J))
    ESTLFI(I,2,J,K) =SATUV2(TEMLFN(I,2,J,K))
    SSLEAF(I,1,K,J)=SATUD2(TEMLFN(I,1,K,J))
    SSLEAF(I,2,J,K)=SATUD2(TEMLFN(I,2,J,K))
ENDIF

179      CONTINUE

        ENDIF

164      CONTINUE
163      CONTINUE

165      CONTINUE

MAXSH=MAXER1
MAXERR=0.0
MAXER1=0.0

2000    CONTINUE
2100    CONTINUE

C      TILL HERE

STORAG=0.0

DO 1300 I=1,ITA,1

    LAYSEN(I)    =0.0
    LAYLEF(I)    =0.0
    STOR(I)      =0.0
    LWPROD(I)    =0.0

    DO 1301 J=1,2,1
        DO 1302 K=1,2,1

            IF (IPR(I,K,J).NE.0) THEN

1          LWLFN(I,1,K,J)= EMSSIV*SBOLTZ
                *(TEMLFN(I,1,K,J)+273.15)**4

1          SENS(I,1,K,J)= HT(I)
                *(TEMLFN(I,1,K,J)-TEMAIR(I))

1          LWLFN(I,2,J,K)= EMSSIV*SBOLTZ
                *(TEMLFN(I,2,J,K)+273.15)**4

1          SENS(I,2,J,K)= HT(I)
                *(TEMLFN(I,2,J,K)-TEMAIR(I))

```



```

1      LEFLUX(I,1,K,J)= HEE(I,1,K,J)
      *(SATUV2(TEMLFN(I,1,K,J))-EAIR(I))

1      LEFLUX(I,2,J,K)= HEE(I,2,J,K)
      *(SATUV2(TEMLFN(I,2,J,K))-EAIR(I))

1      ENERG(I,1,K,J) = LWLFN(I,1,K,J)
      +SENSH(I,1,K,J)
      +LEFLUX(I,1,K,J)
      +FLUXUP(I,1,K,J)
      +NONST(I,1,K,J)

1      ENERG(I,2,J,K) = LWLFN(I,2,J,K)
      +SENSH(I,2,J,K)
      +LEFLUX(I,2,J,K)
      -FLUXBT(I,2,J,K)
      +NONST(I,2,J,K)

1      ERR3(I,1,K,J) = RABL(I,1)+CONDUH(I,1,K,J)
      -ENERG(I,1,K,J)      ! FOR A LEAF SURFACE
1      ERR3(I,2,J,K) = RABL(I,2)+CONDUH(I,2,J,K)
      -ENERG(I,2,J,K)      ! FOR A LEAF SURFACE

      MAXER1= MAX(MAXER1,ERR3(I,1,K,J),ERR3(I,2,J,K))

ENDIF

1      LWPROD(I)= LWPROD(I)
      +LWLFN(I,1,K,J)*REAL(IPR(I,K,J))
      *PR(I,K,J)*LADMID(I)
      +LWLFN(I,2,J,K)*REAL(IPR(I,K,J))
      *PR(I,K,J)*LADMID(I)

1      LAYSEN(I)=LAYSEN(I)
      +DBLE((SENSH(I,1,K,J)+SENSH(I,2,J,K))
      *(PR(I,K,J)*REAL(IPR(I,K,J))*LEAINC(I)))

1      LAYLEF(I)=LAYLEF(I)
      +DBLE((LEFLUX(I,1,K,J)+LEFLUX(I,2,J,K))
      *(PR(I,K,J)*REAL(IPR(I,K,J))*LEAINC(I)))

1      STOR(I)=STOR(I)
      +DBLE((NONST(I,1,K,J)+NONST(I,2,J,K))
      *(PR(I,K,J)*REAL(IPR(I,K,J))*LEAINC(I)))

1302  CONTINUE
1301  CONTINUE

1      LWLAYR(I)=LWPROD(I)*DZ(I)
1      LAYBAL(I)=DBLE((RABL(I,1)+RABL(I,2))*LEAINC(I))
      -LAYSEN(I)-LAYLEF(I)-DBLE(LWLAYR(I))
      -STOR(I)

      STORAG=STORAG+SNGL(STOR(I))

1300  CONTINUE

      TOTLE =0.0
      TOTALQ =0.0

      DO 2400 I=ITA,1,-1

          SH(I) =0.0
          SL(I) =0.0
          ERROL(I)=0.0

          AVGTLF(I)= 0.5*REAL(IPR(I,1,1))*PR(I,1,1)
          *(TEMLFN(I,1,1,1)+TEMLFN(I,2,1,1))
          +0.5*REAL(IPR(I,1,2))*PR(I,1,2)
          *(TEMLFN(I,1,1,2)+TEMLFN(I,2,2,2))
          +0.5*REAL(IPR(I,2,1))*PR(I,2,1)
          *(TEMLFN(I,1,2,1)+TEMLFN(I,2,1,2))
          +0.5*REAL(IPR(I,2,2))*PR(I,2,2)
          *(TEMLFN(I,1,2,2)+TEMLFN(I,2,2,2))

          TOTPRO(I)=PR(I,1,1)+PR(I,1,2)+PR(I,2,1)+PR(I,2,2)

          ITOTPR(I)=REAL(IPR(I,1,1))*PR(I,1,1)
          +REAL(IPR(I,1,2))*PR(I,1,2)
          +REAL(IPR(I,2,1))*PR(I,2,1)
          +REAL(IPR(I,2,2))*PR(I,2,2)

          DO 2403 J=1,2,1
              DO 2404 K=1,2,1

                  IF (IPR(I,J,K).NE.0) THEN

                      REMAIN(I,1,J,K)=0.0
                      REMAIN(I,2,K,J)=0.0

```

```

      DELTAT(I,1,J,K)=TEMLFN(I,1,J,K)-TEMAIR(I)
      DELTAT(I,2,K,J)=TEMLFN(I,2,K,J)-TEMAIR(I)
1     SENFL(I,1,J,K) =DBLE(SENSH(I,1,J,K)*DZ(I)
      *PR(I,J,K)*REAL(IPR(I,J,K))*LADMID(I))
1     SENFL(I,2,K,J) =DBLE(SENSH(I,2,K,J)*DZ(I)
      *PR(I,J,K)*REAL(IPR(I,J,K))*LADMID(I))
1     LEFL(I,1,J,K) =DBLE(LEFLUX(I,1,J,K)*DZ(I)
      *PR(I,J,K)*REAL(IPR(I,J,K))*LADMID(I))
1     LEFL(I,2,K,J) =DBLE(LEFLUX(I,2,K,J)*DZ(I)
      *PR(I,J,K)*REAL(IPR(I,J,K))*LADMID(I))
1     REMAIN(I,1,J,K)=REMAIN(I,1,J,K)
      -SENFL(I,1,J,K)
      -LEFL(I,1,J,K)
1     REMAIN(I,2,K,J)=REMAIN(I,2,K,J)
      -SENFL(I,2,K,J)
      -LEFL(I,2,K,J)
1
SH(I)=SH(I)+SENFL(I,1,J,K)+SENFL(I,2,K,J)
SL(I)=SL(I)+LEFL(I,1,J,K)+LEFL(I,2,K,J)
ELSE
      SENFL(I,1,J,K) =0.0
      SENFL(I,2,K,J) =0.0
      LEFL(I,1,J,K) =0.0
      LEFL(I,2,K,J) =0.0
      REMAIN(I,1,J,K)=0.0
      REMAIN(I,2,K,J)=0.0
ENDIF
2404 CONTINUE
2403 CONTINUE
DO 2406 L=1,2,1
  DO 2407 J=1,2,1
    DO 2408 K=1,2,1
      IF(LEFL(I,L,J,K).LT.0.0) THEN
1         CUMDEW(I,L)=CUMDEW(I,L)
          -SNGL(LEFL(I,L,J,K))*DT
      ENDIF
1         IF((CUMDEW(I,L).GT.0.0).AND.
          (LEFL(I,L,2,J).GT.0.0)) THEN
1             CUMDEW(I,L)=CUMDEW(I,L)
              -SNGL(LEFL(I,L,2,J))*DT
          CUMDEW(I,L)=AMAX1(CUMDEW(I,L),0.)
      ENDIF
2408 CONTINUE
2407 CONTINUE
2406 CONTINUE
      ERROL(I)=RABTOT(I,1)+RABTOT(I,2)
      -SNGL(SH(I))-SNGL(SL(I))-LWLAYR(I)
2400 CONTINUE
DO 2211 I=1,ITA,1
  DO 2212 J=1,2,1
    WAMOUN(I,J) = CUMDEW(I,J)/LAMDA
    CUMDWA(I,J)= CUMDEW(I,J)/(LEAINC(I)*LAMDA)
    FRAC(I,J,2)= CUMDWA(I,J)/(1000.*WFTH(J))
    FRA(I,J,2) = FRAC(I,J,2)
    IF (FRAC(I,J,2).GT.1.) THEN
1       DRTP(I,J) = WAMOUN(I,J)
          -LEAINC(I)*WFTH(J)*1000.
          FRAC(I,J,2) = 1.0
          FRA(I,J,2) = 1.0
          FRAC(I,J,1) = 0.0
          FRA(I,J,1) = 0.0
          INDEXD(I,J,2)=1
    
```

```

      INDEXD(I,J,1)=0
      ELSE IF (FRAC(I,J,2) .GT.0.0001) THEN

          DRIP(I,J)      =0.0
          FRAC(I,J,1)    =1.0-FRAC(I,J,2)
          FRA(I,J,1)     =FRA(I,J,1)
          FRA(I,J,2)     =FRA(I,J,2)
          INDEXD(I,J,1)=1
          INDEXD(I,J,2)=1

      ELSE

          DRIP(I,J)      =0.0
          FRAC(I,J,1)    =1.0
          FRA(I,J,1)     =1.0
          FRA(I,J,2)     =0.0
          INDEXD(I,J,1)=1
          INDEXD(I,J,2)=0

      ENDIF

      ! THERE WILL STILL BE A DRIP DUE
      ! TO DROP RUN OFF FROM THE SURFACE

      VOLUMN(I,J)  = PI*RDIR(I,J)**2*WFTH(J)
      NUMDRP(I,J)  = CUMDWA(I,J)/VOLUMD(I,J)

2212  CONTINUE

      PR(I,1,1) = FRA(I,1,1)*FRA(I,2,1)
      PR(I,1,2) = FRA(I,1,1)*FRA(I,2,2)
      PR(I,2,1) = FRA(I,1,2)*FRA(I,2,1)
      PR(I,2,2) = FRA(I,1,2)*FRA(I,2,2)
      IPR(I,1,1)= INDEXD(I,1,1)*INDEXD(I,2,1)
      IPR(I,1,2)= INDEXD(I,1,1)*INDEXD(I,2,2)
      IPR(I,2,1)= INDEXD(I,1,2)*INDEXD(I,2,1)
      IPR(I,2,2)= INDEXD(I,1,2)*INDEXD(I,2,2)
      TOTPRO(I)=PR(I,1,1)+PR(I,1,2)+PR(I,2,1)+PR(I,2,2)
      ITOTPR(I)=REAL(IPR(I,1,1))*PR(I,1,1)
1      +REAL(IPR(I,1,2))*PR(I,1,2)
1      +REAL(IPR(I,2,1))*PR(I,2,1)
1      +REAL(IPR(I,2,2))*PR(I,2,2)

2211  CONTINUE

      DO 2511 I=1,ITA,1

          TOTLE=TOTLE+SI(I)
          TOTALQ=TOTALQ+SH(I)

2511  CONTINUE

          TRANSP= TOTLE/LAMDA

          RLNTOP  =RLDOWN(ITA)-RLUP(ITA)
          RLNBTM  =RLUP(0)-RLDOWN(0)
          RLNET   =RLDOWN(ITA)-RLDOWN(0)+RLUP(0)-RLUP(ITA)
          RNETOT  = TOTENE+RLNET
          ENERER  =RNETOT-TOTLE-TOTALQ-STORAG
          SOILLN  =RLDOWN(0)-RLUP(0)
          SOILRN  =SOILLN+SOILSN

          IF (ENERER .GT.1.) THEN

      C      DO 3000 I=1,ITA,1
      C      DO 3001 K=1,2,1
      C      DO 3002 J=1,2,1

      C      WRITE(26,*) I,K,J, LWLFN(I,2,K,J), SENSH(I,1,K,J)
      C      1 ,LEFLUX(I,1,K,J), FLUXUP(I,1,K,J), NONST(I,1,K,J)
      C      1 ,ENERG(I,1,K,J), ERR(I,1,K,J), RABL(I,1)
      C      1 ,ERR(I,1,K,J)
      C      1 ,LWLFN(I,2,J,K), SENSH(I,2,J,K), LEFLUX(I,2,J,K)
      C      1 ,FLUXBT(I,2,J,K), NONST(I,2,J,K), ENERG(I,2,J,K)
      C      1 ,ERR(I,2,J,K)
      C      1 ,RABL(I,2), CONDUH(I,1,K,J), CONDUH(I,2,J,K)

      C      WRITE(26,*)
      C      WRITE(26,*)
      C      WRITE(26,*) 'SECOND SEGMENT'

      C      WRITE(26,*) I,LWLFN(I,1,K,J),LWLFN(I,2,J,K), SENSH(I,1,K,J)
      C      1 ,SENSH(I,2,J,K),LEFLUX(I,1,K,J),LEFLUX(I,2,J,K)
      C      1 ,NONST(I,1,K,J),NONST(I,2,J,K)
      C      1 ,ERR(I,1,K,J),ERR(I,2,J,K)

3002  CONTINUE
3001  CONTINUE

      C      WRITE(26,*)

```



```

TOTUP=0.0
TOTUPL=0.0
DO 1801 GITR=ISA+1,0,1
  ROOTUP(GITR)=0.0
1801 CONTINUE
DO 1900 GITRA=1,NUMB,1
EPS(ISA,J) = 0.0
GPN(ISA,J) = 0.0
FPV(ISA,J) = 1.0
DPV(ISA,J) = PSISOL(ISA)*RHO*GR/10E6
CBLOCK(ISA) = EPS(ISA,J)
BBLOCK(ISA) = GPN(ISA,J)
ABLOCK(ISA) = FPV(ISA,J)
DBLOCK(ISA) = DPV(ISA,J)
DO 400 ITRA=1,MAXITR,1
ERRSO=0.0
J=0
ERRMAX=0.0
DO 100 I=ISA+1,ITA,1
  EPS(I,J) = AR(I-1,J)/AR(0,0)*KXYLUM(I-1,J)
1 /(.5*(DZ(I-1)+DZ(I)))
  GPN(I,J) = AR(I,J)/AR(0,0)*KXYLUM(I,J)
1 /(.5*(DZ(I)+DZ(I+1)))
  IF (I.GT.0) THEN
    IF (ITER.EQ.0) THEN
      DPV(I,J) = PSIXYL(I,1,1)/RLS(I)
      +REAL(MS1) * PSIS(I,J,1)/RS(I,J)
      +REAL(MS2)*AVG(I,J)
      /(ELASTI(I,1)+OSMOTI(I,J,1))
      * DZ(I)/DT1*PSIXYL(I,J,1)
    ELSE
      DPV(I,J)=PSIXYL(I,1,2)/RLS(I)
      +REAL(MS1) * PSIS(I,J,1)/RS(I,J)
      +REAL(MS2)* AVG(I,J)
      /(ELASTI(I,1)+OSMOTI(I,J,1))
      *DZ(I)/DT1*PSIXYL(I,J,1)
    ENDIF
    FPV(I,J)= EPS(I,J)+GPN(I,J)
    +1./RLS(I)+REAL(MS1)*1./RS(I,J)
    +AVG(I,J)/(ELASTI(I,1)+OSMOTI(I,J,1))
    *REAL(MS2)*DZ(I)/DT1
  ELSE
    IF((ITER.EQ.0).OR.(INI.EQ.0)) THEN
      CONTRS(I)=0.0 !THEY HAVE TO BE GLOBAL
      SOILRS(I)=0.0 !THEY HAVE TO BE GLOBAL
    ELSE
      CONTRS(I)=0.0 ! contact resistance is zero
      SOILRS(I)=RHO*GR*
      ALOG(RADIUZ(I)/RADIUS(I))
      /(1*DZ(I)*2*PI*KWATER(I)
      *LV(I)*10E6) ! eq. 4.5.12 Gardner (1960)
    ENDIF
    DPV(I,J)=PSISOL(I)*RHO*GR/(10E6
    *PLANTM*(ROOTRS(I)+SOILRS(I)+CONTRS(I)))
    +REAL(MS1)*PSIS(I,J,1)/RS(I,J)
    +REAL(MS2)*AR(I,J)
    /(ELASTI(I,1)+OSMOTI(I,J,1))
    *DZ(I)/DT1*PSIXYL(I,J,1)
    FPV(I,J)=EPS(I,J)+GPN(I,J)+1/
    (PLANTM*(ROOTRS(I)+SOILRS(I)+CONTRS(I)))

```

```

      +REAL(MS1)*1/RS(I,J)+REAL(MS2)*AR(I,J)
      /(ELASTI(I,1)+OSMOTI(I,J,1))
      *DZ(I)/DT1
ENDIF

CBLOCK(I) =EPS(I,J)
BBLOCK(I) =GPN(I,J)
ABLOCK(I) =FPV(I,J)
DBLOCK(I) =DPV(I,J)
100 CONTINUE

C      RS(ITA+1,J) SHOULD BE VERY LARGE
EPS(ITA+1,J)= KXYLUM(ITA,J)/(0.5*DZ(ITA))
GPN(ITA+1,J)=0.0
DPV(ITA+1,J)=REAL(MS2)*AR(ITA+1,J)/(ELASTI(ITA+1,1)
:      +OSMOTI(ITA+1,J,1))
:      *0.01/DT1*PSIXYL(ITA+1,J,1)
C      DPV(ITA+1,J)= 0.0+PSIS(ITA+1,J,1)/RS(ITA+1,J)
C      :      +AR(ITA+1,J)/(ELASTI(ITA+1,1))
C      :      +OSMOTI(ITA+1,J,1))
C      :      * 0.01/DT1*PSIXYL(ITA,J,1)
C      FPV(ITA+1,J)= 0.0+1/RS(ITA+1,J) + EPS(ITA+1,J)+GPN(ITA+1,J)
C      :      +AR(ITA+1,J)/(ELASTI(ITA+1,1)+OSMOTI(ITA+1,J,1))
C      :      * 0.01/DT1
C      FPV(ITA+1,J)= EPS(ITA+1,J)+GPN(ITA+1,J)
:      +REAL(MS2)*AR(ITA+1,J)/(ELASTI(ITA+1,1)
:      +OSMOTI(ITA+1,J,1))
:      * 0.01/DT1
CBLOCK(ITA+1) = EPS(ITA+1,J)
BBLOCK(ITA+1) = GPN(ITA+1,J)
ABLOCK(ITA+1) = FPV(ITA+1,J)
DBLOCK(ITA+1) = DPV(ITA+1,J)
CALL THOM(ITA,ISA,CBLOCK,BBLOCK,DBLOCK,ABLOCK,AUXV)
IF (MS2.EQ.0) THEN
    PSIXYT(ITA+1,0) = PSIXYL(ITA+1,0,1)
ELSE IF (ITER.EQ.0) THEN
    PSIXYT(ITA+1,0) =0.0
ELSE
    PSIXYT(ITA+1,0)=PSIXYL(ITA+1,0,2)
ENDIF
PSIXYL(ISA,0,2)=REAL(AUXV(ISA))
PSIXYL(ITA+1,0,2)=REAL(AUXV(ITA+1))

DIFFER(ITA+1,0) = PSIXYL(ITA+1,0,2)-PSIXYT(ITA+1,0)
DO 150 I=ISA+1,ITA
IF (MS2.EQ.0) THEN
    PSIXYT(I,J) = PSIXYL(I,J,1)
ELSE IF (ITER.EQ.0) THEN
    PSIXYT(I,J) =0.0
ELSE
    PSIXYT(I,J)=PSIXYL(I,J,2)
ENDIF
PSIXYL(I,J,2) = REAL(AUXV(I))
ERROR(I,J) = -FPV(I,J)*PSIXYL(I,J,2)
:      +EPS(I,J)*PSIXYL(I-1,J,2)
:      +GPN(I,J)*PSIXYL(I+1,J,2)+DPV(I,J)
DIFFER(I,J)= PSIXYL(I,J,2)-PSIXYT(I,J)
ERRMAX = MAX(CERRMAX,ABS(DIFFER(I,J)))
ERRSO=MAX(ERRSO,ERROR(I,J))
150 CONTINUE
ITER=1
DO 300 I=1,ITA,1

```

```

EPW(I,0) = 0.0
GPE(I,0) = 0.0
DPH(I,0) = PSIXYL(I,0,2)
FPH(I,0) = 1.00

CBLOCK(0) = EPW(I,0)
BBLOCK(0) = GPE(I,0)
DBLOCK(0) = DPH(I,0)
ABLOCK(0) = FPH(I,0)

DO 200 J=1,5,1
IF (J.EQ.5) THEN
EPW(I,J) = KXYLUM(I,J)/(0.5*(DX(I,J-1)+DX(I,J)))
GPE(I,J) = 0.0
ELSE
EPW(I,J) = KXYLUM(I,J)/(0.5*(DX(I,J-1)+DX(I,J)))
GPE(I,J) = KXYLUM(I,J+1)
1 / (0.5*(DX(I,J)+DX(I,J+1)))
ENDIF
IF (J.EQ.1) THEN
EPW(I,J) = 1. / (BRANCN(I)*RLS(I))
DPH(I,J) = AR(I,J)
: / (ELASTI(I,1)+OSMOTI(I,J,1))
: *REAL(MS2)*DX(I,J)/DT1*PSIXYL(I,J,1)
: +REAL(MS1)*PSIS(I,J,1)/RS(I,J)
:
FPH(I,J) = EPW(I,J)+GPE(I,J)
: +AR(I,J)
: / (ELASTI(I,1)+OSMOTI(I,J,1))
: *REAL(MS2)*DX(I,J)/DT1
: +REAL(MS1)*1./RS(I,J)

ELSE IF (J.LT.5) THEN
DPH(I,J) = AR(I,J)
: / (ELASTI(I,1)+OSMOTI(I,J,1))
: *REAL(MS2)*DX(I,J)/DT1*PSIXYL(I,J,1)
: +REAL(MS1)*PSIS(I,J,1)/RS(I,J)
:
FPH(I,J) = EPW(I,J)+GPE(I,J)+AR(I,J)/
: (ELASTI(I,1)+OSMOTI(I,J,1))
: *REAL(MS2)*DX(I,J)/DT1
: +REAL(MS1)*1./RS(I,J)
ELSE
DPH(I,J) = AR(I,J)
: / (ELASTI(I,1)+OSMOTI(I,J,1))
: *REAL(MS2)*DX(I,J)/DT1*PSIXYL(I,J,1)
: +REAL(MS1)*PSIS(I,J,1)/RS(I,J)
: -AMAX1(SNGL(CSL(I)),0.0)
: / (LAMBDA*RHO*BRANCN(I)*PLANTN)
:
FPH(I,J) = EPW(I,J)+GPE(I,J)+AR(I,J)/
: (ELASTI(I,1)+OSMOTI(I,J,1))
: *REAL(MS2)*DX(I,J)/DT1
: +REAL(MS1)*1./RS(I,J)
ENDIF

CBLOCK(J) = EPW(I,J)
BBLOCK(J) = GPE(I,J)
DBLOCK(J) = DPH(I,J)
ABLOCK(J) = FPH(I,J)

200 CONTINUE

CALL THOM (IHL,ISL,CBLOCK,BBLOCK,DBLOCK,ABLOCK,AUXL)

DO 250 J=1,5,1
IF (MS2.EQ.0) THEN
PSIXYT(I,J) = PSIXYL(I,J,1)
ELSE IF (ITER.EQ.0) THEN
PSIXYT(I,J) = 0.0
ELSE
PSIXYT(I,J) = PSIXYL(I,J,2)
ENDIF

```



```

                PSIXYL(I,J,2)=REAL(AUXL(J))
                DIFFER(I,J) = PSIXYL(I,J,2)-PSIXYT(I,J)
                ERRMAX = MAX(ERRMAX,ABS(DIFFER(I,J)))
250      CONTINUE
                DO 251 J=1,4,1
                ERROR(I,J)=-FPH(I,J)*PSIXYL(I,J,2)
                :           +EPW(I,J)*PSIXYL(I,J-1,2)
                :           +GPE(I,J)*PSIXYL(I,J+1,2)
                :           +DPH(I,J)
                ERR50=MAX(ERR50,ERROR(I,J))

251      CONTINUE
300      CONTINUE
                IF (ERRMAX .LT. CRITR) THEN
                GO TO 500
                ENDIF
                IF ((ERRMAX.GE.CRITR).AND.(MS2.EQ.0)) THEN
                J=0
                DO 901 I=ISA+1,ITA,1
                PSIXYL(I,J,1)=PSIXYL(I,J,2)
                CA(I,J) = VOLUME(I,J)
                :           /(ELASTI(I,2)+OSMOTI(I,J,1))
                :           PSIS(I,J,2)=PSIS(I,J,1)
                :           +1/CA(I,J)*(PSIXYL(I,J,2)-PSIS(I,J,1))
                :           *1/RS(I,J)
                C           PSIS(I,J,1) =PSIS(I,J,2)
2901     CONTINUE
                DO 450 I=1,ITA,1
                DO 1004 J=1,5,1
                PSIXYL(I,J,1)=PSIXYL(I,J,2)
                CA(I,J) = VOLUME(I,J)/(ELASTI(I,2)
                :           +OSMOTI(I,J,1))
                :           PSIS(I,J,2)=PSIS(I,J,1)
                :           +1/CA(I,J)*(PSIXYL(I,J,2)-PSIS(I,J,1))
                :           *1/RS(I,J)
                C           PSIS(I,J,1)=PSIS(I,J,2)
1004     CONTINUE
450      CONTINUE
                ENDIF

400      CONTINUE
500      CONTINUE
                WATERF = WATERF-GPN(0,0)*(PSIXYL(1,0,2)-PSIXYL(0,0,2))
                :           *PLANTN/CUMLAI(0)

CCCCCCCCCCCCCCCCCCCCCCCCCCCCCCCCCCCCCCCCCCCCCCCCCCCCCCCCCCCCCCCC
C  CALCULATION OF THE NEW VARIABLES
CCCCCCCCCCCCCCCCCCCCCCCCCCCCCCCCCCCCCCCCCCCCCCCCCCCCCCCCCCCCCCCC
                J=0
                DO 600 I=ISA+1,ITA,1
                CA(I,J) = VOLUME(I,J)/(ELASTI(I,2)+OSMOTI(I,J,1))
                :           VOLMEN(I,J)=VOLUME(I,J)+(PSIXYL(I,J,2)-PSIS(I,J,1))
                :           *REAL(MS1)*1./RS(I,J)
                :           DOSMO(I,J)=REAL(MS1)*DT1*
                :           (PSIXYL(I,J,2)-PSIS(I,J,1))
                :           /(RS(I,J)*VOLUME(I,J))
                C           STILL SOMETHING IS MISSING

```

```

OSMOTI(I,J,2)=OSMOTI(I,J,1)+DOSMO(I,J)

CAN(I,J)   =VOLMEN(I,J)/(ELASTI(I,2)+OSMOTI(I,J,2))
TIMEPL(I,J)= CA(I,J)*RS(I,J)

IF (MS2.EQ.1) THEN
    PSIS(I,J,2)=PSIS(I,J,1)
    :         +1/CA(I,J)*(PSIXYL(I,J,2)-PSIS(I,J,1))
    :         *1/RS(I,J)
ENDIF

600  CONTINUE
DO 700 I=1,ITA,1
DO 750 J=1,5,1
    CA(I,J)   =VOLUME(I,J)/(ELASTI(I,2)
    :         +OSMOTI(I,J,1))
    VOLMEN(I,J)=VOLUME(I,J)
    :         +REAL(MS1)
    :         *(PSIXYL(I,J,2)-PSIS(I,J,1))
    :         *1/RS(I,J)
    DOSMO(I,J)=REAL(MS1)*DT1*
    :         (PSIXYL(I,J,2)-PSIS(I,J,1))
    :         /(RS(I,J)*VOLUME(I,J))
    OSMOTI(I,J,2)=OSMOTI(I,J,1)
    :         +DOSMO(I,J)
    CAN(I,J)   =VOLMEN(I,J)/
    :         (ELASTI(I,2)+OSMOTI(I,J,2))
    TIMEPL(I,J)= CA(I,J)*RS(I,J)
    IF(MS2.EQ.0) THEN
        PSIS(I,J,2)=PSIS(I,J,1)
        :         +1/CA(I,J)
        :         *(PSIXYL(I,J,2)-PSIS(I,J,1))
        :         *1/RS(I,J)
    ENDIF
750  CONTINUE
700  CONTINUE
DO 800 I=ISA+1,0,1
    ROOTUP(I)=ROOTUP(I)
    :         +(PSISOL(I)*RH0*GR/10E6-PSIXYL(I,0,2))
    :         /(ROOTRS(I)+SOILRS(I)+CONTRS(I))
    TOTUP=TOTUP+ROOTUP(I)
    TOTUPL=TOTUPL+AMAX1(ROOTUP(I),0.0)
800  CONTINUE
    J=0
DO 900 I=ISA,ITA+1,1
    PSIXYL(I,J,1)=PSIXYL(I,J,2)
    PSIS(I,J,1)  =PSIS(I,J,2)
900  CONTINUE
DO 950 I=1,ITA,1
DO 1000 J=1,5,1
    PSIXYL(I,J,1)=PSIXYL(I,J,2)
    PSIS(I,J,1)  =PSIS(I,J,2)
1000 CONTINUE
950  CONTINUE

MS2=1
MS1=1
MAXITR=40
ERRMAG=AMAX1(ERRMAX,ERRMAG)

1900 CONTINUE
    PROD = 0.0

```

```

DO 810 I=ISA+1,0,1
    FRARUP(I) = AMAX1(ROOTUP(I),0.0)/TOTUPL
    PROD = PROD + FRARUP(I)*ALPHAP*PSISOL(ISA)
    *RHO*GR
    ROOTUP(I)=ROOTUP(I)/REAL(NUMB)
810 CONTINUE
    IF (WATERF.LT.0.0) THEN
        ABACON =0.0
    ELSE
        ABACON=PROD/(AMAX1((WATERF/REAL(NUMB)),0.0)+B)
    ENDIF
    IF ((ERRMAX.GE.CRITR)) THEN
        WRITE(*,*) 'AN ERROR WITH THE CONVERGENCE',
        ' OF THE PLANT WATER MOVEMENT'
        WRITE(*,*) ' ERRMAX,ERRMAG = ',ERRMAX,ERRMAG
        WRITE(*,*) ' ERRSO= ',ERRSO
        WRITE(*,*) ' AN ERROR WITH THE CONVERGENCE',
        ' OF THE PLANT WATER MOVEMENT'
        WRITE(26,*) ' ERRMAX= ',ERRMAX
        WRITE(26,*) ' ERRSO= ',ERRSO
    ENDIF
    ENI=1
3000 CONTINUE
    RETURN
    END

```

CC

```

SUBROUTINE RESIS(ITRM,ITRA,FLAG,
1 LEFL,RCUTI,
1 GRASH,NU,REYNOL,NUFORC,NUFREE,
1 LIGHT,UNEW,GAMMAT,FG,AVGTLF,
1 RB,RST,RLEAF,CUMDEW,
1 HT,HE,HEND,POR,VGAS,
1 PSIS,TIME,ABACON)

```

CC

IMPLICIT NONE

```

$INCLUDE:ALIMIT.FOR/L
$INCLUDE:ABLANK.FOR/L
$INCLUDE:ACONST.FOR/L

```

INTEGER ITRM,ITRA,FLAG

```

REAL*8 LEFL(IB:IH,1:2,1:2,1:2)
REAL RCUTI(1:IT,2)
REAL GRASH(0:IT),NU(0:IT),REYNOL(0:IT)
REAL NUFORC(0:IT),NUFREE(0:IT)
REAL LIGHT(0:IH,1:2),UNEW(0:ITB),GAMMAT(1:IT)
REAL FG(1:IT,1:2),AVGTLF(1:IT),RB(0:IT),RST(0:IT,1:2)
REAL RLEAF(1:IT,1:2),CUMDEW(1:IT,1:2)
REAL HT(0:IT),HE(0:IT,1:2,1:2),HEND(1:IT,1:2)
REAL POR(IS:0),VGAS(IS:0)
REAL PSIS(IS:ITB,0:5,1:2)

```

REAL TIME,ABACON

CHARACTER T

```

INTEGER I,J
REAL ETA
REAL DIFF

```

```

REAL GS(1:IT,2)
REAL LCONDU(IT,2)
REAL CO2SET(2,IT)
REAL F1(1:IT,1:2)
REAL F2(1:IT,1:2)

```

```

REAL CRITER(0:IT)
REAL RBOL(0:IT)

REAL BC
REAL ALPHA,GSMIN,DELTA,BETA,GSMAX
REAL DIFFER

$INCLUDE:VALUES.DAT/L

ALPHA=0.254468
DELTA=2.90
BETA=0.000120
GSMIN= 0.0005
ETA = 14.2E-6
DIFF= 20.2E-6

T=CHAR(9)

IF(ITRM .EQ. 0) THEN
  ABACON =0.0
  VGAS(0) =0.0
ENDIF

GSMAX = 0.005

DO 200 I=1,ITA,1
  RCUTI(I,1)=2000.
  RCUTI(I,2)=2000.

  IF(LIGHT(I,1).GT.0.0001) THEN
    F1(I,1)=1.0/(1+100./LIGHT(I,1))
    !The light function for stomatal resistance.
  ELSE
    F1(I,1) =0.0
  ENDIF

  IF(LIGHT(I,2).GT. 0.0001) THEN
    F1(I,2)=1.0/(1+100./LIGHT(I,2))
  ELSE
    F1(I,2)=0.0
  ENDIF

  IF (ITRM.GT.0) THEN
    F2(I,1)= EXP(-BETA*ABACON*EXP(DELTA* PSIS(I,5,2)))
    F2(I,2)= EXP(-BETA*ABACON*EXP(DELTA* PSIS(I,5,2)))
    ! The second term in eq. 4.5.15
  ELSE
    F2(I,1)= EXP(-BETA*ABACON*EXP(DELTA* PSIS(I,5,1)))
    F2(I,2)= EXP(-BETA*ABACON*EXP(DELTA* PSIS(I,5,1)))
  ENDIF

  GS(I,1) = GSMIN+(GSMAX-GSMIN)*F1(I,1)*F2(I,1)
  GS(I,2) = GSMIN+(GSMAX-GSMIN)*F1(I,2)*F2(I,2)

  RST(I,1)=1./GS(I,1)
  RST(I,2)=1./GS(I,2)

  LCONDU(I,1)=GS(I,1)+1/RCUTI(I,1)
  LCONDU(I,2)=GS(I,2)+1/RCUTI(I,2)

  RLEAF(I,1)=1./LCONDU(I,1)
  RLEAF(I,2)=1./LCONDU(I,2)

  REYNOL(I)= UNEW(I)*DLEAF/ETA
  RBOL(I)=CLEAF*(DLEAF/UNEW(I))**(0.5)

  IF (ITRM.EQ.0) THEN
    NU(I) = 1.08*0.89*REYNOL(I)**0.5
  ELSE
    ! Look at Monteith & Unsworth (1990) and Gates (1980)
    DIFFER = AVGTLF(I)-SNGL(TEMAIR(I))
    GRASH(I) = GR * DIFFER
    *DLEAF**3/(273*ETA**2)
    CRITER(I) = GRASH(I)/REYNOL(I)**2
    NUFORC(I) = 1.08*0.89* REYNOL(I)**0.5
  ENDIF
200

```

```

IF (GRASH(I).LT.10E5) THEN

NUFREE(I) = 0.40*(ABS(GRASH(I))*0.7)**0.25
ELSE
NUFREE(I) = 0.13*GRASH(I)**0.33
ENDIF
IF (CRITER(I).GE.16.) THEN
NU(I) = NUFREE(I)
ELSEIF ((CRITER(I).LT.16.).AND.
(CRITER(I).GT.0.1)) THEN
1  NU(I) =AMAX1(NUFREE(I),NUFORC(I))
ELSE
NU(I)= NUFORC(I)
ENDIF
ENDIF
RB(I)= DLEAF/(DIFF*NU(I))
HT(I)=PCP/RB(I)
HE(I,1,1)=PCP/(GAMMA*(0.93*RB(I)+RLEAF(I,1)))
HE(I,2,1)=PCP/(GAMMA*(0.93*RB(I)+RLEAF(I,2)))
HE(I,1,2)=PCP/(GAMMA*0.93*RB(I))
HE(I,2,2)=PCP/(GAMMA*0.93*RB(I))
DO 202 J=1,2,1
HEND(I,J)=HE(I,J,1)
202 CONTINUE
200 CONTINUE
REYNOL(0)= UNEW(1)*DCLOUDS/ETA
IF(ITRM.EQ.0) THEN
RB(0)=CSOILR*(DCLOUDS/UNEW(1))**(0.5)
ELSE
DIFFER =TEMAIR(0)-TEMAIR(1)
1 GRASH(0) = GR*DIFFER
*DCLOUDS**3/(273*ETA**2)
CRITER(0) = GRASH(0)/REYNOL(0)**2
NUFORC(0) = 1.08*0.89* REYNOL(0)**0.5

IF (DIFFER.LT.0.0) THEN
NUFREE(0) = 0.23* (ABS(GRASH(0)))**0.25
ELSEIF (DIFFER.EQ.0.0) THEN
DIFFER =0.2
GRASH(0)= GR*DIFFER*DCLOUDS**3/(273*ETA**2)
NUFREE(0) = 0.5 * (ABS(GRASH(0)))**0.25

ELSEIF (GRASH(0).LE.10E5) THEN
NUFREE(0) = 0.5 * GRASH(0)**0.25
ELSE
NUFREE(0) =0.13*GRASH(0)**0.33
ENDIF
IF (CRITER(0).GE.16.) THEN
NU(0) = NUFREE(0)
ELSEIF ((CRITER(0).LT.16.).AND.
1 (CRITER(0).GT.0.1))THEN
NU(0) =AMAX1(NUFREE(0),NUFORC(0))

```

```

        ELSE
        NU(0)= NUFORC(0)
        ENDIF
    ENDIF
    RB(0)= DCLOUDS/(DIFF*NU(0))

C
    HT(0)=PCP/RB(0)
    RST(0,2)=1000000
    RST(0,2)= DZ(0)/VAPDIF*VGAS(0)**(6./3.)/POR(0)**2
    HE(0,1,2)=PCP/(GAMMA*(0.93*RB(0)+RST(0,2)))

    RETURN
    END

```

CC

```

SUBROUTINE FLUX(FLAG,
: TEMAIN,EAIRNW,NC02,
: STORAH,SH,SL,SINK,
: STORAV,STORAC,
: PCSOIL,VGAS,
: TOTALQ,TOTLE,TOTASE,TOTASQ,SOILLE,
: DT,TIMEW,SOILRN)

```

CC

IMPLICIT NONE

```

$INCLUDE:ALIMIT.FOR/L
$INCLUDE:ABLANK.FOR/L
$INCLUDE:AFUX.FOR/L
$INCLUDE:ACOEFF.FOR/L
$INCLUDE:ACONST.FOR/L

```

SAVE /ACFLUX/,/ACOEFF/

INTEGER FLAG

```

REAL*8 TEMAIN(IS:ITB),EAIRNW(IS:ITB),NC02(IS:ITB),
1 STORAH(IS:IH),
1 SH(IB:IH),SL(IB:IH)
REAL STORAV(IS:IH),STORAC(IS:IH),
1 PCSOIL (IS:0),VGAS(IS:0),
1 DSDT(IS:IH),SINK(IB:IH)

```

REAL TOTALQ,TOTLE,TOTASE,TOTASQ,SOILLE
REAL SOILRN

REAL DT,TIMEW
CHARACTER T

CCCCCCCC

INTEGER I
\$INCLUDE:VALUES.DAT/L

T=CHAR(9)

IF ((FLAG.EQ.0).OR.(FLAG.EQ.1).OR.(FLAG.EQ.2))THEN

DO 1501 I=ISA+1,IHA,1

```

: ANALOG(I)=-FH(I)*TEMAIN(I)+GH(I)*TEMAIN(I+1)
: +EH(I)*TEMAIN(I-1)+DH(I)
: ANELOG(I)=-FLE(I)*EAIRNW(I)+GLE(I)*EAIRNW(I+1)
: +ELE(I)*EAIRNW(I-1)+DLE(I)
: ANAC02(I)=-FC02(I)*NC02(I)+GC02(I)*NC02(I+1)
: +EC02(I)*NC02(I-1)+DC02(I)
FLUXHT(I)= GH(I)*(TEMAIN(I)-TEMAIN(I+1))
FLUXVT(I)= GLE(I)*(EAIRNW(I)-EAIRNW(I+1))
FLUXCT(I)= GC02(I)*(NC02(I)-NC02(I+1))
FLUXHB(I)= EH(I) *(TEMAIN(I-1)-TEMAIN(I))
FLUXVB(I)= ELE(I) *(EAIRNW(I-1)-EAIRNW(I))
FLUXCB(I)= EC02(I)*(NC02(I-1)-NC02(I))

```

```

DELT(I)=(TEMAIN(I)-TEMAIR(I))
DELTV(I)=(EAIRNW(I)-EAIR(I))
DELT(I)=(NC02(I)-C02CON(I))

```

```

IF (I. LE. 0) THEN
    STORAH(I) = PCSOIL(I)*DZ(I)*DELTT(I)/DT
    STORAV(I) = PCP/GAMMA*DZ(I)*VGAS(I)
    *DELTV(I)/DT
    STORAC(I) = VGAS(I)*DZ(I)*DELTC(I)/DT
ELSE
    STORAH(I) = PCP*DZ(I)*DELTT(I)/DT
    STORAV(I) = PCP/GAMMA*DZ(I)*DELTV(I)/DT
    STORAC(I) = DZ(I)*DELTC(I)/DT
ENDIF

ENERLH(I) = FLUXHB(I) - FLUXHT(I) + SH(I) - STORAH(I)
ENERLE(I) = FLUXVB(I) - FLUXVT(I) + SL(I) - STORAV(I)
ENERLC(I) = FLUXCB(I) - FLUXCT(I) - SINK(I)/1.833 - STORAC(I)

IF (I. EQ. 1) THEN
    ENERLE(I) = FLUXVB(I) - FLUXVT(I) + SOILLE + SL(I) - STORAH(I)
ENDIF

IF (I. EQ. 0) THEN
    ENERLH(I) = FLUXHB(I) - FLUXHT(I) + SH(I) - STORAH(I)
    +SOILRN
ENDIF

CFLXHT(I) = FLUXHT(I)*DT
CFLXVT(I) = FLUXVT(I)*DT
CFLXCT(I) = FLUXCT(I)*DT

CFLXHB(I) = FLUXHB(I)*DT
CFLXVB(I) = FLUXVB(I)*DT
CFLXCB(I) = FLUXCB(I)*DT

FLDIVH(I) = (FLUXHB(I) - FLUXHT(I))*DT
FLDIVV(I) = (FLUXVB(I) - FLUXVT(I))*DT
FLDIVC(I) = (FLUXCB(I) - FLUXCT(I))*DT

DHCDT(I) = FLDIVH(I) + SH(I)*DT
DVCDT(I) = FLDIVV(I) + SL(I)*DT

IF (I. EQ. 1) THEN
    DVCDT(I) = FLDIVV(I) + SL(I)*DT + SOILLE*DT
ENDIF

IF (I. EQ. 0) THEN
    DHCDT(I) = FLDIVH(I) + SH(I)*DT + SOILRN*DT
ENDIF

DCCDT(I) = FLDIVC(I) - SINK(I)*DT/1.833

IF (I. GT. 0) THEN
    DELTEM(I) = DHCDT(I)/(PCP*DZ(I))
    DELVPR(I) = DVCDT(I)/(PCP/GAMMA*DZ(I))
    DELCO2(I) = DCCDT(I)/DZ(I)
ELSE
    DELTEM(I) = DHCDT(I)/(PCSOIL(I)*DZ(I))
    DELVPR(I) = DVCDT(I)/(PCP/GAMMA*DZ(I)*VGAS(I))
    DELCO2(I) = DCCDT(I)/(DZ(I)*VGAS(I))
ENDIF

IF (I. GT. 0) THEN
    DELTTE(I) = PCP*DZ(I)*DELTT(I)
    DELTVE(I) = PCP/GAMMA*DZ(I)*DELTV(I)
    DELTCE(I) = DZ(I)*DELTC(I)
ELSE
    DELTTE(I) = PCSOIL(I)*DZ(I)*DELTT(I)
    DELTVE(I) = PCP/GAMMA*DZ(I)*VGAS(I)*DELTV(I)
    DELTCE(I) = DZ(I)*VGAS(I)*DELTC(I)
ENDIF

```

```

STORH=STORH+DELTE(I)
STORV=STORV+DELVE(I)
STORC=STORC+DELTC(I)

STORHT=STORHT+DHCDT(I)
STORVT=STORVT+DVCDDT(I)
STORCT=STORCT+DCCDDT(I)

```

1501 CONTINUE

```

STOREH=0.0
STOREV=0.0
STOREC=0.0

```

```

STORHC=0.0
STORVC=0.0
STORCC=0.0

```

DO 1502 I=1,IHA,1

```

STOREH=STOREH+DELTE(I)
STOREV=STOREV+DELVE(I)
STOREC=STOREC+DELTC(I)

```

```

STORHC=STORHC+DHCDT(I)
STORVC=STORVC+DVCDDT(I)
STORCC=STORCC+DCCDDT(I)

```

1502 CONTINUE

```

STORH=STOREH/DT
STORV=STOREV/DT
STORH2=STORHC/DT
STORV2=STORVC/DT

```

ELSEIF ((FLAG.EQ. 31).OR.(FLAG.EQ.32)) THEN

```

NLF1ST=0.0
NLF1SV=0.0
NLF1SC=0.0

```

DO 100,I=1,IHA, 1

```

NLDLST(I) = PCP*(TEMAIR(I)-TEMAIR(IHA+1))*DZ(I)
NLDLSV(I) = PCP/GAMMA*(EAIR(I)-EAIR(IHA+1))*DZ(I)
NLDLSC(I) = (CO2CON(I)-CO2CON(IHA+1))*DZ(I)

```

```

NLF1ST= NLF1ST + NLDLST(I)
NLF1SV= NLF1SV + NLDLSV(I)
NLF1SC= NLF1SC + NLDLSC(I)

```

100 CONTINUE

ELSEIF (FLAG.EQ. 4) THEN

```

NLF1GT= 0.0
NLF1GV= 0.0
NLF1GC= 0.0

```

DO 200, I=1,IHA,1

```

NLDLGT(I) = PCP*(TEMAIR(I)-TEMAIR(IHA+1))*DZ(I)
NLDLGV(I) = PCP/GAMMA*(EAIR(I)-EAIR(IHA+1))*DZ(I)
NLDLGC(I) = (CO2CON(I)-CO2CON(IHA+1))*DZ(I)

```

```

NLF1GT= NLF1GT + NLDLGT(I)
NLF1GV= NLF1GV + NLDLGV(I)
NLF1GC= NLF1GC + NLDLGC(I)

```

200 CONTINUE

ELSE

WRITE(*,*) 'THERE IS A MISTAKE'

ENDIF

RETURN

END


```

101 CONTINUE
    ELSE

        I2=NINT(REAL(ITA)*0.80)
        DO 10 I= I2+1, IHA, 1
            UINI(I) = USTAR /KARMEN * ALOG ((ZCENTER(I)-DISPL)/ZO)
10    CONTINUE
        I1=NINT(REAL(ITA)*0.25)
        DO 100 I= 1,I1,1
            UINI(I) = USTAR /(100*KARMEN )* ALOG(ZCENTER(I)* 100)
100   CONTINUE
        BA= Z(ITA)/(4*ZO* ALOG(0.25*Z(ITA)/ZO))
        AW =EXP(-BA)* USTAR/KARMEN *ALOG ((Z(ITA)-DISPL)/ZO)
        DO 200 I=I1+1,I2 ,1
            UINI(I) = AW*EXP(BA*ZCENTER(I)/Z(ITA))
200   CONTINUE
        UINI(IHA+1)=USTAR/KARMEN* ALOG((Z(IHA)-DISPL)/ZO)
    ENDIF
    RETURN
    END

```

```

CCCCCCCCCCCCCCCCCCCCCCCCCCCCCCCCCCCCCCCCCCCCCCCCCCCCCCCCCCCCCCCCCCCCCCCC
C

```

```

SUBROUTINE INIT(SOILTM,
: ELASTI,OSMOTI,
: KXYLUM,RLS,RS,
: PSIXYL,PSIS,
: PSISOL,HM,DX,
: VOLUME,TOTDX,
: RADIUS,RDENST,
: TIME,KSOIL,
: SOILIN)

```

```

CCCCCCCCCCCCCCCCCCCCCCCCCCCCCCCCCCCCCCCCCCCCCCCCCCCCCCCCCCCCCCCCCCCCCCCC

```

```

IMPLICIT NONE

```

```

$INCLUDE:ALIMIT.FOR/L
$INCLUDE:ABLANK.FOR/L
$INCLUDE:ACONST.FOR/L

```

```

REAL SOILTM(IS:0),
1 ELASTI(IS:ITB,1:3),OSMOTI(IS:ITB,0:5,1:2),
1 KXYLUM(IS:IH,0:5),RLS(IS:ITB),RS(IS:ITB,0:5),
1 PSIXYL(IS:ITB,0:5,1:2),PSIS(IS:ITB,0:5,1:2),
1 PSISOL(IS:0),HM(IS:0),DX(IS:IH,0:5),
1 VOLUME(IS:IH,0:5),TOTDX(1:IH),
1 RADIUS(IS:0),RDENST(IB:0)

```

```

C REAL TIME,KSOIL
! KSOIL is an assumed soil thermal diffusivity..
CHARACTER T
REAL SATUV2,SATUDZ,X

```

```

CCCCCCC

```

```

INTEGER I,J

```

```

REAL AMP0, TSOILA, OMEGA,PERIOD

```

```

C Amplitude of the soil temperature wave at the soil surface in °C
C Temperature of the soil
C Cyclic frequency.
C period of the wave (daily) respectively.

```

```

1 REAL HEI,VLEAF,VSTEM,CLEAFW,CSTEMW,
,RSLEAF,RSSTEM,RXSTEM,RRROOT

```

```

C HEI height of the plant in m
C VLEAF: volume of the leaves of one plant in m3
C VSTEM: volume of the stem of one plant

```

```

C      CLEFW: leaf capacitance in m3 MPa-1
C      CSTEMW stem capacitance in m3 MPa-1
C      RSLEAF for one leaf in MPa s m-3
C      RSSTEM for whole stem MPa s m-3
C      RXSTEM for whole plant MPa s m-3
C      RROOT for whole root MPa s m-3

C      REAL ELAST1,ELAST2,ELAST3
C      ! Elasticity modulus for the xylum storage

DATA PERIOD/24.0/

T=CHAR(9)

$INCLUDE:VALUES.DAT

READ(36,*) AMP0,KSOIL,TSOILA

CO2CON(IHA+1)=300.

DO 300 I=IHA,1,-1

    TEMAIR(I)= TEMAIR(IHA+1)
    EAIR(I) = EAIR(IHA+1)
    CO2CON(I)=CO2CON(IHA+1)
300    CONTINUE

    OMEGA=2*PI/(PERIOD*60*60)
    PSISOL(ISA)=HM(ISA)+Z(ISA)
    DO 400 I=ISA+1,0,1

        IF (SOILIN .NE.1) THEN

            READ(36,*) SOILTM(I)

            ELSE

                SOILTM(I)=TSOILA
                :
                :      +AMP0
                :      *EXP(-1*(OMEGA/(2*KSOIL)))**0.5*ABS(ZCENTER(I)))
                :      *SIN((OMEGA*TIME*60*60)-(OMEGA/(2*KSOIL)))**0.5
                :      *ABS(ZCENTER(I)))
                :
            ENDIF

            TEMAIR(I)=SOILTM(I)
            EAIR(I)= SATUV2(SNGL(TEMAIR(I)))
            CO2CON(I)=400.0
            PSISOL(I)=HM(I)+ZCENTER(I)
400    CONTINUE

        IF (SOILIN .NE.1) THEN

            READ(36,*) SOILTM(ISA)

            ELSE

                SOILTM(ISA)=TSOILA
                :
                :      +AMP0
                :      *EXP(-1*(OMEGA/(2*KSOIL)))**0.5*ABS(Z(ISA)))
                :      *SIN((OMEGA*TIME*60*60)-(OMEGA/(2*KSOIL)))**0.5
                :      *ABS(Z(ISA)))
                :
            ENDIF

            SOILTM(ISA) =25.0

            TEMAIR(ISA)=SOILTM(ISA)
            EAIR(ISA)= SATUV2(SNGL(TEMAIR(ISA)))
            CO2CON(ISA)=400.0

            READ(36,*) HEI,VLEAF,VSTEM,CLEFW,CSTEMW,
1          RSLEAF,RSSTEM,RXSTEM,RROOT

            READ(36,*) ELAST1,ELAST2,ELAST3

J=0
DO 500 I=ISA,IHA,1

    PSIXYL(I,J,1)= PSISOL(ISA)*RHO*GR/10E6
    PSIS(I,J,1) = PSISOL(ISA)*RHO*GR/10E6
    OSMOTI(I,J,1)=ABS(PSISOL(ISA)*RHO*GR/10E6-0.3)
    KXYLUM(I,J) = HEI/RXSTEM

```

```

        ELASTI(I,1)=ELAST1
        ELASTI(I,2)=ELAST2
        ELASTI(I,3)=ELAST3
500    CONTINUE
        DO 550 I=ISA+1,0,1
            VOLUME(I,0)=PI*RADIUS(I)**2*RDENST(I)
550    CONTINUE
        DO 600 I=1,IHA,1
            RS(I,J)      = RSSTEM*HEI/DZ(I)
            VOLUME(I,0)  = VSTEM*DZ(I)/HEI
600    CONTINUE
        DO 700 I=1,IHA,1
            READ(36,*) DX(I,0),DX(I,1),
1         DX(I,2),DX(I,3),DX(I,4),DX(I,5)
            DO 750 J=1,5,1
                RS(I,J) =RSSTEM*HEI/DX(I,J)
750    CONTINUE
            RLS(I)= DX(I,0)* 2.5*RXSTEM/HEI
C         IT HAS TO BE CORRECTED FOR THE AREA
700    CONTINUE
            PSIXYL(IHA+1,0,1)=PSISOL(ISA)*RHO*GR/10E6
            PSIS(IHA+1,0,1)  =PSISOL(ISA)*RHO*GR/10E6
            OSMOTI(IHA+1,0,1)=ABS(PSISOL(ISA)*RHO*GR/10E6-0.3)
            ELASTI(IHA+1,1)  =ELAST1
            ELASTI(IHA+1,2)  =ELAST2
            ELASTI(IHA+1,3)  =ELAST3
            RS(IHA+1,0)      = 56E6
            RLS(IHA+1)       = 10E8
        DO 650 I=1,IHA,1
            TOTDX(I)=DX(I,0)+DX(I,1)+DX(I,2)
1            +DX(I,3)+DX(I,4)+DX(I,5)
            DO 601 J=1,5,1
                PSIXYL(I,J,1)= PSISOL(ISA)*RHO*GR/10E6
                PSIS(I,J,1)  = PSISOL(ISA)*RHO*GR/10E6
                KXYLUM(I,J)  = KXYLUM(I,0)
                VOLUME(I,J)  = DX(I,J)/TOTDX(I)*VLEAF
                *LEAINC(I)/CUMLA(I,0)
                OSMOTI(I,J,1)=ABS(PSISOL(ISA)*RHO*GR/10E6-0.3)
601    CONTINUE
650    CONTINUE
        J=0
        DO 800 I=ISA,0,1
            RS(I,J)=100E6
800    CONTINUE

        RETURN
        END
        REAL FUNCTION SATUVZ(X)
        IMPLICIT NONE
        REAL X
        SATUVZ=610.7*EXP(17.4*X/(X+239.))
        RETURN
        END

        REAL FUNCTION SATUDZ(X)
        IMPLICIT NONE
        REAL X

```

```

C      SATUD2=4158.6*SATUV2(X)/(X+239)**2
      SATUD2=2539657.*EXP(17.4*X/(X+239.))
1      *.1/(X+239)**2

      RETURN
      END

```

CC

```

      SUBROUTINE RADBOU(TAIR,BAIR,WINDTP,WINDZS,CLOUDN,
1      RLOUT,RLINN,WAYIN,CORR,MINUTE,T,TIMER)

      IMPLICIT NONE

$INCLUDE:ARDBOU.FOR/L
$INCLUDE:ACONST.FOR/L

      SAVE / ARADBOU /
      INTEGER CORR,WAYIN,MINUTE
      REAL WINDTP,CLOUDN,WINDZS
      CHARACTER T

CCCCC
      REAL SATUV2,SATUD2,X
      REAL TAIR,BAIR,DTEMP,WTEMP,SHRTN
C
      REAL RATIO
      REAL SOLARC,SO,TRANAT,SDFSG,R,K
C      ! Solar constant, Extraterrestrial solar radiation, Transmissivity of
C      ! the atmosphere, fraction @@
      REAL ST,SE
C      ! fraction of the value of the amplitude.
      REAL RLOUT,RLINN,HEIM1,HEIM2,FUNK,RSVRT
C      ! outgoing longwave radiation, incoming longwave radiation, heimann 1 and heimann 2
C      ! Funk type netradiometer value, reflected short wave radiation value.
      DATA SOLARC/1370./

$INCLUDE:VALUES.DAT/L

      SINBTA= SIN(LATI*RADE)*SINDE+COS(LATI*RADE)*COS(DECLIN)
1      *COS(RADE*(15*(TIME-12)))

      RATIO=AMAX1((SINBTA/SIN00N),0.0)
      USTAR=(0.25*RATIO)+0.05
      IF (WAYIN.NE.1) THEN
1          READ(29,*)TIMER,WINDZS,WINDTP,DTEMP,WTEMP,SHRTN
          ,RSVRT,FUNK,HEIM1,HEIM2
      ENDIF
      IF (SINBTA.GT.0.0) THEN
          SO = SOLARC*(1+0.033*COS(RADE*360.*DAYNUM/365.))*SINBTA
          TRANAT = A +B * SINBTA
          SGLOBL = SO *TRANAT
          R = 0.847-1.61*SINBTA+1.04* SINBTA**2
          K = (1.47-R)/1.66
          IF (TRANAT.LE. 0.22) THEN
              SDFSG =1.
          ELSE IF (TRANAT.LE.0.35) THEN
              SDFSG =1-6.4*(TRANAT-0.22)**2
          ELSE IF (TRANAT.LE.K) THEN
              SDFSG = 1.47-1.66*TRANAT
          ELSE
              SDFSG = R
          ENDIF
          IF (WAYIN.EQ.1) THEN
              IINI(1)= 0.5*SGLOBL
              IINI(2)= 0.5*SGLOBL
          ELSE
              SHRTN= AMAX1(SHRTN,0.0)
              RSVRT=AMAX1(RSVRT,0.0)

```

```

      IINI(1)= 0.5*SHRTN
      IINI(2)= 0.5*SHRTN
      CLOUDN = 1. -SHRTN/SGLOBL
      RLOUT=-0.95*SBOLTZ*((HEIMA1+HEIMA2)/2.0+273.15)**4
      RLINN=FUNK-(SHRTN-RSHRT)-RLOUT

```

```

ENDIF

```

```

      DIRECT(2)=1-MIN(1.4*SDFSG,1.0)
      DIRECT(1)= 1-(2*SDFSG-MIN(1.4*SDFSG,1.0))

```

```

ELSE

```

```

      IINI(1)  =0.00001
      IINI(2)  =0.00001
      TRANAT   =0.0
      SDFSG    =0.0
      DIRECT(1)=0.0
      DIRECT(2)=0.0

```

```

IF (WAYIN.NE.1) THEN

```

```

      RLOUT=-0.95*SBOLTZ*((HEIMA1+HEIMA2)/2.0+273.15)**4
      RLINN=FUNK-RLOUT

```

```

ENDIF

```

```

ENDIF

```

```

IF (WAYIN.EQ.1) THEN

```

```

IF((TIME.GE.BB).AND.(TIME.LE.SUNSET))THEN

```

```

ST  = SIN(PI*(TIME-BB)/(DAYLNG+2*P))

```

```

IF (TIME.LT.(12+P)) THEN

```

```

      TAIR  = (TMAX-TMIN(1))*ST+TMIN(1)
      RH  = (RHMIN(1)-RHMAX(1))*EXP(-(12+P-BB)/2)
1      +(RHMAX(1)-RHMIN(1))*EXP(-(TIME-BB)/2)/
1      (1-EXP(-(12+P-BB)/2))

```

```

ELSE

```

```

      TAIR  = (TMAX-TMIN(2))*ST+TMIN(2)
      SE  = SIN(PI*(TIME-(12+P))/(2*(12+BB-P)))
      RH  = SE*(RHMAX(2)-RHMIN(1))+RHMIN(1)

```

```

ENDIF

```

```

      BAIR =RH * SATUV2(TAIR)
      BAIR = 2000.

```

```

C

```

```

ELSE IF ((TIME .GT. SUNSET).AND.(TIME.LE.24.0)) THEN

```

```

1      TAIR=(TMIN(2)-TSN*EXP(- (NGHTLN+C)/4)
1      +(TSN-TMIN(2))*EXP(-(TIME-SUNSET)/4))/
      (1-EXP(- (NGHTLN+C)/4))

```

```

      SE  = SIN(PI*(TIME-(12+P))/(2*(12+BB-P)))
      RH  = SE*(RHMAX(2)-RHMIN(1))+RHMIN(1)

```

```

      BAIR=RH *SATUV2(TAIR)

```

```

ELSE

```

```

1      SE  = SIN(PI*(TIME+12-P)/(2*(12+BB-P)))
1      TAIR=(TMIN(1)-TSN*EXP(- (NGHTLN+C)/4)
      +(TSN-TMIN(1))*EXP(-(TIME+NGHTLN/2)/4))/
      (1-EXP(- (NGHTLN+C)/4))

```

```

      RH  = SE*(RHMAX(1)-RHMIN(0))+RHMIN(0)
      BAIR=RH * SATUV2(TAIR)

```

```

ENDIF

```

```

ELSE

```

```

      TAIR =DTEMP

```

```

IF (DTEMP.GT.WTEMP) THEN

```

```

      BAIR =SATUV2(WTEMP)-GAMMA*(DTEMP-WTEMP)

```

```

ELSE

```

```

      BAIR =SATUV2(WTEMP)

```

```

ENDIF

```

```

ENDIF

```

```

RETURN

```

```

END

```

```

C THE COMMON FILES
C Alimit.for
  INTEGER IT,IH,IS,IL,IB,ITB,nla,poly
  1 PARAMETER(IT=24,IH=35,IS=-23,IL=-24
    ,IB=-22,ITB=36,nla=3,poly=5)

C
  .ablank.for
  INTEGER ITA,IHA,ISA
  INTEGER CORR
  REAL*8 TEMAIR(IS:ITB),EAIR(IS:ITB),CO2CON(IS:ITB)
  1 REAL DZ(IS:ITB),Z(IS:IH),ZCENTER(IB:IH),
    LAD(0:IH),LADMID(1:IH),LEAINC(1:IH),CUMLAI(0:IH)
  COMMON //TEMAIR,EAIR,CO2CON,
  1 DZ,Z,ZCENTER,LAD,LADMID,LEAINC,CUMLAI,CORR,
  1 ITA,IHA,ISA

C ABERGE.FOR
  1 REAL FC(IS:0),FQ(IS:0),FO(IS:0),POR(IS:0),
    PCSOIL(IS:0),CHSOIL(IS:0)
  COMMON /ABERGE/ FC,FQ,FO,POR,
  1 PCSOIL,CHSOIL

C ACOEFF.FOR
  REAL*8 EH(IS:ITB),GH(IS:ITB),FH(IS:ITB),DH(IS:ITB),
  1 ELE(IS:ITB),GLE(IS:ITB),FLE(IS:ITB),DLE(IS:ITB),
  1 ECO2(IS:ITB),GCO2(IS:ITB),FCO2(IS:ITB),DCO2(IS:ITB)
  COMMON/ ACOEFF/EH,GH,FH,DH,
  1 ELE,GLE,FLE,DLE,
  1 ECO2,GCO2,FCO2,DCO2

C ACONST.FOR
  REAL PCP,GAMMA,LAMDA,RHO,KW,GR
  REAL CWATER,CQUARZ,CCLAY,CORGNC
  REAL PI
  REAL VAPDIF
  REAL CLEAF,DLEAF,CSOILR,DCLDS
  REAL EMSSIV,SBOLTZ,SOILEM
  real co2dif,mole,RR
  COMMON /ACONST/ PCP,GAMMA,LAMDA,RHO,KW,GR,
  1 CWATER,CQUARZ,CCLAY,CORGNC,
  1 PI,
  1 VAPDIF,
  1 CLEAF,DLEAF,CSOILR,DCLDS,
  1 EMSSIV,SBOLTZ,SOILEM,
  1 co2dif,mole,RR

C AENERG.FOR
  INTEGER INDEXD(IT,2,2),IPR(IT,2,2)
  REAL*8 SENFL(IB:IH,1:2,1:2,1:2),LEFL(IB:IH,1:2,1:2,1:2),
  1 laylef(1:IT),laysen(1:IT),laybal(1:IT),stor(1:it)
  REAL ESTLF(1:IT,1:2,1:2,1:2),DELTAT(1:IT,1:2,1:2,1:2)
  1 LEAFLT(1:IT,1:2),PRC(1:IT,1:2,1:2)
  1 SENSH(1:IT,1:2,1:2,1:2),LEFLUX(1:IT,1:2,1:2,1:2)
  1 LWLFN(1:IT,1:2,1:2,1:2),ENERG(1:IT,1:2,1:2,1:2)
  1 FRA(1:IT,1:2,1:2),TOTCON(1:IT,1:2,1:2)
  1 CUMDWA(1:IT,1:2),VOLUMD(1:IT,1:2),NUMDRP(1:IT,1:2)
  1 ERR2(1:IT,1:2),ER(1:IT,1:2)
  real fluxup(it,1:2,1:2,1:2),fluxbt(it,1:2,1:2,1:2),
  1 linear(it,1:2,1:2,1:2),sourc(it,1:2,1:2,1:2),
  1 nonst(it,1:2,1:2,1:2)
  1 total(it,1:2,1:2,1:2),totae(it,2,2),totaco(1:it)
  REAL RLNET,RLNTOP,RLNBTM,RNETOT,ENERER,
  : CLOUDN,SOILLN,SOILRN,TRANSP,STORAG,
  : THICKN,MAXERR,MAXER1
  COMMON/ AENERG/INDEXD,IPR
  1 ,SENFL,LEFL
  1 ,laylef,laysen,laybal,stor
  1 ,ESTLF,DELTAT,LEAFLT,PR
  1 ,SENSH,LEFLUX,LWLFN,ENERG,FRA,TOTCON
  1 ,CUMDWA,VOLUMD,NUMDRP
  1 ,ERR2,ER,fluxup,fluxbt,linear,sourc
  1 ,nonst
  1 ,total,totae,totaco
  : ,RLNET,RLNTOP,RLNBTM,RNETOT,ENERER

```

```

: , CLOUDN, SOILLN, SOILRN, TRANSP, STORAG
: , THICKN, MAXERR, MAXER1
C
AEQCOE.FOR
REAL*8 DU(0: IH), SH(IB: IH), SL(IB: IH)

REAL LMIX(1: 2, 0: IH), KM(0: IH), Kh(IS: IH),
1 HT(0: IT), HE(0: IT, 1: 2, 1: 2),
1 RB(0: IT), RST(0: IT, 1: 2),
1 SOURCL(1: IH), SOURCH(1: IH), SINK(IB: IH),
1 DSDT(IS: IH)

REAL SOILLE, SOILH, DT

COMMON /AEQCOE/ DU, SH, SL,
1 LMIX, KM, Kh,
1 HT, HE,
1 RB, RST,
1 SOURCL, SOURCH, SINK,
1 DSDT,
1 SOILLE, SOILH, DT
C
AFLUX.FOR
REAL*8 ANALOG(IS: IH), onelog(IS: IH), ANAC02(IS: IH),
1 DELTT(IS: IH), DELTV(IS: IH), DELTC(IS: IH),
1 DELTEM(IS: IH), DELVPR(IS: IH), DELC02(IS: IH),
1 FLDIVH(IS: IH), FLDIVV(IS: IH), FLDIVC(IS: IH)

REAL FLUXHT(IS: IH), FLUXVT(IS: IH), FLUXCT(IS: IH),
1 FLUXHB(IS: IH), FLUXVB(IS: IH), FLUXCB(IS: IH),
1 CFLXHT(IS: IH), CFLXVT(IS: IH), CFLXCT(IS: IH),
1 CFLXHB(IS: IH), CFLXVB(IS: IH), CFLXCB(IS: IH),
1 DHC0T(IS: IH), DVC0T(IS: IH), DCC0T(IS: IH),
1 DELTTE(IS: IH), DELTVE(IS: IH), DELTCE(IS: IH),
1 ENERLH(IS: IH), ENERLE(IS: IH), ENERLC(IS: IH),
1 nldlst(1: IH), nldlsv(1: IH), nldlsc(1: IH),
1 nldlgt(1: IH), nldlgv(1: IH), nldlgc(1: IH)

REAL STOREH, STOREV, STOREC,
1 STORHC, STORVC, STORCC,
1 STORHT, STORVT, STORTC,
1 STORHT, STORVT, STORCT,
1 STORH, STORV, STORH2, STORV2,
1 nflfst, nflfsv, nflfsc,
1 nflfgt, nflfgv, nflfgc,
1 cnlfgt, cnlfgv, cnlfgc,
1 cnlfst, cnlfsv, cnlfsc

COMMON /ACFLUX/ ANALOG, onelog, ANAC02,
1 DELTT, DELTV, DELTC, DELTEM, DELVPR, DELC02,
1 FLDIVH, FLDIVV, FLDIVC, FLUXHT, FLUXVT, FLUXCT,
1 FLUXHB, FLUXVB, FLUXCB, CFLXHT, CFLXVT, CFLXCT,
1 CFLXHB, CFLXVB, CFLXCB, DHC0T, DVC0T, DCC0T,
1 DELTTE, DELTVE, DELTCE, ENERLH, ENERLE, ENERLC,
1 nldlst, nldlsv, nldlsc, nldlgt, nldlgv, nldlgc,
1 STOREH, STOREV, STOREC, STORHC, STORVC, STORCC,
1 STORHT, STORVT, STORTC, STORHT, STORVT, STORCT,
1 STORH, STORV, STORH2, STORV2,
1 nflfst, nflfsv, nflfsc, nflfgt, nflfgv, nflfgc,
1 cnlfgt, cnlfgv, cnlfgc, cnlfst, cnlfsv, cnlfsc
C
AHYDRO.FOR
real*8 ew(is: 0), gw(is: 0), fw(is: 0), DW(is: 0)

REAL hm(is: 0), tortu(is: 0), rhsoil(is: 0),
1 Kwater(is: 0), qwater(is: 0), thetan(is: 0), thetn(is: 0),
1 THETA(is: 0), thetas(is: 0), thetar(is: 0), hmnew(is: 0),
1 Ksatu(is: 0)

real vapflt(is: 0), vapflb(is: 0), vapfdv(is: 0)
REAL lp, mp, np, alpha

REAL hmc(0: nla, 0: poly), depth(0: nla)
real kusa(0: nla, 0: poly)

integer hydrin, indeso(is: 0), rainc

COMMON /AHYDRO/ ew, gw, fw, DW,
1 hm, tortu, rhsoil,
1 Kwater, qwater, thetan, thetn,
1 THETA, thetas, thetar, hmnew,
1 Ksatu,
1 vapflt, vapflb, vapfdv,
1 lp, mp, np, alpha,
1 hmc, depth,
1 kusa,
1 hydrin, indeso, rainc
C
ANRMM.FOR

```



```

REAL LIGHT(0: IH, 1: 2),
1 RAB(1: IH, 1: 2), RABL(1: IH, 1: 2), KAV(1: 3),
1 ENESAB(1: IH, 1: 2), VISIAB(1: IH, 1: 2),
1 TOTENE, RNSHRT, RNSTOP, RNSBTM,
1 SOILSN

COMMON/ ANORMN / LIGHT,
1 RAB, RABL, KAV,
1 ENESAB, VISIAB,
1 TOTENE, RNSHRT, RNSTOP, RNSBTM,
1 SOILSN

c APLANT.FOR

INTEGER BRANCN(0: IH)

REAL DX(IS: IH, 0: 5),
: AR(IS: ITB, 0: 5), ELASTI(IS: ITB, 1: 3),
: OSMOTI(IS: ITB, 0: 5, 1: 2),
: KXYLUM(IS: IH, 0: 5), RLS(IS: ITB), RS(IS: ITB, 0: 5),
: PSIXYL(IS: ITB, 0: 5, 1: 2), PSIS(IS: ITB, 0: 5, 1: 2),
: CA(IS: IH, 0: 5), CAN(IS: IH, 0: 5),
: VOLUME(IS: IH, 0: 5), VOLMEN(IS: IH, 0: 5),
: ROOTUP(IS: 0), CONTRS(IS: 0),
: SOILRS(IS: 0), CSOIL(IS: 0),
: TOTDX(1: IH),
: WATERF, abacon,
: PLANTN, BASEDI,
: timepl(Is: ih, 0: 5)

COMMON /APLANT/BRANCN,
: DX,
: AR, ELASTI,
: OSMOTI,
: KXYLUM, RLS, RS,
: PSIXYL, PSIS,
: CA, CAN,
: VOLUME, VOLMEN,
: ROOTUP, CONTRS,
: SOILRS, CSOIL,
: TOTDX,
: WATERF, abacon,
: PLANTN, BASEDI,
: timepl

c ARDBOU.FOR
INTEGER DAYNUM
REAL SINBTA, LATI, DECLIN, TIME, SINDE,
1 DAYLNG, NGHTLN, RADE,
1 DIRECT(1: 2), Iini(1: 2), RHMAX(1: 2), RHMIN(0: 1), TMIN(1: 2)

REAL TMAX, SUNSET, TSN, RH, BB, P, C,
1 SINOON, USTAR, A, B, SGLOBL

COMMON/ ARARDBOU/ DAYNUM, SINBTA, LATI, DECLIN, TIME, SINDE,
1 DAYLNG, NGHTLN, RADE,
1 DIRECT, Iini, RHMAX, RHMIN, TMIN,
1 TMAX, SUNSET, TSN, RH, BB, P, C,
1 SINOON, USTAR, A, B, SGLOBL

c AROOTD.FOR
REAL RDNST(IB: 0),
: ROOTA(IB: 0), RADIUS(IS: 0), RADIU2(IB: 0),
: LV(IB: 0), ROOTRC(IB: 0), ROOTRS(IB: 0)

REAL ZROOT, TROOTD, SROOTC, F

COMMON /AROOTDN/ RDNST,
: ROOTA, RADIUS, RADIU2,
: LV, ROOTRC, ROOTRS,
: ZROOT, TROOTD, SROOTC, F

c the file Values.dat
PCP =1200.
GAMMA =67.
LAMDA =2.454E6
RHO =1000.
KW =0.597
GR =9.81
CWATER =4.18E6
CQUARZ =2.128E6
CCLAY =2.385E6
CORGNC =2.49E6
PI = 4*ATAN(1.)
VAPDIF =25.E-6
CLEAF=200.
DLEAF=0.05
CSOILR=200.
DCLODS=0.05
EMSSIV=1.0

```

```
C SBOLTZ=5.67E-8
  SOILEM =0.9
  SOILEM =1.0 !DDDDDDDDDD
  co2dif = 15.0e-6
  mole = 0.018 ! kg mole-1
  RR = 8.3144 ! joule mole k-1
```

Symbol	Variable name	Subroutine name & /or Equation number in the program	Units
A	! A coefficient in the atmosphere transmissivity equation ! for light for the simulated site.	RADBOU (-)	
ABACON	! Abscisic acid concentration in the xylem sap.	PLANT	amole m ⁻³
ALPHA	! A coefficient in Van Genuchten model for soil moisture ! characteristics.	HYDRO	
ANACO2	! The sum of the terms in the discretized CO ₂ conservation ! equation i.e. the solution error (Appendix A.2.11).	FLUX	ppmv ms ⁻¹
ANALOG	! The sum of the terms in the discretized sensible heat ! conservation equation i.e. the solution error ! (Appendix A.2.11).	FLUX	Wm ⁻²
ANAMOM	! The sum of the terms in the discretized momentum equation ! i.e. the solution error (Appendix A.2.11).	MOMNTM	m ² s ⁻²
ANELOG	! The sum of the terms in the discretized latent heat ! conservation equation (Appendix A.2.11).	FLUX	Wm ⁻²
AR	! Cross sectional area of the xylem elements in the stem.	PLANT	m ²
AVD1TC	! An average of CO ₂ storage within the canopy air layers ! during One AVGDLT (30 min) period.	MAIN	ppmv ms ⁻¹
AVD1TE	! An average of latent heat storage within the canopy air ! layers during One AVGDLT (30 min) period.	MAIN	Wm ⁻²
AVD1TH	! An average of sensible heat storage within the canopy air ! layers during One AVGDLT (30 min) period.	MAIN	Wm ⁻²
AVDBRN	! An average over an AVGDLT time duration for net radiation ! for the canopy lower boundary (i.e. net radiation soil)	MAIN	Wm ⁻²
AVDH	! An average over an AVGDLT period duration of local ! transport at the canopy top of sensible heat.	MAIN	Wm ⁻²
AVDLE	! An average over an AVGDLT period duration of local ! transport at the canopy top of latent heat.	MAIN	Wm ⁻²
AVDRN	! An average over an AVGDLT period duration for net radiation ! for the canopy layer only (not including the soil).	MAIN	Wm ⁻²
AVDSG	! an average of soil heat flux (at 0.01 m depth) over one ! AVGDLT period.	MAIN	Wm ⁻²
AVDSH	! An average of soil sensible heat flux to the canopy air ! over one AVGDLT period.	MAIN	Wm ⁻²
AVDSLE	! An average of soil latent heat flux to the canopy air ! (soil evaporation) over one AVGDLT period.	MAIN	Wm ⁻²
AVDSRN	! An average of net radiation of the soil over one AVGDLT ! period.	MAIN	Wm ⁻²
AVDSTC	! An average of CO ₂ flux divergence and sources ! for the canopy layer during One AVGDLT (30 min) period.	MAIN	Ppmv
AVDSTE	! An average of latent heat flux divergence and sources ! for the canopy layer during One AVGDLT (30 min) period.	MAIN	Wm ⁻²
AVDSTH	! An average of sensible heat flux divergence and sources ! for the canopy layer during One AVGDLT (30 min) period.	MAIN	Wm ⁻²
AVDSS	! An average of net radiation of the soil over one AVGDLT ! period.	MAIN	Wm ⁻²
AVDTLE	! An average latent heat sources within the canopy over one ! AVGDLT period.	MAIN	Wm ⁻²
AVDTRN	! An average over an AVGDLT period duration for net radiation ! for the canopy top (includes the canopy and the soil).	MAIN	Wm ⁻²
AVDTQ	! An average of sensible heat sources of the canopy over ! one AVGDLT period.	MAIN	Wm ⁻²
AVG1TC	! An average of CO ₂ storage within the canopy air layers ! during one gust cycle period.	MAIN	PPmv ms ⁻¹
AVG1TE	! An average of latent heat storage within the canopy ! air layers during One gust cycle period	MAIN	Wm ⁻²
AVG1TH	! An average of sensible heat storage within the canopy ! air layers during One gust cycle period.	MAIN	Wm ⁻²
AVGBRN	! An average over one gust cycle for net radiation ! for the canopy lower boundary (i.e. net radiation soil)	MAIN	Wm ⁻²
AVGDLT	! An averaging period to be read from an input file ! (in this case, it was 30 minutes).	MAIN	HOURL
AVGH	! An average over one gust cycle of local transport at the ! canopy top of sensible heat.	MAIN	Wm ⁻²
AVGLE	! An average over one gust cycle of local transport at the ! canopy top of latent heat.	MAIN	Wm ⁻²
AVGRN	! An average over one gust cycle for net radiation ! for the canopy layer only (not including the soil).	MAIN	Wm ⁻²
AVGSG	! A time average for soil Heat flux G at 0.01 m depth ! storage and heat flux	MAIN	Wm ⁻²
AVGSH	! A time average over one gust cycle of soil sensible heat ! flux to the air.	MAIN	Wm ⁻²
AVGSLE	! A time average over one gust cycle of soil latent heat ! (evaporation).	MAIN	Wm ⁻²
AVGSRN	! A time average of Average soil net radiation (rn) over ! one gust cycle.	MAIN	Wm ⁻²
AVGSS	! a time average of soil heat storage of the soil top layer ! over one gust cycle	MAIN	Wm ⁻²
AVGSTC	! An average of CO ₂ flux divergence and sources ! for the canopy layer during One gust cycle period.	MAIN	Wm ⁻²
AVGSTE	! An average of sensible heat flux divergence and sources ! for the canopy layer during One gust period.	MAIN	Wm ⁻²

AVGSTH	! An average of sensible heat flux divergence and sources for the canopy layer during One gust cycle period.	MAIN	Wm ⁻²
AVGTLE	! A time average for total sum of latent heat sources for the canopy layer (not including the soil).	MAIN	Wm ⁻²
AVGTLF	! Average temperature of the leaf.	ENERGD	0C
AVGTRN	! An average over one gust cycle for net radiation for the canopy top (includes the canopy and the soil).	MAIN	Wm ⁻²
AVGTQ	! AVERAGE TOTAL sensible heat of the whole canopy.		
B	! A coefficient in the atmosphere transmissivity equation for light at the simulated site.	RADBOU	(-)
BASEDI	! Base diameter of the plants at soil surface.	PLANT	m
BB	! Time of minimum air temperature.	MAIN	hour
BRANCN	! Number of branches per plant segment at different layers.	MAIN/PLANT	(-)
BTNOON	! Angle of the sun elevation at solar noon.	MAIN	rad
BUDLT	! Time interval for boundary condition updated (boundary delt t). In the validation runs, it was 15 minutes.	MAIN	hour
C	! Time delay after sunrise FOR minimum air temperature to occur.	MAIN	hour
CA	! old Capacitance of the plant tissue.	PLANT	m ³ MPa ⁻¹
CAN	! New Capacitance of the plant tissue.	PLANT	m ³ MPa ⁻¹
CAPAC	! Capacitance of the first air layer for water vapour. determined in different ways.	MAIN	Jm ⁻²
CAPAC1	! Capacitance of the first air layer for water vapour.	MAIN	Jm ⁻²
CAPAC2	! Capacitance of the first air layer for water vapour.	MAIN	Jm ⁻²
CAPAC3	! Capacitance of the first air layer for water vapour.	MAIN	Jm ⁻²
CCLAY	! Volumetric heat capacity of clay.	BERGE	J m ⁻³ K ⁻¹
CFLXCB	! Cumulative flux of co2 at a layer bottom within one time step.	FLUX	ppmv.m
CFLXCT	! Cumulative flux of co2 at a layer top within one time step.	FLUX	ppmv.m
CFLXHB	! Cumulative flux of sensible heat at a layer bottom. within one time step.	FLUX	Jm ⁻²
CFLXHT	! Cumulative flux of sensible heat at a layer top within one time step.	FLUX	Jm ⁻²
CFLXVB	! Cumulative flux of vapour at a layer bottom within one time step.	FLUX	Jm ⁻²
CFLXVT	! Cumulative flux of water vapour at a layer top within one time step.	FLUX	Jm ⁻²
CH	! Logical indicator (on or off) to decide the need or not to update the absorbed short wave radiation calculation by going through the subroutine NORMN.	MAIN	(-)
CHECK2	! check of the ratio between time constants of the first and second canopy air layer.		
CHECK4	! sum of vapour flux divergence and sources within the first air layer.	MAIN	Jm ⁻² s ⁻¹
CHSOIL	! Thermal heat conductivity coefficient for soil layers	BERGE	Wm ⁻¹ K ⁻¹
CHOICE	! A logical indicator (yes or no) to determine the choice of a steady or non steady state solution for the leaf	ENERGD	(-)
CLEAF	! Leaf coefficient for boundary layer resistance.	RESIS	(-)
CLOUDN	! Cloudiness (assumed for the whole day).	MAIN/ENERGD	(-)
CN	! Logical indicator (on or off) to decide the need or not to update the absorbed short wave radiation calculation by going through the subroutine NORMN.	MAIN	(-)
CNLFGC	! Cumulative non local flux due to a gust of Co2	FLUX/MAIN	
CNLFGT	! Cumulative non local flux due to a gust of Heat	FLUX/MAIN	
CNLFGV	! Cumulative non local flux due to a gust of water vapour	FLUX/MAIN	
CNLFSC	! Cumulative non local flux due to stability (no gust active) i.e. by the use of critical Richardson number (it did not work) of Co2		
CNLFST	! The same as above , but for heat		
CNLFST	! The same as above but for water vapour.		
CO2CON	! Co2 concentration.	MAIN	ppmv
CO2DIF	! Co2 diffusion coefficient in air.	EQCOEM	m ² s ⁻¹
CONTRS	! Contact resistance between the roots and the soil.	PLANTS	m ⁻¹
CORGNC	! Volumetric heat capacity of soil organic matter.	BERGE	Jm ⁻³ K ⁻¹
CORR	! a integer to determine writing to files (0) or not (else).	MAIN	(-)
COUNT	! counting the number of executing the loop which has an indicator value of 4000. It has a time period of BUDLT.	MAIN	(-)
CQUARZ	! Volumetric heat capacity for Quartz.	BERGE	Jm ⁻³ K ⁻¹
CSOIL	! Inverse of the Slope of the Hm(theta) function (Differential Capacity)		
CSOILR	! Characteristic dimension of soil clods.	HYDRD	m
CUDBRN	! Time Cumulative net radiation at the bottom of the canopy over one AVGDLT period.	RESIS	
CUDCRN	! Time Cumulative net radiation of the canopy over one AVGDLT (30 min) period.	MAIN	Jm ⁻²
CUOSE	! Time Cumulative of soil latent heat flux to the canopy air (soil evaporation) over one AVGDLT period.	MAIN	Jm ⁻²
CUOSG	! Time Cumulative of soil heat flux (at 0.01 m depth) over one AVGDLT period.	MAIN	Jm ⁻²
CUDSH	! Time Cumulative of soil sensible heat flux to the canopy air over one AVGDLT period.	MAIN	Jm ⁻²

CUDSRN	! Time Cumulative net radiation of the soil over one ! AVGDLT period.	MAIN	Jm-2
CUDSS	! Time Cumulative net radiation of the soil over one ! AVGDLT period.	MAIN	Jm-2
CUDTC	! A value for accumulating Co2 flux within time (it was ! not implemented) for AVGDLT		
CUDTLE	! Time Cumulative latent heat sources within the canopy ! over one AVGDLT period.	MAIN	Jm-2
CUDTRN	! Time Cumulative net radiation at the top of the canopy ! over one AVGDLT period.	MAIN	Jm-2
CUDTQ	! Time Cumulative sensible heat sources of the canopy ! over one AVGDLT period.	MAIN	Jm-2
CUMBRN	! Time Cumulative net radiation at the bottom of the ! canopy over one gust cycle.	MAIN	Jm-2
CUMCRN	! Time Cumulative net radiation of the canopy over one ! gust cycle.	MAIN	Jm-2
CUMDEW	! Cumulative dew on the upper (2) and lower (1) leaf ! surfaces expressed in amounts of energy.	ENERGD	Jm ⁻²
CUMDWA	! Cumulative dew at upper (2) and lower (1) leaf surface ! expressed as a wetted area.		
CUMLAI	! Cumulative leaf area index above the upper boundary of ! a certain layer.	NORMN/ ENERGD	(m ² m ⁻²)
CUMTC	! A value for accumulating Co2 flux within time (it was ! not implemented) for one gust cycle.		
CUMTLE	! Time Cumulative latent heat sources of the canopy ! over one gust cycle.	MAIN	Jm-2
CUMTRN	! Time Cumulative net radiation at the top of the canopy ! over one gust cycle.	MAIN	Jm-2
CUMTQ	! Time Cumulative sensible heat sources of the canopy ! over one gust cycle.	MAIN	Jm-2
CUMSE	! Time Cumulative of soil latent heat flux to the canopy ! air (soil evaporation) over one gust cycle.	MAIN	Jm-2
CUMSG	! Time Cumulative of soil heat flux (at 0.01 m depth) ! over one gust cycle.	MAIN	Jm-2
CUMSH	! Time Cumulative of soil sensible heat flux to the ! canopy air over one gust cycle.	MAIN	Jm-2
CUMSRN	! Time Cumulative net radiation of the soil over one ! gust cycle.	MAIN	Jm-2
CUMSS	! Time Cumulative of soil heat storage (within the ! the uppermost 0.01 m depth) over one gust cycle.	MAIN	Jm-2
CUMSLE	! Cumulative soil latent heat flux during a certain ! time interval		
CWATER	! Heat capacity for water	BERGE	Jm ⁻³ K ⁻¹
DAY	! Day number of the year being simulated.	MAIN	(-)
DAYEND	! Day number of the year for the simulation end.	MAIN	(-)
DAYLNG	! Day length in hours.	MAIN	hour
DAYNUM	! Day number of the year for the simulation beginning.	MAIN	(-)
DCCDT	! The sum of time integrated flux divergence and time ! integrated sources of CO2 within a layer over one time ! step.	FLUX	Jm ⁻²
DECLDSD	! Characteristic dimension for soil clods.	RESIS	m
DCO2	! D coefficient for the Co2 conservation equation.	EQCOEM	ppmv ms ⁻¹ or ppmv
DECLIN	! Declination of the sun.	MAIN	rad
DELCO2	! CO2 concentration change within time step determined ! from the continuity equation for a layer.	FLUX	ppmv
DELTAC	! Change in energy content due to water vapour flux ! divergence and the sources within the first air layer ! determined numerically.	MAIN	Jm-2
DELTAT	! Temperature change within a time step.	FLUX	0C
DELTCC	! CO2 concentration change within one time step.	FLUX	ppmv
DELTCE	! CO2 quantity change due to CO2 concentration change ! within time step.	FLUX	ppmv m
DELTEM	! Temperature change within one time step determined ! from the continuity equation for a layer.	FLUX	0C
DELTT	! Air temperature change for a layer within one time step.	FLUX	0C
DELTTTE	! Energy change for a layer due to temperature change ! within one time step.	FLUX	Jm-2
DELTV	! Vapour pressure change for a layer within one time step.	FLUX	Pa
DELTVTE	! Energy change for a layer due to vapour pressure change ! within one time step.	FLUX	Jm-2
DELVPR	! vapour pressure change within one time step determined ! from the continuity equation for a layer.	FLUX	Pa
DEPTH	! The depth of the interface between soil layers with ! different soil moisture characteristics.	HYDRO	m
DH	! D Coefficient of Thomas algorithm for sensible heat ! equation	EQCOEH	Wm ⁻² or 0C
DHCDT	! The sum of time integrated flux divergence and time ! integrated sensible heat sources within a layer over one ! time step.	FLUX	Jm-2
DIRECT	! Direct fraction of the two short wave radiation bands ! the visible (1) and Near Infra Red (2) at canopy top.	RADBDU	(-)
DLE	! D coefficient for Thomas Algorithm for latent heat ! equation.	EQCOEM	Wm ⁻² or Pa
DLEAF	! Characteristic dimension of the leaf.	RESIS	m
DRA	! Momentum sink with canopy layers divided by windspeed.	MOMNTM	ms ⁻¹
DSDT	! Slope of the saturated vapour pressure curve	EQCOEM	Pa K ⁻¹

DT	! Time step for the simulation.	MAIN	s
DT1	! A reduced time step for subroutine PLANT in case of numerical instabilities, due to very thin leaves.	PLANT	s
DTINT	! An integral value for a Time step.	MAIN	s
DTEMP	! dry temperature of the air at the canopy top (6.5 m)	RADBOU	°C
DU	! Wind gradient within height.	MOMNTM	s ⁻¹
DVCDOT	! The sum of time integrated flux divergence and time integrated latent heat sources within a layer over one time step.	FLUX	Jm ⁻²
DW	! The constant term in the discretized equation for liquid water transport within the soil.	HYDRO	ms ⁻¹
DX	! Distance between the nodes along the lateral branch.	PLANT/ INIT	m
DZ	! Thickness of the different layers	MAIN	m
EAIR	! Vapour pressure of air layers at the beginning of each time step.	MAIN/ EQCOEH	Pa
EAIR1	! Vapour pressure of the air for layer 1 (an iterative value)	MAIN	Pa
EAIRS	!		
EAIRNW	! New Calculated vapour pressure of air layers (at the end of time step).	CYCLE1	Pa
ECO2	! lower turbulent coupling coefficient for a layer for Co2	EQCOEM	m s ⁻¹ or (-)
EH	! Sensible heat coupling coefficient with the lower layer (turbulent within the air or thermal conduction within the soil).	EQCOEH	Wm ⁻² K ⁻¹ or (-)
ELASTI	! Elasticity modulus or coefficient of the plant tissues.	INIT	
ELE	! Latent heat coupling coefficient for a layer with the lower one (turbulent for air or diffusion within soil)	EQCOEM	Wm ⁻² Pa ⁻¹ or (-)
ENERER	! Total energy error for the whole canopy layer.	ENERGD	
ENERLC	! Error for a layer in CO2.	FLUX	ppmv ms ⁻¹
ENERLE	! energy error in latent heat for a layer within one time step.	FLUX	Wm ⁻²
ENERLH	! energy error in sensible heat for a layer within one time step.	FLUX	Wm ⁻²
ENERG	! Energy sum for a leaf segment (sum of long wave emission, latent heat, sensible heat, flux from a neighbouring leaf segment and sensible heat storage change).		
ENESAB	! Energy absorbed in the short wave bands per m-2 canopy layer.	NORMN	Wm ⁻²
EMSSIV	! Emissivity of the leaves (1.0)	ENERGD	(-)
ERR	! Difference between WM in two consequent iterations.	MAIN	Wm-2
ERRCAH	! Error in the solution of sensible heat for the whole canopy	MAIN	Wm-2
ERRCAV	! Error in the solution of latent heat for the whole canopy	MAIN	Wm-2
ESAIR	! Saturated vapour pressure for the first air layer	MAIN	Pa
ESAIR2	! Saturated vapour pressure for the first soil layer	MAIN	Pa
EXTRAS	! an extra source (+) which goes into the sensible heat equation in case of over saturation with the next iteration		
EXTRAL	! an extra sink (-) which goes into the latent heat equation in case of over saturation with the next iteration.		
EW	! Coupling coefficient for water flow to the layer below	HYDRO	s ⁻¹
EVAPOT	! Evapotranspiration integrated within one time step	MAIN	Kg m ⁻²
F	! A coefficient for determining root extinction within depth.	ROOTDN	(-)
FACTOR	! a multiplication factor for increasing or decreasing the leaf area density profile from the standard one.	MAIN	(-)
FC	! Volumetric fraction of clay.	BERGE	(-)
FCO2	! F coefficient for Thomas Algorithm for Co2 equation.	EQCOEM	ms ⁻¹ or(-)
FE	! Ratio of soil layer thickness the soil layer above.	EQCOEH	(-)
FG	! Gross photosynthesis	PHOTO	
FH	! F coefficient of Thomas Algorithm for sensible heat equation.	EQCOEH	Wm ⁻² K ⁻¹ or (-)
FLAG	! An integer indicator of the occurrence of a refreshment and due to what reason (shear at canopy top .vs. thermal instability).	MOMNTM	(-)
FLDIVC	! Flux divergence for different layers of CO2 integrated over one time step.	FLUX	ppmv m
FLDIVH	! Flux divergence of Sensible heat for different layers integrated over one time step.	FLUX	Jm ⁻²
FLDIVV	! Flux divergence of Latent(v) heat for different layers. integrated over one time step.	FLUX	Jm ⁻²
FLE	! F coefficient of Thomas algorithm for Latent heat equation for different layers.	EQCOEM	Wm ⁻² Pa ⁻¹ or (-)
FLUXBT	! Flux of Sensible Heat at a leaf segment lower (bottom) boundary.	ENERGD	Wm ⁻²
FLUXCB	! Flux of CO2 at a layer lower (bottom) boundary.	FLUX	ppmv ms ⁻¹
FLUXCT	! Flux of Co2 at the top of different layers.	FLUX	ppmv ms ⁻¹
FLUXHB	! Flux of sensible heat at a layer lower (bottom) boundary.	FLUX	Wm ⁻²
FLUXHT	! Flux of sensible heat at a layer upper (top) boundary.	FLUX	Wm ⁻²
FLUXUP	! Flux of Sensible Heat at a leaf segment upper boundary.	ENERGD	Wm ⁻²
FLUXVB	! Flux of water Vapour at a layer lower (bottom) boundary.	FLUX	Wm ⁻²

FLUXVT	! Flux of water Vapour at a layer upper (top) boundary.	FLUX	Wm^{-2}
FO	! Volumetric fraction of organic matter.	BERGE	(-)
FQ	! Volumetric fraction of Quartz or sand.	BERGE	(-)
FRA	! wet or dry fraction on the upper (2) and lower (1) surfaces of the leaf at different layers.	ENERGD	(-)
FRAC	! wet or dry fraction on the upper (2) and lower (1) surfaces of the leaf at different layers.	ENERGD	(-)
FREQ1	! number of turns for the outside loop with a 3000 index (i.e. number of gust intrusion during BUDLT period)	MAIN	(-)
FREQ2	! number of turns for the inner loop with a 2000 index (i.e. number of time steps within one gust cycle)	MAIN	(-)
FW	! F Coefficient of the Thomas Algorithm for the soil liquid water flux equation.		
GAMMA	! Psychometric constant	MAIN	$Pa K^{-1}$
GAMMAT	! Light compensation point.	PHOTO	
GC02	! Co2 coupling coefficient for a layer with the upper one. (turbulent for air or thermal diffusion within the soil).	EQCOEM	$m s^{-1}$
GH	! Sensible heat Coupling coefficient with the upper layer (turbulent for air or thermal diffusion within the soil).	or (-)	
GL	! Conductivity coefficient for water vapour between the soil and the first air layer	EQCOEH	$Wm^{-2}K^{-1}$
GLE	! latent heat Coupling coefficient with the upper layer (turbulent for air or diffusion for soil).	MAIN	
GR	! Gravitational constant	EQCOEM	$Wm^{-2}Pa^{-1}$
GRASH	! Grashof number determined for the leaves and the soil clods.	or (-)	
GUST	! Gust integer for the run (Yes (1) or no(0))	EQCOEH	$m^2 s^{-1}$
GW	! liquid Water transport coupling coefficient with the upper soil layer.	RESIS/	(-)
		MOMNTM	
		MAIN	(-)
		HYDRO	
HT	! Leaf Convective sensible heat transfer coefficient.	RESIS	$Wm^{-2}K^{-1}$
HE	! Leaf Convective latent heat transfer coefficient.	RESIS	$Wm^{-2}Pa^{-1}$
HEE	! Leaf Convective latent heat transfer coefficient.	RESIS	$Wm^{-2}Pa^{-1}$
HEND	! Leaf Convective latent heat transfer coefficient. in case of dew	RESIS	$Wm^{-2}Pa^{-1}$
HM	! Soil Matric Head at the beginning of each time step.	HYDRO	m
HMC	! coefficients of the hm(theta) polynomial for soil layers.	HYDRO	(-)
HMNEW	! Soil Matric Head at the end of each time step.	HYDRO	m
HYDRIN	! way of inputting the soil moisture characteristics. ((1) van Genuchten model or else a measured function).	HYDRO	(-)
I	! index		(-)
IB	! Number of the soil layers just above the lowest soil layer.	MAIN	(-)
ID	! Probability of non interception for long wave radiation within different canopy layers.	ENERGD	(-)
IEAIR	! Initial vapour pressure of the air (after the gust intrusion).	RADBOU	Pa
IH	! Maximum total number of air layers.	MAIN	(-)
IHA	! Actual total number of layers within the Air.	MAIN	(-)
INI	! Incoming visible (1) and near infrared (2) radiation at the canopy top.	RADBOU	Wm^{-2}
IL	! number of the soil layer below the maximum number simulated domain.	MAIN	(-)
INDEXD	! A logical indicator to determine		(-)
INDEX	! An index (0 or 1) for indication the occurrence of		
INDEXC	! Indicator integer for showing the first air layer solution (i.e. analytically, numerically or the initial rate of water vapour flux from the soil is good enough.	MAIN	(-)
INDESO	! An Index allocating to each soil layer the corresponding soil moisture characteristics functions.	HYDRO	(-)
INDEXI	!		
INDEXS	! An integer which has a value of 1 for the gust intrusion phase and 2 for the quiescence period.	MAIN/	(-)
INI	! integer	MOMNTM	
INIH	! integer		
IPR	! Yes or no (1 or 0) Probability coefficient for wet or dry fraction of leaf surfaces	ENERGD	(-)
IS	! Maximum number of soil layers (negative)		(-)
ISA	! Actual number of soil layers (negative)		(-)
IT	! Maximum number of canopy layers		(-)
ITA	! Actual number of Plant Canopy layers (the highest layer with a leaf area density larger than zero).		(-)
ITB	! Integer for iteration count.		
ITRA	! Iteration number at different parts of the program.		
ITRM	! Number of the time step simulated within the gust cycle.	MAIN	(-)
ITRF	! Iteration number		
J	! integer		(-)
K	! integer		
KAV	! an average extinction coefficient which depends on the leaf class and the zone of the sky.	NORMN	(-)
KH	! Kh values (scalar turbulent diffusivities)		$m^2 s^{-1}$
KM	! Km Values (momentum turbulent diffusivities) between different layers.	MOMNTM	$m^2 s^{-1}$

KSATU	! Water Hydraulic conductivity as a function of moisture content (theta) for different soil layers.	HYDRO	ms ⁻¹
KSOIL	! An assumed soil thermal diffusivity for initialization.	INIT	m ² s ⁻¹
KUSA	! Coefficients of the hydraulic conductivity (theta) function.	HYDRO	
KXYLUM	! Hydraulic conductivity of the plant xylem tissue	INIT	
KW	! Molecular heat transfer coefficient of water		Wm ⁻¹ K ⁻¹
KWATER	! Soil hydraulic conductivity	Hydro	ms ⁻¹
L	! Integer.	MAIN	(-)
LAD	! Leaf area density at the upper interface of different canopy layers (one sided).	MAIN	m ² m ⁻³
LADMID	! Leaf area density at the middle of the layer.	MAIN	(m ⁻¹)
LAMDA	! Latent heat of vapourization	MAIN	(m ⁻¹)
LATI	! Latitude of the simulated site.	MAIN	(m ⁻¹)
LAYBAL	! The canopy air layer energy balance residual (to check for errors very close to zero.	MAIN	J kg ⁻¹
LAYLEF	! one Canopy air layer latent heat		deg
LAYSEN	! one canopy air layer sensible heat		
LOCALC	! Cumulative local transport due to a local gradient of CO2 at the canopy top during one AVGDLT period.	MAIN	Jm ⁻²
LDCALH	! Cumulative local transport due to a local gradient of heat at the canopy top during one AVGDLT period.	MAIN	Jm ⁻²
LDCALV	! Cumulative local transport due to a local gradient of latent heat (v) at the canopy top during one AVGDLT period.	MAIN	Jm ⁻²
LEAFLT	! Leaf segment.	ENERGD	
LEAINC	! Leaf area increments at different layers.	MAIN	(-)
LEFL	! latent heat flux from the leaf to the air		
LEFLUX	! Latent heat flux		
LIGHT	! visible light intensity on the lower (1) and upper(2) surfaces of the leaf in a certain layer.	NORMN	Wm ⁻²
LINEAR	! Linear solution of the energy budget equation.	ENERGD	
LMIX	! Mixing length for a local transport (determined in different ways).	MOMNTM	m
LOCALC	! Cumulative local transport due to a local gradient of CO2 at the canopy top during one gust cycle.	MAIN	ppmv m
LOCALH	! Cumulative local transport due to a local gradient of heat at the canopy top during one gust cycle.	MAIN	Jm ⁻²
LOCALV	! Cumulative local transport due to a local gradient of latent heat (v) at the canopy top during one gust cycle.	MAIN	Jm ⁻²
LOOP	! number of time step within		
LP	! A coefficient in Van Genuchten equation	HYDRO	
LWLFN	! Long wave emission by the leaves (one side)	ENERGD	Wm ⁻²
LV	! root density at (m root per m3 soil) at different layers.	ROOTDN	m ⁻²
MAXER1	! Maximum error in leaf energy solution for different leaf layers.	ENERGD	
MAXERR	!		
MINUTE	! The number of the current simulated gust cycle within the FREQ1	MAIN	(-)
MOLE	! molar weight of water		Kg mole ⁻¹
MP	! A coefficient in van Genuchten model for Soil moisture characteristics.		
MS2	! A logical indicator for a steady or non steady state solution for the leaf temperature.	ENERGD	(-)
NC02	! New CO2 concentration for different layers (at the end time step).	EQCOEM	ppmv
NGHTLM	! Night length in hours.	MAIN	hour
NLA	! Number of soil layers with different soil moisture characteristics.	HYDRO	(-)
NLDLSC	! Nonlocal flux of Co2 from different layers due to stability effects (i.e. Richardson number being less than a critical value) It didn't work. It leads to too much mixing.		
NLDLST	! the same as above except being for heat.		
NLDLSV	! the same as above except being for water vapour.		
NLDLGC	! Nonlocal flux from different layers due to the gust process of Co2 within the gust cycle.		
NLDLGT	! Nonlocal flux of Co2 from different layers due to the gust process of heat within the gust cycle.		
NLDLGV	! Nonlocal flux of Co2 from different layers due to the gust process of water vapour within the gust cycle.		
NLFLSC	! Nonlocal flux from different layers due to the thermal stability or Richardson number being less than a critical value of Co2 within the gust cycle.(it did not work)		
NLFLST	! The same as above but for heat		
NLFLSV	! The same as above but for water vapour.		
NLFLGC	! Integration of NLDLGC over canopy layers.		
NLFLGT	! Integration of NLDLGT over canopy layers		
NLFLGV	! Integration of NLDLGV over canopy layers		
NP	! A coefficient in Van Genuchten Model.	HYDRO	

NUMDLT	! number of BUDLT intervals within one AVGDLT.	MAIN	(-)
NONST	! non steady state change in the leaf energy budget solution.		
NSO	! Ratio of volumetric soil moisture at saturation to soil moisture content.	MAIN/ HYDRO	(-)
NUFORC	! Nusselt number as determined by forced convection regime.	RESIS/	(-)
NUFREE	! Nusselt number as determined by free convection regime.	RESIS/ MOMNTM	(-)
NU	! Nusselt number determined for the leaves and the soil clods.	RESIS/	(-)
NUMDRP	! Number of water drops for the lower and upper surfaces	ENERGD	
ON	! A logical indicator.		
OUTPL	! The period in hours in which output to files is done.	MAIN	hour
OSMOTI	! Osmotic pressure of the plant water.	INIT	MPa
P	! Time in hours after solar noon at which maximum air temperature is observed.	MAIN	hour
PASS	! number of passes for the solution of		
PCP	! Volumetric heat capacity of air at constant pressure	BERGE	$Jm^{-3}K^{-1}$
PCSOIL	! volumetric heat capacity of the soil.	BERGE	$Jm^{-3}K^{-1}$
PHIM1	! stability correction for momentum.	MOMNTM	(-)
PHIH1	! stability correction for heat.	MOMNTM	(-)
PI	! PI (3.1415)	MAIN	(-)
PLANTN	! number of plant per square m^2 .	PLANT	m^{-2}
POLY	! Polynomial coefficients for the soil		
POR	! Soil porosity	HYDRO	(-)
PR	! numerical probability of the leaf upper and lower surfaces being wet or dry.	ENERGD	(-)
PSIS	! Total Water potential (Psi) of the plant storage tissue	PLANT	MPa
PSISOL	! Total soil Water potential (Psi) of the layers far enough from the root surface (osmotic potential assumed zero).	HYDRO	m
PSIXYL	! Total Water Potential (PSI) of the plant xylem Tissue	PLANT	MPa
qwater	! liquid Water flux between different soil layers	Hydro	ms^{-1}
RA	! Time in BUDLT increments.	MAIN	hour
RAB	! Absorbed short wave radiation per unit volume of air	NORMN	Wm^{-3}
RABL	! Absorbed Radiation for m^2 leaf surface (old value)	ENERGD	Wm^{-2}
RABLT	! Absorbed Radiation for m^2 leaf surface (new value)	ENERGD	
RADE	! conversion from degrees to radian.	MAIN	$rad\ deg^{-1}$
RATIO	! ratio of the current sun elevation to its noon elevation	MAIN	(-)
RATIO5	! Ratio of the time step of simulation to the time constant of the first air layer.		
RATIO1	! ratio of turbulent transport at the upper boundary of first air layer to the value of the total of its sum and the soil convective latent heat transfer coefficient.	MAIN	(-)
RATIO2	! ratio of the soil convective latent heat transfer coefficient to the value of the total of its sum and turbulent transport at the upper boundary of first air layer.	MAIN	(-)
RADIUS	! characteristic root radius for different soil layers.	ROOTDN	m
RADIU2	! characteristic distance between neighbouring roots.	ROOTDN	m
RAIN	! Rain indicator for the calculation of soil moistening.	HYDRO	(-)
RAININ	! Indicator for rain fall (was not used).		
RAINM	! Amount of rain for the simulated day in mm	HYDRO	$mm*10^{-3}$
RB	! Boundary layer resistance for the leaf	RESIS	sm^{-1}
RCUTI	! Cuticular resistance for the upper (2) and lower (1) surface of the leaf.	RESIS	sm^{-1}
RDENST	! Root density (per unit soil surface) at different soil layers.	ROOTDN	$m\ m^{-2}$
RDIR	! A characteristic diameter of dew water drops on the leaf upper (2) and lower (1) surfaces.	ENERGD	m
REYNOL	! Reynolds number for the leaves and the soil clods.	RESIS/	(-)
RH	! relative humidity	MOMNTM	
RHMAX	! Maximum relative humidity of the day.	RADBOU	(-)
RHMIN	! Minimum relative humidity of the day.	RADBOU	(-)
RHO	! Density of Water	RADBOU	(-)
RHSOIL	! Relative Humidity of soil air	INIT	$Kg\ m^{-3}$
RICHAR1	! Richardson number determined in case of nogust intrusion at night time (free convection regime within the lower part of the canopy.)	HYDRO	(-)
RICHAR31	! Richardson number determined in case of nogust intrusion during daytime.	MOMNTM	(-)
RICHAR32	! Richardson number determined in case of nogust intrusion during daytime.	MOMNTM	(-)
RLEAF	! Leaf resistance for water transport.	RESIS	sm^{-1}
RLINN	! Incoming long wave radiation at the canopy top.	RADBOU	Wm^{-2}
RLNBTM	! Net long wave radiation at the lower boundary of the canopy (Net long wave for the soil)		
RLNET	! Net long wave radiation for the whole canopy layer		
RLNTOP	! Net long wave radiation at the canopy top (includes the soil).		
RLOUT	! Outgoing long wave radiation at the canopy top.	RADBOU	Wm^{-2}
RLS	! Resistance for water transport between the main stem and the first lateral node.	PLANT/ INIT	$MPa\ sm^{-3}$
RNETOT	! Total absorbed radiative energy (short and long wave)	ENERGD	Wm^{-2}

RNSBTM	! for the canopy layer	NORMN	Wm-2
RNSHRT	! canopy layer Net short radiation at its lower boundary	NORMN	Wm ⁻²
RNSTOP	! Net short wave radiation for all the canopy layer. ! (not including the soil).	NORMN	Wm ⁻²
ROOTA	! Net short wave radiation at the canopy top. ! (includes the soil).	NORMN	Wm ⁻²
ROOTA	! Root area contained within different soil layers.	ROOTDN	m ² (1)
ROOTRC	! Root conductance	ROOTDN	m ³ s ⁻¹
ROOTUP	! Root water uptake from different soil layers	PLANT	MPa ⁻¹
ROOTRS	! Root resistance	ROOTDN	m ⁻³ s MPa
RR	! Gas Constant		
RS	! Resistance for water flux between the storage tissue ! and the xylem vessels in a certain plant segment.	PLANT/ INIT	-
RST	! Stomatal resistance for the upper (2) and lower (1) ! surfaces of the leaf at different layers.	RESIS	sm ⁻¹
RTIME	! time of the simulation in BUDLT increments expressed ! as a real number.	MAIN	hour
RU	! An integer number of the BUDLT interval, within AVGDLT, ! currently simulated.	MAIN	(-)
SATUD2	! Slope of saturated vapour pressure dependence on ! temperature.	SATUD2	Pa K ⁻¹
SATUV2	! Saturated Vapour pressure at air temperature	SATUV2	Pa
SATVAP	! saturated vapour pressure at air temperature.	Pa	
SBOLTZ	! Stephan Boatsmann Constant.	ENERGD	Wm ⁻² K ⁻⁴
SDPRCC	! The same as SDPREC but determined differently as a check.	MAIN	ppmv m
SDPREC	! Storage of CO ₂ during an AVGDLT period.	MAIN	ppmv m
SDPREH	! Storage of sensible heat during an AVGDLT period.	MAIN	Jm ⁻²
SDPREV	! Storage of latent heat during an AVGDLT period.	MAIN	Jm ⁻²
SDPRHC	! The same as SDPREH but determined differently as a check.	MAIN	Jm ⁻²
SDPRVC	! The same as SDPREV but determined differently as a check.	MAIN	Jm ⁻²
SENFL	! Latent heat flux from the leaf to the air.	ENERGD	
SENSH	! Sensible heat flux from the leaf to the air.	ENERGD	
SGLOBL	! Global Radiation.	RADBOU	Wm-2
SH	! sensible heat source within different layers.		
SHEAR	! Shear at about the canopy height (at 2.5 m)	MAIN	s ⁻¹
SINBTA	! Sine of the angle of sun elevation.	RADBOU	(-)
SINDE	! sine of sun declination	MAIN	(-)
SINK	! Sink term for CO ₂ within different canopy layers	PHOTO	
SINODN	! sine of the sun elevation at solar noon time.	MAIN	(-)
SL	! latent heat sources within different layers	ENERGD	Wm ⁻²
SOILEM	! Soil emissivity	ENERGD	(-)
SOILH	! Soil sensible heat flux to the canopy air.	MAIN	Wm ⁻²
SOILIN	! an integer for determining the way of inputting the ! initial soil temperature (measured (1) ! or (any other value) estimated)	MAIN/ INITA	(-)
SOILLE	! Soil latent heat Flux (soil evaporation)	Main	Wm ⁻²
SOILLN	!		
SOILRN	! Soil net radiation.		
SOILRS	! Soil resistance for water transport to the roots.		
SOILSM	! Soil net short wave radiation.	NDRMN	Wm ⁻²
SOILTM	! Initial Soil temperature profile ! (to be read from a file or calculated).	INIT	0 _c
SOURC	! Amount of heat used to raise the temperature of the leaf. ! and for sensible heat.		
SROOTC	! Specific root conductance	ROOTDN	ms ⁻¹ MPa ⁻¹
START	! starting time of the day for the simulation.	MAIN	hour
STOR	!		
STORAC	! rate of storage of CO ₂ within a layer due to ! concentration change within one time step.	FLUX	ppmv.ms ⁻¹
STORAG	! Storage of heat within plant leaves in different ! layers during one time step	ENERGD	
STORAH	! rate of Storage of sensible Heat within a layer ! due to temperature change within one time step.	FLUX	Wm ⁻²
STORAV	! rate of Storage of Latent Heat within a layer ! due to vapour pressure change within one time step.	FLUX	Wm ⁻²
STORCC	! The same as STORREC but determined from the continuity ! equation.	FLUX	ppmv m
STORCT	! THE SAME AS STORTC, but determined from the addition of ! co2 flux divergence and CO ₂ sources.	FLUX	ppmv m
STOREC	! A spatial integral of Co2 quantity due to its ! concentration change over all canopy layers within one ! time step	FLUX	ppmv m
STOREH	! A spatial integral of energy storage due to temperature ! change over all canopy layers within one time step.	FLUX	Jm ⁻²
STOREV	! A spatial integral of energy storage due to vapour ! pressure change over all canopy layers within one ! time step.	FLUX	Jm ⁻²
STORH	! Rate of storage change of sensible heat for all canopy ! layers within one time step.	FLUX	W m ⁻²

STORHZ	! Sum of flux divergence and sources of sensible heat ! for all canopy layers within one time step.	FLUX	$W m^{-2}$
STORHC	! The same as STOREH but determined from the continuity ! equation.	FLUX	$J m^{-2}$
STORHT	! THE SAME AS STORTH, but determined from the addition of ! sensible heat flux divergence and sensible heat sources.	FLUX	$J m^{-2}$
STORTC	! Sum of total daily storage of CO ₂ for the whole system ! determined from CO ₂ change.	FLUX	ppmv m
STORTH	! Sum of total daily storage of sensible heat for the whole ! system determined from temperature change.	FLUX	$J m^{-2}$
STORTV	! Sum of total daily storage of latent heat for the whole ! system determined from vapour pressure change.	FLUX	$J m^{-2}$
STORV	! Rate of storage change of latent heat for all canopy ! layers within one time step.	FLUX	$W m^{-2}$
STORVC	! The same as STOREV but determined from the continuity ! equation.	FLUX	$J m^{-2}$
STORVZ	! Sum of flux divergence and sources of latent heat ! for all canopy layers within one time step.	FLUX	$W m^{-2}$
STORVT	! THE SAME AS STORTV, but determined from addition of ! latent flux divergence and latent heat sources.	FLUX	$J m^{-2}$
STPRCC	! Time integration of the sum of latent heat flux ! divergence and the sources for the canopy layers ! over one gust cycle.	FLUX	ppmv m
STPREC	! CO ₂ storage within the canopy air during one ! gust cycle determined concentration change.	FLUX	ppmv m
STPREH	! Sensible heat storage within the canopy air during one ! gust cycle determined from temperature change.	FLUX	$J m^{-2}$
STPREV	! Latent heat storage within the canopy air during one ! gust cycle determined from vapour pressure change.	FLUX	$J m^{-2}$
STPRHC	! Time integration of the sum of sensible heat flux ! divergence and the sources for the canopy layers ! over one gust cycle.	FLUX	$J m^{-2}$
STPRVC	! Time integration of the sum of latent heat flux ! divergence and the sources for the canopy layers ! over one gust cycle.	FLUX	$J m^{-2}$
SUNSET	! Time of sun set.	MAIN	hour
T	! A Tab (character 9) separator.		
TEMAIN	! New Temperature of the air (at the end of each time step)	MAIN/ EQCOEH	0C
TEMAIR	! air temperature at the beginning of each time step.	MAIN	0C
TEMLFN	! New Temperature of the leaves (at the end of each time ! step).	ENERGD	0C
TEMLF	! Old temperature of the leaves	ENERGD	0C
THETA	! volumetric moisture content of the soil.	HYDRO	(-)
THETAN	! New volumetric moisture content (theta)	HYDRO	(-)
THETAR	! residual volumetric moisture content as defined by ! Van Genuchten (mostly zero).	HYDRO	(-)
THETAS	! Saturated volumetric moisture content of the soil.	HYDRO	(-)
THETN	! New volumetric moisture content of the soil. ! calculated in a different way than THEATN	HYDRO	(-)
THICKN	! Thickness of the leaves.	ENERGD	m
TIME	! Time.		
TIMEC	! Time coefficients.		
TIMEC2	! Time constants for the second air layer.		
TIMEC3	!		
TIMECO	! Time coefficient of the first air layer in contact with ! the soil.	MAIN	s
TIMEG	! Time counter		
TIMEPL	! Time constant for plant parts volume.	PLANT	s
TIMER	! Time (read from a file)		
TIMEW	! Time counter		
TMAX	! Maximum air temperature of the day.	MAIN/ RADBOU	0C
TMIN	! Minimum air temperature of the day	MAIN/ RADBOU	0C
TOTAE	! Error in the solution (the total of in and out is zero) ! for both sides of the leaf.	ENERGD	
TOTALL	! Error in the solution (the total of in and out is zero) ! for one side of the leaf.	ENERGD	
TOTALQ	! Total sum of sensible heat sources within the canopy ! layers (not including the soil).		
TOTCON	!		
TOTENE	! An integration of total absorbed short wave energy for ! all canopy layers.	NORMN	$W m^{-2}$
TOTEVP	! cumulative evapotranspiration for the whole day.	MAIN	$Kg m^{-2}$
TOTLE	! Total sum of latent heat sources within the canopy. ! layers (not including the soil).	MAIN/ ENERGD	$W m^{-2}$
TOTSTC	! Total CO ₂ storage for above the soil layers.	##	
TOTSTE	! Total daily latent heat storage for above the soil layers.	MAIN	$J m^{-2}$
TOTSTH	! Total daily sensible heat storage for above the soil ! layers.	MAIN	$J m^{-2}$
TOTDX	! Total length of the lateral at different layers.	INIT	m
TORTU	! Tortuosity coefficient		(-)
TOTUP	! Total water uptake by plant roots		
TRANSP	! Transpiration.		

TRNST	! Transpiration of the plant canopy within one time step	MAIN	Kg m ⁻²
TROOTD	! Total root length per unit surface soil.	ROOTDN	m m ⁻²
TSN	! air temperature at sunset.	MAIN	0C
U	! Wind speed for different heights. ! (old value within an iterative solution)	MOMNTM	ms ⁻¹
UINI	! initial wind speed used in the iteration.	INITA1	ms ⁻¹
UNEW	! Wind speed for different heights. ! (New value within an iterative solution)	MOMNTM	ms ⁻¹
USTAR	! U* U star (friction velocity).	INIT	ms ⁻¹
VAPDIF	! water vapour diffusion coefficient in air.		m ² s ⁻¹
VAPFLB	! Water vapour flux at the lower boundary of a soil layer.	EQCOEH	Wm ⁻²
VAPFLT	! water vapour flux at the upper boundary of a soil layer.	EQCOEH	Wm ⁻²
VAPFDV	! water vapour flux divergence.	EQCOEH	Wm ⁻²
VGAS	! Volumetric air content (gas filled porosity)		(-)
VISIAB	! Absorbed Visible radiation at different canopy layers.	NORMN	Wm ⁻²
VOLUMD	! Volume of water drops on the upper (2) and lower (1) ! surface of the leaf (at the beginning of the timestep).		
VOLUME	! volume of plant parts (roots, stems) for different ! heights at the beginning of each time step.	PLANT	m ³
VOLMEN	! volume of plants parts for different heights at the ! end of each time step.	PLANTS	m ³
VPDAIR	! canopy air Vapour pressure deficit at different heights		
WAYIN	! Way of inputting the boundary conditions ! ((1) Simulated, else read from a file)	MAIN/ RADBOU	(-)
WATERF	! Water flux between different nodes within the plant	ENERGD	m
WFTH	! Dew water film thickness on the leaf surfaces ! ((1) lower surface and (2) upper surface).		
WINDZ5	! Wind speed at 2.5 m height.	MAIN	ms ⁻¹
WINDTP	! Windspeed at the upper boundary of the simulated domain ! (6.5m).	MAIN	ms ⁻¹
WM	! The new equilibrium water vapour pressure for the first ! air layer as determined by eq.4.2.23.(as determined from ! an iteration).	MAIN	Pa
WME	! The old equilibrium water vapour pressure for the first ! air layer as determined by eq.4.2.23	MAIN	Pa
WTEMP	! Wet bulb temperature at the canopy top.	RADBOU	0C
Z	! Height of the top of different layers.	MAIN	m
ZCENTER	! Height of the centre of different layers	MAIN	m
ZROOT	! depth for the root for determining the root density ! extinction within depth.	ROOTDN	m
XH	! logarithm of the ratio of volumetric soil moisture at ! saturation to volumetric soil moisture content.	HYDRO	(-)
YH	! saturation to actual soil moisture. ! The logarithm of the soil matric head.	MAIN/ HYDRO	(-)
X			

Chapter 6

Measurements & Model Validation

In this chapter, the validity of the model will be checked. Two data sets will be used for this purpose. The first data set has been collected by Van Boxel (Jacobs *et al* 1992) during the growing season of 1986 for a maize experiment and the second data set has been collected by Van Pul during 1988 (Van Pul, 1992).

We will first discuss what is required of a good model.

A brief description of the two data sets will be given and how one of them (Jacobs *et al* 1992) was used to obtain some parameters in the model, while the other one was used to check the model.

In the final part, we will give a comparison for two runs between the simulation and the measurement. The first run is for a three days period. The second one is for seven days in which some functional corrections, based on the results of the first run, have been implemented. We will see the effects of this corrections on the model behaviour and its agreement with the measurements and mention some possibilities for improvement.

6. 1. Introduction:

Validation means checking if a model simulates or comes close to simulating reality. Validation is the last step in the continuous loop of checking a model. Checking a model is checking the basic assumptions in the model, their numerical implementation, the effect of these assumption on the model behaviour and the closeness of the model results to reality. A model which gives close agreement with measurement is not necessarily correct. The basic assumption included in the model should be correct and the agreement with the measurement should also be good.

The problem in a simulation model is that we want to calculate or simulate reality. An abstraction of reality is always required, since we can not simulate everything. Selection of the most significant processes which should be included in a model is so required. An assumption of what is important and what is not, is affected by the viewpoint of the modeller and the way he sees or thinks reality works. This way of seeing reality, by the modeller, also includes how he thinks submodels should be coupled, or what kind of correlations from the lower level or the submodel level to the higher level or the model level should be included and how they should be parameterized. A loop then of selection of the most important processes, as seen by the modeller, their parameterization, modelling (implementing these assumptions in a numerical code) and the results which this selection has on the behaviour of the model and comparison against a good measurement is thus a necessity. Validation and model building in fact includes all these processes.

In a simulation trial, the governing equations concerning heat and mass transfer are not a point of discussion. These equations are always valid. It is the parameterization of the active processes within these equations and the coupling between the different components of the system is what important here. This coupling controls the time constants and its response to intermittency. An example of these are the turbulent transport coefficients for the averaged

equations, the stomatal resistance and root distribution. The first control the coupling between the canopy air layers and the layer of air above, the second controls the coupling of the plants to the air vapour pressure and temperature. The latter control the hydraulic coupling between the soil and the plants and has a feedback on the stomatal resistance. All these processes and how they are controlled and their different parameterizations, depending on the model scale of averaging, is what important.

The selection of which processes and what level of detail is required to achieve validity of models at higher levels requires an insight into which processes in the lower level or submodel processes are decisive in determining the behaviour of the model upper level. This insight can be obtained by studying the governing equations of energy and mass transfer at the higher system level and their solution either mathematically or numerically.

A mathematical attempt to express the solution of these equation in a close to analytical form could help us in determining which parameters in these equations are important in determining the response of the system. All processes in the lower level or submodel processes which affect these parameters should be given careful attention while being included in the submodel components and in the integration upwards.

This way of studying the solution is superior to studying the numerical simulations only, since it gives us more insight to the behaviour of the numerical model, its range of validity or regions of high sensitivities in its domain of solution. The use of this knowledge while building simulation models would save us time in building more accurate models while integrating from a lower level to a higher one. The problem here is that quite often it is not possible to have an analytical form of the solution. In the case of absence of this guidance, and due to the fact that the way of seeing reality by the modeller could be biased, the basic assumptions by the modeller of what is important and what is not and the dependence of the numerical solution results on these assumption, have always to be checked against a good data set.

A numerical study of the sensitivity of the numerical model to its parameters or to the interaction between its submodels is somehow an equivalent means to the mathematical analysis in helping to obtain more valid models. This is quite laborious, and this kind of sensitivity analysis does not give absolute values of the model behaviour since it is a function of the range of the model domain of solution. A contribution of a physical insight into the governing exchange processes, their mathematical representation plus numerical runs are all complementary to each other.

In chapter 1, the importance of obtaining submodels which are valid was discussed. There is a lot of work involved in the integration upwards from different spatial and temporal scales, so the more we can optimize the procedure of integration by analytical insight, the better.

We believe that it is the basic assumptions which have to be checked. We believe that as long as the basic assumptions in a model are correct and the numerical implementations of these assumptions numerically is correct, the model should be able to simulate reality. The first step is the crucial one since the correct numerical implementations of the conservation equation is a programming problem and a choice of a numerical scheme.

6. 2. Validation

In this thesis, a numerical intermittency model for describing heat and mass transfer within the plant canopy and between the canopy, the soil, and the layer of air close above has been introduced. So in validating this model, three things have been done:

- a) checking the basic assumption in the model. In this case, the nature of the dynamic coupling between the canopy air and the layer of air above and the effect of this coupling on the system behaviour.
- b) checking the numerical implementation of the governing equation.
- c) comparing the model runs to an independent data set

a) checking the basic assumption in the model has been done by the use of Van Boxel turbulence data (Jacobs *et al* 1992), collected during 1986 within a maize canopy during few selected days. This data set included a high frequency detailed measurements of the temperature by thermocouples and of wind speed by hot bulb anemometers and by cup anemometers within and above the maize canopy respectively. It also included observation with a three dimensional sonic above and one dimensional sonic within the maize canopy. Also, measurements of R_n were done above the canopy. These measurements were used to obtain a picture of the flow field within and close above plant canopies as have been shown in chapter 3 and 4. These flow field pictures gave us an idea about the depth of intrusion of the gusts (i.e. the refreshment function) and the value of K_m during the quiescence period, as has been explained in 3.6.2. The importance of this intermittency on the behaviour of the system from an analytical point of view has been explained in section 4.2.1. The importance of intermittency on the nonuniformity of the terms has also been discussed in chapter 3. The importance of missing correlation within our interval of averaging on the validity of the available approaches and on *the resulting solution of our equations has been discussed*

In the model, some parameters are needed namely:

- 1) A triggering condition required for the gust process to start and continue occurring. This is represented by a critical shear (0.27 s^{-1} in the first run and 0.20 s^{-1} in the second run) at the canopy top above which the gust process starts. This is somewhat arbitrary but it is shown also by fig. 6.1 in Jie Qiu *et al* (1994). The stability effect on the transport could be considered through increasing or decreasing the gust occurrence frequency. The suggestion of the dependence of the gust frequency on the stability regime is given by Leclerc *et al* (1991).
- 2) An assumption of a degree of refreshment for the air inside the canopy due to a coherent structure intrusion. A complete refreshment of the air inside the canopy was assumed. This is justified by the use of a continuous turbulence measurement within plant canopies collected by Van Boxel (Jacobs *et al* 1992) and the analysis given in section 3.2 and 3.6.1. The analysis of the temperature time domain maps for several days of turbulence measurement showed, that complete refreshment of the air inside the canopy is the dominant pattern.
- 3) A recurrence interval of the gust occurrence. This was assumed constant in the first run. This assumption is not completely correct. It affects the degree of coupling between the canopy air space and the layer of air above, as has been shown by MATHCAD[®] runs. In the

second run, a gust frequency of occurrence depending on wind shear at the canopy top was implemented.

4) The effectiveness of the small-scale transport during the quiescence period on moving the amounts of energy (sensible and latent), which has been delivered by the leaves to the intercanopy air stream, to the layer of air above the canopy. This effectiveness, represented by a local turbulent transport coefficient, will determine the ratio between the storage build-up of the scalar quantities during the quiescence period to that of their local fluxes at the canopy top. The local flux is defined as the flux between the canopy air space and the layer of air above it due to the small size eddies. These small-scale eddies are the ones dominant during the quiescence period. The local flux requires a build-up of a local gradient. This is done according to sect. 3.6.2.

5) A characteristic dimension or a thickness of the first air layer in contact with the soil which is strongly coupled to the soil. At the upper boundary of this air layer, the turbulent transport within the air controls the exchange between this air layer and the layer above it. So, in principle, the turbulent transport will work as a controller on the exchange between the humid air in contact with the soil and the layers of air within the canopy. This thickness was assumed equal to the displacement boundary layer thickness of the soil clods. The characteristic dimensions of the soils were assumed 0.05 m. The displacement boundary layer thickness was assumed about 1 cm thickness. This thickness is very reasonable, assuming a constant wind velocity close to the soil surface of 0.25 ms^{-1} during the quiescence period.

The solution for this air layer and its small time constant in relation to the length of the time step of simulation, especially in the first time step of simulation, led to the use of a semi-analytical solution for this layer (Section 4.4.2).

b) The numerical implementation of the governing equation, in chapter 5, has been checked. i.e. the closure of energy balances, radiative and nonradiative, for different layers and for the whole canopy and their integration within time. There is also the possibility of comparing an analytical form of the model to the numerical results.

c) Once the assumptions mentioned in point (a) are based on reasonable arguments, we started comparing the model runs to an independent data set to compare the measured and simulated behaviour.

6.3 THE DATA SETS USED TO VALIDATE THE MODEL:

Parallel to the measurement by Van Boxel (Jacobs *et al* 1992), there was a continuous measurement campaign of the radiation fluxes, the wet bulb and dry bulb temperatures, but we did not use this data set in the comparison since the highest measurement level was very close to the height of the canopy, so it was considered that the upper boundary of the system is affected by the canopy elements.

The comparison of the numerical model against measurement was done by the use of a second data set collected by Van Pul during his Ph.D. work. A complete description of the data set is given in Van Pul (1992). The aim of the experiment was to determine the fluxes of ozone, nitrogen dioxide, carbon dioxide, momentum, sensible heat and latent heat with the

profile and Bowen ratio techniques. Therefore, profiles of wind velocity, temperature, humidity and the above mentioned gases along with net radiation and soil heat flux were measured. These measurements were made throughout the growing season, i.e. from sprouting of the seeds in May up to two weeks after harvesting time in October. The sensors used in the measurement in the profile are slow response sensors with which a high accuracy of mean quantities is obtained. Values of the mean quantities were kept on tape as 15 minutes averages for the whole season.

For the validation, a period was used in which the crop had its maximum height of 2.2 meters with a corresponding leaf area index of 4 (mid August)

There were two data sets collected parallel within this experiment. The first one is similar to the one collected by Van Boxel, but we could not use it due to a measurement error in the thermocouple measurement. However, the hot bulb anemometers gave an impression of a flow regime similar to the one obtained by analysing of the data set by Van Boxel. We assumed the dynamic picture given by the data set Van Boxel (Jacobs *et al* 1992) valid within the 1988 experiment. The second data set, which is a continuous one, was the one used in the comparison. The upper measurement was at a higher level than that of Jacobs (three times the canopy height). The soil temperature measurements at two heights were compared against the model runs. In these measurements, there were only three depths of soil temperature measurements; the lowest was used as a boundary condition (120 cm depth).

6.3.1 COMPARISON AGAINST MEASURED DATA:

6.3.1.1: The boundary conditions for the simulation run

These boundary conditions are given in the following figures (fig.6.1, 6.2, and 6.3). The zero time coordinate corresponds to 0040 hours UTC, day number 230 of the year 1988. Fig. 6.1, and fig.6.2 show the boundary condition for the windspeed, wet and dry bulb temperatures.

The boundary conditions for radiation:

The incoming short wave radiation was measured using a solarimeter (Kipp & Zonen CM 11) For the incoming long wave radiation, the incoming long wave radiation was calculated from a balance of the net radiometer (Funk), a Heimann for measuring the radiative temperature of the surface during night-time. During daytime in addition to the above, two solarimeters (Kipp), one of them inverted to measure the reflected shortwave radiation, were used to calculate the incoming longwave radiation.

The initialization for the soil temperature profile was done by the use of initial measurements at depths of 0.02, 0.08 and 1.2 meters and a linear interpolation for the depths in between.

The initial soil moisture content was assumed uniform. The initial value was measured gravimetrically for the top soil surface layer (2 cm thickness). The soil moisture characteristics of the different soil layers, i.e. $K(\theta)$ and $hm(\theta)$ (3 layers) were fed into the model.

A leaf area density profile, as measured in the field, was used and is given in the input file (Appendix. 4)

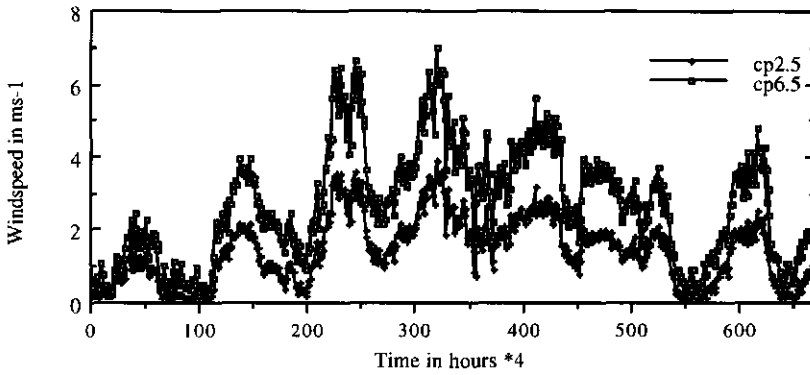


Fig 6.1 The windspeed at 6.5 and 2.5 metres height.

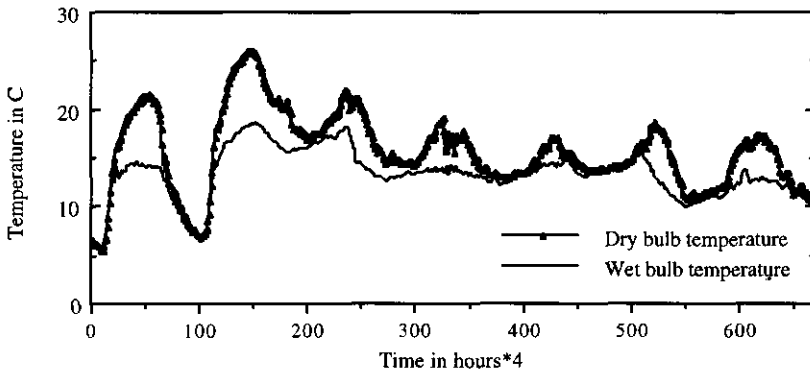


Fig 6.2 The wet and dry bulb temperatures at 6.5 meters height.

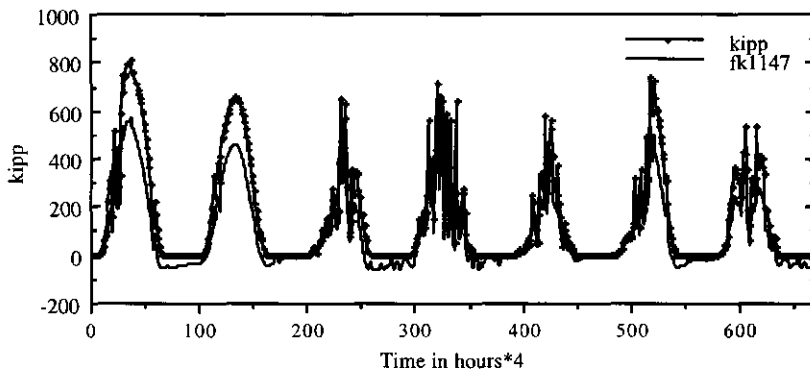


Fig. 6.3 The incoming short and net radiation at 6 meters height.

6.3.2. RESULTS

6.3.2.1. THE FIRST RUN:

6.3.2.1.1 The radiative environment:

Figures 6.4, 6.5 and 6.6 show a good success in simulating the net short wave radiation at the canopy top, the total net radiation and the radiative temperature of the leaves respectively, except in midday (a maximum difference of 20 Wm^{-2} and about 1 C^0 respectively).

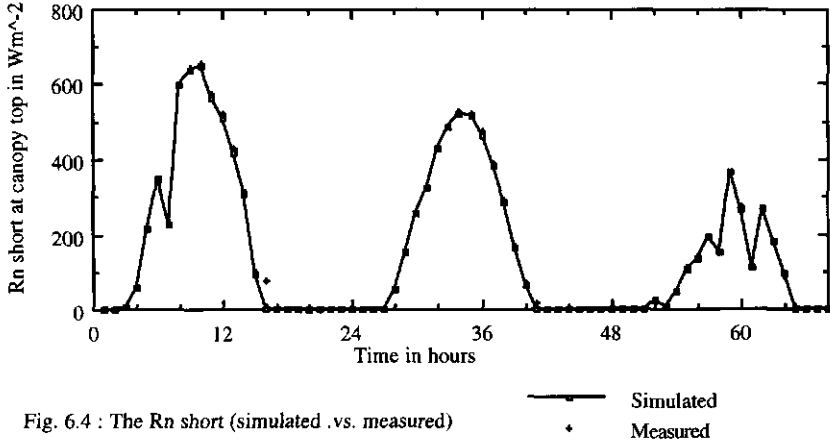


Fig. 6.4 : The R_n short (simulated .vs. measured)

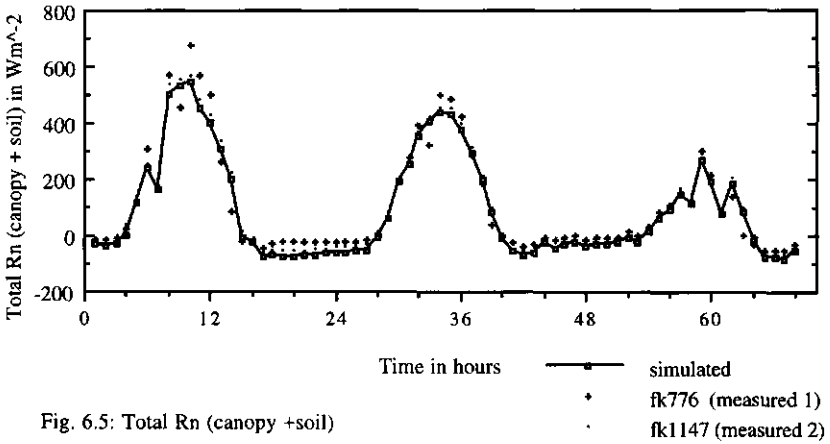


Fig. 6.5: Total R_n (canopy +soil)

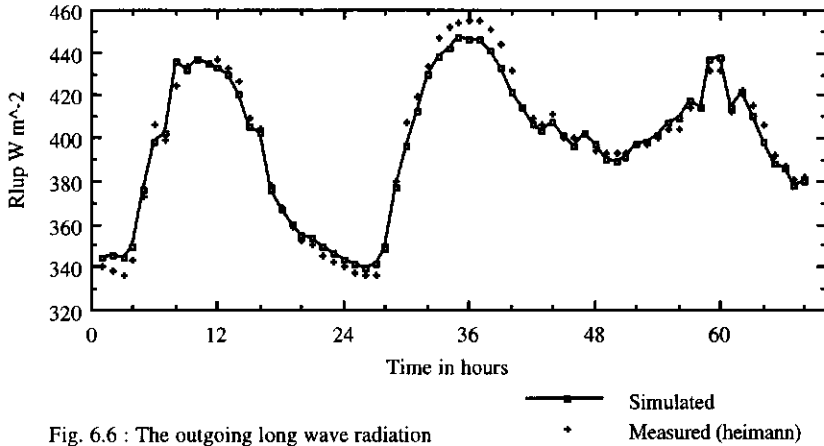


Fig. 6.6 : The outgoing long wave radiation
 5.7 Wm⁻² represents about one degree K error.

6.3.2.1.2 The temperature and the vapour pressure of the air:

The temperature of the air at different heights showed a good agreement between the measured and the simulated. Fig. 6.7 shows the comparison for the heights of 4.5, 2.5, 1.5, 0.5 and 0.1 metres respectively. 1.5 meters height is the height of maximum leaf area density. It seemed from the calculation that there is an underestimation of the temperature of the air , especially at midday.

The vapour pressure simulation at different heights showed an overestimation at all heights, except at the lowest level (0.15 metre) where there is an underestimation. It has a maximum difference of 200 Pa of the vapour pressure between the simulated and the measured at the maximum leaf area density height. The worst situation for the comparison happened for the height of 0.5 meters, with deviations as far as 300 Pa.

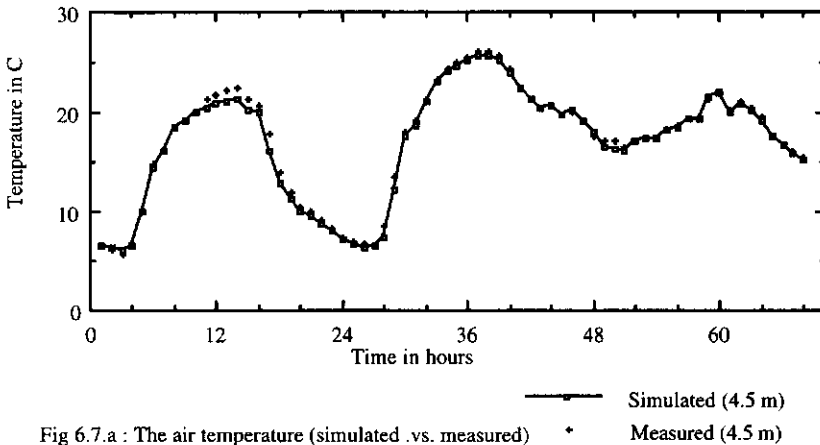


Fig 6.7.a : The air temperature (simulated .vs. measured)

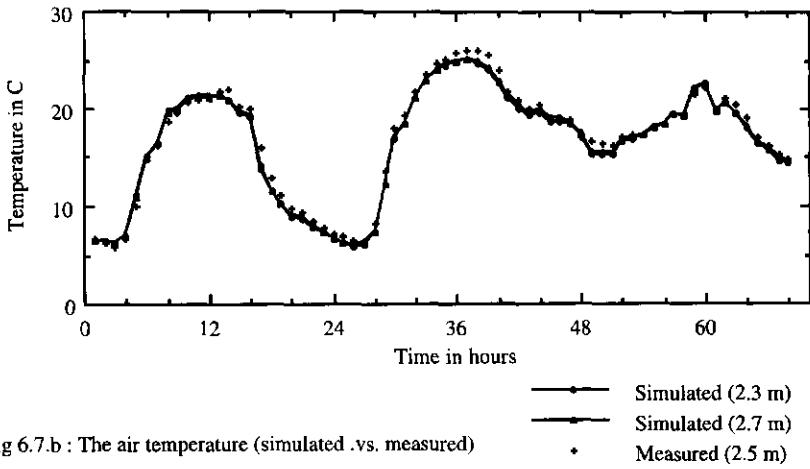


Fig 6.7.b : The air temperature (simulated .vs. measured)

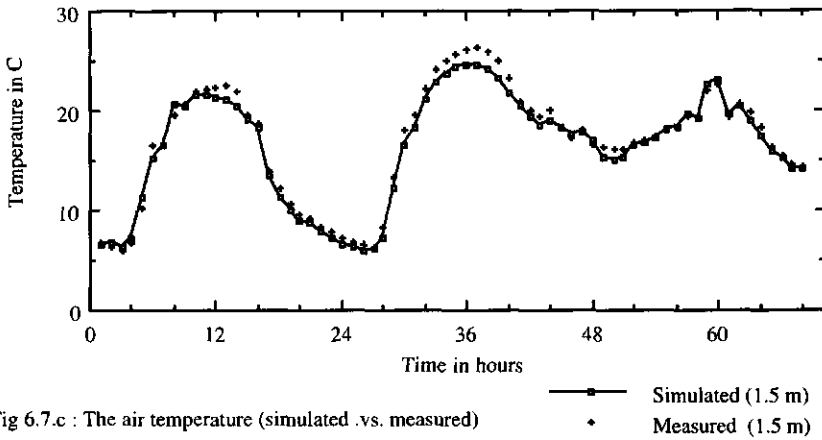


Fig 6.7.c : The air temperature (simulated .vs. measured)

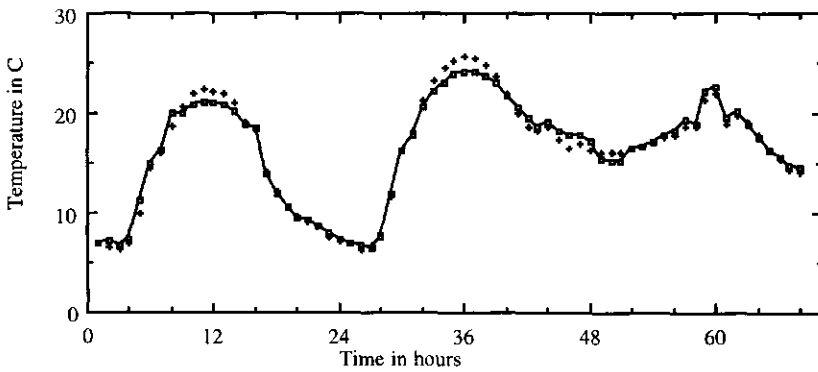


Fig 6.7.d : The air temperature (simulated .vs. measured)

- Simulated (0.50 m)
- Measured (0.50 m)

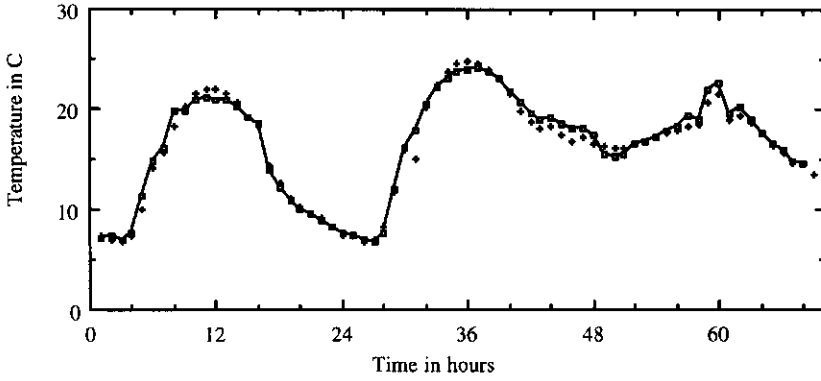


Fig. 6.7.e: The air temperature (simulated .vs. measured)

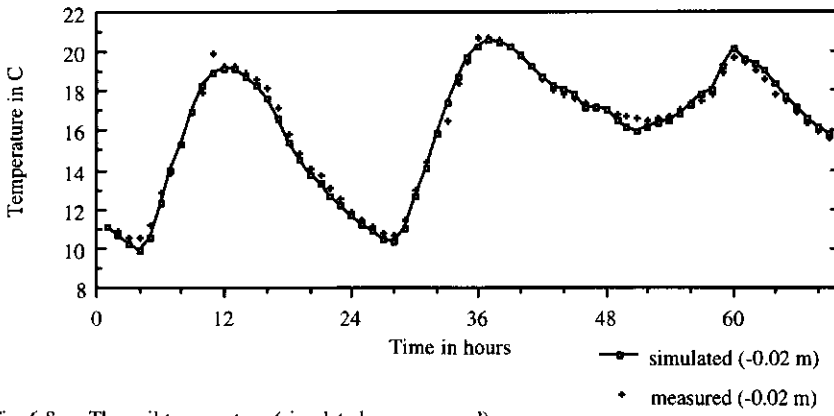


Fig. 6.8.a : The soil temperature (simulated.vs. measured)

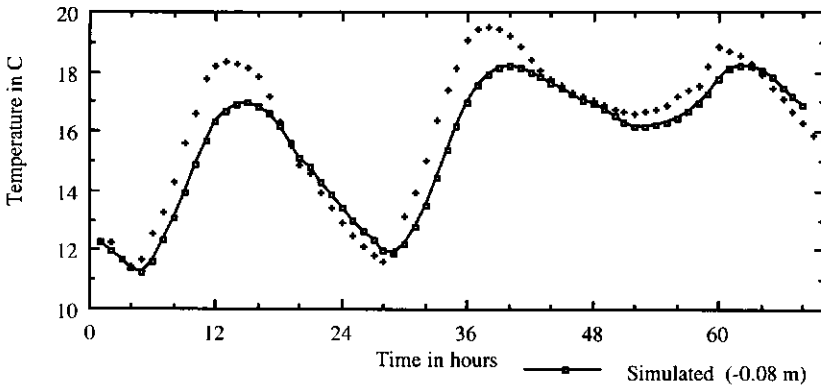


Fig 6.8.b : The soil temperature (simulated .vs. measured)

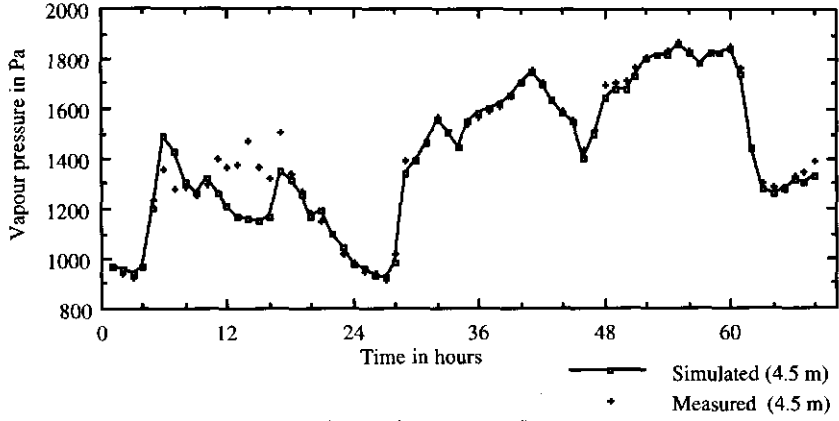


Fig 6.9.a : The air vapour pressure (simulated .vs. measured)

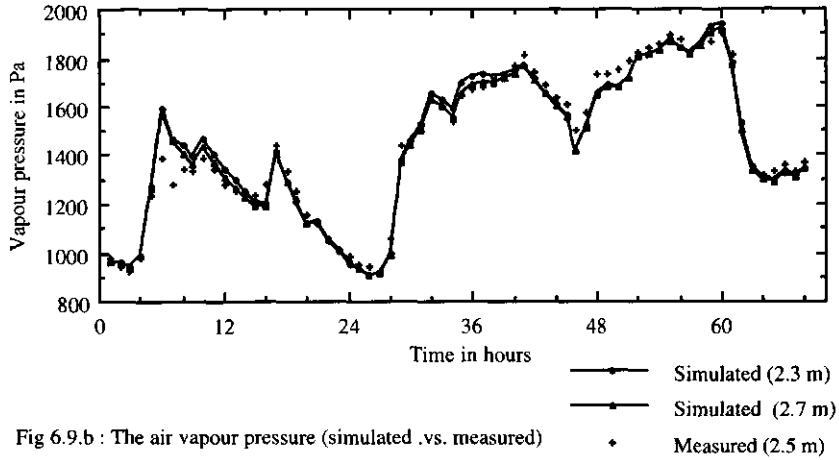


Fig 6.9.b : The air vapour pressure (simulated .vs. measured)

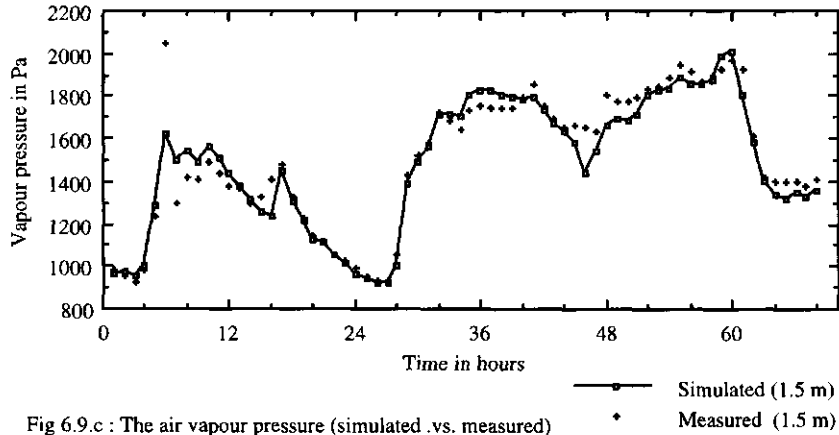


Fig 6.9.c : The air vapour pressure (simulated .vs. measured)

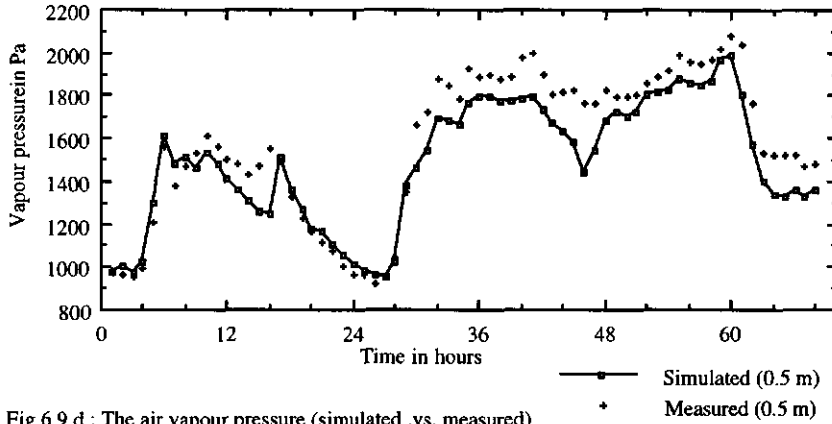


Fig 6.9.d : The air vapour pressure (simulated .vs. measured)

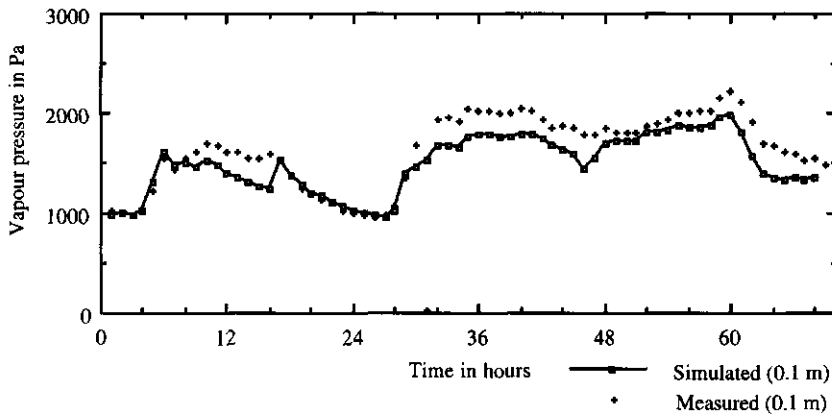


Fig. 6.9. e : The air vapour pressure (simulated .vs. measured)

The simulated soil temperature at 2 cm depth showed a very good agreement with the measured, while for the 8 cm depth there was a phase shift and more damping of the soil temperature wave.

DISCUSSION (THE FIRST RUN):

The explanation of the discrepancy between the measured and simulated values of the temperatures and vapour pressure of the canopy air during different times of the day, we think, is related to the interplay of two factors:

- 1) the frequency of gust intrusion into plant canopies, which was assumed constant, and how much this affected the exchange.
- 2) the values of the modelled stomatal resistance.

The first factor which is dependent on wind shear was assumed constant, once a critical shear at the canopy top was achieved. For the mid-day time periods (e.g. at 35 hours for example), a comparison of the measured and simulated stomatal resistance showed that the simulated stomatal resistance of the lower surface of the leaves came within less than one

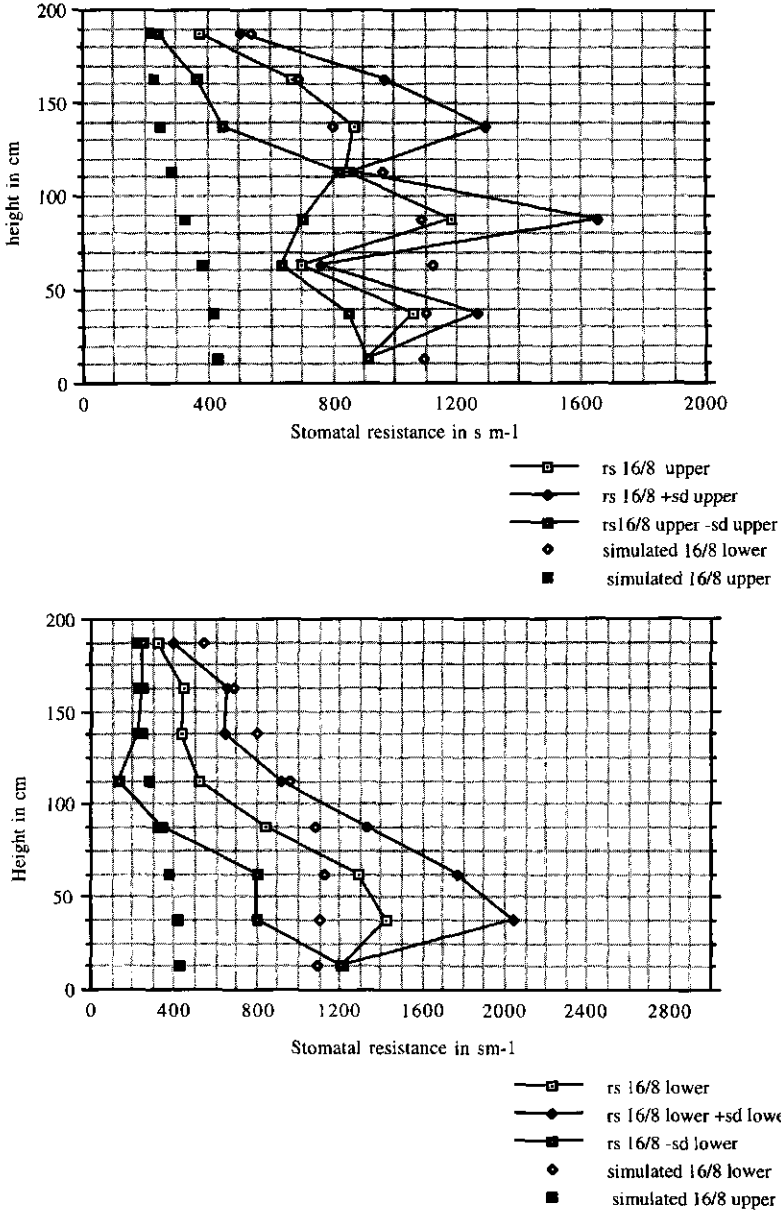


Fig. 6.10 : The stomatal resistance (measured \pm one standard deviation .vs. simulated) for the lower and upper leaf surfaces respectively.

standard deviation of the measured ones. For the upper surface of the leaves, the simulated resistance was about half of the measured one. This is due to an error in the calculation of F1 function which is used to calculate the stomatal response to light. A coefficient of curvature of 40 in stomatal resistance on light was used. This was an underestimation for Maize. That led to the stomatal conductance responding more rapidly to light, especially to medium values of visible light intensity. There was also an error in the distribution in the direct light distribution on the upper and lower surface of the leaves. The leaf angle distribution is assumed spherical. But in the direct light distribution, we assumed that the upper surface of the leaves sees direct light and the lower not. That led to a reduced simulated stomatal resistance for the upper surface of the leaves in comparison to the lower surface.

During the quiescence period, a turbulent transport coefficient which was independent of height and equals $(0.3 \cdot 0.3 \cdot \text{factor})$ was used. This factor was set to 0.35 during the whole period if no gust process occurs, due to low shear during daylight time, or during the quiescence period (if a gust process occurs). During night-time with no gust process occurring, or during the quiescence period if a gust process occurs due to a high shear at the canopy top, this factor was set to 0.20.

The effect of this interplay of the above two mentioned factors is affected by the boundary conditions at the canopy top (i.e. the incoming shortwave radiation, the vapour pressure deficit and shear at the canopy top) since these affect the turbulent transport coefficient and the stomatal resistance. The following explanation could be biased, but it is based on the obtained discrepancies between measured and simulated and tries to relate these to the change in the boundary conditions of the simulated domain. It is a hypothesis.

In the first day of simulation, as can be seen from figures 6.1, 6.2 and 6.3, it was a very sunny, especially in the later part of the day, with very low wind, especially in early part of the day. Fig.6.10 a and b show the stomatal resistance for the first day. There was an underestimation for the stomatal resistance, especially for the lower parts of the canopy since the effect of a lower curvature coefficient shows most noticeably in medium light intensities. The upper leaves would have reached their maximal leaf conductance in higher light intensities, so the effect of the using the wrong parameter of curvature does not show. The reduced stomatal resistance, in the early part of the day, led to high latent heat flux from the leaf to the air in the lower part of the canopy. The assumed coupling through a constant frequency of the gust intrusion was a little bit higher than what it should be (why? This can be seen from reading the third day of simulation), especially in the earlier part of the day. But it seems that it did not compensate the effect of increased latent heat on increasing the vapour pressure deficit of the air which leads to higher leaf temperatures. So, there are two opposing effects: the delivery from the leaves to the air and the transport between different air layers to the upper boundary. The balance was toward the higher delivery.

In the second part of the day, the higher light intensity reduced a little bit the effect of low curvature coefficient probably in the upper parts of the canopy, but not in the lower part of the canopy. So, the effect of lower stomatal resistance was still there. There was also a pickup of wind speed, so probably the intrusion frequency was less than or may be close what it should be. But the reduction of the stomatal resistance did more than compensate this. This led to reducing the vapour pressure, with resulting cooler leaves. This led also to increased latent heat flux from the leaves at the expense of sensible heat flux and a reduced leaf temperature,

but not as severe as in the second day because vapour pressure deficit was lower compared to the second day. This period was at about 10 hours from the beginning of the simulation.

During the night of the first day of simulation (15 till 27 hours from start of simulation), we see from fig. 6.5, fig. 6.6 and fig. 6.7.b and fig. 6.7.c that the simulated R_n was lower than the measured one, and so was the case for simulated outgoing longwave radiation and air temperature. The outgoing longwave radiation is calculated assuming an emissivity of one. What a Heimann sees is a real canopy with an emissivity lower than one, so some of the incoming longwave radiation contributes to the outgoing longwave. This has been considered in the calculation of the incoming longwave boundary condition, but in the simulation of the outgoing longwave an emissivity of one is assumed. If this correction is applied to fig. 6.6, it would make the situation worse. What we see on fig. 6.6 implies cooler canopy than what it should be. We assumed this is due to lower mixing during this night. This led to lower sensible heat flux from the air the radiatively canopy elements. We thought a more active transport should be activated during night time, especially in this low wind speed, so a convective regime should develop within the canopy, which increases the heat flux from the lower parts of the canopy or the warm soil to the radiatively-cooled upper parts of the canopy. We then implemented such a description in the calm nights for the second run. We will discuss the results of this in the second run.

In the second day, the underestimated stomatal resistance, especially with lower incoming solar radiation, led to more transpiration on the account of less sensible heat flux from the leaves to the air and so lower temperature of the leaves. This can be seen, as the simulated air temperature is lower than the measured at all heights. The simulated vapour pressures are also higher than the measured ones, at almost at all heights, except at the lowest level, at all times and at 0.5 m height at most of the time. From the wind speed fig. 6.1, we see that wind speed was such that the assumed critical shear was exceeded most of the time. Maybe, the used gust intrusion was right most of the time, otherwise, if the frequency was higher than what it should be, it would have more than compensated for the increased vapour pressure due to reduced stomatal resistance. The vapour pressure deficit was the highest during that day compared to the whole period. That made the effect of the underestimated stomatal resistance more pronounced.

During the second night, the wind shear at the canopy top was also higher than the first night, with the resulting consequence of enhanced turbulent coupling of the canopy layer to the air above. This increased heat flux from above and below the height of radiatively-cooled canopy elements to that height. So, the simulated total R_n , Radiative temperature and air temperature were better than the previous night. This gave us more justification for the implementation of convective flow regime with the second run.

During the third day, it was very windy day, with high humidity and low radiation intensity. We see that the trend (between 40 and 60 h) in the difference between simulated and measured leaf and air temperature at 1.5 m reversed. At 60 hours the air was more humid than the other two days and light intensity was the lowest, so the effect of the an underestimated stomatal resistance on increasing the latent heat flux from the leaves to the air was not present. The used intrusion of the gust was probably lower than what it should be, since the wind shear at the canopy top was very high. So the refreshment frequency was lower than what it should have been. Humidity of the air was also high. The simulated

temperature of the leaves were higher than the measured ones. This gave us an indication that an gust intrusion once every two and half minutes was less than it should be with this high shear and probably it was a good average value for the second day. In the second run , we varied the frequency of gust intrusions into plant canopies around the inverse of that number.

Concerning the bad agreement between the measured and simulated vapour pressure at height 0.5 and 0.1 metre, we thought that maybe due to the implemented uniform turbulent transport coefficient with height. we are ventilating too much and that leads to the underestimation. So, that is why we thought maybe it is good to implement a vertical velocity variance.

6.3.2.2. THE SECOND RUN

To check the reasoning behind the discrepancy between the measured and the simulated variables, some corrections were implemented in the model.

These included:

- 1) Using the right curvature coefficient in the F1 function for the stomatal resistance dependence on light.
- 2) Correcting the distribution of light on the upper and lower surface of the leaf (look at the code) NORMN subroutine
- 3) A parameterization of the turbulent transport coefficient according to Raupach (1988) implementing a vertical velocity variance.
- 4) We also implemented a gust frequency of intrusion as a function of the shear at the canopy top. This function was rather arbitrary, but we think it is good enough.
- 5) Implementing a free convection regime to describe the exchange processes within the canopy during night-time with low wind speed at the canopy top.

The implemented corrections are shown in the listing in comparison to the old parameterization.

6.3.2.2.1 The radiative environment:

Figures 6.11, 6.12 show very good agreement in simulating the radiative environment of the canopy, but it seemed that there is still a problem with the first night. The outgoing longwave radiation seems higher than the measured, the effect of the emissivity on reducing the simulated outgoing radiation to bring it closer to the measured will make some of this discrepancy disappear. But it seems that the effect of an error in our parameterization of a free convection regime at the first night shows through looking at the temperature of the soil at 0.02m depth. We see there a lower temperature of the soil compared to the previous run. It meant for us that the modelled contribution of soil to warming the canopy air was overestimated. That effect even shows in the soil temperature at 0.08 m. So, there was an overestimation of the contribution of the soil heat flux to warming up the radiatively-cooled canopy elements.

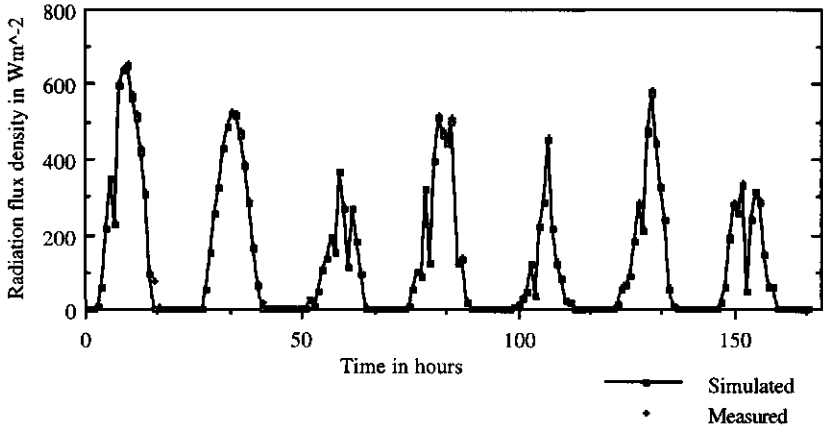


Fig 6.11 The short wave radiation (simulated .vs. measured).

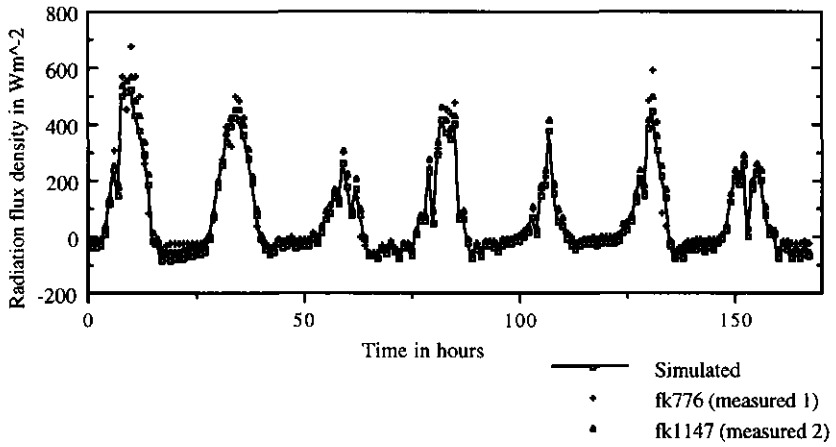


Fig 6.12 Total Rn (canopy +soil).

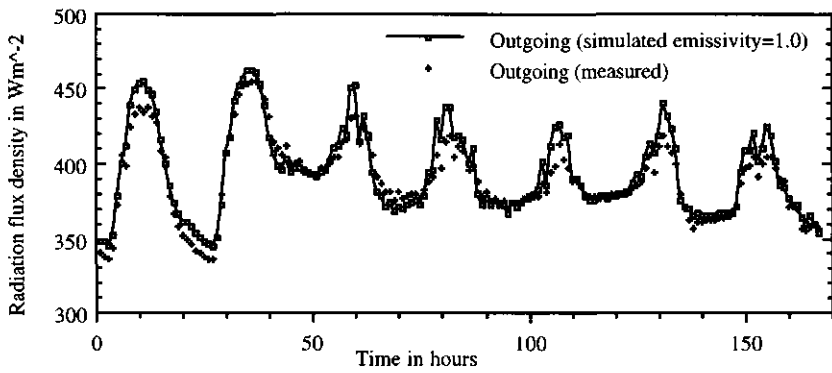


Fig 6.13 The outgoing longwave radiation (simulated .vs. measured).

6.3.2.2.2 *The temperature and vapour pressure of the air:*

The temperatures of the air at different heights show on general a very good agreement between the measured and the simulated for different height for the seven days of simulation, except for two 15 minutes averages at the end of the first and second nights. This discrepancy shows mainly in the figure 6.14.f for the difference between the measured and the simulated. Fig. 6.14 shows the comparison for heights for 4.5, 2.5, 1.5, 0.5 , 0.1. The agreement was very good.

The vapour pressure simulation at different heights showed a much better agreement than the first run between the measured and simulated for 4.5, 2.5 and 1.5 m heights. For the lowest two layers, there were more deviations.

The soil temperature at -.02 behaved worse than the first run, especially during the first night and noontime of the second day.

The soil temperature at -0.08 m was similar in its agreement with the measured temperatures for the first run.

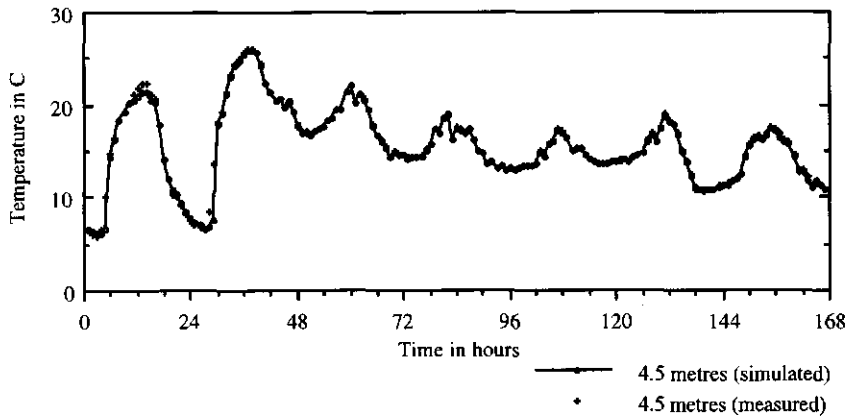


Fig. 6.14.a: The air temperature (simulated .vs. measured).

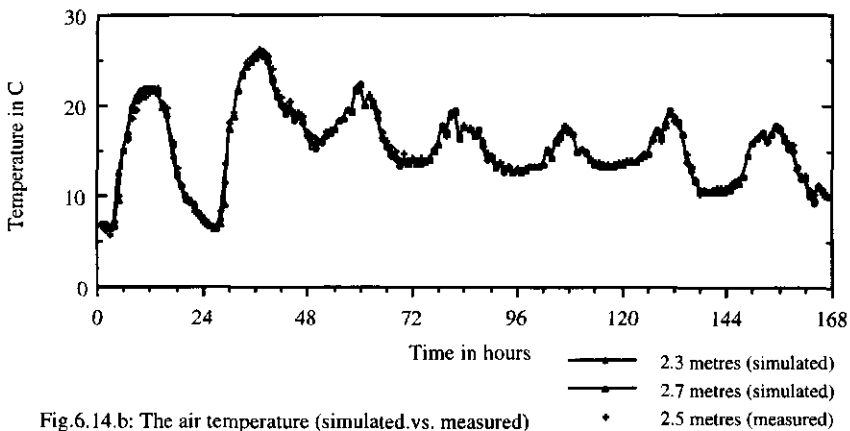


Fig.6.14.b: The air temperature (simulated.vs. measured)

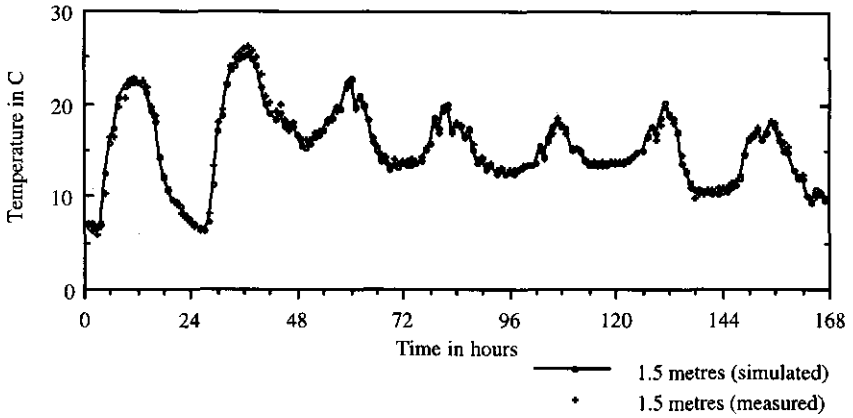


Fig. 6.14.c: The air temperature (simulated .vs. measured).

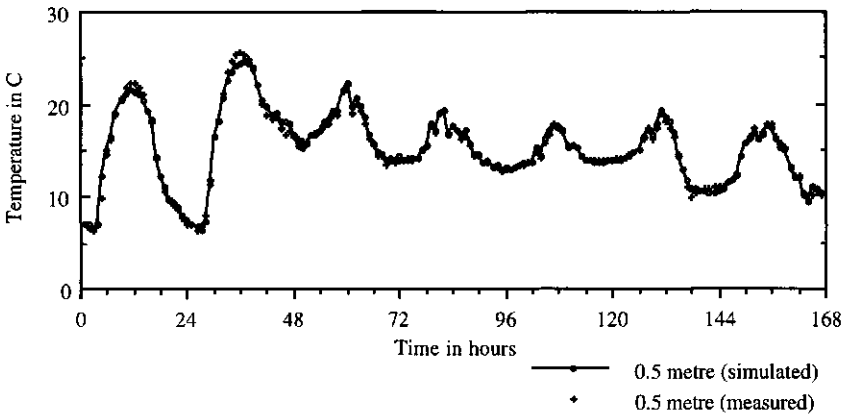


Fig. 6.14.d: The air temperature (simulated .vs. measured).

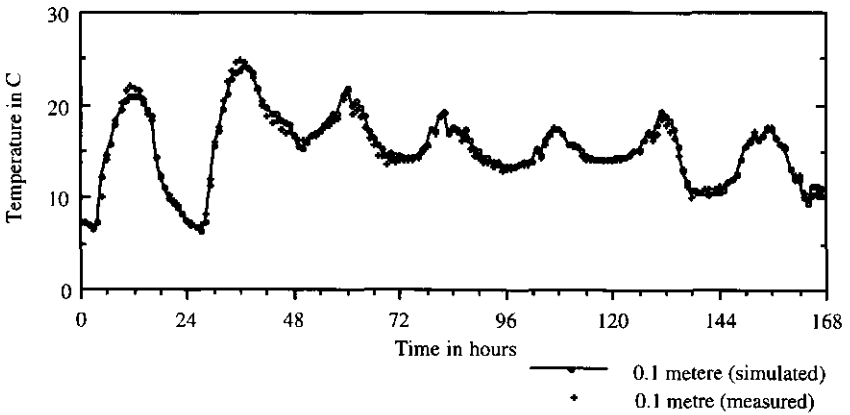


Fig. 6.14.e: The air temperature (simulated .vs. measured).

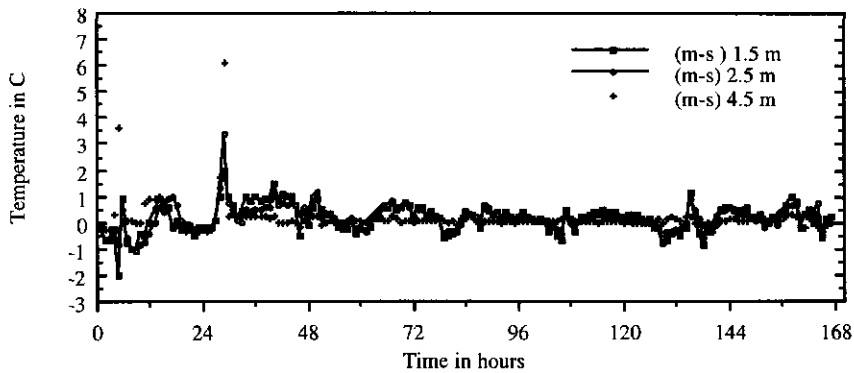


Fig.6.14.f : The difference between the measured and simulated values

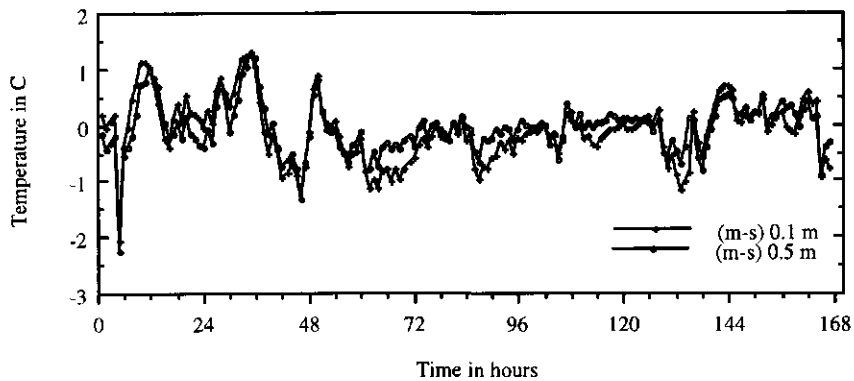


Fig.6.14.g : The difference between the measured and simulated values.

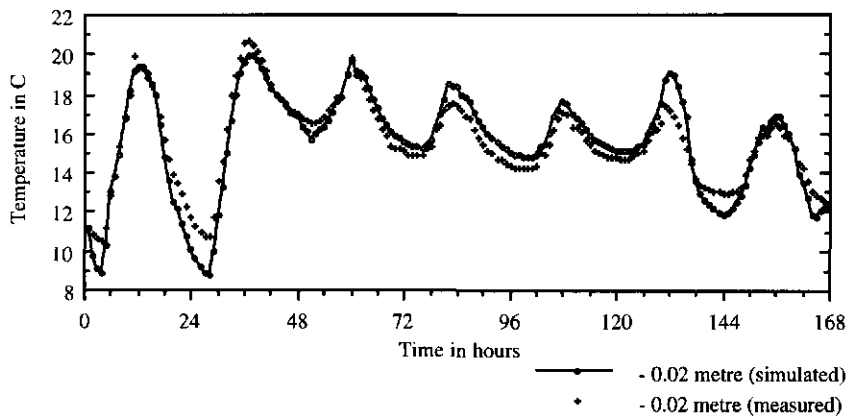


Fig. 6.14.h: The soil temperature (simulated .vs. measured).

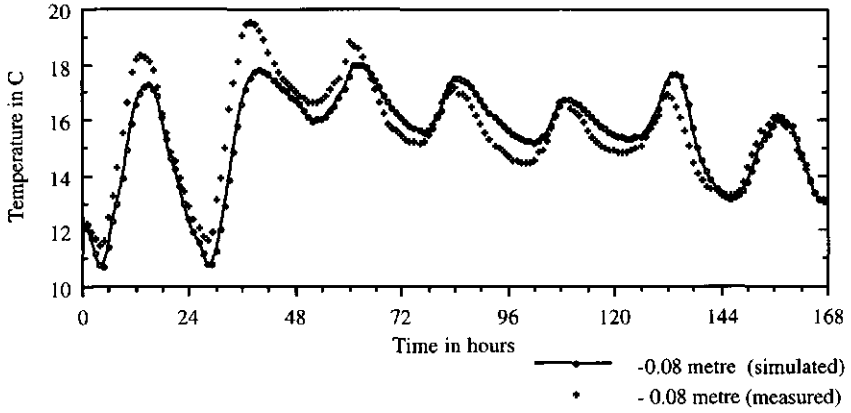


Fig. 6.14.i : The soil temperature (simulated .vs. measured).

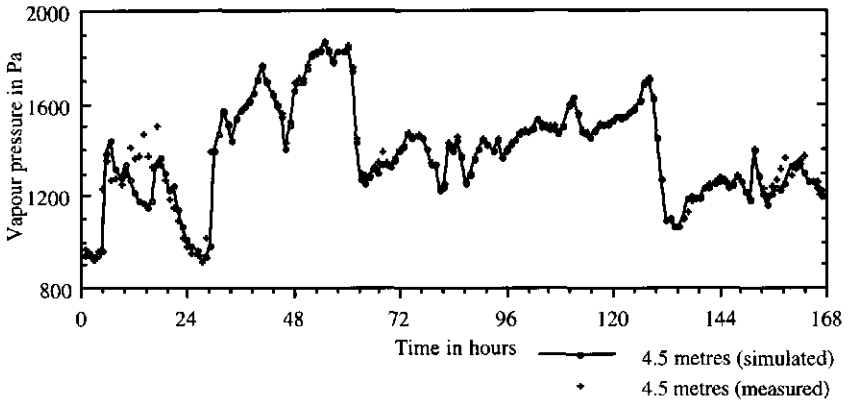


Fig. 6.15.a The air vapour pressure (simulated .vs. measured).

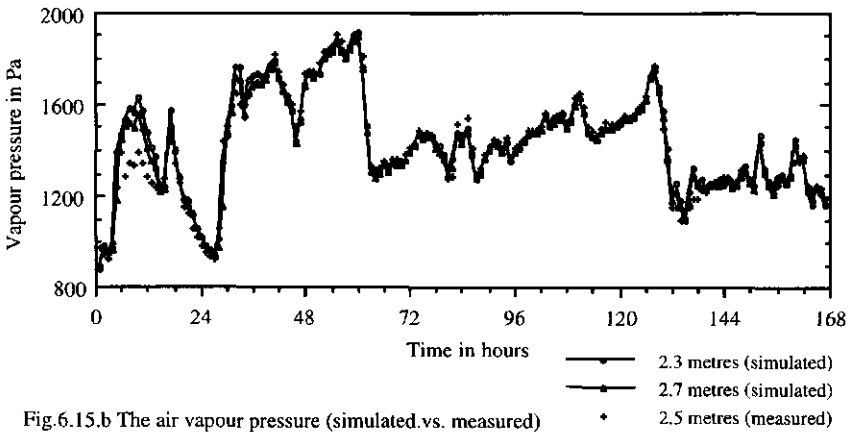


Fig.6.15.b The air vapour pressure (simulated.vs. measured)

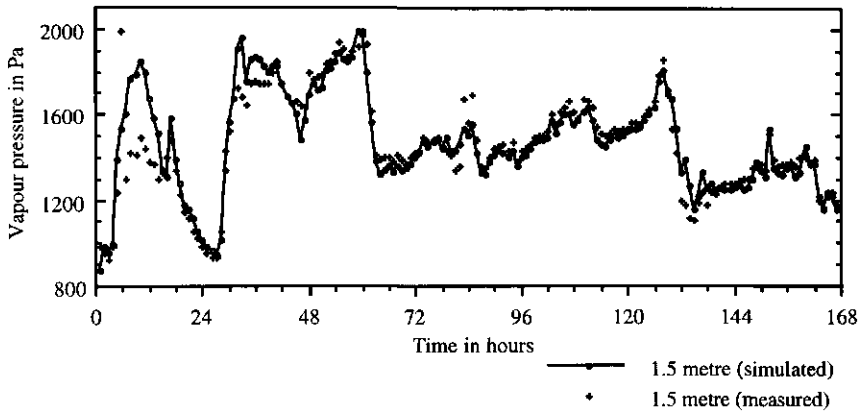


Fig. 6.15.c: The air vapour pressure (simulated .vs. measured).

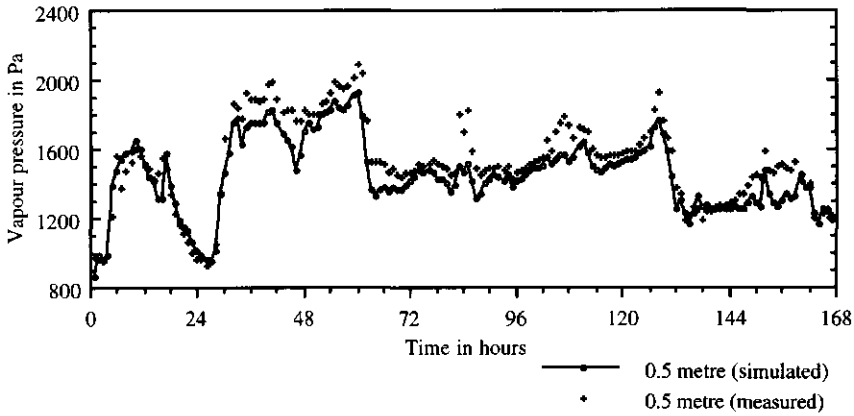


Fig. 6.15.d: The air vapour pressure (simulated .vs. measured).

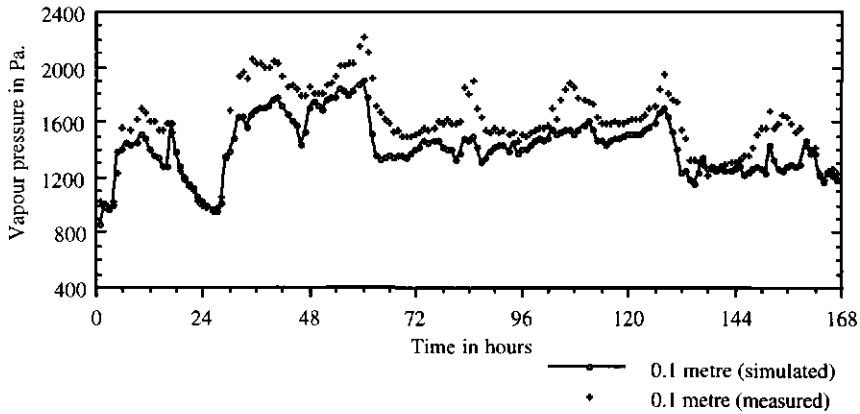


Fig. 6.15.e: The air vapour pressure (simulated .vs. measured).

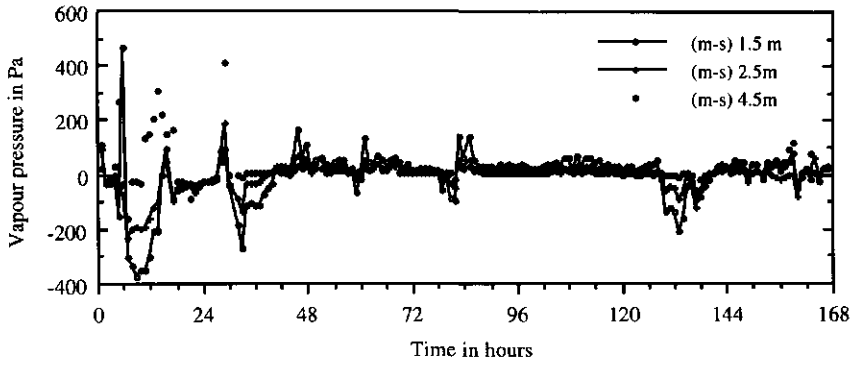


Fig.6.15.f: The difference between the measured and the simulated values.

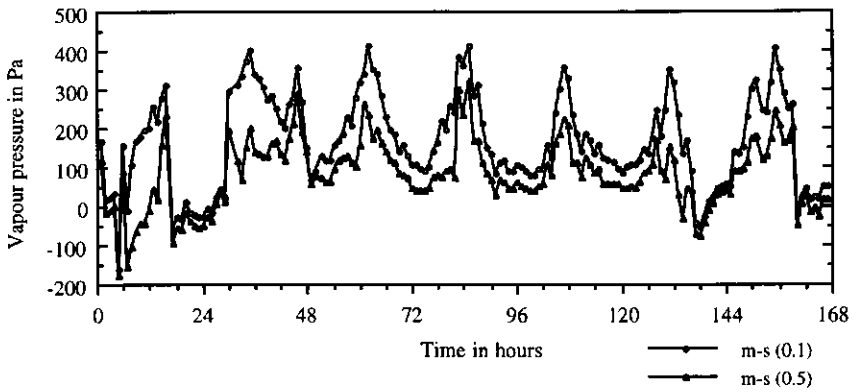


Fig.6.15.g: The difference between the measured and the simulated values

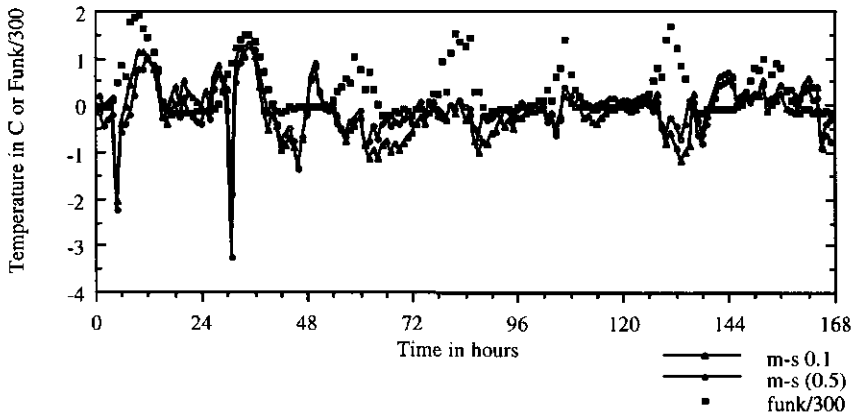


Fig 6.16 The difference between measured and simulated values and measured Rn

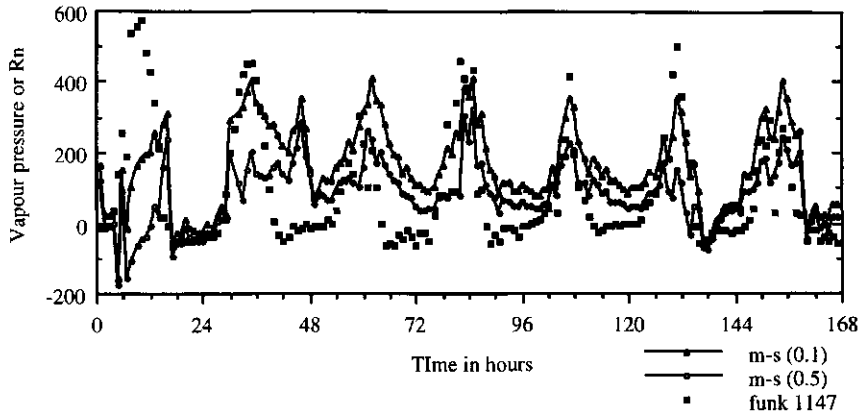


Fig 6.17. The relation between (measured-simulated) difference and measured Rn

DISCUSSION (THE SECOND RUN):

We will discuss the most apparent discrepancies between the measured and the simulated results and show what we think could be a reason.

Looking at the difference between the measured and the simulated curves (fig. 6. 14. f., 6.14.g, 6.15.f. and 6.15.g) for both the temperature and vapour pressure of the air, we see two problems.

The first is that the agreement between the measured and the simulated for the 0.1 and 0.5 m heights is not as good as the other heights.

The second problem is that the agreement between the measured and the simulated gets worse for all heights at mainly two specific periods corresponding to about 5 and 29 hours from the beginning of the simulation.

We will discuss the second problem first.

Concerning the air temperature within these two period, we notice that the measured temperature in the air layers above the canopy (i.e. heights 4.5 and 2.5 metres) are higher than the simulated ones. In the lower part of the canopy (heights 0.1, 0.5 and 1.5 metres), the trend is reversed. These two major deviations between the measured and the simulated coincided with the occurrence of radiative cooling at the upper part of the canopy at the end of the first and second nights. The wind speed at the canopy top was very low (look at fig.6.1). That led to the dynamic decoupling of the canopy layer from the layer of air above the canopy (i.e. the shear was below the assumed minimum value (0.2 s^{-1}), required to initiate the gust process). This reduced the heat flux from the air above to the top of the canopy. The stability corrections for the turbulent exchange coefficient at the layer of air above the canopy accentuated this decoupling. This led to the development a steep temperature gradient at the layer of air above the canopy. In the layers of air below the canopy top, the exchange processes were driven by the warmer soil. We also see from the soil temperature graphs that the simulated soil temperature were also lower than the measured, especially for these two periods. We think that the deviations have to do with the effect of convective flow regime

within plant canopy during the first and second nights. It seemed that the parameterization of the convective regime overestimated the flux from the warm soil to the top of the canopy. The used parameterizations (look in the listing) assumed no hindrance for the convective cells which transport heat from the lower part of the canopy to the radiatively cooled upper part. May be, the plant parts (leaves etc.) would represent some hindrance for that movement and that would represent a reduction for the flux from the lower part of the canopy to the top. This led to the simulated temperature of the air below the radiative cooling height being higher than the measured.

So, the convective flow regime in the lower part of the canopy was contributing much more to the flux while the layers above the canopy were contributing less. So, we think there is a need to correct for the effect of stability on decoupling the air flow above the canopy from that within the canopy during stable conditions. It could also be with low wind shear at the canopy top and radiative cooling, that coherent structures intrude into plant canopies rather sporadically which prevents the severe decoupling of the canopy air layer from the layer above. in the case of low shear, We tried to implement a criterion for an initiation of an ejection of air from the canopy to the layer of air above, in case of the soil being warmer than the radiatively cooled canopy top and also being warmer than the air above the canopy at night. This was done by implementing a critical Richardson concept over a large distance. But this caused far too much mixing.

Concerning the first problem, there seems to be a correlation between the deviation between the measured from the simulated and the value of R_N for the canopy. This is especially true for the vapour pressure deviations all the time and for the temperature deviations at the first three days. We attribute this to the parameterizations for the turbulent transport coefficient, Raupach 1988, which led to low values for the

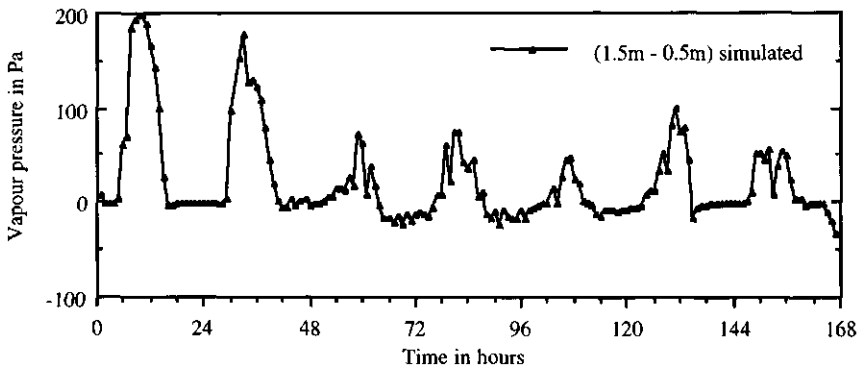


Fig 6.18.f The difference between the simulated values at 1.5 and 0.5 metres

turbulent diffusion of water vapour and heat from the upper parts of the canopy and the soil surface to the heights of 0.1 and 0.5 respectively. This is especially true in the case of water vapour, since the vapour at the soil temperature and the upper part of the canopy is higher than 0.5 m. If turbulent transport was high, it would have allowed more diffusion to the middle layers of the canopy. The gradient in vertical velocity variance was too steep. It led to very low values in the lower parts of the canopy. So, the difference between measured and

simulated is still the same like the first run, but the reason for discrepancy is different. The first is too much diffusion and the second too little diffusion. Concerning the vapour pressure at other heights and times, the deviations between the measured and the simulated were of the order of 100 Pa.

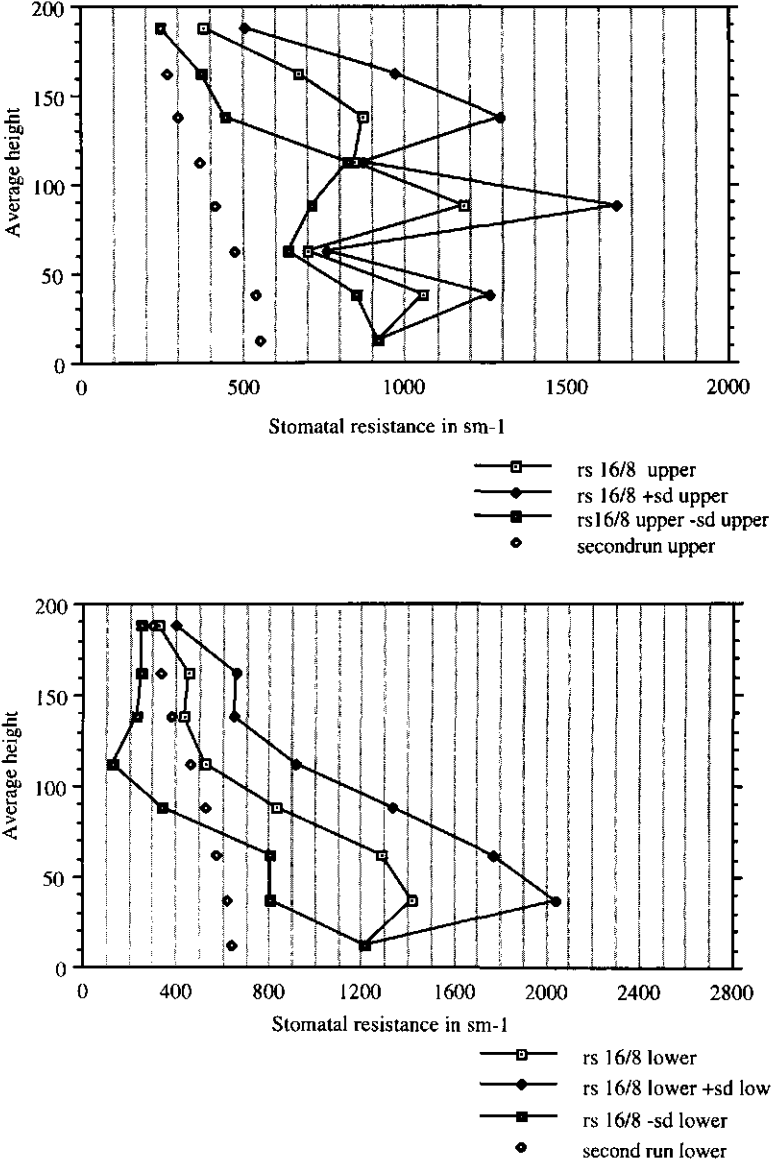


Fig 6.19: The behaviour of the stomatal resistance for the upper and lower surface.

We attribute the better behaviour to the corrected parameterization of the stomatal resistance due to correct distribution of direct light on the upper surface of the leaves, correct curvature coefficient. The effect of these corrections on the measured versus the simulated stomatal resistance is shown on fig. 6.19. It was better than the first run, but not very good either.

The use of a varying gust intrusion into plant canopy was also good in making the model more valid.

The discrepancy between the measured and simulated soil temperatures, we think, is due to a wrong parameterization of the thermal diffusivity of the soil. We see there is stronger damping in the simulated wave with respect to the measured. This could be due to wrong initial moisture content. In the run, we used the value of the gravimetric moisture content measured at 2 cm depth as the initial moisture content for the whole profile. The agreement in the amplitude of the wave in the third, fourth, fifth, sixth and seventh days was better, but there is a delay. We think a better agreement could be to the effect of the amount of rain during these days which was used to humidify the upper layers of the soil. So, it erased any uncertainties concerning the moisture content of the upper soil layers. In the fourth day, rainfall was about 12 mm. (Van Pul 1992) (look at the input file). The re-wetting of the upper soil layers was done at 12.00 noon time of the day in which there was rain (look at HYDRO subroutine). Maybe, that is the reason in the delay.

CONCLUSIONS :

The results of the model validation show in general a very good agreement between the measured and simulated radiative environment and leaf temperature and air temperature. There is, however an interplay between the gust frequency which determines the degree of build-up of the scalar profiles which is allowed to occur and the stomatal resistance which controls the time rate of the profiles build-up for the vapour pressure and temperature. This affects the energy budget solution of the leaves. The turbulent transport parameterization play an important role in controlling the values of the temperature and vapour pressure in the middle layers of the canopy. This interpretation can be seen from the semi-analytical treatment of the canopy, given in chapter 4.2. We think that a better parameterization of these three degrees of freedom will allow even a better simulation of the plant canopy microclimate.

There are a lot of variables in this model which have not been validated (e.g. plant water potential and soil moisture content). They seem to be working but this has not been validated experimentally.

APPENDIX 1. A

Navier Stokes equations constitute a non-linear system of equations. Use of a large time interval averaged value for a term in that system of equations is not the same as the use of a variable in time (fluctuating) term with the same mean. It will not yield the same answer, since the equality

$$\overline{f(x)} = f(\overline{x}) \tag{A1.1 a}$$

does not hold for a nonlinear function. i.e. the mean of a function is not the same as the function of the mean. The problem we have with the large-time interval averaging is that the following invalid assumption is made,

$$\overline{f_1 [\overline{f_0(x)^S}]^l} = f_1 [\overline{f_0(x)^S}]^l \tag{A1.1.b}$$

These two expressions (A1.1.a and A1.1.b) are the same, except that x in A1.1.a is an operator f_0 function in A1.1.b. To show the analogy between this expression and the Reynolds-averaged Navier-Stokes equation, we start with a nonlinear term or a nonlinear operator like $u_j \frac{\partial u_i}{\partial x_j}$. and do the averaging on it. The nonlinearity of this term shows more clearly when $i=j$. When $i \neq j$, u_i is coupled to u_j through the continuity and the pressure correction equation.

Let u_i have two different values A_i, B_i which have to be averaged. There will correspond to these two values of A_i, B_i two different values of $\frac{\partial A_i}{\partial x_j}, \frac{\partial B_i}{\partial x_j}$ and two different values of A_j, B_j depending on the solution of the flow equation. Let us assume, for the time being, that u_i is the instantaneous value or a small volume mean value of u and we want to do the averaging for a larger volume average. The left hand side of the above equality is

$$\frac{1}{2} \left(A_j \frac{\partial A_i}{\partial x_j} + B_j \frac{\partial B_i}{\partial x_j} \right) \tag{A1.2}$$

That represents the average for two values of u_i . Reynolds (1894) has done his averaging by decomposing the value into a mean and a deviation from that mean as given by.

$$\begin{aligned} A_i &= M_i + A_i' \\ A_j &= M_j + A_j' \\ B_i &= M_i + B_i' \\ B_j &= M_j + B_j' \end{aligned}$$

$$\tag{A1.3}$$

where

M_j is the mean of both values A_j, B_j

The mean value of the function i.e. the left hand side of the above equality is

$$\begin{aligned} & \frac{1}{2} \left(A_j \frac{\partial A_i}{\partial x_j} + B_j \frac{\partial B_i}{\partial x_j} \right) = \frac{1}{2} \left((M_j + A_j) \frac{\partial (M_i + A_i)}{\partial x_j} + (M_j + B_j) \frac{\partial (M_i + B_i)}{\partial x_j} \right) \\ & = M_j \frac{\partial M_i}{\partial x_j} + \frac{1}{2} \left(M_j \frac{\partial A_i}{\partial x_j} + A_j \frac{\partial M_i}{\partial x_j} + A_j \frac{\partial A_i}{\partial x_j} \right. \\ & \quad \left. + M_j \frac{\partial B_i}{\partial x_j} + B_j \frac{\partial M_i}{\partial x_j} + B_j \frac{\partial B_i}{\partial x_j} \right) \end{aligned} \tag{A1.4}$$

In the case that u_j is the instantaneous value, the third and the sixth terms inside the brackets represent two values for the Reynolds stress. Increasing the size of the averaging volume to include the largest scale of transport is equivalent to increasing the number of averaged cubes (n is very large). Once there is compliance with eq.3.5.1, this contribution is zero and the sum of Reynolds stress converges. The term $u_j \frac{\partial u_i}{\partial x_j}$ is also non-linear. The total

averaging of the terms i.e. $\overline{u_j \frac{\partial u_i}{\partial x_j}}$ goes into the Reynolds-averaged Navier-Stokes equation,

i.e. the mean non linear momentum equation, due to $\overline{U_j} \frac{\partial \overline{U_j}}{\partial x_j}$ and $u_j \frac{\partial u_i}{\partial x_j}$ in this equation. It is a conservation equation, the total sum of Reynolds stress divergence determines the change in the mean momentum. So, from the above, it seems that the total sum of the Reynolds stress is what matters and how that total sum is achieved should not matter. But what about the nonlinearity of the equation ? There is some circular logic here since the validity of this conservation equation requires certain assumptions in it.

So, in principle, it should not matter how the total sum of Reynolds stress is achieved as long as the requirement for the averaging is achieved.

$$\frac{\partial \overline{U_i}}{\partial t} + \overline{U_j} \frac{\partial \overline{U_i}}{\partial x_j} = \delta_{i3}g + f_c \epsilon_{ij3} \overline{U_j} - \frac{1}{\rho} \frac{\partial \overline{P}}{\partial x_i} + \nu \frac{\partial^2 \overline{U_i}}{\partial x_i^2} - \frac{\partial (\overline{u_i u_j})}{\partial x_j} \tag{A 1.5}$$

$$f_1(\overline{(u_i u_j)^{\Delta t}}) = \int_{t=t_j}^{t_j+\Delta t} \left[-\overline{U_j^{\Delta t}} \frac{\partial \overline{U_i^{\Delta t}}}{\partial x_j} - \delta_{ij} 3g + f_{c\epsilon_{ij} 3} \overline{U_j^{\Delta t}} - \frac{1}{\rho} \frac{\partial \overline{P^{\Delta t}}}{\partial x_i} + \nu \frac{\partial^2 \overline{U_i^{\Delta t}}}{\partial x_i^2} - \frac{\partial (\overline{u_i u_j^{\Delta t}})}{\partial x_j} \right] dt \tag{A 1.6}$$

where Δt is the interval of integration, could be small s or large l . In the right hand side of eq.A1.6, the integration of this equation is equivalent to $f_1(\overline{\quad}^{\Delta t})$ operator in the above expression. The values of the Reynolds stress represent the $\overline{f_0(x)}$ in the above equation, while the effect of this value on the mean momentum is represented by $f_1[\overline{f_0(x)}]$ expression. The superscript next to the $\overline{\quad}^s$ determines the interval of averaging, small or large.

In the derivation of this equation, Reynolds (1894) has shown that the uniformity of the (turbulent ?) signals is a required condition for the validity of the averaging. He has done this through the Taylor expansion of the signals behaviour around the centre of mass of the averaged volume and has shown that to achieve the mean momentum condition, i.e. that the integration of all $\sum \rho u'$, $\sum \rho v'$, $\sum \rho w'$ over all volume or time intervals to be respectively and severally zero, the first order derivatives of the $\overline{u}, \overline{v}, \overline{w}$ within our subvolumes or time intervals with respect to x, y, z should be constant. This is equivalent to assuming that the mean motion is steady, or uniformly varying with time.

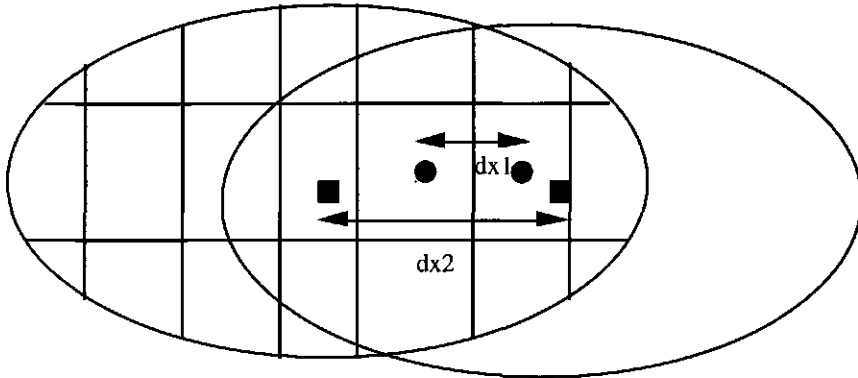


Fig. A.1.1. A variation of the mean signal along a line connecting two control volumes, the first dx_1 is connecting two control volumes which constitute subvolumes in a large control volume.

He concluded “that the closeness of the approximation with which the motion of any system can be expressed as a varying mean-motion together with a relative-motion, which when integrated over a space of which the dimensions are a, b, c , has no momentum increases as the magnitude of the periods of $\overline{u}, \overline{v}, \overline{w}$ in comparison with the periods of u', w', v' and is measured by the relative orders of magnitude to which these periods belong.” This seems to me as a statement of eq.3.5.1. So, did we understand wrong?. What about the legitimacy of

the raised point concerning the behaviour of the terms, as shown through the nonlinearity of the systems of equations and the strong time variations of its terms?

There are two points to answer this. The first, we conclude from Reynolds paper: it depends on the size of subvolumes composing the whole volume of averaging, as shown by the previous graph, to determine what is mean and what is deviation. The variation of the mean signal along the two subvolumes connected by dx_1 represent, with respect to the two larger subvolumes connected by dx_2 , a variation within the larger subdomain one. If condition 3.5 is not achieved yet, in a way, it represents a variation of the turbulent signal along the larger subdomain Or more correctly, it represents the increase in the turbulent signal due to the volume increase from volume 1 to volume 2.

The second is that the separation of the scale required for the validity of averaging is a required condition for all subvolumes which could be averaged. In case of uniform distribution of the length scale, the increase of the turbulent transport with the increase of the volume of averaging or the length of time step will be an increasing function of the spatial dimension or the time interval with a uniform slope. Within this averaging volume, there is an increase of the flux till we reach a plateau. The uniformity of the slope implies uniformity of the term's behaviour within the volume of averaging. The correlation between any two signals will be uniformly distributed. So, Reynolds by specifying this condition of uniformity met also the conditions required for averaging a non-linear equation. The problem happens when there exists a change of the slope or a separation of the scale within our averaging volume.

A uniform distribution of the turbulent transport signals at lower level, i.e. u', c' , will lead to a uniform distribution of the double and triple correlation between variables, i.e. u', c' . This will eliminate the effect of intermittency on the correlation. Two completely non-correlated signals along a certain direction lead to zero turbulent flux in that direction. In the horizontal direction, assuming no mean horizontal component, that implies complete homogeneity of the concentrations or the conserved quantities. In the case of a non-random correlation, which is uniformly distributed, this implies a rather uniform flux in a certain direction (no contribution to the flux divergence along that direction).

For the equality of the above equation A.1.b to be achieved for a nonlinear operator f_1 , it is required that $\overline{f_0(x)^s}$ terms are equal during the short time intervals comprising the large time intervals.

For the equality of the dependent variables in eq.A.1.1.b, the dependent variables have to be equal within our volumes. To have the equality A1.1.b valid, the variance of the $\overline{f_0(x)^s}$ should be zero or a variance minimization principle.

$$\sigma_{f_1}^2 = \frac{\sum_{n=1}^{i-1} \left(\left[\overline{f_0(x)^s} \right] - \left[\overline{f_0(x)^s} \right] \right)^2}{i-1}$$

The derivation of an averaged equation for

$$\left[\overline{f_0(x)^s} \right] - \left[\overline{f_0(x)^s} \right]^s$$

For example, a second order term, $\overline{u_i u_k}$: the derivation of an equation for

$$\overline{(u_i u_k)} = \overline{(u_i u_k)} - \overline{u_i} \overline{u_k}$$

which we try to include in the turbulent transport equation is by multiplying it by its self or by a turbulent transport term which maintains the effect of the deviation. This is similar to a derivation of a higher order term prognostic equation.

The minimization of the variance of this value is achieved, when we have identical volume. Strictly speaking, the equality of eq. A1.1.a is then achieved when we are averaging identical averaging volumes or identical time steps. The variance is then equal to zero. The equality of the terms is the strict required condition for equality of A1.1.b. The effect of variation between the samples shows in the above non-equality.

The sum of $f_1 \left[\overline{f_0(x)^s} \right] - f_1 \left[\overline{f_0(x)^s} \right]^s$ represents the error in the solution due to our approximations. The total difference depends on our system of equation and how much is the difference.

APPENDIX 1.b: Random Walk models.

In a random walk model, we have a problem concerning the effect of coherent structures on the concentration field and whether the derivation of these models include in them an account of the resulting correlation in the motion between particles on the concentration field.

In this appendix, we review the derivation given by Lamb (1980) and we show where a misunderstanding may arise.

THE DERIVATION BY LAMB (1980):

Consider a dispersion experiment in which three particles are released from given points r_{10}, r_{20}, r_{30} at time $t=0$. Once the particles are released, they are carried by the fluid to new locations $r_1(t), r_2(t), r_3(t)$.

Let v be a volume, which we shall call the sample volume, centred at a given point r . The size of v is arbitrary, although we shall assume it is small in the analysis.

The sample volume and particle positions at time t and $t=0$ are illustrated in his fig.A.1.b.1 (which is included here for clarity.)

Lamb(1980) introduces two definitions that will serve as the sole basis of the Lagrangian diffusion equation. The first is the definition of the concentration c itself. He defines

$$c(r,t) \equiv \frac{m(r,t)}{v} \tag{A.1.b.1}$$

where m is the number of particles in v at time t . The second definition is the joint probability density $p(r_1, r_2, r_3, t | r_{10}, r_{20}, r_{30}, t_0)$ that the particles are at the specified points r_1, r_2, r_3 a time t given that they were at r_{10}, r_{20}, r_{30} , respectively, at time $t_0=0$. The function p is a Lagrangian property of u' family and is defined as follows:

$$p(r_1, r_2, r_3, t | r_{10}, r_{20}, r_{30}, t_0) = \lim_{N \rightarrow \infty} \frac{1}{N} \sum_{n=1}^N U_n / (\delta v)^3 \tag{A.1.b.2}$$

$$U_n = \left[\begin{array}{l} = 1 \text{ if the } n\text{-th member of the } u' \text{ family is such that three particles} \\ \text{released at } (r_{10}, r_{20}, r_{30}) \text{ at } t_0=0 \text{ are simulataneously in small} \\ \text{volumes } \delta v \text{ centred at given points } r_1, r_2, r_3 \text{ respectively at} \\ \text{time } t; \\ \\ = 0; \text{ otherwise} \end{array} \right] \tag{A.1.b.3}$$

In the three-particle problem under consideration, the concentration c can have only one of four values at any point in space and time -- $c = m/v$, $m=0,1,2,3$. Then, to determine the probability $w(m)$ that the concentration in the sample volume has the value m/v .

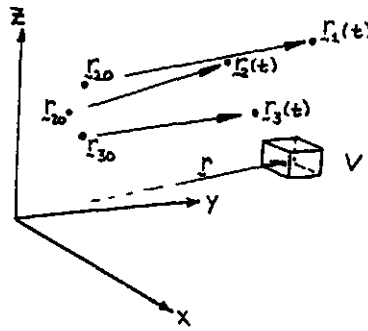


Fig A1.b.1 illustration of the sample volume V and positions for the three particles initially and at time t . taken from Lamb (1980).

Considering first the case of $m=1$ (one particle in the volume), there are three events which can lead to this value: either particle 1 is in v alone, or particle 2 is there alone, or 3 is present in v alone. By virtue of the definition of p we have

$$P_1 = \text{probability of particle 1 in } v \text{ alone} = \int \psi \int \psi \int \psi p_{123} dr_1 dr_2 dr_3 \quad \text{A.1.b.4}$$

where, for brevity

$$p_{123} = p(r_1, r_2, r_3, t | r_{10}, r_{20}, r_{30}, t_0) \quad \text{A.1.b.5}$$

The integration domain represents all space outside the volume v centred at r . v is assumed small enough that p varies little as r_1, r_2, r_3 vary over regions of size v centred at each point. In this case, the inner integral is simply $p_{123} v$.

The integral over ψ can be written in the form

$$\int_{\psi} () dr = \int () dr - \int_v () dr \quad \text{A.1.b.6}$$

where \int denotes integration over all space. Using this equation and the definition of the so called marginal densities p_j and p_{jk} , i.e.

$$p_{jk} \equiv \int p_{jkl} dr_l \quad \text{A.1.b.7}$$

$$p_j \equiv \int p_{jkl} dr_k dr_l \quad \text{A.1.b.8}$$

equation A.1.b.4 is reduced to the form

$$P_1 = \int_v [p_{13} v - p_{123} v^2] dr_3 \quad \text{A.1.b.9}$$

and repeating this operation, we get

$$P_1 = v p_1 - v^2 p_{13} - v^2 p_{12} + v^3 p_{123}$$

The same procedure is repeated for P_2, P_3 A.1.b.10

Since the occurrence in v of any one of the three particles is mutually exclusive of all other possible events, it follows that

$$w(1) = \sum_{n=1}^3 P_n = v (p_1 + p_2 + p_3) - 2 v^2 (p_{12} + p_{13} + p_{23}) + 3 v^3 p_{123} \quad \text{A.1.b.11}$$

The steps leading to the expression for $w(2)$ are similar to those just described, first

$$p_{12} = \text{Probability of particle 1 and 2 only in } v = \int_{v/v} \int_{v/v} p_{123} dr_3 = v^2 p_{12} - v^3 p_{123} \quad \text{A.1.b.12}$$

There are three mutually exclusive pairings of the three particles that give $c=2/v$ -- (1,2), (1,3), (2,3). Consequently

$$w(2) = P_{12} + P_{13} + P_{23} = v^2 (p_{12} + p_{13} + p_{23}) - 3 v^3 p_{123} \quad \text{A.1.b.13}$$

Finally, since all three particles must be in v to cause $c=3/v$, we have

$$w(3) = p_{123} v^3 \quad \text{A.1.b.14}$$

and since $m=0,1,2,3$ are the only 4 possible events,

$$w(0) = 1 - w(1) - w(2) - w(3) \quad \text{A.1.b.15}$$

These are the exact forms of the probability distribution $w(c)$ for this simple model. Now, to determine the ensemble averages or the moments of the concentration. The mathematical expectation of the n order moment is given by:

$$\langle m^n \rangle = \sum_{m=0}^3 m^n w(m) \quad \text{A.1.b.16}$$

The mean concentration, i.e. the zeroth order moment, is given in this three particle system by

$$\langle c \rangle = \langle m \rangle / v = w(1) + 2 w(2) + 3 w(3) \quad \text{A.1.b.17}$$

summing the corresponding expression for $w(1)$, $w(2)$ and $w(3)$, we end up

$$\langle c \rangle = p_1 + p_2 + p_3 \tag{A.1.b.18}$$

i.e. the sum of the marginal densities of the different particles in the system. In Lamb(1975), it is shown that in the limit as the number of particles becomes very large, equation A.1.b.18 becomes equal to

$$\langle C(r,t) \rangle = \int_0^t \int p(r,t | r',t') s(r',t') dr' dt' \tag{A.1.b.19}$$

which is equivalent to eq. 3.7.1a or 3.7.1b.

Here ends the derivation given by Lamb(1980); and now where is the misunderstanding in the derivation and that the effect of coherent structures is thought to be already included?

The joint density function p_{123} , as defined by eq.A.1.b.2 and A.1.b.3, includes in it all the possible correlations between the particle locations after some time since release, which could result due to the effect of different scales of motion, including large scale coherent structures. Small-scale structures do not lead to non-vanishing correlations between particles at different locations or between particles which have a time separation larger than the Lagrangian integral time scale.

The problem is that the marginal density functions p_1 , p_2 , p_3 will not be equal to each other. Since, it is by definition that in the case of independent events, i.e. the event of particle 1 being in location r_1 after time t has nothing to do with particle 2 being in location r_2 after time t , and both of these events or any of them have nothing to do with particle 3 being in location r_3 after time t , requires then the possibility of expressing the function $p(r_1, r_2, r_3, t | r_{10}, r_{20}, r_{30}, t_0)$ as a multiplication of the $p_1 \cdot p_2 \cdot p_3$ which are the marginal density functions for particles 1, 2 and 3 respectively. If the migration of the three particles are correlated, the expressing of $p_{123} = \prod_1^3 p_n$ where $p_1 = p_2 = p_3$ is not possible and the resulting summation in eq. A.1.b.18 is not of identical terms.

If we accept that the fluxes of the scalar quantities represent the migration of particles between different location and that these fluxes resulting from the existence of coherent structures represent correlation between particle emigration at different heights, we end up with the conclusion that the particles motions are correlated and so

$$p(r_1, r_2, r_3, \dots, r_n, t | r_{10}, r_{20}, r_{30}, \dots, r_{n0}, t_0) \text{ can not be expressed as a multiplication of } p_{123\dots n} = p_1 \cdot p_2 \cdot \dots \cdot p_n$$

where

$$p_1 = p_2 = \dots = p_n = p(r, t | r', t')$$

To get a fitting, you need one of these functions to be obtained by fitting.

APPENDIX 2 (A.2):

2.1) The energy equation of the leaves:

The energy budget of the leaves reads as

$$\rho_s C_s V \frac{\partial T_l}{\partial t} = \alpha_r R_s \downarrow A_r - \frac{\rho C_p}{r_{bh}} (T_l - T_a) A_h - \frac{\rho C_p}{\gamma(r_{bv} + r_s)} (e_s(T_l) - e_a) A_l + \left(\epsilon \sigma T_{air,a}^4 - \epsilon \sigma T_{l,a}^4 \right) A_r \quad A.2.1.1$$

assuming

$$e_s(T_l) = e_s(T_{air}) + \frac{\partial e_s}{\partial T} (T_l - T_{air}) \quad A.2.1.2$$

and

$$\left(\epsilon \sigma T_{air,rad,a}^4 - \epsilon \sigma T_{l,a}^4 \right) = 4 \epsilon \sigma T_{air,rad,a}^3 (T_{air,rad} - T_l) \quad A.2.1.3$$

The energy budget equation of the leaves can be put in the following form:

$$\frac{\partial T_l}{\partial t} = \frac{1}{\rho_s C_s V} [\alpha_r R_s \downarrow A_r + 4 \epsilon \sigma T_{air,rad,a}^3 (T_{air,rad} - T_l) - \frac{\rho C_p}{r_{bh}} (T_l - T_{air}) A_h - \frac{\rho C_p}{\gamma(r_{bv} + r_s)} (e_s(T_{air}) - e_a) A_l - \frac{\rho C_p}{\gamma(r_{bv} + r_s)} \frac{\partial e_s}{\partial T} (T_l - T_{air}) A_l] \quad A.2.1.4$$

which can by rearranging the terms be put in the following form

$$\frac{\partial T_l}{\partial t} = \frac{1}{\rho_s C_s V} [\alpha_r R_s \downarrow A_r + 4 \epsilon \sigma T_{air,rad,a}^3 T_{air,rad} + \frac{\rho C_p}{r_{bh}} T_{air} A_h - \frac{\rho C_p}{\gamma(r_{bv} + r_s)} (e_s(T_{air}) - e_{air}) A_l + \frac{\rho C_p}{\gamma(r_{bv} + r_s)} \frac{\partial e_s}{\partial T} T_{air} A_l] - \frac{1}{\rho_s C_s V} [4 \epsilon \sigma T_{air,rad,a}^3 + \frac{\rho C_p}{r_{bh}} A_h + \frac{\rho C_p}{\gamma(r_{bv} + r_s)} \frac{\partial e_s}{\partial T} A_l] T_l \quad A.2.1.5$$

Putting

$$K_{l,T} = \frac{1}{\rho_s C_s V} [4 \epsilon \sigma T_{air,a}^3 A_r + \frac{\rho C_p}{r_{bh}} A_h + \frac{\rho C_p}{\gamma(r_{bv} + r_s)} \frac{\partial e_s}{\partial T} A_l] \quad A.2.1.6$$

and

$$r_R = \frac{\rho C_p}{4 \epsilon \sigma T_{air,rad,a}^3} \quad A.2.1.7$$

and

$$A_r = A_h = A_l = A \quad \text{A.2.1.8}$$

$$\frac{1}{\tau_{l,T}} = K_{l,T} = \frac{\rho C_p}{\rho_s C_s \text{ thickness}} \left[\frac{1}{r_R} + \frac{1}{r_{bh}} + \frac{1}{\gamma(r_{bv} + r_s)} \frac{\partial e_s}{\partial T} \right] \quad \text{A.2.1.9}$$

Defining

$$T_{l,eq} K_{l,T} = \frac{\rho C_p}{\rho_s C_s \text{ thick}} \left[\frac{\alpha_r R_{s\downarrow}}{\rho C_p} + \frac{T_{air,rad}}{r_R} + \frac{1}{r_{bh}} T_a - \frac{1}{\gamma(r_{bv} + r_s)} (e_s(T_{air}) - e_{air}) + \frac{1}{\gamma(r_{bv} + r_s)} s T_{air} \right] \quad \text{A.2.1.10}$$

$$T_{l,eq} = \frac{1}{\left[\frac{1}{r_R} + \frac{1}{r_{bh}} + \frac{1}{\gamma(r_{bv} + r_s)} \frac{\partial e_s}{\partial T} \right]} \left[\frac{\alpha_r R_{s\downarrow}}{\rho C_p} + \frac{T_{air,rad}}{r_R} + \frac{1}{r_{bh}} T_{air} - \frac{1}{\gamma(r_{bv} + r_s)} (e_s(T_{air}) - e_{air}) + \frac{1}{\gamma(r_{bv} + r_s)} \frac{\partial e_s}{\partial T} T_{air} \right] \quad \text{A.2.1.11}$$

The equation for the leaves reads as

$$\frac{\partial T_l}{\partial t} = -K_{l,T} (T_l - T_{l,eq}) \quad \text{A.2.1.12}$$

the solution of which is

$$T_l = T_{l,eq} \left(1 - e^{-\frac{t}{\tau_{l,T}}} \right) + T_{l,initial} e^{-\frac{t}{\tau_{l,T}}} \quad \text{A.2.1.13}$$

2.2) The sensible heat equation of the canopy air layers

The sensible heat balance equation reads as

$$\rho C_p \frac{\partial T_{air}}{\partial t} = -\frac{\partial q}{\partial z} + s_h \quad \text{A.2.2.1}$$

Discretized with respect to space, it reads as

$$\Delta z \rho C_p \frac{\partial T_{air}}{\partial t} = -(q_{i+1} - q_i) + S_h \Delta z \quad \text{A.2.2.2}$$

$$q_1 = \overline{w'c'}_1^{ens} = \left[\overline{w'^2} \tau_L \left\{ 1 - e^{-\frac{t_0-t_1}{\tau_L}} \right\} \right] \frac{\partial \bar{c}_1^{ens}}{\partial z}$$

$$q_{\sum_{i=1}^n} = \int_0^t \overline{w'c'}^{ens} dt = \int_0^t \left[\overline{w'^2} \tau_L \left\{ 1 - e^{-\frac{t_0-t_1}{\tau_L}} \right\} \right]_{top} \frac{\partial \bar{c}_1^{ens}}{\partial z} dt_1$$

$$\bar{q}_{i+1} = \frac{\int_0^t \int_0^t \overline{w'c'}^{ens} dt_1 dt}{t} = \frac{\int_0^t \int_0^t \left[\overline{w'^2} \tau_L \left\{ 1 - e^{-\frac{t_0-t_1}{\tau_L}} \right\} \right]_{top} \frac{\partial \bar{c}_1^{ens}}{\partial z} dt_1 dt}{t}$$

$$\overline{w'c'}^{ens} = \overline{w'^2} \tau_L \left\{ 1 - e^{-\frac{t_0-t_1}{\tau_L}} \right\} \frac{\partial \bar{c}}{\partial z} \quad \text{A.2.2.3}$$

The above equation expresses the development of the flux as a function of time. The ensemble average here means an average over the same time since release or the average of a large number of measurements, taken at the same period after the passage of a gust. The actual flux will be a superposition of different times since release.

The mean flux:

$$\bar{q}_{i+1} = \frac{\int_0^t \overline{w'c'}^{ens} dt}{t} = \frac{\int_0^t \left[\overline{w'^2} \tau_L \left\{ 1 - e^{-\frac{t_0-t_1}{\tau_L}} \right\} \right]_{top} \frac{\partial \bar{c}}{\partial z} dt}{t} \quad \text{A.2.2.4}$$

Putting

$$q_{i+1} = \rho C_p \frac{\overline{w'^2} \tau_L \left\{ 1 - e^{-\frac{t_0-t_1}{\tau_L}} \right\} \frac{\partial \bar{c}}{\partial z} \Big|_{top}}{\delta X_{top}} (T_i - T_{i+1}) \quad \text{A.2.2.5}$$

and

$$q_i = \rho C_p \frac{\overline{w'^2} \tau_L \left\{ 1 - e^{-\frac{t_0-t_1}{\tau_L}} \right\} \frac{\partial \bar{c}}{\partial z} \Big|_{bottom}}{\delta X_{bottom}} (T_{i-1} - T_i) \quad \text{A.2.2.6}$$

leads to

$$\Delta z \rho C_p \frac{\partial T_{air}}{\partial t} = \rho C_p \frac{\overline{w'^2} \tau_L \left\{ 1 - e^{-\frac{t_0 - t_1}{\tau_L}} \right\}_{top}}{\delta X_{top}} (T_{i+1} - T_i) + \rho C_p \frac{\overline{w'^2} \tau_L \left\{ 1 - e^{-\frac{t_0 - t_1}{\tau_L}} \right\}_{bottom}}{\delta X_{bottom}} (T_{i-1} - T_i) + \frac{\rho C_p}{r_{bh}} (T_i - T_i) LAD \Delta z \quad A.2.2.7$$

Rearranging

$$\Delta z \rho C_p \frac{\partial T_{air}}{\partial t} = -\rho C_p \left(\frac{\overline{w'^2} \tau_L \left\{ 1 - e^{-\frac{t_0 - t_1}{\tau_L}} \right\}_{top}}{\delta X_{top}} + \frac{\overline{w'^2} \tau_L \left\{ 1 - e^{-\frac{t_0 - t_1}{\tau_L}} \right\}_{bottom}}{\delta X_{bottom}} + \frac{LAD \Delta z}{r_{bh}} \right) T_i + \rho C_p \left(\frac{\overline{w'^2} \tau_L \left\{ 1 - e^{-\frac{t_0 - t_1}{\tau_L}} \right\}_{top}}{\delta X_{top}} T_{i+1} + \frac{\overline{w'^2} \tau_L \left\{ 1 - e^{-\frac{t_0 - t_1}{\tau_L}} \right\}_{bottom}}{\delta X_{bottom}} T_{i-1} + \frac{T_i LAD \Delta z}{r_{bh}} \right) \quad A.2.2.8$$

In the far field region Of $\frac{z}{\tau_L} > 5$, where τ_L is the Lagrangian time scale which has a

maximum value of 1 sec. The equations reduce to the $\frac{\overline{w'^2} \tau_L}{\delta X_{top}}$

$$\frac{\partial T_{air}}{\partial t} = -\frac{1}{\Delta z} \left(\frac{K_{top}}{\delta X_{top}} + \frac{K_{bottom}}{\delta X_{bottom}} + \frac{LAD \Delta z}{r_{bh}} \right) T_i + \frac{1}{\Delta z} \left(\frac{K_{top}}{\delta X_{top}} T_{i+1} + \frac{K_{bottom}}{\delta X_{bottom}} T_{i-1} + \frac{T_i LAD \Delta z}{r_{bh}} \right) \quad A.2.2.9$$

$$\frac{1}{\tau_{a, T}} = K_{a, T} = \frac{1}{\Delta z} \left(\frac{K_{top}}{\delta X_{top}} + \frac{K_{bottom}}{\delta X_{bottom}} + \frac{LAD \Delta z}{r_{bh}} \right) \quad A.2.2.10$$

$$\frac{\partial T_{air}}{\partial t} = -K_{a,T} T_i + K_{a,T} \frac{\frac{1}{\Delta z} \left(\frac{K_{top}}{\delta X_{top}} T_{i+1} + \frac{K_{bottom}}{\delta X_{bottom}} T_{i-1} + \frac{T_i LAD \Delta z}{\Gamma_{bh}} \right)}{\frac{1}{\Delta z} \left(\frac{K_{top}}{\delta X_{top}} + \frac{K_{bottom}}{\delta X_{bottom}} + \frac{LAD \Delta z}{\Gamma_{bh}} \right)}$$

A.2.2.11

$$\frac{\partial T_{air}}{\partial t} = -K_{a,T} T_i + K_{a,T} T_{air,eq}$$

A.2.2.12

The behaviour of the equation is exponential in a range of values which exceeds the Lagrangian integral time scale by an order of magnitude. The effect of the non-linearity we are considering in the solution is not only a near field effect.

The solution of this equation follows. The assumption of the constancy of $T_{air,eq}$ could be justified by applying the integration for a short timestep in which the values of $T_{air,eq}$ and $K_{a,T}$ are almost constant. For every time step, the values of $T_{air,eq}$ will keep changing. This equation describes the behaviour during such an interval.

$$T_{air} = T_{air,eq} (1 - e^{-\frac{t}{\tau_{a,T}}}) + T_{air,initial} e^{-\frac{t}{\tau_{a,T}}}$$

A.2.2.13

where

$$T_{air,eq}(t) = \left(\begin{aligned} & \frac{\frac{K_{top}}{\delta X_{top}} T_{i+1} + \frac{K_{bottom}}{\delta X_{bottom}} T_{i-1}}{\left(\frac{K_{top}}{\delta X_{top}} + \frac{K_{bottom}}{\delta X_{bottom}} + \frac{LAD \Delta z}{\Gamma_{bh}} \right)} + \frac{\frac{LAD \Delta z}{\Gamma_{bh}} T_i}{\left(\frac{K_{top}}{\delta X_{top}} + \frac{K_{bottom}}{\delta X_{bottom}} + \frac{LAD \Delta z}{\Gamma_{bh}} \right)} \end{aligned} \right)$$

A.2.2.14

There are two time constants for the layer. One active during the gust intrusion and the other during the quiescence period.

2.3) The latent heat equation of the canopy air layers

The latent heat balance equation reads as

$$\frac{\rho C_p}{\gamma} \frac{\partial e_{\text{air}}}{\partial t} = - \frac{\partial q_{le}}{\partial z} + S_{le} \quad \text{A.2.3.1}$$

Discretized with respect to space

$$\Delta z \frac{\rho C_p}{\gamma} \frac{\partial e_{\text{air}}}{\partial t} = - (q_{i+1} - q_i) + S_{le} \Delta z \quad \text{A.2.3.2}$$

Putting

$$q_{e,i+1} = \frac{\rho C_p}{\gamma} \frac{K_{\text{top}}}{\delta X_{\text{top}}} (e_i - e_{i+1}) \quad \text{A.2.3.3}$$

and

$$q_{e,i} = \frac{\rho C_p}{\gamma} \frac{K_{\text{bottom}}}{\delta X_{\text{bottom}}} (e_{i-1} - e_i) \quad \text{A.2.3.4}$$

$$\begin{aligned} \Delta z \frac{\rho C_p}{\gamma} \frac{\partial e_{\text{air}}}{\partial t} &= \frac{\rho C_p}{\gamma} \frac{K_{\text{top}}}{\delta X_{\text{top}}} (e_{i+1} - e_i) + \frac{\rho C_p}{\gamma} \frac{K_{\text{bottom}}}{\delta X_{\text{bottom}}} (e_{i-1} - e_i) \\ &\quad + \frac{\rho C_p}{\gamma(r_{bv} + r_s)} (es(T_i) - e_a) LAD \Delta z \end{aligned} \quad \text{A.2.3.5}$$

Rearranging

$$\begin{aligned} \frac{\partial e_{\text{air}}}{\partial t} &= - \frac{1}{\Delta z} \left(\frac{K_{\text{top}}}{\delta X_{\text{top}}} + \frac{K_{\text{bottom}}}{\delta X_{\text{bottom}}} + \frac{LAD \Delta z}{(r_{bv} + r_s)} \right) e_i \\ &\quad + \frac{1}{\Delta z} \left(\frac{K_{\text{top}}}{\delta X_{\text{top}}} e_{i+1} + \frac{K_{\text{bottom}}}{\delta X_{\text{bottom}}} e_{i-1} + \frac{es(T_i) LAD \Delta z}{(r_{bv} + r_s)} \right) \end{aligned} \quad \text{A.2.3.6}$$

$$\frac{1}{\tau_{a,e}} = K_{a,e} = \frac{1}{\Delta z} \left(\frac{K_{\text{top}}}{\delta X_{\text{top}}} + \frac{K_{\text{bottom}}}{\delta X_{\text{bottom}}} + \frac{LAD \Delta z}{(r_{bv} + r_s)} \right) \quad \text{A.2.3.7}$$

$$\frac{\partial e_{air}}{\partial t} = -K_{a,e} e_i + K_{a,e} \frac{\frac{1}{\Delta z} \left(\frac{K_{top}}{\delta X_{top}} e_{i+1} + \frac{K_{bottom}}{\delta X_{bottom}} e_{i-1} + \frac{LAD \Delta z}{(r_{bv}+r_s)} es(T_1) \right)}{\frac{1}{\Delta z} \left(\frac{K_{top}}{\delta X_{top}} + \frac{K_{bottom}}{\delta X_{bottom}} + \frac{LADMID \Delta z}{(r_{bv}+r_s)} \right)}$$

A.2.3.8

$$\frac{\partial e_{air,i}}{\partial t} = -K_{a,e} e_{air,i} + K_{a,e} e_{air,eq}$$

A.2.3.9

where

$$e_{air,eq}(t) = \left(\frac{\frac{K_{top}}{\delta X_{top}}}{\left(\frac{K_{top}}{\delta X_{top}} + \frac{K_{bottom}}{\delta X_{bottom}} + \frac{LADMID \Delta z}{(r_{bv}+r_s)} \right)} e_{i+1} + \frac{\frac{K_{bottom}}{\delta X_{bottom}}}{\left(\frac{K_{top}}{\delta X_{top}} + \frac{K_{bottom}}{\delta X_{bottom}} + \frac{LAD \Delta z}{(r_{bv}+r_s)} \right)} e_{i-1} + \frac{\frac{LAD \Delta z}{(r_{bv}+r_s)}}{\left(\frac{K_{top}}{\delta X_{top}} + \frac{K_{bottom}}{\delta X_{bottom}} + \frac{LAD \Delta z}{(r_{bv}+r_s)} \right)} es(T_1) \right)$$

A.2.3.10

$$e_{air} = e_{air,eq} (1 - e^{-\frac{t}{\tau_{a,e}}}) + e_{initial} e^{-\frac{t}{\tau_{a,e}}}$$

A.2.3.11

There are two time constants for the canopy air layer. One during the gust intrusion and the other during the quiescence period.

2.4) The vapour pressure deficit of the canopy air layers

$$\Delta z \frac{\rho C_p}{\gamma} \frac{\partial e_{air}}{\partial t} = \frac{\rho C_p}{\gamma} \frac{K_{top}}{\delta X_{top}} (e_{i+1} - e_i) + \frac{\rho C_p}{\gamma} \frac{K_{bottom}}{\delta X_{bottom}} (e_{i-1} - e_i) + \frac{\rho C_p}{\gamma (r_{bv}+r_s)} (es(T_1) - e_a) LAD \Delta z$$

A.2.4.1

$$\Delta z \frac{\rho C_p}{\gamma} \frac{\partial e_{air}}{\partial t} = \frac{\rho C_p}{\gamma} \frac{K_{top}}{\delta X_{top}} (e_{i+1} - e_i) + \frac{\rho C_p}{\gamma} \frac{K_{bottom}}{\delta X_{bottom}} (e_{i-1} - e_i) + \frac{s R_n + \rho C_p D r_h^{-1}}{\gamma^* + s} LAD \Delta z$$

A.2.4.2

$$\Delta z \rho C_P \frac{\partial T_{\text{air}}}{\partial t} = \rho C_P \frac{K_{\text{top}}}{\delta X_{\text{top}}} (T_{i+1} - T_i) + \rho C_P \frac{K_{\text{bottom}}}{\delta X_{\text{bottom}}} (T_{i-1} - T_i) + \frac{\gamma^* R_n - \rho C_P D r_h^{-1}}{\gamma^* + s} \text{LAD } \Delta z$$

A.2.4.3

Multiplying the first equation by $(-\gamma)$ and the second by s ($s = \frac{\partial e_s}{\partial T}$)

$$\Delta z s \rho C_P \frac{\partial T_{\text{air}}}{\partial t} = \rho C_P s \frac{K_{\text{top}}}{\delta X_{\text{top}}} (T_{i+1} - T_i) + \rho C_P s \frac{K_{\text{bottom}}}{\delta X_{\text{bottom}}} (T_{i-1} - T_i) + s \frac{\gamma^* R_n - \rho C_P D r_h^{-1}}{\gamma^* + s} \text{LAD } \Delta z$$

A.2.4.4

$$-\Delta z \rho C_P \frac{\partial e_{\text{air}}}{\partial t} = -\rho C_P \frac{K_{\text{top}}}{\delta X_{\text{top}}} (e_{i+1} - e_i) - \rho C_P \frac{K_{\text{bottom}}}{\delta X_{\text{bottom}}} (e_{i-1} - e_i) - \gamma \frac{s R_n + \rho C_P D r_h^{-1}}{\gamma^* + s} \text{LAD } \Delta z$$

A.2.4.5

$$\begin{aligned} \Delta z \rho C_P \frac{\partial (s T_{\text{air}} - e_{\text{air}})}{\partial t} &= \rho C_P \frac{K_{\text{top}}}{\delta X_{\text{top}}} ((s T_{i+1} - e_{i+1}) - (s T_i - e_i)) \\ &+ \rho C_P \frac{K_{\text{bottom}}}{\delta X_{\text{bottom}}} ((s T_{i-1} - e_{i-1}) - (s T_i - e_i)) \\ &+ \left(s \frac{\gamma^* R_n - \rho C_P D r_h^{-1}}{\gamma^* + s} - \gamma \frac{s R_n + \rho C_P D r_h^{-1}}{\gamma^* + s} \right) \text{LAD } \Delta z \end{aligned}$$

A.2.4.6

$$D(T_a) = e_s(T_a) - e_a \quad \text{A.2.4.7}$$

$$D(T_a) = e_s(T_p) + s T_a - s T_p - e_a \quad \text{A.2.4.8}$$

where T_p is some reference temperature,

Adding and subtracting $e_s(T_p) - s T_p$ to $(s T_{\text{air}} - e_{\text{air}})$ for layer $i+1$ and layer i in the left and right hand side of the equation gives

$$\begin{aligned} \Delta z \rho C_P \frac{\partial D_i}{\partial t} &= \rho C_P \frac{K_{\text{top}}}{\delta X_{\text{top}}} (D_{i+1} - D_i) + \rho C_P \frac{K_{\text{bottom}}}{\delta X_{\text{bottom}}} (D_{i-1} - D_i) \\ &+ \left(s \frac{\gamma^* R_n - \rho C_P D r_h^{-1}}{\gamma^* + s} - \gamma \frac{s R_n + \rho C_P D r_h^{-1}}{\gamma^* + s} \right) \text{LAD } \Delta z \end{aligned}$$

A.2.4.9

dividing the whole equation by s

$$\Delta z \frac{\rho C_p}{s} \frac{\partial D_i}{\partial t} = \frac{\rho C_p}{s} \frac{K_{top}}{\delta X_{top}} (D_{i+1} - D_i) + \frac{\rho C_p}{s} \frac{K_{bottom}}{\delta X_{bottom}} (D_{i-1} - D_i) + \left(\frac{\gamma^* R_n - \rho C_p D r_h^{-1}}{\gamma^* + s} - \frac{\gamma}{s} \frac{s R_n + \rho C_p D r_h^{-1}}{\gamma^* + s} \right) LAD \Delta z \quad A.2.4.10$$

working out the third term between brackets as shown in Chen(1984)

$$\left(\frac{\gamma^* R_n - \rho C_p D r_h^{-1}}{\gamma^* + s} - \frac{\gamma}{s} \frac{s R_n + \rho C_p D r_h^{-1}}{\gamma^* + s} \right) = \frac{\gamma^* R_n - \gamma R_n}{\gamma^* + s} - \frac{\rho C_p D r_h^{-1} + \frac{\gamma}{s} \rho C_p D r_h^{-1}}{\gamma^* + s}$$

$$\frac{\gamma^* R_n - \gamma R_n}{\gamma^* + s} = \frac{\gamma (r_b, v + r_s) R_n - \gamma r_h R_n}{\gamma (r_b, v + r_s) + s r_h} = \frac{\gamma r_s R_n}{\gamma (r_b, v + r_s) + s r_h} = \frac{R_n}{1 + \frac{r_b}{r_s} (1 + \frac{s}{\gamma})}$$

$$= \frac{R_n}{1 + \frac{r_b}{r_s} (\frac{\gamma + s}{\gamma})} = \frac{R_n}{1 + \frac{r_b}{r_s} \alpha} = \frac{r_s \alpha R_n}{r_s \alpha + r_b} \quad A.2.4.11$$

$$- \frac{\rho C_p D r_h^{-1} + \frac{\gamma}{s} \rho C_p D r_h^{-1}}{\gamma^* + s} = - \frac{\rho C_p D (\frac{s + \gamma}{s})}{(\gamma + s) r_b + \gamma r_s} = - \frac{\frac{\rho C_p D}{s}}{r_b + \frac{\gamma}{s + \gamma} r_s} = - \frac{\frac{\rho C_p D}{s}}{r_b + \alpha r_s} \quad A.2.4.12$$

$$\Delta z \frac{\rho C_p}{s} \frac{\partial D_i}{\partial t} = \frac{\rho C_p}{s} \frac{K_{top}}{\delta X_{top}} (D_{i+1} - D_i) + \frac{\rho C_p}{s} \frac{K_{bottom}}{\delta X_{bottom}} (D_{i-1} - D_i) + \left(\frac{r_s \alpha R_n}{r_s \alpha + r_b} - \frac{\frac{\rho C_p D}{s}}{r_b + \alpha r_s} \right) LAD \Delta z \quad A.2.4.13$$

where:

$$\alpha = \left(\frac{\gamma}{\gamma + s} \right) \quad A.2.4.14$$

$$\Delta z \frac{\partial D_i}{\partial t} = \frac{K_{top}}{\delta X_{top}} (D_{i+1} - D_i) + \frac{K_{bottom}}{\delta X_{bottom}} (D_{i-1} - D_i) + \left(\frac{s}{\rho C_p} \frac{r_s \alpha R_n}{r_s \alpha + r_b} - \frac{D_i}{r_b + \alpha r_s} \right) LAD \Delta z \quad A.2.4.15$$

Rearranging :

$$\frac{\partial D_i}{\partial t} = \frac{1}{\Delta z} \left(\frac{K_{top}}{\delta X_{top}} + \frac{K_{bottom}}{\delta X_{bottom}} + \frac{LAD \Delta z}{r_b + \alpha r_s} \right) D_i + \frac{1}{\Delta z} \left(\frac{K_{top}}{\delta X_{top}} D_{i+1} + \frac{K_{bottom}}{\delta X_{bottom}} D_{i-1} + \left(\frac{s}{\rho C_p} \frac{r_s \alpha R_n}{(r_s \alpha + r_b)} \right) LAD \Delta z \right) \quad A.2.4.16$$

$$\frac{1}{\tau_{a,D}} = K_D = \frac{1}{\Delta z} \left(\frac{K_{top}}{\delta X_{top}} + \frac{K_{bottom}}{\delta X_{bottom}} + \frac{LAD \Delta z}{r_b + \alpha r_s} \right) \quad A.2.4.17$$

$$\frac{\partial D_i}{\partial t} = -K_D D_i + \frac{K_D}{\Delta z} \left(\frac{K_{top}}{\delta X_{top}} D_{i+1} + \frac{K_{bottom}}{\delta X_{bottom}} D_{i-1} + \left(\frac{s}{\rho C_p} \frac{r_s \alpha R_n}{(r_b + \alpha r_s)} \right) LAD \Delta z \right) \quad A.2.4.18$$

$$\frac{\partial D_i}{\partial t} = -K_D D_i + K_D \frac{1}{\Delta z} \left(\frac{K_{top}}{\delta X_{top}} D_{i+1} + \frac{K_{bottom}}{\delta X_{bottom}} D_{i-1} + \frac{LAD \Delta z}{(r_b + \alpha r_s)} \left(\frac{s \alpha r_s R_n}{\rho C_p} \right) \right) \quad A.2.4.19$$

$$\frac{\partial D_i}{\partial t} = -K_D D_i + K_D D_{air,eq} \quad A.2.4.20$$

$$D_{air,eq}(t) = \left(\frac{\frac{K_{top}}{\delta X_{top}} D_{i+1} + \frac{K_{bottom}}{\delta X_{bottom}} D_{i-1}}{\left(\frac{K_{top}}{\delta X_{top}} + \frac{K_{bottom}}{\delta X_{bottom}} + \frac{LAD \Delta z}{r_b + \alpha r_s} \right)} + \frac{\frac{LAD \Delta z}{r_b + \alpha r_s} \left(\frac{s \alpha r_s R_n}{\rho C_p} \right)}{\left(\frac{K_{top}}{\delta X_{top}} + \frac{K_{bottom}}{\delta X_{bottom}} + \frac{LAD \Delta z}{r_b + \alpha r_s} \right)} \right) \quad A.2.4.21$$

$$D_{air} = D_{air,eq} \left(1 - e^{-\frac{t}{\tau_{a,D}}} \right) + D_{air,initial} e^{-\frac{t}{\tau_{a,D}}} \quad A.2.4.22$$

$$\left(\frac{s \alpha r_s R_n}{\rho C_p} \right) = \frac{\gamma r_s \frac{s}{\gamma + s} R_n}{\rho C_p} = \frac{\gamma r_s E_{equ}}{\rho C_p} \quad A.2.4.23$$

In this derivation, which is a variant of Chen (1984), there is no need for defining J (saturation heat flux). The system is directly solvable to obtain a D value.

2.5) The Soil temperature equation solution and the effect of intermittency on the change of the boundary condition for the energy equation at the soil surface

Remark: The solution introduced here is standard mathematics, The formulation of the problem (eq. A.2.5.1 to eq. A.2.5.7) and the nonhomogenous solution is done by the author

The soil temperature as function of space (x) and time (t) is formulated as follows:

$$\frac{\partial T_s}{\partial t} = \kappa \frac{\partial^2 T_s}{\partial x^2} + Q(x,t) \quad \text{A.2.5.1}$$

subject to the following boundary conditions:

$$\beta_L \frac{\partial T_s(L,t)}{\partial x} + \alpha_L T_s(L) = f(L,t) \quad \text{A.2.5.1.a}$$

$$\frac{\partial T_s(0,t)}{\partial x} = 0 \quad \text{A.2.5.1.b}$$

and the initial condition

$$T(x,0) = g(x) \quad \text{A.2.5.1.c}$$

where

$$f(L,t) = \alpha_r R_s \downarrow + 4\epsilon\sigma T_{\text{air,rad,a}}^3 T_{\text{air,rad,a}} + \left(\frac{\rho C_p}{r_{bh}} + \frac{\rho C_p s}{\gamma(r_{bv} + r_{s,s})} \right) T_{\text{air}} - \frac{\rho C_p}{\gamma(r_{bv} + r_{s,s})} D_{\text{air}} \quad \text{A.2.5.2}$$

$$\alpha_L = \left(4\epsilon\sigma T_{\text{air,rad,a}}^3 + \frac{\rho C_p}{r_{bh}} + \frac{\rho C_p s}{\gamma(r_{bv} + r_{s,s})} \right) \quad \text{A.2.5.3}$$

$$Q(x,t) = 0 \quad x \leq L \text{ and } t \geq 0 \quad \text{A.2.5.1.d}$$

and g(x) is the initial temperature profile.

The related homogenous problem(A.2.5.4), satisfies a Sturm-Liouville Eigenvalue problem and as such is complete, i.e any piecewise smooth function can be expanded in a series of Eigenfunctions(A.2.5.8). The related homogenous problem is given by :

$$\frac{d^2 \phi_n}{dx^2} + \lambda \phi_n = 0 \quad \text{A.2.5.4}$$

$$\beta_L \frac{d\phi_n}{dx}(L) + \alpha_L \phi_n(L) = 0 \quad \text{A.2.5.4.a}$$

$$\frac{d\phi_n}{dx}(0) = 0 \quad \text{A.2.5.4.b}$$

The Eigenfunction of the related homogenous problem is

$$\phi(x,t) = C_1 \cos \sqrt{\lambda_n} x + C_2 \sin \sqrt{\lambda_n} x \quad \text{A 2.5.5}$$

using the boundary condition at $x=0$ eq.A.2.5.1 , $C_2 = 0$

$$\phi_n = C_1 \cos \sqrt{\lambda_n} x \quad \text{A 2.5.6}$$

where

$$\sqrt{\lambda_n} = \cot(\sqrt{\lambda_n} L) \frac{\alpha L}{\beta L} \quad \text{A 2.5.6.a}$$

The soil temperature can then be expressed as

$$T(x,t) = \sum_{n=0}^{n=\infty} b_n(t) \phi_n(x) \quad \text{A 2.5.7}$$

The equality is actually not valid at $x=L$ since $\phi_n(x)$ satisfies the homogenous boundary condition there while $T(x,t)$ does not. So, the required term by term differentiation of $T(x,t)$ with respect to x is not valid, while the derivative with respect to time is possible (from A.2.5.1 and A2.5.7).

$$\sum_{n=0}^{\infty} \frac{d b_n}{dt} \phi_n(x) = \kappa \frac{\partial^2 T}{\partial x^2} \quad \text{A 2.5.8}$$

$\frac{d b_n}{dt}$ is the coefficients of an Eigenfunction expansion of $\kappa \frac{\partial^2 T}{\partial x^2}$, using the orthogonality of the Eigenfunctions of this expansion

$$\frac{d b_n}{dt} = \frac{\int_0^L \kappa \frac{\partial^2 T}{\partial x^2} \phi_n(x) dx}{\int_0^L \phi_n^2(x) dx} \quad \text{A 2.5.9}$$

Using Green 's formula which states that

$$\int_0^L [u L(v) - v L(u)] dx = \left(u \frac{dv}{dx} - v \frac{du}{dx} \right) \Big|_0^L \quad \text{A 2.5.10}$$

where

L is any Sturm-Liouville operator $L \equiv \frac{d}{dx} (p \frac{d}{dx}) + q$, in this case $q=0$ and $p=1$.

$$\begin{aligned}
 \int_0^L [T \frac{\partial^2 \phi_n}{\partial x^2} - \phi_n \frac{\partial^2 T}{\partial x^2}] dx &= [T \frac{\partial \phi_n}{\partial x} - \phi_n \frac{\partial T}{\partial x}] \Big|_0^L \\
 &= T(L) \frac{\partial \phi_n(L)}{\partial x} - \phi_n(L) \frac{\partial T}{\partial x} - T(L) \frac{\partial \phi_n(0)}{\partial x} + \phi_n(0) \frac{\partial T(0)}{\partial x} = T(L) \frac{\partial \phi_n(L)}{\partial x} - \phi_n(L) \frac{\partial T(L)}{\partial x} \\
 &= -T(L) \frac{\alpha_L}{\beta_L} (\cot \sqrt{\lambda_n} L) \sin \sqrt{\lambda_n} L - \cos(\sqrt{\lambda_n} L) \frac{\partial T(L)}{\partial x} \\
 &= -\frac{1}{\beta_L} \cos \sqrt{\lambda_n} L [\alpha_L T(L) + \beta_L \frac{\partial T(L)}{\partial x}] \\
 &= -\frac{1}{\beta_L} \cos(\sqrt{\lambda_n} L) f(L,t) \tag{A.2.5.11}
 \end{aligned}$$

$$\kappa \int_0^L \phi_n \frac{\partial^2 T}{\partial x^2} dx = -\kappa [T \frac{\partial \phi_n}{\partial x} - \phi_n \frac{\partial T}{\partial x}] \Big|_0^L + \kappa \int_0^L T \frac{\partial^2 \phi_n}{\partial x^2} dx \tag{A.2.5.12}$$

Using equation A.2.5.4

$$\kappa \int_0^L T \frac{\partial^2 \phi_n}{\partial x^2} dx = -\lambda_n \kappa \int_0^L T \phi_n dx \tag{A.2.5.13}$$

and since $b_n(t)$ is the coefficient of an Eigenfunctions expansion of $T(x,t)$, so by definition

$$b_n(t) = \frac{\int_0^L T(t) \phi_n dx}{\int_0^L \phi_n^2(x) dx} \tag{A.2.5.14}$$

$$-\lambda_n \kappa \int_0^L T \phi_n dx = -\lambda_n \kappa b_n \int_0^L \phi_n^2(x) dx \tag{A.2.5.15}$$

Using equation A.2.5.15, A.2.5.9

$$\frac{d b_n(t)}{dt} = \frac{\int_0^L \kappa \frac{\partial^2 T}{\partial x^2} \phi_n(x) dx}{\int_0^L \phi_n^2(x) dx} = \frac{\frac{\kappa}{\beta_L} \cos(\sqrt{\lambda_n} L) f(L,t) - \lambda_n \kappa b_n \int_0^L \phi_n^2(x) dx}{\int_0^L \phi_n^2(x) dx} \tag{A.2.5.16}$$

$$\frac{db_n(t)}{dt} + \lambda_n \kappa b_n(t) = \frac{\kappa \cos(\sqrt{\lambda_n} L) f(L, t)}{\beta_L \int_0^L \phi_n^2(x) dx}$$

A.2.5.17

$$\frac{d(b_n(t) e^{\lambda_n \kappa t})}{dt} = e^{\lambda_n \kappa t} \frac{\cos(\sqrt{\lambda_n} L) f(L, t)}{\rho_s C_s \int_0^L \phi_n^2(x) dx}$$

A.2.5.18

$$b_n(t) = b_n(0) e^{-\lambda_n \kappa t} + e^{-\lambda_n \kappa t} \int_0^t \frac{e^{\lambda_n \kappa \tau} \cos(\sqrt{\lambda_n} L) f(L, \tau)}{\rho_s C_s \int_0^L \phi_n^2(x) dx} d\tau$$

A.2.5.19

$$b_n(0) = \frac{\int_0^L g(x) \phi_n(x) dx}{\int_0^L \phi_n^2(x) dx}$$

A.2.5.20

$$b_n(t) = b_n(0) e^{-\lambda_n \kappa t} + \frac{e^{-\lambda_n \kappa t} \cos(\sqrt{\lambda_n} L)}{\rho_s C_s \frac{L}{2} + \frac{\rho_s C_s}{2\sqrt{\lambda_n}} \sin(\sqrt{\lambda_n} L) \cos(\sqrt{\lambda_n} L)} \left(\int_0^t e^{\lambda_n \kappa \tau} f_1(L, \tau) d\tau + \int_0^t e^{\lambda_n \kappa \tau} f_2(L, \tau) d\tau \right)$$

A.2.5.21

2.6.1) The approximate form:

2.6.1.a) The vapour pressure deficit equation for an n layered canopy.

Our starting point is equation A. 2.4.16, which reads,

$$\Delta z \frac{\partial D_i}{\partial t} = \frac{K_{\text{top}}}{\delta X_{\text{top}}} (D_{i+1}^{t+\Delta t} - D_i^{t+\Delta t}) + \frac{K_{\text{bottom}}}{\delta X_{\text{bottom}}} (D_{i-1}^{t+\Delta t} - D_i^{t+\Delta t}) + \left(\frac{s}{\rho C_p} \frac{r_s \alpha R_n}{(r_s \alpha + r_b)} - \frac{D_i}{r_b + \alpha r_s} \right) \text{LAD } \Delta z \quad \text{A.2.6.1.1}$$

The superscript $t+\Delta t$ means that the values of D are evaluated at the end of each timestep (implicit approach).

$$\frac{\Delta z}{\Delta t} (D_i^{t+\Delta t} - D_i^t) = \frac{K_{\text{top}}}{\delta X_{\text{top}}} (D_{i+1}^{t+\Delta t} - D_i^{t+\Delta t}) + \frac{K_{\text{bottom}}}{\delta X_{\text{bottom}}} (D_{i-1}^{t+\Delta t} - D_i^{t+\Delta t}) + \left(\frac{s}{\rho C_p} \frac{r_s \alpha R_n}{(r_s \alpha + r_b)} - \frac{D_i^{t+\Delta t \text{ or } t}}{r_b + \alpha r_s} \right) \text{LAD } \Delta z \quad \text{A.2.6.1.2}$$

$$\left(\frac{\Delta z}{\Delta t} + \frac{K_{\text{top}}}{\delta X_{\text{top}}} + \frac{K_{\text{bottom}}}{\delta X_{\text{bottom}}} + \frac{\text{LAD } \Delta z}{r_b + \alpha r_s} \right) D_i^{t+\Delta t} = \frac{K_{\text{top}}}{\delta X_{\text{top}}} D_{i+1}^{t+\Delta t} + \frac{K_{\text{bottom}}}{\delta X_{\text{bottom}}} D_{i-1}^{t+\Delta t} + \frac{\text{LAD } \Delta z}{(r_s \alpha + r_b)} \frac{s r_s \alpha R_n}{\rho C_p} \quad \text{A.2.6.1.3}$$

$$\begin{aligned} \frac{K_{\text{top}}}{\delta X_{\text{top}}} D_{i+1}^{t+\Delta t} - \left(\frac{\Delta z}{\Delta t} + \frac{K_{\text{top}}}{\delta X_{\text{top}}} + \frac{K_{\text{bottom}}}{\delta X_{\text{bottom}}} + \frac{\text{LAD } \Delta z}{r_b + \alpha r_s} \right) D_i^{t+\Delta t} + \frac{K_{\text{bottom}}}{\delta X_{\text{bottom}}} D_{i-1}^{t+\Delta t} \\ = - \frac{\text{LAD } \Delta z}{(r_s \alpha + r_b)} \frac{s r_s \alpha R_n}{\rho C_p} \end{aligned}$$

$$E_i D_{i-1}^{t+\Delta t} - F_i D_i^{t+\Delta t} + G_i D_{i+1}^{t+\Delta t} = - C_i \quad \text{A.2.6.1.4}$$

$$F_i = \left(\frac{\Delta z_i}{\Delta t} + \frac{K_{\text{top},i}}{\delta X_{\text{top},i}} + \frac{K_{\text{bottom},i}}{\delta X_{\text{bottom},i}} + \frac{\text{LAD } \Delta z_i}{r_{b,i} + \alpha r_{s,i}} \right) \quad \text{A.2.6.1.4.a}$$

$$E_i = \frac{K_{\text{bottom},i}}{\delta X_{\text{bottom},i}} \quad \text{A.2.6.1.4.b}$$

$$G_i = \frac{K_{\text{top},i}}{\delta X_{\text{top},i}} \quad \text{A.2.6.1.4.c}$$

$$C_i = \frac{LAD \Delta z}{(r_s \alpha + r_b)} \frac{s r_s \alpha R_n}{\rho C_p} + \frac{\Delta z_i}{\Delta t} D_i^t \quad \text{A.2.6.1.4.d}$$

$$\begin{bmatrix} 1 & 0 & 0 & 0 & 0 & 0 \\ E_2 & -F_2 & G_2 & 0 & 0 & 0 \\ 0 & E_3 & -F_3 & G_3 & 0 & 0 \\ 0 & 0 & E_4 & -F_4 & G_4 & 0 \\ 0 & 0 & 0 & E_5 & -F_5 & G_5 \\ 0 & 0 & 0 & 0 & 0 & 1 \end{bmatrix} \begin{bmatrix} D_1 \\ D_2 \\ D_3 \\ D_4 \\ D_5 \\ D_6 \end{bmatrix} = \begin{bmatrix} D_{\text{first air layer}} \\ -C_2 \\ -C_3 \\ -C_4 \\ -C_5 \\ D_{\text{upper boundary}} \end{bmatrix} \quad \text{A.2.6.1.5}$$

$$\mathbf{A} \mathbf{D} = \mathbf{C} \quad \text{A.2.6.1.5.b}$$

$$\mathbf{A}^{-1} \mathbf{A} \mathbf{D} = \mathbf{A}^{-1} \mathbf{C}$$

$$\mathbf{D}_{\text{air,eq}} = \mathbf{A}^{-1} \mathbf{C} \quad \text{A.2.6.1.6}$$

The values of R_n are obtained by initially assuming isothermal condition i.e. the temperature of the leaves are equal to the air temperature which is assumed equal to the boundary above. These values will be updated after the solution of A.2.6.2.5.

2.6.1.b) The temperature of air for an n layered canopy (Penman-Monteith equation) for steady state solution.

In a similar manner to the derivation above for the vapour pressure deficit equation,

$$\Delta z \frac{\partial T_i}{\partial t} = \frac{K_{\text{top}}}{\delta X_{\text{top}}} (T_{i+1}^{t+\Delta t} - T_i^{t+\Delta t}) + \frac{K_{\text{bottom}}}{\delta X_{\text{bottom}}} (T_{i-1}^{t+\Delta t} - T_i^{t+\Delta t}) + \left(\frac{\gamma^* R_n - \rho C_p D r_b^{-1}}{s + \gamma^*} \right) LAD \Delta z \quad \text{A.2.6.2.1}$$

$$\frac{\Delta z}{\Delta t} (T_i^{t+\Delta t} - T_i^t) = \frac{K_{\text{top}}}{\delta X_{\text{top}}} (T_{i+1}^{t+\Delta t} - T_i^{t+\Delta t}) + \frac{K_{\text{bottom}}}{\delta X_{\text{bottom}}} (T_{i-1}^{t+\Delta t} - T_i^{t+\Delta t}) + \left(\frac{\gamma^* R_n - \rho C_p D r_b^{-1}}{s + \gamma^*} \right) LAD \Delta z \quad \text{A.2.6.2.2}$$

$$\begin{aligned} \frac{K_{\text{top}}}{\delta X_{\text{top}}} T_{i+1}^{t+\Delta t} - \left(\frac{\Delta z}{\Delta t} + \frac{K_{\text{top}}}{\delta X_{\text{top}}} + \frac{K_{\text{bottom}}}{\delta X_{\text{bottom}}} \right) T_i^{t+\Delta t} + \frac{K_{\text{bottom}}}{\delta X_{\text{bottom}}} T_{i-1}^{t+\Delta t} \\ = - \left(\frac{\gamma^* R_n - \rho C_p D r_b^{-1}}{s + \gamma^*} \right) LAD \Delta z - \frac{\Delta z}{\Delta t} T_i^t \end{aligned} \quad \text{A.2.6.2.3}$$

$$E_i T_{i-1}^{t+\Delta t} - F_i T_i^{t+\Delta t} + G_i T_{i+1}^{t+\Delta t} = -C_i \quad \text{A.2.6.2.4}$$

$$F_i = \left(\frac{\Delta z_i}{\Delta t} + \frac{K_{\text{top},i}}{\delta X_{\text{top},i}} + \frac{K_{\text{bottom},i}}{\delta X_{\text{bottom},i}} \right) \quad \text{A.2.6.2.4.a}$$

$$E_i = \frac{K_{\text{bottom},i}}{\delta X_{\text{bottom},i}} \quad \text{A.2.6.2.4.b}$$

$$G_i = \frac{K_{\text{top},i}}{\delta X_{\text{top},i}} \quad \text{A.2.6.2.4.b}$$

$$C_i = \left(\frac{\gamma^* R_n - \rho C_P D r_b^{-1}}{s + \gamma^*} \right) \text{LAD} \Delta z + \frac{\Delta z}{\Delta t} T_i^t \quad \text{A.2.6.2.4.c}$$

$$\begin{bmatrix} 1 & 0 & 0 & 0 & 0 & 0 \\ E_2 & -F_2 & G_2 & 0 & 0 & 0 \\ 0 & E_3 & -F_3 & G_3 & 0 & 0 \\ 0 & 0 & E_4 & -F_4 & G_4 & 0 \\ 0 & 0 & 0 & E_5 & -F_5 & G_5 \\ 0 & 0 & 0 & 0 & 0 & 1 \end{bmatrix} \cdot \begin{bmatrix} T_1 \\ T_2 \\ T_3 \\ T_4 \\ T_5 \\ T_6 \end{bmatrix} = \begin{bmatrix} T_{\text{first air layer}} \\ -C_2 \\ -C_3 \\ -C_4 \\ -C_5 \\ T_{\text{upper boundary}} \end{bmatrix}$$

A
T
=
C

A.2.6.2.5

$$\mathbf{A}^{-1} \mathbf{A} \mathbf{T} = \mathbf{A}^{-1} \mathbf{C}$$

$$\mathbf{T} = \mathbf{A}^{-1} \mathbf{C} \quad \text{A.2.6.2.6}$$

In the matrix C, the value of D in different layers are obtained from the solution of A.2.6.1. 6, so the temperature of air at equilibrium can be obtained, and the temperature of the leaves as a function of D by the use of Penman-Monteith equation.

2.6.1.c) The vapour pressure of air for an n layered canopy (Penman-Monteith equation) for steady state solution.

The derivation of this equation follows on the same line as the one for temperature. The terms will be the same except for the source term of latent heat.

$$\mathbf{A}^{-1} \mathbf{A} \mathbf{T} = \mathbf{A}^{-1} \mathbf{C}$$

$$\mathbf{T} = \mathbf{A}^{-1} \mathbf{C} \quad \text{A.2.6.2.a.5}$$

In this case, we solve the nonsteady temperature of the air equation, so $\Delta t \neq \infty$.

2.6.2.b) The vapour pressure of air for an n layered canopy for a non-steady state solution

$$\frac{\Delta z}{\Delta t} (e_i^{t+\Delta t} - e_i^t) = \frac{K_{\text{top}}}{\delta X_{\text{top}}} (e_{i+1}^{t+\Delta t} - e_i^{t+\Delta t}) + \frac{K_{\text{bottom}}}{\delta X_{\text{bottom}}} (e_{i-1}^{t+\Delta t} - e_i^{t+\Delta t}) + \left(\frac{e_s(T_i) - e_i}{(r_{bh} + r_s)} \right) \text{LAD } \Delta z \quad \text{A.2.6.2.b.1}$$

$$\begin{aligned} \frac{K_{\text{top}}}{\delta X_{\text{top}}} e_{i+1}^{t+\Delta t} - \left(\frac{\Delta z}{\Delta t} + \frac{K_{\text{top}}}{\delta X_{\text{top}}} + \frac{K_{\text{bottom}}}{\delta X_{\text{bottom}}} \right) e_i^{t+\Delta t} + \frac{K_{\text{bottom}}}{\delta X_{\text{bottom}}} e_{i-1}^{t+\Delta t} \\ = - \left(\frac{e_s(T_i) - e_i}{(r_{bh} + r_s)} \right) \text{LAD } \Delta z - \frac{\Delta z}{\Delta t} e_i^t \end{aligned} \quad \text{A.2.6.2.b.2}$$

$$E_i e_{i-1}^{t+\Delta t} - F_i e_i^{t+\Delta t} + G_i e_{i+1}^{t+\Delta t} = -C_i \quad \text{A.2.6.2.b.3}$$

$$F_i = \left(\frac{\Delta z_i}{\Delta t} + \frac{K_{\text{top},i}}{\delta X_{\text{top},i}} + \frac{K_{\text{bottom},i}}{\delta X_{\text{bottom},i}} + \frac{\text{LAD } \Delta z}{(r_{bh} + r_s)} \right) \quad \text{A.2.6.2.b.3.a}$$

or

$$F_i = \left(\frac{\Delta z_i}{\Delta t} + \frac{K_{\text{top},i}}{\delta X_{\text{top},i}} + \frac{K_{\text{bottom},i}}{\delta X_{\text{bottom},i}} \right)$$

$$E_i = \frac{K_{\text{bottom},i}}{\delta X_{\text{bottom},i}} \quad \text{A.2.6.2.b.3.b}$$

$$G_i = \frac{K_{\text{top},i}}{\delta X_{\text{top},i}} \quad \text{A.2.6.2.b.3.c}$$

$$C_i = \frac{e_s(T_i)}{(r_{bh} + r_s)} \text{LAD } \Delta z + \frac{\Delta z}{\Delta t} e_i^t \quad \text{A.2.6.2.b.3.d}$$

or

$$C_i = \left(\frac{e_s(T_i) - e_i^t}{(r_{bh} + r_s)} \right) \text{LAD } \Delta z + \frac{\Delta z}{\Delta t} e_i^t$$

$$\begin{bmatrix} 1 & 0 & 0 & 0 & 0 & 0 \\ E_2 & -F_2 & G_2 & 0 & 0 & 0 \\ 0 & E_3 & -F_3 & G_3 & 0 & 0 \\ 0 & 0 & E_4 & -F_4 & G_4 & 0 \\ 0 & 0 & 0 & E_5 & -F_5 & G_5 \\ 0 & 0 & 0 & 0 & 0 & 1 \end{bmatrix} \cdot \begin{bmatrix} e_1 \\ e_2 \\ e_3 \\ e_4 \\ e_5 \\ e_6 \end{bmatrix} = \begin{bmatrix} e_{\text{first soil layer}} \\ -C_2 \\ -C_3 \\ -C_4 \\ -C_5 \\ e_{\text{upper boundary}} \end{bmatrix}$$

A **e** **=** **C**

A.2.6.2.b.4

$$\mathbf{A}^{-1} \mathbf{A} \mathbf{e} = \mathbf{A}^{-1} \mathbf{C}$$

$$\mathbf{e} = \mathbf{A}^{-1} \mathbf{C}$$

A.2.6.2.b.5

In this system of equation, we need the leaf temperature which is equation A.2.1.1.3 and is solved explicitly.

$$T_l = T_{l,eq} (1 - e^{-\frac{t}{\tau_{l,T}}}) + T_{l,initial} e^{-\frac{t}{\tau_{l,T}}}$$

or solved by the use of eq.2.3.8 to eq.2.3.13. (this later solution was used in MATHCAD®)

2.7) The change in the equilibrium temperature of the leaves

Changes in $T_{l,eq}$ due to changes in R_s , R_L do occur, but we take account of them by updating the boundaries whenever a change is detected. $\Delta T_{l,eq}$ changes due to changes in the third, fourth, fifth (i.e due to coherent structures) are the ones considered here. For $\Delta W_m \leq 0$

$$\frac{1}{r_{bh}} T_a - \frac{1}{\gamma(r_{bv}+r_s)} (e_s(T_{air}) - e_a) + \frac{1}{\gamma(r_{bv}+r_s)} \frac{\partial e_s}{\partial T} T_{air} \leq 0 \quad \text{A.2.7.1}$$

$$- \frac{1}{\gamma(r_{bv}+r_s)} \Delta D + \left(\frac{\partial e_s}{\partial T} + \frac{1}{r_{bh}} \right) \Delta T_{air} \leq 0 \quad \text{A.2.7.2}$$

$$\left(\frac{\partial e_s}{\partial T} + \frac{\gamma(r_{bv}+r_s)}{r_{bh}} \right) * \Delta T_{air} \leq \Delta D \quad \text{A.2.7.3}$$

In case of $\Delta D \geq 0$ and $\Delta T_{air} > 0$ (i.e drier warmer air) or $D'' > 0$ and $T'' > 0$ (Quadrant I in fig 4.4). $\Delta D = D_2 - D_1$. D' is with respect to the total mean. We follow the changes of $T_{leaves,eq}$ with respect to the total mean.

$$\text{for } \Delta T_{le,eq} \leq 0 \text{ if } \left(\frac{\partial e_s}{\partial T} + \frac{\gamma(r_{bv}+r_s)}{r_{bh}} \right) \leq \frac{\Delta D}{\Delta T_{air}} \quad \text{Quadrant I in fig 4.3}$$

A.2.7.4

$$\text{for } \Delta T_{l,eq,total} \leq 0 \text{ if } \left(\frac{\partial e_s}{\partial T} + \frac{\gamma(r_{bv}+r_s)}{r_{bh}} \right) \leq \frac{D'}{T'_{air}}$$

A.2.7.5

In case $\Delta D \geq 0$ and $\Delta T_{air} \leq 0$ (i.e drier colder air) or $D'' > 0$ and $T'' \leq 0$ (i.e drier colder air). This represents Quadrant II in fig 4.3.

$$\Delta T_{le,eqli} \leq 0 \text{ if } \left(\frac{\partial e_s}{\partial T} + \frac{\gamma(r_{bv} + r_s)}{r_{bh}} \right) \geq \frac{\Delta D}{\Delta T_{air}} \quad \text{A.2.7.6}$$

$$\Delta T_{le,eqli, total} \leq 0 \text{ if } \left(\frac{\partial e_s}{\partial T} + \frac{\gamma(r_{bv} + r_s)}{r_{bh}} \right) \geq \frac{D'}{T'_{air}} \quad \text{A.2.7.7}$$

which is always true, since the left hand side is always positive. So, $\Delta T_{le,eqli} \leq 0$ is always negative.

In case of ΔD or D' is negative, for the latter in the final stages of buildup and ΔT_{air} or T' is positive. This represents quadrant IV in fig 4.3.

$$\Delta T_{le,eqli} \leq 0 \text{ if } \left(\frac{\partial e_s}{\partial T} + \frac{\gamma(r_{bv} + r_s)}{r_{bh}} \right) \leq \frac{\Delta D}{\Delta T_{air}} \quad \text{A.2.7.8}$$

$$\Delta T_{le,eqli, total} \leq 0 \text{ if } \left(\frac{\partial e_s}{\partial T} + \frac{\gamma(r_{bv} + r_s)}{r_{bh}} \right) \leq \frac{D'}{T'_{air}} \quad \text{A.2.7.9}$$

which can never be satisfied, which means $\Delta T_{le,eqli} \geq 0$ or $\Delta T_{le,eqli, total} \geq 0$

in case of ΔD or D' is negative, and ΔT_{air} or T' is negative. This represents quadrant III in fig 4.3

$$\Delta T_{le,eqli, total} \leq 0 \text{ if } \left(\frac{\partial e_s}{\partial T} + \frac{\gamma(r_{bv} + r_s)}{r_{bh}} \right) \geq \frac{D'}{T'_{air}} \quad \text{A.2.7.10}$$

$$\Delta T_{le,eqli} \leq 0 \text{ if } \left(\frac{\partial e_s}{\partial T} + \frac{\gamma(r_{bv} + r_s)}{r_{bh}} \right) \geq \frac{\Delta D}{\Delta T_{air}} \quad \text{A.2.7.11}$$

A. 2. 8) The fluxes from the leaves to the air (the sources)

The behaviour of the sources as function is given by the following equations:

1) The sensible heat source:

$$H(t)_{\text{leaves}} = \frac{\rho C_p}{r_{bh}} \left((T_{l,eq}(1 - e^{-\frac{t}{\tau_{T,a}}}) + T_{l,initial} e^{-\frac{t}{\tau_{T,a}}}) - (T_{air,eq}(1 - e^{-\frac{t}{\tau_T})} + T_{air,initial} e^{-\frac{t}{\tau_T}}) \right) \quad \text{A 2.8.1}$$

After and during the gust intrusion, the temperature of the air becomes equal to the temperature of air above. Since in this situation $\tau_{T,a}$ is very small, the $T_{air,initial}$ i.e the temperature of the air just before intrusion is completely replaced by the new $T_{air,eq}$ which is equal to the temperature of air above. So, the second term in the large brackets equals $T_{air,top}$ and the temperature of the leaves is equal to $T_{l,initial}$ which may be equal to the equilibrium temperature at the end of the previous cycle.

2) The latent heat source:

$$LE(t) = \frac{\rho C_p}{\gamma(r_{bv} + r_s)} \left(e_s(T_l) - (e_{air,eq}(1 - e^{-\frac{t}{\tau_{a,e}}}) + e_{initial} e^{-\frac{t}{\tau_{a,e}}}) \right) \quad \text{A.2.8.2.1}$$

$$LE(t) = \frac{\rho C_p}{\gamma(r_{bv} + r_s)} \left((e_s(T_a) - (e_{air,eq}(1 - e^{-\frac{t}{\tau_e}}) + e_{initial} e^{-\frac{t}{\tau_e}})) + \frac{\partial e_s}{\partial T_s} (T_s - T_a) \right) \quad \text{A.2.8.2.2}$$

$$LE_{gust} = \frac{\rho C_p}{\gamma(r_{bv} + r_s)} \left(D_{Top} + \frac{\partial e_s}{\partial T_{l, equilibrium}} (T_s - T_a) \right) \quad \text{A.2.8.2.3}$$

A. 2.9) The mean temperature, vapour pressure and vapour pressure deficit of the air

$$\bar{T} = T_{\text{top}} \frac{\Delta t_{\text{gust duration}}}{\text{period}} + T_{\text{air,eq}} \left(1 - \frac{\Delta t_{\text{gust duration}}}{\text{period}} - \frac{4 \tau_{a,T}}{\text{period}} \right) + T_{\text{average}} \frac{4 \tau_{a,T}}{\text{period}}$$

$$T_{\text{average}} = \frac{\text{period}}{4 \tau_{a,T}} \int_{\Delta t_{\text{gust duration}}}^{\Delta t_{\text{gust duration}} + \frac{4 \tau_{a,T}}{\text{period}}} T_{\text{air}} dt$$

$$\bar{e} = e_{\text{top}} \frac{\Delta t_{\text{gust duration}}}{\text{period}} + e_{\text{air,eq}} \left(1 - \frac{\Delta t_{\text{gust duration}}}{\text{period}} - \frac{4 \tau_{a,e}}{\text{period}} \right) + e_{\text{average}} \frac{4 \tau_{a,e}}{\text{period}}$$

$$e_{\text{average}} = \frac{\text{period}}{4 \tau_{a,e}} \int_{\Delta t_{\text{gust duration}}}^{\Delta t_{\text{gust duration}} + \frac{4 \tau_{a,e}}{\text{period}}} e_{\text{air}} dt$$

$$\bar{D} = D_{\text{top}} \frac{\Delta t_{\text{gust duration}}}{\text{period}} + D_{\text{equilibrium}} \left(1 - \frac{\Delta t_{\text{gust duration}}}{\text{period}} - \frac{4 \tau_{a,D}}{\text{period}} \right) + D_{\text{average}} \frac{4 \tau_{a,D}}{\text{period}}$$

A.2.11) Discretization of the transport equations:

The implicitly discretized equation reads as

$$\rho C_p \Delta z \frac{\Theta_j^{t+\Delta t} - \Theta_j^t}{\Delta t} = \rho C_p \frac{K_{top}}{dz_{top}} \left(\Theta_{j+1}^{t+\Delta t} - \Theta_j^{t+\Delta t} \right) - \rho C_p \frac{K_{bottom}}{dz_{bottom}} \left(\Theta_j^{t+\Delta t} - \Theta_{j-1}^{t+\Delta t} \right) + S_h \quad (4.8)$$

which leads to

$$\rho C_p \left(\frac{\Delta z}{\Delta t} + \frac{K_{top}}{dz_{top}} + \frac{K_{bottom}}{dz_{bottom}} \right) \Theta_j^{t+\Delta t} = \rho C_p \frac{K_{top}}{dz_{top}} \Theta_{j+1}^{t+\Delta t} + \rho C_p \frac{K_{bottom}}{dz_{bottom}} \Theta_{j-1}^{t+\Delta t} + S_h^t + \rho C_p \Theta_j^t \frac{\Delta z}{\Delta t} \quad (4.9)$$

where dz stands for the vertical distance between two node points. The subscript denotes an upper or lower neighbouring point. Δz is the thickness of layer J in m . S_h is the source term in $W m^{-2}$. The superscript denotes the time level.

APPENDIX 3 : (List Of Symbols)

Symbol	Quantity	units
A	Event A/ Area of the leaf (one side)/ Area of the soil surface/ Area available for diffusion within a cross section of the soil. <i>Subscripts:</i>	(-) m ² m ² m ²
A _r , A _h , A _l	Areas for energy exchange subscript radiative, sensible heat and latent heat respectively.	m ²
A _a	Apparent area available for diffusion.	m ²
A _e	Actual area available for diffusion	m ²
A _{porosity}	Total porosity projected in a cross section perpendicular to the direction of the flux	(-)
A _{airfilled}	Air filled porosity projected in a cross section perpendicular to the direction of the flux.	(-)
A	Coupling coefficients matrix <i>subscripts:</i>	
A _{gust}	The coupling coefficient matrix determined according to the gust parameterization of K _m values.	
A _{nogust}	The coupling coefficient matrix determined according to the no-gust parameterization of K _m values.	
A _{ij}	Element of the coupling coefficient matrix.	ms ⁻¹
A _{gust,ij}	Element of A _{gust} matrix.	
A _{nogust,ij}	Element of A _{nogust} matrix.	
A ⁻¹	Inverse of coupling coefficients matrix	
B	Event B	
b _n	The coefficient of an Eigen function expansion of the soil temperature function for a certain wave number n.	K or °C
b _n (0)	The initial value of the coefficient of an Eigen function expansion of the soil temperature.	
b _n (t)	The values of the coefficient of an Eigen function expansion of the soil temperature as a function of time.	
C	Concentration of a scalar quantity/ Capacitance of the plant tissue for water/ Capacitance of the leaf for water vapour <i>superscripts:</i>	
C'	Deviation of a concentration from its time mean.	
C ^l	Deviations of a concentration from its time mean or ensemble mean due to large scale fluctuations.	
C ^s	deviations of a concentration from its time mean or ensemble mean due to small scale <i>subscripts:</i>	
C _l	arbitrary constant.	(-)
C _H	lateral heat conduction between neighbouring spots on the same side of the leaf.	
C(z,t)	Concentration as function of height and time.	
C _c (z,t;h,t-s)	Conditional probability density function for a unit source.	(-)

C_p	specific heat capacity of the air (constant pressure)	$J\text{ kg}^{-1}\text{K}^{-1}$
C_l	specific heat capacity of the leaf	$J\text{ kg}^{-1}\text{K}^{-1}$
C_s	specific heat capacity of the bulk soil.	$J\text{ kg}^{-1}\text{K}^{-1}$
C	Constant coefficients matrix for the canopy air system: There are five of these: Three for the approximate form Two for the more exact form. <i>Subscripts:</i>	
C_j	Element of the C column vector.	
$\text{Conduhl}_{\text{leaves, i,l,x,y}}$	Horizontal heat conduction in leaf layer i, on side l with wetness condition x,y	
$\text{CUMLAI}(J)$	cumulative leaf area in the layers above layer J in m^2 leaf \cdot m^{-2} soil. (-) (one side).	
D	vapour pressure deficit i.e. $(e_s(T_{\text{air}}) - e_{\text{air}})$ / Diffusivity for water vapour/ Diameter of water drops. <i>subscripts:</i>	Pa m^2s^{-1} m
\bar{D}	Mean vapour pressure deficit of the air.	Pa
D'	Vapour pressure deficit deviation from the mean (i.e. fluctuations) due to small scale turbulence.	Pa
D''	Vapour pressure deficit deviation from the mean (i.e. fluctuations) due to large scale structures.	Pa
D_1	The sum of mean and small scale fluctuations	Pa
D_{air}	Vapour pressure deficit of the air.	Pa
$D_{\text{air,eq}}$	Equilibrium vapour pressure deficit of the air.	Pa
D_i	Air vapour pressure deficit at a certain layer	Pa
D_{initial}	Initial air vapour pressure deficit just after the gust intrusion.	Pa
$D_{\text{top}}, D_{\text{average}}$	Vapour pressure deficit at about twice the canopy height and the average one during the build-up period respectively.	Pa
D^c	Change of vapour pressure deficit within one time step.	
D_{vapour}	Water vapour diffusivity	m^2s^{-1}
d	Leaf thickness/ Condition of dryness.	m
d_j	Probability of being intercepted for diffuse radiation by the leaf elements in a certain layer.	(-)
D	Vapour pressure deficit matrix (Unknown). <i>subscripts:</i>	Pa
$D_{\text{air,eq}}$	A column vector containing the values of the equilibrium vapour pressure deficit at different layers.	Pa
D_{ini}	A column vector containing the values of the initial vapour pressure deficit.	Pa
$\bar{D}_{\text{gust model}}$	A column vector containing the time averaged values of the vapour pressure deficit determined according to the gust model.	Pa
$\bar{D}_{\text{gust model},i}$	An element of $\bar{D}_{\text{gust model}}$ matrix.	Pa
ds	change of time since release/ surface element bounding a volume.	s m^2
dU	volume element.	m^3
$dz(j)$	thickness of the layer	m
E	evaporation.	$\text{kg m}^{-2}\text{s}^{-1}$
E_{equ}	Equilibrium evaporation	
E_j	Lower turbulent transport coupling coefficient	ms^{-1}

c	internal energy/ extensive quantity/ Vapour pressure <i>Subscripts:</i>	Jm^{-3} Pa
e_2, e_1	vapour pressure at height 2 and 1 respectively.	Pa
e_a, e_{air}	air vapour pressure	Pa
e_{initial}	initial vapour pressure of the air.	
e_i, e_{i+1}, e_{i-1}	vapour pressure of the air at layer $i, i+1$ and $i-1$ respectively.	Pa
e_j	Vapour pressure of the air in layer J .	Pa
e_{air, e_q}	Equilibrium vapour pressure of the air	Pa
$e_{\text{air}, \text{top}}$	vapour pressure high above the canopy top.	Pa
$e_s(T_{\text{air}}), e_s(T_1)$	saturated vapour pressure at T_{air}, T_1 respectively.	Pa
$e_s(T_{\text{leaves}, J})$	Saturated vapour pressure at the mean leaf temperature.	Pa
e	Vapour pressure matrix	Pa
F_i	The layer coefficient	ms^{-1}
f^{-1}	Inverse of gust frequency intrusion into plant canopy.	s
$\overline{f(X)}$	function of the mean variable x .	
$\overline{f(x)}$	mean function of the variable x .	
$f(t)$	function of time.	
$f(L, t)$	The forcing function for radiative and non-radiative energy at the soil surface as a function of time.	Wm^{-2}
$f_1(L, t), f_1$	The radiative forcing at the soil surface as a function of time.	Wm^{-2}
$f_2(L, t), f_2$	The non-radiative forcing at the soil surface as a function of time.	Wm^{-2}
f_b	fraction beam of the short wave radiation at the upper boundary of the canopy.	(-)
Fr	Froude number.	(-)
$f_{\text{upper}, f_{\text{upper}e}}$	The weighing coefficient for the layer $i+1$ in determining the temperature and vapour pressure of layer i respectively.	(-)
$f_{\text{lower}, f_{\text{lower}e}}$	The weighing coefficient for the layer $i-1$ in determining the temperature and vapour pressure of layer i .	(-)
$f_{\text{layer}, f_{\text{layer}e}}$	The weighing coefficient for the leaf elements in a certain layer in determining the layer temperature and vapour pressure respectively.	(-)
G	Soil heat flux.	Wm^{-2}
G_i	Turbulent transport coupling with the upper layer	ms^{-1}
G_{jkl}	Tensorial quantity.	
g	Gravitational acceleration.	m^2s^{-1}
$g(x)$	Initial soil temperature profile.	
H	Sensible heat flux from the leaf to the air per unit leaf surface (one side).	Wm^{-2}
h	Canopy height/ distance shift/ height of release of a source.	m m m
h_m	Matric head.	(m)
I	layer number/ probability.	(-) (-)
$I!$	factorial I .	(-)

$I_{i,k}$	The probability of radiation incident from a direction i being intercepted by leaves with a surface perpendicular to direction k .	(-)
$I_b(J)$	probability that an incident direct radiation <u>will not</u> be intercepted by the leaf elements of layer J.	
$IBBJ$	The cumulative probability that a direct beam <u>will not</u> be intercepted by the leaf elements above Layer J.	(-)
I_d	The probability that an incident radiation (diffuse) will not be intercepted by the leaf elements of layer J.	(-)
	or	
	The probability that an incident radiation from direction i <u>will not</u> be intercepted by the leaf elements of layer J which has a surface with a normal of direction k .	(-)
$I_{d\text{long},J}$	Probability that long wave incident radiation <u>will not</u> be intercepted by the elements of layer J.	(-)
J	Layer number/	(-)
	Total saturation heat flux/	Wm^{-2}
J_v	Vapour flux	Wm^{-2}
J_s	Entropy flux	$Wm^{-2}K^{-1}$
J_{wi}	Mass flux of water flux in its different states	
J'_i	The change of saturation heat flux due to a contribution of a certain layer.	Wm^{-2}
K	Soil hydraulic conductivity/	ms^{-1}
	General turbulent transport coefficient/	m^2s^{-1}
	Extinction coefficient for light/	(-)
	coefficients for air layers and leaf equations	s^{-1}
	<i>Subscripts:</i>	
K_{av} ,	Average extinction coefficients	(-)
$K_{ex,i,\beta}$	Extinction coefficients for leaf angle class i and zone of the sky β .	
K	coefficient for equation.	(-)
	<i>subscripts:</i>	
$K_{l,T}, K_{a,e}, K_{a,T}, K_D$	coefficient for leaf temperature, air vapour pressure and air temperature air vapour pressure deficit respectively.	s^{-1}
K_s	Spherical extinction coefficient/	(-)
	Saturated hydraulic conductivity.	ms^{-1}
K_m	General turbulent transport coefficient/	m^2s^{-1}
	Turbulent transport for momentum.	
K_h	Turbulent transport for sensible heat.	m^2s^{-1}
K_e	Turbulent transport for latent heat.	
K_{top}, K_{bottom}	Turbulent transport coefficients for heat at the top and bottom of an air layer.	m^2s^{-1}
k_u	Molecular diffusivity for momentum.	m^2s^{-1}
k_c	Molecular diffusivity for a scalar c .	m^2s^{-1}
L	Obkhouv length/	m
	characteristic length/	m
	coefficients of the phenomenological equations	

	Length of the soil column from zero to the top of the soil.	m
L(z,t)	Longwave radiation loading as function of height and time.	Wm ⁻²
L _{kj}	A coefficient expressing the effect of the a conjugate force j on the flux of k.(has the units of Flux/conjugate force)	
L _s (z,t)	short wave radiation loading as function of height and time.	Wm ⁻²
LADMID	Leaf area density in the middle of the layer (one side)	(m ⁻¹)
LAI	Lea Area Index (m ² leaf area one side/ m ² Soil)	(-)
	Leaf area increments	(-)
	<i>subscript :</i>	
LAI _k	Leaf area increment with surface perpendicular to direction k.	(-)
LE	Latent heat flux from the leaves to the air.	Wm ⁻²
Ma	Mach Number.	(-)
MAX	A function for the selecting the maximum value out of two numbers.	
n	number of drops per m ⁻² on the upper and lower surface of the leaf/ property under averaging/ frequency./	m ⁻² (-) Hz
n	direction of vector normal to the surface.	
n̄	deviations of the quantity from its mean.	
P	static air pressure	
P(A)	Probability of event A occurring.	(-)
PAI	Plant area Index m ² (leaf + stem area)/m ² soil..	(-)
Pr	probability of occurrence for a certain combination of leaf wetness.	(-)
Pyx	Stress along surface	
Period	period between two consecutive gust intrusions	s
Q(x,t)	Heat sources within the soil	Ks ⁻¹
Q̇	Heat generation due to radiation absorption or chemical reactions.	
q	a Scalar quantity	
q	Heat or scalar flux	
q _i , q _{i+1}	heat flux at the lower boundary and upper boundary of the layer (i) respectively.	Wm ⁻²
q̄	deviations of a scalar quantity from its time mean.	
q _h	sensible heat flux.	
q _{le}	Latent heat flux	
Q _{∑_{i=1}ⁿ i}	flux at a certain boundary between layers which results from the superposition of components fluxes due to the fluxes resulting from plumes with different life times.	
Q̄ _{i+1}	Mean flux at the upper boundary of a layer.	
R	reflected radiation	
	<i>subscripts:</i>	
R _a , R _d , R _s	Absorbed radiation, diffusely reflected and specularly reflected radiation.	(-)
or		
R	Radiation flux density for unit ground surface.	W m ⁻²
	<i>subscripts:</i>	

$R_{\text{abs,total}}$	Total absorbed (short+long) wave radiation within layer J.	Wm^{-2}
$R_{\text{down}, J}$	Down welling long wave radiation flux density at a layer J upper boundary.	
$R_{\text{up}, J}$	Up welling long wave radiation flux density at a layer J upper boundary.	
$R_{\text{abs}, J}$, or $R_{\text{long, absorbed}}$	Absorbed long wave radiation in layer J.	
$R_{\text{Lx}, j}$	Thick layer reflection coefficient for layer j	(-)
$R_{\text{L}} \uparrow$	Long wave radiation leaving a surface	Wm^{-2}
$R_{\text{L}} \downarrow$	Long wave radiation falling on a surface	Wm^{-2}
$R_{\text{x}, t}$	Total incoming radiation flux density at the canopy top of wave band x.	Wm^{-2}
$R_{\text{x}} \downarrow$	down ward radiation flux density.	
$R_{\text{x}} \uparrow$	upward radiation flux density.	Wm^{-2}
$R_{\text{x}, j} \downarrow$	down welling radiation flux density in wave band X at a layer J upper boundary.	Wm^{-2}
$R_{\text{x}, j} \uparrow$	up welling radiation flux density in wave band X at a layer J upper boundary.	Wm^{-2}
R_{n}	Net radiation.	Wm^{-2}
$R_{\text{n}, i}$	Net radiation for a certain layer.	Wm^{-2}
$R_{\text{s}} \downarrow$	Short wave radiation falling on a surface.	Wm^{-2}
$R_{\text{s}} \uparrow$	short wave radiation reflecting from a surface.	Wm^{-2}
R_{short}	Short wave radiation at the canopy top.	
r	resistance/ radius of water drops on the leaf surfaces.	sm^{-1} m
r_1, r_2	Characteristic radius of drops on the lower and upper surface respectively.	m
$r_{\text{bh}}, r_{\text{bv}}, r_{\text{s}}, r_{\text{R}}$	boundary layer resistances for heat, vapour, stomatal resistances and radiative resistance respectively	sm^{-1}
$r_{\text{bv}, j}$	boundary layer resistance for vapour of the leaves in layer j.	sm^{-1}
$r_{\text{bv}, \text{soil}}$	boundary layer resistance for the soil clods	sm^{-1}
$r_{\text{bh}, J}$	boundary layer resistance for heat of the leaves in layer j	sm^{-1}
$r_{\text{leaf}, v, j}$	resistance of the leaves for vapour transfer in layer j.	
r_{local}	turbulent resistance to scalar transport due to local transport.	sm^{-1}
r_{gust}	turbulent resistance to scalar transport due to the gust process.	sm^{-1}
r_{H}	Heat resistance, as defined in Penman-Monteith equation.	sm^{-1}
$r_{\text{s}, s}$	Soil surface resistance to evaporation.	
S	Source strength in a conservation equation/	Wm^{-3} $\text{Kg m}^{-3}\text{s}^{-1}$
S	surface of a leaf or a volume to be averaged/	
S	Volume size or number of ensembles/ number of time intervals used in the averaging/ Relative saturation of the soil/ Storage of heat or mass.	(-)

	<i>subscripts:</i>	
S_0	The chosen volume or number of ensembles or length of time interval.	
S_h, S_e	Sensible heat and latent heat source respectively.	Wm^{-2}
$S(h)$	Source distribution as a function of height.	Wm^{-2}
s	Slope of the saturated vapour pressure as a function of temperature.	$Pa K^{-1}$
T	Temperature	$K, ^\circ C.$
\bar{T}	<i>subscripts :</i> Mean air temperature.	
T_2, T_1	Air temperature at height 2 and 1 respectively.	$^\circ C$
T_a, T_{air}	Air temperature.	$^\circ C$
$T_{air,in}$	Incoming air	
$T_{air,out}$	Outgoing air (ejected air due to gust process)	
$T_{air,J}$	Air temperature at layer J.	$^\circ C$
$\bar{T}_{air,J}$	Mean air temperature at layer J.	$^\circ C$
$T_{air,rad}$	Radiative temperature of the air.	$^\circ C$
$T_{air,rad,a}$	Absolute radiative temperature of the air	K
$T_{air, initial}$	Air temperature just before the gust intrusion or just at the beginning of the quiescence period or at the beginning of each time step.	$^\circ C$ $^\circ C$
$T_{air,top}$	Air temperature high above the canopy top.	$^\circ C$
$T_{l,eq}, T_{air,eq}$	Equilibrium temperature of the leaf and equilibrium temperature of the air respectively.	$^\circ C$
$T_l, T_{leaves,J}$	leaf temperature, or leaf temperature at layer J	$^\circ C$
$\bar{T}_{leaves,J}$	Mean leaf temperature at layer J.	$^\circ C$
T_{leaf}	Absolute leaf temperature	K
$\bar{T}_{leaf,J}$	Mean absolute leaf temperature at layer J.	K
$T_{l,initial}$	Initial temperature of the leaf just after the gust passage or at the beginning of each time step.	$^\circ C$
T_i, T_{i-1}, T_{i+1}	Air temperature at i, i - 1, i+1 layer number.	$^\circ C$
$T_{upper boundary}$	Air temperature at the upper boundary.	$^\circ C$
$T_{first soil layer}$	Temperature of the first soil layer.	$^\circ C$
T_a'	Air temperature deviations from the mean (i.e. fluctuations) due to small scale turbulence.	$^\circ C$
T_a''	Air temperature deviations from the mean (i.e. fluctuations) due to large scale structures.	$^\circ C$
T_L	Lagrangian integral time scale.	s
T_s	Instantaneous surface temperature/ Soil temperature	$^\circ C$ $^\circ C$
T_{dry}	temperature of dry segment of the leaf.	$^\circ C$
T_{wet}	Temperature of wet segment of the leaf.	$^\circ C$
T^c	change of temperature within one time step.	$^\circ C$
$T_l^{t+\Delta t}$	temperature of the leaf at time step $t+\Delta t$.	
T	Temperature of the air matrix (Unknown).	
\bar{T}_{nogust}	<i>subscripts:</i> Matrix containing the average temperature of the air determined according to the no-gust approach.	

$\bar{T}_{\text{gust model}}$	Matrix containing the average temperature of the air determined according to the gust approach.	
$\bar{T}_{\text{nogust model},i}$	The average temperature at layer i determined according to no-gust approach.	
$\bar{T}_{\text{gust model},i}$	The average temperature at layer i determined according to gust approach.	
$T_{\text{ini},i}$	initial temperature at layer i, just after the occurrence of the gust or at the beginning of each time step.	
thickness	leaf thickness.	m
$T_{\text{transx},j}$	Thick layer transmission coefficient for radiation of wave band x. for layer j.	(-)
t	time.	s
t_0, t_1	release time, current time, the difference between them represents the travel time.	s
$U(z)$	Mean wind velocity as function of height (z)	ms^{-1}
U^*	friction velocity.	ms^{-1}
u	Instantaneous wind velocity in direction x. <i>Subscripts</i>	ms^{-1}
u_i, \bar{u}_i, u_i'	instantaneous, mean, deviations of the instantaneous wind velocity from its time mean along direction i	ms^{-1}
u_i^l	deviations due to large scale turbulence.	ms^{-1}
u_i^s	deviations due to small scale turbulence.	ms^{-1}
$\langle \bar{u}_i \rangle, \langle \bar{u}_j \rangle$	volume average of an ensemble mean or the volume average of a time mean for u_i and u_j respectively.	
u_i''	The deviation of a time mean from its volume average or the deviation of an ensemble mean from its control volume average.	
W	wetness condition.	
w	Vertical wind velocity.	ms^{-1}
w'	turbulent vertical wind velocity fluctuations.	ms^{-1}
x	centroid of the averaging domain/ distance along the soil column (positive upwards) and has a zero value at a depth where no flux boundary condition applies/	m
X	Conjugate force	
X_W	Conjugate force for water flux	
X_T	Conjugate force for heat flux	
\bar{x}	average of a certain variable x	
z	height	m
V	leaf volume/	m^3

Soil bulk volume m^3
 wind speed in m seconds. ms^{-1}
 Volume of averaging.

Operators:

$\langle \langle \rangle \rangle$ Spatial averaging
 $\overline{(\)}^{ens}$ ensemble averaging.
 $(\)'$ time deviation or ensemble deviation.
 $(\)''$ spatial deviation

Greek Symbols:

α $\gamma/(\gamma + s)$ (-)
 or the ratio between K_m values for a gust and no-gust model/ (-)
 Coefficient alpha in Van Genuchten model/ m^{-1}
 Air filled porosity of the soil (-)

α_r absorption coefficient for short wave radiation (-)

α_L Radiative and convective heat transfer coefficient $Wm^{-2} K^{-1}$

b inclination of the sun in radians/ rad
 Bowen Ratio (sensible/ latent heat flux)/ (-)
 phenomenological enhancement diffusion coefficient for water vapour/ (-)
 thermal conductivity of the soil $Wm^{-1}K^{-1}$

β_L thermal conductivity at the soil surface. $Wm^{-1}K^{-1}$
 δz vertical distance between the centres of the uppermost soil layer and the layer below it. m

δ_{ij} Kronecker Delta
 $\delta x_{top}, \delta x_{bottom}$ distance between the centre of the layer and the centre of the layer at the top and bottom of this layer. m

ΔZ thickness of the air layer m
 Δ Change of a certain variable
 Δt time step. s
 g psychometric constant $Pa K^{-1}$
 g^* modified psychometric constant $Pa K^{-1}$
 κ Thermal diffusivity of the soil. m^2s^{-1}
 θ volumetric moisture content/ (-)
 Virtual air temperature.

τ_x leaf transmittance of the foliage elements for radiation of wave band x. (-)

$\tau_{l,T}, \tau_{a,T}, \tau_{a,e}, \tau_{a,D}$ leaf thermal time constant, time constants of air temperature, air vapour pressure, and air vapour pressure deficit respectively. s

λ Latent heat of vapourization/ Jkg^{-1}
 Heat conductivity coefficient of the soil or of the leaf./ $Wm^{-1}K^{-1}$
 Eigen value

λ_n Eigenvalue for a certain wave number n

μ dynamic viscosity $kg m^{-1}s^{-1}$
 ρ_x The leaf reflection of the foliage elements for radiation of (-)

	waveband x	
ρ	density of dry air.	kg m^{-3}
ρ_s	density of the leaf material/ bulk density of the soil	kg m^{-3}
$\phi_{i,k}$	the angle between the directions of the incident beam i and the leaf normal k .	rad
ϕ	energy dissipation.	
ϕ_n	Eigen function for a certain wave number n	
Φ	Total porosity.	(-)
ϵ	leaf emissivity (assumed 1.0).	(-)
ϵ_{ijk}	Alternating unit tensor.	
τ_L	Lagrangian integral time scale	s
ν	Kinematic viscosity	m^2s^{-1}
ν_c	molecular diffusivity for a scalar c .	m^2s^{-1}
σ	Stephan-Boltzmann constant (5.67 E-8)	$\text{Wm}^{-2}\text{K}^{-4}$
σ	Entropy production.	$\text{Jm}^{-3}\text{K}^{-1}\text{s}^{-1}$
σ_w	Standard deviation of vertical velocity	ms^{-1}
τ_{ij}	Shear stress	$\text{k}356\text{g m}^{-1}\text{s}^{-1}$.
τ	time since a certain time reference.	s
κ	Soil thermal diffusivity.	m^2s^{-1}

List of Symbols used in MATHCAD @:

i	number of layers.	(-)
j	number of time steps.	(-)
m	number of layers and two boundaries.	(-)
mm	number of time step	
Coeff	The ratio between K_m for a gust and no-gust model.	(-)
$culmlai$	cumulative leaf area density	(-)
$D_{airi,30}$	Vapour pressure deficit of the air at different layers at time step 30.	Pa
D_{meani}	Mean vapour pressure deficit at different heights.	Pa
$delTleqi$	Change in the equilibrium leaf temperature due to the changes in air temperature and vapour pressure within one time step.	
$delTleqiTair$	Change in the equilibrium leaf temperature due to air temperature change within one time step.	
$delTleqiDair$	Change in the equilibrium leaf temperature due to air vapour pressure deficit change within one time step.	
dt	time step of simulation.	s
dzi	Thickness of different canopy layers.	
$eair_{m,j}$	Vapour pressure of the air at different layers m and time steps j (a matrix).	Pa
$eaireqli_{,30}$	equilibrium vapour pressure of the air at different layers at time step 30.	Pa
$Eairmean_i$	Mean vapour pressure of the air.	Pa
$eairtop$	The vapour pressure at the canopy top (upper boundary).	Pa
f_{topti}	The weighing coefficient for the layer $i+1$ in determining the temperature of layer i .	
f_{tope}	The weighing coefficient for the layer $i+1$ in determining the vapour pressure of layer i .	
f_{lowert}	The weighing coefficient for the layer $i-1$ in determining the temperature of layer i .	

f_{lowerc}	The weighing coefficient for the layer $i-1$ in determining the vapour pressure of layer i .	
f_{layert}	The weighing coefficient for the leaf elements in a certain layer in determining the layer temperature.	
f_{layere}	The weighing coefficient for the leaf elements in a certain layer in determining the layer vapour pressure.	
k_{loweri}	Turbulent transport between a layer i and the layer below it.	m^2s^{-1}
k_{topi}	Turbulent transport between a layer i and the layer above it.	m^2s^{-1}
Lad_i	Leaf area density for different layers.	m^{-1}
Leavesfsh	Sensible heat sources within the canopy.	Wm^{-2}
Leaveslh	Latent heat sources within the canopy.	Wm^{-2}
Mean_caireq $_i$	Mean equilibrium vapour pressure of the air.	Pa
Mean_Taireq $_i$	Mean equilibrium temperature of the air	$0C$
Mean_Tleaves $_i$	Mean temperature of the leaves at different layers	$0C$
Mean_Tleaves_eq $_i$	Mean equilibrium temperature of the leaves.	$0C$
Rshort	Short wave radiation load (one side of the leaf).	Wm^{-2}
rbh $_m$	boundary layer resistance for heat at different layers.	sm^{-1}
rbhs	Boundary layer resistance for soil.	sm^{-1}
rsm	Stomatal resistance for different layers.	sm^{-1}
rss	Soil surface resistance for evaporation.	sm^{-1}
Tairmean $_j$	Mean temperature of the air.	$0C$
Tairrad	Radiative temperature of the air.	$0C$
Tairtop	Temperature of the air at the canopy top (upper boundary).	$0C$
Tair $_{m,j}$	Temperature of the air at different heights m and time steps j (a matrix).	$0C$
Tair $_{0,0}$	initial value at soil surface at the beginning of the simulation.	
Tlin $_i$	Initial temperature of the leaves at layer i .	$0C$
Tleaves $_{i,j}$	Temperature of the leaves at different layers i and different time steps (a matrix).	$0C$
Thick	Leaf thickness.	m
Total_load	Total short wave radiation load.	Wm^{-2}
Tsoil	Temperature of the soil (constant during the simulation).	$0C$
Tleaveseq $_{i,30}$	equilibrium temperature of the leaves at different layers at time step 30.	$0C$
Taireq $_{i,30}$	equilibrium temperature of the air at different layers at time step 30.	$0C$

Acronyms

357357

NIR

Near Infrared Radiation

UOC

Uniform overcast sky

i730contribution

The contribution of a certain class of events to the total vertical velocity variance with experiment 730o for J.V. B. Boxel. (scaled)

i730ocount

i1888contribution

The contribution of a certain class of events to the total vertical velocity variance with experiment 18888si for W.A.J. van Pul. (scaled)

i1888count

Number of of events within with experiment 18888si for W.A.J. van Pul (scaled)

relato730o

relative strength of classes of events with 730o experiment

relat18888si

relative strength classes of events with 18888si experiment

860730oRn 4.0

Experiment of Van Boxed inwhich Rn at 4.0 m was measured in 30-7-1986

Appendix 3:

```

*                               Input file for the validation run.
229
232
52.0
0.5 0.25
0.48 0.29 0.5
0.5
0.25
0
0
0
1
22.0 23.0
38.0
0.77 0.82
0.27 0.27
0.0
24 35 -23
1.0
1
24
0.0
0.0001 0.0002
0.5 1.364 1.764           !has been changed
1.7
3.0E4
1.2E-7
12.
0.0007
0.05
-2.40 0.03 0.65 0.00 0.029 -0.1 0.00 1.044e-5 1E-5      !layer C
-2.00 0.03 0.65 0.00 0.029 -0.1 0.00 1.044e-5 1E-5
-1.75 0.03 0.65 0.00 0.029 -0.1 0.00 1.044e-5 1E-5
-1.50 0.03 0.65 0.00 0.029 -0.1 0.00 1.044e-5 1E-5
-1.20 0.03 0.65 0.00 0.029 -0.1 0.00 1.044e-5 1E-5
-1.00 0.03 0.65 0.00 0.029 -0.1 0.00 1.044e-5 1E-5
-0.80 0.03 0.65 0.00 0.029 -0.1 0.00 1.044e-5 1E-5
-0.70 0.03 0.65 0.00 0.029 -0.1 0.00 1.044e-5 1E-5
-0.65 0.03 0.65 0.00 0.029 -0.1 0.00 1.044E-5 1E-5      !layer B3
-0.55 0.03 0.54 0.03 0.098 -0.1 0.00 1.45E-5 1E-5
-0.50 0.03 0.54 0.03 0.098 -0.1 0.00 1.45E-5 1E-5
-0.40 0.03 0.54 0.03 0.098 -0.1 0.00 1.45E-5 1E-5      !layer B2
-0.35 0.03 0.53 0.04 0.19 -0.1 0.00 3.7E-6 1E-5
-0.25 0.03 0.53 0.04 0.19 -0.1 0.00 3.7E-6 1E-5
-0.20 0.03 0.53 0.04 0.19 -0.1 0.00 3.7E-6 1E-5      !layer A1
-0.15 0.03 0.53 0.04 0.19 -0.1 0.00 3.7E-6 1E-5
-0.12 0.03 0.53 0.04 0.19 -0.1 0.00 3.7E-6 1E-5
-0.10 0.03 0.53 0.04 0.19 -0.1 0.00 3.7E-6 1E-5
-0.08 0.03 0.53 0.04 0.19 -0.1 0.00 3.7E-6 1E-5
-0.05 0.03 0.53 0.04 0.19 -0.1 0.00 3.7e-6 1E-5
-0.03 0.03 0.53 0.04 0.19 -0.1 0.00 3.7E-6 1E-5
-0.02 0.03 0.53 0.04 0.19 -0.1 0.00 3.7e-6 1E-5
-0.01 0.03 0.53 0.04 0.19 -0.1 0.00 3.7E-6 1E-5
0.00 0.03 0.53 0.04 0.19 -0.1 0.00 3.7E-6 1E-5
0.00 0.0 2
0.01 0.012 2
0.04 0.47 2
0.05 0.06 2
0.10 0.12 2
0.20 0.23 2
0.30 0.62 2
0.40 1.07 2
0.50 1.53 2
0.65 2.25 2
0.70 2.33 2
0.80 2.51 2
0.85 2.60 2
0.90 2.69 2
0.95 2.79 2
1.00 2.87 2
1.10 3.06 2
1.25 2.89 2

```


Summary

The aim of the work is to describe heat and mass transfer between the soil, the plant canopy and the layer of air close above. This transfer has a very intermittent nature, due to the existence of large scale coherent structures in the layer of air close above the canopy. The periodic passage of these coherent structures at the canopy top and their large length scale with respect to the canopy height, lead to the refreshment of the air within the canopy with fresh air from far well above the canopy. This makes the coherent structures responsible for a dominant fraction of heat and mass exchange between the canopy air and the layer of air close above. Coherent structures are also responsible for a large fraction of momentum exchange between the canopy air layer and the layer of air close above. There is a gap of knowledge concerning the effect of these coherent structures on the soil canopy system as a whole. This study was dedicated to the investigation of the effect of these coherent structures on the long-time behaviour of the canopy soil system represented by the soil temperature and moisture regimes.

This present research involves five steps:

1) Formulating a numerical multi-layered canopy-soil model which takes into account radiative and non-radiative energy and mass exchange between the different components of the canopy-soil-atmosphere system. In that model, an emphasis was given to the effect of intermittency in the exchange processes on the behaviour of the soil system while, giving at the same time ample consideration to other processes which are also significant such as stomatal resistance and soil resistance to evaporation. The consideration of intermittency in a direct way makes the model unique since it is the first attempt to formulate, on basics of fluid mechanics, an intermittency approach for describing heat and mass transfer within plant canopies (El-Kilani *et al* 1994 a,b). The theoretical formulation gives a solid basis in Fluid mechanics for the gust approach as first explained by Goudriaan (1989) and suggested by El-Kilani (1989) and El-Kilani (1991).

2) Addressing the earlier attempts to consider this process in an indirect way such as by, higher order closure models or random walk models. An analysis in a qualitative or quantitative way shows some of the limitations of these approaches.

3) A mathematical analysis of the canopy air -soil system governing equations is used, to obtain a physical insight into the significance of the intermittency of the processes of heat and mass exchange on the behaviour of the canopy soil system and its dynamics. The mathematical analysis shows that the interaction between coherent structures and the canopy leads to the appearance of a non-linearity in the canopy-soil system behaviour. This nonlinear behaviour necessitates an intermittent approach to the canopy-soil system. This nonlinearity is analysed and its effect on the long-term behaviour of the system is considered.

4) A sensitivity analysis of the equations describing the system and also of a simplified model of the system shows the effect of several parameters on the time constants of the lower canopy air layers, and how the time period between gust intrusions affects the behaviour of the system.

5) A validation of the developed model against existing data sets was done. The results of the model show a very good agreement with the measurements. The values of the parameters

needed to run the model are not difficult to obtain and have a theoretical justification. The model represents a significant improvement over the existing models but requires intensive calculation.

We will cover the five steps underlined above, and mention the main points achieved or conclusions obtained from this study.

1) Formulating a numerical multi-layered canopy soil model

This part is covered in chapter 2, sect. 3.6, Sect. 4.1.2, Sect. 4.4, Sect. 4.5, Sect.4.6 and chapter 5.

The solution of the canopy and soil climate requires, for the canopy air layers, the solution of a set of averaged turbulent transport equations. The time interval and the space domain over which the averaging is done determine the kind of correlations which have to be parameterized. There are several variants for averaging the conservation equations. In the problem under consideration, an averaging procedure was introduced which separates between the large scale turbulent fluctuations and the small scale ones. The large scale turbulent velocity and scalar fluctuations are due to the existence of coherent structures in the flow field. These coherent structures, depending on their length scale and the mechanism of their generation and destruction, keep moving around the flow field, so that their effect on the momentum, heat and mass transfer all over the domain is significant. The small scale turbulent velocity and scalar fluctuations are the ones due to small scales of motion. These scales are mainly active during the quiescence period or occupy the regions between the large scale moving-around coherent structures.

The introduced averaging procedure, takes directly account of intermittency and the resulting feedback on the system behaviour. The averaging procedure leads to the appearance of correlations between the large scale and small scale turbulence and canopy inhomogeneities for both the momentum and the scalar equations. The defined averaging volumes, the averaging procedures, lead to terms in the averaged equations that are easier to parameterize.

In the case of a homogeneous canopy, we get four terms, which do not vanish in the ensemble average or in the time average. These terms represent the turbulent fluxes of momentum and scalars due to large scale, small scale and interaction fluxes. The first is mainly active during the period of the gust intrusion into the plant canopy, while the second is active during the quiescence period. The interaction fluxes are important terms in the period around (i.e. before and after) the passage of the coherent structures at the canopy top.

For the scalar equation, the parameterization for the large scale turbulent flux and the two interaction fluxes is done by assuming a refreshment function which gives the change of the scalar storage just before the intrusion of the gust till the end of the passage period. This gives an integrated value for the flux divergence at the end of the coherent structure passage.

Since we assume some degree of refreshment of the air within the canopy due to the passage of the coherent structure, the value of the turbulent transport coefficient during the quiescence period will be very important in determining the storage buildup within the air inside the canopy. With the arrival of the next coherent structure, the storage change will represent the value of the gust flux. So, a valid parameterization of the turbulent transport coefficient during the quiescence period is very important in determining the profiles and the sources within the canopy. We have assumed a complete refreshment which is not far from reality, as is shown

from an analysis of the time domain maps of windspeed and temperature within a maize canopy (Chapter 3)

To obtain a value for that turbulent transport coefficient, a frequency distribution analysis on the ratio of the instantaneous (1 second average) vertical velocity variance to the mean vertical velocity variance was used. We considered this ratio as an indicator of the behaviour of the K_M value.

It is shown for two time series, each of a duration of about 7 hours, that during about 70% of the time, the measured instantaneous w'^2 was less than the mean and contributed less than 20% to the total w variance. On the other hand, gusts occupying less than 10% of the time, contributed about 60% to the total variance. It is shown from the analysis, that the K_M value during the quiescence period was about 27% of the commonly used parameterization.

It is shown that this method of parameterizing the K_M value reflects the sequence of events characteristic of a coherent structure passage cycle (i.e. depletion during the passage of the coherent structure and buildup during the quiescence period). This was done by the use of the ratio between the instantaneous w'^2 to the mean which clearly corresponded with the disappearance of temperature islands and the increase in the absolute windspeed in the time domain maps.

In chapter 2, the solution of the energy budget for the leaves is used to parameterize the interaction terms between the leaf and the air which result from the volume averaging procedure of the turbulent transport equations within a multiply interconnected air space.

In Sect. 4.4, the decoupling of the energy equation at the soil surface is done through the calculation of the ratio of the time step of simulation to the time constant of the first air layer in contact with the soil. Depending on this ratio, either an analytical solution of the equilibrium vapour pressure of that air layer is used for decoupling the energy equation, or a numerical solution is used. The soil surface resistance to evaporation is calculated from the soil total porosity and its air filled porosity.

The decoupling of the energy equation at lower layers within the soil is done through the calculation of the water vapour flux divergence within different soil layers.

The calculation of the water flux between different soil layers, either in its liquid or vapour states, is done to calculate the soil water potential. This potential will affect the sensitivity of the stomata to the leaf water potential through the production by the plant roots of soil moisture dependent Abscisic acid (ABA).

A complete submodel for plant water movement is introduced.

2) Addressing earlier attempts

This part is covered in Sect. 3.3 and Sect. 3.7.

These attempts lie mainly under two different categories: Higher order Eulerian closure models or Lagrangian random walk models.

In a large-time-interval averaged Eulerian model, the direction of the flux and minus the gradient do not fit. Trying to counteract this problem is by increasing the order of the closure. This is done by taking account of the turbulent transport term in the higher order equations and the effect of this on the gradient of the turbulent flux in the lower order equation.

One of the assumptions here is that all the terms within these equations have a constant averaged value during the time step of simulation. It is shown from the analysis of some papers and some data sets, that this is far from reality. Due to the high nonlinearity of these equations, we expect that the time fluctuating behaviour of the terms will give a different solution than the same terms having non fluctuating values with the same mean.

It appeared that the assumption of retaining the lost information, due to averaging, by going higher with the closure is not correct. This is due to the role of the coherent structures in correlating the fluxes i.e. creating correlations at higher order which is not counteracted by the role of pressure in destroying these correlations. The role of the pressure in destroying these correlations is centred around the passage of the inclined shear layer at the canopy top. In canopy flow, the ratio between the pressure smearing distance/ distance between coherent structure is much less than one. This automatically invalidates some assumptions for closing the higher order terms.

Another problem is also the requirement for the validity of averaging a nonlinear equation. Reynolds averaging has a requirement concerning the uniformity of the terms within the period of averaging. The high variation in time or space of the signals make the fulfilment of this requirement in doubt.

Therefore, the validity of the obtained results from second and higher order closure models for canopy flow must be doubted.

Another approach used in modelling canopy flow is Lagrangian modelling which simulates the trajectories of a large number of independently moving particles and sums up the results as representing the mean concentration profile within the canopy.

The superposition of the concentration field overlooks the fact that the intrusion of the coherent structure into plant canopy leads to the creation of correlation between motion of the particles all over the canopy height. So, the particles are not moving independently all the time. This correlation should be subtracted from the total superposition.

The argument that random walk models take account already of the correlation between particles motions due to coherent structure existence in the flow field, is discussed in the objection to the theoretical derivation of Lamb (1980) in Appendix 1.b.

The problem is that the joint density function for a large number of particles cannot be expressed as a multiplication of marginal density functions for all the particles which are equal to each other.

An approach for superposition of the concentration fields, as seen by a sensor which is immersed in the flow field and which starts to see progressively older clouds, is suggested in this thesis, to take account of this process.

3) A mathematical analysis of the canopy-soil system governing equations

This part is covered in Sect. 4.2.

The aim of this part was to answer, in a semi-analytical way, if a constant turbulent transport coefficient will result in the same mean temperature and vapour pressure of the air as a fluctuating turbulent transport coefficient which has the same value of the mean. It is analysed if this leads to a difference on the soil heat flux and the soil temperature profile.

For the canopy air system, this analysis involved transforming four coupled partial differential equations describing the system behaviour into ordinary ones. These are the leaf temperature, air temperature, vapour pressure and vapour pressure deficit equations. It is shown from the analysis that after a gust intrusion into a plant canopy, the leaf temperature, air temperature, vapour and vapour pressure deficit approach asymptotically a steady state solution which is a linear function of the transport coefficient. So, in the early stages of the solution development toward equilibrium, there will be a non linear dependence on the turbulent transport coefficient due to the exponential behaviour of the equations. Use of a large time averaged turbulent transport coefficient is not similar to the use of a non averaged one which has the same mean. The importance of this nonlinearity on the mean behaviour of the canopy depends on the ratio between the period between two consecutive gust intrusions in relation to the canopy air time constants. If this ratio ranges between 0.5 to 3.0, the canopy will always be in the nonlinear part of the solution. Depending on the dominance of this process, the canopy system could be in the nonlinear domain of the solution for a significant part of the time.

Due to the changes within time of the ratio between the inverse of the gust intrusion frequency into the plant canopy to the time constants of the systems, the canopy system will be scanning, within time, different regions in the nonlinear or linear part of the solution. The frequency of gust intrusions into plant canopies is assumed to be dynamically controlled i.e. controlled by the shear at the canopy top while the time constants of the canopy air layers are affected mainly by the stomatal resistance of the plants and how it is controlled (e.g. water potential in the soil and light etc.). So, an irrigation cycle will span the different regions of the nonlinear and linear dependence of the solution.

It is also shown, that the above mentioned nonlinearity exceeds by at least one time order of magnitude the near field effect, as explained by Raupach (1989) or Finningan (1985), in their criticism of the use of K_m theory to describe canopy turbulent transport processes. So, the non linearity in the canopy system is not only due to the near field effect.

The next step in the mathematical analysis was analysing the response of the soil to this nonlinearity. It is shown from a mathematical solution of the nonhomogeneous problem of the soil temperature profile that the soil integrates the effect of intermittency in the values of the coefficients of an Eigenfunction expansion of the soil temperature i.e. Fourier series expansion.

It is shown from the mathematical expression for these coefficients that they see all sources of intermittency; either due to changes in the radiative forcing or changes in the temperature and vapour pressure deficit of the air close to the soil surface.

Each value of the coefficients of the Eigenfunction expansion of the soil temperature is composed of an initial component which decays exponentially within time and a component which integrates both the radiative forcing signals and the nonradiative forcing signals (i.e. the air temperature and vapour pressure deficit close to the soil surface). The nonradiative forcing is the one affected by coherent structures.

The rate of decay for the initial component and for previous intermittencies decreases at a much faster rate for the higher wave numbers. It is also shown that the effect of intermittencies on the coefficients of the Eigenfunction expansion expresses itself in the same way in all wave numbers. So the effect of intermittency needs to be studied for one wave number only. The

effect of intermittency on the integrated value of the non radiative forcing quantifies the effect of intermittency on the soil. The mathematical solution integrates all the details of intermittencies in the radiative and nonradiative forcing.

4) A sensitivity analysis

This part is covered in Sect. 4.2.1.2.b , 4.2.2 , 4.2.3, 4.2.4 and 4.3.

To simplify the analysis and to obtain a physical insight to the effect of the intermittency on the system, we assumed a separation in the time scale of the response of the air layers and the soil layers. That allowed us to integrate the effect of the nonlinearity on the mean temperature and vapour pressure deficit of the air layers close to the soil and feed that effect into the equations describing the coefficients of an Eigenfunction expansion of the soil temperature. To calculate the mean temperature and vapour pressure deficit of the air layers close to the ground, a combination of several situations was assumed.

The first of these were: a steady state and nonsteady state situations. In the steady state (what we call the approximate form) situation, the effect of the heat storage change with the canopy elements was ignored while in the nonsteady state (what we call the more exact form), that effect was accounted for.

The second of these, either a single layer canopy or a multi-layered canopy was assumed. In the single layer canopy, the canopy layer was assumed well mixed while in the multi-layered canopy, several layers each having a different leaf area density and turbulent transport coefficients were assumed. In the nonsteady solution, only a multi-layered canopy was used.

In the calculation of the mean temperature and vapour pressure deficit, a constant K_m value was assumed. This K_m value was four times higher for the no-gust model than that for the gust model. In the gust model, most of the contribution to the K_m value occurs during the gust intrusion phase, while in the quiescence period, the value of K_m is much lower than the mean of the no-gust model. In the gust model, an initial profile after the passage of the coherent structure profile was set equal to the temperature and vapour pressure at about twice the canopy height.

In the case of single layer, and the approximate form solution, the results show that the gust model had a higher value of the nonradiative forcing on the soil due to the lower turbulent transport coefficient which couples the leaf temperature more to the radiation forcing than to the temperature and the vapour pressure of the air well above the canopy. This will increase the equilibrium temperature of the leaves. That will have a feedback on the temperature and the vapour pressure of the canopy air since the coupling coefficients of the sources within the air layers to the air temperature and vapour pressure is higher in the gust model compared to the no-gust model. The end result is that unless that the period between consecutive gust intrusions is small compared to the time constant of the canopy air, the lower mixing during the quiescence period will increase the temperature and the vapour pressure of the air in comparison to a no-gust model. The well mixed layer assumption will lead to the increase in the temperature and vapour pressure of the air, being felt at the soil surface. This will increase the mean nonradiative forcing at the soil surface and will counteract the effect of the refreshment, due to the gust intrusion, on relieving the nonradiative forcing on the soil.

In the approximate form, for a multi-layered canopy, it is shown that the inverse matrix which controls the equilibrium solution of the air layers have its inner elements multiplied, for the case of a gust model, by the ratio of the K_m value in the no-gust model to the K_m value in the gust model. This matrix has to be multiplied by a C matrix which expresses the source terms within each canopy layer. This C matrix, depending on which system (Vapour pressure deficit or air temperature system), is independent of the solution. This means a relative reduction in the role of the upper and lower boundaries of the simulated domain to the equilibrium solution and a higher contribution of the inner layers to the solution at a certain height. The lower mixing during the quiescence period leads then to the establishment of a higher influence of the inner C elements to the temperature and vapour pressure of the air within a certain layer in comparison to a no-gust model in which a higher value of the turbulent transport coefficient is active all the time. Whether this leads, in the case of vapour pressure deficit equation, to a higher or a lower vapour pressure deficit than that of the boundaries depends on the stomatal resistance and R_n profile.

In the more exact solution, only a multilayered model was used. This was done either by the use of a Mathcad program or a simplified complete numerical model. The Mathcad code was using the same method of solution for the leaf temperature, air temperature and vapour pressure as in the more detailed numerical model. It has less number of layers and was run only for a short period (i.e. three gust cycles which have a period of 150 seconds each). The soil surface temperature was assumed constant and the effect of the gust process was integrated on the value of the nonradiative forcing and the boundary condition for the soil heat flux. These Mathcad runs are also part of the sensitivity analysis discussed in the next point. The simplified complete numerical model is exactly the same as the model given in chapter 5, except that it has no feed back of the soil dryness on the solution (i.e. the soil surface resistance to evaporation was assumed zero all the time i.e. 11 days run).

The results from the Mathcad runs show that for the soil heat flux and the nonradiative forcing on the soil surface, a lower leaf area density in the lower parts of the canopy and a lower turbulent transport coefficient increase the difference between the gust and no-gust model. This relates to increasing the time constant of the lowest air layer and decreasing the ratio between the inverse of the gust intrusion frequency into plant canopy and the time constant of the lowest air layers close to the soil. The effect of air introduced by the gust on relieving the nonradiative forcing on the soil surface will be felt at the soil surface.

The results of the simplified complete numerical model, which was run for a typical hot summer day in Egypt, show a significant difference between the gust and no-gust parameterization on the soil temperature and the soil heat flux. That difference at noon time were about -9 C in the air temperature for the gust minus the no-gust model and higher vapour pressure deficit (+1000 Pa for the gust minus the no-gust) in the lower part of the canopy. The gust intrusion period was constant and equals 1.5 minutes. The reason behind this high difference was the large time constant of the lower air layers close to the soil. This large time constants were due to the used turbulent parameterizations, the lower leaf area density in the lower part of the canopy and the higher stomatal resistance which was light dependent.

The results of the Mathcad runs show that it is possible that there is no difference in the forcing on the soil surface, while there is one in the energy partition on plant surfaces.

A complete analysis of the interaction between the leaves and the air for typical situations representing different climatic regions is also done. The dynamics of that interaction and the importance of the nonsteady term on the solution are shown. It is shown the state variables of the air (i.e. the temperature, vapour pressure and vapour pressure deficit) and the sources follow within the whole gust cycle an exponential behaviour.

In sect. 4.3, it is shown from the scaling of the large-time averaged flux equation that the source vertical velocity correlation, which results from the interaction between the air which comes into plant canopies and the source, has the same order of magnitude as the production term of the flux, So an account of that correlation due to the intrusion of coherent structures should be included.

5) Validation of the developed model

This part is covered in Chapter 6.

The results of the model validation show in general a very good agreement between the measured and simulated radiative environment and leaf temperature and air temperature. There is, however an interplay between the gust frequency which determines the degree of buildup of the scalar profiles which is allowed to occur and the stomatal resistance which controls the time rate of the profiles buildup for the vapour pressure and temperature. This affects the energy budget solution of the leaves. The turbulent transport parameterization play also an important role in controlling the values of the temperature and vapour pressure in the middle layers of the canopy. A better parameterization of the gust frequency, stomatal resistance and turbulent transport will allow even a better simulation of the plant canopy microclimate.

Samenvatting

Het doel van het onderzoek is het beschrijven van het transport van warmte en massa tussen de bodem, plant en de atmosfeer direct boven het gewas. Dit transport heeft een sterk intermitterend karakter t.g.v. de aanwezigheid van grootschalige coherente structuren in de luchtlag aangrenzend aan het gewas. De periodieke passage van deze coherente structuren aan de bovenkant van het gewas en haar grote lengteschaal ten opzichte van de gewashoogte, leidt tot de verversing van lucht binnen het gewas met lucht van ver boven het gewas. Dit maakt de coherente structuren verantwoordelijk voor het overheersende deel van het transport van warmte en massa van de lucht binnen het gewas en de lucht daar boven. Coherente structuren zijn ook verantwoordelijk voor een groot deel van het impulstransport tussen gewaslaag en de lucht daar boven. Er bestaat een leemte in kennis omtrent het effect van deze coherente structuren op het transport binnen het systeem bodem, gewas en atmosfeer. Deze studie is gewijd aan het onderzoek van het effect van deze coherente structuren op het langetermijn gedrag van de van de bodemtemperatuur en het -vochtregime.

Het onderzoek omvat vijf stappen:

1) Het formuleren van een numeriek meer-lagen gewas-bodemmodel

Dit model houdt rekening met zowel stralingstermen als andere energetische termen en houdt rekening met de massa-uitwisseling tussen het bodem-gewas-atmosfeer systeem. In het model is veel aandacht geschonken aan het intermitterende karakter van het transportmechanisme en het effect hiervan op het gedrag op de bodem. Ook is rekening gehouden met andere van belang zijnde processen zoals het gedrag van stomataire weerstand van de planten en de bodemweerstand. Het direct meenemen van intermittentie in het transportmechanisme maakt het model uniek want het is de eerste keer dat, op basis van de stromingsleer, dit is meegenomen in het transportmechanisme voor massa, impuls en warmte (El-Kilani, 1994a,b). De theoretische formuleringen betreffende de vlagbenadering zijn gebaseerd op de basisvergelijkingen uit de stromingsleer zoals dat aanvankelijk verklaard is door Goudriaan (1989) en voorgesteld is door El-Kilani (1989, 1991).

2) Bespreking van benaderingen van anderen

Veelal is dit proces op een indirecte manier benaderd, bijvoorbeeld met behulp van hogere orden sluitingsmodellen of random walk modellen. In een kwalitatieve of kwantitatieve analyse worden de beperkingen van deze benaderingen aangetoond.

3) Een mathematische analyse van de vergelijkingen voor het bodem-gewas-atmosfeer systeem

Deze analyse is toegepast om inzicht te krijgen in het belang van intermittentie voor de uitwisselingsprocessen van warmte, massa en haar dynamica. De mathematische analyse laat zien, dat de interactie tussen coherente structuren en het gewas leidt tot het optreden van niet-lineariteiten in het gewas-bodem-systeem. Dit niet-lineaire gedrag maakt het noodzakelijk deze intermittentie ook in het systeem in te brengen. Deze niet-lineariteit is geanalyseerd alsmede het gedrag hiervan op het systeem op de lange termijn.

4) Een gevoeligheidsanalyse

Het systeem wordt beschreven en besproken en er wordt een vereenvoudigd systeem gegeven, dat het effect van verschillende parameters laat zien op de tijdconstanten van de onderste lagen van het gewas. Tevens is het effect op het systeem van de periode tussen twee vlagen beschreven.

5) Een validatie van het model

Deze is uitgevoerd met bestaande gegevensbestanden. De modelsimulaties geven een zeer goede overeenkomst met de metingen. De waarden van de modelparameters die nodig zijn om het model te draaien zijn eenvoudig te verkrijgen en hebben ook een fysische betekenis. Het huidige model is een aanzienlijke verbetering t.o.v. reeds bestaande modellen maar vereist wel veel rekentijd. De bovenstaande punten worden vervolgens kort besproken.

Ad 1) Het formuleren van een numeriek meer lagen gewas-bodemmodel.

Dit deel bevat hoofdstuk 2 en 5, en de paragrafen 3.6, 4.1.2, 4.4, 4.5 en 4.6. De oplossing voor de gewasklimatologie vereist voor de gewaslaag de oplossing van een stelsel gemiddelde turbulente transportvergelijkingen. Het tijdsinterval en het ruimtedomein waarover de middeling wordt uitgevoerd bepaalt de soort correlaties welke moeten worden geparаметriseerd. Er zijn verschillende varianten voor het middelen van de behoudswetten. In het onderhavige geval is er een middelingsmethode ingevoerd, welke onderscheid maakt tussen de grote en de kleine schaal van de turbulentie. De grote schaal van de turbulente snelheidscomponenten en scalaire grootheden worden veroorzaakt door de coherente structuren van het stromingsveld. Deze coherente structuren blijven, afhankelijk van hun lengteschaal en het mechanisme dat deze genereert en afbreekt, bewegen in het stromingsveld, zodat het effect hiervan op de impuls, warmte en massa over het gehele domein belangrijk is. De kleine schaal turbulente snelheidscomponenten en scalaren worden veroorzaakt door de kleinschalige bewegingen. Deze schalen zijn voornamelijk actief gedurende de kalme periode of in de gebieden tussen de grootschalige structuren.

De ingevoerde middelingsprocedure houdt direct rekening met de intermittentie en de hieruit voorkomende terugkoppeling op het systeem. De middelingsprocedure leidt tot het ontstaan van correlaties tussen de grote en kleine schaal van de turbulentie en inhomogeniteiten in het gewas voor zowel voor de impuls- als de scalaire vergelijkingen. Het gedefinieerde middelingsvolume geeft extra termen in de gemiddelde vergelijkingen die eenvoudig zijn te parametriseren.

In het geval van een homogeen gewas krijgen we zo vier extra termen. Deze termen representeren de turbulente fluxen van impuls en scalaire grootheden ten gevolge van de grote schaal, de kleine schaal en de interacties hiertussen. De eerste term is meestal actief gedurende de periode dat een vlaag in het gewas binnendringt, terwijl de tweede actief is gedurende de kalme periode. De interactieve fluxen zijn belangrijke termen gedurende de overgangperiodes.

Voor de scalaire vergelijkingen zijn de parametrisaties voor de grote schaal turbulentie en de twee interactieve fluxen verkregen door het invoeren van een z.g. verversingsfunctie welke de verandering van de scalaire opslagterm geeft, juist voordat de, vlaag het gewas

binnendringt tot het eind van de passage van de vlaag. Dit geeft een geïntegreerde waarde voor de divergentie van de flux op het einde van de passage van de coherente structuur.

Omdat we een zekere mate van verversing van lucht binnen het gewas veronderstellen ten gevolge van de passage van de coherente structuur, zal de waarde van de turbulente uitwisselings-coëfficiënt gedurende de kalme periode erg belangrijk zijn voor het bepalen van de opslag van warmte en waterdamp binnen het gewas. Bij de aankomst van de volgende coherente structuur, zal de verandering van de opslag overeenkomen met de waarde van de flux van de betreffende grootheid tijdens vlaagperiode. Dus een geldige parametrisering van de turbulente transportcoëfficiënt gedurende de kalme periode is zeer belangrijk voor het bepalen van de profielen en bronnen/putten van de betreffende grootheden. Er is een volledige verversing verondersteld, hetgeen dicht bij de werkelijkheid komt zoals is aangetoond in hoofdstuk 3.

Om een numerieke waarde te krijgen voor deze uitwisselingscoëfficiënt, is een analyse van de frequentieverdeling gemaakt tussen de verhouding van de momentane ($1s$ gemiddeld) verticale snelheidscomponent en de verticale snelheidsvariantie. Deze verhouding beschouwen we als een indicator voor het gedrag van de K_m -waarde.

Voor twee tijdreeksen, ieder van een duur van ongeveer 7 uur, is aangetoond dat gedurende ongeveer 70% van de tijd, de gemeten momentane w'^2 minder was dan de gemiddelde bijdrage en minder dan ongeveer 20% bij droeg aan de totale w variantie. Aan de andere kant nemen de vlagen minder dan 10% van de tijd in beslag, maar dragen ongeveer 60% bij aan de totale variantie. Uit de analyse wordt aangetoond, dat de K_m -waarde gedurende de kalme periode ongeveer 27% was van de waarde waarmee gewoonlijk wordt geparameteriseerd.

Aangetoond is dat deze parametrisatiemethode van de K_m -waarde het verloop van de gebeurtenissen weergeeft, karakteristiek voor de passage van een vlaag; met andere woorden ledigen/verversen gedurende de passage van de vlaag en de opbouw gedurende de kalme periode). Dit is uitgevoerd door gebruik te maken van de verhouding tussen de momentane w'^2 tot het gemiddelde, hetgeen duidelijk overeen blijkt te komen met het verdwijning temperatuur "eilandjes" en de toename van de absolute windsnelheid in het tijdsdomein.

In hoofdstuk 2, wordt de oplossing voor de energiebalans voor de bladeren gebruikt om de interactieve fluxen tussen blad en lucht te parametriseren, hetgeen het resultaat is van de ruimtelijke middelingsprocedure van de turbulente transportvergelijkingen binnen een meervoudig verbonden luchtruimte.

De ont koppeling van de energievergelijking aan het bodemoppervlak, in paragraaf 4.4, is verkregen door het berekenen van de tijdstap van de simulatie en de tijdconstante van de eerste luchtlaag welke in contact staat met de bodem. Afhankelijk van deze verhouding wordt ofwel een analytische evenwichtoplossing voor de dampspanning gebruikt voor de ont koppeling van de energievergelijking ofwel wordt er een numerieke oplossing gebruikt. De oppervlakteweerstand voor verdamping wordt berekend uit de totale porositeit van de bodem and de met lucht gevulde porositeit.

De ont koppeling van de energievergelijking voor de lagere bodemlagen is uitgevoerd door het berekenen van de divergentie van de waterdampflux in de verschillende bodemlagen. Het berekenen van de waterflux tussen de verschillende bodemlagen, zowel in de vloeibare fase als in de dampfase, is uitgevoerd m.b.v. de waterpotentiaal. Deze potentiaal

zal de gevoeligheid van de stomata van de bladeren beïnvloeden door de productie van Abscissinezuur ABA door plantenwortels onder invloed van bodemvocht. Een volledig submodel voor de waterbeweging in de plant is geïntroduceerd.

Ad 2) Bespreking benaderingen van anderen

Dit onderdeel wordt besproken in par. 3.3 en 3.7.

Hierin zijn voornamelijk twee richtingen in aan te geven: Hogere orde Euleriaanse sluitingsmodellen en Lagrangiaanse random walk modellen.

In een Euleriaans model over een lange periode, komt het teken van de gradiënt niet overeen met de richting van de fluxen. Om dit probleem op te lossen wordt overgegaan naar een hogere orde sluiting. Dit gebeurt door gebruik te maken van de turbulente transporttermen in de hogere orde vergelijkingen en het effect hiervan op de gradiënt van de turbulente flux in de lagere orde vergelijking.

Een van de veronderstellingen is hierbij dat alle termen van deze vergelijkingen een constant gemiddelde hebben gedurende het simulatie-interval. Uit de analyse van enkele artikelen en gegevensbestanden wordt aangetoond dat dit verre van de werkelijkheid is. Ten gevolge van de hoge mate van niet-lineariteit van de vergelijkingen moeten we verwachten dat het fluctuerende gedrag in de tijd van deze termen een andere oplossing geeft dan dezelfde termen die geen fluctuerende waarde t.o.v. het gemiddelde hebben.

Het blijkt dat de aanname dat de bij middeling verloren informatie terug zou komen door gebruik te maken van een hogere orde sluiting niet juist is. Dit komt door het effect van de coherente structuur op de kruiscorrelaties, met andere woorden het creëren van correlaties bij hogere orden welke niet tegengewerkt worden door de druktermen die deze correlaties willen vernietigen. De rol van de druk om deze correlaties te vernietigen is speelt vooral rondom de passage van een hellende schuifspanningslaag aan de bovenkant van het gewas. Bij de stroming in het gewas is de verhouding tussen de afstand waarover drukfluctuaties worden uitgesmeerd en de afstand tussen coherente structuren veel kleiner dan één. Dit maakt automatisch enige veronderstellingen ongeldig bij het gebruik van hogere orde sluiting.

Een ander probleem is de geldigheid van de middelingsprocedure bij niet-lineaire vergelijkingen. Reynoldse middeling vereist uniformiteit van de termen binnen de middelingsperiode. De hoge mate van variatie in de tijd of in de ruimte noopt tot twijfel aan deze veronderstellingen.

Daarom moet getwijfeld worden aan de geldigheid van het resultaat dat verkregen wordt met tweede en hogere orde sluitingen.

Een andere manier van modellering binnen gewassen is gebruik te maken van de Lagrangiaanse modellering, welke de trajectoriën simuleert van een groot aantal onafhankelijk bewegende deeltjes en deze op te tellen als eindresultaat.

Deze optelling ziet echter over het hoofd dat bij het binnendringen van een coherente structuur in een gewas er een sterke correlatie aanwezig is tussen al de deeltjes binnen het gewas. De deeltjesbeweging gedurende een zekere tijd is dus beslist niet onafhankelijk. Deze correlatie moet van de totale superpositie worden afgetrokken.

Het argument dat random walk modellen al rekening houden met de correlatie tussen de deeltjes t.g.v. het aanwezig zijn van coherente structuren in het stromingsveld, wordt

besproken in Lamb (1980). De moeilijkheid is dat de gezamenlijke dichtheidsfunctie voor een groot aantal deeltjes niet uitgedrukt kan worden als een vermenigvuldiging van marginale dichtheidsfuncties welke aan elkaar gelijk zijn.

Een benadering voor de superpositie van concentratievelden, zoals dat gevoeld wordt door een sensor in een stromingsveld en die steeds oudere concentratiewolken ziet, wordt in dit promotieverslag voorgesteld.

Ad 3) Een mathematische analyse van de vergelijkingen voor het bodem gewas systeem.

Paragraaf 4.2 behandelt op een semi analytische wijze, de vraag of een constante turbulente transportcoëfficiënt zal resulteren in dezelfde gemiddelde temperatuur en dampdruk als een fluctuerende turbulente transport coëfficiënt met een zelfde gemiddelde waarde. Bekeken wordt of deze twee benaderingen leiden tot verschillen in de bodemwarmtestroom en het bodemtemperatuurprofiel.

Voor het gewas-atmosfeer systeem betekent dat 4 gekoppelde partiële differentiaalvergelijkingen getransformeerd zijn in gewone differentiaal vergelijkingen, waarbij het hier gaat om de vergelijkingen voor bladtemperatuur en luchttemperatuur, de dampdruk en het dampdrukdeficit. Met deze analyse wordt gedemonstreerd, dat na het binnendringen van een windvlaag in het gewas, de blad- en luchttemperatuur, de dampdruk en dampdrukdeficit asymptotisch naderen tot een evenwichtstoestand, die een lineaire functie is van de turbulente transportcoëfficiënt. In de loop naar deze evenwichtstoestand, zal er echter een niet-lineaire afhankelijkheid van de turbulente transportcoëfficiënt bestaan ten gevolge van het exponentiële gedrag van de vergelijkingen. Het gebruik van een gemiddelde waarde voor een turbulente transportcoëfficiënt is dus niet hetzelfde als een fluctuerende waarde met hetzelfde gemiddelde. Het belang van de niet-lineariteit op het gemiddelde gedrag van het gewas hangt af van de verhouding tussen het interval van twee opeenvolgende binnendringende windvlagen en de tijdconstanten van de lucht in het gewas. Ligt deze verhouding tussen de 0.5 en 3.0, dan zal de oplossing voor binnen het gewas zich altijd in het niet-lineaire gedeelte van de oplossing bevinden. Afhankelijk van het belang van dit proces kan de oplossing zich, voor een aanzienlijke periode van de tijd, in het niet lineaire domein bevinden.

De frequentie waarmee windvlagen het gewas binnendringen wordt dynamisch bepaald door de windschering aan de top van het gewas. De tijdconstanten van de luchtlagen binnen het gewas daarentegen, worden voornamelijk bepaald door de stomataire weerstand van de planten en hoe deze wordt beheerst (b.v. water potentiaal in de bodem en lichtintensiteit).

Tevens wordt aangetoond dat de genoemde niet-lineariteit de grootte van het nabije veld effect met minimaal één orde overtreft. Het nabije veld effect, wordt beschreven door Raupach (1989) en Finnigan (1985) in hun kritiek op het gebruik van Km-theorie bij de beschrijving van turbulente transportprocesses binnen een gewas.

De volgende stap van de mathematische analyse is het beschrijven van de reactie van de bodem op deze niet-lineariteit. De wiskundige oplossing van het niet homogene probleem van het bodemtemperatuurprofiel laat zien dat de bodem het effect van intermittentie integreert in de waarden van de coëfficiënten van een Eigenfunctie ontwikkeling van de bodemtemperatuur; met andere woorden een Fourier reeks ontwikkeling.

Wiskundige uitdrukkingen voor deze coëfficiënten, demonstreren dat alle bronnen van intermittentie worden waargenomen, enerzijds door veranderingen in straling of anderzijds door veranderingen in temperatuur of dampdrukdeficit van de lucht vlak bij het grondoppervlak. Elke waarde van de coëfficiënten van de eigenfunctie ontwikkeling voor de bodemtemperatuur bestaat uit een initieel en een integrerend bestanddeel. De eerste neemt exponentieel af in de tijd en de tweede integreert de opgelegde straling en andere grootheden, zoals de luchttemperatuur en het dampdrukdeficit nabij het grondoppervlak. Het zijn deze laatste grootheden die beïnvloed worden door coherente structuren.

De afnamesnelheid van de initiële componenten en de afname van de invloed van voorgaande intermittenties gaan voor de hogere golfgetallen veel sneller. Een ander effect van intermittenties op de coëfficiënten van de Eigenfunctieontwikkeling is dat deze zich voor alle golfgetallen op een zelfde manier uitdrukken. Het effect van intermittentie hoeft dus maar voor één golfgetal bestudeerd te worden. Het effect van intermittentie op de geïntegreerde waarde van de drijvende krachten anders dan straling kwantificeren het effect van intermittentie op de bodem. De wiskundige oplossing integreert alle details van de aandrijvende krachten van intermittentie.

Ad 4) Een gevoeligheidsanalyse

Paragraaf 4.2.1.2.b. tot en met 4.3 behandelt de gevoeligheidsanalyse. Om de analyse te vereenvoudigen en om fysisch inzicht te verkrijgen in het effect van intermittentie op het systeem, hebben we aangenomen dat er onderscheid is in de tijdschaal waarin de luchtlagen en bodemlagen reageren. Dit stelt ons in staat het effect van de niet-lineariteit op de gemiddelde temperatuur en dampdruk van de luchtlagen nabij het grondoppervlak te integreren en deze te gebruiken om de vergelijkingen te beschrijven van coëfficiënten van de Eigenfunctieontwikkeling van de bodemtemperatuur. Om de gemiddelde bodemtemperatuur en het dampdrukdeficit van de luchtlagen nabij het grondoppervlak te berekenen, worden een combinatie van verschillende situaties aangenomen.

De eerste combinatie is een evenwichts- en een niet-evenwichtstoestand. In de evenwichtstoestand wordt het effect van veranderende warmteopslag met de gewas elementen verwaarloosd, maar wordt in de niet-evenwichtstoestand wel meegenomen. Een tweede combinatie is een één-laag of een meer-lagen gewas. In het eerste geval is aangenomen dat de lucht in het gewas goed gemengd is. Bij het tweede geval is aangenomen dat iedere laag een verschillende bladoppervlaktedichtheid en turbulente uitwisselingscoëfficiënt heeft. Bij de niet-evenwichtstoestand is alleen een meer lagen model gebruikt.

Bij de berekening van de gemiddelde temperatuur en dampdrukdeficit, is een constante K_m waarde aangenomen. Deze waarde is ongeveer vier maal zo groot in het één windvlagen model ten opzichte van het windvlagen model. In het windvlagen model is tijdens het binnendringen van een vlaag de bijdrage aan K_m het grootst, terwijl gedurende een kalme periode K_m veel kleiner is dan de gemiddelde K_m in het één windvlagen model. In het windvlagen model wordt, na de passage van een coherente structuur, het initiële profiel gelijk gemaakt aan de temperatuur en dampdruk die heerst op ongeveer 2 maal de gewashoogte.

In het geval van de combinatie met één enkele laag en de combinatie met een evenwichtstoestand, laat het resultaat zien dat het windvlagen model een hogere waarde geeft voor de aandrijving anders dan straling op de bodem als gevolg van een lagere turbulente transportcoëfficiënt. Deze maakt dat de blad temperatuur meer afhankelijk van is stralingsaandrijving dan van de temperatuur en de dampdruk van de lucht ver boven het gewas. Dit zal de evenwichtstemperatuur van de bladeren doen toenemen. Dit zal weer gevolgen hebben voor de temperatuur en dampdruk van de lucht, immers de afhankelijkheidscoëfficiënten van de bronnen van temperatuur en dampdruk in de luchtlagen is groter in het windvlagen model dan in het géén windvlagen model. Het eindresultaat is dat, tenzij de periode tussen twee opeenvolgende binnendringende windvlagen klein is ten opzichte van de tijdconstante van lucht in het gewas, de lagere menging tijdens een kalme periode de temperatuur en dampdruk van de lucht zal laten stijgen ten opzichte van het géén windvlagen model. De aanname van de goed gemengde laag zal leiden tot een toename in de temperatuur en dampdruk van de lucht, waargenomen door het grondoppervlak. Dit zal de gemiddelde niet-stralingsaandrijving aan het grondoppervlak laten toenemen waarna dit het effect van verversing door het binnendringen van de windvlaag zal tegenwerken door een niet-stralings aangedreven forcering op de bodem uit te oefenen.

In de evenwichtstoestand, voor een meer lagen gewas, laat een inverse matrix, die de evenwichtsooplossing van de luchtlagen controleert, zien dat bij een vlagen model de binnenste elementen vermenigvuldigd zijn met de verhouding tussen de K_m -waarde in een géén vlagen model en de waarde van K_m in een vlagen model. Deze matrix moet vermenigvuldigd worden met een C-matrix, die de brontermen in elke laag van het gewas vertegenwoordigen. Deze C-matrix is onafhankelijk van de oplossing. Dit betekent een relatieve vermindering van de rol van de onderste en bovenste randvoorwaarden van het gesimuleerde domein en een grotere bijdrage van de binnenste lagen tot de oplossing op een bepaalde hoogte. De geringere menging gedurende de kalme periode leidt dan tot het bereiken van een grotere invloed van de binnenste elementen van de C-matrix op de temperatuur en dampdruk van de lucht op een zekere hoogte, in vergelijking met een géén vlagen model waarin constant een hogere waarde voor de turbulente transportcoëfficiënt actief is. Of dit leidt, in het geval van de dampdruk vergelijking, tot een hogere of lagere dampdrukdeficit dan die aan de randen, hangt af van de stomataire weerstand en het netto straling profiel.

In een meer exacte oplossing, is alleen een meer lagen model gebruikt. Dit is gebeurd behulp van MathCad, een mathematisch computerprogramma, of een gesimplificeerd compleet numeriek model. Het MathCad programma gebruikt dezelfde oplossingsmethode voor zowel de bladtemperatuur, de luchttemperatuur als de dampdruk. Het heeft minder lagen en simuleert een kortere periode dan het numerieke model. De bodem temperatuur is constant genomen en het effect van het binnendringen van de vlagen is geïntegreerd in de waarde van de niet-stralings forcering en de randvoorwaarden voor de bodemwarmtestroom. Deze MathCad runs zijn onderdeel van de gevoeligheidsstudie die in het volgende besproken wordt. Het numerieke model is hetzelfde als in hoofdstuk 5, behalve de invloed van de droogte van de bodem op de oplossing. Met andere woorden, de bodemweerstand voor verdamping is altijd nul genomen.

Het resultaat van de MathCad runs laten zien dat voor de bodemwarmtestroom, de niet-straling forcering op het bodemoppervlak een lagere bladoppervlaktedichtheid in de onderste lagen van het gewas en een lagere turbulente uitwisselingscoëfficiënt het verschil tussen vlagen en een géén vlagen model laat toenemen. Dit staat in verband met het verhogen van de tijdconstante van de onderste luchtlagen en het verhogen van de verhouding tussen de inverse van het binnendringen van de vlag in het gewas en de tijd constante van de onderste luchtlag nabij het grondoppervlak.

Het resultaat van het gesimplificeerde complete numerieke model, die een typische warme zomer dag in Egypte simuleert, laat een significant verschil zien in de vlag en géén vlag parametrisatie op de bodemwarmtestroom en de bodemtemperatuur. Het verschil rond 12 uur in de middag, lag rond -9°C en $+1000\text{ Pa}$ voor het vlag model ten op zichte van géén vlag model, voor respectievelijk de temperatuur en de dampdruk in de onderste lagen van het gewas. Hierbij is de periode van het binnendringen constant gehouden en op 1.5 minuut gesteld. De oorzaak van dit grote verschil ligt in de grote tijd constante van de onderste luchtlagen nabij de grond. Deze is zo groot ten gevolge van de gebruikte turbulente parametrisatie, de lagere blad oppervlakte dichtheid in de onderste lagen van het gewas en een hogere licht afhankelijke stomataire weerstand.

Het resultaat van de MathCad run laat zien dat het mogelijk is dat er geen verschil is in de forcering van de grond, maar wel in de partitie van het plantoppervlak.

Een complete analyse van de interacties tussen de bladeren en de lucht voor typische klimatologische situaties is ook geanalyseerd. De dynamica van deze interactie en het belang van de niet-stationaire termen op de oplossing wordt aangetoond. De toestandsvariabelen (o.a. de temperatuur, de dampdruk en -deficit) en de bronnen, volgen binnen een gehele vlaagcyclus een exponentieel gedrag.

In paragraaf 4.3 wordt getoond uit schaling van de lange-tijd-gemiddelde fluxvergelijking dat de correlatie van de verticale bronsnelheid, die het resultaat is van de interactie tussen de lucht die het gewas binnentreedt en de bron, dezelfde orde van grootte heeft als de produktieterm voor de flux. Dit betekent dat bij het binnendringen van coherente structuren deze correlatie moet worden meegenomen.

Ad 5) Validatie van het ontwikkelde model.

Dit onderdeel wordt behandeld in hoofdstuk 6. Het resultaat van de modelvalidatie vertoont in het algemeen een zeer goede overeenkomst tussen de gemeten en gesimuleerde stralingsomgeving, de blad- en luchttemperatuur. Er is echter interactie tussen de vlaagfrequentie, die de mate van de opbouw van de scalaire profielen bepaalt, en de stomataire weerstand, die bepalend is voor het verloop van de opbouw van temperatuur en dampdruk. Dit bepaalt de oplossing van de energiebalans van de bladeren. De parametrisatie van het turbulente transport speelt een belangrijke rol voor de waarde van de temperatuur en dampdruk in de middelste lagen van het gewas. Een betere parameterisatie van frekwentie van de vlagen, de stomataire weerstand en het turbulente transport zal een nog betere simulatie opleveren van het gewasmicroklimaat.

انتقال الحرارة و البادئة بيني و داخل النظم المكون من التربة و الغطاء النباتي و الطبقة من الغلاف الجوي القريبة من الغطاء النباتي، معالجة نظرية و التحقق من صحتها.

ملخص

إن الهدف من هذا العمل هو وصف انتقال الحرارة و البادئة بيني التربة و الغطاء النباتي و الطبقة الهوائية من الغلاف الجوي القريبة من الغطاء النباتي. إن هذا الانتقال ذو طبيعة متلاطعة نظراً لتواجد كياناته أو دوامات هوائية كهيرة النطاق الجحبي في تلك الطبقة الهوائية. إن المردود الدوري لتلك الكيانات الهوائية بالقرب من قمة الغطاء النباتي وطاقته الجحبي الكبير بالنسبة لارتفاع الغطاء النباتي يؤدي إلى استبدال الهواء الموجود داخل الغطاء النباتي و الذي تر شحنته بكميات من الحرارة و الرطوبة بهواء جديد من ارتفاع أكبر بكثير من ارتفاع النباتات. هذا يجعل تلك الكتل الهوائية المتحسسة مسئولة عن أغلب التبادل للحرارة و البادئة بيني الهواء الموجود داخل الغطاء النباتي و الهواء الموجود أعلى منه. إن تلك الدوامات الهوائية مسئولة أيضاً عن جزء كبير من تبادل كمية الحركة بين الغطاء النباتي و الطبقة الهوائية من الغلاف الجوي القريبة منه. إن هناك فجوة في معرفتنا لتأثير تلك الكيانات الهوائية على التربة و الغطاء النباتي ككل، ولذلك فإن تلك الدراسة تر توجيهها لدراسة تأثير تلك الكيانات الهوائية على سلوك التربة و الغطاء النباتي على المدى الطويل مثلاً ذلك بالسلك الحراري و الرطوبي للتربة.

إن البحث الحالي يتمثل في خمس خطوات:

(١) بناء موديل أو نموذج رقمي عديد الطبقات، لتربة ذات غطاء نباتي، يأخذ في الحسبان التبادل الأشعاعي و الغير اشعاعي للطاقة و البادئة بيني و داخل أجزاء ذلك النظم المكون من التربة و الغطاء النباتي و الطبقة السفلى من الغلاف الجوي. لقد تم التركيز في هذا النموذج على تأثير التلطعية في انتقال البادئة و الطاقة على سلوك التربة و في نفس الوقت تر إعطاه اهتمام كاف لبعض العمليات الأخرى ذات الأهمية على سلوك النظم مثل المقاومة الشجرية للنباتات و مقاومة التربة للبحر. إن أخذ التلطعية في الحسبان بصورة مباهرة يجعل الموديل فريد في نوعه حيث إنه المحاولة الأولى لوضع أو تأسيس موديل تلتطعية على أساس من ميكانيكا الموائع لوصف انتقال البادئة و الطاقة داخل الغطاء النباتي (الكيلاني و آخرون ١٩٩٤ ب،). إن التمهيد النظري للنموذج يحظى أساساً صلب من ميكانيكا الموائع لطريقة الأحلل الهوائي، كما تر وصفها لأول مرة بواسطة جودريل ١٩٨٩، و كما تر إقتراحها بواسطة الكيلاني ١٩٨٩ و الكيلاني ١٩٩١.

(٢) معالجة الطرق السابقة المستخدمة لوصف تلك العملية بصورة غير مباشرة مثل: النمذج أو الموديلات العالمة لإغلاق و نماذج السريان العشوائي. إن التحليل الوصف و الكمي لكلا النوعي من النمذج يظهر بعض عيوب أو توجه القصور لتلك المعالجات أو الطرق.

(٣) لقد تم استخدام التحليل الرياضي للمعادلات الرياضية الواصفة لنظم التربة و الغطاء النباتي لكي نحصل على فهم أو تقدير فيزيائي لتأثير التلطعية في انتقال البادئة و الطاقة على سلوك نظم التربة و الغلاف النباتي و ديناميكية تفاعلهم. إن التحليل الرياضي يظهر أن التفاعل بين الكيانات الهوائية و الغلاف النباتي يؤدي إلى ظهور نوع من عدم الخطية في سلوك التربة و الغلاف النباتي. إن هذا السلوك الغير الخطي يحتمر إستخدام معالجة تلتطعية للنظم المكون من التربة و الغطاء النباتي. لقد تر تحليل عدم الخطية تلك و دراسة تأثيرها على النظم.

(٤) دراسة حساسية للمعادلات الواصفة للنظم و أيضاً لنموذج مبسط للنظم. لقد أظهرت دراسة الحساسية تلك تأثير بعض العوامل على الثوابت الزمنية لطبقات الهواء الدنيا من الغلاف النباتي و كيف أن الفترة الزمنية بيني مرور الكيانات الهوائية تؤثر على سلوك النظم.

(٥) إجراء فحص لصحة الموديل أو النموذج الرقمي المقترح بمقارنته بالقياسات الفعلية لتجربتيين حقيقيتين. لقد أظهرت نتائج الموديل تطابق جيد للغاية مع القياسات الحقيقية. إن البرمترات المطلوبة لتجربة ذلك النموذج الرقمي ليس من الصعب اشتقاقها كما أن لها أساس نظري. إن النموذج المقترح يمثل تحسن معدود عن الموديلات المتاحة حالياً ولكنه يتطلب حسابات مكثفة.

سوف تقوم اللى بتغطية كل تلك الخطوات الخمس بصورة مفصلة و ذكر النقاط الأساسية التي تر اجزائها و الاستنتاجات التي تر التحصل عليها من تلك الرسالة.

(١) بناء موديل أو نموذج رقمي عديد الطبقات لتربة ذات غطاء نباتي;

هذه الغلظة تمت تغطيتها في الفصل الثاني من الرسالة و جزء ٦.٣ و جزء ٢.١٠.٤ و جزء ٤.٠٤ و جزء ٥.٤ و جزء ٦.٤ والفصل الخامس.

إن الحصول على حل لمناخ الغطاء النباتي والتربة يخطب، لطبقته الهواء داخل الغطاء النباتي، حل فئة من المعادلات للتغير المتوسط المستخدمة لوصف انتقال المادة والطاقة وكمية الحركة داخل وسط مائع ذو حركة دوامية (الهول). إن الفترة الزمنية أو الحيز المكاني الاتي يتر عليهما حساب القيم المتوسطة يحدد نوع الارتباطات الناتجة بين المتغيرات المطلوب حسابها والاتي يجب ايجاد تعبيرات لوصفها. توجد عدة طرق لاتخذ قيم متوسطة لتلك المعادلات. وفي المهكلة نبحث (الاعتبار، فلقد تم اقتراح طريقة لاتخذ المتوسطات لتلك المعادلات تفصل بين الانجرافات الكبيرة عن المتوسط والانجرافات الصغيرة عن المتوسط. إن الانجرافات الكبيرة عن المتوسط (التذبذبات) في سرعة الهول (كمية متجهة) وفي تركيز الكميات القياسية (الحرارة أو الرطوبة أو ثاني أكسيد الكربون) تنتج نتيجة لوجود لحر كاس الدوامية كبيرة الحجر في حقل السرياني. إن الحركات الدوامية أو الكيانات الهوائية كبيرة الحجر، متوافقاً ذلك على نطاقهم الحجمي وعلى ميكانيكة نهااتهم وفتاتهم، تظل تتحرك خلال كل الحقل ولذلك فإن تأثيرهم على انتقال كمية الحركة والمادة يصبح معدوم أو همل في كل أرجاء الحقل. أما الانجرافات الصغيرة في السرعة والتركيز فإنها ترجع إلى نطاقات الحركة الصغيرة. تنشط تلك الحركات الصغيرة خلال فترة الهدوء النسبي بين فترات مرور الكيانات الهوائية في قمة الغطاء النباتي أو في الأماكن الواقعة بين موافق تواجد الكيانات الهوائية كبيرة الحجر.

إن طريقة أخذ المتوسطات المقترحة لاتخذ في الحسبي بطريقة مباشرة التقطعية وتأثيرها على سلوك النخل. تؤخذ تلك الطريقة إلى ظهور نوع من الارتباطات بين الحركات الاضطرابية الكبيرة الحجر والصغيرة و النباينات المكانية داخل أجزاء الغطاء النباتي في كل من معادلات بقلة كمية الحركة و الكميات القياسية. تؤخذ الحجوم التي تتحرك عليها عملية أخذ المتوسطات وطريقة أخذ تلك المتوسطات إلى الحصول على كميات في المعادلات المتوسطة أسهل في إيجاد تعابير كمية لها.

وفي حالة وجود غطاء نباتي متجانس؛ فإننا نحصل على أربعة كميات أو مقادير لاتتلاهي في عملية أخذ المتوسط لعهد من المكررات أو في عملية أخذ المتوسط الزمني. تلك الكميات تمثل السريان أو الفيض الاضطرابي أو الدوامي لكل من كمية الحركة والكميات القياسية نتيجة لطاقتهم الحركة الكبيرة والصغيرة والتفاعل بينهم. يدهش المقادير الأولى خلال عملية إلتحام الكيانات الهوائية للغطاء النباتي بيدها يدهش المقادير الثاني خلال فترة الهدوء النسبي التي تسود بين فترات إلتحام الكيانات الهوائية للغطاء النباتي. إما الفيض الناتج من التفاعل بين نطاقات الحركة الكبيرة والصغيرة، فيكون هاماً في الفترة التي تسبق وتلي مرور الكيانات الهوائية عند قمة الغطاء النباتي.

فيما يتعلق بمعادلة بقلة الكميات القياسية، فإن التعبير المستخدم لوصف السرياني الاضطرابي الناتج عن الكيانات الهوائية الكبيرة الحجر و السرياني الناتج عن التفاعل بين نطاقات الحركة الكبيرة والصغيرة 'بني' على أساس إستخدام دالة تعرف مقدار لإحلال الهوائى والتي تحظى مقدار التغير في مقدار الكمية القياسية المحزنة داخل الغطاء النباتي من بداية إلتحام الكيانات الهوائية للغطاء النباتي وحتى نهايتها. هذا التغير يعطى قيمة لفرق السرياني بين أعلى أو طبقاً وأسفلها في نهاية فترة مرور الكيانات الهوائية.

ونظراً لأننا نفترض درجة معينة من تجديده الهواء داخل الغطاء النباتي نظراً لمرور الكيانات الهوائية، فإن قيمة معامل الإلتحام الاضطرابي خلال فترة الهدوء النسبي سوف تكون هامة للغاية في تحديد مقدار التذبذب للحرارة والمادة (الكميات القياسية) داخل الغطاء النباتي. ويقدم الكيان الهوائي الثاني، فإن التغير في تلك الكميات المحزنة سوف تشكل الفيض الناتج من مرور الكيان الهوائي. ولذلك فإن إستخدام تعبير سليم أو صحيح للمعامل الاضطرابي خلال فترة الهدوء النسبي همل جداً في تحديد مقدار القطاعات والمصادر والطاقة والمادة داخل الغطاء النباتي. لقد إقترضا في ذلك النموذج تجديده كامل للهول ويبدو من القياسات أن ذلك لإفتراض غير مجاف للحقيقة، كما يبدو ذلك من تحليل الخواص الزمانية لسرعة الرياح و الحرارة داخل حقل ذرة (فصل ٣).

لكي نحصل على تغير لتلك المعامل، فلقد تم إجراء تحليل إحصائي للتوزيع التكراري الواضح للنسبة بين القيم اللحظية والقيم المتوسطة لتباين السرعة الرأسية للرياح. لقد إعتبرنا تلك النسبة كمؤشر لتصرف معامل الإلتحام الاضطرابي.

ولقد تبين من ذلك التحليل لعينتين زمنيتين، كل منهما تمثل سبع ساعات من القياسات، أنه خلال حوالي ٧٠٪ من الوقت فإن القيم اللحظية المقاسة لتباين السرعة الرأسية للرياح كانت أقل من القيمة

المتوسطة وساهمت بأقل من ٢٠٪ من إجمالي مجموع تباين السرعة الرأسية للرياح. بينما الفجوات الهوائية أو الجركات الهوائية الشديدة الناجمة من مرور الكيانات الهوائية احتلت أقل من ١٠٪ من الوقت الكلي ولكنها ساهمت بحوالي ٦٠٪ من إجمالي مجموع تباين السرعة الرأسية للرياح. لقد أظهر من التحليل أن مقدار معامل الانتقال لإضطرابي خلال فترة الهذوء النسبي يبلغ حوالي ٢٧٪ من التعابير الشائعة الاستعمال.

لقد أظهر أيضا أن تلك الطريقة لوضع تعابير لوصف قيمة معامل الانتقال لإضطرابي تعكس ترتيب الأحداث المختلفة لطور مرور الكيانات الهوائية (أي هورة الاستنزاف لبحزوي الكيانات القياسية في طبقات هواء الغطاء النباتي ثم يليه ذلك البحزوي خلال فترة الهذوء النسبي). لقد تم إثبات ذلك عن طريق إستخدام النسبة بين القيم اللحظية والقيم المتوسطة لتباين السرعة الرأسية للرياح وتوافقها الزمني مع كلا من غياب مناطق الحرارة العالية ومناطق زيادة سرعة الرياح في الجرائط الزمنية. وفي فصل ٢، فلقد تم إستخدام ميزانية الطاقة لأوراق النبات لوضع تعابير كمية لوصف المقادير الناجمة من التفاعل بين أوراق النبات والهواء. تنتج تلك المقادير من عملية أخذ المتوسطات الحجمية لمعادلات الانتقال لإضطرابي لحجم من الهواء عميق الارتباطية. وفي قسم ٤-٤، فإن التجزئة للطاقة المفتوحة عند سطح التربة إلى طاقة هامة للبحر وطاقة صاعدة قد تم أخذها في الحسبان عن طريق حساب النسبة بين الخطوة الزمنية للجاذبية و الثابت الزمني للطبقة الهوائية الأولى المجاورة لسطح التربة. وتبعاً لمقدار تلك النسبة، فإنه يتم إستخدام إما حل تحليلي للإيجاد قيمة ضغط بخار الماء المتزاد في الطبقة الهوائية الأولى أو يتم إستخدام حل رقمي لحساب ذلك الضغط البخاري وهكذا يمكن الفصل بين معادلاتي الجرولة الكاملة والصاعدة. ولقد تم حساب مقاومة التربة للبحر عن طريق إستخدام المسامية الكلية للتربة ومساميتها الهوائية.

أما بالنسبة للفصل بين تلك المعادلتين في داخل طبقات التربة، فلقد تم ذلك عن طريق حساب الفرق في قيض بخار الماء بين قمة وقاعدة طبقات التربة المختلفة.

إن حساب سريان أو قيض الماء بين طبقات التربة المختلفة إما في حالته السائلة أو الغازية يُستخدَم في حساب الجهد الرطوبي للتربة. هذا الجهد الرطوبي للتربة سوف يؤثر على حساسية شعور الورقة للجهد الرطوبي للورقة عن طريق إنتاج جذور النبات لكميات من حمض الأرسنيك. وتتوقف مقادير تلك الكميات المنتجة على الجهد الرطوبي للتربة. لقد تم أيضا وضع نموذج فرعي كامل لوصف حركة الماء داخل النبات.

٢) مخاطبة المحاولات السابقة:

لقد تم تغطية ذلك الجزء في جزء ٢-٣ و ٧-٢.

تقع المحاولات السابقة لوصف ذلك الانتقال أو التبادل بين الغطاء النباتي والطبقة الدنيا من الغلاف الجوي تحت طائفتين أساسيتين: النماذج الأيرلوية (التي تصف حزم هوائي ثابت) العالية الأرتفاع والنماذج الجواندينية (التي تصف حزم هوائي متحرك) ذات السريان العشوائي. في النماذج الأيرلوية التي تمت عملية أخذ المتوسطات لها على فترة زمنية طويلة، فإن إنتاج السريان وسالب إنتاج مدرج التركيز لا يتفق. إن محاولة حل تلك المشكلة تتم بزيادة مستوى الأرتفاع للموديل. يتم ذلك عن طريق الأخذ في الحسبان للمقدار الواصف للانتقال الاضطرابي في معادلات الرتبة العالية وتأثير ذلك المقدار على مدرج الأرتقال الاضطرابي في المعادلة الأدنى. إن واحد من الافتراضات الأساسية في تلك المعادلات أن كل المقادير داخل تلك المعادلات لها قيمة متوسطة ثابتة خلال الخطوة الزمنية للجاذبية. لقد أظهرنا من تحليل بعض الأبحاث المشهورة أن ذلك الافتراض أبعد ما يكون عن الحقيقة. ونظراً لعدم التغطية العالية لتلك المعادلات، فإننا نتوقع أن يعطى السلوك المتذبذب لتلك المقادير خلافاً لتلك المعادلات عن نفس المقادير في حالة كونها ذات قيمة ثابتة مساوية لقيمة المتوسط.

ويبدو أن الافتراض بإسترجاع المعلومات المفقودة، نتيجة لعملية أخذ المتوسطات، بإلارتقاء بمستوى الأرتقال إفتراض غير صحيح. ويرجع ذلك إلى دور الكيانات الهوائية في تكوين ارتباطات بين السريانات (أي تكوين ارتباطات على مستوى أعلى) لا يتم معادلتها بدور ضغط الهواء الاستاتيكي في تحطيم تلك الارتباطات. إن دور ضغط الهواء الاستاتيكي في تحطيم تلك الارتباطات يكون مركزاً حول موضع مرور طبقة القص البائنة في قمة الغطاء النباتي. وفي حقل السربلي للهواء داخل الغطاء

النبات، فإن النسبة بين المسافة التي يتقدم فيها الضغط بتدعيم أو مسح الارتباطات إلى المسافة بين الكيانات الهوائية المتتالية أقل بكثير من واحد، هذا بصورة أتوماتيكية يجعل بعض الارتباطات المستخدمة لتألق المقادير العالية غير صحيحة.

والمشكلة الأخرى التي تظهر في حالتنا هذه هو واحد من الاشتراطات المطلوبة لأخذ المتوسطات للمعادلات الغير خطية. إن أخذ المتوسطات تبعاً لطريقة رينولدز يتطلب اشتراط معينين فيما يتعلق بانتظام سلوك المقادير خلال الفترة الزمنية التي يتم عليها أخذ المتوسط. إن التباين الشديد الزماني و/أو المكاني للمقادير المتأخذ لها المتوسطات يجعل إستيفاء ذلك الشرط أمراً موضع شك. ولذلك، فإن صحة تلك النتائج المحصل عليها، لوصف السريان للغطاء النباتي، من النماذج شائبة الارتباط أو الأعلى من ذلك لابد أن تكون محل شك.

والموديلات الجرانجية هي طريقة أخرى مستخدمة لوصف السريان داخل الغطاء النباتي وهي تحاكي مسار عدد كبير من الجزيئات المستقلة في حركتها وتجميع النتائج لمواقع تواجد الجزيئات باعتبارها مشكلة لتقاطع التركيز المتوسط داخل الغطاء النباتي. إن إضافة تحول التركيز لتحط كبير من الجزيئات يتغاضى عن أي اختراق أو دخول الكيانات الهوائية داخل الغطاء النباتي يؤدي إلى تواجد ارتباطات بين حركة الجزيئات على طول ارتفاع الغطاء النباتي. ولذلك فإن الجزيئات لا تتحرك بصورة مستقلة طول الوقت. إن هذه الارتباطات يجب طرحها من المجموع الكلي.

إن المجادلة بأن موديلات الحركة الهوائية تأخذ بصورتها الحالية في الحساب الارتباطات بين الجزيئات الناتجة عن تواجد الكيانات الهوائية المتشابهة في حقل السريان تم مناقشتها في الإعتراض على الاشتقاق النظري المعطى بواسطة لامب (١٩٨٠) في ملحق ١.ب.

والمشكلة في اشتقاق لامب (١٩٨٠) تتمثل في أن دالة الكثافة الاحتمالية المشتركة لتحديد كبير من الجزيئات لا يمكن التعبير عنها كحاصل ضرب لحوال الكثافة الحدية أو الجانبية لكل الجزيئات والتي تكون مسوية كل منها للأخر.

ولقد تم إقتراح طريقة لجمع تحول التركيز، كما يتم وظيفتها بواسطة مؤثر حساس مغزور في حقل التركيز والذي يبدأ بالتدرج في رؤية سحابات الغدر مجزأة - نتيجة وجود مصادر للطاقة أو المادة- لكي تأخذ في الحساب تلك الارتباطات.

٣) التحليل الرياضي للمعادلات الحاكمة لنظام الغطاء النباتي والتربة.

لقد تمت تغطية ذلك الجزء في جزء ٢.٤

إن الهدف من ذلك الجزء هو الإجابة بصورة تحليلية أو رياضية، عما إذا كان معامل إنتقال إضطرابي ثابت زمنياً سوف يؤدي إلى الحصول على نفس التغير المتوسط للحرارة أو ضغط بخار الماء للهواء كعامل إنتقال إضطرابي متذبذب زمنياً ولكي له نفس المتوسط. ولقد تم أيضاً تحليل إن كان ذلك يؤدي إلى إختلاف في قيمة السريان الحراري والتقاطع الحراري للتربة.

بالنسبة لنظام الهواء داخل الغطاء النباتي، فإن التحليل الرياضي تتعلق بتحويل أربع معادلات تفاضلية جزئية واصفة للنظام إلى معادلات تفاضلية عادية. إن هذه المعادلات هي معادلة حرارة الورتقة، معادلات حرارة وضغط بخار الماء للهواء ومعادلة لنقص ضغط بخار الماء للهواء. ولقد تبين من التحليل أن بعد دخول كيان هوائي إلى داخل الغطاء النباتي، فإن حرارة الورتقة والهواء والضغط البخاري للهواء ونقص ضغط التبخر لبخار الماء للهواء تأخذ في الارتداد اللاحق من قيم تمثل الجبل الثابت. هذا الجبل الثابت هو حالة خطية في معاملات الانتقال الاضطرابي. ولذلك فإنه في المراحل الأولى لارتداد الجبل نحو

القيم المبتدئة للجبل الثابت (الارتداد)، سوف يكون هناك إعتناء غير خطي على معاملات الانتقال الاضطرابي نظراً لسلوك الأسي للمعادلات. وبالتالي فإن إستخدام قيمة متوسطة لمعامل الانتقال الاضطرابي على فترة زمنية طويلة لن تعطي نفس الجبل (حرارة النبات والهواء وضغط بخار الماء للهواء) كاستخدام التغير المتوسط لسلوك الغطاء النباتي تعتمد على النسبة بين الفترة الزمنية للدخول المتعاقب للكيانات الهوائية داخل الغطاء النباتي إلى الثوابت الزمنية لطبقات هواء الغطاء النباتي. فإذا كانت تلك النسبة في حدود ٢ إلى ٣، فإن الغطاء النباتي سوف يكون دائماً في الجزء الغير خطي من الجبل. ومتوافقاً على مدى سيادة تلك العملية، فإن نظام الغطاء النباتي قد يظل في النطاق الغير خطي من الجبل لجزء معدود من الوقت.

ونظراً للتغيرات خلال الوقت للنسبة بين معكوس التردد الزمني بالنسبة للثوابت الزمنية للظلم، فإن نظام الغطاء النباتي سوف يسمح مع الوقت بمناطق مختلفة في السلوك الغير خطي والخطي للجل. ولقد افترض أن التردد الزمني لدخول الكيانات لدخول الغطاء النباتي يتم التحكم فيه بصورة ديناميكية أي أنه يتوقف على مقدار نقص الريح عند قمة الغطاء النباتي بينما الثوابت الزمنية لطبقات الهواء داخل الغطاء النباتي تتأثر بصورة أساسية بالملامحة الشجرية للنباتات والعوامل التي تتحكم فيها (مثلاً الجهد الرطوبي للتربة والضوء إلخ). ولذلك فإن دوراً في سوف تغطي المناطق المختلفة للأعمدة الغير خطي والخطي للجل.

ولقد تبين أن عمر الخطية تتجاوز زمناً بنسبة عشر مرات على الأقل خطية حقل التركيب القريب ، كما تم شرحها بواسطة وويج (١٩٨٩) أو فنيجالي (١٩٨٥) ، في إعتقادهم لاستحتمل نظرية معامل التوصيل (نظرية ك) في وصف عمليات الانتقال الاضطرابي داخل الغطاء النباتي. ولذلك فإن عمر الخطية داخل الغطاء ليست راجعة فقط لتأثير الحقل القريب.

إن الخطوة التالية في التحليل الرياضي كانت تحليل إستجابة التربة لعدم الخطية تلك. ولقد تبين من الحل الرياضي للمهكلة الغير متجانسة للقطع الحراري للتربة أن التربة تكامل تأثير النقطعية في قيم المعاملات الخاصة لمفكوك ذوال أيثنى لحرارة التربة أي مفكوك ذوال ثورييه. ولقد تبين من التعبير الرياضي لتلك المعاملات أنهم يروا كل مطرد أو صور النقطعية، سوله كانت راجعة لتغيرات في التجميد الإشعاعي أو راجعة لتغيرات في حرارة الهواء القريب من سطح التربة أو نقص ضغط بخار ماء عن التهب.

تتكون كل قيمة لتلك المعاملات لمفكوك ذوال أيثنى لحرارة التربة من جزء ابتدائي يتناقص بصورة أسية مع الزمن وجزء آخر يكامل سلوك التجميد الإشعاعي والتجميد الغير إشعاعي (حرارة الهواء القريب من سطح التربة أو نقص ضغط بخار ماء عن التهب). والتجميد الغير إشعاعي هو الذي يتأثر بالكيانات الهوائية المتناسكة.

إن معدل الأحتضار للجزء الابتدائي للنقطعيات السابقة في الماضي يكون أعلى لأرقام الموجة العالية. ولقد تبين أيضاً أن تأثير النقطعية على معاملات مفكوك أيثنى يعبر عن نفسه بنفس الصورة في جميع قيم أرقام الموجة. ولذلك فإن الأحتياج لدراسة تأثير النقطعية يتم في رقم موجة واحد فقط. إن تأثير النقطعية على القيمة التكاملية للتجميد الغير إشعاعي تحدد كمياً تأثير النقطعية على التربة. إن الحل الرياضي يكامل كل تفاصيل النقطعية في التجميد الإشعاعي والغير إشعاعي.

٤) دراسة حساسية

لقد تم تغطية ذلك الجزء في فصل ٢.١.٢.٤ ، ٢.٢.٤ ، ٢.٣.٤ ، ٤.٢.٤ ، ٣.٤ لكي نسط التحليل ولكي نحصل على فهم أو تصور فيزيائي لتأثير النقطعية على النظام، فلقد افترضنا فصل في النطاق الزمني لاستجابة سلوك طبقات هواء الغطاء النباتي وسلوك طبقات التربة للنقطعية. لقد سمح لنا ذلك بأنحد تكامل تأثير عمر الخطية على متوسط حرارة الهواء القريب من سطح التربة ونقص ضغط بخار ماء عن التهب وإطلعنا ذلك التأثير للمعادلات الواصفة لمعاملات مفكوك ذوال أيثنى لحرارة التربة. ولكي نحسب القيم المتوسطة لحرارة الهواء القريب من سطح التربة ونقص ضغط بخار ماء عن التهب، فلقد تم افتراض توليفة من عدة مواقف.

أول تلك المواقف: افتراض تواجد حل إتراني أو حل متغير مع الزمن. في حالة الحل الإتراني (وهو ما نطلق عليه حل تقريبي) فإنه تم تجاهل التغير في تخزين الحرارة داخل أجزاء النبات بينما في الحل المتغير (وهو ما نطلق عليه حل أكثر دقة) ، فإن ذلك التأثير قد تم أخذه في الحسبان.

وفي الافتراض الثاني السابق ذكره فإنه يتم معاملة الغطاء النباتي ككونه وحيد الطبقة أو عديد الطبقات. وفي حالة غطاء نباتي وحيد الطبقة، فإن تم افتراض أن تلك الطبقة جيدة الخلط بينما في حالة الغطاء النباتي عديد الطبقات، فإنه تم افتراض عدة طبقات لكل منها كثافة ووقتية مختلفة ومعامل انتقال اضطرابي، وفي حالة الحل المتغير فإنه تم فقط افتراض غطاء نباتي عديد الطبقات.

وفي حساب متوسط درجة حرارة الهواء ونقص ضغط بخار ماء عن التهب، فإنه تم إستحتمل قيمة ثابتة زمناً لمعامل الانتقال الاضطرابي. ولقد كانت تلك القيمة أكبر بمقدار أربع مرات لموديل عمر تواجد النفخة الهوائية (نموذج عمر الإحلال الهوائي) عنها في موديل النفخة الهوائية (نموذج الإحلال وفي نموذج الإحلال الهوائي، فإن أغلب المساهمة لمعامل الانتقال الاضطرابي تحدث خلال طور

إنتحار الكيان الهوائي المتماسته للغطاء النباتي ببينما في فترة الهواء النسيج التي تتعقب ذلك، فإن قيمة معامل الانتقال الاضطرابي تكون أقل بكثير عن متوسط نظيرتها في نموذج عدم الإرحلال الهوائي. وفي نموذج الإرحلال الهوائي، فإن القطع الابتدائي لحرارة وضغط بخار الماء للهواء المستخدم في الحسابات بعد مرور الكيان الهوائي كان مساوياً لحرارة وضغط بخار الماء للهواء على ارتفاع يبلغ ضعف ارتفاع الغطاء النباتي.

وفي توليفة غطاء نباتي وحيد الطبقة و حل تقديبي، فإن النتائج هي أن نموذج الإرحلال الهوائي أعطى تقييم أكبر للتحميل الغير إشعاعي على التربة عن نظيره نظراً للتغير الأقل لمعامل الانتقال الاضطرابي والتي تؤدي الى ربط درجة حرارة الورقة أكثر بالتحميل الإشعاعي عن ربطها بدرجة حرارة وضغط بخار الماء للهواء عالياً فوق الغطاء النباتي. هذاسوف يزيد درجة الحرارة الارتزانية للورقة. سوف يكون لذلك تأثير رجعي على حرارة وضغط بخار الماء للهواء داخل الغطاء النباتي نظراً لأن معاملات الربط لمصدر الطاقة والهدأة مع طبقات الهواء تكون أعلى في نموذج النخلة الهوائية عنها في نموذج عدم تواجد النخلة الهوائية. والنتيجة النهائية أنه إذا لم تكن الفترة الزمنية بين مرور كيانين هوائيين متعاقبين صغيرة بالمقارنة بالخواص الزمنية لطبقات الهواء، فإن الخلط الهوائي الضعيف خلال فترة الهواء النسيج سوف يزيد حرارة وضغط بخار الماء للهواء داخل الغطاء النباتي بالمقارنة بنموذج عدم تواجد النخلة الهوائية. وبالتالي فإن افتراض الخلط الجيد للطبقة الوحيدة للغلاف النباتي سوف يؤدي الى أن تلك الزيادة في درجة الحرارة وضغط بخار الماء للهواء سوف تحدث على سطح التربة.

وفي توليفة الحل التقريبي وغطاء نباتي عميق الطبقات، فإنه يمكن إظهار أن المصفوفة العكسية التي تتحكم في الحل الارتزاني لطبقات الهواء، عناصرها الداخلية مضروبة في حالة نموذج الإرحلال الهوائي برتر بمثل النسبة بين قيمة معامل الانتقال الاضطرابي لنموذج عدم الإرحلال الهوائي إلى تلك لنموذج الإرحلال الهوائي. هذه المصفوفة يجب ضربها بمصفوفة (ش) مجازاً بمصفوفة الشايفس والتي تشير عن مقادير المضار داخل كل طبقة في الغلاف النباتي. هذه المصفوفة (ش) متوافقة على أي نظام معادلات تقوم بحل (نظير نقص ضغط بخار الماء عن التهبج للهواء أو حرارة الهواء)، غير معتمدة على الحل النهائي. إن ذلك يعني خفض نسبي لدور الحدود العليا والسفلى للنظام المحاكى في الحل الارتزاني ومساهمة أعلى لطبقات الهواء الداخلية للحل في طبقة معينة.

إن الخلط الداخلي الأقل خلال فترة الهواء النسيج يؤدي إلى حدوث تأثير أعلى للعناصر الداخلية في المصفوفة (ش) لحرارة وضغط بخار الماء للهواء في طبقة معينة بالمقارنة لنموذج عدم الإرحلال الهوائي والذي فيه تكون نتيجة أعلى لمعامل الانتقال الاضطرابي نهيفة طول الوقت. أماما كان ذلك يؤدي إلى في قيمة أعلى أو أقل لنقص ضغط بخار الماء للهواء عن التهبج عن تلك في الحدود للنظير، فإن ذلك يتوافق على قطاعا المقاومة الشغرية والإشعاع الصافي.

وفي حالة الأكثر دقة، فإنه تم فقط إستخدام نموذج عميق الطبقات. لقد تم ذلك بإستخدام برنامج ماشكاد، نوع من برامج الكمبيوتر التي يمكن إستخدامها لحل ورسم حلول المشاكل الرياضية، أو نموذج رتبي مبسط. ولقد إستخدم البرنامج المبني بالمشكاد نفس طريقة الحل لدرجة حرارة الورقة وحرارة وضغط بخار الماء للهواء كالنموذج الرتبي، ولقد احتوى برنامج المشكاد على عدد أقل من الطبقات وتم تجريبه لفترة زمنية أقصر (في لمدة ثلاث ساعات لحوث النخلة الهوائية، كل منها تستغرق 100 ثانية). ولقد إفتراضاً أن حرارة التربة ثابتة خلال تلك الفترة وتم تكامل تأثير النخلة الهوائية على قيمة التجميل الغير إشعاعي وحرط الحدود لسريان الجوارح للتربة. وتكون تجريبات المشكاد جزءاً من دراسة الحساسية للنظير التي سنناقشها في النقطة التالية. إن النموذج الرتبي المبسط هو نفسه بالضبط كالنموذج الرتبي في الفصل الخامس، ماعدا أنه ليس به تأثير رجعي لجفاف سطح التربة على الحل (أي أنه تم افتراض أن ملاومة التربة للبحر صفر طول فترة المحاكاة (1 يوم)).

إن النتائج من ماشكاد تظهر أن بالنسبة لسريان الجوارح للتربة والتجميل الغير إشعاعي على سطح التربة، فإن كثافة ورتبية منخفضة في الجزء السفلي من الغطاء النباتي ومعامل الانتقال الاضطرابي الأقل تزيد الفرق بين نموذج الإرحلال وعدم الإرحلال الهوائي. وهذابرجح إلى زيادة الثابت الزمني للطبقة الهوائية الدنيا من الغلاف النباتي وتقليل النسبة بين مقلوب التردد الزمني لاختراق الكيانات الهوائية للغطاء النباتي إلى الثابت الزمني لأحد طبقات الهواء القريبة من سطح التربة. وبالتالي فإن تأثير الهواء المتخذ بواسطة النخلة الهوائية على تخفيف التجميل الغير إشعاعي على سطح التربة سوف تحدث عند سطح التربة.

أما النتائج من النموذج الكامل المبسط، والذي تمت تجريبه ليوم صيف حار شائع الجردوث في مرجح

تظهر فرق معنوي بين إقتراضات كلا من الدفحة الهوائية وعدم تواجد الدفحة الهوائية على حرارة التربة والسريريان الحراري للتربة. ولقد بلغ الفرق في وقت الظهيرة ٩- درجات مئوية للفرق في درجة حرارة الهواء بين نموذجي الدفحة الهوائية وعدم تواجد الدفحة الهوائية ونقص تهوية يتنازل الماء للهواء على (+) ١٠٠٠ بسكال للفرق بين نموذجي الدفحة الهوائية وعدم تواجد الدفحة الهوائية) في الجزء السفلي من الغطاء النباتي. ولقد كانت فترة إستقرار الأوراق لتكرار حدوث الدفحة الهوائية ١,٥ دقيقة. ولقد كلى السبب في هذا الفرق الكبير بين النموذجين راجعاً إلى التواهب الزمنية الكبيرة لطبقات الهواء السفلي القريبة من سطح التربة. ولقد كانت تلك التواهب الزمنية الكبيرة راجعة إلى الإلبيم المستخدمة لمعامل الإلتقال الأرضي، الكثافات الورقية المنخفضة في الجزء السفلي من الغطاء النباتي والمقاومة الشجرية العالية والتي كانت دالة لهدية الضوء.

وتظهر تجربات الماشكاد أنه من الممكن أن لا يكون هناك إختلاف في التجميل الطاقى على التربة مع وجود إختلاف في التقسيم للطاقة على أسطح النباتات.

ولقد تم إجراء تحليل كامل للتفاعل بين الأوراق و الهواء لمؤلف نباتية مميزة لمناطق مناخية مختلفة. ولقد أظهرت الديناميكيات لتلك التفاعل وأهمية المقدر الغير ثابت على الجذ. ولقد أظهرنا أيضاً أن المتغيرات الواضحة لحالة الهواء (أي حرارة الهواء وضغط بخار الماء به ونقص ضغط بخار الماء به من التهوية) والمصادر للطاقة والمدة تنبع خلال كل فترة دورة مرور الكيانات الهوائية سلوكه لسي. وفي قسم ٢.٤؛ فلقد أظهرنا من عملية الوزن النسبي للمقادير في معادلة السريان الأرضي المتخوذ عليها المتوسط لفترة طويلة أن الارتباط بين المعامل للطاقة والرطوبة والسرعة الرأسية للرياح، والذي يحتاج من التفاعل بين الهواء الذي يأتي إلى داخل الغطاء النباتي والمصدر، له نفس الكمية كالمقادير المنتجة للسريان. ولذلك فإنه يجب أخذ ذلك الارتباط نتيجة لدخول الكيانات الهوائية إلى داخل الغطاء النباتي في الحسبان.

(٦) النتائج من صحة النموذج المطور.

لقد تمت تغطية ذلك الجزء في فصل ٦.

إن نتائج التحقق من صحة النموذج انظر بوجه علم تطابق جيد للغاية بين كل من البيئة الإشعاعية وحرارة الأوراق وطبقات الهواء. لقد كان هناك على أي حال تفاعل بين تردد دخول الكيانات الهوائية للغطاء النباتي والذي تحدد درجة البله المسبوح بها لقطاعات الكيانات القياسية وبين المقاومة الشجرية التي تتحكم في المعدل الزمني للبناء للقطاعات لضغط بخار الماء وحرارة الهواء. هذا يؤثر على حل ميزانية الطاقة لأوراق النبات. إن إقتراضات النقل الأرضي تلعب دوراً هاماً في التحكم في تغير الحرارة وضغط بخار الماء في الطبقات الوسطى للغطاء النباتي. إن هدف أفضل لتردد مرور الكيانات الهوائية والمقاومة الشجرية والإلتقال الأرضي سوف تسمح حتى بدرجة أفضل من محاكاة المناخ الدقيق للغطاء النباتي.

REFERENCES:

- Arlery, R., 1970. The Climate of France, Belgium, The Netherlands and Luxembourg. In *Climates of Northern and Western Europe*, *World Survey of Climatology*, Vol. 5 (eds.) C. C. Wallen, Elsevier, Amsterdam.
- Balocchi, D., 1992. A lagrangian random-walk model for simulating water vapour, CO₂ and sensible heat flux densities and scalar profiles over and within a soybean Canopy. *Boundary Layer Meteorology*, **61**: 113-144.
- Bar-Yosef, B., and Lambert, J. R., 1981. Corn and cotton root growth in response to soil impedance and water potential. *Soil Science Society of America Journal*, **45**, 930-
- Bear, J., and Bachmat, Y., 1990. *Introduction to modelling of transport phenomena in porous media*. Kluwer Academic Publishers, Dordrecht.
- Berge, H. F. M., 1990. *Heat and Mass Transfer in bare topsoil and the lower Atmosphere*. Pudoc Simulation monogram 33, Pudoc, Wageningen.
- Bergström, H., and Högström, U., 1989. Turbulent exchange above a pine forest II. Organized structures. *Boundary Layer Meteorology* **49**, 231-263.
- Beursenks, J. E. M., Winkels, H.J., de Wolf, J. and Dekker, C.G.C. 1994. Trends of priority pollutants in the Rhine during the last fifty years. *Water Science Technology*, **29**, no.3, 77-85.
- Blackwell, P. S., and Wells, E. A., 1983. Limiting oxygen flux densities for oat root extension. *Plant Soil*, **73**, 129-
- Bolt, G. H., and Groenevelt, P. H., 1972. Coupling between transport processes in porous media. *Proceedings 2nd IAHR-ISSS symposium on the fundamentals of transport phenomena in porous media*. Geulph, Ontario.
- Campbell, G. S., 1977 *An introduction to environmental biophysics*. Springer-Verlag, New York, Heidelberg Science Library.
- Cary, J. W., 1965. Water flux in moist soil : Thermal versus suction gradients. *Soil Science* **100**: 168-175.
- Chen., J., 1984. *Mathematical Analysis and Simulation of Crop Micrometeorology*. Ph.D thesis, Wageningen Agricultural University, The Netherlands.
- Cantwell, B. J. , 1981. Organized Motion in turbulent flow, *Annual Review of Fluid Mechanics* , **13**:457-515.
- Conklin, P. S., and Konner, K. R., 1994. The role of static pressure fluctuations in the structure of turbulence within a hardwood forest canopy. *Proceedings of the 21st conference on Agricultural and Forest Meteorology held in San Diego, California. 7-11 March, 1994.* 175-178.
- Cuwo, working group 5. 1990. Sediment quality in the Netherlands (in Dutch) Ministry of Transport and PublicWorks, The Hague, pp. 57-58.
- De Jong, M. A., 1989. Analyse van gemeten stomataire weerstanden aan snijmais op proef-veld Sinderhoeve gedurende het seizoen 1987 (An Analysis of the measured stomatal resistance of a maize canopy in the experimental site Sinderhoeve during the season 1987), KEMA, Divisie Onderzoek en Ontwikkeling. report 00606-MOB 89-3248, Arnhem 65 p.
- De Jong, M. A., and Schoofs, M. J., 1989. Analyse van gemeten stomataire weerstanden aan snijmais op proef-veld Sinderhoeve gedurende het seizoen 1988 (An analysis of the measured stomatal resistance of a maize canopy in the experimental site Sinderhoeve during the season 1988), KEMA, Divisie Onderzoek en Ontwikkeling. report 515514-MOB 89-3323, Arnhem 56 p.
- Den Dulk, J. A., 1989. The interpretation of remote sensing: a feasibility study. Ph. D. thesis. Wageningen Agricultural University. The Netherlands.

- Denmead, O. T., and Bradley, E. F., 1985. Flux gradient relationships in a forest canopy. In: *The Forest-atmosphere interaction*, eds Hutchinson, B. A. and Hicks, B.B. pp. 421-442. D. Reidel, New York.
- Dexter, A. R., 1987. A stochastic model for the growth of roots in tilled soils. *Journal of Soil Science* 29, 102-
- Drazin, P. G., and Reid, W. H., 1981. *Hydronamic Stability*. Cambridge University Press, Cambridge.
- El-Kilani, R. M. M., 1989: Heat and mass transfer within plant canopies; a first order closure model extended with a non locality term. M.Sc. thesis submitted in partial fulfilment of the M.Sc. Degree in Water Management, at Wageningen Agricultural University, Specialization: Agrohydrology.
- El-Kilani, R. M. M., 1991: Some aspects of energy exchange processes in a plant canopy. *Proceedings of the 20th Conference On Agricultural & Forest Meteorology*, Sep. 10-13 1991, Salt Lake City, Utah, pp. 3-6.
- El-Kilani, R. M. M., Jacobs, A. F. G., and van Boxel, J. H., 1994 a: Intermittent canopy turbulent transport, correlations time domain maps and the resulting inherent inadequacy of using large time averaged second order closure to describe canopy turbulent transport processes, *Proceedings of the 21st Conference On Agricultural & Forest Meteorology*, March 7-11 1994, San Diego, California, pp. 80-83.
- El-Kilani, R. M. M., Jacobs, A. F. G., and van Boxel, J. H., 1994 b. An intermittent model for describing heat and mass transfer within plant canopies. *Proceedings of 21st Conference On Agricultural & Forest Meteorology*, March 7-11 1994, San Diego, California, pp. 76-79.
- Finnigan, J. J., 1979. Turbulence in waving wheat II. Structure of momentum transfer. *Boundary Layer Meteorology*, 16, 213-236.
- Finnigan, J. J., 1985. Turbulent transport in flexible plant canopies. In: *The Forest-atmosphere interaction*, eds Hutchinson, B. A. and Hicks, B.B. pp. 443-480. D. Reidel, New York
- Finnigan, J. J., and Raupach, M. R., 1987. Transfer Processes in Plant Canopies in Relation to Stomatal Characteristics. In: *Stomatal Function*, eds Zeiger, E., Farquhar, G. D. and Cowan, I. R., pp.385-429. Stanford University Press, Stanford, California.
- Flesch, T. K., and Wilson, J. D., 1992. A two dimensional trajectory simulation for nongaussian inhomogenous turbulence within plant canopies. *Boundary layer Meteorology*. 61:349-374.
- Gao, W., Shaw, R. H., and Paw U, K. T., 1989. Observation of organized structure in turbulent flow within and above a forest canopy. *Boundary Layer Meteorology*, 47:349-377.
- Gardner, W. R., 1960. Dynamic aspects of water availability to plants. *Soil Science* 84, 63,
- Gates, D. M., 1980. *Biophysical Ecology*. Springer-Verlag, New York.
- Genuchten, M. Th. van, 1980. A closed-form equation for predicting the hydraulic conductivity of unsaturated soils. *Soil Science Society of America Journal*. 44:892-898.
- Gerwitz, A., and Page, E.R., 1974. An empirical mathematical model to describe plant root systems, *Journal of Applied ecology*, 11, 773
- Glinski, J., and Lipiec, J., 1990. *Soil physical conditions and plant roots*. CRC Press Inc, Boca Raton, Florida.
- Griffiths, J. J., and Soliman, K. H., 1972. The Northern Desert. In *Climates of Africa, World Survey of Climatology*, Vol. 10. (eds.) J.J. Griffiths. pp. 75-132. Elsevier. Amsterdam.
- Goudriaan, J., 1977. *Crop Micrometeorology: a simulation study*. Pudoc. Centre for Agricultural Publishing and Documentation. Wageningen . The Netherlands.
- Goudriaan, J., 1982. Potential production processes. In: *Simulation of plant growth and crop productivity* eds Penning de Vries, F. W. T. and van Laar, H. H. Pudoc. Wageningen.

- Goudriaan, J., 1988. The bare bones of leaf-angle distribution in radiation models for canopy photosynthesis and energy exchange. *Agricultural and Forest Meteorology*, **43**, 155-169.
- Goudriaan, J., 1989. Simulation of micrometeorology of crops, some methods and their problems, and few results. *Agricultural and Forest Meteorology*, **47**, 239-.
- Gowing, D. J. G., Jones, H. J., and Davies, W. J., 1993. Xylem- transported abscisic acid: the relative importance of its mass and its concentration in the control of stomatal aperture. *Plant, Cell and Environment* **16**, 453-459.
- Hemdan, G., 1961. Agricultural Development in Egypt. In: *History of Land Use in Arid Zones*. UNESCO (the title of the article and the book have been translated from an arabic reference).p 119-142.
- Hendricks, A. J., 1994. Monitoring and estimating concentrations and effects of micronutrients in the Rhine delta: Chemical analysis, biological laboratory assays and field observations. *Water Science Technology*., vol **29**, no 3, pp. 223-232.
- Hendricks, A. J., Maas-Diepeveen, J. L., Noordsij, A., and van der Gaag, M. A., 1994. Monitoring response to XAD-concentrated water in the rhine: a major part of the toxic compounds remains unidentified. *Water Research*, **28**, 581-598.
- Hillel, D., and Toplaz, H., 1976. Simulation of root growth and its effect on the pattern of soil water uptake by a nonuniform root system. *Soil Science*, **121**, 307
- Hillel, D., 1993. *Out of the earth. Civilization and the life of the soil*, Aurum Press, London. 321 p.
- Ho, C. M., and Hurre, P., 1984. Perturbed free Shear Layers. *Annual Review of Fluid Mechanics*. **16**, 365-424.
- Jacobs, A. F. G., and Van Boxel, J. H., 1988. Changes of the displacement height and roughness length of maize during a growing season. *Agricultural and Forest Meteorology*, **42**; 53-62.
- Jacobs, A. F. G., Van Boxel, J. H., and Shaw, R. H., 1992. Horizontal and vertical distribution of air temperature in vegetation canopy. *Netherlands Journal of Agricultural Sciences*, **40**, 359-372.
- Jacobs, A. F. G., Van Boxel, J. H., and El-Kilani, R. M., 1994. Nighttime free convection characteristics within a plant canopy. *Boundary Layer Meteorology*, **71**, 375-391.
- Jacobs, C. M. J., 1994. Direct Impact Of Atmospheric CO₂ Enrichment on Regional Transpiration. Ph. D. thesis. Wageningen Agricultural University.
- Jury, W. A., Gardner, W. R., and Gardner, W. H., 1991. *Soil Physics* (fifth edition), Wiley Inc, New York.
- Katchalsky, A., and Curran, P., 1965. *Nonequilibrium thermodynamics in Biophysics*. Harvard University Press. Cambridge. Massachusetts.
- Kaviany, M., 1990. *Principles of convective heat transfer*. Mechanical engineering series. Springer Verlag. New York.
- Kramer, P. J., and Boyer, J. H., 1995. *Water relations of plants*. Academic press, San Diego, New York.
- Krischer, O., and Rohnalter, H., 1940. Wärmeleitung und Dampfdiffusion in feuchten Gutern. *Verein Deutsch. Ing. Forschungsheft* **402**: 1-18.
- Lamb, R. G., 1980. Mathematical principles of turbulent diffusion modelling. In: *Atmospheric Planetary Boundary Layer physics*, eds. Longhetto, A. pp.173-210. Elsevier, Amsterdam.
- Legg, B. J., and Raupach, M. R., 1982. Markov-chain simulation of particle dispersion in inhomogenous flows: The mean drift velocity induced by a gradient in eulerian velocity variance. *Boundary Layer Meteorology*, **24**, 3-13.

- Leclerc, M. Y., and Beissner, K. C., Shaw, R.H., den Hartog, G. and Neumann, H. H., 1991. The influence of buoyancy on third order turbulent velocity statistics within a deciduous forest. *Boundary Layer Meteorology* **55**: 109-123.
- Li, Z. J., Miller, D. R., and Li, J. D. 1985. A first order closure scheme to describe counter-gradient transport in plant canopies. *Boundary Layer Meteorology* , **33**: 77-83.
- Meyers, T. P., and Paw U, K. T., 1987. Modelling the plant canopy micrometeorology with higher-order closure principles. *Agricultural and Forest Meteorology* , **41**, 143-163.
- Millington, J. R., and Quirk, J. P., 1961. Permeability of porous solids. *Trans. Faraday. Soc.* **57**:1200-1207
- Misra, R. K., Alston, A. M., and Dexter, A. R., 1988. Root growth and phosphorus uptake in relation to the size and strength of soil aggregates. II. Predictions by a stochastic model. *Soil Till. Res.* , **11**,117
- Molz, F. J., and Ferrier, J. M., 1982. Mathematical treatment of water movement in plant cells and tissue: a review 1982. *Plant, Cell and Environment*, **5**, 191-206.
- Monteith, J. L., and Unsworth. M. H., 1990. *Principles of Environmental physics.* (second edition). Arnold, London.
- Norman, J. M., 1979. Modelling the complete crop canopy. In: *Modification of the aerial environment of crops* , eds B. Barfield and J. Garber, pp. 249-277, St. Joseph, Michigan, Am. Soc. Agric. Engr. Monogram no.2 , ASAE.
- Norman., J. M., 1982. Simulation of microclimates: In: *Biometeorology in integrated Pest Management* eds Hatefield, J. and Thomason, I., pp.65-99. Academic Press, New York.
- Onsager, L., 1931. Reciprocal relations in irreversible processes . *Phys. Rev.*, **37**: 405-2426.
- Patankar, S. V., 1980. *Numerical heat transfer and fluid flow* . Series in computational methods in mechanics and thermal sciences , Hemisphere Publishing Company, London.
- Paw U, K. T., 1987. Mathematical analysis of the operative temperature and energy budget. *Journal of Thermal Biology* , **12** nr.3, 227-233.
- Paw U., K. T., and Gao, W., 1988. Applications of solutions to non-linear energy budget equations. *Agricultural and Forest Meteorology*, **43**, 121-145.
- Paw. U, K. T., Brunet, Y., Collineau, S., Shaw, R.H., Maitani, T., Qiu, J., and Hipps, L.,1992. On coherent structures in turbulence above and within agricultural plant canopies. *Agricultural and Forest Meteorology*, **61**, 55-68.
- Penman, H. L., 1948. Natural evaporation from open water, bare soil and grass. *Proceedings of the Royal Society of London, A*, **194**, 120-145.
- Perrier, A., 1976 Etude et essai de modelisation des échanges de masse et d'énergie au niveau des couverts vegetaux . These de Doctorat d'Etat Université de Paris VI Avril 1976, Paris 240 pp.
- Pickard, W. F., 1980. The ascent of sap in plants. *Prog. Biophys and molec Biolo* **37**, 181-229.
- Philip, J. R., and de Vries, D. A., 1957. Moisture movement in porous material under temperature gradient. *Transactions of the American Geophysical Union* **38**:222-231.
- Pockman, W. T., Sperry, J. S., and O'Leary, J. W., 1995. Sustained and significant negative water pressure in the xylum, *Nature*. **378**, 715-716.
- Press, H. J., Teukolsky, S. A., Vetterling, W.T., and Flannery, B. P., 1992. *Numerical Recipes in Fortran The art of scientific computing.* Cambridge University Press.

- Qiu, J., Paw U, K. T., and Shaw, R. H., 1994. Pseudo-wave analysis of turbulence patterns in three vegetation layers. *Proceedings of the 21 Conference on Agricultural and Forest Meteorology, March 7-11, 1994, San Diego, California*. P. 80-83
- Raupach, M. R., 1988. Canopy Transport Processes In: *Flow and transport in Natural Environments: Advances and Applications*, W. L. Steffen and O.T. Denmead (eds). Springer-Verlag, Berlin, pp 95-127.
- Raupach, M. R., 1989. A practical Lagrangian method for relating scalar concentrations to source distributions in vegetation canopies. *Quarterly Journal of Royal Meteorological Society*, **115**, 609-632.
- Raupach, M. R., Finnigan, J. J., and Brunet, Y., 1989. Coherent eddies in vegetation canopies. *Proceedings of the Fourth Australian Conference on Heat and Mass Transfer*, Christchurch, New Zealand, 9-12 May, University of Canterbury, Christchurch, New Zealand, pp. 75-90.
- Reynolds, O., 1894. On the dynamical theory of incompressible viscous fluids and the determination of the criterion. *Phil. Trans. Roy. Soc. A* **186**, 123-164.
- Said, R., 1993. *River Nile: Geology, Hydrology and Utilization*. Pergamon Press, Oxford.
- Seager, J. C. Reed and P. Scott, 1995. *The State of The Environment Atlas*. Penguin.
- Schols, J., 1984. The determination of turbulent structures in the atmospheric surface layer. Ph.D. Thesis. Wageningen Agricultural University.
- Scholander, P. F., Hammel, H. T., Hemmingsen, E. A., and Bradstreet, E.D., 1964. Hydrostatic pressure and osmotic potential in leaves of mangroves and some other plants. *Proceedings of the National Academy of Sciences USA*, **52**, 119-125.
- Shaw, R. H., Ward, D. P., and Aylor, D. E., 1979. Frequency of occurrence of fast gust of wind inside a corn canopy. *Journal of Applied Meteorology*, **16**, 167-171.
- Shaw, R. H., Tavanger, J., and Ward, D. P., 1983. Structure of the Reynolds stress in a canopy layer. *Journal of Climate and Applied Meteorology*, **22**, 1922-1931.
- Shaw, R. H., and Mccarteny; H. A., 1985. Gust penetration into plant canopies. *Atom. Environ.* **19**, 827-830
- Shaw, R. H., 1985. On diffusive and dispersive fluxes in forest canopy. In: *The Forest-Atmosphere Interaction*, eds Hutchinson, B. A. and Hicks, B.B. pp. 407-419. D. Reidel, New York.
- Shaw, R. H., Paw U, K. T., Zhang, X. J., Gao, W., Den Hartog, G., and Neumann, H. H., 1990: Retrieval of turbulent pressure fluctuations at the ground surface beneath a forest. *Boundary Layer Meteorology*, **50**, 319-338.
- Shaw, R. H., and Zhang, X. J., 1992. Evidence of pressure forced turbulent flow in a forest. *Boundary Layer Meteorology*, **58**, 273-288.
- Sloof, W., 1983. Rijn, Lek, Waal, IJssel en uiterwaarden onder invloed van ingrepen en verontreinigingen. In: *Rijnwaterin Nederland*, Hekstra, G. P. and Joenje, W. (eds), Oecologische Kring, Arnhem, The Netherlands, pp. 13-31.
- Sukanto, M., 1969. Climate of Indonesia. In : *Climates of Northern and Eastern Asia*, eds Arkwa, H. World survey of climatology, Vol. 8 . pp.215-231. Elsevier, Amsterdam.
- Spitters, C. J. T., Toussaint, H. A. J. M., and Goudriaan, J., 1986. Separating the diffuse and direct component of global radiation and its implications for modelling canopy photosynthesis.. Part 1. Components of incoming radiation. *Agricultural and Forest Meteorology* **38**, p. 217-2329.
- Stull, R. B., 1988. *An Introduction to Boundary Layer Meteorology*, Kluwer Academic Publishers, Dordrecht.

- Tardieu, F., 1993. Will increases in our understanding of soil-root relations and root signaling substantially alter water flux models. *Phil. Trans. R. Soc. Lond. B.* **341**, 57-66.
- Tardieu, F., and Davies, W. J., 1993. Integration of hydraulic and chemical signalling in the control of stomatal conductance and water status of draughted plants. *Plant, Cell and Environment* **16**: 341-349.
- Tardieu, F., Zhang, J., and Gowing, D. J. G., 1993. Stomatal control by both [ABA] in the xylem and leaf water status: a test of a model for draughted or ABA-fed field-grown maize. *Plant, Cell and Environment* **16**: 413-420.
- Taylor, G. I., 1921a. Diffusion by continuous movements. *Proceedings of the London Mathematical Society*, ser. 2 Vol **20**: 196-212
- Taylor, G. I., 1921b. Diffusion by continuous Movements; In: *G. I. Taylor Scientific Papers* eds Batchelor. G. K., pp. 172-184.
- Taylor, S. A., and Cary, J. W., 1964. Linear equations for the simultaneous flow of matter and energy in a continuous soil system. *Soil Science Society of America Proceedings* **28**: 167-172.
- Tollmien, W., 1929. Nachr. Ges. Wiss. Gottingen, Math. Phys. Klasse, **21** ,
- Tollmien, W., 1931 N. A. C. A . Techn. Mem. Nr. 609
- Van Boxel, J. H., 1988. Transportprocessen binnen en vlak boven gewassen. Eindrapportage van een tweejarig onderzoek. (Internal report.) Dept. of Meteorology, Wageningen Agricultural University., Wageningen, The Netherlands.
- Van Heemst, H. D. J., 1988: Plant data Values required for simple crop growth simulation models: Review and bibliography. Simulation Report CABO-TT nr. 17.
- Van Pul, W. A. J., 1992. *The flux of ozone to a maize crop and the underlying soil during a growing season.* ph.d thesis, wageningen agricultural university, the netherlands.
- Vries, D. A. de., 1963. Thermal properties of soils. In : *Physics of Plant Environment* , ed. W. R. van Wijk. North Holland Publishers, Amsterdam.
- Vries, D. A. de., 1975. Heat transfer in soils. In: *Heat and mass transfer in the biosphere.* eds. N. H. Afgan & D. A. DeVries , Scripta books.
- Zimmermann, U., Haase, A., Lanbein, D., and Meinzer, F., 1993. Mechanism of long distance water transport in plant: a re-examination of some paradigms in the light of new evidence. *Phil. Trans. R. Soc. Lond. B.* **341**, 19-31.
- Zimmermann, M. H., 1983. *Xylem structure and ascent of sap.* Springer. Berlin.
- Weeks, L. V., Richards, S. J., and Letty, J., 1968. Water and salt transfer in soil resulting from thermal gradients. *Soil Science Society of America Proceedings.* **32**: 193-197.
- Wilczak, J. M., 1984. Large scale eddies in the unstably stratified atmospheric surface layer. Part I: velocity and temperature Structure. *Journal of Atmospheric Sciences.* **41**, No. 24, 3537-3550.
- Wilson, N. R., and Shaw, R. H., 1977. A higher order closure model for canopy flow. *Journal of Applied Meteorology*, **16**, 1197-1205.
- Wilson, J. D., Thurtell, G. W., and Kidd, G. E., 1981. Numerical simulation of particle trajectories in inhomogenous turbulence. II. Systems with variable turbulent velocity scale. *Boundary Layer Meteorology*, **21**, 423-441.
- Wilson , J. D., and Sawford, B. L., 1996. Review of Lagrangian Stochastic models for trajectories in the turbulent atmosphere *Boundary layer Meteorology* **78**, 191-210.

Curriculum Vitae

In the end of 1956, Suez war broke out between Egypt and Israel, France and England. Suez canal was closed and ships have to take the route of the Cape of Good Hope. On an Egyptian ship, there was an Egyptian engineer sailor who was invited with his colleagues for a reception by the Moslem community in Cape Town. During that reception, this engineer met the girl which would become his future wife. He later brought her to Egypt. From that marriage, Rushdi Mohammed Mohammed El-Kilani was born in Alexandria, Egypt on 12 December 1958 as the first of three brothers.

After finishing high school examination in 1987, he joined the faculty of Agriculture, Cairo University. He graduated four years later with an average final grade "very good" specialising in Soil Science. He was later asked by the Soil science department of that faculty to work as a teaching assistant.

After joining the army for a period of fifteen month, starting in January 1983, he took the responsibility of doing research and teaching within this department.

In August 1984, he enrolled for an M.Sc. degree in Soil science and Plant mineral nutrition. During the period of August 1984- June, he finished a course load of 14 courses , 11 of them are post graduate. He also did a field experiment.

In August 1987, he got the opportunity to join the ninth M. Sc. Course in Soil Science and Water Management in the Wageningen Agricultural University (WAU), The Netherlands. He graduated in June 1989 with distinction. He specialised in Water Management: Agrohydrology. His M.Sc. thesis was titled: Heat and Mass Transfer within Plant Canopies: A first order closure model extended with a non-locality term.

In the period of Nov. 1989, he worked for VROM on extending a two dimensional wind flow model around wind breaks with a scalar to describe the effect of windbreaks on the dispersion of smell coming out from animal sheds. The study was entitled: A first order closure model for estimating the effect of windbreak on passive scalar dispersion.

His Ph.D. study started officially in June 1990. The modelling work was mainly finished by September 1992. From Sept. 1992, till March 1994, analysis was done on the some available data set with the Meteorology Department, WAU. Also during the same period, a qualitative analysis of the limitation of the second and higher order closure models and random walk models was done. During the same period, some early parts of the mathematical analysis were done. From March 1994 till June 1996, the rest of the mathematical analysis, including the soil solution, the MATHCAD runs and the validation runs were completed.

During his Ph.D. Study years, he built a publications list of 12 articles (9 non refereed as a main author in proceedings and 3 refereed as a co-author in periodicals).